ACTA CHIMICA

ACADEMIAE SCIENTIARUM HUNGARICAE

ADIUVANTIBUS

L. ERDEY, K. POLINSZKY, G. SCHAY

AC

R. BOGNÁR, GY. BRUCKNER, Z. CSŰRÖS, T. ERDEY-GRÚZ, Z. FÖLDI, M. FREUND, Á. GERECS, GY. HARDY, J. HOLLÓ, Á. KISS, M. KORACH, F. MÁRTA, F. NAGY, J. PROSZT, E. PUNGOR, Z. SZABÓ, P. TÉTÉNYI, L. VARGHA, K. VAS

REDIGIT

B. LENGYEL

TOMUS 57 FASCICULUS 1

AKADÉMIAI KIADÓ, BUDAPEST

1968

ACTA CHIM. ACAD. SCI. HUNG.

ACTA CHIMICA

A MAGYAR TUDOMÁNYOS AKADÉMIA KÉMIAI TUDOMÁNYOK OSZTÁLYÁNAK IDEGEN NYELVŰ KÖZLEMÉNYEI

SZERKESZTI

LENGYEL BÉLA

TECHNIKAI SZERKESZTŐK

DEÁK GYULA és TAKÁCS VILMOS

Az Acta Chimica német, angol, francia és orosz nyelven közöl értekezéseket a kémiai tudományok köréből.

Az Acta Chimica változó terjedelmű füzetekben jelenik meg, egy-egy kötet négy füzetből áll. Évente átlag négy kötet jelenik meg.

A közlésre szánt kéziratok a szerkesztőség címére (Budapest 112/91 Műegyetem) küldendők.

Ugyanerre a címre küldendő minden szerkesztőségi levelezés. A szerkesztőség kéziratokat nem ad vissza.

Az Acta Chimica előfizetési ára kötetenként belföldre 120 Ft, külföldre 165 Ft. Megrendelhető a belföld számára az „Akadémiai Kiadó"-nál (Budapest V., Alkotmány utca 21. Bankszámla 05-915-111-46), a külföld számára pedig a „Kultúra" Könyv- és Hírlap Külkereskedelmi Vállalatnál (Budapest I., Fő utca 32. Bankszámla: 43-790-057-181) vagy annak külföldi képviseleteinél és bizományosainál.

Die Acta Chimica veröffentlichen Abhandlungen aus dem Bereiche der chemischen Wissenschaften in deutscher, englischer, französischer und russischer Sprache.

Die Acta Chimica erscheinen in Heften wechselnden Umfanges. Vier Hefte bilden einen Band. Jährlich erscheinen 4 Bände.

Die zur Veröffentlichung bestimmten Manuskripte sind an folgende Adresse zu senden:

Acta Chimica
Budapest 112/91 Műegyetem

An die gleiche Anschrift ist auch jede für die Redaktion bestimmte Korrespondenz zu richten.

Abonnementspreis pro Band: 165 Forint. Bestellbar bei dem Buch- und Zeitungs-Außenhandels-Unternehmen »*Kultúra*« (Budapest I., Fő utca 32. Bankkonto Nr. 43-790-057-181) oder bei seinen Auslandsvertretungen und Kommissionären.

ACTA CHIMICA

ACADEMIAE SCIENTIARUM HUNGARICAE

ADIUVANTIBUS

L. ERDEY, K. POLINSZKY, G. SCHAY

AC

R. BOGNÁR, GY. BRUCKNER, Z. CSŰRÖS, T. ERDEY-GRÚZ, Z. FÖLDI, M. FREUND, Á. GERECS, GY. HARDY, J. HOLLÓ, Á. KISS, M. KORACH, F. MÁRTA, F. NAGY, E. PUNGOR, Z. SZABÓ, P. TÉTÉNYI, L. VARGHA, K. VAS

REDIGIT

B. LENGYEL

TOMUS 57

AKADÉMIAI KIADÓ, BUDAPEST

1968

ACTA CHIMICA

TOMUS 57

Fasciculus 1 : 1968
Fasciculus 2 : 1968
Fasciculus 3 : 1968
Fasciculus 4 : 1968

INDEX

ALTENBURG, K.: Zur Anwendung einiger Konformationsregeln auf Cyclohexylamine 101
BAITZ, E. s. SZŐKE, S.
BALOGH, A. s. FÁY, L.
BÁN, M. und CSÁSZÁR, J.: Untersuchung der Elektronenanregungsvorgänge und der Bindungsverhältnisse der Komplexe von $3d^n$ Elementen mit der Ligandenfeldmethode, III. Monacido-, trans-Diacido- und cis-Diacido-Kobalt (III)- und Chrom (III)-Komplexe 153
BÁRDY, M. s. LEMPERT-SRÉTER, M.
Book reviews 453
BRAUN, T. s. TÖLGYESSY, J.
BURGER, K., PJNTÉR, B., PAPP-MOLNÁR, E. and NEMES-KÓSA, S.: The Chemistry of Mixed Ligand Complexes, III. The Effect of Water Activity on the Stability of the Bis-Dimethyglyoximato-Diiodo-Cobaltate(II) Mixed Complex 363
BURGER, K., VÉRTES, A. and PAPP-MOLNÁR, E.: The Nephelauxetic Series and the Order of the Mössbauer Parameters of Iron Complexes 257
COHEN-ADAD, R., TRANQUARD, A. et MARCHAND, A.: Sur quelques problèmes posés par l'étude, à température élevée, des équilibres liquide-solide dans les systèmes contenant un constituant volatil 69
CSÁSZÁR, J. s. BÁN, M.
ЧОРДАШ, Л.: Программирование для звм типа »Урал-2« для рентгеноструктурного анализа 1. Суммирование двухмерных рядов фурье 147
(CSORDÁS, L.: X-ray Diffraction Calculations on the Electronic Computer "Ural-2", I. Summation of Fourier Series with two Variables) 147
DOLESCHALL, G., HORNYÁK, GY., LÁNG, L., LEMPERT, K. and ZAUER, K.: 1,2,4-Triazines and Condensed Derivatives, VI. Synthesis of 6-methyl-7H-thiazolo (3,2-b) (1,2,4) thiazine-3 (2H)-dione and 2-methyl-6,7-dihydro-3H, 8H-(1,3) thiazino (3,2-b) (1,2,4) triazine-3,8-dione 191
ЕЛЕК, А. и САБО, Э: Анализ вольфрама методом нейтронной активации, II. определение содержания натрия и калия 385
(ELEK, A. and SZABÓ, E.: Investigation of Tungsten by Neutron-Activation Analysis, II. Determination of the Sodium and Potassium Content) 385
ERDEY-GRÚZ, T. und KUGLER, E.: Über den Wanderungsmechanismus von Wasserstoff- und Hydroxylionen, VIII. Einfluß der Zusammensetzung von Glycerin-Wasser-Gemischen auf die elektrische Leitfähigkeit und Viskosität von gelöstem HCl, KOH, KF und KCl bei 5 und 25° C 301
ERDEY, L. s. GÁBOR-KLATSMÁNYI, P.
FARKAS, L. s. WAGNER, H.
FÁY, L. and BALOGH, A.: Determination of Reaction Order Rate Constants on the Basis of the Parameter Estimation of Differential Equations 391
FEHÉR, I. s. NÁRAY-SZABÓ, I.
FODOR, M. s. POKÓ, Z.
FREUND, M. s. MARKÓ, L.
GÁBOR-KLATSMÁNYI, P., INCZÉDY, J. and ERDEY, L.: The Use of Ammonium Sulphosalicylate as Complexing Agent in Ion Exchange Chromatography, II. Stability of the Sulphosalicylate Complexes of Copper(II), Nickel(II) and Cobalt(II) at 80° C 5

GÉCZY, I.: Synthetische lineare Polymere, XXVIII. Zusammenhang zwischen einzelnen spezifischen Eigenschaften der in der Kettenmitte Heteroatome oder Atomgruppen enthaltenden oligomeren polymerhomologen Verbindungen und ihrer Molekülgröße 345
GENAEVA L. I. s. LAVRUKHINA, A. K.
GERECS, Á. s. RUFF, F.
GÖNDÖS, G. s. MATKOVICS, B.
HANKOVSZKY, O. H. and HIDEG, K.: Benzanoles, VI. O-Alkylation of 2-(Hydroxyphenyl)- and 2-(Hydroxy-Benzyl) Benzanoles 219
HANKOVSZKY, O. H. s. HIDEG, K.
HARGITTAI, I.: Investigation of the Molecular Structure of Sulphuryl Chloride by Sector Microphotometer Electron Diffraction 403
HIDEG, K. and HANKOVSZKY, O. H.: Benzazepines, III. Preparation of 1H,-2,3-Dihydro-6,7-Benzo-(1,5)-Diazepines and their Reduction to 1H,2,3,4,5-Tetrahydro-6,7-Benzo-(1,5)-Diazepines 213
HIDEG, K. s. HANKOVSZKY, O. H.
HÖRHAMMER, L. s. WAGNER, H.
HORNYÁK, GY. s. DOLESCHALL, G.
INCZÉDY, J. s. GÁBOR-KLATSMÁNYI, P.
KAJTÁR, J. s. KUTASSY, S.
KALLÓ, D.: Die katalytisch kinetische Deutung der scheinbar reversiblen Dreieckreaktion erster Ordnung der Butenisomerisierung 313
KASKAROV, L. L. s. LAVRUKHINA, A. K.
KLIVÉNYI, F. s. VINKLER, L.
KOLESOV, G. M. s. LAVRUHINA, A. K.
KÓSA, I. s. SOHÁR, P.
KOTSIS, T. s. NÁRAY-SZABÓ, I.
KUCSMAN, Á., RUFF, F., SÓLYOM, S. und SZIRTES, T.: Bindungssystem der N-Acyl-sulfilimine, VI. Konjugativer Effekt der S-Methyl-N-p-tolylsulfonyl-sulfilimingruppe .. 205
KUGLER, E. s. ERDEY-GRÚZ, T.
KUTASSY, S., KAJTÁR, J. und MEDZIHRADSZKY-SCHWEIGER, H.: Eine einfache Mikromethode zur Bestimmung der tert. Butyloxycarbonyl-Schutzgruppe verschiedener Aminosäuren und ihrer Derivate 113
LÁNG, L. s. DOLESCHALL, G.
ЛАВРУХИНА, А. К., КАШКАРОВ, Л., КОЛЕСОВ, Г. М., ГЕНАЕВА, Л.И.: Изучение распределения редких элементов между различными фазами каменных метеоритов методом нейтроно-активацинного анализа 353
LAVRUKHINA, A. K. KASKAROV, L. L., KOLESOV, G. M. and GENAEVA, L. I.: Investigation of the Distribution of Rare Elements between the Various Phases of Stone Meteorites by Neutron Activation Analysis) 353
LÉGRÁDI, L.: Mechanism of Adsorption Indication, III. 4-(4'-Nitrophenylazo)-1-naphthol, a New Adsorption Indicator 241
LÉGRÁDI, L.: Mechanism of Adsorption Indication, IV. Combination of the Fajans Indication with the Acid—Base Principle 247
LEMPERT, K. s. DOLESCHALL, G.
LEMPERT-SRÉTER, M. and BÁRDY, M.: 1,5-Diketones, IV. Synthesis of Some New Isobenzopyrylium Anhydrobases 181
LENGYEL, T.: Investigations on Ion Exchange Equilibria with Radioactive Tracer Method, XII. Determination of the Successive Formation Constants of α-Hydroxyisobutyrate Complexes of Europium 291
MAGYAROSY, I. s. NÁRAY-SZABÓ, I.
MARCHAND, A. s. COHEN-ADAD, R.
МАРДАШЕВ, Ю., С.: К кинетике дегидрирования C_6H_{12} над никелевыми катализаторами 83
(MARDASHEW, YU. S.: Kinetics of Dehydrogenation of C_6H_{12} on Nickel Catalysts) .. 83
MARKÓ, L. et FREUND, M.: L'utilisation des oléfines plus élevées de craquage dans l'oxosynthèse 445
MATKOVICS, B., GÖNDÖS, G. and TARÓDI, B.: Rearrangements of Steroids, V. Schmidt Reaction and Beckmann Rearrangement of Estrone and of its Derivatives (Preliminary Communication) 109
MEDZIHRADSZKY-SCHWEIGER, H. s. KUTASSY, S.
MISHRA, M. B. and NIGAM, H. L.: Complex Formation between Uranyl (VI) and Thiopropionic Acid 1

NÁRAY-SZABÓ, I., MAGYAROSY, I., KOTSIS, T. und FEHÉR, I.: Untersuchung der chemischen Vorgänge bei der Kalkbehandlung des Rotschlammes 377
NEMES-KÓSA, S. s. BURGER, K.
NIGAM, H. L. s. MISHRA, M. B.
NÓGRÁDI, M. s. WAGNER, H.
NOVÁK, L. s. SZÁNTAY, Cs.
PAÁL, T. s. ZSADON, B.
PAPP-MOLNÁR, E. s. BURGER, K.
PINTÉR, B. s. BURGER, K.
POKÓ, Z., FODOR, M. and SZABÓ, E.: Formation, Thermal Decomposition and Structure of the System UO_3—H_2O, III. Thermal Decomposition of β-$UO_3 \cdot 2H_2O$ Produced from γ-UO_3 275
PULAY, P.: On the Parameter Form of Force Constant Matrix, VII. The Closest Assignment Force Constant Matrix 373
RUFF, F., SCHUSTER, I. und GERECS, Á.: Protonenresonanzspektroskopische Untersuchungen und Bildung von O-Acetyl-D-gluconsäure-, — D-mannonsäure- und — D-xylonsäure-(1,5)-lacton-2,4-dinitro-phenylhydrazon 101
RUFF, F. s. KUCSMAN, Á.
SCHUSTER, I. s. RUFF, F.
SELIGMANN, O. s. WAGNER, H.
SOHÁR, P. s. SZÁNTAY, Cs.
SOHÁR, P. and KÓSA, I.: NH Stretching Vibration Bands at Wave Numbers Lower than 3000 cm^{-1}, V. Cyclic Dimeric Structures, V. Quinazolone Derivatives 411
SOHÁR, P.: NH Stretching Vibration Bands at Wave Numbers Lower than 3000 cm^{-1}, VI. Cyclic Dimeric Structures, VI. Hydantoin Derivatives 425
SOLYMOSI, F.: Thermal Stability of Chlorine Oxy-Salts in the Solid State, IV. Kinetics and Mechanism of the Thermal Decompositions of Alkali Perchlorates 11
SOLYMOSI, F.: Thermal Stability of Chlorine Oxy-Salts in the Solid State, V. Thermal Decomposition of Some Divalent Metal Perchlorates 35
SÓLYOM, S. s. KUCSMAN, Á.
STRELISKY, J. s. WAGNER, H.
SZABÓ, E. s. ELEK, A.
SZABÓ, E. s. POKÓ, Z.
SZÁNTAY, Cs., NOVÁK, L. and SOHÁR, P.: Chemistry of Heterocyclic Pseudobasic Aminocarbinols, XXXIV. Notes on the Synthesis on "Quantril" and on the Tautomerism of β-Oxo-Carboxamides 335
SZÁSZ, K.: Determination of Mass Transfer Coefficients in the Extraction of Medicinal Plants with an Organic Solvent 225
SZIRTES, T. s. KUCSMAN, Á.
SZŐKE, S. and BAITZ, E.: The Potential Energy Functions of Diatomic Molecules (Halides and Hydrides of the Groups Ia and IIa) 129
TARÓDI, B. s. MATKOVICS, B.
TÖLGYESSY, J., BRAUN, T. and VARGA, S.: Some Problems Concerning the Application of Radioactive Kryptonates as Complexometric Indicators 265
TÖRÖK, F.: On the Parameter form of Force Constant Matrix, VI. On the Common Force Constant Matrices of Isotopic Molecules 141
TRANQUARD, A. s. COHEN-ADAD, R.
VARGA, S. s. TÖLGYESSY, J.
VARSÁNYI, G.: Characteristic Normal Vibrations of Benzene Derivatives, III. Correlation among the Frequency and Vibrational Form of the Out-of-Plane CH Vibrations ... 51
VERMES, B. s. WAGNER, H.
VÉRTES, A. s. BURGER, K.
VINKLER, L. and KLIVÉNYI, F.: Recent Results Concerning the Reaction of Aromatic Thiolsulfinates with Dinitrochlorobenzene 91
WAGNER, H., SELIGMANN, O., HÖRHAMMER, L., NÓGRÁDI, M., FARKAS, L., STRELISKY, J. and VERMES, B.: Investigation on the Keto-Enol Tautomerism of O-Hydroxy-Dibenzoylmethanes by Nuclear Magnetic Resonance 169
ZAUER, K. s. DOLESCHALL, G.
ZSADON, B. und PAÁL, T.: Über die quantitative polarographische Bestimmung des Morphingehalts von Mohnkapseln 323

Acta Chimica Academiae Scientiarum Hungaricae Tomus 57 (1), pp. 1—4 (1968)

COMPLEX FORMATION BETWEEN URANYL(VI) AND THIOPROPIONIC ACID

M. B. MISHRA and H. L. NIGAM

(Chemical Laboratories, University of Allahabad, Allahabad)

Received May 29, 1967

Thiopropionic acid (hereafter abbreviated as TPA) has been described as a ligand towards transition metal ions [1—5], but no systematic study of its donor characteristics has been reported. Particular interest is attached to the system UO_2(VI)-TPA. In the present work an effort has been made to gather some information, at least in a semi-quantitative manner, regarding the complex formation between uranyl(VI) and TPA. Potentiometric studies in solution reveal 1 : 2 UO_2(VI) : TPA stoichiometry. The complex has been isolated as a yellow solid which shows the same composition. It has been characterized by infrared and magnetic measurements.

Experimental

Apparatus and materials

All the chemicals used were *AnalaR (BDH)* reagent grade. TPA was an *Evans (Chemetics Inc., N. Y.)* product of 99.2% purity. Its freshly prepared solutions were used whenever needed and were standardized iodometrically. Magnetic measurements were done by *Gouy*'s method, using mercury(II) tetrathiocyanatocobaltate(II) as calibrating agent.

The electronic spectra were recorded on a *Perkin—Elmer model*-350 spectrophotometer using KBr discs. The IR spectra were obtained with a *Perkin—Elmer model*-350 automatic recording spectrophotometer, in Nujol mull.

pH titrations were done with a *Leeds* and *Northrup* pH-meter supplied with an all-purpose glass electrode, operated at 220 V mains. Potentiometric titrations were carried out in nitrogen atmosphere, and on dilute solutions to avoid volume corrections. Sodium perchlorate and perchloric acid were added to maintain constant ionic strength. Different mixtures of metal ion, ligand and the buffer were titrated against standard alkali. A plot of the pH against the volume of alkali used gave S-shaped curves, which were utilized for the evaluation of the composition and the stepwise stability constants.

Preparation of the compound

125 ml of 0.1 *M* TPA was added to 25 ml of 0.1 *M* uranyl nitrate solution, the pH of the reacting solutions being 4.5. Immediately after the addition of TPA, a deep yellow colouration appeared. The yellow solution on warming gave a pale yellow precipitate. This was filtered off, washed three or four times with water, then with acetone, and dried at 80°. The complex was insoluble in water and in organic solvents. It decomposed on heating above 250°.

$[UO_2(C_3H_5O_2S)_2 \cdot (H_2O)_2]$; diaquo-bis-thiopropionato-uranate. Calcd. C 13.9; H 2.7; U 46.10; S 10.4. Found C 9.01; H 2.14; U 46.3; S 10.6%.

Results and discussion

Potentiometric studies in solution reveal the 1 : 2 UO_2(VI) : TPA stoichiometry. As is apparent from Fig. 1, a shift of 1.00 ml is observed in curves *B* and *C*. 1.00 ml of NaOH is required for the neutralization of the third hydro-

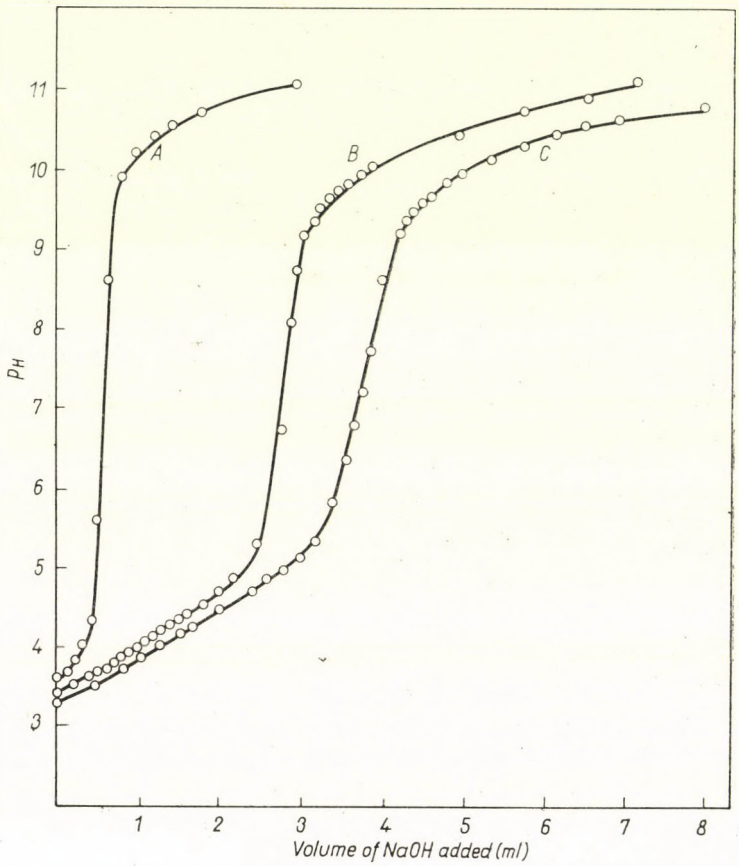

Fig. 1. (A) 5 ml 0.1 *M* $NaClO_4$ + 5 ml 0.01 *M* $HClO_4$ + 140 ml water, *(B)* 5 ml 0.1 *M* $NaClO_4$ + 5 ml 0.01 *M* $HClO_4$ + 25 ml 0.01 *M* TPA + 115 ml water, *(C)* 5 ml 0.1 *M* $NaClO_4$ + 5 ml 0.01 *M* $HClO_4$ + 25 ml 0.01 *M* TPA + 5 ml 0.01 *M* UO_2(VI) + 110 ml water. Strength of NaOH = 0.1 *M*

gen ion, released during complexation with TPA. This volume of NaOH corresponds to the strength of the metal ion utilized in complexation. The equivalence between the metal ion and NaOH is found to be 1 : 2. Again, since one molecule of NaOH will neutralize one proton of TPA, the equivalence between the metal and TPA is found to be 1 : 2. The stepwise stability constants log K_1 and log K_2, have been evaluated by the method of BJERRUM [9] as modified by IRVING and ROSSOTTI [10] (Table I).

Analyses of the solid complex for its metal, sulphur, carbon and hydrogen contents confirm the 1 : 2 UO_2(VI) : TPA stoichiometry. The complex is diamagnetic, as expected [8]. The absorption spectra (in KBr disc [6]) show four peaks; 17250 cm^{-1}, 20600 cm^{-1}, 23250 cm^{-1} and 30200 cm^{-1}. Owing to lack of information on the spectra of UO_2(VI) complexes and the complex nature of splitting of energy levels, band assignments could not be made.

Table I

pH	$\bar{n}$	P_L	Stepwise stability constants
4.00	0.34	— 4.0345	
4.50	0.55	— 5.0170	
5.00	1.09	— 5.9686	
5.50	1.37	— 7.0309	log $K_1 = 3.7$
6.00	1.67	— 7.9098	log $K_2 = 7.4$
6.50	1.70	— 8.9064	
7.00	1.86	— 9.9541	
7.50	1.91	—10.9508	

The infrared spectrum of TPA shows bands corresponding to S—H, C=O, C—O, and C—S stretching vibrations at 2577 cm^{-1}, 1712 cm^{-1}, 1429 cm^{-1}, respectively. In the complex under investigation, the band corresponding to S—H (2577 cm^{-1}) disappeared, whereas the band corresponding to C=O stretching vibrations was observed to have shifted to the lower frequency of 1655 cm^{-1}. The band corresponding to C—O stretching frequencies was observed to have shifted to a higher frequency, 1434 cm^{-1}, indicating further stretching of the bond. The disappearance of the band corresponding to the S—H frequency and the lowering of the C—S stretching frequency indicate the coordination through the sulphur atom, whereas the lowering of the C=O stretching frequency indicates coordination through the carbonyl oxygen (C=O) of the carboxylic group. JONES [8] has observed that the uranyl group itself has a band appearing between 900—950 cm^{-1}, which in the present case is found to appear at 938 cm^{-1}, indicating the presence of the uranyl group. The bands at 3278 cm^{-1} and 3639 cm^{-1} in the infrared spectra of the complex are due to coordinated water molecules.

On the basis of these observations it seems that thiopropionic acid acts as a bidentate ligand in this eight-coordinated uranium complex.

*

The authors are thankful to authorities of *N. C. L. Poona, India*, for providing laboratory facilities for the spectral measurements. Thanks are also due to *CSIR, New Delhi, India*, for the award of fellowship *M. B. M.*

SUMMARY

Potentiometric studies in solution have revealed the formation of a 1 : 2 metal : ligand [UO_2(VI) : TPA] complex (where TPA stands for thiopropionic acid). The stepwise stability constants are log $K_1 = 3.7$ and log $K_2 = 7.4$, and the corresponding free energy of formation is —5.13 cal. (at 30° C). The complex has been isolated as a yellow solid which shows the same composition as in solution. It has been characterized by infrared and magnetic measurements.

REFERENCES

1. Lyons, E.: Anal. Chem. **27,** 1813 (1955).
2. Fernando, Q., Freiser, H.: J. Am. Chem. Soc. **80,** 4928 (1958).
3. Burke, R. W., Yoe, J. H.: Talanta **10,** 1267 (1963).
4. Clark, E. R.: J. Inorg. Nucl. Chem. **25** (4), 354 (1963).
5. Bear, J. L., Choppin, G. R., Quaglino, J. V.: J. Inorg. Nucl. Chem. **25** (5), 513 (1963).
6. Stimson, M. M., O'Donell, M. J.: J. Am. Chem. Soc. **74,** 1805 (1952).
7. Belova, V. I., Syrkin, Y. K., Narkov, V. P., Tsapkina, I. V.: Zhur. Neorg. Khim. **6,** 495 (1961).
8. Llewellyn, H., Jones, H.: Spectrochim. Acta **10,** 395 (1958).
9. Bjerrum, J.: "Metal ammine formation in aqueous solution". P. Hasse & Son. Copenhagen.
10. Irving, H. M., (Mrs.) Rossotti, H. S.: J. Chem. Soc. **1954,** 294.

M. B. Mishra
H. L. Nigam
University of Allahabad, Allahabad 2, India

Acta Chimica Academiae Scientiarum Hungaricae Tomus 57 (1), pp. 5—9 (1968)

THE USE OF AMMONIUM SULPHOSALICYLATE AS COMPLEXING AGENT IN ION EXCHANGE CHROMATOGRAPHY, II

STABILITY OF THE SULPHOSALICYLATE COMPLEXES OF COPPER(II), NICKEL(II) AND COBALT(II) AT 80°C

P. GÁBOR-KLATSMÁNYI, J. INCZÉDY and L. ERDEY

(Institute for General and Analytical Chemistry of the Technical University, Budapest)

Received August 10, 1967

In our earlier paper [1] an ion-exchange chromatographic method was described for the separation and photometric determination of transition metal ions.

The metal ions were separated using ammonium sulphosalicylate eluting solutions of pH 5, at 80°.

In connection with these separations, the determination of the stability constants of the sulphosalicylate complexes of the transition metals at 80° seemed to be of interest.

The method of ion exchange can be usefully employed for the investigation of the sulphosalicylate complexes of bivalent metal ions. Metal ions form 1 : 1 and 1 : 2, negatively charged complexes with sulphosalicylate ions which in principle, are not bound by the cation exchanger. Since the ligand is much larger than the metal ion, the penetration of the ligand into the resin phase is negligible even at higher concentrations.

As virtually only the free metal ions are bound by the cation exchanger, the distribution coefficient of the metal ion in the presence of a complexing agent depends, besides the ion-exchange equilibrium, only on the ligand concentration and stability of the complexes formed. When a series of experiments is performed in which the ligand concentration is varied while the concentration of the counter ion is kept constant by the addition of an indifferent alkali salt, and the distribution coefficients are determined, the stability constants of the complexes can be calculated from the distribution coefficients and ligand concentrations [2].

In the absence of a complexing agent — if the activity coefficients are disregarded — the distribution coefficient of the bivalent ion may be calculated as follows:

$$d = K^x \left(\frac{(Na)}{[Na]} \right)^2 \qquad (1)$$

where K^x is the apparent ion-exchange equilibrium constant of the metal and sodium ions, and (Na) and $[Na]$ denote the concentrations of sodium ions in the resin and solution, respectively.

In the presence of a complexing agent the distribution coefficient is as follows:

$$D = K^x \left(\frac{(Na)}{[Na]} \right)^2 \Phi \tag{2}$$

where Φ is the mole fraction of the free metal ion.

If the concentration of sodium ions is kept constant during the series of experiments, and the distribution coefficients are determined at varying ligand concentrations and also in the absence of a complexing agent, the $\frac{D}{d}$ quotients will be equal to the reciprocal of Φ belonging to the given ligand concentration. It means that

$$\frac{d}{D} = 1 + [L]\beta_1 + [L]^2\beta_2 = \frac{1}{\Phi} \tag{3}$$

where $[L]$ is the concentration of free ligand and β_1 and β_2 are the complex products of the 1 : 1 and 1 : 2 complexes, respectively.

The complex products can be evaluated by the graphical method of LEDEN [3] if the corresponding $\frac{D}{d}$ and $[L]$ values are known.

We have determined the distribution coefficients by means of an ion exchange column, from the results of elution experiments, similarly as we have done earlier [1]. The eluting solutions that were used contained various amounts of a complexing agent, but the ionic strength was invariably 0.5, the pH 5, and the temperature 80°, in all experiments. The concentration of the eluted metal ion was negligible in all cases compared to that of the complexing agent.

The free ligand concentration was calculated by means of the following equation:

$$[L] = \frac{C_L}{\alpha_H} \tag{4}$$

where C_L is the analytical concentration of sulphosalicylic acid in the eluent, and α_H is the protonation function of the ligand:

$$\alpha_H = 1 + [H]\frac{1}{k_3} + [H]^2\frac{1}{k_2 k_3} + [H]^3\frac{1}{k_1 k_2 k_3} \tag{5}$$

where k_1, k_2 and k_3 are the dissociation constants of sulphosalicylic acid.

Since the dissociation constants of sulphosalicylic acid at 80° were not known, we determined them by pH-metric titration. The following values were found for the dissociation constants:

$$\log k_1 = -1.52$$
$$\log k_2 = -2.30$$
$$\log k_3 = -10.47 \ (80°;\ I = 0.5)$$

Experimental

Ion-exchange column. An ion exchange column of 6.5 mm diameter and 120 mm length was prepared of *Amberlite CG*-120 (100—200 mesh) ion-exchange resin. The resin was transformed into the sodium form by 1 *M* sodium chloride solution, and washed out with water. Water of 80 ° temperature from a thermostat was circulated in the heating jacket of the column.

Stock solutions containing copper(II), nickel(II) and cobalt(II) ions. 0.01 *M* solutions were prepared from analytical grade salts (see reference [1]).

Eluting solutions. A 0.5 *M* solution was prepared from recrystallized sulphosalicylic acid, and a known amount of it adjusted to pH 5 at 80° by means of concentrated sodium hydroxide solution. The solution was finally diluted to 0.25 *M*.

0.5 *M* sodium perchlorate solution was prepared by neutralizing 1 *M* perchloric acid to pH 5, and diluting the solution to appropriate volume.

The eluting solutions were prepared from these two solutions so that the ionic strength was 0.5 in each case.

Determination of the dissociation constants of sulphosalicylic acid. The pH-metric titrations were performed by means of a *Radelkisz* (Hungary) precision pH-meter, with glass and saturated calomel electrodes. The pH-meter was calibrated at 80° with solutions of known pH. The following solutions were used: 0.05 *M* potassium tetraoxalate (pH 1.77); 0.05 *M* potassium hydrogen phtalate (pH 4.16); potassium hydrogen tetrate saturated at 25° (pH 3.61); 0.01 *M* borax solution (pH 8.89) [4].

50 ml 0.01 *M* sulphosalicylic acid containing 0.5 *M* sodium perchlorate was pipetted into a titrating flask equipped with a heating jacket, and titrated at 80° with 0.1 *M* sodium hydroxide standard solution, under stirring and nitrogen bubbling. The pH values measured by the pH-meter were recorded during the titration. The dissociation constants of sulphosalicylic acid were calculated from the titration curve and from the ionic product of water (log K = = —12.60 [5]), using the graphical method of SCHWARZENBACH *et al.* [6].

Determination of distribution coefficients. The elution experiments were performed, the metal ions in the effluent determined and the volumetric distribution coefficients calculated from experimental data (position of peak in the elution diagram; volume of column; void fraction), as described earlier [1]. The distribution coefficients found are given in Table I.

Table I

Volumetric distribution coefficients of copper(II), nickel(II) and cobalt(II) ions on cation exchange resin, at 80°C and at varying eluent compositions.

(Ionic strength = 0.5)

Sodium sulphosalicylate, mole/l (pH 5)	Distribution coefficients		
	D_{Cu}	D_{Ni}	D_{Co}
0.25	2.0	25.2	24.7
0.15	3.6	34.2	33.6
0.10	5.1	40.3	40.8
0.05	10.1	49.0	52.8
0.025	18.4	—	—
0.000	62.2	59.9	69.1

Results and discussion

The $\frac{d}{D}$ quotients were calculated from the results of experiments carried out using eluting solutions with and without a complexing agent. The free

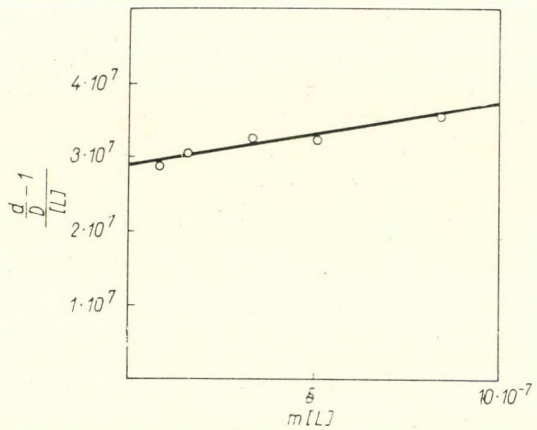

Fig. 1. Determination of the complex products of copper(II) sulphosalicylate complexes from the distribution coefficients by graphical method

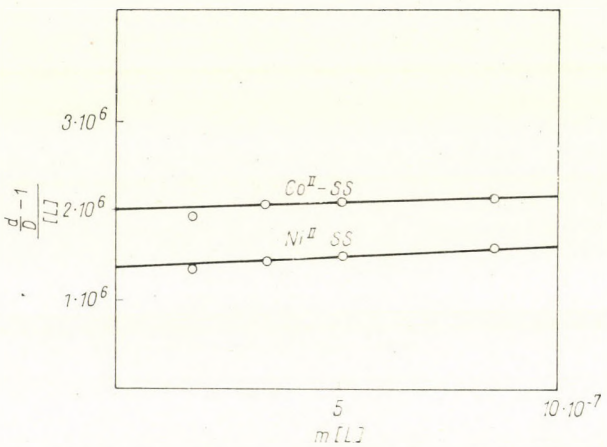

Fig. 2. Determination of the complex products of nickel(II) and cobalt(II) sulphosalicylate complexes from the distribution coefficients by graphical method

ligand concentrations belonging to the $\frac{d}{D}$ values were calculated by means of Eq. (4). Then the values of $\frac{\frac{d}{D} - 1}{[L]}$ were plotted against the free ligand concentration, $[L]$, according to LEDEN (see Figs 1 and 2). Taking Eq. (3) into account, the intercept of the line gives β_1, while the slope gives β_2. The latter could only be determined with some uncertainty because of the small number of measurements. The following values were found for the complex products by the graphical method:

For the system copper(II)–sulphosalicylate:

$$\log \beta_1 = 7.46 \pm 0.2$$
$$\log \beta_2 = 12.9 \pm 0.5$$

For the system nickel(II)–sulphosalicylate:

$$\log \beta_1 = 6.15 \pm 0.2$$
$$\log \beta_2 = 11.3 \pm 0.5$$

For the system cobalt(II)–sulphosalicylate:

$$\log \beta_1 = 6.3 \pm 0.2$$
$$\log \beta_2 = 11.1 \pm 0.5$$

The above data afford information on the calculation of ion-exchange chromatographic procedures performed at 80°.

SUMMARY

The dissociation constants of sulphosalicylic acid have been obtained by pH-metric titration, and the complex products for the copper(II), nickel(II) and cobalt(II) sulphosalicylate complexes determined from ion-exchange distribution experiments at 80° C, at an ionic strength of 0.5. The following data were found: dissociation constants

$\log k_1 = -1.52$; $\log k_2 = -2.30$; $\log k_3 = -10.47$.

Products for the copper(II) complexes:
$\log \beta_1 = 7.46 \pm 0.2$; $\log \beta_2 = 12.9 \pm 0.5$.
Products for the nickel(II) complexes:
$\log \beta_1 = 6.15 \pm 0.2$; $\log \beta_2 = 11.3 \pm 0.5$.
Products for the cobalt(II) complexes:
$\log \beta_1 = 6.3 \pm 0.2$; $\log \beta_2 = 11.1 \pm 0.5$.

REFERENCES

1. Inczédy, J., Gábor-Klatsmányi, P., Erdey, L.: Acta Chim. Acad. Sci. Hung. **50,** 105 (1966).
2. Schubert, J., Russel, E. R., Myers, J. L. S.: J. Biol. Chem. **185,** 387 (1950).
3. Leden, I.: Z. Phys. Chem. **A188,** 160 (1941).
4. Bates, R. G.: J. Res. nat. Bur. Standards **59,** 261 (1957).
5. Harned, H. S., Robinson, R. A.: Trans. Faraday Soc. **36,** 973 (1940).
6. Schwarzenbach, G., Willi, A., Bach, R. O.: Helv. Chim. Acta **30,** 1303 (1947); Schwarzenbach, G., Ackermann, H.: Helv. Chim. Acta **31,** 1029 (1948).

Piroska Gábor-Klatsmányi
János Inczédy
László Erdey
Budapest, XI., Gellért tér 4.

Acta Chimica Academiae Scientiarum Hungaricae Tomus 57 (1), pp. 11—33 (1968)

THERMAL STABILITY OF CHLORINE OXY-SALTS IN THE SOLID STATE, IV*

KINETICS AND MECHANISM OF THE THERMAL DECOMPOSITION OF ALKALI PERCHLORATES

F. SOLYMOSI

(Reaction Kinetical Research Group of the Hungarian Academy of Sciences, Szeged)

Received July 5, 1967

Introduction

The thermal decomposition of alkali perchlorates was first studied by MARVIN and WOOLAVER [1] with thermogravimetric methods. Similar investigations were performed later by GORDON and CAMPBELL [2], as well as by MARKOVITZ *et al.* [3, 4]. In their investigations these authors established the temperature of the onset of decompositions, and MARKOVITZ *et al.* even registered the heat changes occurring during decomposition, by means of differential thermal analysis (DTA), and determined the approximate melting points of the substances.

Detailed kinetic measurements were performed mainly on potassium perchlorate. The decomposition has been described by GLASNER and WEINDENFELD [5] using the modified *Prout—Tompkins* rate equation. BIRCUMSHAW [6] was the first to point out that the reaction is kinetically extremely complex, and that the fusion of the substance, the potassium chlorate formed during the decomposition and the accumulated decomposition product (potassium chloride) play a significant role in the decomposition. HARVEY *et al.* [7] described the decomposition of potassium perchlorate with two first order equations; one refers to a decomposition taking place in the solid phase and the other to that in the molten phase. The activation energy of the reaction — similarly to the temperature of the decomposition — is given rather differently by the different authors. GLASNER and SIMCHEN [8] found 69 kcal in vacuum, and HARVEY *et al.* 70.5 kcal for the reaction in both phases. In contrast to this, RODGERS and WASSINK [9] obtained 98.4 kcal for the solid-phase decomposition, and 80.7 for that in the molten phase. The effect of different contaminations on the stability of potassium perchlorate has been pointed out by SIMCHEN [10].

A detailed study of the decomposition of lithium perchlorate has been carried out by MARKOVITZ and BORYTA [11]. Decomposition starts at temperatures high above the melting point of lithium perchlorate, at about 390°; it

* Part III: Z. phys. Chem. N. F. **57**, 1 (1968).

is of autocatalytic character and follows the *Prout—Tompkins* rate equation. For the activation energy of the acceleration period and for the deceleration stage 52.2 kcal and 62 kcal respectively, have been measured.

The purpose of the present study has been to form a general picture about the stability of perchlorates, about the role of structural and physical properties in determining the stability, and to ascertain the possible mechanism of the decomposition. To this end, detailed kinetical measurements have been made concerning the decomposition of alkali perchlorates and some bivalent metal perchlorates, supplemented with differential thermal analytical investigations, measurements and calculations of the physical properties and bonding of the compounds. In the present paper we report on the results obtained with alkali perchlorates.

Experimental

Preparation of perchlorates

(a) $LiClO_4$: $HClO_4$ was added to Li_2CO_3 in equivalent amount, and $LiClO_4$ was recrystallized from the solution.
(b) $NaClO_4$: commercial pure $NaClO_4$ was recrystallized from redistilled water, dried at 110°, and powdered.
(c) $KClO_4$: *Merck c.p.* product was used.
(d) $RbClO_4$: $HClO_4$ was added to *(BDH)* $RbNO_3$. The solution was evaporated, and the obtained solid several times recrystallized.
(e) $CsClO_4$: A hot solution of Cs_2SO_4 *(BDH)* was poured into a solution of $Ba(ClO_4)_2$ with constant stirring. The precipitate of $BaSO_4$ was filtered off and $CsClO_4$ was recrystallized from the filtrate.

Measuring procedure

The kinetic measurements were performed in the apparatus shown in Fig. 1. A small glass boat was used to hold the substance to be investigated. Before the experiment the reacting vessel was evacuated to 10^{-4}—10^{-5} torr, keeping the boat which contained the substance, in the cold part of the vessel. At the start of the measurement the boat was pushed into the heated part of the vessel by means of a magnet. The pressure of gases formed in the decomposition was continuously measured by glass or mercury manometers.

The thermogravimetric and differential thermal analyses of the compounds were made with a PAULIK—PAULIK—ERDEY derivatograph.

Results

Of the alkali perchlorates the decomposition of the lithium and, especially, of the potassium salt had been the subject of a detailed kinetic study. However, for a better comparison with the stabilities of other alkali perchlorates, our experiments were also extended to the study of decomposition of lithium and potassium perchlorates.

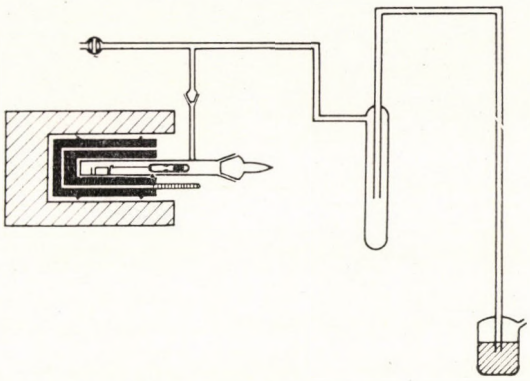

Fig. 1. Vacuum apparatus for studying the decomposition of perchlorates

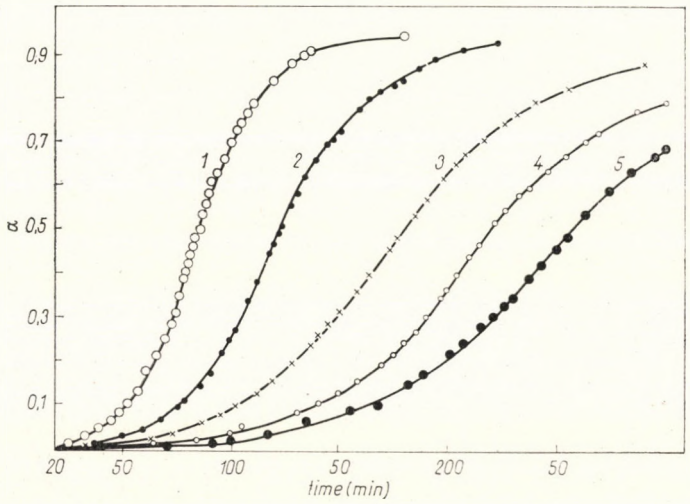

Fig. 2. α-t curves of the decomposition of lithium perchlorate. 1. 430.5°C; 2. 425°C; 3. 420°C; 4. 415°C; 5. 411°C

Decomposition of lithium perchlorate

The melting of lithium perchlorate occurs at 247°; the decomposition of the compound takes place with a measurable velocity only at about 400°. Fig. 2 shows some $\alpha - t$ curves.

$\alpha = p_t/p_f$; p_t is the pressure measured at t time, p_f is the final pressure.

The reaction is preceded by a comparatively long time lag. The curves are autocatalytic. The rate maximum appeared at about 50% conversion. The decomposition of lithium perchlorate is represented by Eq. 1,

$$LiClO_4 = LiCl + 2\,O_2 \tag{1}$$

but some chlorine (1—2%) was also found in the gaseous product. To establish whether the decomposition goes through the formation of chlorate and chlorite, the reaction was stopped at different times and analysis of a sample carried out. In the initial period of the decomposition about 1.5—2.5% lithium chlorate was found. Lithium chlorite, however, was not detected.

The *Prout—Tompkins* rate equation was used to calculate the rate constants.

$$\log \frac{\alpha}{1-\alpha} = k_{1;2}\,t + C_{1;2} \tag{2}$$

The applicability of the equation is illustrated by Fig. 3.

The temperature dependence of the rate constants of the acceleration period was 52.6 kcal, while 41 kcal was obtained for the decay period. The rate constant of the latter period was also determined by a first order equation,

$$\log \frac{1}{1-\alpha} = k_{3;4}\,t + C_2 \tag{3}$$

which described the decomposition after $\alpha = 0.4$ (Fig. 3). The value of the activation energy in this case is 43.9 kcal.

Table I

Kinetic data of the thermal decomposition of lithium perchlorate

Temperature, °C	$k_1 \cdot 10^2$ (min.$^{-1}$)	$k_3 \cdot 10^2$ (min.$^{-1}$)	$k_4 \cdot 10^2$ (min.$^{-1}$)
430.5	3.08	1.58	1.3
426	2.11	1.08	0.9
425	2.05	1.06	0.93
420	1.5	1.0	0.61
415	1.25	0.67	0.52
411	1.06	0.71	0.53
Activation energy, kcal/mole	52.6	41.0	43.9
Frequency factor (min.$^{-1}$)	$6.58 \cdot 10^{14}$	$8.83 \cdot 10^{14}$	$5.12 \cdot 10^{11}$

k_1; $\alpha = 0.01$—0.45
k_2; $\alpha = 0.45$—0.95
k_4; $\alpha = 0.4$—0.93

The activation energy obtained for the acceleration period is near to that obtained by MARKOVITZ and BORYTA, while the activation energy of the decay period in our experiments appeared to be much lower.

Kinetic data are contained in Table I.

Decomposition of sodium perchlorate

The decomposition of sodium perchlorate has been studied in the range 490—515°. $\alpha - t$ curves are plotted in Fig. 4.

The reaction is autocatalytic. The rate maximum is shifted towards the later phase of decomposition ($\alpha = 0.38—0.68$), as the reaction temperature is

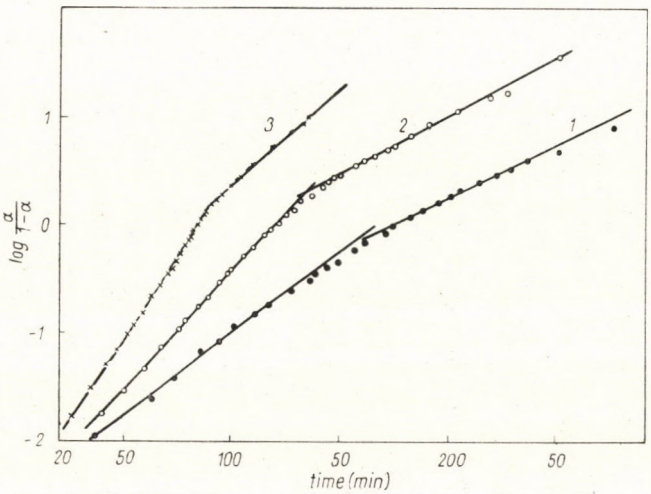

Fig. 3. Kinetical analysis of the decomposition of lithium perchlorate by the *Prout-Tompkins* equation 1. 420° C; 2. 426° C; 3. 430.5° C

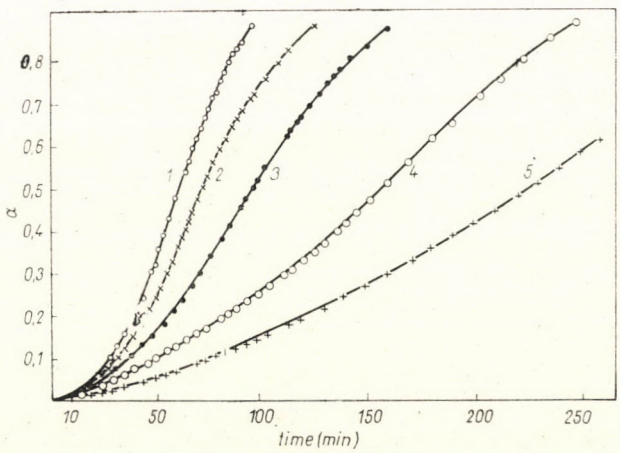

Fig. 4. α-t curves of the decomposition of sodium perchlorate. 1. 515°C; 2. 510°C; 3. 505°C; 4. 500°C; 5. 490°C

increased. The decomposition is preceded by a time lag of a few minutes only, which is practically independent of the temperature. The reaction takes place according to the equation:

$$NaClO_4 = NaCl + 2\ O_2 \qquad (4)$$

No traces of chlorine were found. A mathematical analysis of the $\alpha - t$ curves was attempted by the *Prout—Tompkins* equation, which described the complete reaction (Fig. 5).

The activation energy of the acceleration period is 57.3 kcal, while that of the decay period is 57 kcal. The mathematical analysis of the decay period

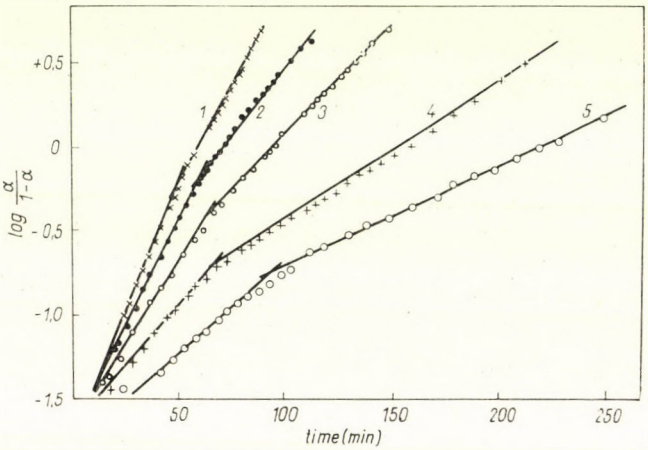

Fig. 5. Kinetical analysis of the decomposition of sodium perchlorate by the *Prout-Tompkins* equation. 1. 515°C; 2. 510°C; 3. 505°C; 4. 500°C; 5. 490°C

was performed by the first order equation and by the "contracting cube" formula:

$$1-(1-\alpha)^{1/3} = k_5 t \qquad (5)$$

The first order equation yielded a straight line in a rather narrow range of the decomposition ($\alpha = 0.5-0.85$) only. The value of the activation energy was 59 kcal. Equation (5) was valid in the range $\alpha = 0.35-0.9$. The temperature dependence of the rate constants (k_5) gave activation energy values similar to those obtainable from the temperature analysis of k_2. Kinetical data are summarized in Table II.

The effect of sodium chloride, the solid residue of the decomposition, was also studied. Fig. 6 shows some measurements. The decomposition in the presence of sodium chloride started with maximum rate and the half-time of the reaction was considerably decreased.

Table II

Kinetic data of the thermal decomposition of sodium perchlorate

Temperature, °C	$k_1 \cdot 10^3$ (min.$^{-1}$)	$k_3 \cdot 10^3$ (min.$^{-1}$)	$k_4 \cdot 10^3$ (min.$^{-1}$)	$k_5 \cdot 10^3$ (min.$^{-1}$)
490	11.1	5.8	5.05	1.91
500	14.7	8.0	7.98	3.25
505	20.0	12.9	11.6	4.20
510	25.4	15.8	16.0	5.50
515	30.6	22.3	17.0	8.43
Activation energy kcal/mole	57.3	57.1	59.2	62.6
Frequency factor (min.$^{-1}$)	$2.7 \cdot 10^{14}$	$1.57 \cdot 10^{14}$	$4.89 \cdot 10^{14}$	$1.7 \cdot 10^{15}$

k_1; $\alpha = 0.003$—0.3
k_2; $\alpha = 0.3$ —0.8
k_4; $\alpha = 0.55$ —0.95
k_5; $\alpha = 0.35$ —0.9

Decomposition of potassium perchlorate

The decomposition of potassium perchlorate began at a higher temperature than that of sodium perchlorate. Measurements were carried out in the range of 549 and 576°. The reaction equation is:

$$KClO_4 = KCl + 2\,O_2. \qquad (6)$$

The decomposition starts with a short deceleratory period followed by an autocatalytic reaction. The rate maximum appears at about $\alpha = 0.5$.

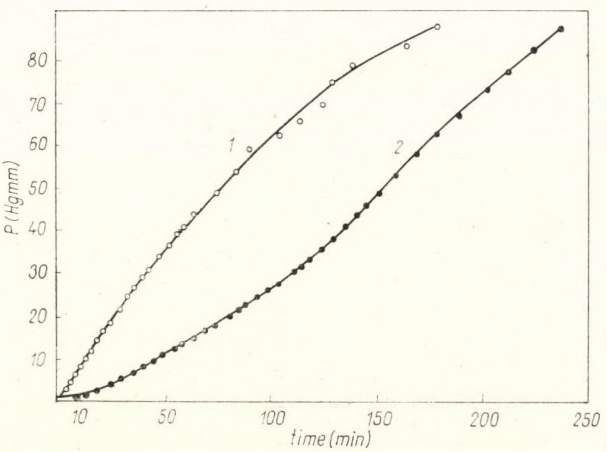

Fig. 6. Thermal decomposition of sodium perchlorate in the presence of sodium chloride at 500°C. 1. $NaClO_4$: NaCl molar ratio 1 : 1, 2. Pure $NaClO_4$

The mathematical treatment of the $\alpha - t$ curves was done by the former equations.

The first order equation, similarly to the results of HARVEY *et al.*, yielded two straights. Although the rate constants calculated from the second phase are about 15 times larger than those of the first phase practically the same activation energy, 70 kcal, was obtained for both phases. In the present case the temperature dependence of the rate constants of the *Prout—Tompkins* equation cannot be evaluated. Kinetical data are summarized in Table III.

The effect of the reaction product has been studied in this case, too, but was found to be considerably less than with sodium perchlorate.

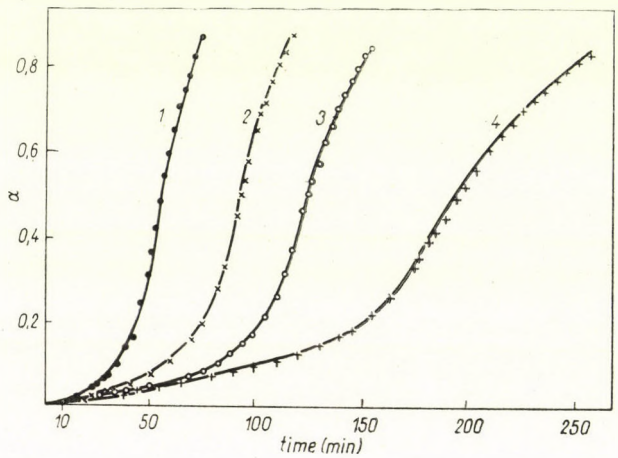

Fig. 7. α-t curves of the decomposition of potassium perchlorate. 1. 570°C; 2. 565°C; 3. 560°C; 4. 549°C

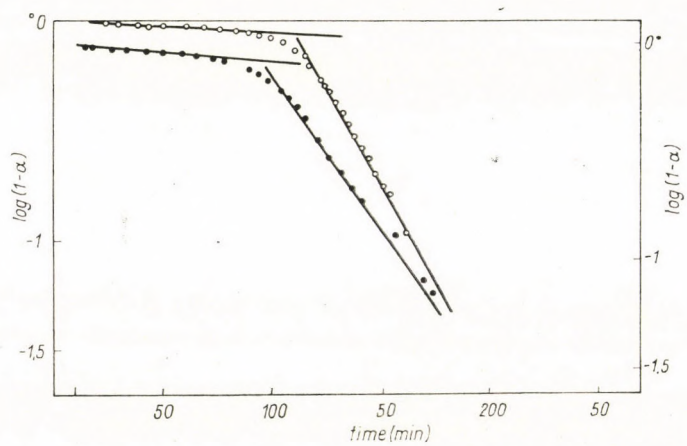

Fig. 8. Kinetical analysis of the decomposition of potassium perchlorate by the first order equation. • 560° C, ○ 555°C

Table III

Kinetic data of the thermal decomposition of potassium perchlorate

Temperature, °C	$k_3 \cdot 10^4$ (min.$^{-1}$)	$k_4 \cdot 10^3$ (min.$^{-1}$)	$k_5 \cdot 10^3$ (min.$^{-1}$)
549	5.1	8	4
555	9	13	6.3
560	5.8	17	8.92
565	10.8	26.2	11.5
570	16	28	14.6
575	20	31.7	18.1
Activation energy, kcal/mole	69.05	71.5	75.4
Frequency factor (min.$^{-1}$)	$1.16 \cdot 10^{15}$	$1.05 \cdot 10^{17}$	$5.54 \cdot 10^{17}$

k_3; $\alpha = 0$ —0.15
k_4; $\alpha = 0.3$ —0.9
k_5; $\alpha = 0.28$—0.95

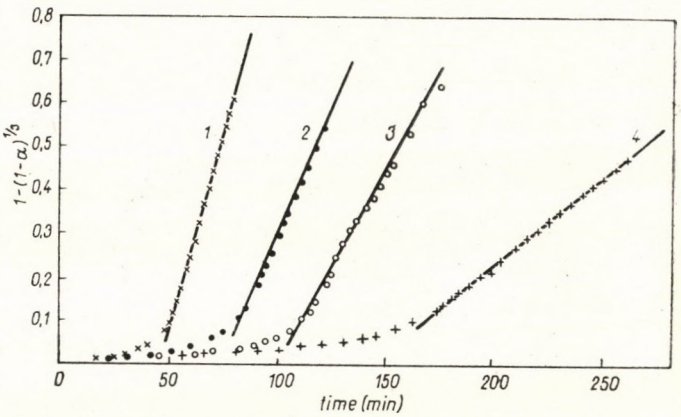

Fig. 9. Kinetical analysis of the decomposition of potassium perchlorate by the formula $1\text{-}(1\text{-}\alpha)^{1/3} = k_5 t$. 1. 575°C; 2. 565°C; 3. 560°C; 4. 549°C

Decomposition of rubidium perchlorate

The decomposition of rubidium perchlorate was studied in the range 547 to 569°. The reaction began immediately, without a time-lag, and resulted in the formation of rubidium chloride.

$$RbClO_4 = RbCl + 2\ O_2 \qquad (7)$$

The decomposition — as in the case of potassium perchlorate — started with a slow decay period.

In this case, too, the reaction could be readily described by two first order equations, from $\alpha = 0.01$ to $\alpha = 0.28$ and from $\alpha = 0.4$ to $\alpha = 0.93$. The rate constants, especially k_2, as the function of $1/T$ showed some scattering. The activation energies are: 70.5 and 66.8 kcal. The decomposition was surprisingly well described by the *Prout—Tompkins* equation, which yielded a straight line practically covering the whole decomposition ($\alpha = 0.06 - 0.96$). The value of the activation energy is 71.3 kcal.

In the range $\alpha = 0.2 - 0.95$, *i.e.* for the second decay process, Eq. (5) gave a straight line. The value of the activation energy is 72 kcal.

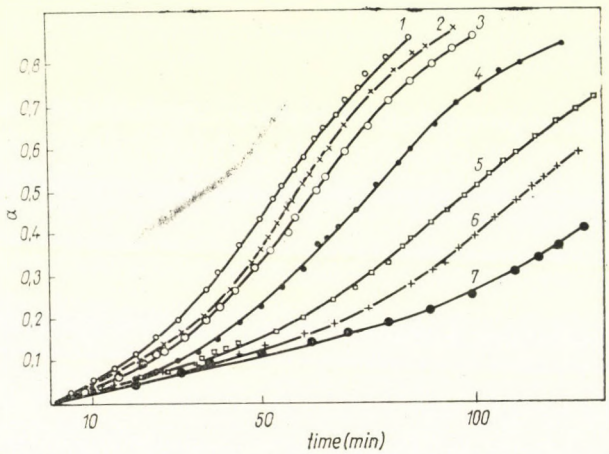

Fig. 10. α-t curves of the decomposition of rubidium perchlorate.
1. 569°C; 2. 566°C; 3. 563°C; 4. 558°C; 5. 556° C; 6. 552°C; 7. 547°C

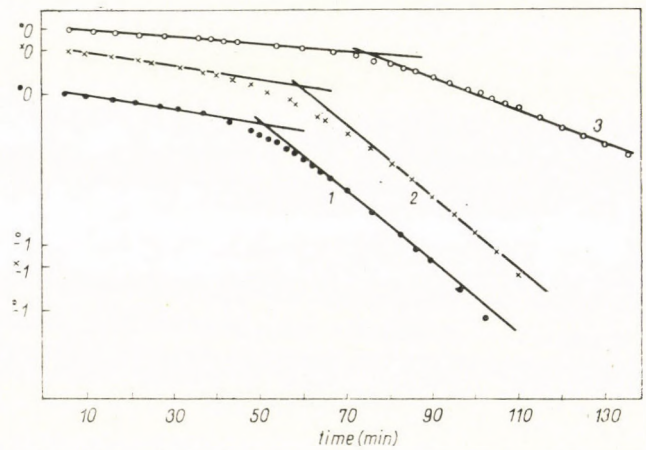

Fig. 11. Kinetical analysis of the decomposition of rubidium perchlorate by the first order equation. 1. 566°C; 2. 563°C; 3. 556°C

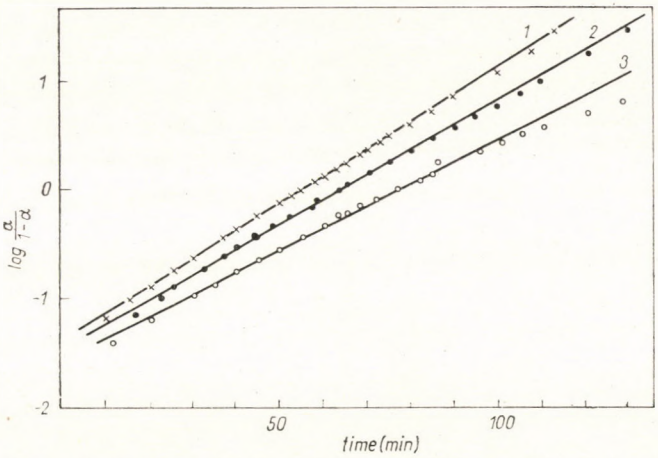

Fig. 12. Kinetical analysis of the decomposition of rubidium perchlorate by the *Prout-Tompkins* equation. 1. 569°C; 2. 563°C; 3. 558°C

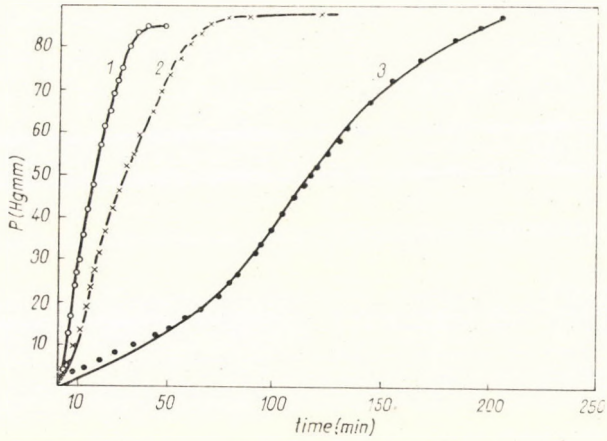

Fig. 13. The thermal decomposition of rubidium perchlorate in the presence of rubidium chloride. 1. $RbClO_4$: RbCl molar ratio 1 : 1; 2. molar ratio 10 : 1; 3. Pure $RbClO_4$

The addition of rubidium chloride to rubidium perchlorate altered the character of the reaction here too, and considerably increased the rate of decomposition. The effect of rubidium chloride is illustrated by Fig. 13. Kinetical data are summarized in Table IV.

Decomposition of cesium perchlorate

The decomposition temperature of cesium perchlorate was lower than that of rubidium perchlorate, and even lower than that of potassium perchlorate. Measurements were taken between 528 and 558°. The decomposition equation is:

$$CsClO_4 = CsCl + 2\ O_2 \qquad (8)$$

Table IV

Kinetic data of the thermal decomposition of rubidium perchlorate

Temperature, °C	$k_1 \cdot 10^2$ (min.$^{-1}$)	$k_3 \cdot 10^3$ (min.$^{-1}$)	$k_4 \cdot 10^3$ (min.$^{-1}$)	$k_5 \cdot 10^3$ (min.$^{-1}$)
547	0.92	1.14	5.94	2.84
552	1.25	1.66	9.1	4.09
556	1.45	1.66	7.93	4.25
558	2.05	2.96	11.5	5.06
563	2.26	3.25	16.6	6.97
566	2.53	3.44	16.4	8.15
569	2.52	3.64	18.7	8.40
Activation energy kcal/mole	71.3	70.4	66.8	72.3
Frequency factor (min.$^{-1}$)	$1.03 \cdot 10^{17}$	$8.19 \cdot 10^{15}$	$4.28 \cdot 10^{15}$	$4.02 \cdot 10^{16}$

k_1; $\alpha = 0.03$—0.85 $\quad$ k_4; $\alpha = 0.40$—0.92
k_3; $\alpha = 0.01$—0.28 $\quad$ k_5; $\alpha = 0.20$—0.95

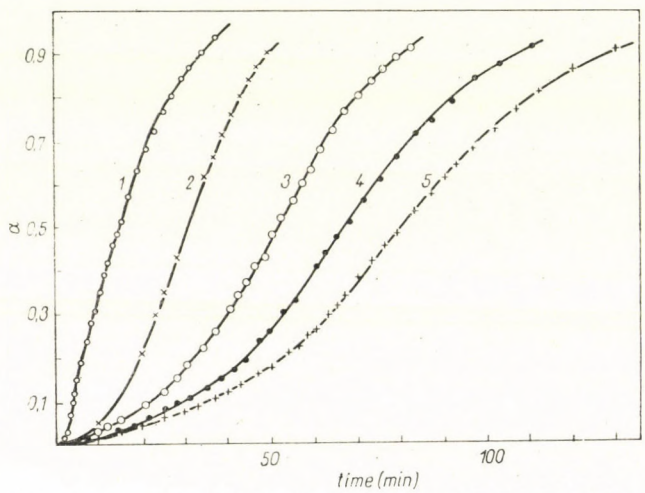

Fig. 14. α-t curves of the decomposition of cesium perchlorate.
1. $CsClO_4$; CsCl(2:1) 534°C; 2. 558°C; 3. 542°C; 4. 538°C; 5. 534°C

The process of the decomposition is similar to that of rubidium perchlorate. The rate maximum appeared, at each temperature, at about $\alpha = 0.45$. The mathematical analysis of the decomposition curves was carried out by the former equations. By plotting the result according to the first order equation, a well defined straight can be obtained only at about $\alpha = 0.23$. The activation energy of the decomposition for this phase is 68.7 kcal.

Between $\alpha = 0.35$—0.95 the decomposition was well described by Eq. (3). The value of the activation energy is 57 kcal. The *Prout—Tompkins* equation, in the range $\alpha = 0.05$—0.93 except at 528°, yielded one straight line.

Because of the difficulties in evaluating the initial phase, we also attempted to determine the activation energy from the temperature dependence of the times elapsed between the different phase of decomposition, $\alpha = 0.025$ to 0.05. The activation energies thus obtained ranged from 67 to 70 kcal.

Cesium chloride markedly accelerated the reaction (Fig. 14). Kinetical data are shown in Table V.

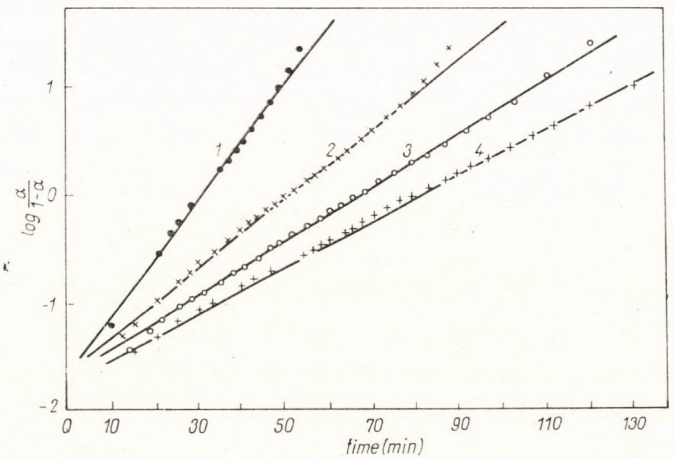

Fig. 15. Kinetical analysis of the decomposition of cesium perchlorate by the *Prout-Tompkins* equation. 1. 558°C; 2. 542°C; 3. 538°C; 4. 534°C

Table V

Kinetic data of the thermal decomposition of cesium perchlorate

Temperature, °C	$k_1 \cdot 10^2$ (min.$^{-1}$)	$k_3 \cdot 10^3$ (min.$^{-1}$)	$k_4 \cdot 10^3$ (min.$^{-1}$)	$k_5 \cdot 10^3$ (min.$^{-1}$)
528	(1.27)	(0.763)	13.5	5.45
534	2.13	1.85	15.4	7.14
538	2.45	2.63	17.9	8.08
542	3.21	3.03	25.1	10.8
558	5.35	8.5	41.3	20.0
Activation energy, kcal/mole	52.0	68.7	(48.3)	57.1
Frequency factor (min.$^{-1}$)	$2.68 \cdot 10^{12}$	$8.44 \cdot 10^{15}$	$(1.25 \cdot 10^{11})$	$2.12 \cdot 10^{13}$

k_1; $\alpha = 0.1$ —0.70
k_3; $\alpha = 0.01$—0.25
k_4; $\alpha = 0.52$—0.91
k_5; $\alpha = 0.30$—0.95

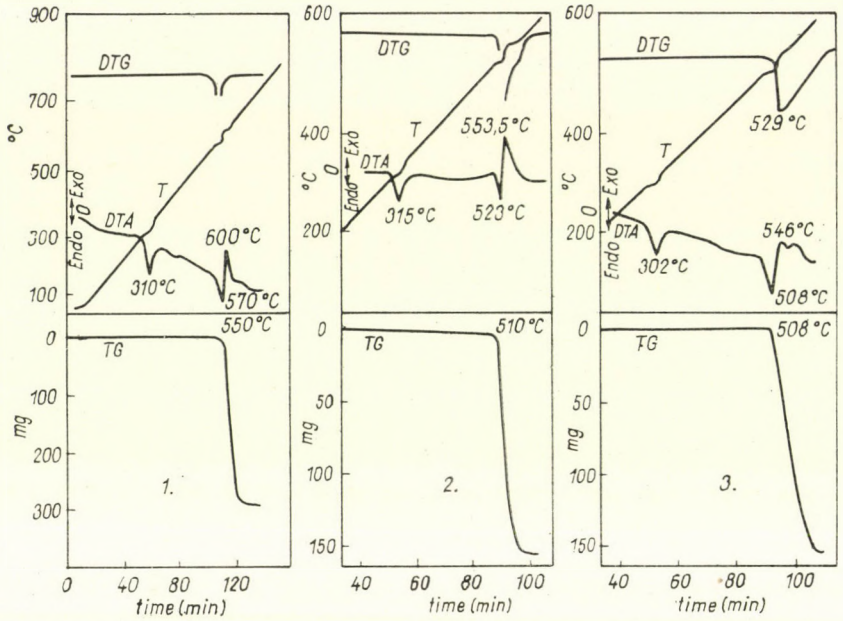

Fig. 16. Derivatograms of potassium perchlorate. Heating rate 6°/min. 1. Pure $KClO_4$, 2. $KClO_4$:KCl, 50:50, 3. $KClO_4$:KCl, 70:30 mole-%

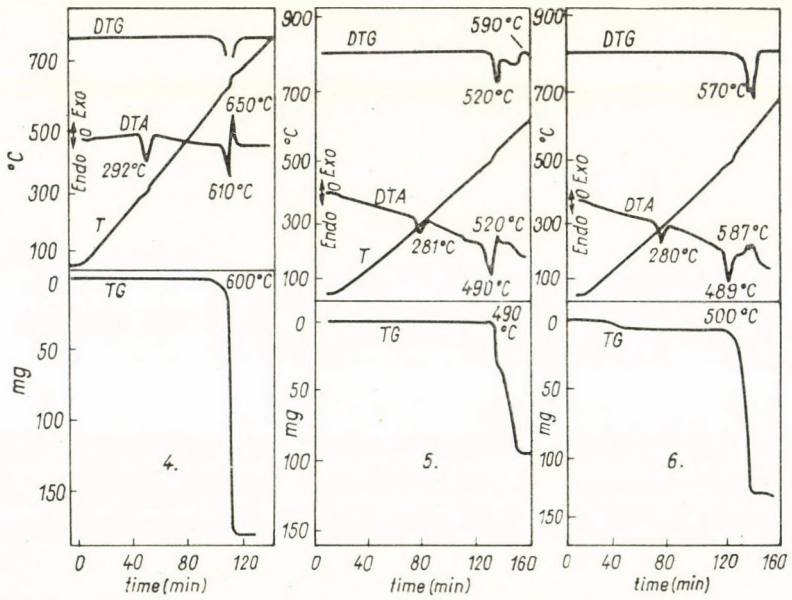

Fig. 17. Derivatograms of rubidium perchlorate. Heating rate 6°/min. 1. Pure $RbClO_4$, 2. $RbClO_4$:RbCl, 50:50, 3. $RbClO_4$:RbCl, 70:30 mole-%

Derivatographic investigations

In the introduction it was mentioned that the method of differential thermal analysis was widely applied in the study of the thermal properties of pure alkali perchlorates. The primary aim of the present investigations was to determine the effect exerted by alkali chloride (the solid decomposition product) on the melting point and the stability of the compounds. Investigations were done with pure perchlorates and with mixtures containing 10, 30 and 50 mole-% chloride. Some of the data are shown in Figs 16 and 17, and in Table VI.

Table VI

Thermal behaviour of alkali perchlorates in the presence of alkali chlorides
Derivatographic investigations

$LiClO_4$: LiCl, mole-%	Melting point, °C	t, °C*	$NaClO_4$: NaCl, mole-%	Melting point, °C	t, °C*	$CsClO_4$: CsCl, mole-%	Melting point, °C	t, °C*
100 : 0	247	450	100 : 0	471	507	100 : 0	571	570
90 : 10	243	420	90 : 10	428	500	90 : 10	500	480
70 : 30	246	390	70 : 30	415	485	70 : 30	447	460
50 : 50	251	390	50 : 50	423	485	50 : 50	550	500

* Temperature of the onset of decomposition
The heating rate was 6°/min.

The results indicate that, with the exception of lithium perchlorate, the chlorides markedly lower the melting point of perchlorates and also the temperature at which decomposition begins. Addition of lithium chloride to lithium perchlorate influences the melting point only slightly, but it also exerts a marked effect on the decomposition of the substance.

Structure and physical properties

Prior to discussing the kinetic results, and interpreting the differences in the stability of perchlorates, the most important data on the structure and physical properties of perchlorates will be summarized.

The crystal structure of alkali perchlorates at low temperature is rhombohedral, and at high temperature is cubic. Lithium perchlorate is an exception as it melts in the low temperature modification.

The lattice constants of the compounds, the Cl—O and O—O distances are given according to BRAEKEN's and HARANG's measurements in Table VII [12]. In order to establish a correlation between the stability and structural properties of perchlorates, the so-called "free-space" of the perchlorates has

been calculated. This characteristic can be defined as the difference between the volume of the crystal per ion pair calculated from the density (a value obtained from X-ray experiments) and the combined volumes of the ions as calculated from accepted ionic radii [13]. For these calculations the volume of the perchlorate ion was taken as 33.2 Å^3 taking this ion to be a nearly regular tetrahedron with the chlorine atom in the centre. The mean of the chlorine—oxygen distance was taken as 1.46 Å. It appears from the table that the "free space" increases from lithium to caesium perchlorate.

The melting point of the compounds increases from lithium to rubidium, but the melting point of caesium perchlorate is lower than that of potassium perchlorate. The magnetic susceptibility and density of the compounds increase with the size of the cation.

There is not, however, any marked difference in the refractive indices of the compounds. The solubility of the substances in water does not show any particular trend (that of sodium perchlorate being the largest), but it decreases in organic solvents from lithium to caesium. An extremely large decrease of solubility appears for potassium perchlorate. Some characteristic data are listed in Table VII.

Table VII

Some data of the structure and physical properties of alkali perchlorates

Compound	Cryst. trans., °C	Melting point, °C	Radius of cation, Å	Distance		Lattice parameter, α	*Free space* ion pair Å^3	Density	Refractive index
				Cl—O Å	O—O Å				
$LiClO_4$	—	247	0.68				37.5	2.40	1.4700
$NaClO_4$	305	471	0.98	0.85	1.39	7.08	43.0	2.49	1.4651
$KClO_4$	300	585	1.33	1.26	2.06	7.50	47.8	2.51	1.4746
$RbClO_4$	270	588	1.49	1.30—1.48	2.12—2.42	7.70	54.6	3.01	1.4708
$CsClO_4$	221	571	1.65	1.35—1.53	2.2—2.51	7.98	64.1	3.32	1.4781

Discussion

Decomposition products

The decomposition of alkali perchlorates takes place at high temperature, but, with the exception of lithium perchlorate, the decompositions occur in a relatively narrow temperature range (500—575°). The alkali perchlorates decompose according to the equation:

$$MClO_4 = MCl + 2\,O_2 \qquad (1)$$

The only exception is lithium perchlorate, as here a small amount of chlorine is also which indicates the occurrence of the following reaction:

$$2\ LiClO_4 = Li_2O + Cl_2 + 3.5\ O_2 \qquad (2)$$

The fact that the decomposition of alkali perchlorates, in contrast to a number of divalent metal perchlorates, takes place by the first reaction, is in accordance with thermodynamic considerations, as it was shown by MARKOVITZ [23].

Kinetical characteristics of the reactions

The decomposition reactions are preceded by a short time lag, the length of which decreases with an increase in temperature. The decomposition of lithium and sodium perchlorates is a characteristic autocatalytic reaction, which is well described by the *Prout—Tompkins* equation. The decomposition of potassium, cesium and rubidium perchlorates start with a short deceleratory period, followed by an acceleration and then another deceleratory reaction. Both deceleratory reactions fit the first-order rate law. The value of the rate constant (k_4) of the second decay period is much larger (by about one order of magnitude) than the rate constant for the first period (k_3). The deceleratory reaction after the rate maxima also fits the contracting cube formula but we do not think that this has any physical meaning. It should be mentioned that the mathematical analysis of the decomposition of rubidium and cesium perchlorates by the *Prout—Tompkins* equation resulted in one straight line for the whole decomposition, in spite of the different stages of the reaction mentioned above. This, in our opinion, is only fortuitous, and does not reflect the complex character of the decomposition.

On the basis of the melting points and the decomposition temperature of the substances it was expected that lithium perchlorate, and sodium perchlorate, partly decompose in the molten phase. It was observed, however, that potassium, rubidium and cesium perchlorates also melted in the course of their decomposition, much below the melting points of the pure substances. The probable reason for this is that chloride formed during the decomposition gives an eutectic with the remaining perchlorate. The compositions of the eutectics produced with perchlorates and chlorides were not established, but the marked effect of the presence of chlorides on the melting points and stabilities of perchlorates were well exhibited by the differential thermal analysis (Table VI).

Considering these facts, the autocatalytic character of the decomposition of perchlorates seems to be in some connection with their melting. The initial long decay period in the decomposition of potassium, rubidium and cesium perchlorates can be attributed to the slow decomposition in the solid state. However, due to the effect of the reaction products (chlorides), the melt-

ing of perchlorates soon begins and consequently the rate of decomposition increases. (It has long been known that the melting of solids gives rise to a great increase of the decomposition rate.) After complete liquidification, the rate of decomposition corresponds again to the first-order rate law. When the chlorides were mixed in advance with the perchlorate salts, the process of decomposition changed. The perchlorates melted at the very beginning of the decomposition, the autocatalytic character of the reaction was missing, and the decomposition started with maximum rate. Accordingly, the catalytic effect of chlorides is apparent. The fact, however, that the decomposition of lithium perchlorate, which occurs in the molten phase, is also autocatalytic, and nevertheless, lithium chloride accelerates this decomposition, indicates that chloride might have some effect on the molten phase reaction in the other cases, too.

Mechanism of decomposition

The values of activation energy, calculated from the temperature dependence of the rate constants obtained by different kinetical equations, fell in the range of 60—70 kcal. In accordance with the results of earlier authors, the activation energies for the solid and molten phase decompositions do not differ markedly, but in the latter case the frequency factor is much larger. This indicates that the mechanism of the decomposition of perchlorates is essentially similar, and the rate determining step, independently of the phases, is the same for every compound. The larger frequency factor obtained in the molten perchlorates is most likely the result of the larger mobility of the perchlorate ion. The decomposition of perchlorates is probably composed from the following reactions. In the first step

$$MClO_4 \overset{k_1}{\rightleftharpoons} MClO_3 + \frac{1}{2} O_2 \tag{3}$$

metal chlorate and oxygen are formed. The metal chlorate then decomposes partly into chloride and oxygen:

$$MClO_3 \overset{k_2}{\rightleftharpoons} MCl + \frac{3}{2} O_2, \tag{4}$$

and partly disproportionates into perchlorate and chloride:

$$MClO_3 \overset{k_3}{\rightleftharpoons} \frac{3}{4} MClO_4 + \frac{1}{4} MCl \tag{5}$$

The occurrence of this latter reaction is indicated by our experiments with chlorates [14]. Above 500° the thermal decomposition of alkali chlorates

(Reaction 4) is rapid, nevertheless the formation of perchlorate (Reaction 5) was observed even at this temperature. It is also possible that the decomposition of chlorate into chloride does not take place in one step, but first chlorite is formed which then decomposes into chloride:

$$MClO_3 \overset{k_4}{\rightleftharpoons} MClO_2 + \frac{1}{2} O_2 \tag{6}$$

$$MClO_2 \overset{k_5}{\rightleftharpoons} MCl + O_2 \tag{7}$$

While the chlorate intermediate was found in every alkali perchlorate, chlorite was not detected at all. The most likely explanation for this seemed to be that at high temperatures chlorites would decompose extremely rapidly into chloride and oxide. We have shown [15], however, that alkali chlorites do not decompose even in this temperature range into oxygen and chloride, but instantaneously disproportionate into chlorate and chloride:

$$MClO_2 \overset{k_6}{\rightleftharpoons} \frac{2}{3} MClO_3 + \frac{1}{3} MCl\,. \tag{8}$$

Considering that alkali chlorates are less stable compounds than perchlorates ($k_2 > k_1$) and that their amount never exceeds 2—3% during the reaction, it can be assumed that the decomposition of all alkali perchlorates (Reaction 3) is the rate-determining step. This step involves the rupture of the Cl—O bond. The dissociation energy of the Cl—O bond (about $\sim$ 60 kcal) is in good agreement with the activation energies found experimentally.

A further proof for this mechanism can be obtained by calculating the endothermic heat of the reaction of this step [7]. On the basis of the standard enthalpy of formation of perchlorates and chlorates, and assuming only a slight difference in their heat capacities, we get for ΔH° the values listed in the fourth column of Table VIII. The values are much less than the activation energies determined experimentally. However, when the formation of atomic oxygen ($\Delta H_f^\circ = 59.2$ kcal) is assumed, the data shown in the last column are obtained. These values, with the exception of that for lithium perchlorate, agree very well with the measured activation energies.

Besides the rupture of the Cl—O bond, one can suppose that the electron transfer reaction between the anion and the cation is the rate determining step of the decomposition:

$$M^+ + ClO_4^- = M + ClO_4 \tag{9}$$

The electron transfer reaction plays an important part in the decomposition of a number of ionic compounds, such as alkali azides [16]. Of the perchlorates,

the decomposition of ammonium perchlorate was supposed to take place between 200—300° according to this mechanism [17].

The energy required for the transfer of an electron from the anion to the cation in ionic crystals can be calculated from spectroscopic data. The calculation was performed on potassium perchlorate. The absorption edge of alkali perchlorates is about 6 eV [18]. The low frequency dielectric constant (K) of potassium perchlorate is 5.9, and its refractive index (n) is 1.4746. From these data, by the following equation

$$E_T = E_0 \frac{K_0}{K} \; ; \quad K_0 = n^2$$

(where E_0 is the optical activation energy, K_0 = the high frequency dielectric constant) the thermal activation energy was found to be 2.21 eV (51 kcal). Since this value is much less than the activation energy of the decomposition,

Table VIII

Compound	$\Delta H°$ $MClO_4$	$\Delta H°$ $MClO_3$	$\Delta H°$ reaction	$\Delta H°$ reaction
$LiClO_4$	— 91.77	—70	21.7	80.9
$NaClO_4$	— 92.18	—85.7	6.5	65.7
$KClO_4$	—103.6	—93.5	10.1	69.3
$RbClO_4$	—103.87	—93.8	10.0	69.2
$CsClO_4$	—103.86	—96.0	7.8	67.0

we are of the opinion that the possibility of an electron transfer reaction can be excluded. The decomposition products (chloride and oxygen) also make an electron transfer reaction unlikely because in this case chlorine dioxide and chlorine should have been formed in the decomposition of the perchlorate radical or in the reaction between the alkali metal and the perchlorate radical.

It should be mentioned here that the thermal decomposition of sodium, potassium and caesium perchlorates has been studied by CABANÉ and BÉNARD [19], and they have found 28, 30 and 35 kcal activation energies. These values agreed with those measured for the self-diffusion of the perchlorate ion in these compounds. From this result it was concluded that the rate determining process of the thermal decomposition was the diffusion of the perchlorate ion. In the present case the values of activation energy are much larger. As CABANÉ and BÉNARD performed the kinetical measurements in the ranges 330—420°, 375—480° and 388—470°, where there are only very slight decompositions, it is very probable that the activation energies they obtained refer to the surface reactions.

Factors influencing the stability of alkali perchlorates

In spite of the fact that the temperature range of the decomposition of alkali perchlorates is relatively narrow, there are well defined differences between the decomposition temperatures of these compounds. To characterize the stability of the substances, the temperature values have been calculated from the *Arrhenius* diagrams, where the rate constant of the decompositions (k_5) reaches the value of $5 \cdot 10^{-3}$. This characteristic temperature, as it can be seen from Table IX, increases from lithium to rubidium but it is lower for cesium.

As factors influencing the stability of perchlorates one must consider the structural properties of the compounds, their physical constants and the character of the prevailing bonds. These properties are summarized in Table VII. Some other data on the polarizability of the cation, cation polarizing power, the effective electric field strength of the cations, the ionic character of the bonds, the polarity of the Cl—O bond and the ionization potential of alkali metals, are given in Table IX.

Table IX

Some characteristic data of the cations and the type of bonding in alkali perchlorates

Compound	Ionization potential, eV	Polarizability of cation	Polarizing power of cation, e/r	F^*	Ionic character of the bond, %	Polarizability of oxygen ion %	t °C
$LiClO_4$	5.390	0.03	1.667	2.915	67.8	20.3	410
$NaClO_4$	5.138	0.41	1.053	2.407	68.9	25.3	508
$KClO_4$	4.339	1.33	0.752	1.661	73.2	25.4	547
$RbClO_4$	4.176	1.98	0.676	1.423	74.1	30.1	560
$CsClO_4$	3.893	3.34	0.592	1.303	75.5	26.1	526

$F^* = \frac{Z^*}{r^2}$; where F^* = effective electric field strength of the cation

Z^* = effective nuclear charge (LAKATOS [20])

t_0 = characteristic temperature, where $k_5 = 5 \cdot 10^{-3}$/min.

The ionic character of the bond was calculated by SANDERSON's method [21] and the polarizability of oxygen ion by LAKATOS [22].

Evaluating the stability of perchlorates in the light of these data, it can be stated that the more ionic a compound, the greater its stability. The effective electric field strength of the cations affects the stability of perchlorates in a similar way. Especially in the case of divalent metal perchlorates this proved to be a more convenient basis to characterize the effect of the cations than their polarizing power. The increase of the effective electric field strength of the cat-

ions results in a decrease of the temperature of the decomposition. The only exception is cesium perchlorate, as its characteristic temperature is lower than that of the potassium salt. The same stability order was found by MARKOVITZ *et al.* [3] using the technique of differential thermal analysis and thermogravimetry. The striking behaviour of cesium perchlorate was explained by its lower melting point compared to that of the potassium and rubidium salts. Since the melting of the compounds, as proved by general experience, results in an increase in the decomposition rate of the solids, this last explanation seems probable. In our opinion, however, the origin of the strange behaviour both in melting and stability of cesium perchlorate is to be found in the large size of the cesium ion and, consequently, in its more marked polarizability. This is reflected in the polarity of the Cl—O bond which is less in the case of cesium perchlorate than in rubidium perchlorate (Table IX).

It is worth-while noting that, on the basis of the data listed in Tables VII and IX, the order of stabilities is opposite to that of the so-called "free space" of the compounds. This "free space" proved to be a very important factor in the radiolysis of inorganic compounds [13]. A larger "free space" as a rule, also means a larger G value. This can be explained by the fact that the a larger "free space" assures an easier escape of the gaseous products formed in radiolysis. In the present case it follows from the divergent run of the "free space" and stability of the compounds that the favourable effect of increasing the "free space" is overcompensated by the change in the properties of the compounds found previously as decisive for the decomposition. In other words, in the thermal decomposition of alkali perchlorates the formed gaseous products escape more easily, compared to the chemical reaction. From these results it also can be deduced that the mechanisms of the thermal decomposition and of reactions occurring on the effect of radiation are different. Thermal decomposition takes place mostly on the crystal surfaces and at the interfaces between the solid reaction products and the perchlorate, while the reactions effected by radiation may occur inside the crystals as well. Thus the escape of the gaseous products is more important in the latter case.

*

The author wishes to express his thanks to Mr. Gy. BRAUN and Mrs. F. TAKÁCS for their helpful assistance in the experiments.

SUMMARY

The decomposition of lithium and sodium perchlorate occur in the molten phase, while that of the perchlorates of potassium, rubidium and cesium start in the solid phase but continue in the molten phase. The melting of these perchlorates during the decomposition is ascribed to eutectic formation between the perchlorate and the reaction products. The decomposition of the first two salts is well described by the *Prout-Tompkins* equation. The decomposition of the other compounds fits with two first order equations. The first one refers to the slow

solid state reaction, and the second one to the much faster molten phase decomposition. The activation energy of the reactions fell into the range of 60—70 kcal. It is assumed that the rate determining step in the decomposition of alkali perchlorate is the rupture of Cl—O bond.

Some derivatographic and kinetic measurements were also carried out concerning the effect of the reaction products on the decompositions. From the kinetic data the stability order of the compounds has been determined and this order is discussed on the basis of the collected physical and chemical constants of the cations and the character of the bonds.

REFERENCES

1. MARVIN, G. G., WOOLAVER, L. B.: Anal. Chem. **17,** 474 (1945).
2. GORDON, S., CAMPBELL, C.: Anal. Chem. **27,** 1102 (1955).
3. MARKOVITZ, M. M.: J. Phys. Chem. **61,** 505 (1957); J. Phys. Chem. **62,** 827 (1958).
4. MARKOVITZ, M. M., BORYTA, D. A.: J. Phys. Chem. **64,** 1711 (1960); J. Phys. Chem. **69,** 1114 (1965).
5. GLASNER, A., WEIDENFELD, L.: J. Am. Chem. Soc. **74,** 2467 (1952).
6. BIRCUMSHAW, L. L., PHILLIPS, R. T.: J. Chem. Soc. **1953** 703.
7. HARVEY, A. E., EDMISON, M. T., JONES, E. O., SEYBERT, R. A., CATTO, K. A.: J. Am. Chem. Soc. **76,** 3270 (1954).
8. GLASNER, A., SIMCHEN, A. E.: Bull. soc. chim. [5] **18,** 233 (1951).
9. RODGERS, T. A., WASSINK, A.: Final Summary Report. University of Arkansas, Contract No. DA-23-072-ORD. 1958.
10. SIMCHEN, A. E.: J. phys. Chem. **65,** 1093 (1961).
11. MARKOVITZ, M. M., BORYTA, D. A.: J. phys. Chem. **65,** 1419 (1961).
12. BRAEKEN, H., HARANG, L.: Z. Krist. **75,** 588 (1930).
13. PRINCE, L. A., JOHNSON, E. R.: J. phys. Chem. **69,** 377 (1965).
14. SOLYMOSI, F., BÁNSÁGI, T.: Acta Chim. Acad. Sci. Hung., **56.** 337 (1968).
15. SOLYMOSI, F., BÁNSÁGI, T.: Acta Chim. Acad. Sci. Hung., **56.** 251 (1968).
16. BOWDEN, F. P., YOFFE, A. D.: Fast Reactions in Solids. Butterworths, London, 1958.
17. GALWEY, A. K., JACOBS, P. W. M.: Proc. Roy. Soc. A **227,** 115 (1954).
18. TELTOW, A.: Z. phys. Chem. B **40,** 397 (1938).
19. CABANÉ, J., BÉNARD, J.: Bull. soc. chim. France **36** (1961).
20. LAKATOS, B.: Magyar Kém. Foly. **65,** 1 (1959).
21. SANDERSON, R. T.: J. Chem. Educ. **29,** 539 (1952); **31,** 238 (1954); **32,** 140 (1955).
22. LAKATOS, B.: Magyar Kém. Foly. **69,** 409 (1963).
23. MARKOVITZ, M. M.: J. Inorg. Nucl. Chem. **25,** 407 (1963).

Frigyes SOLYMOSI; Szeged, Rerrich tér.

Acta Chimica Academiae Scientiarum Hungaricae Tomus 57 (1), pp. 35—50 (1968)

THERMAL STABILITY OF CHLORINE OXY-SALTS IN THE SOLID STATE, V

THERMAL DECOMPOSITION OF SOME DIVALENT METAL PERCHLORATES

F. SOLYMOSI

(Reaction Kinetical Research Group of the Hungarian Academy of Sciences, Szeged)

Received July 6, 1967

Introduction

In a previous paper we reported a study on the characteristics of the decompositions of alkali perchlorates and on the factors which determine the thermal stability of these salts [1]. It has been found that the stability order of the compounds is determined by the ionic character of the bond and the effective electric field strength of the cations. In the present paper we give an account of the results of our investigations extended to the perchlorates of some divalent metals, *i.e.* barium, magnesium, lead, cadmium and zinc.

The decomposition of the perchlorates of divalent metals has not yet been studied kinetically and, in general, there are very few data about the stability of the above compounds. ZINOVJEV and TSHUDINOVA [2] studied the decomposition of the perchlorates of alkali-earth metals by means of differential thermal analysis and thermal gravimetry. On the thermogram of magnesium perchlorate they found exothermic effects at 410 and 499°. The reaction began as soon as the first exotherm appeared. The decomposition of barium perchlorate started at 480°, but the salt had melted previously.

Experimental

Materials

Magnesium perchlorate: The commercial salt *(Sterling)* was dried at 200° C until it reached constant weight.

Barium perchlorate: *Riedel p.a.* product was used, which had been dried at 250°.

Cadmium perchlorate: A solution of sodium hydroxide *p.a.* was poured into an aqueous solution of cadmium nitrate *p.a.* while constantly stirring. The cadmium hydroxide was filtered off and dried at 140—150°. This product was dissolved in equivalent perchloric acid, and the cadmium perchlorate was crystallized. The material obtained was purified by several recrystallizations. The cadmium perchlorate containing water of crystallization was dehydrated at 200°. The preparation of zinc perchlorate was similar to that of cadmium perchlorate.

In the preparation of lead perchlorate, lead carbonate was used as the starting material, it was added in small quantities to perchloric acid. The solution was slightly warmed and constantly stirred. The crystallized lead perchlorate was twice recrystallized from distilled water, dried in vacuum for 3 to 4 hrs. at 100—115°, and finally for 4 hrs. at 200°.

Measuring procedure

As the perchlorates dehydrated in the above way were extremely hydroscopic, before the kinetic experiments they were pre-treated at 150° in the reaction vessel for 30 minutes in vacuum.

The kinetic measurements were done in the same way as in the case of alkali perchlorates. The chlorine and chlorine dioxide formed during the reaction were frozen out by liquid air in a cooled vessel, and only the pressure of the oxygen was measured. At the end of the experiment, the chlorine and chlorine dioxide were determined iodometrically.

Experimental results

Barium perchlorate

The decomposition of barium perchlorate was studied in the range 440—480°. According to the gas analysis, barium perchlorate, similarly to alkali perchlorates, decomposes into chloride and oxygen:

$$BaClO_4 = BaCl_2 + 2\,O_2. \qquad (1)$$

In order to detect any intermediate product that might have formed during the decomposition, the experiment was interrupted at different times, and an analysis of a sample was performed. In the initial phase of the reaction a few per cents of barium chlorate was found, which had decomposed before the decomposition of barium perchlorate was complete. The $\alpha - t$ curves were different from those of alkali perchlorates. After a short time lag, an extremely rapid reaction took place, during which about 50% of the material decomposed. This phase was followed by a very slow reaction. This behaviour is characteristic especially of experiments performed at higher temperatures, *e.g.*, in the range 450—480°. At 440° and 445° the extent of the fast reaction was essentially smaller, while that of the slow decomposition was considerably large. The $\alpha - t$ curves obtained at different temperatures are plotted in Fig. 1.

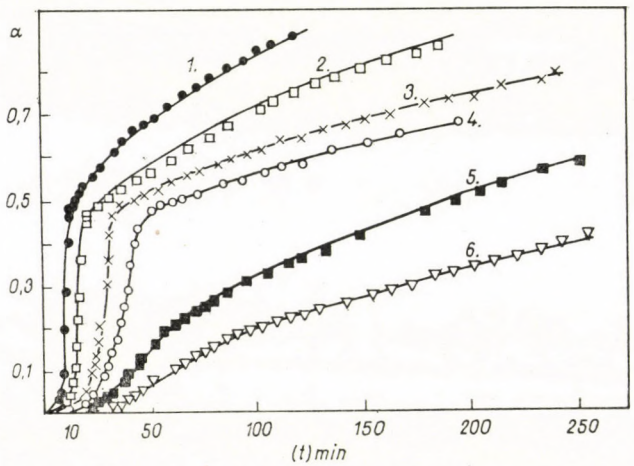

Fig. 1. α-t curves of the decomposition of barium perchlorate (1) 480° C; (2) 469° C; (3) 455° C; (4) 450° C; (5) 445° C; (6) 440° C

The rate constants were calculated by means of the *Prout—Tompkins* equation:

$$\log \frac{\alpha}{1-\alpha} = k_{1,2}\, t + C_1\,, \tag{2}$$

and the first-order equation:

$$\log \frac{1}{1-\alpha} = k_3\, t + C_2\,. \tag{3}$$

The results by the *Prout—Tompkins* equation are shown in Fig. 2.

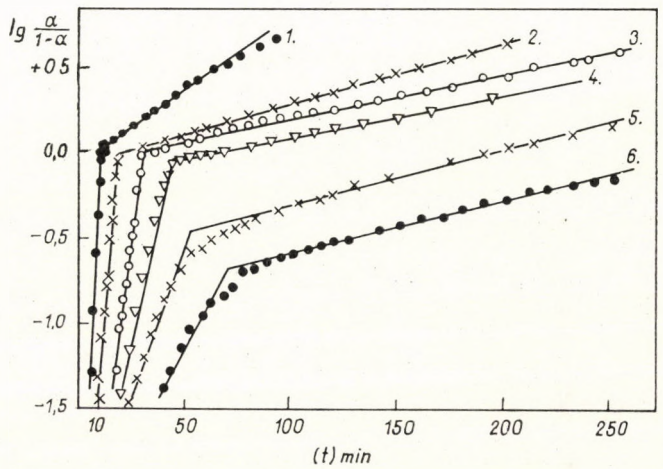

Fig. 2. Kinetical analysis of the decomposition of barium perchlorate by the *Prout-Tompkins* equation. (1) 480° C; (2) 465° C; (3) 455° C; (4) 450° C; (5) 445° C; (6) 440° C

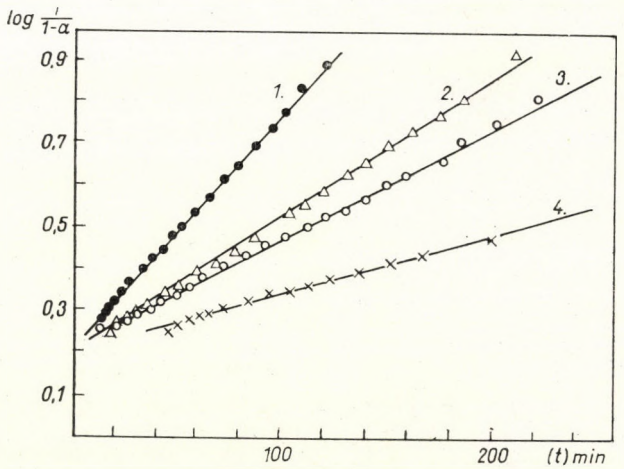

Fig. 3. Kinetical analysis of the decomposition of barium perchlorate by the first-order equation. (1) 480° C; (2) 469° C; (3) 465° C; (4) 450° C

The first straight almost completely reflects the rapid phase of the decomposition, while the second refers to the range of $\alpha = 0.4-0.95$. The activation energy of the first period is 60.2 kcal, and that of the slow period is 52.2 kcal.

The first-order equation proved to be suitable for describing the second period only.

The value of the activation energy is 46.7 kcal. Mathematical analysis of the decay period was attempted by the "contracting cube" formula:

$$1-(1-\alpha)^{1/3} = k_4 t, \tag{4}$$

and straights were obtained in the range of $\alpha = 0.45-0.9$.

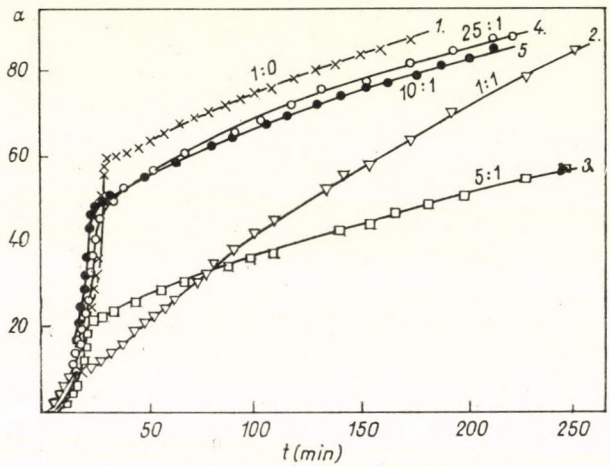

Fig. 4. Effect of barium chloride on the decomposition of barium perchlorate. The molar ratios of barium perchlorate to barium chloride are indicated on the curves (1) 455° C; (2) 458° C; (3) 455° C; (4) 455° C; (5) 455° C

It was assumed that the peculiar run of the $\alpha - t$ curves could be due to the effect of the reaction products formed. To explore this, the effect of barium chloride previously admixed to barium perchlorate was studied in detail. The $p - t$ curves obtained in the presence of different quantities of barium chloride are shown in Fig. 4.

With the addition of barium chloride the reaction started somewhat sooner, while the rate of the acceleration period decreased. At a barium perchlorate: barium chloride molar ratio of 5 : 1 this decrease was larger than 50%. However, the second period of the decomposition of the barium perchlorate took place at a practically unchanged rate. In a mixture of 1 : 1 molar ratio, the initial rapid phase was rather short, while the following reaction, in which decomposition took place at a markedly higher rate than in the previous case, became perceptibly longer. Kinetic data are summarized in Table I.

Table I

Kinetic data for the decomposition of barium perchlorate

No.	Temperature, °C	$k_1 \cdot 10^2$ (min.$^{-1}$)	$k_2 \cdot 10^3$ (min.$^{-1}$)	$k_3 \cdot 10^4$ (min.$^{-1}$)	$k_5 \cdot 10^4$ (min.$^{-1}$)
87	440	2.64	3.03	8.6	5.7
90	445	(3.26)	3.15	13.1	7
86	450	5.38	2.34	13	8.3
88	455	9.29	2.63	17	9.7
89	460	12.4	3.2	22	11
91	465	15.2	3.4	25	12.7
93	469	16.7	4.8	32	16
85	480	31.1	9	55	26
Activation energy kcal.		60.2	52.2	46.7	(41.5)
Frequency factor, min.$^{-1}$		$1.11 \cdot 10^{17}$	$1.19 \cdot 10^{13}$	$1.89 \cdot 10^{11}$	$2.77 \cdot 10^{9}$

k_1; $\alpha = 0.02$—0.4
k_2; $\alpha = 0.4$—0.9
k_3; $\alpha = 0.4$—0.5
k_5; $\alpha = 0.45$—0.9

Magnesium perchlorate

The kinetic measurements were made between 368 and 400°. According to the analysis of the gaseous and solid products of the reaction, the decomposition of magnesium perchlorate can be characterized by two reactions:

$$Mg(ClO_4)_2 = MgCl_2 + 4\ O_2 \tag{5}$$

$$Mg(ClO_4)_2 = MgO + Cl_2 + 3.5\ O_2. \tag{6}$$

As calculated from the quantity of the chlorine formed, about 35% of the substance decomposes according to the second reaction. No traces of chlorate could be detected, but some undecomposed magnesium perchlorate was found in the residue. The run of the $\alpha - t$ curves was rather irregular, especially from $\alpha = 0.5$. This indicated the complex nature of the reaction, and foreshadowed the difficulties of the mathematical evaluation of the decomposition.

Of the kinetic equations, the first order and the "contracting tube" formula were found to be the best applicable. These equations, as it is seen in Fig. 6 give rise to a straight between $\alpha = 0.1$—0.7.

The temperature dependence of the rate constants satisfied the *Arrhenius* equation. The activation energy is 41 kcal. Kinetic data are summarized in Table II.

Table II

Kinetic data for the decomposition of magnesium perchlorate

No.	Temperature, °C	$k_3 \cdot 10^3$ (min.$^{-1}$)	$k_5 \cdot 10^3$ (min.$^{-1}$)
15	382	6.0	4.1
14	386	5.9	4.35
13	392	7.84	5.2
11	400	13.3	7.53
10	408	19.2	12.8
Activation energy, kcal.		41.2	40.1
Frequency factor, min.$^{-1}$		$3.31 \cdot 10^{11}$	$8.33 \cdot 10^{10}$

k_3 ; $\alpha = 0.07—0.75$ k_5 ; $\alpha = 0.10—0.70$

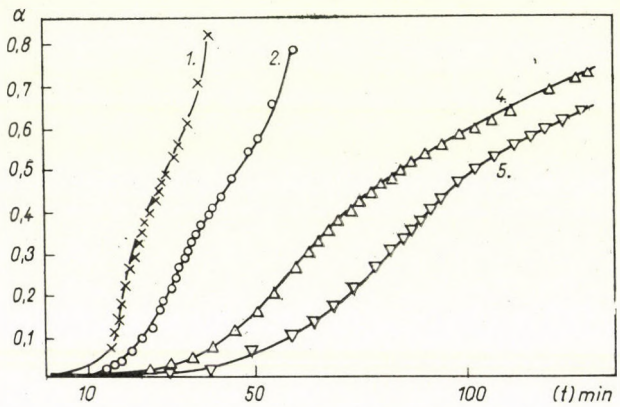

Fig. 5. α-t curves of the decomposition of magnesium perchlorate. (1) 408° C; (2) 400° C; (3) 386° C; (4) 382° C

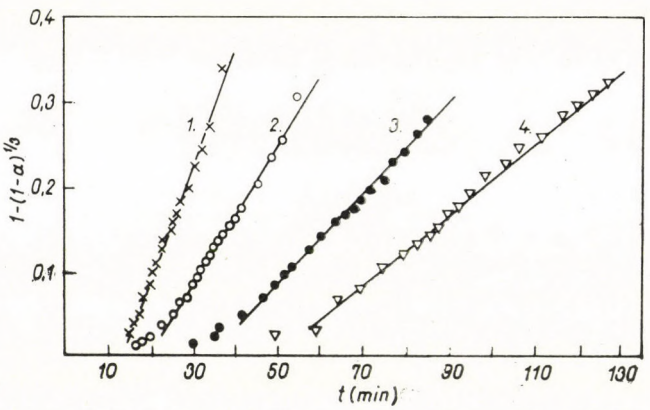

Fig. 6. Kinetical analysis of the decomposition of magnesium perchlorate by the $1-(1-\alpha)^{1/3} = k_5 t$ equation. (1) 408° C; (2) 400° C; (3) 392° C; (4) 382° C

Cadmium perchlorate

The decomposition of cadmium perchlorate was studied in the range between 377 and 403°. The solid residue of the decomposition consisted of cadmium chloride and a slight amount of cadmium oxide. The decomposition can be described by the following two equations:

$$Cd(ClO_4)_2 = CdCl_2 + 4\ O_2 \tag{7}$$

$$Cd(ClO_4)_2 = CdO + Cl_2 + 3.5\ O_2. \tag{8}$$

The quantity of the chlorine formed shows that the decomposition occurs according to the second reaction up to about 3%. Traces of cadmium

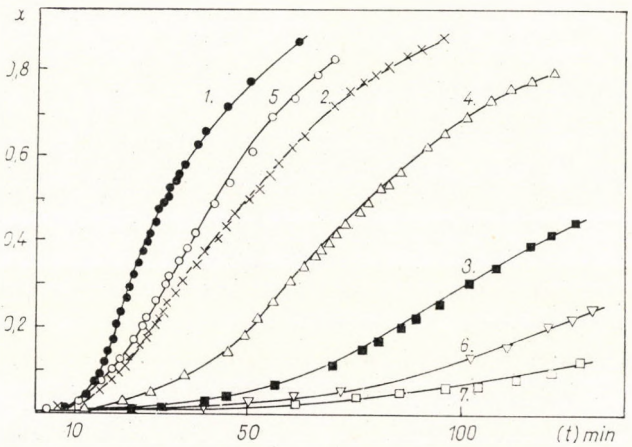

Fig. 7. α-*t* curves of the decomposition of cadmium perchlorate (1) 403° C; (2) 400° C; (3) 396° C; (4) 392° C (5) 385° C; (6) 381° C; (7) 377° C

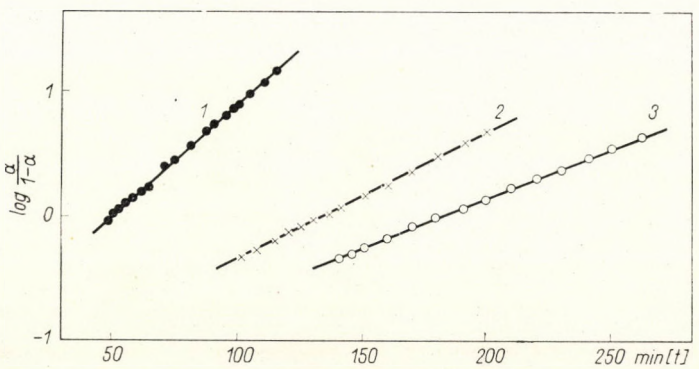

Fig. 8. Kinetical analysis of the decomposition of cadmium perchlorate by the *Prout-Tompkins* equation. (1) 396° C; (2) 385° C; (3) 381° C

Table III

Kinetic data for the decomposition of cadmium perchlorate

No.	Temperature, °C	$k_2 \cdot 10^3$ (min.$^{-1}$)	$k_5 \cdot 10^3$ (min.$^{-1}$)
9	377	7.1	1.4
8	381	7.6	2.4
5	385	10.6	3.05
6	392	14.2	4.95
2	396	18.3	6.03
7	400	24.6	8.31
1	403	28.8	9.57
Activation energy, kcal.		54.0	54.7
Frequency factor, min.$^{-1}$		$1.16 \cdot 10^{14}$	$5.07 \cdot 10^{15}$

k_2 ; $\alpha = 0.3$—0.9 k_5 ; $\alpha = 0.3$—0.95

chlorate were not found. The decomposition is autocatalytic, and it is preceded by a time lag. The rate maximum appeared at $\alpha = 0.2-0.3$ depending on the temperature. The rate constants were calculated by means of the previous equations. At higher temperatures, Eq. (4) yielded straights in the range of $\alpha = 0.3-0.95$ and the first-order equation in the range of $\alpha = 0.23-0.8$.

At lower temperatures, *i.e.* below 392°, a kinetical analysis of the measurements was more difficult, since the above rate equations, especially the first-order equation, was valid only for a narrower range of the decomposition.

The kinetical analysis of the $\alpha - t$ curves was also attempted by the *Prout–Tompkins* equation. The equation did not give satisfactory results for the acceleration period, but it well described the decay period of the decomposition (Fig. 8). From the temperature dependence of the rate constants calculated by the "contracting cube" formula, an activation energy of 54.7 kcal was obtained. The temperature dependence of the *Prout–Tompkins* rate constants (k_2) yielded 54 kcal.

In this case, also, the effects of cadmium chloride and cadmium oxide, *i.e.* the solid residues of the decomposition, on the reaction were studied. Of the two materials cadmium chloride had an accelerating effect.

The kinetical results are shown in Table III.

Zinc perchlorate

Of the perchlorates studied, the decomposition of zinc perchlorate started at the lowest temperature. The reaction was investigated in the range 280—310°. Here, the decomposition can be characterized again by two equations:

$$Zn(ClO_4)_2 = Zn(Cl)_2 + 4\,O_2 \qquad (9)$$

$$Zn(ClO_4)_2 = ZnO + Cl_2 + 3.5\ O_2. \qquad (10)$$

The reactions take place to almost the same extent. The $\alpha - t$ curves are plotted in Fig. 9. The gas formation, in contrast to the case of cadmium perchlorate, started after a few minutes time lag. To determine the rate constant, the first-order equation was used. It is valid between $\alpha = 0.04 - 0.75$.

The activation energy is 38.2 kcal. Equation (3) describes the decomposition in a similar range: in this case the activation energy is 40.0 kcal.

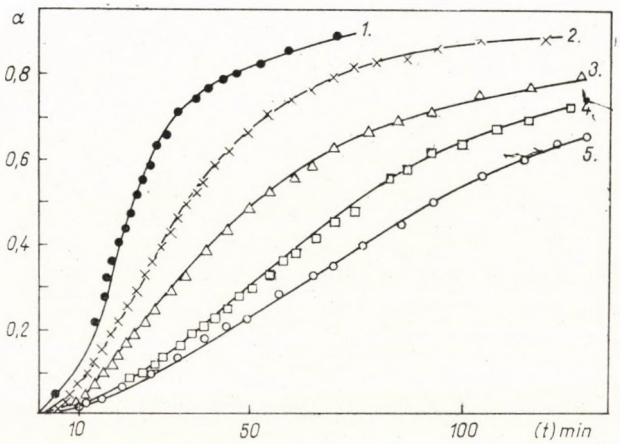

Fig. 9. α-t curves of the decomposition of zinc perchlorate, (1) 310° C; (2) 300° C; (3) 296° C; (4) 290° C; (5) 285° C

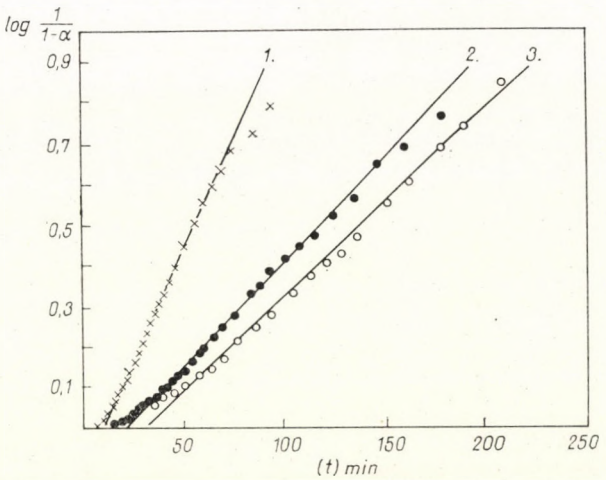

Fig. 10. Kinetical analysis of the decomposition of zinc perchlorate by the first order equation (1) 303° C; (2) 290° C; (3) 285° C

Table IV

Kinetic data for the decomposition of zinc perchlorate

No.	Temperature, °C	$k_3 \cdot 10^3$ (min.$^{-1}$)	$k_5 \cdot 10^3$ (min.$^{-1}$)
31	285	4.8	2.57
30	290	5.17	3.05
27	296	6.8	4.70
28	303	11.5	7.24
29	308	14.2	8.40
32	310	20.8	12.4
Activation energy, kcal.		38.2	40.7
Frequency factor, min.$^{-1}$		$3.73 \cdot 10^{12}$	$2.11 \cdot 10^{13}$

k_3 ; $\alpha = 0.04$—0.75 k_5 ; $\alpha = 0.01$—0.75

Formation of zinc chlorate was not observed during the reaction. From studying the effect of the reaction products, it appeared that zinc oxide had practically no influence on the decomposition, while zinc chloride definitely inhibited the reaction in a 1 : 1 molar ratio. Kinetic results are summarized in Table IV.

Lead perchlorate

The decomposition of lead perchlorate was studied in the temperature range of 320—355°. The decompisition occurred mainly by the reaction

$$Pb(ClO_4) = PbCl_2 + 2\ O_2 \qquad (11)$$

and the reaction

$$Pb(ClO_4)_2 = PbO + Cl_2 + 3.5\ O_2 \qquad (12)$$

Table V

Kinetic data for the decomposition of lead perchlorate

No.	Temperature, °C	$k_3 \cdot 10^3$ (min.$^{-1}$)	$k_5 \cdot 10^3$ (min.$^{-1}$)
23	330	4.01	2.24
22	336	5.69	3.04
20	340	7.64	4.64
19	345	9.05	6.00
17	350	11.82	8.85
18	355	16.14	10.32
Activation energy, kcal.		42.4	46.3
Frequency factor, min.$^{-1}$		$9.76 \cdot 10^{12}$	$6.07 \cdot 10^{13}$

k_3 ; $\alpha = 0.005$—0.86 and $\alpha = 0.15$—0.7 resp. k_5 ; $\alpha = 0.04$—0.7

played a lesser role. No transitional formation of lead chlorate was found. The run of the $\alpha - t$ curve is similar to that of zinc perchlorate.

The mathematical analysis of the curves was done by the above rate equations. At higher temperatures the first-order equation described the reaction practically from its beginning to $\alpha = 0.86$. At lower temperatures two stages were obtained. The first and longer phase was valid in the range $\alpha = 0.15-0.7$. Equation (3) yielded a straight in the range $\alpha = 0.04-0.7$.

The value of the activation energies is 42.4 kcal, and 46.3 kcal, respectively.

The kinetic data are shown in Table V.

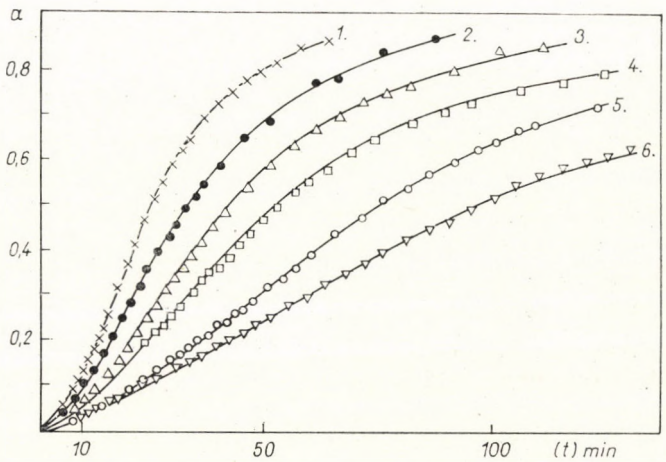

Fig. 11. α-t curves of the decomposition of lead perchlorate.
(1) 355° C; (2) 330° C; (3) 345° C; (4) 340° C; (5) 336° C; (6) 330° C

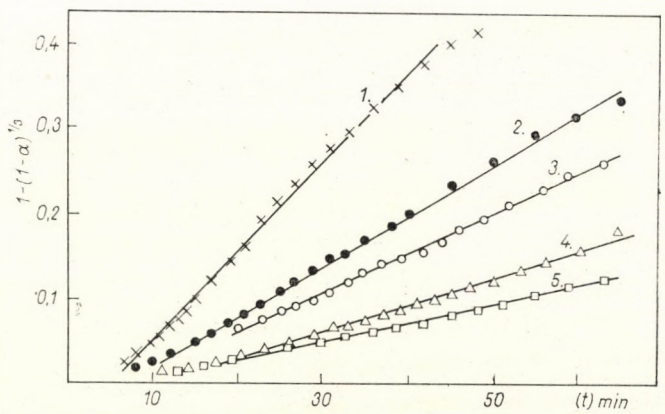

Fig. 12. Kinetical analysis of the decomposition of lead perchlorate by the $1-(1-\alpha)^{1/3} = k_3 t$ equation. (1) 355° C; (2) 345° C; (3) 340° C; (4) 336° C; (5) 330° C

Discussion

The decomposition of the perchlorates of the divalent metal ions investigated took place at a lower temperature than that of alkali perchlorates. On the basis of the characteristics of the decompositions, the materials can be divided into three groups:

(a) In the case of barium perchlorate, the behaviour differs from that of other perchlorates by its extremely fast reaction taking place after the short, slow decomposition. In this fast period about 50% of the material is consumed. It could be supposed that the acceleration of the reaction was due to the melting of the material. The melting point of the pure material is 472°. According to our observations, however, barium perchlorate melts at about 450° during the initial part of decomposition. This shows that for reducing the melting point of barium perchlorate, a comparatively small quantity of barium chloride is sufficient. It may mean that the eutectic composition is shifted towards barium perchlorate. After a decomposition of about 50%, the material becomes stable again, and the rate of decomposition decreases; this is probably due to the accumulation of barium chloride, and to the consequent resolidification of barium perchlorate.

Results in accordance with the above considerations were also obtained when barium chloride was first admixed to the barium perchlorate. In the presence of barium chloride the decomposition began sooner; however, barium chloride definitely inhibited the development of the fast reaction, and decreased its extent. This effect became greater with the increase of the quantity of barium chloride.

(b) Special attention must be given to the behaviour of magnesium perchlorate. In the course of the reaction there was no phase change, and the reaction occurred throughout in the solid. Despite this, the run of the $\alpha - t$ curves was rather irregular, which was probably due to the fact that the decomposition took place stepwise (see later).

(c) The decompositions of the perchlorates of lead, cadmium, and zinc are similar, being mildly autocatalytic. All the three materials melted in the course of the reaction.

The behaviour of the materials described above also appeared in the kinetic evaluation of the decomposition. The *Prout–Tompkins* equation gave two straights characterizing the decomposition of barium perchlorate. One referred to the fast molten-phase reaction, and the other to the much slower solid-phase decomposition. The monomolecular decay equation and the "contracting cube" formula seemed to be suitable only for describing the second, slow decomposition. After the initial rate maximum, however, these equations described the decomposition of the perchlorates of magnesium, cadmium, lead and zinc, to about $\alpha = 0.8$.

Similarly to the characteristics of alkali perchlorates, the decomposition products of barium and cadmium perchlorates are, almost exclusively, metal chloride and oxygen. Only 5.5% chlorine was found even in the decomposition of lead perchlorate. The main reaction equation is:

$$Me(ClO_4)_2 = MeCl_2 + 4\ O_2.$$

Table VI

Equivalent heats of formation for chlorides and oxides (kcal.)

Chlorides	$H^0_{298/n}$	Oxides	$H^0_{298/n}$	$(H^0_{Cl}—H^0_O)_{298/n}$
$BaCl_2$	—102.78	BaO	—66.5	—36.28
$MgCl_2$	— 76.6	MgO	—71.83	— 4.75
$CdCl_2$	— 46.5	CdO	—30.6	—15.9
$ZnCl_2$	— 49.7	ZnO	—41.7	— 8.0
$PbCl_2$	— 42.92	PbO	—26.2	—16.72

n = valency of the cations.

The decomposition of magnesium and zinc perchlorates likewise yield chloride and oxide, but here the process

$$Me(ClO_4)_2 = MeO + Cl_2 + 3.5\ O_2$$

also occurs.

The direction of the decomposition of divalent metal perchlorates is in accordance with the expectation of MARKOWITZ [6]; namely, if the free energy data are not available, the equivalent enthalpies of formation of the possible reaction products may be used as guides to formulating the expected reaction residue. As Table VI shows, the equivalent heat of formation of barium, cadmium and lead chlorides, is much greater (negative) than that of the oxide. In the case of magnesium and zinc perchlorates, when the decomposition is bi-directional, the difference between the heat of formation of the chlorides and oxides is essentially smaller.

In contrast to alkali perchlorates, the activation energies of the decompositions of these salts differ considerably from each other. The value of the activation energy obtained for the decomposition of barium and cadmium perchlorates was nearly 60 kcal. This was the case when the decomposition took place in the direction of the formation of chloride and oxygen. An activation energy of about 40 kcal. was obtained in the other three cases, when the decomposition was bi-directional. Here, as with alkali perchlorates, it may also be assumed that the first step of the decomposition is the formation of chlorate:

$$Me(ClO_4)_2 = Me(ClO_3)_2 + O_2 \qquad (1)$$

which is followed by the reactions

$$Me(ClO_3)_2 = Me(ClO_2) + O_2 \tag{2}$$

and

$$Me(ClO_2)_2 = MeCl + 2\ O_2. \tag{3}$$

In addition to the above processes, the disproportionation of chlorates to perchlorates can also take place:

$$4\ Me(ClO_3)_2 = 3\ Me(ClO_4)_2 + MeCl_2. \tag{4}$$

Formation of chlorate was detected only in the decomposition of barium perchlorate. No chlorate or chlorite was found in the decomposition of the rest of the perchlorates. Very few data are known in the literature concerning the stability of chlorates and chlorites.

According to our investigations, barium chlorite is converted into barium chlorate in the range 130—160° without gas evolution, while above 195° it explodes [3]. The decomposition of barium chlorate begins at about 400°, but as well as the decomposition, the transformation to barium perchlorate also takes place [4]. The decomposition of the lead chlorate starts at 195°, and after a long induction period, it takes place at a very high rate [4]. The explosion of lead chlorite occurs at 112° [3].

The stabilities of the chlorates of zinc and cadmium are not known, but considering the above data it is possible that the above reactions (2), (3) and (4) are in every case faster than the first step. So it seems very likely that the rate-determining step is the first one, which involves the rupture of the Cl—O bond. This mechanism is valid first of all for the decomposition of barium and cadmium perchlorates.

The decomposition of the rest of the perchlorates is more complex. ZINOVJEV and THSUDINOVA [2], on the basis of thermogravimetric and DTA investigations, described the decomposition of magnesium perchlorate by the following reaction scheme:

$$2Mg\begin{matrix}OClO_3\\OClO_3\end{matrix} = Cl_2O_7 + O\begin{matrix}Mg{-}OClO_3\\Mg{-}OClO_3\end{matrix} \tag{5}$$

$$Cl_2O_7 = Cl_2 + 3.5\ O_2 \tag{6}$$

$$O\begin{matrix}MgOClO_3\\MgOClO_3\end{matrix} = O\begin{matrix}MgCl\\MgCl\end{matrix} + 2\ O_2 \tag{7}$$

Our experiments performed with magnesium perchlorate under isothermic conditions seem to support the stepwise decomposition. In the other cases,

neither the derivatographic studies (not expounded in detail here), nor the measurements conducted under isothermic conditions point to a stepwise decomposition.

According to the above scheme, 2 moles of perchlorate give 1 mole of chlorine. The quantity of chlorine found during our experiments was in every case smaller than this, which means that either reactions (1), (2) and (3) take place parallel to the above, or that the chlorine formed reacts with the metal oxide:

$$MgO + Cl_2 = MgCl_2 + \frac{1}{2} O_2 . \qquad (8)$$

Table VII

Some characteristic data of the cations and compounds

Compound	Melting point, °C	Radius of cation, Å	Ionization potential, eV	Polarizability of cation	F^*	Ionic character of the bond, %	Refractive index	t_0, °C
$Ba(ClO_4)_2$	470	1.35	10.00	2.5	—	45.1	1.5327	440
$Mg(ClO_4)_2$	600	0.78	15.03	—	5.444	35.7	—	393.1
$Cd(ClO_4)_2$		1.03	16.90	1.8	5.750	22.6	1.486	392.6
$Zn(ClO_4)_2$		0.83	17.96	0.8	6.654	19.6	1.501	297.8
$Ph(ClO_4)_2$		1.25	15.03	4.9	3.876	17.3	1.587	341.9

$F^* = \frac{Z^*}{r^2}$ where F^* = effective electric field strength of the cation
r = radius of cation
Z^* = effective nuclear charge
t_0 = characteristic temperature where $k_5 = 5 \cdot 10^{-3}$/min.

It is not possible to evaluate the kinetics and the detailed mechanism of the decomposition of magnesium and zinc perchlorate on the basis of the measurements performed until now. This can only be done when it is technically possible to have a continuous registration of the quantity of the chlorine formed, in addition to measuring the pressure of the oxygen. (At present the decomposition of the materials is followed by measuring only the pressure of the oxygen formed.) One must also learn the characteristics of the reactions between chloride and oxygen, and oxide and chlorine, respectively.

To describe the stability of the perchlorates, the temperature value was also calculated where the rate constant of the decomposition is $5 \cdot 10^{-3}$/min. As a basis for comparison, the rate constants of the "contracting cube" formula were chosen, as they can be determined satisfactorily in every case. The stability order of the divalent perchlorates was the following: barium—magnesium—cadmium—lead—zinc.

Some data concerning the bonds and the characteristics of the cations are summarized in Table VII.

The study of alkali perchlorates has revealed that the stability of the compounds is determined by the ionic character of the bond between the metal ion and the complex anion, and the polarizing power of the cations. This conclusion is valid — with the exception of lead perchlorate — for the divalent metal perchlorates, and also when comparing the thermal behaviour of alkali and divalent metal perchlorates. The stability of the salts decreases with the decrease in the percentage of ionic character of the bond and with the increase of the effective electric field strength of the cations.

In our earlier experiments the decomposition of silver perchlorate was also studied [5]. The ionic character of silver perchlorate is 36.2% and the effective electric field strength of the silver ion is 3.394. On the basis of the above, the stability of silver perchlorate must fall between that of barium and lithium perchlorate. The characteristic temperature determined from the kinetic data was 420°, which, according to expectations, is, indeed, between the characteristic temperatures of the decompositions of the above two compounds.

The author's thanks are due to Mr. Gy. BRAUN and Mrs. F. TAKÁCS for their assistance in the experiments.

SUMMARY

The thermal decomposition of barium, magnesium, cadmium, zinc and lead perchlorates has been studied. Barium and cadmium perchlorates decomposed to chloride and oxygen, while the decomposition of the other salts resulted in chlorides, oxides and different gases. The decomposition of the substances can be described by different equations, and the rate constants and the activation energies of the reaction have been calculated. The stability order of the perchlorate salts has also been determined and it decreases in the order: barium—magnesium—cadmium—lead—zinc. This order is interpreted by the effective electric field strength of the cations and the ionic character of the compounds.

REFERENCES

1. SOLYMOSI, F.: Acta Chim. Acad. Sci. Hung. (In press).
2. ZINOVJEV, A. A., TSHUDINOVA, L. J.: Zhur. Neorg. Khim. **1**, 1722 (1956).
3. SOLYMOSI, F., BÁNSÁGI, T.: Acta Chim. Acad. Sci. Hung. **56**, 251 (1968).
4. SOLYMOSI, F., BÁNSÁGI, T.: Acta Chim. Acad. Sci. Hung. **56**, 337 (1968).
5. SOLYMOSI, F.: Z. Phys. Chem. N. F. **57**, 1 (1968).
6. MARKOVITZ, M. M.: J. Inorg. Nucl. Chem. **25**, 407 (1963).

Frigyes SOLYMOSI; Szeged, Rerrich tér.

Acta Chimica Academiae Scientiarum Hungaricae Tomus 57 (1), pp. 51—67 (1968)

CHARACTERISTIC NORMAL VIBRATIONS OF BENZENE DERIVATIVES, III

CORRELATION AMONG THE FREQUENCY AND VIBRATIONAL FORM OF THE OUT-OF-PLANE CH VIBRATIONS

G. VARSÁNYI

(Department of Physical Chemistry of the Technical University, Budapest, and Central Research Institute for Chemistry of the Hungarian Academy of Sciences, Budapest)

Received July 21, 1967

Introduction

In two previous papers [1, 2], there was discussed the correlation between the frequency and vibrational form of radial skeletal vibrations and in-plane CH bending modes. In the present work the correlation existing between the frequency and vibrational form of the out-of-plane CH vibrations, and, on the other hand, the spectroscopic properties of the substituents will be treated. YOUNG, DU VALL and WRIGHT [3] called attention to the analytical importance of the spectral range between 1700 and 2000 cm^{-1}. This is the region where the combination tones, and occasionally the overtones of the out-of-plane CH vibrations appear. Since the out-of-plane CH frequencies themselves are first of all characteristic of the site of substitution, the frequencies and intensities of their combination tones are rather constant in the infrared spectra.

The relation between the out-of-plane CH vibration of the lowest frequency, the so-called umbrella vibration, and the number of the adjacent unsubstituted hydrogens of the aromatic ring has been discovered by a number of well-known research workers. Their results have been summarized by BELLAMY [4]. The frequency of the umbrella vibration of benzene is 673 cm^{-1} (according to BRODERSEN and LANGSETH [5]). In monosubstituted benzene derivatives, where there are five unsubstituted adjacent hydrogen atoms, the corresponding frequency range is 730—770 cm^{-1}, according to COLTHUP [6] (disregarding strongly electron-attracting substituents). The umbrella vibration frequency of *ortho*-disubstituted benzenes is found between 735 and 770 cm^{-1} (four adjacent hydrogens), while for *meta*-disubstituted and *vic*-trisubstituted benzene derivatives the corresponding frequency range is 750—810 cm^{-1}. In the latter type there are only three adjacent hydrogens left unsubstituted. In the cases of *para*-di-, *asym*-tri-, and *ortho*-tetrasubstitution (two adjacent hydrogens), the frequency range is 800—860 cm^{-1}, while finally in all those substitution types where only isolated hydrogens can be found, the umbrella vibration occurs between 860 and 900 cm^{-1}. VAN BINST, DAVIS, SMIT and

MARTIN [7] determined the interaction force constants of the umbrella vibration in different solvents. According to their calculations, *e.g.* in CS_2 as the solvent, the frequency values are the following, in the order of the decreasing number six to one of adjacent unsubstituted hydrogens: 675, 716, 736, 762, 804 and 865 cm^{-1}.

Interpretation of the frequency course according to the principle of orbital-following

In the umbrella vibration all hydrogen atoms move in the same phase. If the carbon atoms preserve their sp^2 planar hybridization state during the vibration, the C—C bonds must be "bent". The bending of the bonds, however,

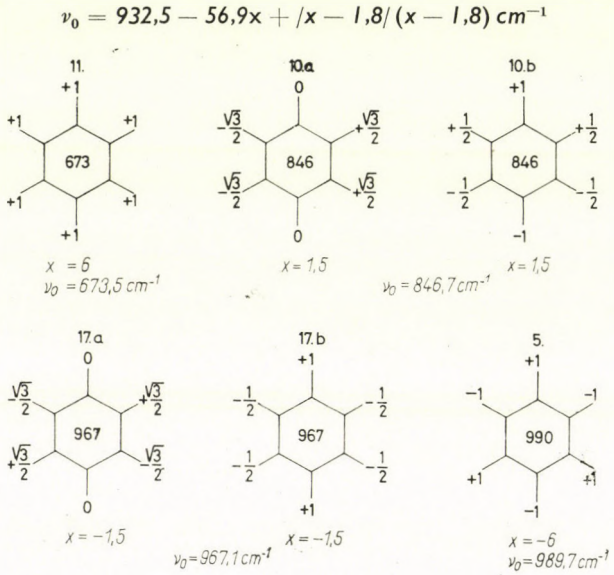

Fig. 1

does not involve an essential decrease of the orbital overlap (the orbitals "follow" one another), so that the force constant of the out-of-plane vibration is smaller than it is in those modes where the adjacent hydrogens are displaced out-of-plane from their equilibrium positions. In the latter case the C—C bond directions will tend apart while the planar hybrid sp^2 character is retained, which leads to an increase of the force constant.

In order to provide a semi-quantitative explicit description of the orbital-following, a parameter can be defined: $\sum_{i=1}^{N} A_i A_i'$, where A_i and A_i' are the vibra-

tional amplitudes of the two adjacent hydrogens, resp. belonging to the i-th C—C bond, and the summation extends over the N number of the C—C bonds connecting the unsubstituted adjacent methine groups. When the presence of more than one substituent gives rise to more than one isolated methine chains in the aromatic ring, the parameter should be completed by the expression: $x = \sum_{i=1}^{N} A_i A_i' \left(1 + \frac{\delta}{3}\right)$, where $\delta = 0$, if there is no second methine chain, while $\delta = 1$ if there is such a chain. The latter case occurs only for para disubstitution. Fig. 1 depicts the six out-of-plane CH vibrations of benzene using normalized amplitudes, and the corresponding x values are given. The frequency data are taken from the work of BRODERSEN and LANGSETH [5].

The interpolation formula given below reproduces very well the out-of-plane CH frequencies of benzene:

$$\nu_0 = 932.5 - 56.9\,x + |x - 1.8|(x - 1.8)\text{cm}^{-1} \qquad (1)$$

The calculated values are: $\nu_{011} = 673.5$; $\nu_{010} = 846.7$; $\nu_{017} = 967.1$; and $\nu_{05} = 989.7$ cm^{-1}.

The effect of substitution on the frequencies of the perpendicular CH vibrations

KROSS, FASSEL and MARGOSHES [8] have reported that the frequency of the umbrella vibration increases with the $-M$ effect of the substituent. According to their interpretation, the sp^2 hybridized ground state interacts with the sp^3 state in the out-of-plane CH vibrations, in which the hydrogen would not be found in the plane of the ring. The interaction results in a decrease of the bending frequency and force constant. If the π-electron density is reduced on the carbon atom carrying the hydrogen, the interaction energy is reduced as well, which can be described illustratively by saying that the activation energy for the transition into the sp^3 state is increased, whereby the bond becomes more rigid towards bending, the force constant and the frequency are increased. The decisive role of the π-electrons is proved by the observation that although the cyano and nitro groups have similar electronegativities, the cyano group is negative due mainly to inductive effect, while the nitro group has in addition a very important $-M$ effect, so that the latter gives rise to a greater increase of the frequency of the umbrella vibration. A similar trend in the frequencies can be observed for the other out-of-plane CH vibrations.

MARGOSHES and FASSEL [9] established for monoatomic substituents that the frequency can be linearly correlated with the reduced mass of the substituent. The only minor defect in this theory is that it also applies to deuterobenzene, although the 778 cm^{-1} frequency of the latter does not belong to

the umbrella vibration. The above relation does not hold for polyatomic substituents. A similar opinion was expressed by THOMPSON *et al.* [10, 11], who obtained 725 cm^{-1} for monosubstitution using an infinitely large reduced mass in the calculations.

BELLAMY [12] drew a parallel between the frequencies of the carbonyl- and umbrella vibrations of carbonyl derivatives. By simplifying this theory,

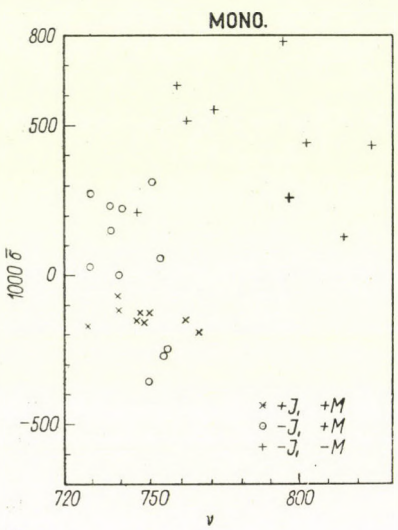

Fig. 2a

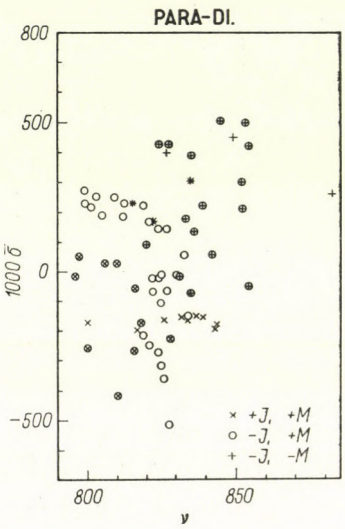

Fig. 2b

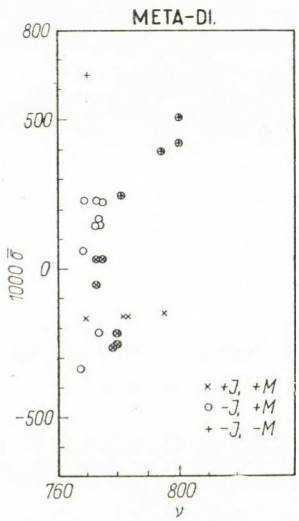

Fig. 2c

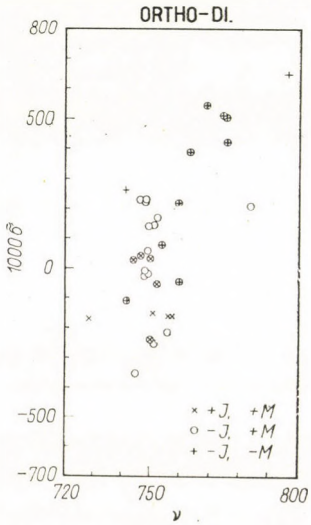

Fig. 2d

it can be stated that the lower the carbonyl frequency of the substituent containing the carbonyl group, *i.e.* the greater its $-M$ effect, the higher the frequency of the umbrella vibration. Unfortunately, this is not always true, and the application of this theory to the umbrella vibration of benzoyl chloride, methyl benzoate and ethyl benzoate led to some fallacious assignments by the above author.

GRIFFITHS and DERWISH [13] interpreted the effect of negative substituents on the frequency of the umbrella vibration by an electrostatic steric effect. They corrected the force constant with the term $e_H^+ \cdot e_M^-/r^3$, in which expression e_H^+ and e_M^- are the charges of the hydrogen and the substituent, resp., while r is the distance between them. Plotting ν^2 as a function of e_M^-/r^3, one obtains a straight line.

BELLAMY [14] plotted the sum of the *Hammett* σ values of the substituents for *meta* and *para* disubstitution and for symmetric trisubstitution as a function of the frequency; on the basis of some available values he found a nearly linear relationship. The slope of the three straight lines was approximately the same.

According to the present investigation, it is not possible to give such a straight correlation between the *Hammett* σ values and the frequency of the umbrella and other out-of-plane CH vibrations, as it could be expected on the ground of the paper of BELLAMY [14]. As an illustration, Fig. 2 shows the frequencies of the umbrella vibration of mono-, and disubstituted benzene derivatives as a function of the *Hammett* σ values. It is seen that the description of the frequencies as a linear function of the σ values is a very rough approximation. It was found that the frequencies can be better correlated with the so-called "spectroscopic momenta" given by PLATT [15]. These momenta are proportional to the intensity square-root of the first ultraviolet band systems of substituted benzenes, and as such they are unambiguously related to the transition moments. According to experience, the intensity of the interactions between the states sp^2 and sp^3 and the spectroscopic momenta are correlated. The more positive the spectroscopic moment of the substituent, the lower the frequency of not only the umbrella vibration but also of the out-of-plane CH vibrations in general.

Since the effect of the substituent increasing the interaction between the states sp^2 and sp^3 influences the carbon atoms, for the characterization of this effect we may introduce a parameter related to the carbon atoms: $y = \sum_{j=1}^{6} |A_{j-1} + 2\,A_j + A_{j+1}|$, where A_j is the amplitude of the j-th carbon atom, normalized for the amplitude of the hydrogen attached to it while A_{j-1} and A_{j+1} denote the amplitudes of the adjacent carbon atoms. For the amplitude of the carbon atom carrying the substituent, the arithmetical mean of the amplitudes of the two adjacent carbon atoms, normalized with respect to the hydrogen,

was taken. (In first approximation the amplitude of the carbon atom carrying the substituent was considered equal to zero.) Thus, *e.g.*, for the 10*a* (17*a*) vibration of 2,6-disubstituted benzenes (Fig. 3) we have: for C—1 0; for C—2 and C—6 2; for C—3 and C—5 2.5; and finally for C—4 0 again. In this case $y = 9$.

The quantity proportional to the number of substituents was taken into account as an additive term to the average spectroscopic momentum. It was also taken into account that substituents of identical orientation effect in *meta* positions bring about alternating polarity on the carbon atoms, resulting in a state of higher energy and in a stronger interaction with the sp^3 state.

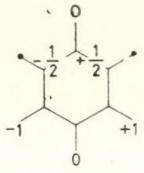

Fig. 3

Considering all these aspects, the following interpolation formula is proposed for all out-of-plane CH vibrations of all benzene derivatives:

$$\nu = \nu_0 - \frac{y}{16}(10n + 5m + \overline{M}), \tag{2}$$

where ν_0 is the frequency defined in Eq. (1), n is the number of substituents, m is the number of pairs of substituents in the *meta* positions having the same orientation effect, and $\overline{M}$ is the average spectroscopic momentum.

Monosubstitution

In the case of a light* substituent the out-of-plane CH vibrations of monosubstituted benzenes can be traced back to normal vibrations 5, 10a, 10b, 11 and 17a of benzene (17b is strongly coupled to 16b, and can be qualified as a CX vibration). In the case of heavy substituents, vibration 10b is classified as CX mode, therefore instead of the latter it is vibration 17b that is considered as out-of-plane CH vibration. In benzene the vibrational forms of 10b and 17b

* A substituent is called "light" if its atomic weight is less than 25 [1]. Contrary to what has been stated in paper [1], where it was the mass of the first atom that was important in polyatomic substituents, in the present case the total mass of the whole substituting group should be considered owing to the stronger coupling of the out-of-plane vibrations. Exceptions are those substituent groups (*e.g.*, ethyl group) in which free rotation is possible about the first atom, since the extremely low frequency of these cannot couple with the out-of-plane CX vibration.

are different, but if zero amplitude is calculated for the hydrogens in positions 3 and 5, the forms of the two vibrations will become identical. This means that in vibration 10b (17b) depending on the substituent, the amplitude directions of the hydrogens in positions 3 and 5 can be different as compared with the other hydrogen atoms. BELL, THOMPSON and VÁGÓ [10] calculated the normal coordinates of the out-of-plane vibrations according to the valence force field model. The scheme for the CH vibrations of symmetry b_1 can be seen in Fig. 4.

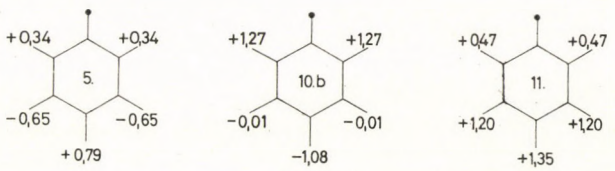

Fig. 4

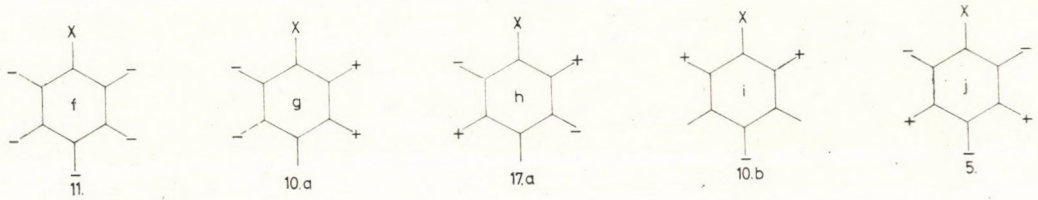

Fig. 5

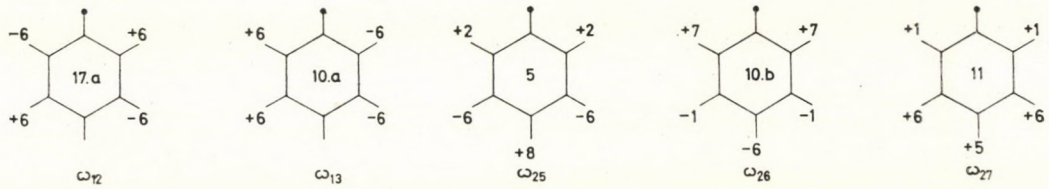

Fig. 6

The first figure corresponds to vibration 5, the second one to normal mode 10b, while the third figure corresponds to vibration 11. In normal mode 10b, however, the amplitudes of the hydrogens in positions 3 and 5 are smaller by two orders of magnitude than those of the others, so that by a slight change the form of the vibration can transform to that of 17b. It is also important to point out that the amplitudes of the *ortho*-positioned hydrogens are essentially smaller than those of the other three H-atoms in the "umbrella" vibration 11. The vibrational forms *f*, *g*, *h*, *i* and *j* given by WHIFFEN [16] are shown in Fig. 5. The vibrational forms given by SCHMID, BRANDMÜLLER and NONNENMACHER [17] are very similar to those given by BELL *et al.* Here again the 3,5-positioned hydrogens in vibration 10b have much smaller amplitudes than the others,

and the situation is similar for the hydrogens in positions 2 and 6 in vibration 11 (Fig. 6). BOGOMOLOV's vibrational forms [18] are shown in Fig. 7. The figures display the same characteristics as all the cases discussed so far. SHIMANOUCHI, KAKIUTI and GAMO [19] published the relative amplitudes of the out-of-plane CH vibrations of symmetry b_1, according to which Fig. 8 has been here constructed. There is no great difference in the amplitudes of the hydrogens in vibration 11, but the hydrogens in positions 3 and 5 have again the smallest amplitudes in vibration 10b. The amplitudes in Figs 4 and 8 are normalized with respect to the amplitudes of the umbrella vibration, taken as units.

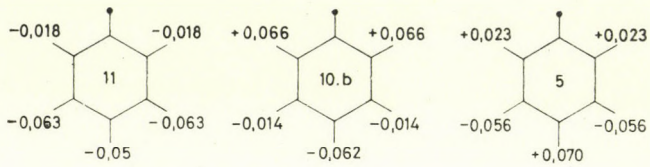

Fig. 7

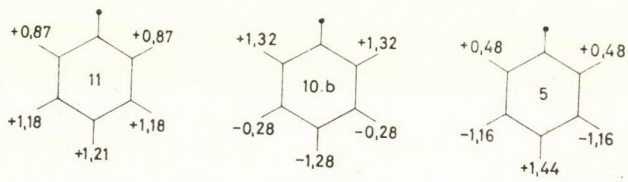

Fig. 8

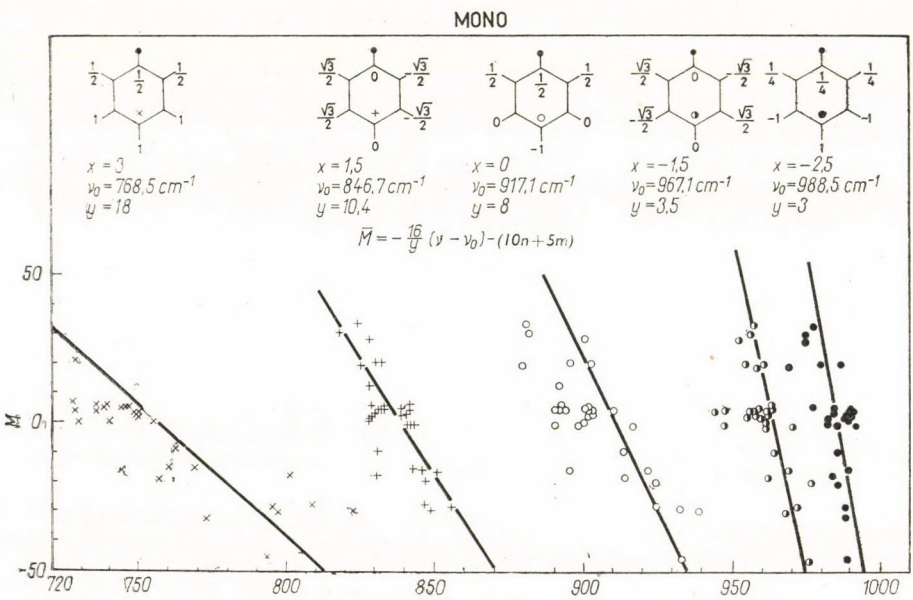

Fig. 9

In Fig. 9 the frequencies of the out-of-plane CH vibrations of monosubstituted benzene derivatives, taken from the literature, are given, while on the ordinate axis the spectroscopic momentum is plotted. The averaged normalized amplitudes are given for each normal vibration, together with the corresponding x and y values. The equation of the straight lines derived from Eq. (2) is the following:

$$\overline{M} = -\frac{16}{y}(\nu - \nu_0) - (10n + 5m) \tag{3}$$

Disubstitution

In *para* disubstitution the vibrational forms are given by the symmetry properties of the point group V_h. The amplitudes of the four out-of-plane CH vibrations, their x and y values, and literature frequency data with the straight lines given by Eq. (3) are shown in Fig. 10.

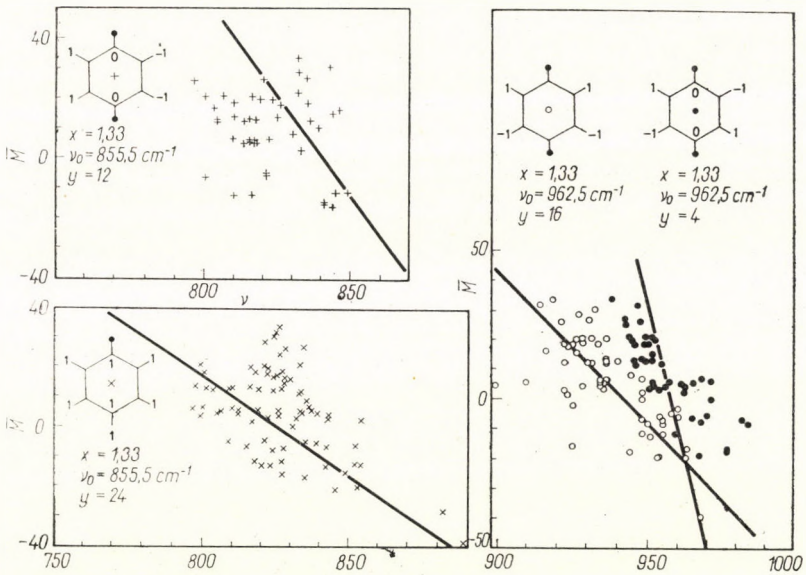

Fig. 10

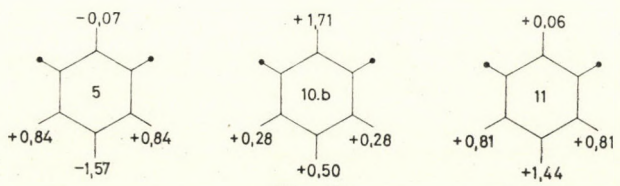

Fig. 11

In *meta* disubstitution BELL, THOMPSON and VÁGÓ [10] gave, in the order of decreasing frequencies, the vibrational forms calculated by the use of the valence force field for b_1 symmetry vibrations (Fig. 11). The amplitude directions of the hydrogens are the same in the second and third forms but the absolute values are different. The middle (10b or 17b) is essentially the out-of-plane vibration of the hydrogen in position 1, while the right-hand figure is the in-phase vibration of the 3,4,5 hydrogens (11). In Fig. 12 the same vibra-

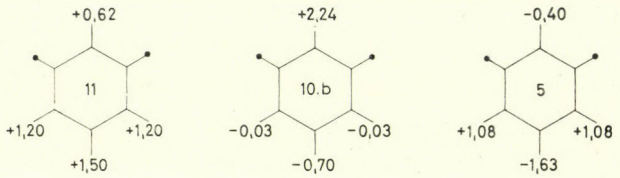

Fig. 12

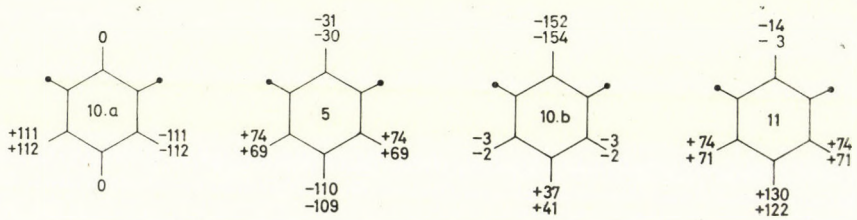

Fig. 13

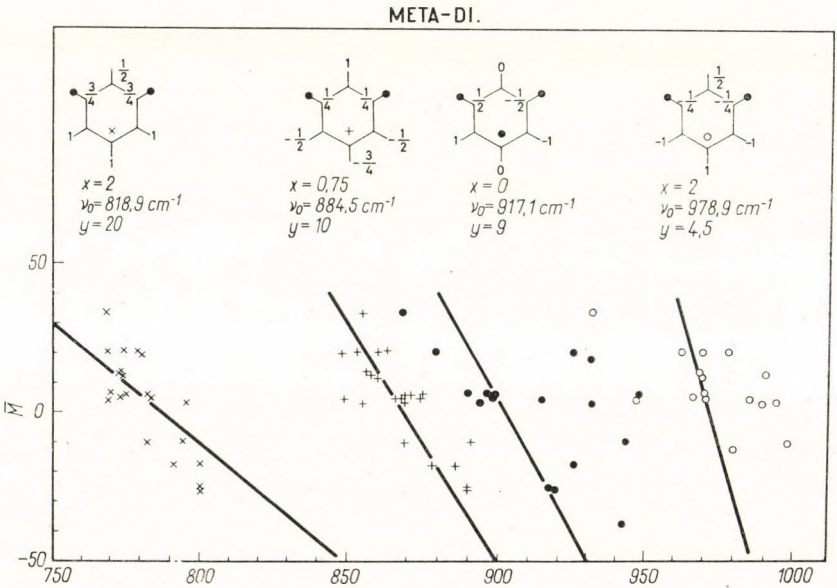

Fig. 14

tions are given with the amplitudes calculated by SHIMANOUCHI, KAKIUTI and GAMO [19]. It can be seen that in the opinion of the above authors, the vibration in which the amplitude of the hydrogen in position 1 is predominating corresponds to the form of vibration 10b. According to both THOMPSON *et al.* and SHIMANOUCHI *et al.*, the hydrogen in position 1 vibrates with a small but opposite amplitude as compared with the corresponding vibration in benzene. In Figs 11 and 12 the amplitudes are normalized with respect to the umbrella

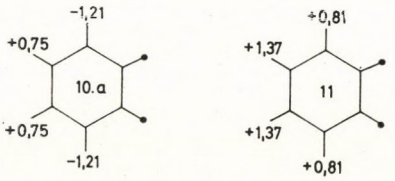

Fig. 15

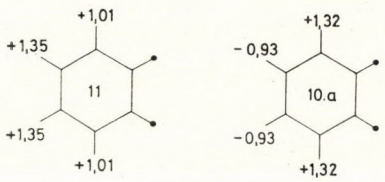

Fig. 16

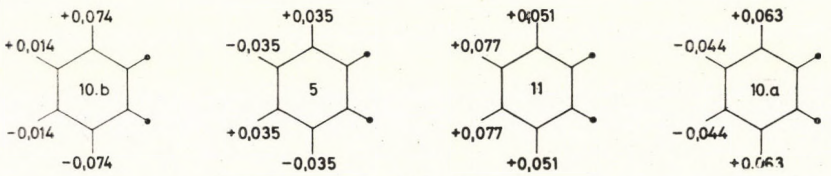

Fig. 17

vibration of benzene. In Fig. 13, the vibrational forms calculated by NONNENMACHER and MECKE [20] are shown for *meta*-difluoro- and dichlorobenzene. The amplitudes are given in 0.001 Å units. Fig. 14 gives the literature frequency data, schematic amplitudes, x and y parameters, and the straight lines according to Eq. (3) as well. In order to give a consistent representation, the correction $5m$ is calculated in each case for the axis intersection of the straight lines; but when the two substituents have different orientation effects, in order to compensate for this, their $\overline{M}$ values were also corrected by $5m$.

In *ortho* disubstitution the phase combinations of the four hydrogens are given: $++++$, $++--$, $+--+$ and $+---+$. In the vibrations 10a and 17a of benzene the amplitudes of the hydrogens in positions 1,4 are zero, but in the above types a finite amplitude value has been attributed to them.

KATRITZKY and JONES [21] gave the schematic vibrational form, denoting them by IX—XII, although not in the right sequence, since they put the form of vibration 5 into the third place according to a decreasing frequency order, in spite of the fact that this has the highest frequency of the four vibrations. BELL, THOMPSON and VÁGÓ [10] gave only the diagram for the two vibrations of b_1 symmetry, indicating also the relative magnitudes of the amplitudes (Fig. 15). Very similar relative amplitudes have been given by SHIMANOUCHI, KAKIUTI and GAMO [19] (Fig. 16). The corresponding calculated frequencies

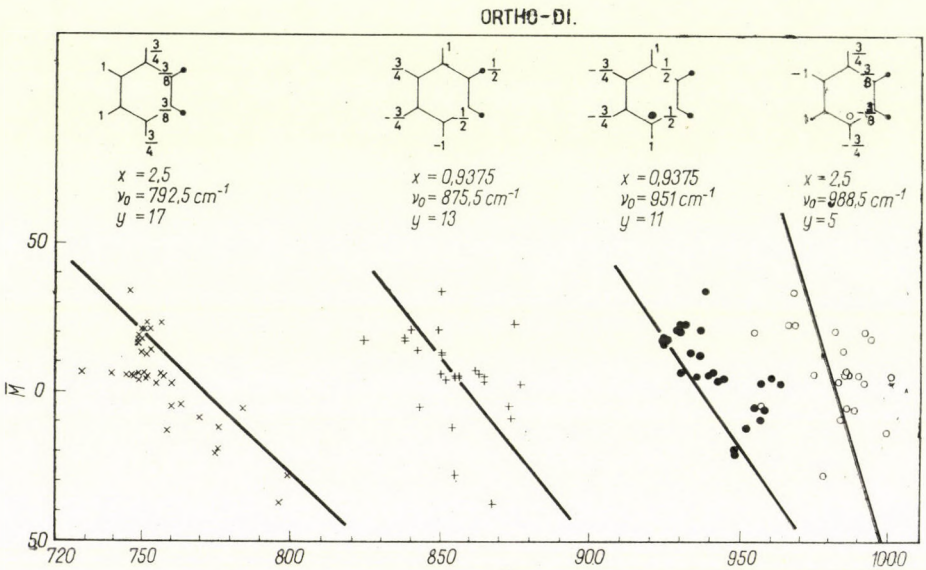

Fig. 18

are 950 and 740 cm^{-1}, in the sequence of the figures. BOGOMOLOV [22] gave the amplitudes of all four vibrations in Å units for *ortho*-xylene (Fig. 17). The schematic vibrational forms and literature frequency data, together with the straight lines according to Eq. (3) for *ortho*-disubstituted benzenes are shown in Fig. 18.

Trisubstitution

There are only a few frequency data available for the out-of-plane CH vibrations of trisubstituted benzene derivatives. The schematic vibrational forms, frequencies and straight lines for symmetric trisubstitution are shown in Fig. 19.

Fig. 20 shows some of the frequencies, the vibrational forms assigned, and the straight lines for some vicinally trisubstituted benzenes. The out-of-

plane CH vibrational forms, for symmetric trisubstitution, given by BELL, THOMPSON and VÁGÓ [10], are shown in Fig. 21. The first of these is the out-of-phase vibration of the adjacent hydrogens, and the third one is the in-phase mode of the same. The vibration shown in the middle corresponds to the out-of-

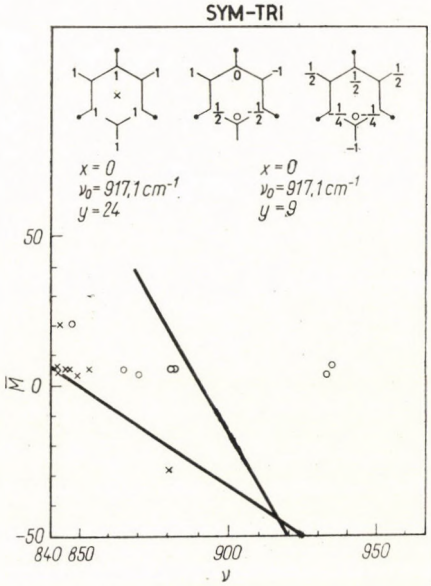

Fig. 19

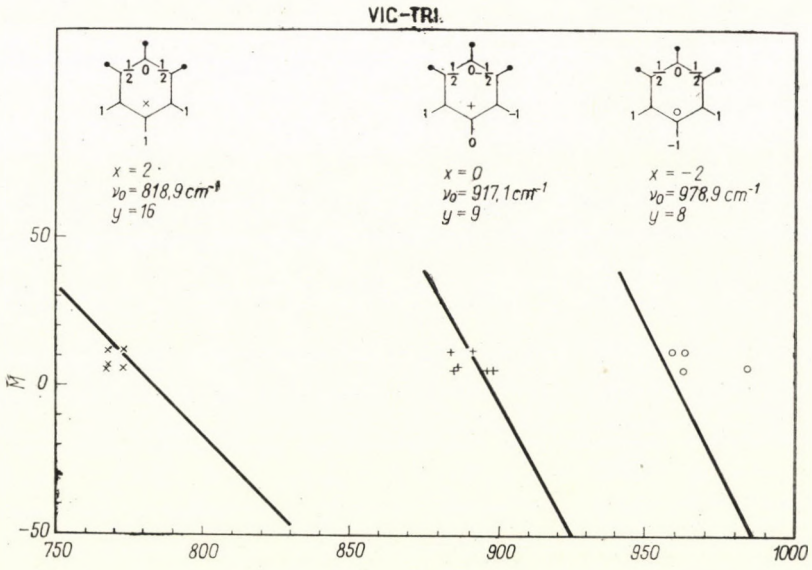

Fig. 20

plane vibration of the isolated hydrogen atom. The sequence of the figures is that of decreasing frequencies. The vibrational forms given by COLE and THOMPSON [11] are somewhat different, specifically the amplitudes of the two adjacent

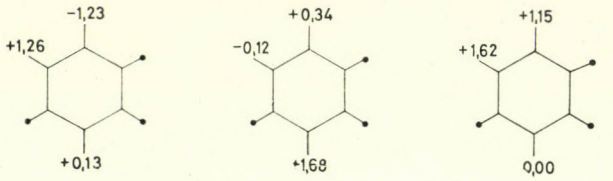

Fig. 21

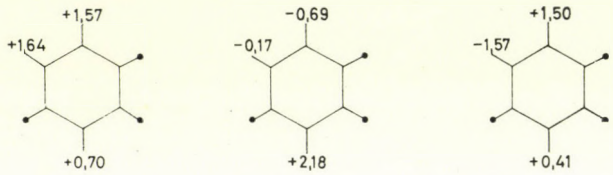

Fig. 22

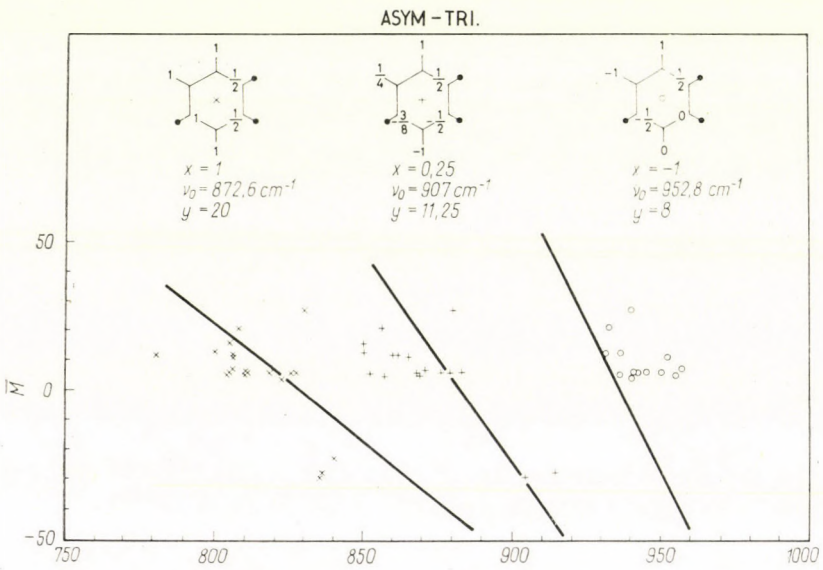

Fig. 23

hydrogens are in-phase in the out-of-plane vibration of the isolated hydrogen. The same authors hold the view that the hydrogen in position 4 vibrates with a small amplitude but in opposite phase in the vibration of lowest frequency. They calculated the frequency 830 cm^{-1} for the in-phase vibration of the two adjacent hydrogens. This is the same as the frequency of the umbrella vibration

of symmetry b_{3u} in *para*-disubstitution, in which mode all hydrogens move in-phase. For this reason it does not seem unjustified to assign this frequency to vibration 11 in asymmetric trisubstitution, assuming that also in this mode the isolated hydrogen in position 4 vibrates with an amplitude of the same

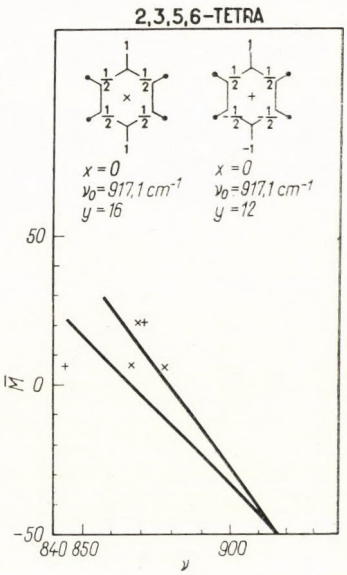

Fig. 24

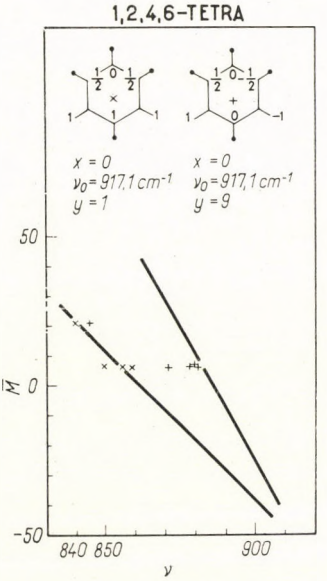

Fig. 25

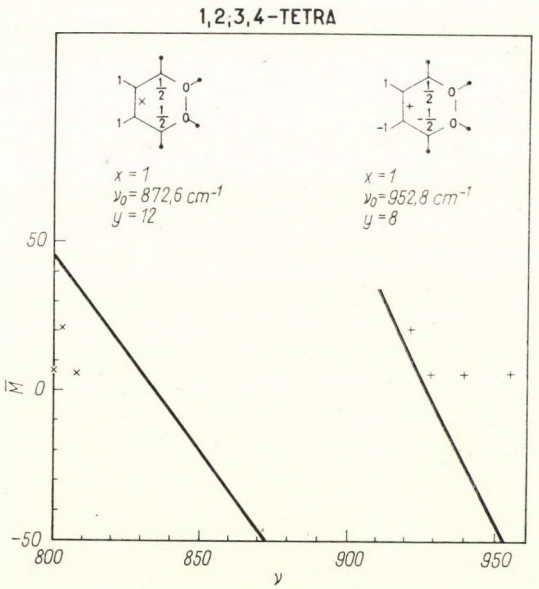

Fig. 26

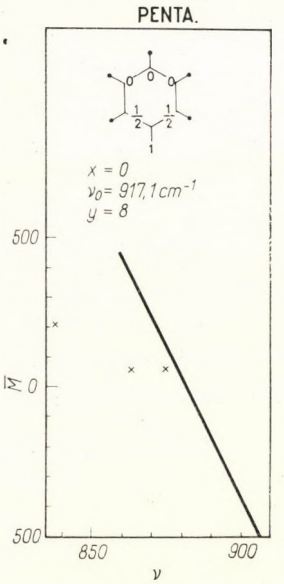

Fig. 27

direction. The out-of-plane CH amplitudes calculated by SHIMANOUCHI, KAKIUTI and GAMO [19] are in accordance with this assumption (Fig. 22). The schematic vibrational forms of asymmetrically trisubstituted benzene derivatives, the corresponding frequencies and straight line plots are shown in Fig. 23.

Tetra- and pentasubstitution

There are even less literature data available for these derivatives. The frequency graphs similar to the previous ones have the numbering 24—27.

In the Figures here there are also given some spectroscopic momenta that were not reported by PLATT [15]. These values have been estimated in this work on the basis of the intensity of the first band system in the ultraviolet spectra of the compounds concerned (except for nitrobenzene). The supplementary data are summarized in Table I.

Table I

Some additional data for the spectroscopic momenta given by PLATT [15]

Substituent	*M*	Substituent	*M*
OC_2H_5	+29	NSO	— 9
NH_2	+20	CH_2CN	—10
$N(CH_3)_2$	+20	CH_2I	—12
$N(C_2H_5)_2$	+20	Ac	—15
OAc	+13	CHO	—16
SH	+ 6	$CONH_2$	—27
SCH_3	+ 5	$COOCH_3$	—29
SC_2H_5	+ 4	$COOC_2H_5$	—29
NCS	+ 3	COF	—30
NCO	+ 1	COCl	—32
C≡CH	0	COBr	—33
CH_2NCS	0	NO_2	—45
CH_2OH	— 3		

SUMMARY

The frequency course of the out-of-plane CH vibrations of benzene derivatives is interpreted by the theory of orbital-following. With the help of a parameter defined in this work, the frequencies of the out-of-plane CH vibrations of benzene are exactly reproduced. Substituents increase the interaction of the states sp^2 and sp^3, and thereby, in general decrease the frequencies. The spectroscopic momentum defined by PLATT proved to be the best characterizing property for this effect. A general formula has been elaborated with the help of the parameter containing the spectroscopic momentum for all out-of-plane CH frequencies of all benzene derivatives.

REFERENCES

1. VARSÁNYI, G.: Acta Chim. Acad. Sci. Hung. **50,** 225 (1966).
2. VARSÁNYI, G.: ibid. **50,** 237 (1966).
3. YOUNG, C. W., DU VALL, R. B., WRIGHT, N.: Anal Chem. **23,** 709 (1951).
4. BELLAMY, L. J.: The Infrared Spectra of Complex Molecules. Methuen, London, 1958.
5. BRODERSEN, S., LANGSETH, A.: Mat. Fys. Skr. Kong. Dansk. Vid. Selsk. **1,** 1 (1956).
6. COLTHUP, N. B.: J. Opt. Soc. Amer. **40,** 397 (1950).
7. VAN BINST G., DAVIS, E. A., SMIT, D., MARTIN, R. H.: Conference held on the VIII th European Congress of Molecular Spectroscopy, Copenhagen, 1965.
8. KROSS, R. D., FASSEL, V. A., MARGOSHES, M.: J. Am. Chem. Soc. **78,** 1332 (1956).
9. MARGOSHES, M., FASSEL, V. A.: Spectrochim. Acta **7,** 14 (1955).
10. BELL, R. P., THOMPSON, H. W., VÁGÓ, É. E.: Proc. Roy. Soc. London G **192,** 498 (1948).
11. COLE, R. H., THOMPSON, H. W.: Trans. Far. Soc. **46,** 103 (1950).
12. BELLAMY, L. J.: J. Chem. Soc. **1955,** 4221.
13. GRIFFITHS, V. S., DERWISH, G. A. W.: J. Mol. Spec. **13,** 393 (1964).
14. BELLAMY, L. J.: J. Chem. Soc. **1955,** 2818.
15. PLATT, J. R.: J. Chem. Phys. **19,** 263 (1951).
16. WHIFFEN, D. H.: J. Chem. Soc. **1956,** 1350.
17. SCHMID, E. W., BRANDMÜLLER, J., NONNENMACHER, G.: Z. Elektrochem. **64,** 726 (1960).
18. BOGOLOV, A. M.: Opt. Spek. **9,** 311 (1960).
19. SHIMANOUCHI, T., KAKIUTI, Y., GAMO, I.: J. Chem. Phys. **25,** 1245 (1956).
20. NONNENMACHER, G., MECKE, R.: Spectrochim. Acta **17,** 1049 (1961).
21. KATRITZKY, A. R., JONES, R. A.: J. Chem. Soc. **1959,** 3670.
22. BOGOMOLOV, A. M.: Opt. Spek. **10,** 322 (1961).

György VARSÁNYI; Budapest XI., Műegyetem rkp. 3/9.

Acta Chimica Academiae Scientiarum Hungaricae Tomus 57 (1), pp. 69—82 (1968)

SUR QUELQUES PROBLÈMES POSÉS PAR L'ÉTUDE, A TEMPÉRATURE ÉLEVÉE, DES ÉQUILIBRES LIQUIDE-SOLIDE DANS LES SYSTÈMES CONTENANT UN CONSTITUANT VOLATIL

R. COHEN-ADAD, A. TRANQUARD et A. MARCHAND

Laboratoire de Chimie 1er Cycle II — Faculté des Sciences — Lyon (69)

Reçu le 15 septembre 1967

L'étude des équilibres liquide-solide d'un système contenant un constituant volatil présente des difficultés de plus en plus grandes, à mesure que la température s'élève au-dessus du point d'ébullition de la solution saturée, sous la pression atmosphérique.

Ceci est dû essentiellement aux pressions élevées qui se développent dans l'enceinte contenant le système et qui entraînent un certain nombre d'inconvénients:

— impossibilité, le plus souvent, d'agiter de façon efficace les mélanges;
— détitrement;
— risques de condensations sur les parties froides de l'appareil . . .

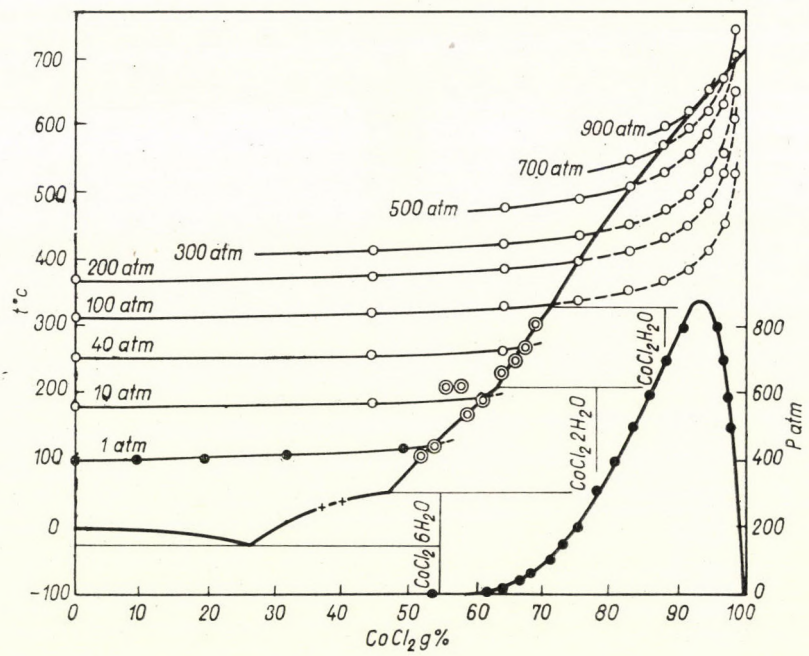

Fig. 1

Dans ce travail, l'influence des facteurs les plus gênants a été étudiée dans le but de préciser les caractéristiques de l'appareillage à utiliser. Différents modèles de bombes d'analyse thermique, de solubilité ou de mesure de tensions de vapeur adaptés à l'étude de ces systèmes ont pû être construits.

Tous les calculs ont été effectués dans le cas particulier du système binaire eau-$CoCl_2$, représenté dans la figure 1, qui a fait l'objet d'une étude sous pression jusqu'à la température de 350° C [1].

Trois hydrates se manifestent: $CoCl_2$, 6 H_2O; $CoCl_2$, 2 H_2O et $CoCl_2$, H_2O. L'hexahydrate donne, avec la glace, une eutexie à −27,3°C pour une composition de 26 g de sel pour 100 g de mélange.

Une péritexie se manifeste à +51,25° C correspondant à l'équilibre:

$$CoCl_2,\ 6\ H_2O \rightleftharpoons CoCl_2,\ 2\ H_2O + \text{liq.}$$

Aux hydrates $CoCl_2$, 2 H_2O et $CoCl_2$, H_2O correspondent des fusions non congruentes à 206,1° C et 335° C.

Le sel anhydre fond à 720° C.

La solution saturée bout à 120,2° C sous 760 mm de mercure, pour une teneur de 53,7% de $CoCl_2$.

Calcul de la pression

Une grande partie du diagramme précédent n'est accessible que par une étude sous pression. Avant d'aborder l'étude d'un tel système, il était donc nécessaire de calculer, même de façon approximative, l'ordre de grandeur des pressions dans les tubes de mesure, de façon à construire un appareillage possédant une résistance mécanique suffisante.

Deux difficultés se manifestent alors:

. d'une part, on ne connaît rien des propriétés thermodynamiques des mélanges étudiés,

. d'autre part, un domaine important du système se situe au-dessus du point critique de l'eau.

Il est cependant possible de faire un calcul grâce aux hypothèses simplificatrices suivantes:

1°) — On admet que la solution est idéale et que la pression de vapeur du sel est négligeable. Si X est la fraction molaire du sel et P_0 la pression de vapeur saturante de l'eau, la pression de vapeur de la solution est:

$$P = P_0(1 - x)$$

2°) — La courbe de tensions de vapeur d'eau est extrapolée au-dessus de la température critique.

3°) — La vapeur d'eau se comporte comme un gaz parfait.

4°) — Les résultats sont présentés dans la figure 1. Sur le même diagramme sont tracées les isobares donnant les températures des solutions saturées en fonction de la concentration, les courbes des équilibres liquide — solide du système $CoCl_2$, H_2O et la courbe exprimant la pression de vapeur de la solution saturée en fonction de la composition du mélange.

Ces calculs, bien que très approximatifs, conduisent à un ordre de grandeur valable. On peut s'en rendre compte en comparant les résultats qu'ils fournissent avec les données expérimentales lorsque celles-ci existent. Par exemple, pour le système NaCl, H_2O les mesures de KEEVIL [2] conduisent à une pression de 388,7 bars pour une température de 600° C.

Pour le système $CoCl_2$—H_2O, la pression maximale atteinte dans le tube de mesure est de l'ordre de 900 bars, si on ne dépasse pas trop les températures de fin de fusion.

Détitrement des mélanges

Lorsqu'on chauffe un échantillon de composition déterminée dans une enceinte hermétiquement close, une masse d'eau de plus en plus importante se vaporise, à mesure que la température augmente et il en résulte un accroîssement de la concentration en sel.

La concentration a (g pour cent de mélange) de la solution en équilibre avec la vapeur, à une température T, s'exprime par la formule:

$$(m - M)RT\,p_0 - mVP_0\,a^2 + 100\,m(MVP_0 - RT_{p0}) - \\ - (m - M)RTp_0a_0 + 100\,mRTp_0a_0 = 0$$

où p_0 est la masse de l'échantillon de départ et a_0 sa concentration (g de sel pour cent), M est la masse molaire du solvant, m celle du soluté, V est le volume mort offert à la vapeur, P_0 est la pression de vapeur saturante du constituant volatil et R la constante des gaz parfaits.

La figure 2 présente les résultats du calcul dans le cas du système binaire eau—$CoCl_2$ pour un mélange de masse $p_0 = 10$ g et une composition de départ $a_0 = 44{,}5$ pour cent de sel.

Les courbes de détitrement ont été tracées pour différentes valeurs du volume mort. Lorsque V est suffisamment grand, elles rencontrent le liquidus du binaire eau-$CoCl_2$.

Au cours de l'analyse thermique à l'échauffement, on observe donc, dans ce cas, un accident exothermique correspondant à l'apparition d'une phase solide, puis, à température plus élevée, un accident endothermique traduisant sa disparition.

Dans la figure 3 sont tracées les courbes d'analyse thermique directe à l'échauffement que l'on pourrait observer, pour un échantillon à 44,5% de $CoCl_2$, pour les valeurs de 0, de 50 et de 1000 ml du volume mort.

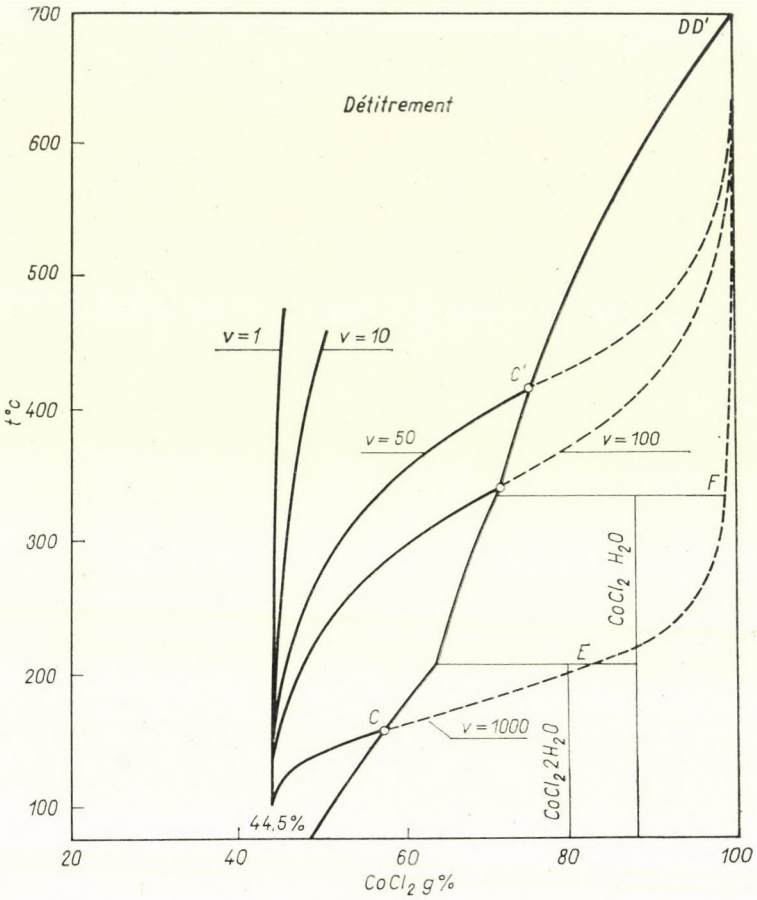

Fig. 2

Le palier A,A,A'' correspond à la péritexie:

$$CoCl_2,\ 6\ H_2O \rightleftharpoons CoCl_2,\ 2\ H_2O$$

à 51,25° C;

l'accident B, B', B'' traduit la disparition des derniers cristaux de $CoCl_2,\ 2\ H_2O$.

Si le volume mort est nul, la courbe d'analyse thermique ne présente aucun autre accident.

Pour $V = 50$ ml, au point C', on note l'apparition de cristaux de $CoCl_2$ anhydre et en D', nouvelle fusion.

Pour $V = 1000$ ml, la courbe est plus compliquée: en C, apparition de cristaux de $CoCl_2,\ 2\ H_2O$, en E (206,1° C), péritexie:

$$CoCl_2,\ 2\ H_2O \rightleftharpoons CoCl_2,\ H_2O + \text{liq.}$$

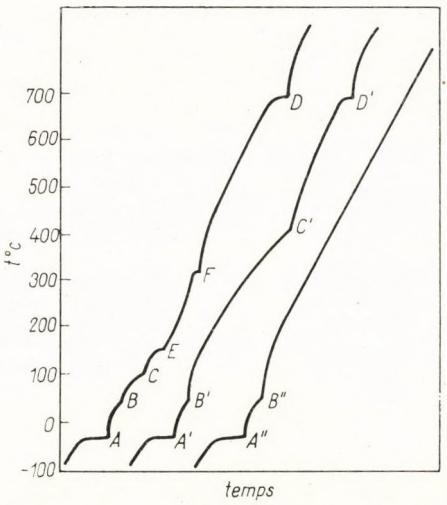

Fig. 3

En *F* (335° C), péritexie du monohydrate et en *D*, disparition des derniers cristaux de $CoCl_2$ anhydre.

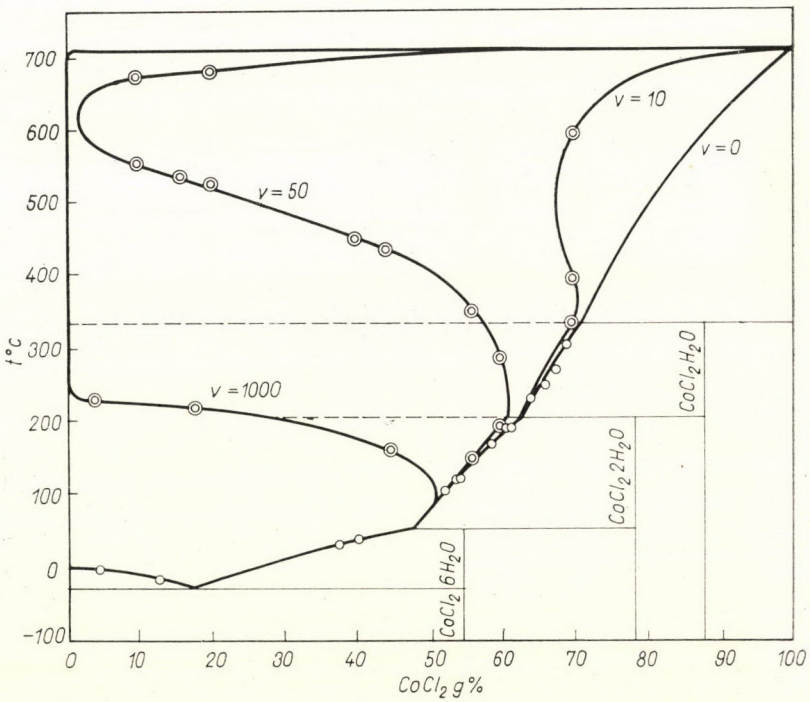

Fig. 4

Diagramme apparent des équilibres liquide-solide

Si on représente la température des accidents thermiques en fonction de la composition du mélange initial, on obtient un diagramme (figure 4) ou le liquidus est déformé et d'autant plus que le volume mort offert à la vapeur est plus grand.

Par exemple, pour $V = 1000$ ml, la solubilité apparente du sel devient de plus en plus faible à mesure que la température augmente, s'annule pratiquement au-dessus de 200° C, puis rejoint, suivant une horizontale, la température du fusion du sel.

Pour $V = 50$ ml, la déformation du liquidus ne devient sensible qu'au-dessus de 200° C.

Dans tous les cas, on observe les paliers correspondant aux péritexies bien au-delà de leur domaine normal d'existence.

Dispositifs experimentaux

L'appareillage nécessaire pour étudier de tels systèmes doit posséder des caractéristiques que nous avons essayé de réunir:

Analyse thermique

Pour l'étude de systèmes contenant de l'eau, nous avons utilisé des tubes scellés en verre lorsque la température ne dépasse pas 200°C. Le volume mort y est du même ordre de grandeur que celui de l'échantillon et le détitrement reste assez faible pour être négligé.

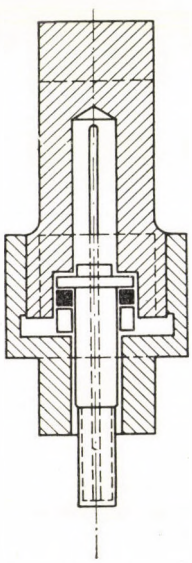

Fig. 5

Entre 200 et 500°C, de bons résultats sont obtenus avec des bombes en acier inoxydable du modèle représenté par la figure 5 et déjà décrites dans des publications antérieures [3], [4].

La bombe se compose de deux parties essentielles:

— un corps massif, capable de résister à une pression de 500 bars et comportant un filetage extérieur;

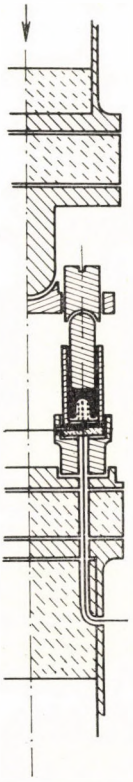

Fig. 6

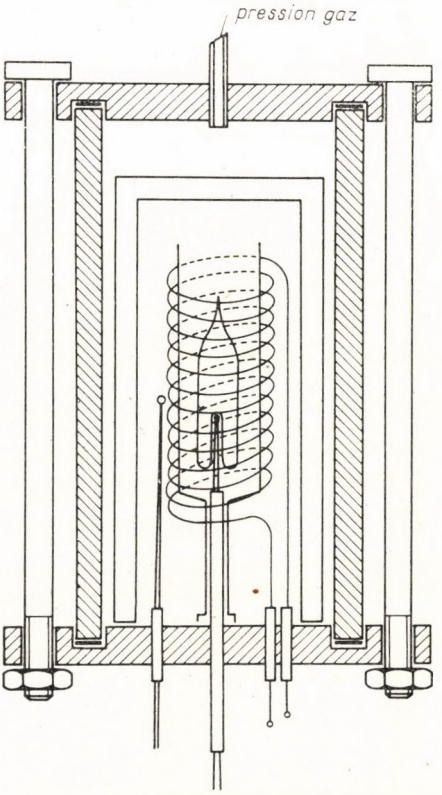

Fig. 7

— un dispositif de fermeture constitué d'un bouchon fileté qui vient se visser sur le corps de la bombe et d'une pièce centrale. Un anneau d'acier jouant le rôle de multiplicateur de pression et un joint de cuivre complètent l'ensemble. Ce mode de fermeture, réalisé suivant les indications de BRIDGMAN [5] a donné toute satisfaction. Un doigt de gant adapté à la pièce centrale permet d'introduire un thermocouple au sein du mélange étudié et d'en suivre la température.

Dans ces bombes, le volume mort est assez réduit. On ne peut pas le supprimer complètement et ce n'est, d'ailleurs, pas souhaitable car la dilatation du mélange à l'échauffement provoquerait alors, dans l'appareil, des pressions dangereuses et incontrôlables.

Vers 500°C, des problèmes purement technologiques apparaîssent tels que fluage des métaux, scellement de surfaces fortement pressées l'une sur l'autre, fusion des brasures . . . Deux types d'appareils susceptibles de résoudre ces difficultés ont été étudiés:

Le premier est à chauffage par l'extérieur. Il est représenté sur la figure 6. Il comprend un tube laboratoire, en forme de cylindre, capable de résister à une pression de 3000 bars et un piston mobile dans ce cylindre. Le mélange à étudier, disposé dans une petite cupule en plomb est placé dans le tube et comprimé par enfoncement du piston, grâce à un vérin pneumatique. A la compression, la cupule de plomb est écrasée et sert de joint d'étanchéité.

Le tube laboratoire ainsi que les deux tubes témoins nécessités par les mesures d'analyse thermique différentielle sont comprimés par le même vérin grâce à un répartiteur de pression à rotules. La température est suivie au moyen de thermocouples placés sous les tubes.

Cet appareil, construit en acier inoxydable 18/8 Mo, permet d'effectuer des mesures d'A.T.D., sans volume mort, pour des pressions pouvant atteindre 2500 bars. Le plomb convient parfaitement pour les cupules recevant les échantillons mais limite la température d'utilisation à 327°C. D'autres matériaux, à plus haut point de fusion, sont actuellement à l'étude. Cependant, en raison des risques de fluage, un tel appareil ne peut guère travailler au-delà de 600° C.

Le second type d'appareil (figure 7) est à chauffage par l'intérieur. Il est constitué d'une enceinte métallique massive, refroidie extérieurement et capable de résister à la pression désirée. A l'intérieur, on place un tube scellé au centre d'un petit four électrique tubulaire. Des passages sont ménagés dans l'enceinte pour le doigt de gant du couple thermoélectrique et l'alimentation du four.

La tension de vapeur du mélange étudié qui tend à faire exploser le tube est contrebalancée par une pression extérieure de gaz comprimé dans l'enceinte. Enfin, l'utilisation de tubes scellés en métal mou et à parois très minces permet de supprimer la phase vapeur.

Solubilités

Jusqu'à 350° C, les mesures sont faites dans la bombe à renversement mise au point par ROLLET et BOUAZIZ [6], représentée dans la figure 8.

Elle est constituée essentiellement de deux parties:

— une enveloppe métallique *A*, *B*, *C* étanche prolongée vers le haut et vers le bas par deux tourillons;

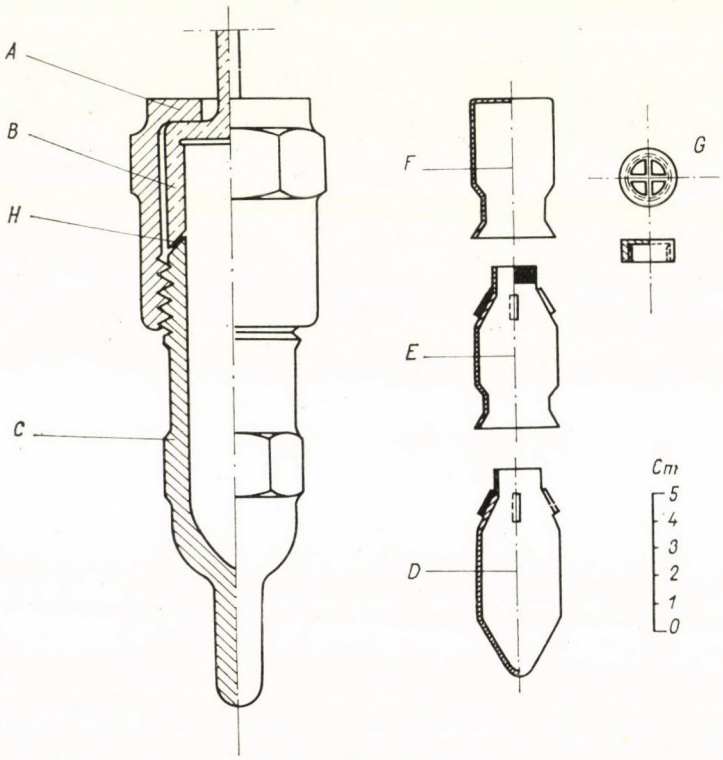

Fig. 8

— l'intérieur fait de trois éléments, s'emboîtant les uns dans les autres. Le premier *D* est un récipient dans lequel est obtenu l'équilibre, le second *E* est destiné à filtrer le mélange et le troisième *F* sert à récupérer la solution saturée. L'agitation est produite en faisant tourner la bombe sur son axe par une série d'impulsions. On sépare le solide de la solution saturée en retournant la bombe.

Un autre dispositif utilisé est un appareil à prélèvement direct [7] représenté dans la figure 9. Il comprend une enveloppe métallique dans laquelle l'équilibre liquide — solide est réalisé et un dispositif à prélèvement constitué par une pipette également métallique vissée sur

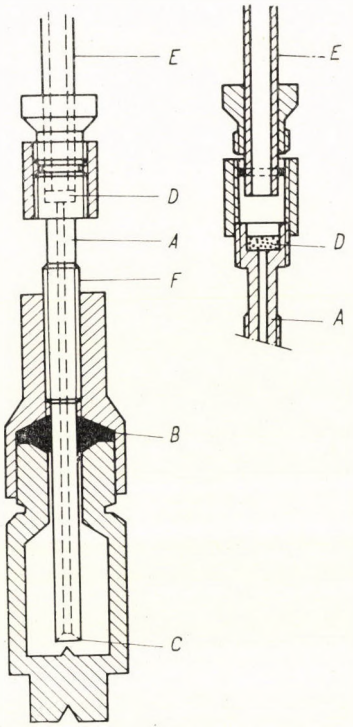

Fig. 9

le corps de la bombe. L'étanchéité est obtenue par un joint de téflon, ce qui limite la température d'emploi de cet appareil. La pipette comporte un filtre en métal fritté et elle est obturée, à son extrémité inférieure, par une mince feuille d'argent brasée sur le tube. L'équilibre atteint, on fait descendre la pipette, ce qui provoque le déchirement de la membrane d'argent sur une pointe d'acier disposée au fond de l'enveloppe. La suppression projette alors le mélange dans la pipette.

Mesure de la pression de vapeur

Deux appareils sont actuellement en cours d'essais:

Le premier est représenté dans la figure 10 et dérive du modèle décrit par BESSOUAT [8]. Il est constitué de deux enceintes étanches séparées par un soufflet métallique. L'échantillon est placé dans le compartiment extérieur. On fait le vide dans l'appareil. A une température donnée, la pression de vapeur de l'échantillon peut être équilibrée par de l'azote: le déplacement du soufflet,

dû à cette pression, permet, par l'intermédiaire d'une tige métallique, l'ouverture ou la fermeture d'un contact électrique ce qui commande l'introduction d'azote dans l'enceinte intérieure.

La lecture de la pression à l'équilibre se fait sur un manomètre placé sur la canalisation d'azote.

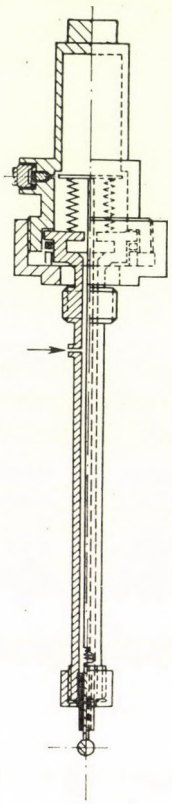

Fig. 10

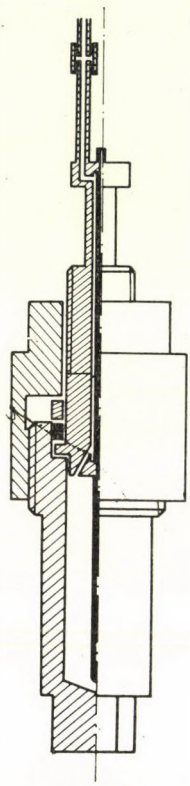

Fig. 11

Un autre appareil (figure 11) est constitué d'une bombe, reliée par un long tube capillaire à un volant de quelques litres permettant de maintenir une pression fixée à l'avance pendant toute la durée d'une manipulation. Un thermocouple, placé au niveau de l'échantillon, permet d'en suivre la température.

Lorsque le mélange en cours d'étude est chauffé progressivement, sa tension de vapeur augmente jusqu'à atteindre la pression extérieure imposée. Une ébullition se produit alors et on observe un accident thermique sur la courbe température — temps. On laisse l'ébullition se poursuivre, il y a départ de solvant vers un piège et la température monte régulièrement jusqu'à

atteindre un palier correspondant à l'ébullition de la solution saturée. La figure 12 donne un exemple de courbe pour un mélange $CoCl_2 - H_2O$:

A: dissolution du dernier cristal de dihydrate;
B: ébullition de la solution diluée;
C: ébullition de la solution saturée;
D: péritexie $CoCl_2$, 2 $H_2O \rightleftharpoons CoCl_2$, H_2O + liq.
E: décomposition du monohydrate $CoCl_2$, $H_2O \rightleftharpoons CoCl_2$ + vap.

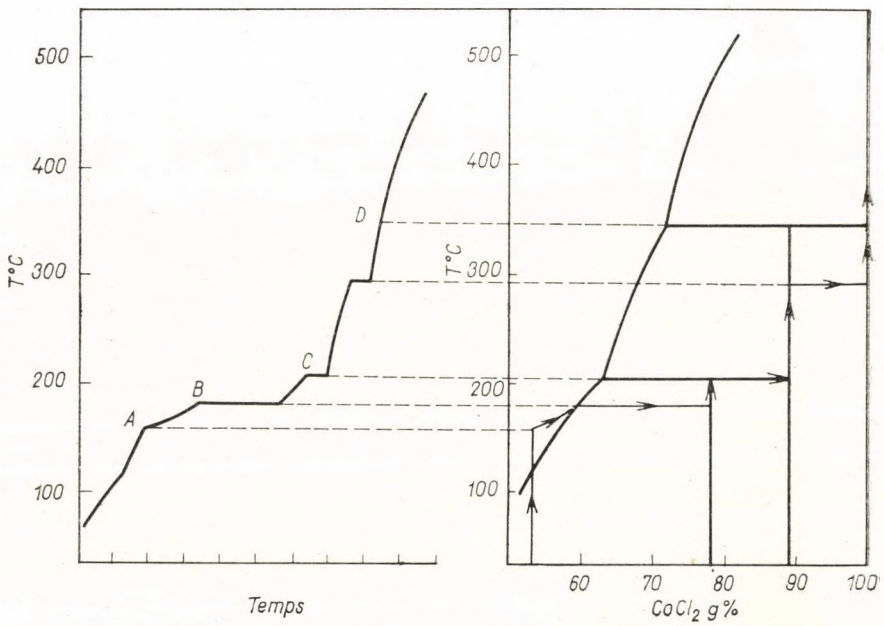

Fig. 12

Si on effectue une série de mesures à pression constante pour des mélanges de composition variable, le diagramme température d'ébullition — composition présente une brisure lorsque la solution devient saturée, ce qui permet de déterminer un point de la courbe de liquidus du système.

Résultats

Dans ce paragraphe sont condensés quelques résultats obtenus sous pression à l'aide des dispositifs décrits précédemment.

Système eau-chlorure de cobalt (figure 1)

Le diagramme est établi en totalité jusqu'à 350°C, seule reste à déterminer la branche d'anhydre.

Système eau-carbonate thalleux (figure 13)

La plus grande partie du diagramme n'est pas accessible sous la pression atmosphérique. Une étude d'analyse thermique sans phase vapeur, à 800 bars, de la zone concentrée a permis de préciser convenablement le diagramme [9].

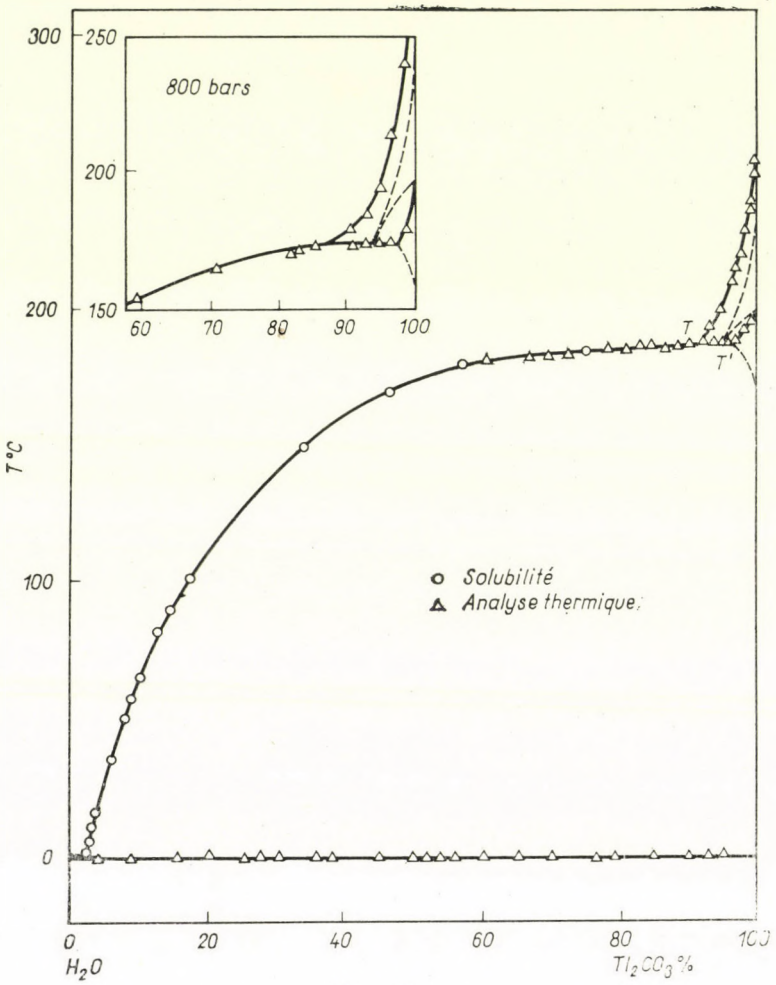

Fig. 13

Fusion du fluorure d'ammonium

Comme l'ont montré Erdey, Gál et Liptay [10], NH_4F sublime sans fondre quand on le chauffe sous la pression atmosphérique et le phénomène s'accompagne d'une dissociation $NH_4F \rightleftharpoons NH_3 + HF$.

L'acide fluorhydrique se recombine partiellement à NH_4F, pour donner NH_4F, HF.

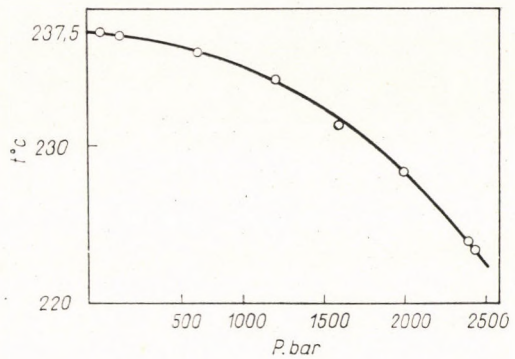
237,5
t°c 230
220
500
1000
1500
2000
2500
P. bar

Fig. 14

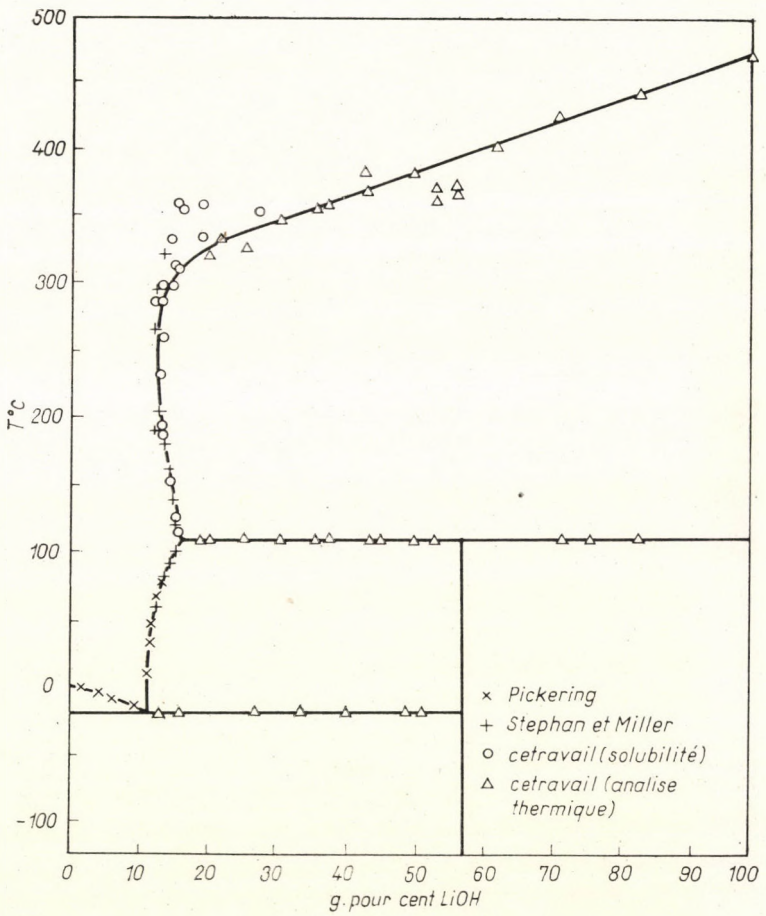
500
400
300
T°C 200
100
0
-100
0
10
20
30
40
50
60
70
80
90
100
g. pour cent LiOH
× Pickering
+ Stephan et Miller
o cetravail (solubilité)
Δ cetravail (analise thermique)

Fig. 15

Une étude, sans phase vapeur, sous une pression suffisamment élevée, permet une détermination correcte de la température de fusion: la figure 14 présente les résultats obtenus. Une extrapolation jusqu'à la pression atmosphérique conduit à une température de fusion de 237,5°C.

Système eau-lithine (figure 15) [11]

L'étude a pû être conduite en totalité par des mesures d'analyse thermique dans une bombe et par des mesures de solubilité sous pression. Seul un monohydrate se manifeste.

RÉSUMÉ

L'étude des équilibres liquide-solide des systèmes contenant un constituant volatil présente des difficultés nombreuses dûes à l'augmentation de pression dans les tubes laboratoire.

Dans ce travail, l'influence des facteurs les plus importants est examinée dans le but de définir l'appareillage le mieux adapté aux problèmes considérés.

Différents modèles d'appareils d'analyse thermique ou de solubilité sous pression sont décrits et leurs conditions d'emploi précisées.

Les résultats expérimentaux obtenus dans quelques cas particuliers sont développés à titre d'exemples.

BIBLIOGRAPHIE

1. COHEN-ADAD, R., SAID, J., SAUGIER, M. TH. et SEBAOUN, A.: en cours de publication aux C. R. Acad. Sc. Paris.
2. KEEVIL J. Am. Chem. Soc. **64,** p. 841—850 1942.
3. TRANQUARD, A.: Thèse Lyon 1965.
4. TRANQUARD, A.: Rev. Chim. Min. **2,** p. 435 1965.
5. BRIDGMAN, The Physics of High Pressure, Bell and Sons London 1958.
6. BOUAZIZ, Thèse Paris 1961.
7. FERLIN, Thèse Lyon 1965.
8. BESSOUAT, R., CHAVANEL, H., ELBERG, S.: Phys. Appl. Suppl. n° 3 **24,** 1963 p. 39A.
9. CARBONNEL, L., TRANQUARD, A. et BOINON, M. J.: C. R. Acad. Sc. Paris **264** p. 1180—1967.
10. ERDEY, L., GÁL, S. et LIPTAY, G.: Talanta II p. 913 1964.
11. ROLLET, A. P. et COHEN-ADAD, R.: Rev. Chim. Min. **1** p. 451 1964.

Roger COHEN-ADAD
Aymond TRANQUARD
Alain MARCHAND

Laboratoire de Chimie 1er Cycle II
Faculté des Sciences
Lyon (69), France

Acta Chimica Academiae Scientiarum Hungaricae Tomus 57 (1), pp. 83—89 (1968)

К КИНЕТИКЕ ДЕГИДРИРОВАНИЯ C_6H_{12} НАД НИКЕЛЕВЫМИ КАТАЛИЗАТОРАМИ

Ю. С. МАРДАШЕВ

(Московский государственный ордена трудового красного знамени, педагогический институт им. В. И. Ленина)

Поступило 15. IX. 1967 г.

Кинетические уравнения, описывающие протекание гетерогенной каталитической реакции в проточной системе, даны в работах [1—3]. Эти уравнения основаны на следующих допущениях:

а) скорость установления адсорбционного равновесия больше скорости реакции*;

б) поверхность катализатора однородна или квазиоднородна [1]. Некоторое различие в подходе к методу вычисления кинетических параметров из опытных данных между работами [1] и [2, 3] заключается в том, что в последних работах не вводится постулат о квазиоднородности поверхности и предполагается, что решение уравнения справедливо во всем интервале степеней превращения y от 0 до 1. Отсюда различны и способы решения кинетического уравнения в работах [1] и [2, 3]. В методике [1] предполагается, что при небольших степенях превращения в интервале $0 < y \leq 0{,}1$ или $y < 0{,}3$ можно произвести упрощение формул, что позволяет экспериментально довольно просто определять кинетические параметры, например, по способу бинарных смесей. Второй способ основан на графическом решении кинетического уравнения путем изучения влияния изменения скорости потока на скорость реакции [2, 3].

Постулат а) рассматривается в работах [1, 4]. Рассмотрим подробнее постулат б). Совершенно очевидно, что поверхности реальных адсорбентов неоднородны. Однако, как следует из работы [5], поверхности металлов при хемосорбции часто ведут себя как лэнгмюровские. В случае квазиоднородной поверхности предполагается, что для всех участков активной поверхности:

$$Z_r = Z_0 \exp\left[\frac{\lambda_r - \lambda_1}{RT}\right], \qquad (1)$$

Z_r — относительный адсорбционный коэффициент продукта r; λ_r, λ_1 — теплоты адсорбции соответственно продукта и реагирующего вещества, R —

* Диффузионные факторы исключаются.

газовая постоянная, T — температура °K, Z_0 — энтропийный член. Если теплоты адсорбции линейно изменяются с заполнением поверхности (случай логарифмической изотермы), то для соблюдения условия (1) интервал неоднородности для реагирующего вещества и для вещества r должен быть одинаков.

При решении кинетического уравнения по методу [1] предполагается, что при небольших степенях превращения торможение образующимися продуктами реакции не должно искажать кинетики реакции.

Почему необходимо проводить исследование в узком интервале степеней превращения? Мы полагаем, что это необходимо по двум причинам: при исследовании скорости реакции в широком интервале степеней превращения мы неизбежно будем изучать реакцию на разном удалении от положения равновесия. Тогда, согласно принципу линейности в термодинамике необратимых процессов [6], скорость реакции (скорость приближения системы к равновесию) должна меняться, по мере приближения системы к положению равновесия. Это связано с тем, что разность химических потенциалов на разном расстоянии от равновесия различна. Далее скорость реакции на поверхности заполненной лишь в небольшой степени продуктом реакции, и на поверхности заполненной в значительной степени, должна быть различной. Это связано не только с эффектом уменьшения доли активной поверхности, но и с эффектом значительного изменения физической природы поверхности. Отсюда способ решения кинетического уравнения, предложенный в работах [2, 3], может приводить к константам, которые лишены того физического смысла, который в них вкладывался при выводе уравнения. Действительно, экспериментальное решение кинетического уравнения по способу, предложенному в [2], часто дает константу $\beta = 1$, что лишено физического смысла. Подробный анализ обоих способов и некоторые кинетические особенности даны в [12].

Как показали исследования [1], кинетика дегидрогенизации над металлическими катализаторами не зависит от давления и для случая циклогексана подчиняется уравнению:

$$(Z_2 + 3Z_3)\, A_1 \ln \frac{A_1}{A_1 - m} - (Z_2 + 3Z_3 - 1)\, m = K, \qquad (2)$$

где Z_2 — относительный адсорбционный коэффициент C_6H_6,
Z_3 — относительный адсорбционный коэффициент H_2,
A_1 — скорость подачи циклогексана, m — количество прореагировавших молей,
K — константа скорости. С помощью уравнения Аррениуса по температурной зависимости $\ln K$ и $\ln m$ нами вычислялись истинные и кажу-

щиеся энергии активации E и Q. Преобразуя уравнение (2) к виду, удобному для решения по способу, предложенному в [2] получаем:

$$A_1 \ln \frac{1}{1-y} - \beta y A_1 = \alpha \quad , \tag{3}$$

где

а) $$\beta = \frac{Z_2 + 3Z_3 - 1}{Z_2 + 3Z_3} , \tag{4}$$

б) $$\alpha = \frac{K}{Z_2 + 3Z_3} .$$

По температурной зависимости $\ln \alpha$ нами вычислялись энергии активации q.

Экспериментальная часть

Кинетика дегидрогенизации C_6H_{12} изучалась нами над Ni на различных носителях при температурах 270—320°. Все катализаторы содержали 23,5% Ni. Методика работы описана ранее [7].

Из литературы известно, что в нашем случае реакция тормозится C_6H_6 [8] и не тормозится H_2 [9].

В таблице 1 приведены величины Q и E. Нетрудно видеть, что величины Q и E для большинства катализаторов близки. Исключение представляет Ni/силикагель. Как было показано [10], это связано с зависимостью Z_2 от степени превращения. В этом случае Z_2 вычислялась по реакции со смесями, бедными бензолом, что соответствовало интервалу степеней превращения $y \leq 0{,}1$.

В статических условиях справедлива формула:

$$v = \frac{d[C_6H_6]}{dt} = \frac{\text{const.}}{[C_6H_6]^n} \tag{5}$$

Можно показать, что в случае формального применения этого уравнения к нашему случаю получается формула, связывающая степень торможения n с величинами E и Q:

$$\frac{E}{Q} = n + 1 . \tag{6}$$

При выводе (6) и (5) мы предполагали, что $v \sim \exp\left[-\frac{Q}{RT}\right]$ и $[C_6H_6] \sim$ $\sim m \sim \exp\,[-Q/RT]$; $\text{const.} \sim \exp\,[-E/RT]$.

Таблица I*

Номер образца	Катализатор	Q ккал/моль	E ккал/моль	n	Z_2
1	Ni/Al_2O_3	9,8	12,8	0,4	3,9
2	Ni/силикагель	4,8	14,0	1,8	7,3
3	Ni/Al_2O_3	10,0	13,0	0,3	2,0
4	Ni/кизельгур	11,0	13,7	0,2	2,1
5	Ni/Al_2O_3	10,8	13,0	0,2	2,1
6	Ni/-чернь	7,0	13,0	0,9	—

* Специальными опытами было установлено, что диффузионные факторы не имели место.

Вычисленные таким образом степени торможения приведены в таблице 1. Нетрудно видеть, что при значительном торможении (Ni/силикагель) величина кажущейся энергии активации значительно отличается от истинной. В этом случае при решении кинетического уравнения по способу [1] необходимо проводить исследования при степенях превращения $y \leq 0{,}1$; тогда торможение не искажает кинетики, что позволяет определить Z_2.

Нетрудно видеть, что большим величинам Z_2 соответствует большая степень торможения, что соответствует физическому содержанию этих констант.

В таблице II приведены результаты решения кинетического уравнения по способу [2], для двух, наиболее отличающихся друг от друга, катализаторов. Нетрудно видеть, что энергии активации q в данном случае оказались практически одинаковыми и $q > E$. Последний результат связан с тем обстоятельством, что графическая экстраполяция, применяемая в способах [2, 3], не может быть осуществлена дальше равновесных значений y. В следующей графе приведены величины с учетом равновесия, которые близки к Q, определяемым по способу Баландина. Поскольку $Z_{2,3} \neq f(T)$ [7], постольку независимо от физического смысла коэффициентов уравнения (3), q должно быть равно E. Однако, для этого необходимо точно знать константу равновесия в нашем температурном интервале 270—230°. Мы использовали данные работы[11], которые относятся к интервалу 230—277°. Существенным в данном случае является понижение величины q при учете равновесия.

Таблица II

Номер образца	q ккал/моль	q_p ккал/моль	β	α	α_p
2	17,0	11,0	1,0	$0{,}8 \cdot 10^{-5}$	$1{,}1 \cdot 10^{-5}$
4	18,0	11,0	0,95	$17{,}5 \cdot 10^{-5}$	$47{,}5 \cdot 10^{-5}$

Далее из таблицы II следует, что коэффициент β из уравнения (3) близок к 1. Укажем на обстоятельство, которое в нашем случае может приводить к $\beta \approx$ I. Способ (2,3) предполагает значения $y \geqslant 0{,}5$. Для катализатора Ni/силикагель, обнаружено $Z_2 = f(y)$ при $y > 0{,}10$, причем с увеличением y Z_2 быстро растет. В этом случае при $y \sim 0{,}5$ имеем $Z_2 \sim 20$—30 [10]. Отсюда из уравнения 4 а) следует ($Z_3 \sim 0{,}2$) $\beta = 0{,}96$. В последних двух графах таблицы II преведены величины α, определенные графически по способу [2], и α_p, рассчитанные из уравнения 4 б) с использованием Z и K, определенных по методу [1]*. Нетрудно видеть, что величины α и α_p совпадают по порядку. Принимая по внимание вышеизложенное о различии между методами [1] и [2, 3], можно признать это соответствие удовлетворительным.

Таблица III

Номер образца	$K \cdot 10^6$	x в %
1	21	14
2	6	4
3	20	12
4	129	65
5	33	35

Если сопоставить величины K для рассматриваемых катализаторов, то относительные активности оказались приблизительно такими же, как и в случае, когда за активность принимался процент дегидрирования x, см. табл. III. Причем наибольшее соответствие наблюдается для первых трех контактов, когда процент дегидрирования невелик и торможение не искажает результат. Относительные активности у двух последних контактов по K и по x значительно отличаются. В этом случае лучше судить об относительной активности катализатора по константе скорости. В том же случае, когда мы желаем сопоставить активность серии катализаторов по x, то сопоставление необходимо проводить в узком интервале степеней превращения (лучше при $y < 0{,}3$), чтобы исключить значительное влияние торможения продуктами. Интересно было сопоставить относительные активности по K, α и x для катализаторов № 2 и № 4: K(№ 4): K (№ 2) = 129 : 6 $\approx$ 22; α (№ 4) : α (№ 2) = 17,5 : 0,8 $\approx$ 22; x (№ 4) : x (№ 2) = 65 : 4 $\approx$ 16.

Таким образом, сопоставление относительной активности по константам скорости в методах [1] и [2, 3] идентичны.

Представляло интерес оценить число активных мест на единицу поверхности, используя уравнение теории абсолютных скоростей [13]:

$$v = C_g C_s \frac{\sigma}{\sigma^*} \frac{1/2\, sh^5\, e^{-3}\, e^{-E/RT}}{8\pi^2 (8\pi^3 I_A I_B I_C)^{1/2} (2\pi M)^{3/2} (kT)^{5/2}} \qquad (7)$$

* Впервые такое соответствие было обнаружено А. Е. Агрономовым на примере реакции разложения изо-C_3H_7OH над ZnO.

где C_s — концентрация активных центров,
C_g — число адсорбированных на единицу поверхности молекул,
σ, σ^* — числа симметрии соответственно реагирующей молекулы и активного комплекса,
s — координационное число активного центра,
I_A, I_B, I_c — три момента инерции молекулы,
k — константа Больцмана,
M — массы молекулы,
h — постоянная Планка,
E — энергия активации.

Оценим некоторые величины в формуле (7): $s = 4$ [13], $\sigma = 6$ (D_{3d} симметрия кресла молекулы C_6H_{12}), $\sigma^* = 12$ (D_{gh} симметрия плоского шестиугольника молекулы C_6H_{12}), $I_A \approx I_B \approx I_c = 5 \cdot 10^{-40}$ г · см² (обычная величина для симметричных многоатомных молекул, небольшая погрешность в данном случае на скажется значительно на порядке величины C_s), $C_g = 10^{14}$ (10^{17})*. Для Ni/кизельгура опыт дает $v = 8 \cdot 10^{-10}$ моль · сек$^{-1}$ · см$^{-2}$. Отсюда C_s оказывается равным 10^{11} (10^8) на 1 см². Эта величина намного ниже величины $C_s \sim 10^{15} - 10^{14}$, которая обычно приводится в литературе [13, 15]. По-видимому это связано с тем, что процесс является неадиабатическим. Введение трансмиссионного коэффициента $\varkappa \sim 10^{-5}$ приводит к хорошему согласию рассчетной величины C_s с данными из литературы. В работе [16] исследовался никель без носителя. Величина v, рассчитанная нами по данным [16] для той же реакции, оказалась равной $3 \cdot 10^{-12}$ моль · сек$^{-1}$ · см$^{-2}$. Рассчитывая отсюда C_s по формуле (7) ($E = 9\,600$ кал/моль [16]), получаем в адиабатическом случае $C_s \sim 10^{10}$ (10^7). Аналогичный рассчет для никелевых катализаторов без носителя, но разного способа приготовления, по данным работ [17, 18] дает $C_s \sim 10^{11} - 10^{12}$. Этот результат свидетельствует в пользу представления о резонансно-дисперсионном характере каталитических сил [19]. Действительно, катализатор Ni/кизельгур содержит железо [20], которое должно влиять на электронное состояние никеля в данном катализаторе. Т. к. концентрация активных мест на 1 см² для массисного никеля и никеля на кизельгуре оказалось практически одной и той же, то можно думать, что роль хемосорбционной составляющей в активном комплексе невелика и что главную роль играют резонансные молекулярные комплексы [19]. В пользу этого предложения говорит также величина $\lambda \sim 10$—20 ккал/моль [17, 18], характерная для молекулярных комплексов.

* C_g рассчитана по [14], λ для C_6H_{12}, принято 10 ккал/моль, для значения в скобках $\lambda = 20$ ккал/моль, что соответствует опытным данным для разных образцов никелевых катализаторов [18].

РЕЗЮМЕ

Для сопоставления каталитической активности по степени превращения следует использовать небольшой интервал степеней превращения $< 0{,}3$. Из сопоставления концентрации активных мест массивного никеля и никеля на кизельгуре можно предполагать, что главную роль в активном комплексе играют молекулярные комплексы дисперсионно-резонансного характера.

SUMMARY

The degree of conversion can be used for comparison of catalytic activities only when it is smaller than 0.3. The comparison of the concentration of active sites on compact nickel with that on Ni-kieselgur leads to the assumption that dispersion–resonance–type molecular complexes play an important role in the activated complex.

ЦИТИРОВАННАЯ ЛИТЕРАТУРА

1. *Баландин, А. А.:* «Мультиплетная теория катализа» т. 2, МГУ, М. 1964.
2. *Фрост, А. В.:* Вест. МГУ, № 3—4, 111 (1946).
3. *Панченков, Г. М.:* Учен. зап. МГУ, *в.* **174**, 53 (1955).
4. *Баландин, А. А., Нейман, М. Б., Богданова, О. К., Исагулянц, Г. В., Щеглова, А. П., Попов, Е. И.:* Изв. АН СССР (ОХН), № 2, 157 (1957).
5. *Бонч-Бруевич, В. Л., Гласко, В. Б.:* Вестн. МГУ, № 5, 91 (1958).
6. *Де Гроот, С. Р.:* «Термидинамика необратимых процессов», стр. 9, Изд. Тех.-теор. лит. М., 1956.
7. *Агрономов, А. Е., Баландин, А. А., Мардашев, Ю. С.:* ДАН, **127,** 325 (1959).
8. Herbo, C., J. Chim. Phys., **47,** 445 (1950).
9. *Флид, Р. М., Коган, М. Я.:* ЖФХ., **24,** 1409 (1950).
10. *Агрономов, А. Е., Баландин, А. А., Мардашев, Ю. С.:* ДАН, **131,** 1120 (1960).
11. *Жаркова, В. Р., Фрост, А. В.:* Ж. О. Х., **2,** 534 (1942).
12. *Баландин, А. А., Матюшенко, В. Х.:* Ж. Ф. Х., **37,** 115 (1963).
13. *Глестон, С. Г., Лейдлер, К., Эйринг, Г.:* «Теория абсолютных скоростей реакций», 361, М. ИИЛ, 1948.
14. *Бур, Я. Д.:* «Динамический характер адсорбции» М. 1962 г.
15. *Вассерберг, В. Э.:* Доктор. диссерт. М. 1965 г.
16. Tétényi, P., Babernics, L., Rethő, A., Acta Chim. Hung. **28,** 375 (1961).
17. Tétényi, P., Babernics, L., Guczi, L., Schächter, K., [16], **40,** 387 (1964).
18. Tétényi, P., Schächter, K., Babernics, L., [16], **42,** 227 (1965).
19. *Мардашев, Ж. С.:* Ж. Ф. Х., **39,** 1817 (1965).
20. *Агрономов, А. Е., Мардашев, Ю. С.:* Ж. Ф. Х., **35,** 2047 (1961).

Ю. С. МАРДАШЕВ, Москва, М. Пироговская, дом 1.

Acta Chimica Academiae Scientiarum Hungaricae Tomus 57 (1), pp. 91—100 (1968)

RECENT RESULTS CONCERNING THE REACTION OF AROMATIC THIOLSULFINATES WITH DINITROCHLOROBENZENE

E. VINKLER and F. KLIVÉNYI

(Institute of Pharmaceutical Chemistry, Medical University, Szeged)

Received October 8, 1966
In revised form May 23, 1967

Our previous communication [1] dealt with the cleavage of thiolsulfinates (**I**) with 2,4-dinitrochlorobenzene (**II**). Our investigations showed that the corresponding 2,4-dinitrophenylarylsulfide (**III**) can be isolated as the main product.

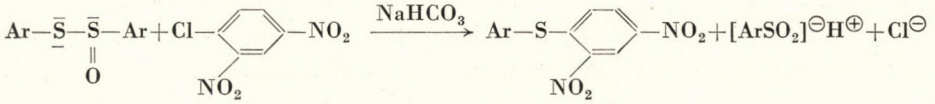

I II III

(a) Ar = C_6H_5; (b) Ar = p—CH_3 — C_6H_4; (c) Ar = p—Cl—C_6H_4.

From this result the conclusion was drawn that the sulfur-sulfur of the molecule is split heterolytically by the reagent, so that the bonding electron pair remains attached to the sulfur atom which is not connected to an oxygen atom. Thus, it is the sulfenyl sulfur atom which acts as the nucleophilic centre in the thiolsulfinate molecule, and its attack introduces the reaction resulting in the splitting off of the chloride anion. This finding seemed to be inconsistent with the investigations of LEANDRI and TUNDO [2]. These authors established in similar reactions of thiolsulfonates (**IV**) the formation of the corresponding 2,4-dinitrophenylarylsulfones (**V**), and concluded that it is the sulfonyl sulfur atom which has the stronger nucleophilic character in aromatic thiolsulfonates.

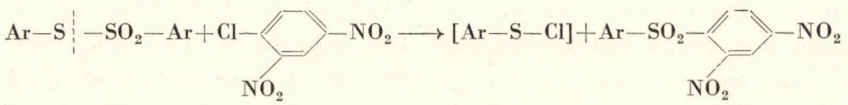

IV II VI V

Probably these considerations prompted BARNARD and PERCY [3] to reproduce our experiments, repeating the reaction of phenylbenzene- (**Ia**) and p-chlorophenyl-p-chlorobenzenethiolsulfinate (**Ic**) with dinitrochlorobenzene. Processing by chromatography gave the corresponding sulfoxides (45 and 8%, respectively), sulfides (16 and 62%) and sulfones (0 and 26%) as the isolated

main products. These authors concluded that the high quantity of sulfoxide — indubitably formed by a primary reaction — is indicative of the stronger nucleophilic character of the sulfinyl sulfur atom. The high quantity of sulfide obtained in our experiments is formed, according to their interpretation by the disproportionation before cleavage of the thiolsulfinate molecule into disulfide and thiolsulfonate. The subsequent reaction of these compounds with dinitrochlorobenzene would yield sulfide and sulfone as secondary products. Another possibility pointed out by BARNARD and PERCY is the hydrolysis of sulfenyl chloride (Ar—S—Cl), produced by primary cleavage, which gives a secondary product (*e.g.*, disulfide), and the latter reacts with dinitrochlorobenzene to yield sulfide.

The same authors also carried out experiments in which — as contrary to our work — the reagents were not used in equimolecular quantity. For one mole of thiolsulfinate, the quantity of the aryl halide and of sodium hydrogen carbonate was almost two moles. Under these conditions, the formation of 39% of sulfoxide was observed in the case of the dichloro derivative (**Ic**).

After the publication of the paper of BARNARD and PERCY, we repeated our earlier work and completed them by several model experiments.

In these model experiments, we tried to replace sodium hydrogen carbonate by sodium acetate, magnesium oxide, and sodium hydrogen phosphate, and to use dinitrofluorobenzene instead of dinitrochlorobenzene. The reaction was not influenced substantially by these reagents, which caused only quantitative changes. However, the reagents and experimental conditions reported in our earlier publication proved to be the most suitable for carrying out the reaction. At lower temperatures the reaction proceeds only partly or not at all. In the processing of the reaction products, the method of the British authors was used, and care was taken to observe exactly all experimental conditions (quantity of adsorbent, composition of solvent, etc.).

The experimental results reported in our earlier communication [1] were modified or completed by this different mode of processing.

In order to fully elucidate this reaction of thiolsulfinates, first the degree of disproportionation had to be established. For this purpose, experiments were carried out with our three model compounds under the usual experimental conditions, however, in the absence of aryl halide and sodium hydrogen carbonate. It was found that the degree of decomposition was about 0.5% for the (*p*-tolyl) compound (**Ib**), while it was 13 and 55% for the *p*-chlorophenyl derivative (**Ic**) and for phenylthiolsulfinate (**Ia**), respectively. Thus the tolyl derivative is the most suitable for drawing theoretical conclusions concerning the cleavage reaction.

The following facts have been established in our investigations:

1. The products of the cleavage of all the three thiolsulfinates are disulfide sulfide and sulfone. Sulfoxide could be isolated only in the case of the *p*-tolyl derivative (**Ib**).

2. In the case of **Ib**, the quantity of sulfide (41%) is more than that of the sulfoxide (21%).

3. In the presence of sodium hydrogen carbonate, but in the absence of aryl halide, not disproportionation but hydrolysis takes place under identical experimental conditions in all cases, giving rise to disulfide and sulfonic acid (*cf.* [1]).

4. Under identical experimental conditions and in the presence of sodium hydrogen carbonate, half the quantity of the aryl sulfenyl chlorides (*e.g.*, **VI**) is converted into thiolsulfinate, the other half into disulfide.

On the basis of these experimental results, the compounds produced in the cleavage of thiolsulfinates upon the action of 1 mole of dinitrochlorobenzene and sodium hydrogen carbonate have been studied. Under these conditions, the course of the reaction becomes more perspicuous, as the secondary reaction of dinitrochlorobenzene in excess is eliminated. Moreover, when the model experiments are made with the *p*-methyl derivative (**Ib**), which is known to suffer disproportionation to a small degree (0.5%), this inconvenient side reaction is also eliminated.

In the splitting of **Ib**, the sulfoxide (21%) is formed beyond doubt as a primary reaction product, besides sulfenyl chloride.

Both our previous investigations [1] and model experiments substantiate the fact that the disulfide (43%) (**VIII**) is formed by the alkaline hydrolysis of the sulfenyl chloride (**VI**).

The sulfide (**III**) (41%) may also be formed by the cleavage of the disulfide when acted upon by dinitrochlorobenzene, that is to say, by a secondary reaction. However, since 81% of this disulfide remains unchanged in the presence of sodium hydrogen carbonate and dinitrochlorobenzene, and only 15.5% of sulfide can be isolated, it follows that the predominant part of the sulfide, the difference ($41 - 15.5 = 25.5\%$) is formed by primary reaction, by the splitting of thiolsulfinate.* Thus, the quantity of sulfide of this latter origin is higher, but, at least not less than equal to the quantity of the sulfoxide.

Our model experiments showed that dinitrochlorobenzene and sulfinic acid (**VII**) gave — under identical experimental conditions — sulfone in a high yield (96%). On the other hand, only a relatively small amount of sulfone (5%) could be isolated in the cleavage reaction. This experiment proves that the primary reaction of thiolsulfinate with the aryl halide proceeds at a higher rate, than the secondary reaction leading to the sulfone. Therefore, the predominant part of the aryl halide reacts during the primary process, and only a small part of it can give rise to secondary reactions.

Similar experiments were carried out with the phenyl- (**Ia**) and the *p*-chlorophenyl- (**Ic**) thiolsulfinates, which disproportionate to a higher degree. As contrary to the findings of BARNARD and PERCY, no sulfoxide could be isolated from the reaction mixture formed in the cleavage of these compounds.

* In this calculation, the difference between the molecular weights of thiolsulfinate and disulfide was not taken into consideration.

The quantity of sulfide was found to be 57 and 64.5%, respectively. From the corresponding disulfides 19.9 and 64.5% of sulfide, respectively, was formed by the analogous reaction.

With the compounds **Ia** and **Ic**, the quantity of sulfone was found to be 10.2 and 18.4%, respectively.

Most probably, the absence of sulfoxide formation may be attributed to the fact that already before cleavage into sulfoxide, these two thiolsulfinates suffer hydrolysis or decomposition by disproportionation into disulfide, sulfinic acid and sulfonic acid. It follows that these thiolsulfinates are unsuitable for an investigation of the primary products formed in the cleavage with dinitrochlorobenzene. It is to be assumed that under the experimental conditions applied by BARNARD and PERCY, the formation of sulfoxide in the case of the two mentioned thiolsulfinates was due to the higher aryl halide concentration, which favours the cleavage reaction proceeding simultaneously with hydrolysis and disproportionation.

We think, therefore, that in the case of phenyl- and *p*-chlorophenylthiolsulfinates both primary and secondary reaction products are present. With regard to these two compounds, our opinion agrees with the findings of BARNARD and PERCY.

However, the British authors did not investigate the splitting reaction of *p*-tolylthiolsulfinate, but considered it to be analogous to the reaction of the two compounds. In view of the fact that this analogy does not hold true according to our investigations, the criticism of the British authors of our interpretation of the reaction cannot be accepted.

It seems probable on the basis of the experimental results that the nucleophilic character of the thiolsulfinate molecule cannot be assigned exclusively to the sulfenyl or the sulfinyl sulfur atom.

The remarkable reactivity of *p*-tolyltoluenethiolsulfinate is due probably to the hyperconjugation effect of the *p*-methyl group (such an effect cannot play a part in the case of the analogous phenyl and *p*-chlorophenyl derivatives). This effect increases the nucleophilic character of the sulfur atom linked to the aromatic group. At the same time, it is to be assumed that an increase in the nucleophilic character of the sulfur atoms favours cleavage more strongly than promotes hydrolysis or disproportionation.

The reaction scheme summarized in the following table of formulas illustrates the processes taking place in the reaction of *p*-tolyltoluenethiolsulfinate with 2,4-dinitrochlorobenzene.

Table of formulas

(Reaction scheme)

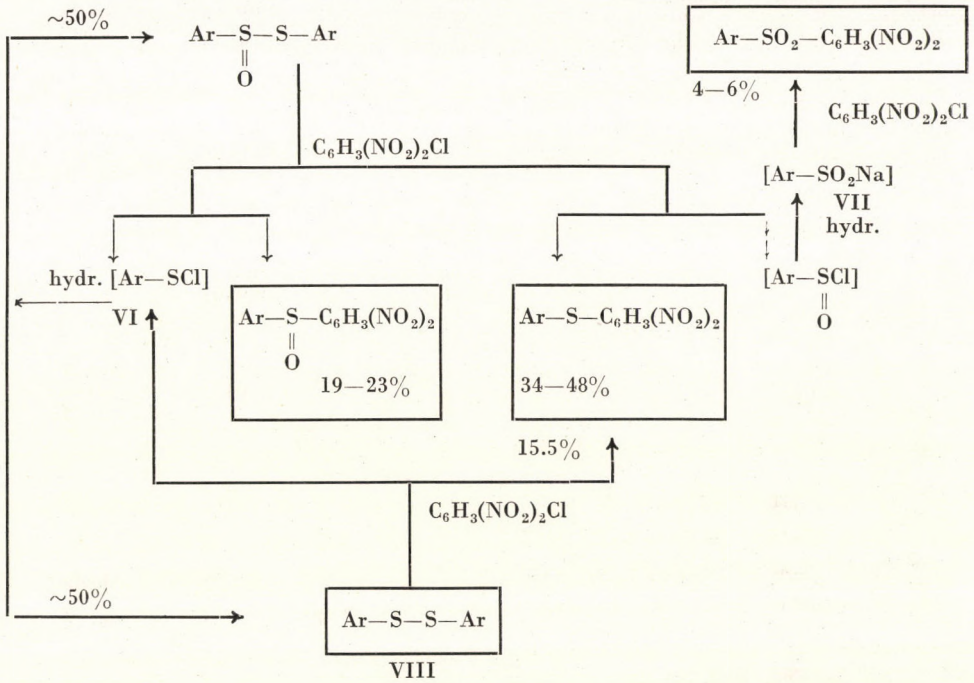

Experimental

(Melting points are uncorrected)

Procedure: The reactants are dissolved in the solvents using the quantities, given in Tables I and II. The reaction mixture is placed immediately on a steam bath, and refluxed for 1 hr. After rapid cooling to room temperature, the mixture is poured, with stirring, into about 2 l. of water. After a short period of standing, the solidified reaction product is filtered off. After drying, the raw product is dissolved in a minimum volume of a 1 : 1 mixture of benzene and petroleum ether, and poured into a chromatographic column (diameter 20—25 mm), packed with an adequate quantity (90—110 g for about 7—10 g of the crude product) of activated silica gel. Elution is effected successively with petroleum ether, a 1 : 1 mixture of petroleum ether and benzene, and finally, with chloroform. (The solvent is changed when the eluate dripping down has become colourless, or does not contain measurable quantities of the substances.) The fractions of identical composition are combined, and the weighed substances are recrystallized from methanol or ethanol (unless other solvent is indicated).

Note: Yields were calculated from the results of five parallel experiments, and refer to the crude fractions. The percentage yields — unless indicated otherwise — are reffered to the compounds **Ia**, **Ib** and **Ic**.

Analysis of the compounds listed in Table I

Experiment No. 1.

(a) identical with an authentic sample.

(b) $C_{13}H_{10}O_4N_2S$ (290.14). Calcd. S 11.05. Found S 11.1%.

(c) $C_{13}H_{10}O_5N_2S$ (306.14) Calcd. C 50.97; H 3.29. Found C 51.30 H 3.20%.

(d) $C_{13}H_{10}O_6N_2S$ (322.14) Calcd. S 9.95. Found S 9.80%.

Table I*

Experiment, No.	Thiolsulfinate, Ib g (M)	Dinitrochlorobenzene, g (M)	Other reactants, g (M)	$NaHCO_3$ g (M)	Solvent, ml
1	3.9 (0.015)	3.0 (0.015)	—	1.2 (0.015)	Alcohol: water 80 : 16
2	—	—	**VI** 2.38 (0.015)	1.2 (0.015)	Alcohol: water 80 : 16
3	3.9 (0.015)	—	—	1.2 (0.015)	Alcohol: water 80 : 16
4	3.9 (0.015)	—	—	—	Alcohol: water 80 : 16
5	—	2.0 (0.01)	**VIII** 2.46 (0.01)	0.84 (0.01)	Alcohol: water 80 : 16
6	—	2.0 (0.01)	**VII** 1.56 (0.01)	0.84 (0.01)	Alcohol: water 80 : 16

* Formulas of the compounds shown in the table: **VI**: p—$CH_3 \cdot C_6H_4 \cdot SCl$;

Experiment No. 2.
(a) as above.
(f) identical with an authentic sample.
Experiment No. 3.
(a) as above.
(e) $C_{15}H_{18}O_3N_2S_2$ (338.43). Calcd. C 53.23; H 5.36. Found C 53.14; H 5.16%.
Experiment No. 4.
(a) as above
(f) 1 identical with an authentic sample.
2 as above.

Isolated substances						M. p., °C
a.	b.	c.	d.	e.	f.	
Disulfide, g (%)	Sulfide, g (%)	Sulfoxide, g (%)	Sulfone, g (%)	Sulfonic acid, g (%)	Other products, g (%)	
0.7—1 (18.9—17.1)	1.5—2.1 (34.4—48.2)	0.9—1.0 (19.6—23)	0.2—0.3 (4.1—6.2)	—	—	(a) 44— 45 (b) 100—101 (c) 136—138 (d) 185—186
0.8 (43.3)	—	—	—	—	**Ib** 0.8 (40.6)	(a) 44— 45 (f)104 petrol. ether: benzene (3 : 1)
2.1	—	—	—	1.8 (From the aqueous solution)	—	(a) 44— 45 (e) Characterization as S-benzylisothiuronium sulfate, 179—181 (from aqueous alcohol)
0.02 (0.5)	—	—	—	Traces	① **IX** 0.01 (0.2) ② **Ib** 3.5 (89.7)	(a) 44—45 (f) ① 176—77 (f) ② 103—104 Petrol. ether: benzene (3 : 1)
2.0 (81) partly as unchanged substance	0.45 (15.5)	—	—	—	**X** 0.85 (40%) referred to dinitrochlorobenzene	(a) 44—45 (b) 101 (f) 86— 87
—	—	—	3.1 (96.2)	—	—	(d) 185—186

IX: p—$CH_3 \cdot C_6H_4 \cdot SO_2 \cdot S \cdot C_6H_4 \cdot CH_3 \cdot p$; **X**: 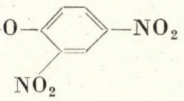

Experiment No. 5.

(a) as above

(b) identical with an authentic sample.

(f) identical with an authentic sample.

Experiment No. 6.

(d) identical with an authentic sample.

Analysis of the compounds listed in Table II.

Experiment No. 1.

(a) identical with an authentic sample.

(b) $C_{12}H_8O_4N_2S$ (262.1). Calcd. S 11.61. Found S 11.75%

Table II

Experiment No.	Thiolsulfinate g (M)	Dinitrochlorobenzene, g (M)	Other reactants, g (M)	$NaHCO_3$ g (M)	Solvent, ml
1	**Ia** 2.3 (0.01)	2.0 (0.01)	—	0.8 (0.01)	Alcohol: water 80 : 16
2	**Ic** 4.5 (0.015)	3.0 (0.015)	—	1.2 (0.015)	Alcohol: water 80 : 16
3	—	2.0 (0.01)	$(C_6H_5S)_2$ 2.2 (0.01)	0.8 (0.01)	Alcohol: water 80 : 16
4	—	2.0 (0.01)	$(p\text{-}ClC_6H_4S)_2$ 2.9 (0.01)	0.8 (0.01)	Alcohol: water 80 : 16
5	**Ia** 2.3 (0.01)	—	—	—	Alcohol: water 80 : 16
6	**Ic** 4.5 (0.015)	—	—	—	Alcohol: water 100 : 20
7*	**Ib** 0.55	0.88	—	0.36	Ethanol: water 7 : 0.7

* Under the experimental conditions applied by BARNARD–PERCY

Formula of the compound shown in the table: **XI:** $HO-C_6H_3(NO_2)_2$;

(d) identical with an authentic sample.
(f) identical with an authentic sample.

Experiment No. 2.

(a) identical with an authentic sample.
(b) $C_{12}H_7O_4N_2SCl$ (310.6). Calcd. S 10.32. Found S 10.20%.
(d) identical with an authentic sample.

Experiment No. 3.

(a) as above.
(b) as above.

Isolated substances						M. p., °C
a.	b.	c.	d.	e.	f.	
Disulfide, g (%)	Sulfide, g (%)	Sulfoxide, g (%)	Sulfone, g (%)	Sulfonic acid, g (%)	Other products g (%)	
0.5 (22.9)	1.5 (57.2)	—	0.3 (10.2)	—	**XI** 0.3	(a) 60— 61 (b) 118 (d) 157 (f) 113
0.75 (17)	3.0 (64.5)	—	0.80 (18.4)	—	—	(a) 70— 71 (b) 120—123 (d) 168—170
2.45 — partly as unreacted substance	0.55 (19.9)	—	—	—	—	(a) 60—61 (b) 118
1.7 (—) partly as unreacted substance	2.0 (64.5)	—	—	—	**X** 0.2	(a) 70— 71 (b) 120—122 (f) 86— 87
1.2 (55)	—	—	—	—	**Ia** 1g (42.7) as unreacted subst.	(a) 60—61 (f) 67—68
0.6 (13.2)	—	—	—	—	**Ic** 3.6 (79.2) as unreacted subst.	(a) 70—71 (f) 96—98
0.1 (19.3)	0.4 (32.8)	0.2 (31.1)	0.3 (44.4)	—	**X** 0.1ᵘ	See Table I

Experiment No. 4.
(a) as above.
(b) as above.
(f) identical with an authentic sample.
Experiment No. 5.
(a) as above.
(f) identical with an authentic sample.
Experiment No. 6.
(a) as above.
(f) identical with an authentic sample.

We wish to thank Dr. E. CSAPÓ-BARTOS for the analyses.

SUMMARY

The cleavage of benzene-, *p*-toluene- and *p*-chlorobenzenethiolsulfinic acid phenyl-, *p*-tolyl- and *p*-chlorophenyl esters with 2,4-dinitrochlorobenzene in alkali hydrocarbonate solutions was investigated by the authors and subsequently by BARNARD and PERCY. It was found that exact conclusions concerning the direction and degree of the cleavage can be drawn only in the case of the *p*-tolyl compound. This compound, as contrary to the other two analogues, practically does not disproportionate under the conditions of the reaction. Using an equimolecular quantity of dinitrochlorobenzene, side reactions, which would interfere with the study of the course of the reaction, can be eliminated. Model experiments carried out under such conditions have proved the predominant role not only of the sulfoxide but also of the sulfide formed in the primary reaction. It has been shown that the principal part of dinitrochlorobenzene reacts at a relatively high rate in the primary process, and only a small part is available for secondary reactions. It is to be assumed on the basis of these experimental results that the nucleophilic character of the thiolsulfinate molecule is not to be attributed exclusively to the S(II) and S(IV) sulfur atoms.

REFERENCES

1. VINKLER, E., KLIVÉNYI, F.: Acta Chim. Acad. Sci. Hung. **22**, 348 (1960).
2. LEANDRI, G., TUNDO, A.: Ann. di Chimica **44**, 255 (1954).
3. BARNARD, D., PERCY, J.: J. Chem. Soc. **1962**, 1667.

Elemér VINKLER, Ferenc KLIVÉNYI } Szeged, Eötvös-u. 2. Hungary

Acta Chimica Academiae Scientiarum Hungaricae Tomus 57 (1), pp. 101—110 (1968)

ZUR ANWENDUNG EINIGER KONFORMATIONSREGELN AUF CYCLOHEXYLAMINE

K. ALTENBURG

(Institut für Physikalische Chemie der Deutschen Akademie der Wissenschaften zu Berlin, Berlin-Adlershof)

Eingegangen am 16. Juni 1967

I. Einleitung

In einer vorangegangenen Mitteilung [1] (im folgenden mit [1] zitiert) war, ausgehend von einer theoretischen Deutung der Abhängigkeit der Siedetemperaturen isomerer Alkane von der Form der Moleküle [2], eine Deutung verschiedener, zur Konformations- und Konfigurationsanalyse cyclischer Alkane benutzter Regeln gegeben worden. Weiterhin wurden einige neue, universell anwendbare und auch für stellungsisomere Verbindungen gültige Beziehungen über die Zusammenhänge zwischen Konstitution und physikalischen Eigenschaften angegeben. Danach wird die Abhängigkeit verschiedener physikalischer Eigenschaften von der Form der Moleküle im wesentlichen durch die Abhängigkeit dieser Eigenschaften vom quadratischen Mittelwert des Radius [3] eines Moleküls, der dem mittleren Trägheitsmoment eines Moleküls entspricht [4], bestimmt.

FELTKAMP u. Mitarbeiter [5] haben in der letzten Zeit eine Reihe stereoisomerer Cyclohexylamine dargestellt, deren Siedetemperaturen, Dichten und Brechungsindizes bestimmt und die Ergebnisse anhand der AUWERS–SKITA-schen Regeln in der von VAN BEKKUM u. Mitarbeitern [6] gegebenen Form diskutiert. Mit diesem experimentellen Material ist es möglich, die Anwendbarkeit der in [1] gewonnenen Ergebnisse auf diese Stoffklasse zu prüfen. Eine derartige Prüfung ist von grundsätzlichem Interesse, da die Cyclohexylamine polar und zum Teil zur Bildung von Wasserstoffbrücken fähig sind. Bei einer solchen Verbindungsklasse ist am ehesten ein Versagen der bisher nur für unpolare Kohlenwasserstoffe geprüften Beziehungen zu erwarten.

II. Zur Berechnung der quadratischen Mittelwerte der Radien der Cyclohexylamine

Eine wesentliche Rolle bei der Deutung der Abhängigkeit physikalischer Eigenschaften isomerer Verbindungen von der Form der Moleküle spielt der quadratische Mittelwert des Radius, so daß auf dessen Berechnung zunächst kurz eingegangen sei (vgl. hierzu [3]).

Der quadratische Mittelwert des Radius eines Moleküls ist durch folgende Beziehung definiert:

$$\overline{R^2} = \frac{1}{N} \sum_i \overline{r_i^2}. \tag{1}$$

Hierbei sind N die Zahl der (gleichen) Bausteine und r_i der Abstand des i-ten Bausteines vom Schwerpunkt des Moleküls. Der mit 2/3 M ($M \mathrel{\hat{=}}$ Molekulargewicht) multiplizierte Wert von $\overline{R^2}$ entspricht dem mittleren Trägheitsmoment des Moleküls [4]. Durch elementare Umformungen [3a] folgt aus Gl. (1)

$$\overline{R^2} = \frac{1}{N^2} \sum_i \sum_{j>i} \overline{s_{ij}^2}, \tag{2}$$

wobei s_{ij} der Abstand des i-ten vom j-ten Baustein des Moleküls ist. Kennt man die Abstände der Bausteine des Moleküls voneinander, so kann man den quadratischen Mittelwert des Radius elementar berechnen, indem man die Häufigkeit der einzelnen in einem Molekül vorkommenden Abstände abzählt, mit dem quadratischen Mittelwert des Abstandes multipliziert und sämtliche Werte addiert. Nach dieser Methode wurden unter Benutzung des Modells der „frei drehbaren Valenzwinkelkette" (freie Drehbarkeit um jede Einfachbindung unter Berücksichtigung des Tetraederwinkels) für eine große Anzahl acyclischer und cyclischer Alkane die quadratischen Mittelwerte der Radien berechnet [3].

Die Cyclohexylamine unterscheiden sich von den entsprechenden Cyclohexylderivaten in ihrem Kerngerüst durch die unterschiedliche Länge der C—N-Bindung. Prinzipiell ist es möglich, die quadratischen Mittelwerte der Radien unter Berücksichtigung unterschiedlicher Bindungslängen (und Bindungswinkel) zu berechnen [3b]. Die numerischen Rechnungen werden dadurch jedoch wesentlich umfangreicher. Da sich die Bindungslängen der C—C- und der C—N-Bindungen (1,54 Å bzw. 1,47 Å [7]) nicht wesentlich unterscheiden, kann man, wie an anderer Stelle [8] gezeigt wurde, in den Aminen näherungsweise die quadratischen Mittelwerte der Radien der Cyclohexanderivate übernehmen, deren C-Atome die gleiche Anordnung aufweisen, wie die schweren Atome der interessierenden Cyclohexylamine; d. h. es entspricht:

X-Methylcyclohexylamin $\mathrel{\hat{=}}$ 1.X-Dimethylcyclohexan
N-Methyl-X-methylcyclohexylamin $\mathrel{\hat{=}}$ 1-Äthyl-X-methylcyclohexan
N.N-Dimethyl-X-methylcyclohexylamin $\mathrel{\hat{=}}$ 1-Isopropyl-X-methylcyclohexan
und
X-tert.-Butylcyclohexylamin $\mathrel{\hat{=}}$ 1-Methyl-X-tert.-Butylcyclohexan

Die quadratischen Mittelwerte der Radien dieser Cyclohexane wurden früheren Veröffentlichungen [3d, 3e] entnommen und sind in Tab. I zusammengestellt.

Tabelle I

Quadratische Mittelwerte der Radien R, bezogen auf die Länge einer C-C-Einfachbindung a_1, Dichte ϱ bei 20 °C, Brechungsindex n bei 20 °C, Molrefraktion R_D und gemessene bzw. berechnete Siedetemperaturen t_{sex} bzw. t_{sth} für Cyclohexylamine***

Substanz	Form	$\overline{R^2}/a_1^2$	ϱ [g cm^{-3}]	n	R_D [cm^3 Mol^{-1}]	t_{sex} [° C]	t_{sth} [° C]
2-Methyl-cyclohexylamin	*cis*	1,2917	0,8710	1,4607	35,645	151,8	150,9
	trans	1,4167	0,8550	1,4541	35,862	148,8	146,6
3-Methyl-cyclohexylamin	*cis*	1,5260	0,8545	1,4518	35,726	149,5	150,4
	trans	1,3594	0,8646	1,4569	35,652	150,8	149,9
4-Methyl-cyclohexylamin	*cis*	1,3750	0,8695	1,4570	35,410	150,5	153,2
	trans	1,5833	0,8492	1,4508	35,880	149,2	149,6
N-Methyl-2-methyl-cyclohexylamin	*cis*	1,5967	0,8607	1,4570	40,260	162,6	164,2
	trans	1,6955	0,8486	1,4531	40,533	161,4	160,2
N-Methyl-3-methyl-cyclohexylamin	*cis*	1,8820	0,8396	1,4500	40,726	163,6	161,6
	trans	1,7174	0,8478	1,4518	40,470	161,1	160,5
N-Methyl-4-methyl-cyclohexylamin	*cis*	1,7394	0,8500	1,4531	40,466	163,0	162,8
	trans	1,9808	0,8418	1,4511	40,704	164,3	166,7
N.N-Dimethyl-2-methyl-cyclohexylamin	*cis*	1,7867	0,8598	1,4605	45,093	178,5	178,5
	trans	1,8667	0,8448	1,4519	45,100	170,3	170,9
N.N-Dimethyl-3-methyl-cyclohexylamin	*cis*	2,0989	0,8406	1,4518	45,317	176,2	176,7
	trans	1,9389	0,8394	1,4509	45,303	172,3	169,8
N.N-Dimethyl-4-methyl-cyclohexylamin	*cis*	1,9644	0,8453	1,4531	45,177	174,5	174,9
	trans	2,2222	0,8360	1,4490	45,321	177,3	178,1
4-tert.-Butyl-cyclohexylamin	*cis*	2,1047	0,8716	1,4670	49,435	210,1	207,8
	trans	2,3691	0,8660	1,4645	49,525	211,2	213,5

* Um vergleichbare Werte zu erhalten, wurden sämtliche Siedetemperaturen auf einen Druck von 725 Torr umgerechnet.

** Sämtliche experimentellen Werte s. [5].

Die im folgenden betrachteten substituierten Cyclohexylamine existieren jeweils in zwei verschiedenen Konfigurationen (*trans*- bzw. *cis*-Form). Jede Konfiguration kann grundsätzlich wiederum in zwei verschiedenen Konformationen vorliegen: di-äquatorial oder di-axial bzw. äquatorial-axial bzw. axial-äquatorial. Aus energetischen Gründen ist im ersten Falle die di-äquatoriale Anordnung die stabilere, im zweiten Fall dagegen diejenige, bei der die größere Gruppe die äquatoriale Stellung einnimmt. Die stabilere Form hat jeweils den größeren Radius.

III. Physikalische Eigenschaften und Radius

In [1] waren die Zusammenhänge zwischen Molekülform und Radius einerseits und Radius und physikalischen Eigenschaften der Cyclohexane andererseits abgeleitet worden. Im folgenden sei gezeigt, daß diese Beziehungen auch für die Cyclohexylamine gelten.

III.1 Molvolumen und Dichte

An anderer Stelle [9] war gezeigt worden, daß die Molvolumina der Methylcyclohexane mit gleicher Zahl äquatorialer bzw. axialer Methylgruppen linear mit dem Quadrat des Radius wachsen. Für das Molvolumen V_M isomerer Methylcyclohexane gilt folgende Beziehung

$$V_M = k_o + k_n n_s + k_R \frac{\overline{R^2}}{a_1^2} \tag{3}$$

Hierbei sind n_s die Zahl der Methylgruppen, $\overline{R^2}/a_1^2$ der auf die Länge a_1 einer C—C-Einfachbindung bezogene quadratische Mittelwert des Radius und k_o, k_n und k_R Konstanten, die von der Konformation der betreffenden Verbindung (und der Temperatur) abhängen.

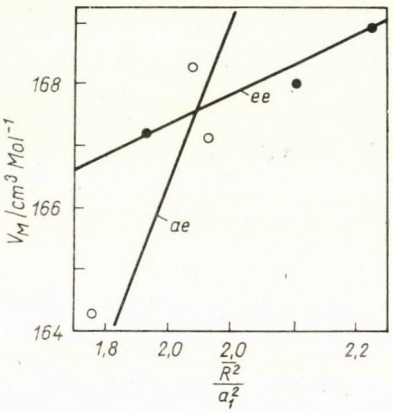

Abb. 1. Abhängigkeit der Molvolumina von N.N-Dimethyl-X-methylcyclohexylaminen vom quadratischen Mittelwert des Radius. Die eingezeichneten Geraden entsprechen der Gl. (3)

Trägt man analog die Molvolumina isomerer Cyclohexylamine als Funktion von $\overline{R^2}/a_1^2$ auf (s. Abb. 1), so liegen die Punkte für Verbindungen mit gleicher Konformation der Substituenten (*ae* bzw. *ee*) auf (sich schneidenden) Geraden mit positiver Neigung. Im allgemeinen liegen die Punkte der Verbindungen der Konformation *ae* links, die der Verbindungen der Konformation *ee* rechts vom Schnittpunkt der Geraden.* In diesen Fällen haben die Verbindun-

* Ausnahmen sind auf Grund der Radienverhältnisse bei den 3-Alkylcyclohexylaminen möglich. Bei diesen Verbindungen können die Punkte der Konformation (*ae*) rechts vom Schnittpunkt liegen, so daß u. U. die Verbindung mit dem größeren Radius das kleinere Molvolumen aufweist. Dies ist bei den N.N-Dimethyl-3-methylcyclohexylaminen der Fall.

Eine derartige Umkehrung ist nur bei den 1.3-Verbindungen zu erwarten. Bei den 1.2-Verbindungen liegt die *cis*-Verbindung (Konformation *ae*) wesentlich unterhalb des Schnittpunktes der Geraden, während bei den 1.4-Verbindungen die *trans*-Verbindung (Konformation *ee*) wesentlich oberhalb des Schnittpunktes liegt.

gen der Konformation *ee* größere Molvolumina und damit kleinere Dichten als die konfigurationsisomeren Verbindungen der Konformation *ae*.

Die Beziehung (3) gilt sinngemäß auch für die Alkylcyclohexylamine. n_s entspricht in diesem Falle der Zahl der schweren Atome in den Seitenketten des Cyclohexylamins. Eine Ausgleichsrechnung ergibt für das Molvolumen der Alkylcyclohexylamine (bei 20 °C) folgende Werte für die Konstanten der Gl. (3):

Konformation	cm³ Mol⁻¹	cm³ Mol⁻¹	cm³ Mol⁻¹
ae	72,474	10,712	26,840
ee	92,717	16,303	4,635

III.2 Siedetemperatur

Wie bereits von verschiedener Seite [6] betont und in [1] theoretisch begründet wurde, besteht zwischen der Konfiguration von Cyclohexylverbindungen und deren Siedetemperaturen kein unmittelbarer, eindeutiger Zusammenhang.

Die Siedetemperatur (im Druckbereich von 100 bis 1000 Torr) ergibt sich, wie in [1] gezeigt wurde, aus dem durch eine stoffspezifische Konstante erweiterten Theorem der korrespondierenden Zustände zu

$$t_s = A_d + 4{,}98508\, M\varrho + 37{,}708\, \frac{\overline{R^2}}{a_1^2}, \tag{4}$$

wobei A_d eine für jede Gruppe von isomeren Verbindungen charakteristische (druckabhängige) Konstante, M das Molekulargewicht und $\varrho = d_4^{20}$ die Dichte bei 20 °C ist. Für die Siedepunktsdifferenz zweier isomerer Verbindungen folgt hieraus

$$\Delta t_s = t_{s2} - t_{s1} = 4{,}98508\, M(\varrho_2 - \varrho_1) + 37{,}708 \left(\frac{\overline{R_2^2}}{a_1^2} - \frac{\overline{R_1^2}}{a_1^2} \right). \tag{5}$$

Da, wie in III.1 dargestellt wurde, die konfigurationsisomere Verbindung mit dem größeren Radius im allgemeinen die kleinere Dichte aufweist, haben die beiden Terme der Gl. (5) verschiedenes Vorzeichen. In den meisten Fällen überwiegt der erste Term; die Verbindung mit dem größeren Radius hat dann die niedrigere Siedetemperatur. Es sind jedoch einige Fälle bekannt (s. [1] Abschn. 3.1), in denen der zweite Term überwiegt. In diesen Fällen hat entgegen der erweiterten AUWERS—SKITAschen Regel die Verbindung mit dem größeren quadratischen Mittelwert des Radius die höhere Siedetemperatur.

Zur Konfigurationsanalyse geeigneter als die Siedetemperatur sind zwei Funktionen, die aus Gl. (4) folgen. Unmittelbar ergibt sich, daß

$$t_s - 4{,}98508\, M\varrho = f_d\left(\frac{\overline{R^2}}{a_1^2}\right) = A_d + 37{,}708\,\frac{\overline{R^2}}{a_1^2} \tag{6}$$

eine eindeutige Funktion des quadratischen Mittelwertes des Radius ist. An anderer Stelle [10] wurde weiterhin gezeigt, daß man in Gl. (4) anstelle der Dichte den Brechungsindex n bei 20° C (für die D-Linie) einführen kann. Für die Siedetemperatur gilt dann

$$t_s = A_n + 10{,}168\, Mn + 36{,}025\,\frac{\overline{R^2}}{a_1^2}\,. \tag{7}$$

Hieraus folgt analog zur Gl. (6)

$$t_s - 10{,}168\, Mn = f_n\left(\frac{\overline{R^2}}{a_1^2}\right) = A_n + 36{,}025\,\frac{\overline{R^2}}{a_1^2}\,. \tag{8}$$

Zur Prüfung der Beziehungen (6) und (8) sind in Abb. 2 bzw. 3 $f_d(\overline{R^2}/a_1^2)$ bzw. $f_n(\overline{R^2}/a_1^2)$ als Funktion von $\overline{R^2}/a_1^2$ für verschiedene isomere Cyclohexylamine dargestellt. Die Neigung der eingezeichneten Geraden entspricht dem Wert $\operatorname{tg}\alpha_d = 37{,}708$ (Gl. (6)) bzw. $\operatorname{tg}\alpha_n = 36{,}025$ (Gl. (8)). Die ursprünglich für acyclische Alkane abgeleiteten Beziehungen gelten also auch quantitativ für die Cyclohexylamine. Die Abbildungen zeigen, daß eine eindeutige Zuordnung von Konfigurations- und Stellungsisomeren möglich ist, wenn $\Delta\,\overline{R^2}/a_1^2 = R_2^2/a_1^2 - \overline{R_1^2}/a_1^2 \geqslant 0{,}1$ ist. Diese Voraussetzung ist für sämtliche Konfigurationsisomere erfüllt.

Weiterhin wurden zur Prüfung der oben angegebenen Beziehungen die Siedetemperaturen der Cyclohexylamine mittels Gl. (4) berechnet.* In Tab. II sind diese Werte den experimentellen Werten [5] gegenübergestellt. Die Vorzeichen der Differenzen der berechneten und der experimentell bestimmten Siedetemperaturen konfigurationsisomerer Verbindungen stimmen bis auf einen Fall überein.** Die Cyclohexylamine verhalten sich bezüglich der Siedetemperaturen ebenso wie die Cyclohexanderivate.*** Dies erscheint erstaunlich, da diese Amine polar sind, und die primären und sekundären Amine darüber hinaus zur Bildung von Wasserstoffbrücken befähigt sind. Man muß jedoch folgendes berücksichtigen. An anderer Stelle [11] wurde gezeigt, daß die Ab-

* Die Konstante A_n hat dabei die Werte —389,30; —441,91; —494,35 und —546,21.

** Dies sind die 3-Methylcyclohexylamine. Hierbei ist folgendes zu berücksichtigen. Die Differenz der Siedetemperaturen ergibt sich als Differenz zweier großer Zahlen. Ein Fehler von 0.001 gcm^{-3} bei der Dichtemessung bedingt eine Unsicherheit der berechneten Siedetemperatur von $\approx$ 0.5°.

*** Die von FELTKAMP und THOMAS [5] an Hand der AUWERS–SKITAschen Regel geführten Diskussionen über das unterschiedliche Verhalten der Siedepunktsdifferenzen konfigurationsisomerer Cyclohexylamine wird damit gegenstandslos.

Tabelle II

Vergleich der Anwendungsbereiche der verschiedenen Beziehungen zur Konstitutionsaufklärung

Beziehung	Definition	Experimentell z. bestimmende Größen	Anwendungsbereich
$f_d\,(\overline{R}^2/a_1^2)$	Gl. (6)	t_S; ϱ	Konfigurationsisomere, Stellungsisomere sofern $\Delta\,\overline{R}^2/a_1^2 \geqslant 0{,}1$
$f_n\,(\overline{R}^2/a_1^2)$	Gl. (8)	t_S; n	desgl.
Molrefraktion		n; ϱ	Konfigurationsisomere
Dichte		ϱ	Konfigurationsisomere*
Brechungsindex		n	desgl.

* Ausnahmen sind bei den 3-Alkylcyclohexylaminen möglich.

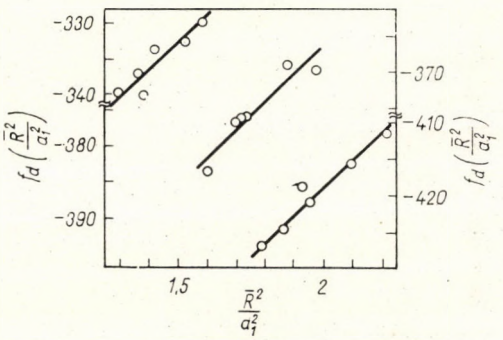

Abb. 2. Die Abhängigkeit der Funktion $f_d\,(\overline{R}^2/a_1^2)$ von $\overline{R}^2/a_1^2$ für X-Methylcyclohexylamine, N-Methyl-X-methylcyclohexylamine und N.N-Dimethyl-X-methylcyclohexylamine (von oben nach unten). Die eingezeichneten Geraden entsprechen der Gl. (4)

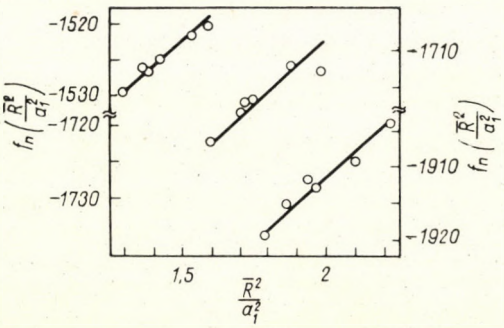

Abb. 3. Die Abhängigkeit der Funktion $f_n(\overline{R}^2/a_1^2)$ von $\overline{R}^2/a_1^2$ für X-Methylcyclohexylamine, N-Methyl-X-methylcyclohexylamine und N.N-Dimethyl-X-methylcyclohexylamine (von oben nach unten). Die eingezeichneten Geraden entsprechen der Gl. (7)

hängigkeit der physikalischen Eigenschaften von der Form der Moleküle in erster Linie eine Folge der unterschiedlichen Potentiale der abstoßenden zwischenmolekularen Kräfte ist. Die Dipolkräfte und die durch die Wasserstoffbrückenbindungen bedingten Kräfte beeinflussen im wesentlichen die anziehenden zwischenmolekularen Kräfte. Sie finden ihren Ausdruck in den Koeffizienten A_d bzw. A_n der Gl. (4) bzw. (7). Beim Vergleich der Eigenschaften isomerer Verbindungen fallen diese Koeffizienten jedoch heraus.

III.3 Molrefraktion und Brechungsindex

Auch Molrefraktion und Brechungsindex hängen von der Form der Moleküle ab und sind deshalb prinzipiell zur Konstitutionsermittlung geeignet. In einer vorangegangenen Mitteilung [12] war gezeigt worden, daß für die Molrefraktion R_D gesättigter Kohlenwasserstoffe folgende zur Gl. (4) analoge Beziehung gilt:

$$R_D = \frac{n^2 - 1}{n^2 + 2} \cdot \frac{M}{\varrho} = R_0 - 0{,}098065\, M\varrho + 0{,}1726\, \frac{\overline{R^2}}{a_1^2} \qquad (9a, b)$$

mit

$$R_0 = 5{,}0068\, n_c + 0{,}3694\, n_H$$

n_c bzw. n_H sind hierbei die Zahl der Kohlenstoff- bzw. Wasserstoffatome der betreffenden Verbindung. Ein Vergleich der Koeffizienten der Gl. (9) mit denen der Gl. (4) ergibt, daß der Einfluß der Molekülform auf die Molrefraktion wesentlich geringer ist als auf die Siedetemperatur. Aus diesem Grunde ist auch die aus Gl. (9) folgende, zu den Gln. (6) bzw. (8) analoge Beziehung

$$R_D + 0{,}098065\, M\varrho = f_R\left(\frac{\overline{R^2}}{a_1^2}\right) \qquad (10)$$

weniger zur Konformationsanalyse geeignet als die Beziehung (6) bzw. (8).*

Wie in III. 1 gezeigt wurde, hat bei Konfigurationsisomeren im allgemeinen die Verbindung mit dem größeren quadratischen Mittelwert des Radius die kleinere Dichte. Wegen des negativen Vorzeichens des Dichteterms addieren sich beide Terme der Gl. (9). Die Molrefraktion konfigurationsisomerer Verbindungen ist deshalb eine eindeutige Funktion des quadratischen Mittelwertes des Radius. Von zwei konfigurationsisomeren Verbindungen hat stets die mit dem größeren quadratischen Mittelwert des Radius die größere Molrefraktion. Wie Tab. I, in der die experimentell bestimmten Molrefraktionen den mittels Gl. (9) berechneten** gegenübergestellt sind, zeigt, ist dies stets der Fall.

* Unterscheidet sich die Größe $\overline{R^2}/a_1^2$ zweier isomerer Verbindungen um 0,2 Einheiten, so bedingt dies einen Unterschied von $\approx 0{,}035$ Einheiten in $f_R(\overline{R^2}/a_1^2)$. Dies ist vergleichbar mit der Fehlergrenze der meisten Messungen der Molrefraktion.

** In diesem Fall ist R_0 in Gl. (9b) durch einen Term $4{,}4620\, n_N$ ($n_N \triangleq$ Zahl der Stickstoffatome) zu ergänzen.

Es besteht schließlich noch die Möglichkeit, den Brechungsindex unmittelbar zur Konstitutionsermittlung heranzuziehen. Löst man Gl. (9) nach n auf, so erhält man

$$n = \sqrt{\frac{1+2x}{1-x}} \quad \text{mit} \quad x = \frac{R_D\,\varrho}{M} \quad \text{und} \quad R_D = R_D\left(\varrho;\ \frac{\overline{R^2}}{a_1^2}\right). \qquad (11)$$

Betrachtet man zwei isomere Verbindungen, so ist $n_2 \approx n_1$ und $\varrho_2 \approx \varrho_1$. Eine Reihenentwicklung ergibt für die Differenz der Brechungsindizes in erster Näherung

$$n_2 - n_1 = \left(\frac{dn}{d\varrho}\right)_{n_1} (\varrho_2 - \varrho_1) + \ldots .$$

Führt man die Differentiation unter Berücksichtigung der Gln. (3) und (9) aus, so erhält man

$$n_2 - n_1 \approx \frac{3}{2}\,\frac{1}{n_1(1-x_1)^2}\,\frac{1}{M}\left[\frac{dR_D}{d\varrho}\,\varrho + R_D\right](\varrho_2 - \varrho_1). \qquad (12)$$

Eine Abschätzung zeigt, daß bei den hier betrachteten Verbindungen stets $\left(\frac{dR_D}{d\varrho}\,\varrho\right) < R_D$ ist. Damit sind sämtliche in Gl. (12) eingehenden Terme positiv; die Differenz der Brechungsindizes ist damit im wesentlichen den Dichtedifferenzen proportional. Für den Brechungsindex gilt somit sinngemäß das für die Dichte in III.1 Gesagte. Von konfigurationsisomeren Verbindungen hat im allgemeinen die Verbindung mit dem größeren quadratischen Mittelwert des Radius den kleineren Brechungsindex. Ausnahmen sind — analog zur Dichte — bei den 3-Alkylcyclohexylaminen möglich.

IV. Vergleich der verschiedenen Methoden

Ein Vergleich der in III. zur Konstitutionsermittlung auf Grund der physikalischen Eigenschaften beschriebenen Methoden (s. Tab. II) ergibt, daß die Aussagefähigkeit der Funktionen $f_d(\overline{R^2}/a_1^2)$ [Gl. (6)] bzw. $f_n(\overline{R^2}/a_1^2)$ [Gl. (8)] am größten ist. Die Gl. (6) ist theoretisch fundierter; für die praktische Anwendung ist jedoch Gl. (8) überlegen, da die Bestimmung des Brechungsindex mit vergleichbarem experimentellem Aufwand mit größerer Genauigkeit möglich ist als die der Dichte.

Die Molrefraktion liefert ebenfalls eindeutige Aussagen über die Zuordnung der Konfigurationsisomeren; eine Zuordnung der Stellungsisomeren ist aus den in III.3 genannten Gründen nicht möglich. Mittels Dichte und Brechungsindex können ausschließlich Konfigurationsisomere zugeordnet werden. Aus den oben genannten Gründen ist der Brechungsindex hierfür die geeignetere Größe.

ZUSAMMENFASSUNG

Es wird gezeigt, daß die für acyclische und cyclische Alkane abgeleiteten Beziehungen zwischen Siedetemperatur, Dichte und Brechungsindex einerseits und dem quadratischen Mittelwert des (Trägheits-) Radius andererseits auch auf isomere Cyclohexylamine anwendbar sind. Die Möglichkeiten der Konformationsanalyse der Cyclohexylamine mittels Siedetemperatur, Dichte, Brechungsindex und einiger hieraus abgeleiteter Funktionen werden diskutiert.

LITERATUR

1. ALTENBURG, K.: Brennstoff-Chem. **47,** 331 (1966).
2. ALTENBURG, K.: Brennstoff-Chem. **47,** 100 (1966).
3. ALTENBURG, K.: *a)* Kolloid-Z. **178,** 112 (1961); Kolloid-Z. u. Z. Polymere **189,** 144 (1963); *b)* Z. physik. Chem. **228,** 120 (1965); *c)* Z. physik. Chem. **230,** 13 (1965); *d)* Z. physik. Chem. **231,** 77 (1966); *e)* Z. physik. Chem. **234,** 136 (1967).
4. TAYLOR, J. W.: J. chem. Physics **16,** 257 (1948).
5. Zusammenfassung der Ergebnisse: FELTKAMP, H. und THOMAS, K. D.: Liebigs Ann. Chem. **685,** 148 (1965).
6. VAN BEKKUM, H., VAN VEEN, A., VERKADE, P. E. und WEPSTER, B. M.: Recueil Trav. chim. Pays-Bas **80,** 1310 (1961).
7. LANDOLT-BÖRNSTEIN: Zahlenwerte und Funktionen. 6. Aufl., Springer-Verlag, Berlin—Göttingen—Heidelberg, 1951. 1. Band, 2. Teil, S. 16.
8. ALTENBURG, K.: Z. Chem. **7,** 164 (1967).
9. ALTENBURG, K.: Z. physik. Chem. **231,** 274 (1966).
10. ALTENBURG, K.: Z. Chem. **7,** 116 (1967).
11. ALTENBURG, K.: Z. Elektrochem., Ber. Bunsenges. physik. Chem. **65,** 805 (1961).
12. ALTENBURG, K. und GEY, E.: Z. physik. Chem. (im Druck).

K. ALTENBURG; 1199 Berlin-Adlershof, Rudower Chaussee 5, DDR

Acta Chimica Academiae Scientiarum Hungaricae Tomus 57 (1), pp. 111—118 (1968)

PROTONENRESONANZSPEKTROSKOPISCHE UNTERSUCHUNGEN UND BILDUNG VON O-ACETYL-D-GLUCONSÄURE-, -D-MANNONSÄURE- UND -D-XYLONSÄURE-(1,5)-LACTON-2,4-DINITRO-PHENYLHYDRAZON

F. RUFF,* I. SCHUSTER** und Á. GERECS

(Lehrstuhl für Chemische Technologie der Eötvös Loránd Universität, Budapest)

Eingegangen am 21. Juni 1967

Es wurde von uns früher beschrieben, daß sich bei der acetylierenden Ringspaltung aus den, eine Pyranose-Struktur besitzenden O-Acetyl-2,4-dinitrophenyl-»hydrazonen« von D-Glucose, D-Mannose und D-Xylose als Nebenprodukt je eine Verbindung von unbekannter Struktur bildete, wenn zum Essigsäureanhydrid ein wenig Chinolin (oder Pyridin) zugegeben wurde [1, 2]. Durch Mikroanalyse bzw. infrarot-spektroskopische Untersuchungen konnte festgestellt werden, daß diese Nebenprodukte in dem Dinitro-phenylhydrazin-Anteil nur eine NH-Gruppe enthalten, und daß das Glucose- und Mannose-Derivat 4, das Xylose-Derivat aber 3 Acetylgruppen besitzt. Die im Infrarot-Spektrum dieser Nebenprodukte bei 1670 cm^{-1} befindliche Bande von kleiner Intensität wurde der C=N Doppelbindung zugeordnet. Da aber die Bande dieser Doppelbindung im Spektrum des offenkettigen O-Pentaacetyl-D-glucose-, D-Mannose- bzw. O-Tetraacetyl-D-xylose-2,4-dinitrophenylhydrazons bei 1600 cm^{-1} erscheint, mußte angenommen werden, daß zwischen diesen Doppelbindungen charaktermäßig ein Unterschied besteht.

Weitere Aufschlüsse über die Struktur der betreffenden Verbindungen konnten von den kernresonanzspektroskopischen Untersuchungen erwartet werden. Auf Grund dieser erwiesen sich die erwähnten Nebenprodukte als O-Acetyl-aldonsäure-⟨1,5⟩-lacton-2,4-dinitro-phenylhydrazone. Neben den Acetylierungsnebenprodukten wurden parallel auch die betreffenden O-Acetyl-2,4-dinitro-phenylhydrazone von offenkettiger (I) und von Pyranose-Struktur (II) untersucht.

Vor der eingehenden Analyse der NMR-Spektren der betreffenden Verbindungen kann allgemein folgendes festgestellt werden. Bei der kleinsten Feldstärke (δ = 11,50—9,50 ppm) erscheint das Signal des Protons von der dem aromatischen Ring benachbarten NH-Gruppe. Die Signale der Protonen des aromatischen Anteiles im Bereich δ = 7,80—9,50 ppm zeigen die erwartete Aufspaltung, wogegen die Protonen des Monose-Anteiles im Bereich δ = 6,30—3,50 ppm ein kompliziertes System bilden.

* Lehrstuhl für Organische Chemie der Eötvös Loránd Universität, Budapest.
** Organisch-Chemisches Institut der Universität, Wien.

Die Protonen der Acetylgruppen bei $\delta = 2{,}60-2{,}00$ ppm geben meistens mehrere Signale, deren Aufspaltung aber bezüglich der räumlichen Stellung der Acetylgruppen keine weiteren Schlüsse mehr gestattet. Die Regeln von LEMIEUX und Mitarb. [3] konnten in diesem Fall nicht verwendet werden. Ähnliche Schwierigkeiten hatte auch ARNDT [4] bei der Untersuchung von

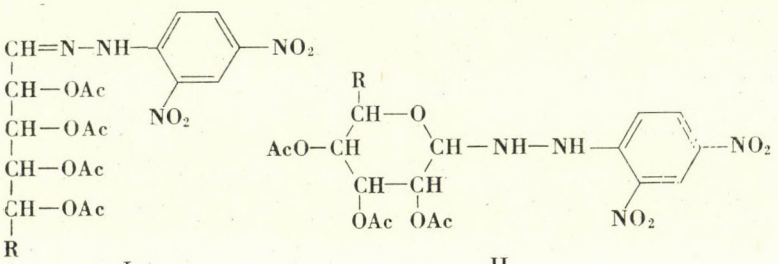

I

R = H, CH_2OAc

II

R = H, CH_2OAc

Glucopyranose-Derivaten. In unserem Fall wurde die Lage dadurch noch komplizierter, daß in den O-Acetyl-Hydrazonen von Pyranose-Struktur beide Anomere und auch diese in mehreren Konformationen anwesend sein können.

Untersuchung der offenkettigen O-Acetyl-monose-2,4-dinitro-phenylhydrazone (I)

Offenkettige O-Acetyl-monose-phenylhydrazone wurden mit NMR-Spektroskopie bisher nur von WOLFROM und Mitarb. untersucht [5]. Für unsere Arbeit erwiesen sich die Angaben von CURTIN und Mitarb. über die 2,4-Dinitrophenylhydrazone von Aldehyden und Ketonen [6] als besonders wertvoll, mit denen die von uns bestimmten chemische Verschiebungen der Protonen von C-1, NH und dem aromatischen Ring (Tab. I) übereinstimmen.

Das Signal des einzigen NH-Protons erschien infolge der mit der NO_2-Gruppe gebildeten Wasserstoffbrücke und der Nähe der C=N Gruppe bei sehr kleiner Feldstärke (Abb. 1). Neben den Signalen der Protonen des aromatischen Ringes befindet sich bei $\delta = 7{,}50$ ppm das Signal des Protons von C-1. Dieses Proton ist nur mit dem Proton von C-2 gekoppelt, dementsprechend zeigt dieses Signal eine Dublett-Aufspaltung von einer Kopplungskonstante 4—6 cps. Aus den Signalen der Protonen der aliphatischen Kette konnten bei den Hexose-Derivaten die Protonen von C-5 und C-6, bei dem Xylose-Derivat die von C-4 und C-5 identifiziert werden, welche bezüglich der CH_2-Gruppe ein ABX-System bilden. Bei größerer Feldstärke erscheinen die Signale der ein AB-System bildenden Protonen der CH_2-Gruppe (8 Linien). Die Protonen von C-5 (Hexose) bzw. C-4 (Pentose), welche den X-Anteil des Systems bilden,

Tabelle I

Chemische Verschiebung der Protonen der offenkettigen O-Acetyl-monose-2,4-dinitro-phenyl-hydrazone (δ, ppm)

Die Stelle der Protonen	Xylose-Der.	Glucose-Der.	Mannose-Der.
NH	11,23	11,28	11,21
Aromatischer Ring	9,18	9,18	9,17
	8,46	8,46	8,45
	7,95	7,99	8,02
C—1	7,54	7,60	7,51
C—2, C—3	5,70	5,70	5,65
C—4	5,57	5,54	5,65
C—5	4,30	5,20	5,24
C—6		4,27	4,24
Acetylgruppen	2,15	2,15	2,10
	2,10	2,03	2,05
	2,05		

zeigen anstatt des erwarteten Sextetts eine größere Aufspaltung, da diese nicht nur mit den Protonen von C-6 bzw. C-5, sondern auch mit dem Proton von C-4 bzw. C-3 gekoppelt sind. Überdies erscheinen im Bereich der Signale von Protonen des X-Anteiles noch die der Protonen von C-2 und C-3 in der Pentose bzw. von C-2, C-3 und C-4 in einer Hexose. Zahlenmäßig konnte also nur der AB-Anteil des ABX-Spektrums ausgewertet werden. Die Resultate wurden in der Tab. II zusammengefaßt.

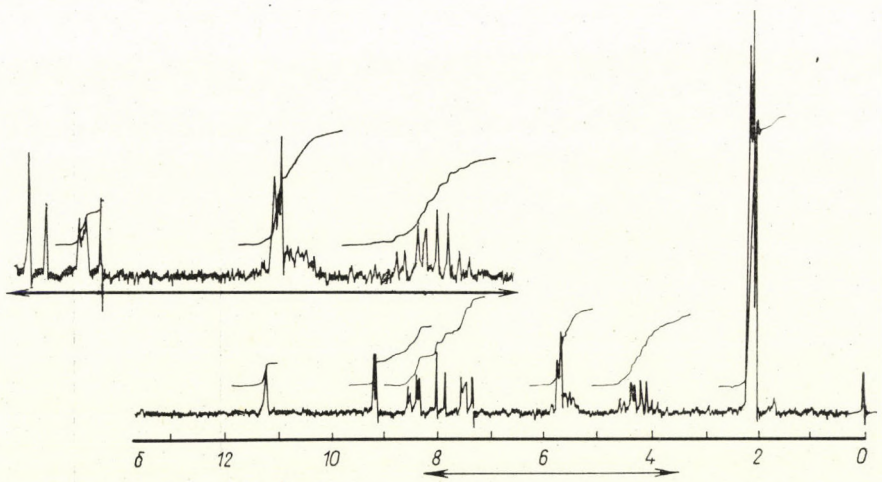

Abb. 1. NMR Spektrum des O-Tetraacetyl-D-xylose-2,4-dinitro-phenylhydrazons

Tabelle II

	J_{AB}	$\nu_0 \delta_{AB}$	$J_{AX}-J_{BX}$
O-Tetraacetyl-D-xylose-H*	12 cps	20,8 cps	2,3 cps
O-Pentaacetyl-D-glucose-H	12 cps	10,5 cps	2,3 cps
O-Pentaacetyl-D-mannose-H	12 cps	8,0 cps	3,6 cps

* H = 2,4-dinitro-phenylhydrazon

Untersuchung der O-Acetyl-monose-2,4-dinitro-phenylhydrazone von Pyranose-Struktur (II)

Unsere Resultate der NMR-Spektren von den entsprechenden D-Glucose-, D-Mannose- und D-Xylose-Derivaten wurden in Tab. III zusammengefaßt. Das Signal des Protons der neben dem aromatischen Ring befindlichen NH-Gruppe erschien bei größerer Feldstärke als bei den Verbindungen von offenkettiger Struktur, da in den Pyranose-Derivaten auch das andere Stickstoffatom ein Proton besitzt. Erwartungsgemäß zeigte sich kein an ein Kohlenstoffatom einer Doppelbindung angeschlossenes Proton. Aus der integralen Intensität der Signale der Protonen des Monose-Anteiles schien es, als wären im Monose-Anteil des D-Glucose- und D-Mannose-Derivates 8, des D-Xylose-Derivates aber 7 Protonen anwesend. Da aber in den entsprechenden Monose-Anteilen nur 7 bzw. 6 Protonen zu finden sind, ergibt sich, daß das Proton von

Tabelle III

Die chemische Verschiebung der Protonen der O-Acetyl-aldopyranose-2,4-dinitro-phenylhydrazone (δ, ppm)

Die Stelle der Protonen	Xylose-Der.	Glucose-Der.	Mannose-Der.
NH neben dem aromatischen Ring	9,72	9,75	9,72
Aromatischer Ring	9,14	9,13	9,14
	8,36	8,35	8,37
	7,59	7,60	7,76
NH neben dem Monose-Anteil und Monose-Anteil	5,79—3,04	5,57—3,87	5,74—3,80
Acetylgruppen	2,17	2,17	2,25
	2,03	2,12	2,13
		2,03	2,10
			2,07
			2,00

der zu C-1 benachbarten NH-Gruppe auch in diesem Bereich erscheint. Die Signale konnten den einzelnen Protonen nicht zugeordnet werden, da dieses Signal-System zu kompliziert ist (Abb. 2). Möglicherweise sind beide Anomere und auch diese in mehreren Konformationen anwesend.

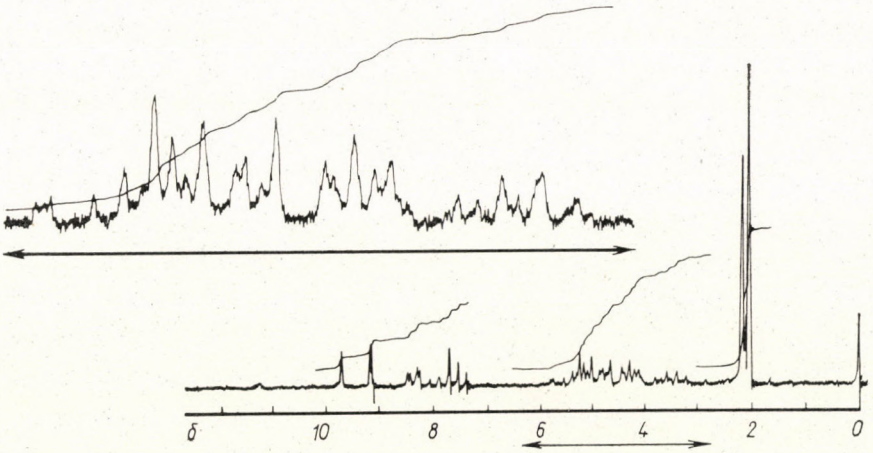

Abb. 2 NMR Spektrum des O-Triacetyl-D-xylose-2,4-dinitro-phenylhydrazons.

O-Acetyl-D-gluconsäure-, D-mannonsäure- und D-xylonsäure-⟨1,5⟩-lacton--2,4-dinitro-phenylhydrazon (III, IV, V, VI)

Im Spektrum dieser Verbindungen zeigt das Signal des Protons der dem aromatischen Ring benachbarten NH-Gruppe ähnliche chemische Verschiebung wie bei den offenkettigen Verbindungen (**I**) (Abb. 3, Tab. IV). Neben den Signalen der Protonen des aromatischen Anteiles erscheint kein Signal von einer CH Gruppe, d. h. auf C-1 befindet sich kein Proton; der Hydrazin-Anteil

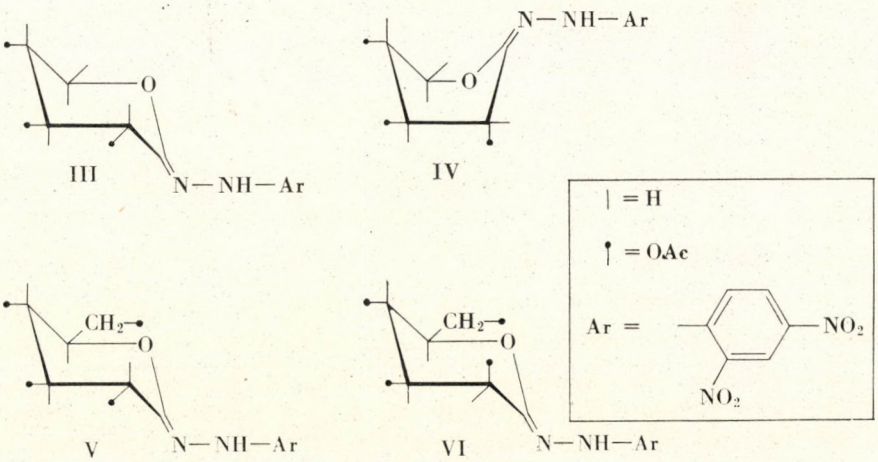

ist also mit einer C=N Doppelbindung an den Monose-Anteil gebunden. Im Xylose-Derivat enthält der Kohlenhydrat-Rest 5, im Glucose- und Mannose-Derivat aber 6 Protonen. Die integrale Intensität der Absorptionssignale der Acetylgruppen stimmen mit den durch Mikroanalyse erhaltenen bzw. berechneten Acetylzahlen überein.

Auf Grund dieser Feststellungen ergeben sich für die betreffenden Verbindungen Strukturen wie auf Seite 115 dargestellt.

Aus diesen Strukturen kann auch teilweise die Aufspaltung der Signale der Protonen des Monose-Anteiles erklärt werden. Im Spektrum des Xylose-Derivates (**III**) erscheint z. B. das Signal des Protons von C-2 als ein Dublett

Tabelle IV

Die chemische Verschiebung der Protonen der O-Acetyl-aldonsäurelacton-2.4-dinitro-phenyl-hydrazone (δ, *ppm*)

Die Stelle der Protonen	Xylose-Der.	Glucose-Der.	Mannose-Der.
NH	11,33	11,47	11,52
Aromatischer Ring	9,15	9,18	9,23
	8,38	8,43	8,45
	7,84	7,90	7,94
C—2	5,77	5,67	6,14
C—3, C—4	5,25	5,30	5,48
C—5	4,57	4,84	4,65
C—6		4,47	4,51
Acetylgruppen	2,23	2,22	2,63
	2,13	2,14	2,22
		2,10	2,17
			2,11

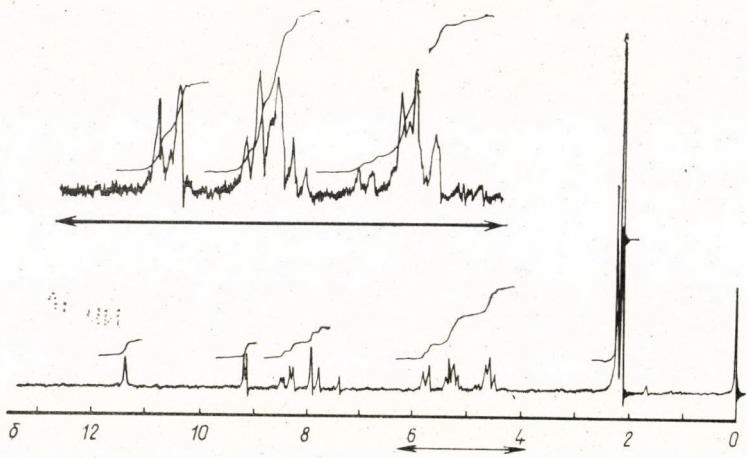

Abb. 3 NMR Spektrum des O-Triacetyl-D-xylonsäure-(1,5)lacton-2,4-dinitro-phenylhydrazons

mit 6 cps Kopplungskonstante, in Übereinstimmung mit der Lage, daß C-3 nur ein Proton besitzt, wobei die Größe der Kopplungskonstante die axiale-axiale Stellung dieser Protonen beweist. Bei größerer Auflösung (Abb. 3) erscheinen zwischen den Signalen des Dublettes in einer Entfernung von 2 cps zwei Signale von kleiner Intensität, welche der Anwesenheit der Konformation **IV** zugeschrieben werden können, wo die Protonen von C-2 und C-3 axiale-äquatoriale Stellung aufnehmen. Die Zuordnung der Signale der Protonen von C-3 und C-4 war noch nicht durchführbar. Die CH_2-Gruppe erscheint als AB-Anteil eines ABX-Systems ($J_{AB} = 12$ cps, $\nu_0\,\delta_{AB} = 11{,}2$ cps, $J_{AX} - J_{BX} = 4{,}4$ cps).

Die Analyse der NMR-Spektren des entsprechenden D-Glucose- und D-Mannose Derivates (**V** bzw. **VI**) führte zu ähnlichen Ergebnissen (Tab. IV).

Die Bildung der Lacton-hydrazone III—VI

In unserer vorigen Mitteilung über die Bildung dieser Verbindungen wurde beschrieben, daß sich aus den O-Acetyl-pyranose-2,4-dinitro-phenylhydrazonen mit Essigsäureanhydrid bei 80—100° diese Verbindungen bilden, wenn zum Essigsäureanhydrid ein wenig Chinolin (oder Pyridin) zugegeben wurde, wobei als Hauptprodukt das offenkettige O-Acetyl-monose-2,4-dinitro-phenylhydrazon erhalten wurde [2]. Aus den NMR-spektroskopischen Untersuchungen folgt, daß diese Lacton-hydrazone sich aus den Hydrazonen mit Pyranose-Struktur durch Abspaltung von 1 Mol Wasserstoff bilden. Diese Umwandlung kann eventuell dem Einfluß der aromatischen Nitro-Gruppe zugeschrieben werden. Die Struktur dieser Lacton-hydrazone steht im Einklang mit der Beobachtung, daß diese sich aus den offenkettigen O-Acetyl-monose-hydrazonen nicht bilden.

In Kenntnis der obigen Tatsachen konnten die betreffenden Lactonhydrazone auch durch Oxydation erhalten werden. Die Oxydation wurde in Essigsäure mit 0,1 *n* $KMnO_4$, in Anwesenheit von wäßriger Schwefelsäure durchgeführt. Als Beispiel wird die Oxydation von O-Tetraacetyl-D-mannose-2,4-dinitro-phenylhydrazon beschrieben, weil sich in diesem Fall die besten Resultate ergaben.

Beschreibung der Versuche

Oxydation von O-Tetraacetyl-D-mannose-2,4-dinitro-phenylhydrazon

0,523 g O-Tetraacetyl-D-mannose-2,4-dinitro-phenylhydrazon wurden bei Zimmertemperatur in 12 ml Eisessig gelöst, die Lösung wurde mit 2 ml 10%iger Schwefelsäure und danach in 0,5—1,0-ml-Portionen mit 21 ml 0,1 *n* $KMnO_4$ versetzt. Es konnte kein Endpunkt beobachtet werden. Die Lösung wurde mit 100 ml Wasser verdünnt und der entstandene Niederschlag mit Äthylacetat extrahiert. Rückstand der mit $NaHCO_3$ neutralisierten Äthylacetat-Lösung: 0,502 g; aus 37 ml Methanol umkristallisiert: 0,360 g, Fp.: 176—177°, $[\alpha]_D^{20} = -111{,}5°$ ($CHCl_3$, c = 0,879).

Das Produkt eines anderen Versuches: Fp.: 176—177°, $[\alpha]_D^{20} = -107{,}9°$ ($CHCl_3$, c = 0,816). Fp. des bei der Acetylierung als Nebenprodukt erhaltenen Produktes: 178° [2]. Die auf verschiedenem Weg dargestellten Substanzen gaben keine Schmelzpunktdepression.

$C_{20}H_{22}N_4O_{13}$ (526,428). Ber. C 45,63%; H 4,21%; N 10,64%. Gef. C 45,61%, 45,74%; H 4,13%, 4,15%; N 10,61%, 10,68%.

In unserer Mitteilung [2] wurde für dieses Mannose-Derivat irrtümlicherweise das spez. Drehungsvermögen des Rohproduktes (—94,8°) angegeben. Durch Umkristallisieren erhöhte sich der Schmelzpunkt nicht, dagegen ergab sich folgendes spez. Drehungsvermögen: $[\alpha]_D^{20} = -111{,}2°$ ($CHCl_3$, c = 0,0836).

Auf ähnliche Weise wurden auch die entsprechende D-Glucopyranose- und D-Xylopyranose-Derivate oxydiert. Aus 0,520 g O-Tetraacetyl-D-glucopyranose-2,4-dinitro-phenylhydrazon wurden 0,087 g (Fp.: 192—194°; Fp. des Nebenproduktes der Acetylierung [2] 197°) und aus 0,458 g O-Triacetyl-D-xylopyranose-2,4-dinitro-phenylhydrazon wurden 0,185 g (Fp.: 192—194°; Fp. des Nebenproduktes der Acetylierung [2] 194—195°) einmal umkristallisiertes entsprechendes Lacton-hydrazon erhalten.

Die Spektren wurden auf einem *Varian A-60-A*-Instrument in Deuterochloroform bei Zimmertemperatur aufgenommen. Als innerer Standard diente Tetramethylsilan (TMS).

*

Wir danken auch an dieser Stelle Herrn Prof. F. WESSELY, daß er einem von uns (F. RUFF) die Durchführung der NMR-spektroskopischen Untersuchungen ermöglichte.

Frau M. BALOGH danken wir für die Mikroanalysen und Frau M. BARTA für die wertvolle Hilfe.

ZUSAMMENFASSUNG

Es wurde durch protonenresonanzspektroskopische Untersuchungen festgestellt, daß sich aus O-Acetyl-D-glucopyranose-, -D-mannopyranose- und -D-xylopyranose-2,4-dinitrophenylhydrazon durch ringspaltende Acetylierung, in Anwesenheit von wenig Chinolin (oder Pyridin), als Nebenprodukt das entsprechende O-Acetyl-aldonsäure-⟨1,5⟩-lacton-2,4-dinitrophenylhydrazon bildete. Diese Lactonhydrazone wurden auch durch Oxydation mit $KMnO_4$ aus den gleichen Ausgangsverbindungen erhalten.

LITERATUR

1. GERECS, Á., FÓTI, A.: Acta chim. Acad. Sci. hung. **35,** 217 (1963).
2. GERECS, Á., FÓTI, A., RUFF, F.: Acta chim. Acad. Sci. hung. **42,** 145 (1964).
3. LEMIEUX, R. U., KULLNIG, R. K., BERNSTEIN, H. J., SCHNEIDER, W. G.: J. Am. Chem. Soc. **79,** 1005 (1957).
4. ARNDT, O.: Annalen **695,** 176 (1966).
5. WOLFROM, M. L., FRAENKEL, G., LINEBACK, D. R., KOMITSKY, F.: J. Org. Chem. **29,** 457 (1964).
6. CURTIN, D. V., GOURSE, J. A., RICHARDSON, W. H., RINEHART, K. L.: J. Org. Chem. **24,** 93 (1959).

Ferenc RUFF; Budapest VIII. Múzeum krt. 4/b.
Inge SCHUSTER; Wien IX. Währingerstraße 38.
Árpád GERECS; Budapest VIII. Múzeum krt. 6—8.

Acta Chimica Academiae Scientiarum Hungaricae Tomus 57 (1), pp. 119—122 (1968)

REARRANGEMENTS OF STEROIDS, V

SCHMIDT REACTION AND BECKMANN REARRANGEMENT OF ESTRONE AND OF ITS DERIVATIVES

(PRELIMINARY COMMUNICATION)

B. MATKOVICS, G. GÖNDÖS and B. TARÓDI

(Institute of Organic Chemistry, A. József University Szeged)

Received July 21, 1967

Subsequent to the investigations of REGAN and HAYES [1], we studied the chemical properties of the 17-aza-17a-oxo-D-homosteroids and 17a-aza-17-oxo-D-homosteroids which can be prepared from estrone and its derivatives. The thin-layer chromatographic properties of these compounds have already been summarized [2].

In this communication, we are dealing with the Schmidt reaction and with the *Beckmann* rearrangement of estrone (*i.e.* of 3-hydroxyestra-1,3,5-(10)-triene-17-one) and of its derivatives.

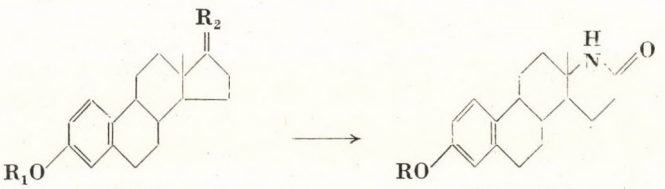

I—VIII. **IX—XII**

IX : R = H; **XI** : R =
X : R = CH_3 ; **XII** : R = $COCH_3$

I: R_1 = H; R_2 = 0 (estrone)
II: R_1 = H; R_2 = N.OH (estrone-17-oxime)
III: R_1 = CH_3 ; R_2 = 0 (estrone-3-methylether)
IV: R_1 = CH_3 ; R_2 = N.OH (estrone-3-methylether-17-oxime)
V: R_1 = (cyclopentyl radical); R_2 = 0 (estrone-3--cyclopentylether)
VI: R_1 = $\}-\langle$ (C_5H_9) R_2 = N.OH (estrone-3-cyclopentylether-17--oxime)
VII: R_1 = CO · CH_3; R_2 = 0 (estrone-3-acetate)
VIII: R_1 = CO · CH_3; R_2 = N.OH (estrone-3-acetate-17-oxime)

Our investigations, in part, may be summerized by the chart of formulas given below.

The Schmidt reaction was carried out with the ketones **I, III, V** and **VII**, while the Beckmann rearrangement was effected with the oximes **II, IV, VI** and **VIII**, in the presence of *p*-acetamidobenzenesulphonyl chloride, in pyridine or thionyl chloride [3]. The lactams obtained as products in both these reactions

were compared, and their structures were proved by reducing them to known D-homo-aza-steroids. In the Beckmann rearrangement of **II** and **VIII**, small amounts of the seco-nitriles **XIII** and **XIV** were also obtained. The Schmidt

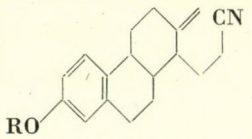

XIII—XIV

XIII: R = H; **XIV**: R = CO · CH_3

reaction of the ketones was carried out by several methods. The best route proved to be the reaction with a benzene solution of titrated hydrazoic acid, at room temperature, in the presence of concentrated sulphuric acid [4]. Interestingly, in the case of estrone and its derivatives, the Schmidt reaction gave the same D-homolactams, as main products, which were obtained in the Beckmann rearrangements. This is in contrast to our experiences made with other compounds, *e.g.* with 6-ketoandrostane-3 β, 17 β-diol-diacetate [5]. However, another lactam was formed as a by-product in minute amounts. (The structures of these lactams will be discussed later.)

The structures of the unsaturated seco-nitriles **XIII** and **XIV** were proved by converting them, by alkaline hydrolysis, into the corresponding secocarboxylic acids [3]. In addition, the unsaturated nitrile structure was unequivocally proved by the infrared spectra of the seco-nitriles **XIII** and **XIV**.

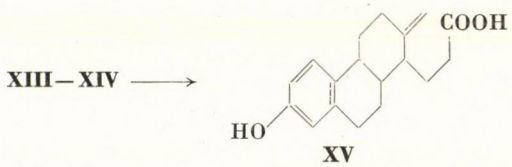

XV

The 17a-aza-17-oxo-D-homosteroids were converted with lithium aluminium hydride into the corresponding 17a-aza-D-homosteroid (**XVI**) which was, in turn treated with acetic anhydride to obtain the N-acetyl-D-homosteroid (**XVII**). In each case, the same 17a-aza-D-homoestra-1,3,5-(10)-triene-3-acetate N-acetyl derivative was isolated as the end product.

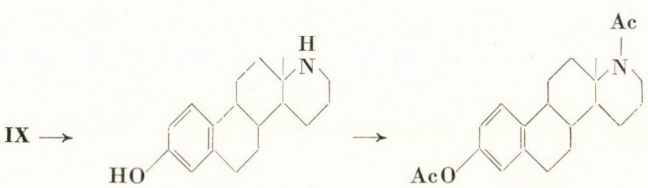

XVI **XVII**

On the basis of the reaction with concentrated sulphuric acid, the D-homolactam, formed in the Beckmann rearrangement and isolated in addition to the D-homolactams formed as the main products of the Schmidt reaction of **I, III, V** and **VII**, has presumably the following structure:

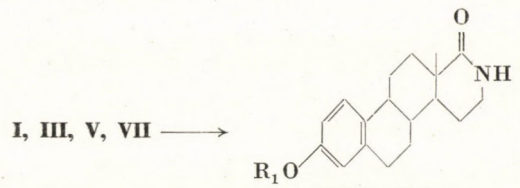

XVIII—XIX

Discussion of the experimental results

In the case of estrone, as mentioned above, the Schmidt rearrangement gives 17a-aza-D-homoestra-1,3,5-(10)-triene-3-ol-17-one (**IX**) as the main product, which can be isolated in the Beckmann rearrangement. However, small amounts of another D-homolactam (**XVIII**) are formed. In the case of compound **II**, our attempts to isolate the stereoisomeric oximes failed. REGAN *et al.* are probably right in assuming that compound **II** melting over a broad range contains, instead of the isomeric pair of ketoximes, the ketoxime mixed with some of its hydrated forms, or that this is a case of polymorphism depending on the crystallizing solvent. In the case of the 17-oximes of **III, IV, VI** and **VIII**, we succeeded in isolating the stereoisomeric modifications by means of our usual technique of column and thin-layer chromatography.

As regards the Beckmann rearrangement of **II**, we isolated, in addition to **IX**, the unsaturated seco-nitrile **XIII**. This points to the fact that a Beckmann rearrangement "of second order" takes place in the case of **II** as well [3, 6]. The same phenomenon was also observed in the Beckmann rearrangement of **VIII** where, in addition to **XII, XIII** and **XIV** could be isolated. Interestingly, in the case of the 17-oximes of the alkyl ethers (**IV, VI**), the formation of nitriles could not be detected. The Schmidt reaction of **III** and **V** gave the 17a-aza-17-oxo-D-homoestra-1,3,5-(10)-triene-3-yl ethers **X** and **XI** as main products, besides some unchanged initial substance. Of these products, the structure of **X** is already known [1], while the structure of **XI** could be reduced, by applying a mild hydrolysis, to that of **IX**.

The other group (**XVIII** to **XXI**) of the D-homolactams, which can be frequently detected only in minute amounts, loses CO in hot concentrated sulphuric acid. Thus, these compounds presumably are hydrolyzed to products which contain a tertiary carboxyl group.

SUMMARY

In order to prepare D-homolactams, various ethers and the acetate of estrone (**I, III, V, VII**) were subjected to Schmidt reaction. A similar technique was followed in the case of the oximes of the mentioned 17-ketones (**II, IV ,VI** and **VIII**), with the difference that the D-homolactams were prepared here by Beckmann rearrangement. Both rearrangements gave, as main products, the same 17a-aza-17-oxo-D-homoestra-1,3,5-(10)-triene-3-ol or its partly known, partly novel derivatives. In the case of **II** and **VIII**, the Beckmann rearrangement of "first order" was followed by a "second order" reaction, as proved by the isolation of the unsaturated seco-nitriles **XIII** and **XIV**, and of the unsaturated seco-carboxylic acid **XV** derived from this product. The formation of 17-aza-17a-oxo-D-homoestra-1,3,5-(10)-triene-3-ol and of its derivatives points to differences in the conditions of the Schmidt reaction and in stabilization of the intermediary products [7].

REFERENCES

1. REGAN, B. M., HAYES, F. N.: J. Am. Chem. Soc. **78,** 639 (1956).
2. MATKOVICS, B., GÖNDÖS, GY.: Microchem. J. (In press.)
3. MATKOVICS, B., GÖNDÖS, GY., TEGYEY, ZS.: Magyar Kém. Foly. **72,** 303 (1966).
4. WOLFF, H.: Org. Reactions **3,** 307 (1946).
5. MATKOVICS, B., TEGYEY, ZS.: Acta Chim. Acad. Sci. Hung. (In press.)
6. FERRIS, A. F.: J. Org. Chem. **25,** 12 (1960).
7. GÖNDÖS, GY., MATKOVICS, B.: Lecture presented at the Conference of the Hungarian Chemical Society, Pécs, August 24—26, 1967. (Lecture abstract p. 82) (In Hungarian).
8. SHOPPEE, C. W., LACK, R. E., ROY, S. K.: J. Chem. Soc. **1963,** 3767.

Béla MATKOVICS
György GÖNDÖS
Béla TARÓDI

Szeged, Dóm tér 8.

Acta Chimica Academiae Scientiarum Hungaricae Tomus 57 (1), pp. 123—127 (1968)

EINE EINFACHE MIKROMETHODE ZUR BESTIMMUNG DER TERT. BUTYLOXYCARBONYL-SCHUTZGRUPPE VERSCHIEDENER AMINOSÄUREN UND IHRER DERIVATE

S. KUTASSY, J. KAJTÁR und H. MEDZIHRADSZKY-SCHWEIGER

(Organisch-Chemisches Institut der L. Eötvös Universität, Budapest)

Eingegangen am 7. September 1967

Eine der wichtigsten Aminoschutzgruppen, die in die Peptidchemie Eingang gefunden haben, ist die *tert.* Butyloxycarbonylgruppe (BOC-Gruppe). Im Laufe von Peptidsynthesen ist die genügende Reinheit der Zwischenprodukte, z. B. der BOC-Derivate der Aminosäuren oder Peptide bzw. ihrer Ester eine wesentliche Forderung. Es ist vor allem angezeigt sich zu vergewissern, ob die Blockierung der Aminogruppe auf quantitative Art erfolgt ist. Darüber gibt die übliche Elementaranalyse nicht immer genügenden Aufschluß, da zwischen der elementaren Zusammensetzung der Zwischenprodukte mit freier und blockierter Aminogruppe oft nur ein geringer Unterschied besteht. Die Möglichkeit einer unmittelbaren Bestimmung der BOC-Gruppe gewährt somit eine verläßlichere Reinheitsprüfung der BOC-Derivate als ihre Elementaranalyse.

Zur Bestimmung der BOC-Gruppe läßt sich ihre Spaltbarkeit durch Säuren [1] verwerten, die folgend verläuft:

$$(CH_3)_3C-O-\overset{\overset{O}{\|}}{C}-HNCHCOOH+HX \longrightarrow (CH_3)_2C=CH_2+XH_3NCHCOOH+CO_2$$
$$\qquad\qquad\qquad\qquad\quad \underset{R}{|} \qquad\qquad\qquad\qquad\qquad\qquad\quad \underset{R}{|}$$

Dabei wird Isobutylen nicht quantitativ gebildet, da z. B. in salzsaurem Medium (X=Cl) auch die Entstehung von *tert.* Butylchlorid (selbstredend auf Kosten des Isobutylens) nachweisbar ist [2]. Hingegen wird Kohlendioxyd quantitativ freigesetzt und kann somit als Maß der BOC-Gruppe dienen, umsomehr, als zur Bestimmung des Kohlendioxyds mehrere verläßliche Methoden entwickelt worden sind.

Im Laufe von Peptidsynthesen wird zur Abspaltung der BOC-Gruppe, d. h. zur Regenerierung der Aminogruppe zumeist Trifluoressigsäure ($X=CF_3COO$) oder Salzsäure (X=Cl) angewandt. Die Reaktion verläuft schon bei Raumtemperatur und ist in der Regel in einigen Minuten beendet. Die im Überschuß angewandte Trifluoressigsäure dient zugleich als Lösungsmittel, während bei Anwendung von Salzsäure Benzol, Diäthylphosphit oder Äthylacetat als Lösungsmittel gebraucht werden kann [3].

Bei präparativen Arbeiten ist die leichte Entfernbarkeit durch Destillation der angewandten Säure erwünscht, hingegen läßt sich die genaue Bestimmung des frei gewordenen Kohlendioxyds nur dann auf einfache Art durchführen, wenn zur Spaltung der BOC-Gruppe eine schwerflüchtige Säure herangezogen wird. Salzsäure und Trifluoressigsäure kamen deshalb nicht in Frage, gut bewährt hat sich aber Schwefelsäure. Um die Löslichkeit der BOC-Derivate zu sichern, wurde ein Schwefelsäure-Alkohol-Wasser Gemisch (2 : 1 : 1 Raumteile) angewandt.

Als Reaktionsgefäß konnte das zur Bestimmung der Aminosäure- und Peptidhydrazide dienende Gerät [4] verwendet werden; das entwickelte Kohlendioxyd wurde einerseits gravimetrisch, andererseits maßanalytisch bestimmt. Im ersten Fall wurde ein mit Natronasbest gefülltes Absorptionsröhrchen nach PREGL [5], im zweiten Fall — wie bei der Bestimmung der Carbobenzyloxygruppe [6] — eine alkoholische Cyclohexylaminlösung zum Abfangen des Kohlendioxyds angewandt. Wie bekannt, bildet das Kohlendioxyd in alkoholischer Lösung mit Cyclohexylamin das Cyclohexylammoniumsalz der N-Cyclohexylcarbaminsäure ($C_6H_{11}HNCOOH_3NC_6H_{11}$), dessen Menge mit Hilfe einer 0,02 N Natriummethylatlösung, unter Anwendung von Thymolblau als Indikator, maßanalytisch bestimmt werden kann. Vor der Spaltung des BOC-Derivats wird die Luft aus der Apparatur mit kohlensäurefreiem Stickstoff verdrängt, der später auch zum Hineinspülen des entstandenen Kohlendioxyds in das Absorptionsgefäß dient.

Enthält die Substanz außer BOC-Gruppen auch andere Aminoschutzgruppen vom Typ eines Urethans, wie z. B. N-Carbobenzyloxygruppen, so kann das beschriebene Verfahren zur selektiven Bestimmung der BOC-Gruppen nicht verwendet werden, da durch Schwefelsäure auch N-Carbobenzyloxygruppen unter Entwicklung von Kohlendioxyd zersetzt werden. Zur selektiven Spaltung der BOC-Gruppe ist die Trifluoressigsäure geeignet, die aber wegen ihrer Flüchtigkeit vom entstandenen Kohlendioxyd getrennt werden müßte, wollte man dieses bestimmen. PATCHORNIK und SHALITIN [7] haben bei ihrer maßanalytischen Kohlendioxydbestimmung zum Abfangen der sauren Begleitstoffe des Kohlendioxyds alkoholische Pyridinlösung verwendet, jedoch hat sich dieses Verfahren beim Versuch, die BOC-Gruppe neben der N-Carbobenzyloxygruppe (durch selektive Spaltung der ersteren mit Trifluoressigsäure) zu bestimmen, nicht bewährt. Hingegen ließ sich die aus dem Reaktionsgefäß vom Gasstrom mitgerissene Trifluoressigsäure durch eine mit Aceton-Kohlensäure stark gekühlte (−70°) Falle leicht abfangen, d. h. vom Kohlendioxyd trennen.

Zu Serienanalysen ist die Spaltung mit Schwefelsäure und gravimetrische Bestimmung des Kohlendioxyds am besten geeignet. Die Spaltung mit Trifluoressigsäure haben wir wegen der Umständlichkeit des Verfahrens nur zur selektiven Bestimmung der BOC-Gruppe neben der N-Carbobenzyloxygruppe herangezogen.

Durchführung der Bestimmung

a) Gravimetrisches Verfahren

Als Reaktionsgefäß kann das zur Bestimmung der Hydrazide konstruierte Gerät (Abb. 1) dienen. Das mit Henkel versehene Wägegläschen, in das man 15—20 mg der zu untersuchenden Substanz eingewogen hat, wird an den Platinhaken des eingeschliffenen Glasstopfens gehängt, dann der Stopfen in seinen Schliff hineingesetzt. An das andere Ende des Reaktionsgefäßes, das mit 2 ml Schwefelsäurelösung (Schwefelsäure : Alkohol : Wasser 2 : 1 : 1 Raumteile) beschickt worden ist, werden nach einander zwei Preglsche Absorptionsröhrchen angeschlossen. Die Füllung des ersten Röhrchens besteht aus mit Phosphorpentoxyd imprägnierten Siedesteinchen, des zweiten aus Natronasbest. Nun läßt man zuerst 10 Minuten lang einen langsamen Stickstoffstrom durch die Apparatur streichen und wägt nachher das CO_2-Absorptionsröhrchen ab. Nach wiederholter Anschaltung dieses Röhrchens läßt man durch Umdrehen des Glasstopfens das Wägegläschen in die Säurelösung fallen. Nachdem sich die Substanz aufgelöst und die Gasentwicklung aufgehört hat, läßt man durch den Apparat noch weitere 20—25 Minuten den Stickstoffstrom streichen. (Im Falle schwer löslicher Substanzen wird die Säure gelinde erwärmt.) Diese Zeit genügt zum vollständigen Hinausspülen und Abfangen des entwickelten Kohlendioxyds, so daß die Gewichtszunahme des Absorptionsröhrchens bestimmt werden kann.

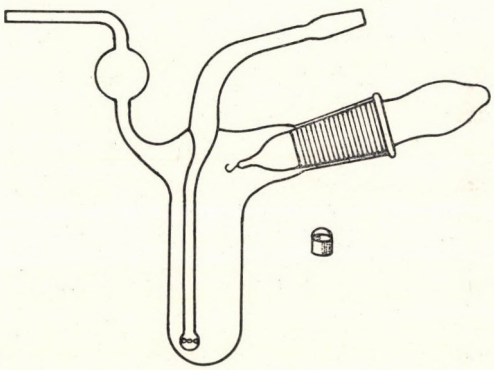

Abb. 1

b) Massanalytisches Verfahren

Die Spaltung der BOC-Gruppe wird wie unter a) durchgeführt, nur verwendet man anstatt des mit Natronasbest beschickten Absorptionsröhrchens ein Rohr, das mit einem 1 : 3-Gemisch von Cyclohexylamin und absol. Alkohol benetzte Glasspiralstückchen enthält. Nach beendeter Reaktion und Überspülung des Kohlendioxyds in die Reagenslösung wird diese mit der beim Blindversuch (s. unten) angewandten Menge absol. Alkohols in einen Kolben hineingespült und nachher, in Anwesenheit einer 0,2%igen Thymolblau-Indikatorlösung, mit einer nach Fritz und Lisicki [8] bereiteten 0,02 N Natriummethylatlösung titriert. Dazu dient am zweckmäßigsten eine Mikrobürette; das Kohlendioxyd der Luft muß selbstredend auch während der Titrierung ausgeschlossen werden. Wegen der Empfindlichkeit der Reagenslösung ist es angezeigt, einen Blindversuch durchzuführen und dessen Ergebnis als Korrektion in Betracht zu ziehen.

c) Spaltung mit Trifluoressigsäure

Man arbeitet nach dem gravimetrischen Verfahren, nur wird Trifluoressigsäure anstatt der alkoholisch-wäßrigen Schwefelsäure gebraucht und zwischen das erste Absorptionsröhrchen und das Reaktionsgefäß eine aus drei leeren Waschfläschchen bestehende, in ein mit Aceton-Kohlensäure gefülltes Dewar-Gefäß getauchte Falle zum Kondensieren der mitgeschleppten Säuredämpfe angewendet.

Substanz*	Summenformel	Mol. gew.	CO_3% ber.	CO_3% gefunden				BOC% ber.	BOC% gefunden			
				gravimetrisch		maßanalytisch			gravimetrisch		maßanalytisch	
BOC-Gly	$C_7H_{13}O_4N$	175,2	25,12	25,00;	25,09	25,04;	24,93	57,65	57,27;	57,55	57,48;	57,21
BOC-Ser-N_2H_3	$C_8H_{17}O_4N_3$	219,2	20,07	19,79;	19,86	20,01;	20,13	46,07	45,41;	45,57	46,22;	45,94
BOC-Pro	$C_{10}H_{17}O_4N$	215,2	20,45	20,74;	20,56	20,22;	20,56	46,93	47,60;	47,17	46,40;	47,17
BOC-Ala	$C_8H_{15}O_4N$	189,2	23,26	23,16;	23,06	23,13;	23,24	53,38	53,15;	52,92	53,10;	53,34
BOC-Val. DCHA	$C_{22}H_{42}O_4N_2$	398,6	11,04	11,07;	11,25	11,02;	11,08	25,34	25,40;	25,81	25,28;	25,43
BOC-Gln. DCHA	$C_{22}H_{41}O_5N_3$	427,6	10,29	10,50;	10,43	10,24;	10,43	23,62	24,10;	23,93	23,50;	23,93
BOC-Met. DCHA	$C_{22}H_{42}O_4N_2S$	430,6	10,22	10,08;	10,02	10,16;	10,00	23,45	23,14;	23,00	23,32;	22,96
BOC-Phe. DCHA	$C_{26}H_{42}O_4N_2$	446,6	9,85	9,73;	9,84	9,67;	9,62	22,62	22,33;	22,58	22,20;	22,10
BOC-Glu(OBut). DCHA	$C_{26}H_{48}O_6N_2$	484,7	9,08	9,20;	9,04	8,97;	9,17	20,84	21,13;	20,75	20,61;	21,06
BOC-Asp(OBut)	$C_{13}H_{23}O_6N$	289,3	15,21	15,40;	15,32	15,04;	15,11	34,91	35,35;	35,16	34,53;	34,66
BOC-Asp(OBut). DCHA	$C_{25}H_{46}O_6N_2$	470.6	9,35	9,34;	9,23	9,41;	9,32	21,46	21,20;	21,44	21,40;	21,61
BOC-Glu(OBzl). DCHA	$C_{29}H_{46}O_6N_2$	518,7	8,48	8,42;	8,50	8,40;	8,41	19,47	19,32;	19,52	19,30;	19,32
BOC-Ser(OBzl). DCHA	$C_{27}H_{44}O_5N_2$	476,6	9,23	9,12;	9,23	9,09;	9,14	21,20	20,94;	21,20	20,88;	21,00
Z-Lys(BOC)-OMe	$C_{20}H_{30}O_6N_2$	394,5	22,31	22,57;	22,66	22,29;	22,46					
Z-Lys(BOC)-OMe	$C_{20}H_{30}O_6N_2$	394,5	11,15	10,95;	10,98			25,60	25,13;	25,20		

* Siehe Fußnote auf S. 127.

Die mit Hilfe der drei Verfahren gewonnenen Ergebnisse sind in der Tabelle zusammengefaßt. Als Testsubstanzen wurden in unserem Institut synthetisierte Verbindungen herangezogen; von ihrer Reinheit haben wir uns durch Anwendung anderer Analysen überzeugen können. In der Tabelle sind die mit den Verfahren a) und b) erhaltenen Meßergebnisse einerseits auf den CO_2-Gehalt, andererseits auf den *tert.* Butyloxycarbonyl-Gehalt der Substanz, in Prozente umgerechnet, angegeben. Im Falle der Analyse vom Z-Lys (BOC)-OMe* ist nur auf den CO_2-Gehalt umgerechnet worden, da das aus der N-Carbobenzyloxygruppe und aus der *tert.* Butyloxycarbonyl-Gruppe stammende Kohlendioxyd zusammen gemessen wurde. Die letzte Zeile der Tabelle enthält die nach selektiver Spaltung mit Trifluoressigsäure bestimmte BOC-Gruppe in CO_2- und auch in BOC-Prozenten angegeben.

Herrn Prof. V. BRUCKNER sei für die Anregung dieser Arbeit und für die wertvollen Ratschläge auch an dieser Stelle gedankt.

ZUSAMMENFASSUNG

Es wird eine einfache Bestimmung der BOC-Gruppe beschrieben, die darauf beruht, daß sich diese Gruppe in alkoholischer Lösung mittels Schwefelsäure unter Freisetzung von Kohlendioxyd spalten läßt. Das Kohlendioxyd kann gravimetrisch oder maßanalytisch bestimmt werden.

LITERATUR

1. ANDERSON, G. W., MCGREGOR, A. C.: J. Am. Chem. Soc. **79,** 6180 (1957).
2. SCHRÖDER, E., LÜBKE, K.: "The Peptides". Academic Press, New York, 1965. Vol. I. p. 39.
3. SCHRÖDER, E., LÜBKE, K.: "The Peptides". Academic Press, New York, 1965. Vol. I. p. 39.
4. MEDZIHRADSZKY-SCHWEIGER H.: Acta Chim. Acad. Sci. Hung. **34,** 213—216 (1962).
5. PREGL-ROTH: "Quantitative organische Mikroanalyse". Springer Verlag, 1958, S. 46.
6. MEDZIHRADSZKY-SCHWEIGER, H., KAJTÁR, J.: Acta Chim. Acad. Sci. Hung. **42,** 317 (1964).
7. PATCHORNIK, A., SHALITIN, Y.: Anal. Chem. **33,** 1887 (1961).
8. FRITZ, J. S., LISICKI, N. M.: Anal. Chem. **23,** 589 (1951).

Sára KUTASSY
Judit KAJTÁR
Hedvig MEDZIHRADSZKY-SCHWEIGER

Budapest VIII., Múzeum krt. 4/b.

* Die Abkürzungen richten sich nach den Vorschlägen der *Comission on Biochemical Nomenclature* (J. Biol. Chem. **241**, 527 (1966).

INDEX

INORGANIC AND ANALYTICAL CHEMISTRY — ANORGANISCHE UND ANALYTISCHE CHEMIE — НЕОРГАНИЧЕСКАЯ И АНАЛИТИЧЕСКАЯ ХИМИЯ

MISHRA, M. B. and NIGAM, H. L.: Complex Formation Between Uranyl (VI) and Thiopropionic Acid 1

GÁBOR-KLATSMÁNYI, P., INCZÉDY, J. and ERDEY, L.: The Use of Ammonium Sulphosalicylate as Complexing Agent in Ion Exchange Chromatography, II. Stability of the Sulphosalicylate Complexes of Copper (II), Nikkel (II) and Cobalt (II) at 80° C 5

PHYSICAL CHEMISTRY — PHYSIKALISCHE CHEMIE — ФИЗИЧЕСКАЯ ХИМИЯ

SOLYMOSI, F.: Thermal Stability of Chlorine Oxy-Salts in the Solid State, IV. Kinetics and Mechanism of the Thermal Decomposition of Alkali Perchlorates 11

SOLYMOSI, F.: Thermal Stability of Chlorine Oxy-Salts in the Solid State, V. Thermal Decomposition of Some Divalent Metal Perchlorates 35

VARSÁNYI, G.: Characteristic Normal Vibrations of Benzene Derivatives, III. Correlation Among the Frequency and Vibrational Form of the Out-of-Plane CH Vibrations 51

COHEN-ADAD, R., TRANQUARD, A. et MARCHAND, A.: Sur quelques problèmes posés par l'étude, à temperature élevée, des equilibres liquide-solide dans les systèmes contenant un constituant volatil 69

Мардашев, Ю. С.: К кинетике дегидрирования C_6H_{12} над никелевыми катализаторами 83

ORGANIC CHEMISTRY — ORGANISCHE CHEMIE — ОРГАНИЧЕСКАЯ ХИМИЯ

VINKLER, E. and KLIVÉNYI, F.: Recent Results Concerning the Reaction of Aromatic Thiolsulfinates with Dinitrochlorobenzene 91

ALTENBURG, K.: Zur Anwendung einiger Konformationsregeln auf Cyclohexylamine ... 101

RUFF, F., SCHUSTER, I. und GERECS, Á.: Protonenresonanzspektroskopische Untersuchungen und Bildung von O-Acetyl-D-gluconsäure-, -D-mannonsäure- und -D-xylonsäure-(1,5)-lacton-2,4-dinitro-phenylhydrazon 111

MATKOVICS, B., GÖNDÖS, G. and TARÓDI, B.: Rearrangements of Steroids, V. Schmidt Reaction and Beckmann Rearrangement of Estrone and of its Derivatives (Preliminary Communication) 119

KUTASSY, S., KAJTÁR, J. und MEDZIHRADSZKY-SCHWEIGER, H.: Eine einfache Mikromethode zur Bestimmung der tert. Butyloxycarbonyl-Schutzgruppe verschiedener Aminosäuren und ihrer Derivate 123

Printed in Hungary

A kiadásért felel az Akadémiai Kiadó igazgatója — Műszaki szerkesztő: Farkas Sándor

A kézirat nyomdába érkezett: 1968. IV. 16. — Terjedelem: 11.50 (A/5) ív, 86 ábra

68.65463 Akadémiai Nyomda, Budapest — Felelős vezető: Bernát György

ACTA CHIMICA

ТОМ LVII — ВЫП. 1

РЕЗЮМЕ

Изучение образования комплекса между уранилом(VI) и тиоприпионовой кислотой

М. Б. МИШРА и Х. Л. НИГАМ

На основе потенциометрических измерений было обнаружено образование комплекса между UO_2(VI) и ТРА (где ТРА — тиопропионовая кислота) с отношением компонентов металл: диганд = 1 : 2, со ступенчатыми константами стабильности $\log K_1 = 3{,}7$ и $\log K_2 = 7{,}4$ и со свободной энергией образования, равной —5,13 кал (при 30° С). Комплекс удалось изолировать в твердом состоянии, которое представляет собой желтое вещество с тем же составом, что и в растворе. Комплекс характеризовался с помощью ИК и магнитных измерений.

Применение сульфосалицилата аммония как комплексообразователя в ионообменной хроматографии, II. Константы стабильности комплексов сульфосалицилатов меди II), никеля(II) и кобальта(II) при 80° С

П. ГАБОР, Я. ИНЦЕДИ и Л. ЭРДЕИ

С помощью pH-метрического титрования определялись константы диссоциации сульфосалициловой кислоты, а на основе экспериментальных данных по распределению на ионообменниках определялись константы стабильности комплексов сульфосалицилатов с медью(II), никелем(II) и кобальтом(II) при 80° С и при ионной силе, равной 0,5. Были получены следующие значения: константы диссоциации $\log K_1 = -1{,}52$ и $\log K_2 = -2{,}30$ и $\log K_3 = -10{,}47$; константы стабильности комплексов с медью(II) $\log \beta_1 = 7{,}46 \pm 0{,}2$ и $\log \beta_2 = 12{,}9 \pm 0{,}5$; константы стабильности комплексов с никелем(II) $\log \beta_1 = 6{,}15 \pm 0{,}2$ и $\log \beta_2 = 11{,}3 \pm 0{,}5$; и константы стабильности комплексов с кобальтом(II) $\log \beta_1 = 6{,}3 \pm 0{,}2$ и $\log \beta_2 = 11{,}1 \pm 0{,}5$.

Термическая стабильность солей с анионами, содержащими кислород и хлор, в твёрдом состоянии IV. Кинетика и механизм термического разложения перхлоратов щелочных металлов

Ф. ШОЙМОШИ

Разложение перхлоратов лития и натрия происходит в расплавленной фазе, в то время как разложение перхлоратов калия, рубидия и цезия начинается уже в твердой фазе и продолжается в расплавленной фазе. Плавление этих перхлоратов в течение разложения приписывалось образованию эвтектики между перхлоратом и продуктами реакции. Разложение первых двух солей хорошо описывается уравнением Прута—Томпкинса. Разложение же других соединений описывается двумя уравнениями первого порядка. Первое относится к медленной твердофазной реакции, а второе — к намного более быстрой реакции в расплавленной фазе. Энергия активации этих реакций лежит в

пределах 60—70 ккал. Полагалось, что ступенью определяющей скорость разложения перхлоратов щелочных металлов, является разрыв связи Cl—O.

Проводились также некоторые дериватографические и кинетические измерения для выяснения влияния продуктов реакции на разложение. Из кинетических данных определялся порядок стабильности этих соединений, и последний обсуждался на основе известных физических и химических констант катионов и характера связей.

Термическая стабильность солей с анонимами, содержащими кислороды хлор, в твёрдом состоянии. V. Термическое разложение перхлоратов некоторых двухвалентных металлов

Ф. ШОЙМОШИ

Изучалось термическое разложение перхлоратов бария, магния, кадмия, цинка и свинца. Перхлораты бария и кадмия разлагаются до хлоридов и кислорода, в то время как разложение остальных солей приводит к образованию хлоридов, окисей и различных газов соответственно. Разложение веществ описывается различными уравнениями, на основании которых были рассчитаны константы скорости и энергия активации реакции. Определялась также и степень стабильности перхлоратных солей, и было найдено, что последняя уменьшается в следующем порядке: барий, магний, кадмий, свинец, цинк. Этот порядок обсуждался с точки зрения эффективной силы электрического поля катионов и ионного характера соединений.

Характеристические нормальные колебания производных бензола, III. Корреляция между формой и частотой перпендикулярных колебаний CH

ДЬ. ВАРШАНИ

Ход частот перпендикулярных CH колебаний в производных бензола объясняется теорией следования орбиты. С помощью одного определенного параметра точно воспроизводились частоты перпендикулярных колебаний CH в бензоле. Заместители повышают взаимодействие между состояниями sp^2 и sp^3 и тем самым, обычно, уменьшают частоту. Наилучшим показателем этого эффекта оказался спектроскопический момент, введенный Платтом. С помощью нового параметра, содержащего спектроскопический момент, была разработана общая формула для всех перпендикулярных частот CH в производных бензола.

Изучение некоторых проблем в области фазовых равновесий жидкостó-твердое тело при высоких температурах для систем, содержащих летучие вещества

Р. КОЭН-АДАД, А. ТРАНКАРД и А. МАРШАН

Изучение фазовых равновесий жидкость-твердое тело для систем, содержащих летучие вещества, сталкивается с большими трудностями, принимая во внимание высокие требования к лабораторным установкам, связанные с повышенным давлением.

В данной работе изучалось влияние наиболее важных факторов с целью разработки наиболее подходящего оборудования.

Описываются различные типы установок для термического анализа или растворения под давлением и определяются условия их применимости.

Новые данные относительно взаимодействия эфиров тиолсульфиновых кислот с динитрохлорбензолом

Э. ВИНКЛЕР и Ф. КЛИВЕНИ

Авторами, а также Барнаром и Перси [3] изучалась реакция расщепления фенил,-п-толуил и п-хлорфениловых эфиров бензол-, п-толуол- и п-хлорбензол-тиолсульфиновых кислот в присутствии 2,4-динитрохлорбензола в щелочном бикарбонатном растворе. Было установлено, что о направлении и степени разложения можно точно судить лишь в случае п-толуиловых соединений. Это соединение, в противоположность двум другим аналогам, в условиях реакции практически не диспропорционируется. Используя эквимолекулярные количества динитрохлорбензола, можно исключить побочные реакции, затрудняющие изучение основной реакции. Модельные исследования, проведенные в таких условиях, доказали, что не только сульфоксид, но и основное количество сульфида образуется в первичном процессе. Было также доказано, что основное количество динитрохлорбензола реагирует с относительно большой скоростью, и лишь небольшое количество последнего принимает участие во вторичных реакциях.

На основе экспериментальных данных кажется вероятным, что нуклеофильный характер молекулы тиолсульфината нельзя приписывать только S(II) и S(IV) атомам серы.

Применение некоторых конформационных правил к циклогексиламинам

К. АЛЬТЕНБУРГ

Было показано, что зависимость между температурой кипения, плотностью и показателем преломления, с одной стороны, и средней квадратичной (инерционного радиуса, с другой стороны, выведенная для ациклических и циклических алканов, применяется и для изомерных циклогексиламинов. Обсуждается возможность конформационного анализа циклогексиламинов с помощью температуры кипения, плотности, показателя преломления и некоторых функций, выведенных из этих величин.

Получение и исследование методом ЯМР ⟨1,5⟩-лактон-2,4-динитрофенилгидразона О-ацетил-D-глюконовой, -D-маннoновой, -D-ксилоновой кислот

Ф. РУФФ, И. ШУСТЕР и А. ГЕРЕЧ

С помощью исследований методом ЯМР было установлено, что из 2,4-динитрофенилгидразона О-ацетил-D-глюкопиранозы, -D-маннопиранозы и -D-ксилопиранозы путем ацетилирования с размыканием кольца и в присутствии небольших количеств хинолина (или пиридина) в качестве побочного продукта образуется ⟨1,5⟩-лактон-2,4-динитрофенилгидразон соответствующей О-ацетил-альдоновой кислоты. Тот же самый лактонгидразон образуется и при окислении тех же самых исходных соединений перманганатом калия.

Упрощенный микрометод для определения защитной группы *трет.*-бутилоксикарбонила в различных аминокислотах и их производных

Ш. КУТАШИ, Й. КАЙТАР и Х. МЕДЗИХРАДСКИЙ-ШВАЙГЕР

Авторами описывается простой метод для определения *трет.*-бутилоксикарбонильной группы (BOC). Под влиянием серной кислоты в спиртовой среде эта защитная группа отщепляется с выделением эквивалентного количества двуокиси углерода. Образующаяся двуокись углерода определялась либо гравиметрическим, либо титриметрическим путем.

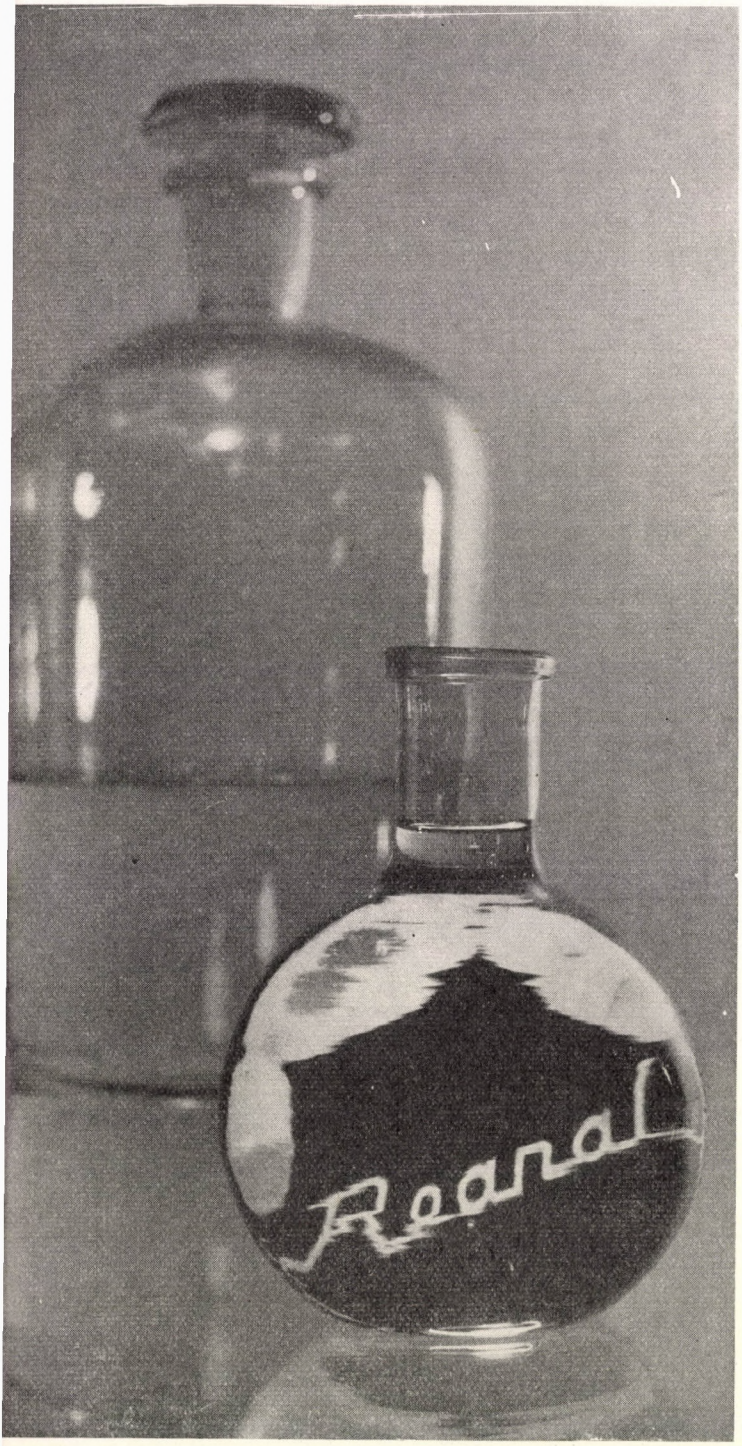

ANORGANISCHE UND ORGANISCHE FEINCHEMIKALIEN

Garantiert reine Reagenzien für analytische Zwecke

Laboratoriumspräparate für die Forschung und Technik

Biochemikalien:

Aminosäuren und Derivate · Peptide und Derivate · Enzyme · Nukleoproteide · Purine

Indikatoren

Tetrazoliumsalze

Präparate für Mikroskopie und Biologie

Kohlenhydrate

»Selecton«-Reagenzien für Komplexometrie

Radioaktive (markierte) Verbindungen

R E A N A L FABRIK FÜR FEINCHEMIKALIEN

Budapest · Ungarn

INFORMATION
UND LITERATUR
VON **MEDIMPEX**
BUDAPEST 5 . POSTFACH 126

Novelties in chemical literature published by AKADÉMIAI KIADÓ, Publishing House of the Hungarian Academy of Sciences, Budapest

I. NÁRAY-SZABÓ

INORGANIC CRYSTAL CHEMISTRY

In Russian • Approx. 510 pages • 200 figures • Cloth

The results of research for more than half a century on the structure of crystals are presented in this book in terms of regular arrays of atoms, ions or molecules. The chemical formulae thought previously formalistic are represented as definite three-dimensional lattices. The structures are illustrated by a number of artistic figures, the majority of which is new. The system of elements and inorganic compounds, discussed strictly following the periodic table, gives a survey of inorganic chemistry on this basis for the first time.

PROCEEDINGS OF THE NINTH CONFERENCE OF THE SILICATE INDUSTRY

Ed. by F. TAMÁS

In English • Approx. 960 pages • Cloth

This volume contains the papers and contributions read at the Ninth Conference, held in November, 1967, Budapest, grouped — in alphabetical order of Authors' names — in the traditional sections: Basic Science, Cement, Ceramic, Glass, Quarrying, Refractories.

1828—1968

AKADÉMIAI KIADÓ

PUBLISHING HOUSE OF THE HUNGARIAN ACADEMY OF SCIENCES BUDAPEST

The Acta Chimica publish papers on chemistry in English, German, French and Russian.

The Acta Chimica appear in volumes consisting of four parts of varying size, 4 volumes being published a year.

Manuscripts should be addressed to

Acta Chimica
Budapest 112/91 Műegyetem

Correspondence with the editors should be sent to the same address.

The rate of subscription is 165 forints a volume. Orders may be placed with "*Kultúra*" Foreign Trade Company for Books and Newspapers (Budapest I., Fő utca 32. Account No. 43-790-057-181) or with representatives abroad.

Les Acta Chimica paraissent en français, allemand, anglais et russe et publient des mémoires du domaine des sciences chimiques.

Les Acta Chimica sont publiés sous forme de fascicules. Quatre fascicules seront réunis en un volume (4 volumes par an).

On est prié d'envoyer les manuscrits destinés à la rédaction à l'adresse suivante:

Acta Chimica
Budapest 112/91 Műegyetem

Toute correspondance doit être envoyée à cette même adresse.

Le prix de l'abonnement est de 165 forints par volume.

On peut s'abonner à l'Entreprise pour le Commerce Extérieur de Livres et Journaux «*Kultúra*» (Budapest I., Fő utca 32. Compte-courant No. 43-790-057-181) ou à l'étranger chez tous les représentants ou dépositaires.

«*Acta Chimica*» издают трактаты из области химической науки на русском, французском, английском и немецком языках.

«*Acta Chimica*» выходят отдельными выпусками разного объема. 4 выпуска составляют один том. 4 тома публикуются в год.

Предназначенные для публикации рукописи следует направлять по адресу:

Acta Chimica
Budapest 112/91 Műegyetem

По этому же адресу направлять всякую корреспонденцию для редакции.

Подписная цена «*Acta Chimica*» — 165 форинтов за том. Заказы принимает предприятие по внешней торговле книг и газет «*Kultúra*» (Budapest I., Fő utca 32. Текущий счет № 43-790-057-181) или его заграничные представительства и уполномоченные.

51,— Ft

Reviews of the Hungarian Academy of Sciences are obtainable at the following addresses:

ALBANIA

Ndermarja Shtetnore e Botimeve
Tirana

AUSTRALIA

A. Keesing
Box 4886, GPO
Sydney

AUSTRIA

Globus Buchvertrieb
Salzgries 16
Wien I

BELGIUM

Office International de Librairie
30, Avenue Marnix
Bruxelles 5

Du Monde Entier
5, Place St. Jean
Bruxelles

BULGARIA

Raznoiznos
1, Tzar Assen
Sofia

CANADA

Pannonia Books
2, Spadina Road
Toronto 4, Ont.

CHINA

Waiwen Shudian
Peking
P. O. B. 88

CZECHOSLOVAKIA

Artia
Ve Směčkách 30
Praha 2

Poštovná Novinová Služba
Dovoz tisku
Vinohradská 46
Praha 2

Mad'arská Kultura
Václavské nám. 2
Praha I

Poštová Novinová Služba
Dovoz tlače
Leningradská 14
Bratislava

DENMARK

Ejnar Munksgaard
Nörregade 6
Copenhagen

FINLAND

Akateeminen Kirjakauppa
Keskuskatu 2
Helsinki

FRANCE

Office International de Documentation et Librairie
48, rue Gay Lussac
Paris 5

GERMAN DEMOCRATIC REPUBLIC

Deutscher Buch-Export und Import
Leninstraße 16
Leipzig 701

Zeitungsvertriebsamt
Clara Zetkin Straße 62
Berlin N. W.

GERMAN FEDERAL REPUBLIC

Kunst und Wissen
Erich Bieber
Postfach 46
7 Stuttgart S.

GREAT BRITAIN

Collet's Holdings Ltd.
Dennington Estate
London Rd.
Wellingborough. Northants.

Robert Maxwell and Co. Ltd.
Waynflete Bldg. The Plain
Oxford

HOLLAND

Swetz and Zeitlinger
Keizersgracht 471—487
Amsterdam C

Martinus Nijhof
Lange Voorhout 9
The Hague

INDIA

Current Technical Literature
Co. Private Ltd.
India House OPP
GPO Post Box 1374
Bombay I

ITALY

Santo Vanasia
Via M. Macchi 71
Milano

Libreria Commissionaria Sansoni
Via La Marmora 45
Firenze

JAPAN

Nauka Ltd.
92, Ikebukur O-Higashi 1-chome
Toshima-ku
Tokyo

Maruzen and Co. Ltd.
P. O. Box 605
Tokyo-Central

Far Eastern Booksellers
Kanda P. O. Box 72
Tokyo

KOREA

Chulpanmul
Phenjan

NORWAY

Johan Grundt Tanum
Karl Johansgatan 43
Oslo

POLAND

RUCH
ul. Wronia 23
Warszawa

ROUMANIA

Cartimex
Str. Aristide Briand 14—18.
Bucureşti

SOVIET UNION

Mezhdunarodnaya Kniga
Moscow G—200

SWEDEN

Almquist and Wiksell
Gamla Brogatan 26
Stockholm

USA

Stechert Hafner Inc.
31, East 10th Street
New York, N. Y. 10003

Walter J. Johnson
111, Fifth Avenue
New York, N. Y. 10003

VIETNAM

Xunhasaba
19, Tran Quoc Toan
Hanoi

YUGOSLAVIA

Forum
Vojvode Mišića broj 1
Novi Sad

Jugoslovenska Knjiga
Terazije 27
Beograd

5. VIII. 1968

Index: 26.027

ACTA CHIMICA

ACADEMIAE SCIENTIARUM HUNGARICAE

ADIUVANTIBUS

L. ERDEY, K. POLINSZKY, G. SCHAY

AC

R. BOGNÁR, GY. BRUCKNER, Z. CSŰRÖS, T. ERDEY-GRÚZ, Z. FÖLDI, M. FREUND, Á. GERECS, GY. HARDY, J. HOLLÓ, Á. KISS, M. KORACH, F. MÁRTA, F. NAGY, E. PUNGOR, Z. SZABÓ, P. TÉTÉNYI, L. VARGHA, K. VAS

REDIGIT

B. LENGYEL

TOMUS 57 FASCICULUS 2

AKADÉMIAI KIADÓ, BUDAPEST

1968

ACTA CHIM. ACAD. SCI. HUNG.

ACTA CHIMICA

A MAGYAR TUDOMÁNYOS AKADÉMIA KÉMIAI TUDOMÁNYOK OSZTÁLYÁNAK IDEGEN NYELVŰ KÖZLEMÉNYEI

SZERKESZTI

LENGYEL BÉLA

TECHNIKAI SZERKESZTŐK

DEÁK GYULA és HARASZTHY-PAPP MELINDA

Az Acta Chimica német, angol, francia és orosz nyelven közöl értekezéseket a kémiai tudományok köréből.

Az Acta Chimica változó terjedelmű füzetekben jelenik meg, egy-egy kötet négy füzetből áll. Évente átlag négy kötet jelenik meg.

A közlésre szánt kéziratok a szerkesztőség címére (Budapest 112/91 Műegyetem) küldendők.

Ugyanerre a címre küldendő minden szerkesztőségi levelezés. A szerkesztőség kéziratokat nem ad vissza.

Az Acta Chimica előfizetési ára kötetenként belföldre 120 Ft, külföldre 165 Ft. Megrendelhető a belföld számára az „Akadémiai Kiadó"-nál (Budapest V., Alkotmány utca 21. Bankszámla 05-915-111-46), a külföld számára pedig a „Kultúra" Könyv- és Hírlap Külkereskedelmi Vállalatnál (Budapest I., Fő utca 32. Bankszámla: 43-790-057-181) vagy annak külföldi képviseleteinél és bizományosainál.

Die Acta Chimica veröffentlichen Abhandlungen aus dem Bereiche der chemischen Wissenschaften in deutscher, englischer, französischer und russischer Sprache.

Die Acta Chimica erscheinen in Heften wechselnden Umfanges. Vier Hefte bilden einen Band. Jährlich erscheinen 4 Bände.

Die zur Veröffentlichung bestimmten Manuskripte sind an folgende Adresse zu senden:

Acta Chimica
Budapest 112/91 Műegyetem

An die gleiche Anschrift ist auch jede für die Redaktion bestimmte Korrespondenz zu richten.

Abonnementspreis pro Band: 165 Forint. Bestellbar bei dem Buch- und Zeitungs-Außenhandels-Unternehmen »*Kultúra*« (Budapest I., Fő utca 32. Bankkonto No. 43-790-057-181) oder bei seinen Auslandsvertretungen und Kommissionären.

Acta Chimica Academiae Scientiarum Hungaricae Tomus 57 (2), pp. 129—140 (1968)

THE POTENTIAL ENERGY FUNCTIONS OF DIATOMIC MOLECULES

(HALIDES AND HYDRIDES OF THE GROUPS IA AND IIA)

S. SZŐKE and E. BAITZ

(Central Research Institute for Chemistry of the Hungarian Academy of Sciences, Budapest)

Received August 28, 1967

The validity of the potential energy function

$$U = D_e\left(1 - e^{-\gamma \frac{(r-r_e)^2}{r}}\right)[1 + af(r)] \tag{1}$$

constructed mainly on the basis of data of covalent diatomic molecules, may be extended to apply to ionic cases, too [1]. In Eq. (1) U is the potential energy, D_e is the dissociation energy, $r - r_e$ is the displacement coordinate, and a denotes the LENNARD-JONES parameter [2]. γ can be defined by the following relation:

$$\gamma = \frac{1}{2} d \left(\frac{e_1 e_2}{D_e}\right) \tag{2}$$

where d is a proportionality constant, and e_1, e_2 are the electronegativities, according to PAULING [3]. The correctness of Eq. (1) was checked in the usual way, by reproducing values of the anharmonicity ($\omega_e x_e$) and the rotational-vibrational coupling constants (α_e); the calculated values were compared to those obtained with the aid of the RITTNER potential equation, which is actually the most preferred formula in the literature. Besides checking the correctness of the equation, our other purpose was to study the performance of the LENNARD-JONES [2] constants.

The way for extension of Eq. (1) consists simply in the changing of the value of the proportionality constant

$$d = \frac{k_e r_e}{(e_1 e_2 D_{12})^{1/2}} \tag{3}$$

where k_e denotes the force constant, r_e is the interatomic distance, e_1 and e_2 are the electronegativities of the individual atoms, and D_e is the dissociation energy.

The aim of the present work has been the investigation of the behaviour of the halides and subhalides of Groups Ia and IIa, respectively. The analysis

deals with molecules in the gaseous state, which have predominantly ionic character.

The interatomic distances and dissociation energies of the diatomic molecules studied are generally large. The mean electronegativities and the force constants have the lowest values in diatomic cases.

Alkali halides

The potential energy functions of the molecules were studied in the gaseous state, on the basis of the high temperature spectra. Besides the determination of the values of d, the magnitude of the LENNARD-JONES parameters is of considerable interest.

The low values of the force constants can be traced back to similar values of the alkali metal molecules. The interatomic distances are in part low as compared with the covalent radii.

VARSHNI and SHUKLA [4] studied the potential functions of these molecules. They selected the RITTNER potential [5] applicable to ionic bonds to investigate energy relations.

The potential function was given in the following form:

$$U = -\frac{e^2}{r} - \frac{e^2(\alpha_1 + \alpha_2)}{2r^4} - \frac{2e^7 \alpha_1 \alpha_2}{r^7} - \frac{c}{r^6} + A \exp\left(-\frac{r}{\varrho}\right) \qquad (4)$$

where e = charge of an electron
r = interatomic distance
α_1, α_2 = polarizability of the ions
c = *van der Waals* parameter
A and ϱ are constants determined by the equilibrium data.

VARSHNI and SHUKLA used the ionic dissociation energies in their calculations:

$$D_i = D_e + I - E \qquad (5)$$

where D_i = ionic dissociation energy
I = first ionization potential
E = electron affinity.

In order to justify the validity of the basic function, VARSHNI and SHUKLA calculated the D_e, $\omega_e x_e$ and α_e values. The D_e's were taken from a publication of BREWER and BECKET [6].

Alkali metal and alkali hydride molecules

When studying the behaviour of the alkali halide molecules, it seemed worth-while to compare the relations $kr/(e_1 e_2 D)^{1/2}$ of alkali hydrides and alkali halides.

Alkali metal molecules can be studied at high temperature in the gaseous state. They are characterized by large interatomic distances and by small dissociation energies and force constants. The latter values are much smaller than expected even on the basis of the low dissociation energy values.

Alkali metal atoms are able to perform bonds with each other. The parameters of these mixed alkali molecules — mainly the force constants — are nearly the same as those of homonuclear molecules which is characteristic of covalency.

In *alkali hydrides* the hydrogen atom is the negative pole, its ionization potential being considerably larger than that of alkali elements. The dissociation energies are well equalized, having values somewhat lower than the mean value corresponding to the metal and the hydrogen molecules, indicating partial ionic character. The interatomic distances are considerably lower than in alkali molecules: the electron of the hydrogen atom is built into the valence shell, causing significant contraction in the interatomic distance.

Subhalides of alkaline earth metals

These are molecules in gaseous state, the behaviour of which can be studied only at elevated temperatures. Their dissociation energy values were determined by HERZBERG from the infrared spectra [7], and by BLUE, GREEN, BAUTISTA and MARGRAVE on the basis of mass spectral measurements [8, 9]. Some dissociation energy values were obtained by GURVICH et al.[10] and VEDENEYEV et al. [11] on the basis of high temperature equilibrium data. The reliability of the different data was investigated by KRASNOV and KARASEVA [12] using the RITTNER potential. These authors estimated the interatomic distances of certain molecules on the basis of VARSHNI's calculations. They compiled the most probable dissociation energy values in their paper.

Alkaline earth metal subhydrides

The subhydrides of Group IIa as well as the corresponding halides are formed through the hybridization of the $2s$ electrons of the metal molecule.

The Ia and IIa hydrides do not differ very much from each other with respect to dissociation energy and interatomic distances, however, there are considerable differences in the normal frequencies, involving a great deviation in the force constants.

The d value dependence in the halides and hydrides of Group Ia and the subhalides and subhydrides of Group IIa

The relations of the parameters characterizing the bond strength, given as the proportionality constant d, can, in first approximation, be considered constant within the individual groups. The values, according to the above

sequence, are the following: 0.138, 0.152, 0.221 and 0.213. These magnitudes are correct if the energies are given in kcal/mole, the bond lengths in Å, force constants in mdyne/Å, and the electronegativities are considered to be dimensionless numbers.

The data of *alkali halides* are compiled in Table I. Our calculations were made with the numerical values applied by VARSHNI and SHUKLA in the

Table I

Proportionality constants of alkali halides

	D_i	r	k	d
NaCl	128.0	2.361	1.086	0.139
KBr	109.4	2.821	0.738	0.133
KI	102.3	3.048	0.611	0.131
LiF	178.3	1.564	2.502	0.147
NaBr	123.6	2.502	0.935	0.132
LiCl	148.0	2.021	1.415	0.136
CsF	136.0	2.345	1.305	0.157
CsI	97.6	3.315	0.543	0.137
RbCl	108.8	2.787	0.795	0.137
RbBr	105.1	2.945	0.692	0.133
KF	134.2	2.170	1.385	0.145
NaI	116.6	2.711	0.770	0.129
NaF	149.0	1.926	1.761	0.147
CsCl	107.8	2.906	0.748	0.144
CsBr	104.7	3.072	0.652	0.140
KCl	113.2	2.667	0.851	0.138
LiBr	142.9	2.170	1.205	0.131
LiI	134.3	2.392	0.972	0.127
RbF	128.9	2.2703	1.2521	0.140
RbI	98.4	3.177	0.575	0.130
	average:			0.138
	mean deviation:			4.18%

RITTNER potential calculations. Table II gives a good picture about the slight but regular change of the d values. These values decrease from Li to Rb, and from F to I regularly. In the Cs row the regular decrease, as compared to the other halides, is no longer observed. (We mention in advance that this behaviour is repeated, in a rather analogous fashion, in the case of alkaline earth halides.)

The d values of *alkali hydrides* are given in Table III. They do not differ very much from the corresponding values of the halides. The bonding in alkali

halides is established by *s* and *p* electrons, while in hydrides there are bonds with two *s* electrons.

In the *alkaline earth subhalides* the bond is made by *sp* hybrid and *p* electrons. In these groups difficulties are encountered in the calculations owing to the unreliability of the experimental data.

Table II

Regular tendency in the proportionality constants

	F	Cl	Br	I
Li	0.147	0.136	0.131	0.127
Na	0.147	0.139	0.132	0.129
K	0.145	0.138	0.133	0.131
Rb	0.140	0.137	0.133	0.130
Cs	0.157	0.144	0.140	0.137

The probability of the right values can be justified by careful analysis; such analyses have been reported by KRASNOV and KARASEVA. In order to check their results, we calculated the *d* values with their data, and compared them with the *d* values obtained using other experimental values given by different authors [7, 8, 9, 10, 11]. The *d* values calculated from the two sets of data obtained in different ways, are shown in Table IV. The factors calculated from the dissociation energies proposed by KRASNOV and KARASEVA are

Table III

Proportionality constants of alkali hydrides

	k	r	$(e_1e_2)^{\frac{1}{2}}$	D	d
LiH	1.026	1.596	1.448	58	0.148
NaH	0.781	1.887	1.376	47	0.156
KH	0.561	2.244	1.296	43	0.148
RbH	0.545	2.376	1.296	41	0.156
CsH	0.467	2.494	1.212	42	0.148
Average:					0.152

better equalized, having smaller dispersion, and seem therefore to be more acceptable. As in the case of alkali halides, we give a comparison in Table V. The tendencies and deviations agree in the two groups of molecules. In some places irregularities are found arising from slightly unreliable data.

Table IV

Proportionality constants of alkaline earth subhalides

	k	r	D^a	D^b	d^a	d^b
BeF	5.767	1.365	159.8	140.0	0.255	0.272
BeCl	3.025	1.700	110.0	110.0	0.231	0.231
BeBr	2.612*	1.930	—	100.0	—	0.246
BeI	2.143*	2.130	—	88.0	—	0.251
MgF	3.216	1.750	105.0	120.0	0.251	0.236
MgCl	1.815	2.200	89.8	90.0	0.222	0.222
MgBr	1.514	2.360	73.9	74.0	0.227	0.227
MgI	1.170*	2.560	—	55.0	—	0.234
CaF	2.614	2.020	124.8	125.0	0.297	0.236
CaCl	1.504	2.439	62.9	105.0	0.267	0.207
CaBr	1.270	2.600	65.85	90.0	0.244	0.209
CaI	1.051*	2.800	64.5	75.0	0.232	0.215
SrF	2.300	2.120	125.5	126.0	0.218	0.218
SrCl	1.345	2.580	68.84	108.0	0.241	0.193
SrBr	1.146	2.740	63.77	90.0	0.235	0.198
SrI	0.923	2.940	49.96	80.0	0.243	0.193
BaF	2.163	2.240	133.76	134.0	0.221	0.220
BaCl	1.282	2.750	61.93	110.0	0.273	0.205
BaBr	1.108	2.910	64.46	100.0	0.253	0.203
BaI	0.874*	3.110	—	85.0	—	0.197
Average:						0.221

* VARSHNI's data [4]
D^a experimental data given by KRASNOV and KARASEVA [12]
D^b recommended values by KRASNOV and KARASEVA [12]

Table V

Regular tendency in the proportionality constants

	F	Cl	Br	I
Be	0.272	0.231	0.246	0.251
Mg	0.235	0.222	0.227	0.234
Ca	0.236	0.207	0.209	0.215
Sr	0.218	0.193	0.198	0.193
Ba	0.220	0.205	0.203	0.197

It can be inferred from the data of Table IV that for BeF the dissociation energy (160 kcal/mole), suggested by KRASNOV and KARASEVA is the more probable value. By using this, the d factor remains regularly in the line.

An analysis was also made concerning the corresponding values of subhydrides (Table VI). It is easy to see that these differ only moderately from the former ones (0.221 for the halide, and 0.213 for the hydride). It follows from

Table VI

Proportionality constants of alkaline earth subhydrides

	k	r	$(e_1e_2)^{\frac{1}{2}}$	D [12]	d
BeH	2.263	1.343	1.775	53	0.235
MgH	1.277	1.731	1.587	46	0.205
CaH	0.977	2.002	1.448	39.2	0.215
SrH	0.857	2.145	1.448	38	0.205
BaH	0.809	2.232	1.374	41	0.204
Average:					0.213

this fact that it is not very important whether the other bonding partner is an s or a p electron beside the sp hybrid electron.

Values of the Lennard-Jones a and b parameters

A general feature of the potential energy functions is that they do not describe the lower and higher energy levels with the same accuracy. The original LIPPINCOTT function [13] is therefore to be completed by the supplementary term given in Eq. (1). The LENNARD-JONES supplementary term [3] is also useful when employing electronegativity data.

The potential energy assumptions prescribe that the functions have to reproduce spectroscopic constants not given in the starting expression [14]. The criterion for recalculation of the $\omega_e x_e$ and α_e terms is that the a and b parameters must be of the same magnitude in the given bond type. Expanding the $[1 + af(r)]$ expression in power series and neglecting term higher than order three, we have the following expression:

$$1 + af(r) = 1 + (-1)a\{(r_e/r)^6[1 - \exp(-b^2\gamma\Delta r^2\, r^{11}/r_e^{12})]^{1/2} - \\ - (r_e/r)^{12}[1 - \exp(-b^2\gamma\Delta r^2 r^{11}/r_e^{12})]\} \qquad (6)$$

The parameters a and b can be given according to the analysis of DUNHAM solving the SCHRÖDINGER equation [15]. The following expression can be

Table VII

Lennard-Jones parameters of alkali halides

	ab	*b*	*a*
NaCl	1.125	1.065	1.056
KBr	1.120	1.016	1.102
KJ	1.084	1.000	1.084
NaBr	1.085	1.093	0.993
LiCl	1.010	1.068	0.946
CsI	1.154	1.002	1.152
RbCl	1.133	1.009	1.122
RbBr	1.121	1.036	1.082
KF	1.164	1.029	1.131
LiF	1.111	1.077	1.032
NaF	1.225	1.182	1.036
NaI	1.037	0.960	1.080
KCl	1.126	1.035	1.088
RbI	1.174	1.135	1.034
CsCl	1.147	1.049	1.093
CSBr	1.180	1.174	1.005
LiBr	0.986	0.981	1.005
RbF	1.113	0.929	1.198
Average:	1.116	1.047	1.069
Mean deviation:	3.88%	5.0%	4.61%

Table VIII

Lennard-Jones parameters of alkali hydrides

	ab	*b*	*a*
LiH	0.484	1.046	0.463
NaH	0.518	0.977	0.530
KH	0.431	0.912	0.473
RbH	0.529	1.036	0.511
CsH	0.506	0.975	0.519
Li^2H	0.494	1.067	0.463
K^2H	0.531	1.000	0.531
Average :	0.499	1.002	0.498

Table IX

Lennard-Jones parameters of alkaline earth subhydrides

	ab	*b*	*a*
BeH	0.430	1.200	0.358
MgH	0.489	0.943	0.519
CaH	0.425	1.167	0.364
SrH	0.433	1.210	0.358
BaH	0.438	1.120	0.391
Mg^2H	0.510	0.990	0.515
Average:	0.454	1.105	0.418

Table X

Spectroscopic constants of alkali halides

	$\omega_e x_e$ exptl.	$\omega_e x_e$ calc.	Deviation %	$10^4\ \alpha_e$ exptl.	$10^4\ \alpha_e$ calc.	Deviation %
NaCl	1.755	1.75	0.3	16.248	16.17	0.5
KBr	0.758	0.741	2.2	4.048	4.037	0.3
KI	0.574	0.574	0	2.678	2.763	3.2
NaBr	1.16	1.24	6.9	9.41	9.684	2.4
LiCl	4.2	4.791	14.1	80.122	86.84	8.4
CsI	0.254	0.235	7.5	0.683	0.66	2.6
RbCl	0.856	0.816	4.7	4.536	4.467	1.5
RbBr	0.463	0.456	1.5	1.86	1.845	0.9
KF	2.4	2.253	6.1	23.346	23.7	1.5
LiF	8.895	9.127	2.6	241	243	0.8
LiBr	3.53	3.89	9.7	56.402	63.96	13.4
NaF	3.4	3.327	2.1	45.59	41.58	8.8
NaI	0.964	0.987	2.3	6.48	6.97	7.5
KCl	1.167	1.141	2.2	7.89	7.825	0.8
RbF	1.9	1.758	7.5	15.223	15.263	3.2
RbI	0.335	0.334	0.3	1.095	1.044	4.7
CsCl	0.740	0.667	9.9	3.37	3.27	2.9
CsBr	0.360	0.340	5.6	1.241	1.177	5.2
Average:			4.74			3.8

derived:

$$\frac{\alpha_e \omega_e}{6B_e^2} = ab\,(\gamma r_e)^{1/2} \tag{7}$$

$$\frac{\frac{5}{4}\left(-1-\frac{\alpha_e\omega_e}{6B_e^2}\right)^2 - \frac{2\omega_e x_e}{3B_e} - 1 + \frac{\gamma r_e}{2} - \frac{3}{2}a\cdot b\,(\gamma r_e)^{1/2}}{a\cdot b\,\gamma r_e} = b \tag{8}$$

Solving the equations gives for alkali halides 1.047 as the average LENNARD-JONES b parameter, and 1.116 as the ab parameter; the same parameters in the covalent area are: 1.061 and 0.562 (Table VII).

A further study on alkali hydrides gave about 1.0 for the LENNARD-JONES b parameter and 0.5 for a. Hydrogen and the hydride molecules deviate from ordinary behaviour almost in all chemical-physical parameters, therefore a few per cent deviation is in accordance with the general rule of the constant

Table XI

Spectroscopic constants of alkali hydrides

	$\omega_e x_e$ exptl.	$\omega_e x_e$ calc.	Deviation %	α_e exptl.	α_e calc.	Deviation %
LiH	23.2	24.50	5.6	0.2132	0.22	3.2
NaH	19.72	19.25	2.4	0.135	0.125	7.4
KH	14.65	13.97	4.6	0.0673	0.0783	16.3
RbH	14.15	14.42	1.9	0.072	0.067	6.9
CsH	12.6	12.31	2.3	0.057	0.0558	2.1
Li^2H	13.228	13.921	5.2	0.09198	0.0929	1.0
K^2H	7.6	7.49	1.4	0.028	0.0264	5.7
Average:			3.3			6.1

character of parameter b. In Table VIII ab and b data of deuterides are also shown; here we found the experimental parameters to be reliable.

Analogous calculations were made with alkaline earth metals using data of the hydrides as well as that of magnesium deuteride.

The LENNARD-JONES parameters for alkaline earth hydrides are a: 0.418; ab: 0.454; b: 1.105 (Table IX).

In the case of alkaline earth subhalides, reliable experimental data were found only for BeF. The following values were obtained a: 0.748; b: 0.969; ab: 0.725.

Calculations were also made to find the anharmonicity and rotational-vibrational coupling constants. The calculated and experimental data are shown in Tables X, XI, XII. They unambiguously justify the correctness of our potential energy assumption.

Table XII

Spectroscopic constants of alkaline earth subhydrides

	$\omega_e x_e$ exptl.	$\omega_e x_e$ calc.	Deviation %	α_e exptl.	α_e calc.	Deviation %
BeH	35.5	38.99	9.8	0.3	0.317	5.7
MgH	31.5	26.95	14.4	0.167	0.155	7.2
CaH	19.5	20.76	6.5	0.096	0.094	2.1
SrH	17	19.1	12.4	0.0814	0.0853	4.8
BaH	16	16.35	2.2	0.0655	0.068	3.8
Mg^2H	16.09	14.27	11.3	0.0654	0.0592	9.5
Mean deviation:			9.43			5.5

Discussion of the results

These studies about the characteristic $kr/(e_1 e_2 D_{12})^{1/2}$ values of hydrides and halides of alkali metals, and subhydrides and subhalides of alkaline earth metals have shown that these values are independent of the ionic-covalent character, and they are constant for certain groups of molecules. Though the different molecular properties change gradually in accordance with a not strictly defined relation of the periodic system, the above-mentioned ratio seems to remain constant, depending only on the electrons participating in the bond.

In the halide and hydride groups treated above, the metal takes part with *s* or *sp* hybrid electrons in the bond, giving rise to linkages of *s*—*p* or *sp*—*p* and *s*—*s* or *sp*—*s* character.

According to experience, the *d* values depend preponderantly on the metal component, and it is nearly indifferent whether the partner is taking part in the bond with an *s* or *p* electron.

Informative calculations have also been made on hydride and halide molecules of Group Ib. The *d* values found were in the range of 0.2, and they seem to be independent of the *s* or *p* bonding electron of the hydrogen or halogen atom. These molecular parameters are apparently not entirely reliable, therefore the calculations are not given in this paper.

For the *d*'s of *p*—*p* bonds in the covalent area, we have obtained values of about 0.28, which are nearly of the same magnitude as in the cases of molecules with an *s*—*p* link.

The average deviation of the *d* values is $\pm 4.18\%$ for alkali halides. The LENNARD-JONES *b* values are within about $\pm 10\%$ constant. The *a*'s can be considered constants to about the same extent.

By recalculating the $\omega_e x_e$ and α_e data, we wished to determine whether the potential energy functions of general validity or the more specific Rittner potential can afford better agreement for the energy levels. The anharmonicity of the halide molecules of Group Ia as well as the rotational-vibrational coupling constants can be calculated from the functions of type (1) more precisely than from the Rittner equation. The average deviations are in the first case 4.7% for $\omega_e x_e$ and 3.8% for α_e, while the corresponding values from the ionic relations are 5.5 and 5.2%. For the Ia and IIa hydrides both, the calculated and experimental values are given; on the basis of the standard deviations it has been found that Eq. (1) with the d values given satisfies the conventional conditions on the potential energy in this field, too.

SUMMARY

The

$$d = k_e r_e (e_1 e_2 D_e)^{1/2}$$

values, characteristic for bond types and useful for potential energy studies, have been calculated for alkali and alkaline earth hydride and halide molecules. The LENNARD-JONES parameters, a and ab, are given; these have been found constant within the range of 4.6 and 3.9% respectively in the different bond types. The assumption that parameter b is a constant being independent of the bond type, has been justified. Comparison has been made between potential energy functions arising from different principles and conclusions can be drawn that the LIPPINCOTT type functions are satisfactory in the ionic as well as in the covalent area.

REFERENCES

1. SZŐKE, S.: Acta Chim. Acad. Sci. Hung. **51,** 183 (1967)
2. LENNARD-JONES, J. E.: Proc. Roy. Soc. (London) A **106,** 463 (1924)
3. PAULING, L.: The Nature of Chemical Bond. Cornell Univ. Press, Ithaka, New York, 1960
4. VARSHNI, Y. P., SHUKLA, R. C.: J. Mol. Spect. **16,** 63 (1965)
5. RITTNER, E. S.: J. Chem. Phys. **19,** 1030 (1951)
6. BREWER, L., BECKET, E.: Chem. Rev. **61,** 425 (1961)
7. HERZBERG, G.: Molecular Spectra and Molecular Structure. Van Nostrand, New York, 1950
8. BLUE, G., GREEN, J., BAUTISTA, R., MARGRAVE, J.: J. Phys. Chem. **67,** 877 (1963)
9. BLUE, G., GREEN, J., BAUTISTA, R., MARGRAVE, J.: Bull. Amer. Phys. Soc. **8,** 112 (1963)
10. GURVICH, L. V. et al.: Thermodynamic properties of individual substances. Izd. An. SSSR, Moscow (1962)
11. VEDENEYEV, V. I. et al.: Bond Energies, Ionization Potentials and Electron Affinities. Edward Arnold Ltd., London, 1966
12. KRASNOV, K. Sz., KARASEVA, N. V.: Optika i spektr. **19,** 30 (1965)
13. LIPPINCOTT, E. R.: J. Chem. Phys. **21,** 2070 (1953)
14. LIPPINCOTT, E. R., SCHROEDER, R.: J. Chem. Phys. **23,** 1131 (1955)
15. DUNHAM, J. L.: Phys. Rev. **41,** 713 (1932)

Sándor SZŐKE
Eszter BAITZ
} Budapest II., Pusztaszeri út 57 —69.

Acta Chimica Academiae Scientiarum Hungaricae Tomus 57 (2), pp. 141—145 (1968)

ON THE PARAMETER FORM OF FORCE CONSTANT MATRIX, VI.*

ON THE COMMON FORCE CONSTANT MATRICES OF ISOTOPIC MOLECULES

F. TÖRÖK

(Institute of General and Inorganic Chemistry, L. Eötvös University, and Research Group for Inorganic Chemistry of the Hungarian Academy of Sciences, Budapest)

Received September 15, 1967

In the BORN—OPPENHEIMER approximation, the forces between atoms, and consequently, the force constants can be regarded as unchanged in molecules differing only in isotopic substitution. At the same time, however, the normal frequencies of isotopic molecules are modified. In this way, further data can be obtained concerning the force field of molecules.

With the help of the parametric representation described in our earlier works [1, 2, 3], for the sake of simplicity, the case of isotopic molecules will be examined where the symmetry of the two molecules remains unchanged on isotopic substitution.

Let

$$G^{(1)} F^{(1)} L^{(1)} = L^{(1)} \Lambda^{(1)}, \quad G^{(2)} F^{(2)} L^{(2)} = L^{(2)} \Lambda^{(2)}$$

be the secular equations of the two molecules, where the G and F matrices are defined by WILSON [4]; Λ is a diagonal matrix whose elements can be easily computed in the knowledge of the normal frequencies; and L denotes a matrix consisting of the eigenvectors of matrix GF. Henceforth the elements of matrices $G^{(1)}$, $G^{(2)}$, $\Lambda^{(1)}$ and $\Lambda^{(2)}$ are supposed to be known.

As it has been pointed out [1], instead of the non-symmetric matrix GF, the use of the symmetric matrix gFg (where $g = G^{1/2}$) is much more convenient. Therefore, the secular equations above are converted into the forms:

$$g^{(1)} F^{(1)} g^{(1)} U^{(1)} = U^{(1)} \Lambda^{(1)} \quad \text{and} \quad g^{(2)} F^{(2)} U^{(2)} = U^{(2)} \Lambda^{(2)}$$

where $U^{(1)}$ and $U^{(2)}$ are orthogonal matrices.

Assuming the BORN—OPPENHEIMER approximation to hold, and using the formula described in our earlier work [1], all the matrices F satisfying the secular equations of both molecules can be formed as follows:

$$F = (g^{(1)})^{-1} U^{(1)} \Lambda^{(1)} (U^{(1)})' (g^{(1)})^{-1} = (g^{(2)})^{-1} U^{(2)} \Lambda^{(2)} (U^{(2)})' (g^{(2)})^{-1} \qquad (1)$$

where U' is transpose of U.

* Part V: Acta Chim. Acad. Sci. Hung. **56**, 285 (1968).

It is to be noted that $U^{(1)} = U^{(2)}$ would be possible with the same F only if the two matrices the eigenvectors of which are contained by matrices $U^{(1)}$ and $U^{(2)}$, were commutatives, *i. e.*:

$$g^{(1)} F g^{(1)} g^{(2)} F g^{(2)} = g^{(2)} F g^{(2)} g^{(1)} F g^{(1)}$$

As $g^{(1)} \neq g^{(2)}$, the equation above is incorrect. FREEMAN has arrived at a similar conclusion [5].

Let it be remarked that matrix L in the form $L = gU$ cannot be considered as decomposed into two factors, one of which is matrix g expressing the mixing of the inner (symmetry) coordinates in the normal coordinates, and the other matrix U characterizing the mixing caused by matrix F. This can be seen from the fact that in the case of isotopic molecules $U^{(1)} \neq U^{(2)}$, though $F^{(1)} = F^{(2)}$.

In the following, the relation (1) will be transformed in order to see better the connection between matrices $U^{(1)}$ and $U^{(2)}$ satisfying Eq. (1).

Using the notation

$$S = g^{(1)} (g^{(2)})^{-1} U^{(2)} \Lambda^{(2)} (U^{(2)}), \quad (g^{(2)})^{-1} g^{(1)} .$$

From Eq. (1) we get:

$$S U^{(1)} = U^{(1)} \Lambda^{(1)} .$$

This means that the $U^{(2)}$ belonging to the examined common F matrices is such that the matrices S formed by $U^{(2)}$ and matrix $G^{(1)} F^{(1)}$ have the same eigenvalues. In this way, on the basis of the known relation between the roots and coefficients of the secular equation, we have the following equation system:

$$\begin{gathered} \sum_{k=1}^{n} \lambda_k^{(1)} = \sum_{t=1}^{n} S_{tt} \\ \sum_{k<k'}^{n} \lambda_k^{(1)} \lambda_{k'}^{(1)} = \sum_{t<t'}^{n} (S_{tt} S_{t't'} - S_{tt'} S_{t't}) \qquad (2) \\ \cdots\cdots\cdots\cdots\cdots\cdots \\ \lambda_1^{(1)} \lambda_2^{(1)} \ldots \lambda_n^{(1)} = |S| \end{gathered}$$

where $\lambda_1^{(1)}, \lambda_2^{(1)}, \ldots, \lambda_n^{(1)}$ are the elements of the diagonal matrix $\Lambda^{(1)}$, and $|S|$ is the determinant of matrix S. Equation system (2) consists of n equations. In the last of the equations the elements of matrix $U^{(2)}$ do not occur, and by developing this last equation, the REDLICH—TELLER product rule can be obtained:

$$\begin{aligned} \lambda_1^{(1)} \lambda_2^{(1)} \ldots \lambda_n^{(1)} &= \frac{|g^{(1)}||g^{(1)}|}{|g^{(2)}||g^{(2)}|} |\Lambda^{(2)}| = \\ &= \frac{|G^{(1)}|}{|G^{(2)}|} \lambda_1^{(2)} \lambda_2^{(2)} \ldots \lambda_n^{(2)} \end{aligned}$$

Equation system (2) means further $(n-1)$ restrictions for the $\binom{n}{2}$ parameters [1] giving matrix $U^{(2)}$. Consequently, matrices F satisfying the secular equations of both isotopic molecules can be formed as the function of

$$\binom{n}{2} - (n-1) = \binom{n-1}{2}$$

parameters.

Because of the complexity of equation system (2), further methods have been developed for the examination of the common matrices F.

In our previous work [3] the method of "mapping" the force field was described. In a similar sense, the common F matrix of the isotopic molecules can be "mapped", *i. e.*, F matrices can be computed with systematically changed values of the $\binom{n-1}{2}$ independent parameters. In order to be able to perform this method, a simpler relation between all the parameters and the independent ones must be found.

Let us suppose that following the method described in our earlier work [1], or with the help of relations given by JOHANSEN [6], a matrix F satisfying both secular equations has been found. Let then the parameters be changed in small steps in such a way that the new matrix F belonging to these parameters should again correspond to both molecules. Let the parameters belonging to matrix $U^{(1)}$ be changed. Matrix

$$F = (g^{(1)})^{-1}\, U^{(1)}\, \Lambda^{(1)}\, (U^{(1)})'\, (g^{(1)})^{-1}$$

obtained in this way, obviously reproduces the frequencies of the first molecule properly, but it must be ensured that the frequencies of the other molecule are also given by this F matrix. This means that the changes in elements of F are only allowed if the relations

$$\Delta\lambda_i^{(2)} = \sum_{k,j=1}^{n} \frac{\partial\lambda_i^{(2)}}{\partial F_{kj}} \Delta F_{kj}^{(1} = 0 \qquad (3)$$

$$i = 1,\ 2,\ \ldots, n$$

hold, where $\Delta F_{kj}^{(1)}$ is a small change of the matrix element F_{kj}. Using the known relations (*e.g.*, [7])

$$\frac{\partial\lambda_i}{\partial F_{kj}} = 2L_{ji}L_{ki} \text{ if } k \neq j \text{ and } \frac{\partial\lambda_i}{\partial F_{kk}} = L_{ki}^2$$

$$k = 1, 2, \ldots, n$$

Eq. (3) can be converted into the form:

$$\Delta\lambda_i^{(2)} = \sum_{k,j=1}^{n} L_{ji}^{(2)} L_{ki}^{(2)} \Delta F_{kj}^{(1)} = 0$$
$$i = 1, 2, \ldots, n$$

Changing the parameters in sufficiently small steps, the equation

$$\Delta F_{kj} = \sum_{r<s=2}^{n} \frac{\partial F_{kj}}{\partial \alpha_{rs}} \Delta\alpha_{rs}$$

is valid in a good approximation, and

$$\Delta\lambda_i^{(2)} = \sum_{k,j=1}^{n} L_{ji}^{(2)} L_{ki}^{(2)} \sum_{r<s}^{n} \frac{\partial F_{kj}^{(1)}}{\partial \alpha_{rs}^{(1)}} \Delta\alpha_{rs}^{(1)} =$$

$$= \sum_{r<s=2}^{n} \Delta\alpha_{rs}^{(1)} \sum_{k,j}^{n} L_{ki}^{(2)} L_{ji}^{(2)} \frac{\partial F_{kj}^{(1)}}{\partial \alpha_{rs}^{(1)}} = 0$$
$$i = 1, 2, \ldots, n$$

The equation system consists of n equations, but if the product rule is fulfilled and $n-1$ frequencies have remained unchanged, the n-th cannot be changed, either. Thus we can take into consideration $n-1$ equations of the equation system above, in order to express $n-1$ parameters as a function of the other $\binom{n-1}{2}$ parameters.

According to this, using the method of "mapping", the values of the parameters belonging to a common matrix F are to be modified. The values of one or several of the $\binom{n-1}{2}$ independent parameters will be changed to a small extent; then the values of the further $n-1$ parameters can be determined with the help of equation system (4). Thus having all the $\binom{n}{2}$ parameter values, the elements of the following matrix F can be determined. Going on with the procedure, the matrices F corresponding to the systematically changed values of the independent parameters can be obtained.

Our method, which is suitable for the determination of the maximum and minimum (*i. e.* extreme) values of force constants, has been described in a previous work [3]. This process offers a possibility for the determination of the extreme values with accessory conditions, namely that the force constants have to remain between prescribed limits. This method also permits to find the extreme values of the F matrices suitable for isotopic molecules. The dif-

ference as compared with the process described in [3] lies only in the fact that now further conditions, namely that $\Delta\lambda_i^{(2)} = 0$ $(i = 1, 2, \ldots n)$ must be fulfilled.

SUMMARY

It is proved that matrices F fulfilling the secular equations of order n of two isotopic molecules can be formed by $\binom{n-1}{2}$ parameters. An equation system is given for the determination of independent parameters. The given relations permit the calculation of the common matrices F belonging to systematically varied values of independent parameters and the determination of the extreme values of elements of common matrix F.

REFERENCES

1. PULAY, P., TÖRÖK, F.: Acta Chim. Acad. Sci. Hung. **44**, 287 (1965)
2. PULAY, P., TÖRÖK, F.: Acta Chim. Acad. Sci. Hung. **47**, 273 (1965)
3. TÖRÖK, F., PULAY, P.: Acta Chim. Acad. Sci. Hung. **56**, 285 (1968)
4. WILSON, E. B., DECIUS, J. C., CROSS, P. C.: Molecular Vibrations. McGraw-Hill Book Co., Inc. 1955.
5. FREEMAN, D. E.: J. Mol. Spectr. **22**, 305 (1967)
6. JOHANSEN, H.: Z. Phys. Chem. **227**, 305 (1964)
7. GRIBOV, P. A.: Грибов, П. А.: Введение в теорию и расчет колебательных спектров многоатомных молекул. Изд. Ленинградского Университета. 1965

Ferenc TÖRÖK; Budapest VIII., Múzeum krt. 6/8.

Acta Chimica Academiae Scientiarum Hungaricae Tomus 57 (2), pp. 147—152 (1968)

ПРОГРАММИРОВАНИЕ ДЛЯ ЭВМ ТИПА «УРАЛ-2» ДЛЯ РЕНТГЕНОСТРУКТУРНОГО АНАЛИЗА I.

СУММИРОВАНИЕ ДВУХМЕРНЫХ РЯДОВ ФУРЬЕ

Кафедра Экспериментальной физики университета им. Л. Этвэша

Л. Чордаш

Поступило 30 сент. 1967 г.

Одной из самых больших технических проблем в рентгеноструктурном анализе является большой объем расчетов. Очень часто применяется суммирование рядов Фурье с двумя переменными и для определения электронной плотности в кристалле и для исследования функции Паттерсона.

Электронную плотность в кристалле можно разложить в трехмерный ряд Фурье, где коэффициентами ряда являются структурные амплитуды рассеянных рентгеновских лучей кристаллом. Функция Паттерсона совпадает с выше упомянутым выражением за исключением коэффициентов. Расчет трехмерного ряда даже и на средних ЭВМ требует такую большую затрату времени, что обычно считается только двухмерный ряд-двухмерная проекция или двухмерное сечение трехмерного ряда.

Симметрия проекции зависит от пространственной группы кристалла. Различаются 17 плоских групп (17 различных проекций). Соответственные им ряды Фурье являются тоже различными, поэтому для расчетов в различных плоских группах требуются отдельные программы. Построение и проверка программы являются всегда очень трудоемкими, особенно для таких машин, как и Урал-2, для которой программы закодированы цифровым кодом в действительных адресах. Поэтому мы стремились вырабатывать программу, применяемую для решений различных задач.

Была выбрана плоская группа $p2$. Двухмерный ряд в общем (центросимметричном) случае имеет следующий вид:

$$f(x,y) = \sum_{h\,0}^{\infty} \sum_{k\,-\infty}^{\infty} A(hk) \cdot \cos 2\pi(hx + ky)$$

В плоской группе $p2$ амплитуды $A(hk) \neq A(h\bar{k})$ ($\bar{k}$ пишется вместо $-k$), поэтому ряд можно делить на две части:

$$f(x,y) = \sum_{h\,0}^{\infty} \sum_{k\,0}^{\infty} A(hk) \cdot \cos 2\pi\,(hx + ky) +$$

$$+ \sum_{h\,0}^{\infty} \sum_{k\,0}^{\infty} A(h\bar{k}) \cdot \cos 2\pi\,(hx - ky)$$

или в другой форме:

$$f(x,y) = \sum_{h}^{\infty}{}_{0} \sum_{k}^{\infty}{}_{0} \left[A(hk) + A(h\bar{k})\right] \cdot \cos 2\pi\, hx \cdot \cos\, 2\pi\, ky -$$

$$- \sum_{h}^{\infty}{}_{0} \sum_{k}^{\infty}{}_{0} \left[A(hk) - A(h\bar{k})\right] \cdot \sin 2\pi\, hx \cdot \sin 2\pi\, ky\,.$$

Для плоской группы ***pmm*** вид ряда проще (так как $A(hk) = A(h\bar{k})$):

$$f(x,y) = \sum_{h}^{\infty}{}_{0} \sum_{k}^{\infty}{}_{0} A(hk) \cdot \cos 2\pi\, hx \cdot \cos 2\pi\, ky.$$

Программа была составлена исходя из этих формул. Исходные данные: $A(hk)$, $A(h\bar{k})$, или только $A(hk)$. Максимальная величина h равна 20, а величина $k_{\max}$ может быть любая (у нас было $k_{\max} = 38$).

В запоминающем устройстве машины сохраняется таблица косинусов, $\cos n\,.\,3°$ (n = целое число), от 0° до 180°. Машина выбирает из этой таблицы нужную величину косинуса или синуса. «Шаг» Δx и Δy, на которые элементарная ячейка разделена, равен 3° и 6° ($2\pi/120$ или $2\pi/60$), либо в обоих направлениях, либо в одном направлении 3°, а в другом 6°.

Перед численными данными передаются машине команды о тех переменных, как $h_{\max}$, $k_{\max}$ и соответственно им длины циклов, «шаги» Δx, Δy, и в случае необходимости, и добавочные команды для других плоских групп.

Основной рачет ведется по формуле $f(xy)$ для плоской группы $p2$. Во-первых считается выражение

$$A(hk) \pm A(h\bar{k})$$

и накопляется на месте $A(hk)$ и $A(h\bar{k})$. Первое суммирование (внутренний цикл) идет по k, отдельно для k четных и нечетных индексов (x и y постоянные). Если обозначим результаты первой суммы (отдельно для всех h) через

$$C_{2n} = \sum_{k}{}_{k=2n} \left[A(hk) + A(h\bar{k})\right] \cdot \cos 2\pi\, ky\,,$$

$$C_{2n+1} = \sum_{k}{}_{k=2n+1} \left[A(hk) + A(h\bar{k})\right] \cdot \cos 2\pi\, ky$$

и через S_{2n}, S_{2n+1} соответственно для второй части выражения (с синусами) тогда амплитуды второго суммирования по h (внешний цикл) равны:

$$C_{2n} \pm C_{2n+1}$$

$$S_{2n+1} \pm S_{2n}$$

(отдельно для четных и нечетных индексов h). Такое разделение необходимо для получения функций $f(x, y)$ не только в интервалах 0°—90°, но и в интервалах 0°—180°, 0°—360°. В результате этих процессов получаются 8 данных. Их суммирование с различными знаками дает функцию $f(x, y)$ в следующих точках:

$$f(x, y),\ f(1/2 - x, y),\ f(1/2 + x, y),\ f(1 - x, y),\ f(x, 1/2 - y),$$
$$f(1/2 - x, 1/2 - y),\ f(1/2 + x, 1/2 - y),\ f(1 - x, 1/2 - y).$$

(В действительности, x, y не считаются в градусах, но в относительных единицах.) После выписывания этих величин продолжается расчет на всех x, (y остается постоянной), потом суммирование начинается с начала на следующую величину y.

ЭВМ «Урал-2» имеет внешнее управление, это — ключ «23». С помощью этого ключа (тумблер на пульте управления) меняется программа для других плоских групп. Например для плоской группы ***pmm*** функция $f(x, y)$ имеет вышеуказанную формулу. Исходные данные $A(hk)$ и суммирование ведется только по косинусам. Здесь первый ключ «23» запрещает образование

$$A(hk) \pm A(h\bar{k})$$

и второй ключ выключает суммирование по синусам.

Асимметрическая часть элэментарной ячейки на половину меньше вышеописанной, поэтому третий ключ командирует выписку результатов только в точках:

$$f(x, y),\ f(1/2 - x, y),\ f(x, 1/2 - y),\ f(1/2 - x,\ 1/2 - y).$$

Для плоской группы ***pgg*** функция $f(x, y)$ пишется в следующей форме:

$$f(x, y) = \sum_h \sum_k \sum_{h+k=2n} A(hk) \cdot \cos 2\pi hx \cdot \cos 2\pi ky -$$

$$- \sum_h \sum_k \sum_{h+k=2n+1} A(hk) \cdot \sin 2\pi hx \cdot \sin 2\pi ky$$

[так как при $h + k = 2n$, $A(hk) = A(h\bar{k})$
и при $h + k = 2n + 1$, $A(hk) = -A(h\bar{k})$].

Здесь исходные данные 1/2. $A(hk)$ в естественном порядке h и k. Машина вначале перепишет амплитуды на место $A(h\bar{k})$ с неизменными знаками для $h + k = 2n$ и с противоположными знаками для $h + k = 2n + 1$.

Образуя теперь выражение

$$A(hk) \pm A(h\bar{k}),$$

на месте $A(hk)$ получается $A(hk)$ для $h + k = 2n$ и нуль для $h + k = 2n + 1$, а на месте $A(h\bar{k})$ нуль, для $h + k = 2n$ и $A(hk)$ для $h + k = 2n + 1$. Меняя еще несколько команд во внутреннем цикле, оставляется каждый второй член суммы. Позиции ключей «23» будут:

первый : включено
второй : включено
третий : выключено

(требуются только результаты 1—4).

С помощью такого типа управления программа пригодна для 11-ти плоских групп электронной плотности и для всех проекций функции Паттерсона, и машина не выполняет много лишних операций. Переменяя несколько команд, мы уже использовали программу тоже и для такого ряда, как

$$\sum_h \sum_k A(hk) \cdot \cos 2\pi hx \cdot \sin 2\pi ky .$$

Такой задачей была определение взвешенной (обобщенной) проекции электронной плотности.

Результаты расчета получаются или на быстродействующей выписывающей машине или перфорируются на бумажную ленту (в связи с четвертым и пятым ключем).

Контроль за правильностью работы машины решается так, что определяется функция $f(x, y)$ еще в точках $f(x = 96°, y)$ и $f(x, y = 96°)$. Эти данные уже повторяются из-за симметрии кристалла. Значение $f(0, 0)$ вычисляется с ручной машиной.

Длительность выполнения программы находится в диапазоне 5—15 минут в зависимости от длины ряда и «шагов» Δx и Δy.

Автор выражает искреннюю благодарность за оказанную помощь сотрудникам Вычислительного Центра Университета и д-ру Дьердь Менцел за ценные советы.

ЛУТЕРАТУРА

1. Айнберг, В. Д., Гавриленко, Е. Т., Сабсович, Л. Л.: Программирование для электронных вычислительных машин типа «Урал», Москва 1966.
2. Порай-Кошиц, М. А.: Практический курс рентгеноструктурного анализа том II. Москва 1960.

László Csordás; Budapest, VIII., Múzeum krt. 6/8.

Схема программы

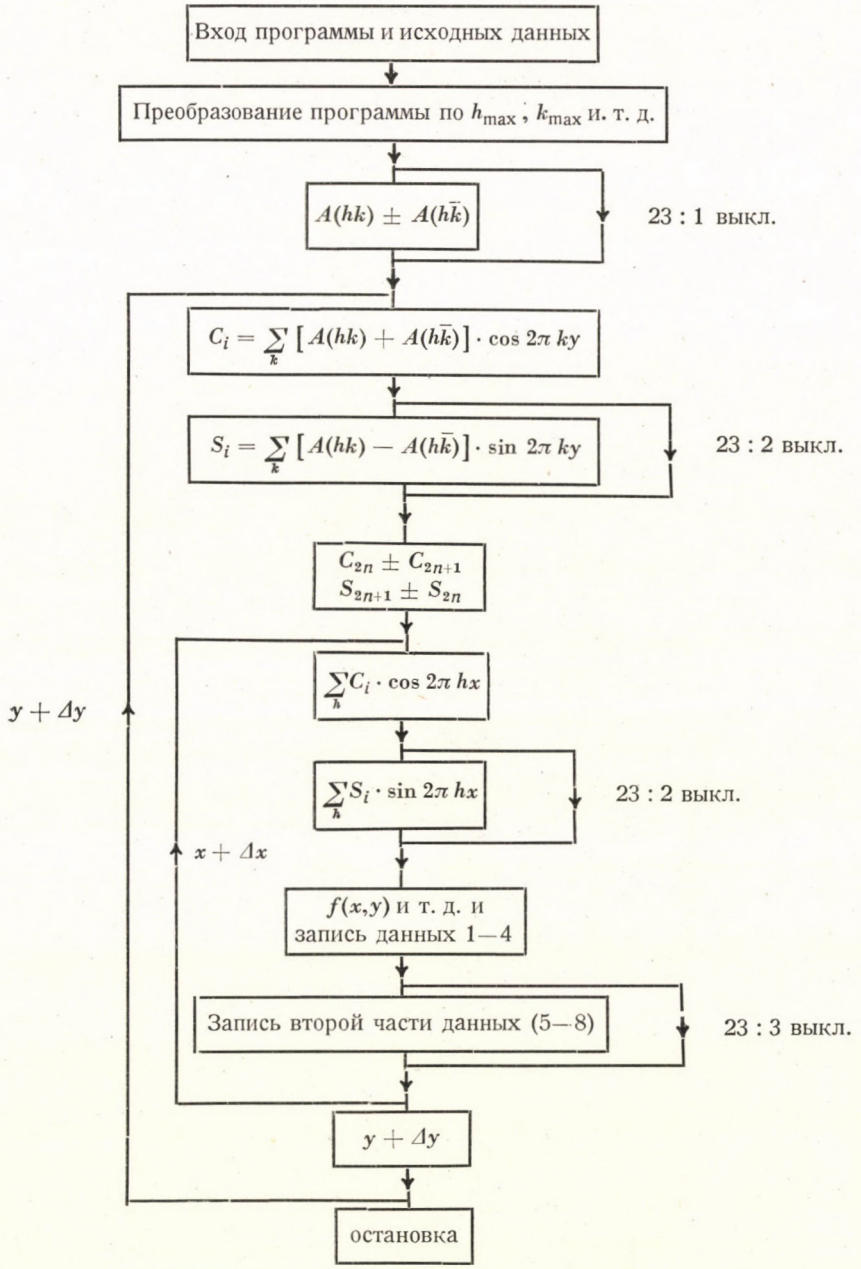

РЕЗЮМЕ

Одной из чаще всего применяющихся расчетов в рентгеноструктурном анализе является суммирование рядов Фурье. На *Кафедре Экспериментальной Физики была выработана* программа суммирования двухмерных рядов для ЭВМ типа «*Урал*-2», на машинном языке с цифровым кодом. Вид ряда и сам расчет зависит от симметрии кристалла. Программа пригодна для 11-ти из всех 17-ти возможных плоских групп. Исходные данные $A(hk)$, $A(h\bar{k})$ или только $A(hk)$ и h_{max}, k_{max}. Максимальная величина h может быть 20, а k_{max} любая. «Шаг» Δx и Δy, на которые разделена элементарная ячейка, равен $2\pi/120$ или $2\pi/60$ либо в обеих направлениях, либо в одном направлении равен $2\pi/120$, а в другом $2\pi/60$. Основой программы является использование «штрипсов» Биверса и Липсона. Величины косинусов и синусов выбираются из таблицы, находящейся в запоминающем устройстве машины. Результаты расчета получаются или на быстродействующей выписывающей машине, или перфорируются на бумажную ленту.

SUMMARY

In structural analysis by x-ray diffraction, one of the most often used methods of calculation is the summation of Fourier series. In the *Institute for Experimental Physics*, the program of the summation of Fourier series with two variables has been prepared in machine code for the electronic computer type "*URAL*—2". The form of the series, and consequently also the computation are dependent on the symmetry of the crystal. Of the possible 17 plane groups, this program can be used with 11 groups. Starting data are $A(hk)$, $A(h\bar{k})$ or only $A(hk)$ and h_{max} k_{max}, the possible maximum value of h being 20, while that of k_{max} is arbitrary. The "steps" Δx, Δy, into which the elemental cell is divided, are $2\pi/120$ or $2\pi/60$ either in both directions, or $2\pi/120$ in one of the directions, and $2\pi/60$ in the other. The program is based on the Beevers—Lipson strips. The cosine and sine values are selected by the machine from a table stored in the memory. The output may be printed out on a quick-printer or punched on a tape.

Acta Chimica Academiae Scientiarum Hungaricae Tomus 57 (2), pp. 153—168 (1968)

UNTERSUCHUNG DER ELEKTRONENANREGUNGS-VORGÄNGE UND DER BINDUNGSVERHÄLTNISSE DER KOMPLEXE VON $3d^n$ ELEMENTEN MIT DER LIGANDEN-FELD-METHODE, III.

MONOACIDO-, TRANS-DIACIDO- UND CIS-DIACIDO-KOBALT(III)- und CHROM(III)-KOMPLEXE

M. BÁN und J. CSÁSZÁR

(Physikalisch-Chemisches Institut der Attila József Universität, Szeged)

Eingegangen am 3. November 1967

Zahlreiche Forscher beschäftigten sich bereits mit der experimentellen [1—6] und theoretischen [7—9] Untersuchung der spektroskopischen Eigenschaften von Cr^{3+}- und Co^{3+}-Monoacidopentaamin-, *trans*- und *cis*-Diacidotetraamin-Komplexen. Die bei der Symmetrieerniedrigung von O_h auf D_{4h}, C_{4v}, C_{2v} in manchen Fällen auftretende Bandenspaltung wurde nachgewiesen und gedeutet. Solche Berechnungen jedoch, die bei *cis*-Verbindungen auf Grund der effektiven C_{2v}-Symmetrie erfolgten oder mit Hilfe deren die charakteristischen Parameter der *cis*- und *trans*-Diacidoverbindungen ($X \neq Y$) berechnet wurden, sind in der Literatur kaum zu finden (s. z. B. [10]).

In einer unserer früheren Arbeiten beschäftigten wir uns mit der Struktur, der Absorptionsspektra, den Anregungsvorgängen und Bindungsverhältnissen von Co^{3+}- und Cr^{3+}-Komplexen oktaedrischer (O_h) Symmetrie [11]. Diese auf der Ligandenfeldtheorie beruhenden Berechnungen wurden auch auf Moleküle von $[Me(NH_3)_5X]$-, *cis*, *trans*-$[Me(en)_2X_2]$- und *cis*, *trans*-$[Me(en)_2XY]$-Typ (Me = Cr^{3+}, Co^{3+}) ausgebreitet; über die Resultate wird nachstehend berichtet.

Theoretischer Teil

a) Das d^6-Problem

Für jene Komplexe (Monoacido- und *trans*-Diacido-Verbindungen), die quantummechanisch mit der tetragonalen (D_{4h}, C_{4v}) Perturbation des Oktaeders beschrieben werden können, ist das in Abb. 1 dargestellte Spaltschema gültig. Für *cis*-Komplexe wird angenommen, daß sie trotz ihrer formell rhombischen Symmetrie (C_{2v}) praktisch als tetragonal behandelt werden können [12], so daß auch hier das obige Schema der Termaufspaltung gültig ist. Wenn die tetrago-

nale Perturbation klein ist, was im folgenden angenommen wird, müssen statt $^1E_g^1$ und $^1E_g^2$ die linearen Kombinationen

$$^1E_g^+ = \frac{\sqrt{3}}{2}\,{}^1E_g^1 + \frac{1}{2}\,{}^1E_g^2 \tag{1a}$$

und

$$^1E_g^- = \frac{1}{2}\,{}^1E_g^1 - \frac{\sqrt{3}}{2}\,{}^1E_g^2 \tag{1b}$$

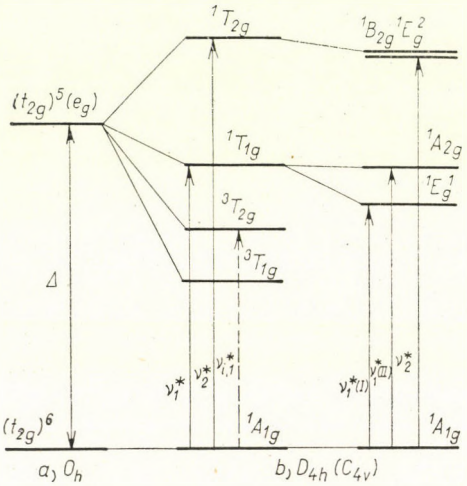

Abb. 1. Energieniveau-Diagramm und die wichtigsten Übergänge der Co^{3+}-Komplexe mit O_h- und $D_{4h}(C_{4v})$-Symmetrie

verwendet werden [13, 8*a*]. Die Einelektronen-Bahnenergien sind

$$E(a_{1g}) = \varepsilon_0 + 6Dq - 2Ds - 6Dt\,, \tag{2a}$$

$$E(b_{1g}) = \varepsilon_0 + 6Dq + 2Ds - Dt\,, \tag{2b}$$

$$E(b_{2g}) = \varepsilon_0 - 4Dq + 2Ds - Dt\,, \tag{2c}$$

$$E(e_g) = \varepsilon_0 - 4Dq - Ds + 4Dt\,, \tag{2d}$$

wobei Dq das oktaedrische Ligandenfeld-Parameter ist, Ds und Dt hingegen für die tetragonale Perturbation charakteristische Parameter sind [8a, 14, 15]. Unter Verwendung der Zusammenhänge (1) und (2), der Ligandenfeld-Potentiale D_{4h} und C_{4v} [14, 15] sowie der entsprechenden Mehrelektron-Wellenfunktionen [13] ergeben sich für die einzelnen Zustände die folgenden Energieausdrücke:

$$E_l(^1A_{1g}) = -24Dq + 14Dt\,, \tag{3a}$$

$$E_l(^1E_g^+) = -14Dq + 21/4Dt\,, \tag{3b}$$

$$E_l(^1A_{2g}) = -14Dq + 14Dt\,, \tag{3c}$$

$$E_l(^1B_{2g}) = -14Dq - 4Ds + 9Dt\,, \tag{3d}$$

$$E_l(^1E_g^-) = -14Dq + 2Ds + 31/4Dt\,. \tag{3e}$$

Im weiteren werden auch noch die die gegenseitige Wechselwirkung der Elektronen beschreibenden Energieausdrücke benötigt. Diese erhält man aus den diagonalen Elementen [17] der entsprechenden elektrostatischen Matrizen [16]:

$$E_e(^1A_{1g}) = 5B + 8C\,, \tag{4a}$$

$$E_e(^1T_{1g}) = 5B + 7C\,, \tag{4b}$$

$$E_e(^1T_{2g}) = 21B + 7C\,. \tag{4c}$$

So erhält man für die einzelnen Elektronenübergänge

$$\nu_1^*(\mathrm{I}) = {}^1E_g^+ \leftarrow {}^1A_{1g} = 10Dq - 35/4Dt - C\,, \tag{5a}$$

$$\nu_1^*(\mathrm{II}) = {}^1A_{2g} \leftarrow {}^1A_{1g} = 10Dq - C\,, \tag{5b}$$

$$\nu_2^*(\mathrm{I}) = {}^1B_{2g} \leftarrow {}^1A_{1g} = 10Dq - 4Ds - 5Dt + 16B - C\,, \tag{5c}$$

$$\nu_2^*(\mathrm{II}) = {}^1E_g^- \leftarrow {}^1A_{1g} = 10Dq + 2Ds - 25/4Dt + 16B - C\,. \tag{5d}$$

Für den oktaedrischen Parameter ergibt sich

$$Dq = 1/6R_4(xy,z)\,. \tag{6}$$

Für Monoacido- und *trans*-Diacidoverbindungen erhält man für die Parameter *Ds* und *Dt* [14, 15]:

$$C_{4v} \begin{cases} Ds = 1/7[2R_2(xy) - R_2(z) - R_2'(z)]\,, & (7) \\ Dt = 1/21[2R_4(xy) - R_4(z) - R_4'(z)]\,, & (8) \end{cases}$$

$$D_{4h}(X=Y) \begin{cases} Ds = 2/7[R_2(xy) - R_2(z)]\,, & (9) \\ Dt = 2/21[R_4(xy) - R_4(z)]\,, & (10) \end{cases}$$

während im Falle von *cis*-Verbindungen der spezifisch für C_{2v}-Symmetrie erhaltene Zusammenhang [14] auch zum Ausdruck von *Dt* verwendet wird:

$$Dt = 1/168[19R_4(xy) - 3R_4'(xy) - 8R_4(z) - 8R_4'(z)]\,. \tag{11}$$

In den Formeln (7)—(10) ist

$$R_l(xy, Z) = 8/45 \cdot \varepsilon \cdot e \cdot f \cdot G_l \,, \tag{12}$$

wobei ε, e, bzw. Z die Ladung des Ligands, des Elektrons und des Zentralions,

$$f = \frac{Z}{3a_0} \tag{13}$$

und

$$G_l = \int_0^\infty (fr)^6 \frac{r_<^l}{r_>^{l+1}} \cdot e^{-2fr} \cdot dr \tag{14}$$

ist.

Laut unserer Erfahrungen wird ν_2^* bei Co^{3+}-Komplexen nie aufgespaltet, doch kann ν_1^* bei Monoacido-, *trans*-Diacido- und manchmal sogar bei *cis*-Diacidoverbindungen in zwei Komponente aufgelöst werden. Beim Spalten oder nicht Spalten von ν_1^* gestalten sich die entsprechenden Parameter folgend:

Für den Wert von Dt ergibt sich unter Berücksichtigung von (6) für alle drei Verbindungsgruppen

$$Dt = 4/35 \left[\nu_1^*(O_h) - \nu_1^*(I)\right], \tag{15}$$

wenn ν_1^* (I) und ν_1^* (II) getrennt werden können. Falls nicht, d.h. ν_1^* (I) = $= \nu_1^*$ (II) $\equiv (\nu_1^*)$, dann ist

$$Dt = 8/35[\nu_1^*(O_h) - \nu_1^*] \,. \tag{16}$$

Ds kann stets auf Grund des Zusammenhangs

$$Ds = 5/24 Dt \tag{17}$$

berechnet werden.

Beim Spalten von ν_1^* ergeben sich die folgenden Werte für Dq:

$$C_{4v} : Dq(z) = Dq(O_h) - 2/5[\nu_1^*(O_h) - \nu_1^*(\mathrm{I})] \,, \tag{18}$$

$$D_{4h}(X = Y) : Dq(z) = Dq(O_h) - 1/5[\nu_1^*(O_h) - \nu_1^*(\mathrm{I})] \,, \tag{19}$$

$$C_{2v} : Dq(z) = Dq(O_h) - 28/11 Dt \,. \tag{20}$$

Wenn ν_1^* nicht aufgelöst werden kann, dann steht in (18) 4/5 statt 2/5, und in (19) 2/5 statt 1/5. Wenn bei *trans*- bzw. *cis*-Verbindungen $X \neq Y$ ist, so ergeben sich die folgenden Werte:

$$Dq(z) = \frac{4Dq\,(O_h) - 7Dt - 2Dq(z')}{2}\,, \tag{21}$$

$$Dq'\,(xy) = \frac{11Dq(O_h) - 8Dq(z) - 28Dt}{3}\,, \tag{22}$$

und

$$Dq(z) = \frac{11Dq\,(O_h) - 3Dq'\,(xy) - 28Dt}{8}\,. \tag{23}$$

Der Parameter C kann stets aus dem Zusammenhang

$$C = 10Dq(O_h) - \nu_1^*(\mathrm{II}) \tag{24}$$

erhalten werden, während B auf Grund der Formeln (5c) und (5d) sowohl für Monoacido- als auch für *trans*- und *cis*-Verbindungen aus dem Zusammenhang

$$B = \frac{6\nu_2^* - 60Dq\,(O_h) + 6C + 35Dt}{96} = \\ = \frac{\nu_2^* - 10Dq\,(O_h) + C(O_h) + 5Dt + 4Ds}{16} \tag{25}$$

berechnet werden kann.

b) Das d^3-Problem

Die mathematische Behandlung der bei diesen Verbindungen auftretenden Probleme ist sehr ähnlich wie die der vorangehend diskutierten Probleme. Der Unterschied besteht darin, daß im Termschema (Abb. 2) Quadruplett-Zustände vorliegen, der Grundterm die Symmetrie $^4B_{1g}$ besitzt, ferner daß für den oktaedrischen Fall die Reihenfolge von $^4T_{1g}$ und $^4T_{2g}$ und für den tetragonalen Fall die der entsprechenden Spaltprodukte vertauscht ist. Die *Dt*-Werte in Verbindung mit der tetragonalen Perturbation sind mit den für Fall d^6 angegebenen identisch (Formeln 15 und 16).

Als ein wesentlicher Unterschied ist zu erwähnen, daß sich bei einigen *trans*-Diacido-Cr^{3+}-Komplexen auch ν_2^* spaltet, und die dabei zu erwartenden Elektronenübergänge folgend beschrieben werden können:

$$\nu_1^*(\mathrm{I}) \quad = {}^4E_g^+ \leftarrow {}^4B_{1g} = 10Dq - 35/4Dt\,, \tag{26a}$$

$$\nu_1^*(\mathrm{II}) \quad = {}^4B_{2g} \leftarrow {}^4B_{1g} = 10Dq\,, \tag{26b}$$

$$\nu_2^*(\mathrm{I}) \quad = {}^4A_{2g} \leftarrow {}^4B_{1g} = 10Dq + 12B - 4Ds - 5Dt\,, \tag{26c}$$

$$\nu_2^*(\mathrm{II}) \quad = {}^4E_g^- \leftarrow {}^4B_{1g} = 10Dq + 12B + 2Ds - 25/4Dt\,. \tag{26d}$$

Falls sich ν_2^* nicht spaltet, kann Ds mit der Formel (15), und wenn die Lage von $\nu_2^*(\mathrm{I})$ und $\nu_2^*(\mathrm{II})$ bestimmt werden kann, mit der Formel

$$Ds = \frac{4[\nu_2^*(\mathrm{II}) - \nu_2^*(\mathrm{I})] + 5Dt}{24} \tag{27}$$

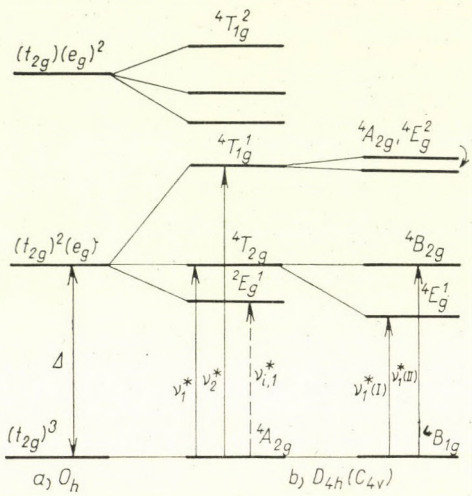

Abb. 2. Termschema der Cr^{3+}-Komplexe mit O_h- sowie $D_{4h}(C_{4v})$-Symmetrie, mit den wichtigsten Übergängen

berechnet werden. Für $Dq(z)$ und $Dq(xy)$ sind die für die entsprechenden Symmetrien abgeleiteten Gleichungen (18) — (23) die betreffenden Feststellungen gültig. Unter Verwendung von (26c) und (26d) ist

$$B = \frac{4\nu_2^*(\mathrm{II}) + 2\nu_2^*(\mathrm{I}) - 60Dq(O_h) + 35Dt}{72} =$$

$$= \frac{2[\nu_2^*(\mathrm{II}) - \nu_1^*(\mathrm{I})] + [\nu_2^*(\mathrm{I}) - \nu_1^*(O_h)]}{36}. \tag{28}$$

Wenn $\nu_2^*(\mathrm{I}) = \nu_2^*(\mathrm{II}) \equiv (\nu_2^*)$, dann ist auf Grund von (15,) (16) und (17), aber auch aus (28)

$$B = \frac{\nu_2^* - 10Dq(O_h) + 4Ds + 5Dt}{12}. \tag{29}$$

Diskussion

Die spektralen Daten einiger Monoacidopentaamin-, *trans*-Diacido-($X = Y$), *cis*-Diacido-($X = Y$), *trans*- bzw. *cis*-Diacido-($X \neq Y$) Verbindungen sowie die aus diesen Daten berechneten charakteristischen Parameter sind in den Tabellen I—V zusammengefaßt.

Auf Grund der zahlreichen Versuchsdaten kann festgestellt werden, daß bei den Monoacido-, *trans*-Diacido-Co^{3+}- und -Cr^{3+}-Verbindungen in der überwiegenden Mehrzahl der Fälle ν_1^* gut auswertbar aufgespaltet oder zumindest so stark deformiert wird, daß die Bestimmung der Lage der beiden Komponenten $\nu_1^*(I)$ und $\nu_1^*(II)$ — eventuell mittels Kurvenanalyse — keine Schwierigkeit verursacht. Bei Co^{3+}-Komplexen liegen $\nu_1^*(II)$ und die Bande $\nu_1^*[^1T_{1g} \leftarrow {}^1A_{1g}]$ der Grundverbindungen einander sehr nahe. Die Bande $\nu_1^*(I)$ ist dem Übergang $^1E_g^+ \leftarrow {}^1A_{1g}$ zugeordnet. $\nu_1^*(I)$ und $\nu_1^*(II)$ können gut unterschieden werden, wenn die Lage von X (Y) in der spektrochemischen Reihe der oktaedrischen Komplexe von der von NH_3 (oder von »en») wesentlich verschieden ist. Falls dieser Unterschied klein ist, kann bloß eine Verbreitung von ν_1^* beobachtet werden. Bei *cis*-Diacidoverbindungen kann ν_1^* mit guter Annäherung als symmetrisch betrachtet werden.

Tabelle I[a]

Spektraldaten und berechnete Parameter der Komplexe vom Typ $[Co(NH_3)_5X]^{n+}$ *und* $[Cr(NH_3)_5X]^{n+}$

No.	X	$\nu_1^*(I)$	$\nu_1^*(II)$	ν_2^*	Dq	Dt	Ds	B	β
				a) Co^{3+}-Verbindungen					
1.	Cl^-	18 720	21 400	27 500	1566	266	55,4	500	0,47
2.	H_2O	20 500		30 400	2058	126	26,3	630	0,59
3.	OH^-	19 000	21 050	27 100	1678	234	48,8	463	0,43
4.	NCS^-	20 600		27 150	2138	103	21,5	419	0,38
5.	NO_2^-	21 750		30 800	3058	—160	—33,3	551	0,52
6.	Br^-	18 220	21 800	?	1366	323	67,3	—	—
7.	F^-	19 450	21 800	28 270	1858	183	38,1	518	0,49
8.	SO_3^{--}	20 500	22 250	28 000	2278	63	13,1	457	0,43
9.	N_3^-	19 320		27 150	1114	395	82,2	525	0,49
10.	CN^-	22 700		30 600	3818	—377	—78,5	459	0,43
				b) Cr^{3+}-Verbindungen					
11.	Cl^-	19 400	22 100	26 620	1310	240	50,0	543	0,57
12.	Br^-	19 050	21 800	26 500	1170	280	58,3	553	0,58
13.	J^-	18 500	21 500	—	949	343	71,5	—	—
14.	H_2O	19 360	22 280	27 820	1292	245	51,0	646	0,68
15.	OH^-	18 320	21 080	25 850	879	363	75,6	539	0,57
16.	NCS^-	20 350		~27 000	1229	263	54,8	586	0,62
17.	ONO^-	20 730		~26 800	1534	176	36,7	527	0,56
18.	N_3^-	20 080	22 850	~27 210	1583	162	33,8	471	0,50

[a] Mit Ausnahme von β sind sämtliche Werte in cm^{-1} angegeben.

Während bei Co^{3+}-Verbindungen die Aufspaltung von ν_2^* in keinem einzigen Fall vollständig eindeutig nachgewiesen werden konnte, ist die Aufspaltung dieser Bande bei einigen *trans*-Diacido-Cr^{3+}-Komplexen [18] mit Sicherheit feststellbar. Hier können $\nu_2^*(I)$ und $\nu_2^*(II)$ den Übergängen (26c) und (26d) zugeordnet werden; die Intensität von $\nu_2^*(II)$ ist im allgemeinen kleiner als die von $\nu_2^*(I)$.

Auf Grund der gemessenen bzw. berechneten *Dq* und β-Werte können für Monoacidoverbindungen die folgenden spektrochemischen und nephelauxetischen Reihen aufgestellt werden:

Co^{3+}-Verbindungen

$$Dq: \quad CN^- > NO_2^- > SO_3^{--} > NCS^- > H_2O > C_3H_5O_2^- > F^- > NO_3^- >$$

$$> TFA > OH^- > SO_4^{--} > CO_3^{--} > \left|\begin{matrix} DClA \\ TClA \end{matrix}\right| > \left|\begin{matrix} MClA \\ MBrA \\ DBrA \end{matrix}\right| > OCHO^- >$$

$$> Cl^- > CH_3CO_2^- > NH_2CO_2^- > S_2O_3^{--} > C_2O_4^{--} > Br^- > N_3^- > J^- > PO_4^{3-}$$

$$\beta: NCS^- < \left|\begin{matrix} CN^- \\ SO_3^{--} \\ OH^- \end{matrix}\right| < \left|\begin{matrix} Cl^- \\ C_2O_4^{--} \\ S_2O_3^{--} \end{matrix}\right| < \left|\begin{matrix} C_3H_5O_2^- \\ CO_3^{--} \end{matrix}\right| < \left|\begin{matrix} F^- \\ N_3^- \end{matrix}\right| < NO_3^- <$$

$$< \left|\begin{matrix} MClA,\ NH_2CO_2^- \\ CH_3CO_2^-,\ OCHO^- \\ NO_2^- \end{matrix}\right| < \left|\begin{matrix} PO_4^{3-},\ DClA,\ DBrA, \\ MBrA,\ TClA \end{matrix}\right| < \left|\begin{matrix} SO_4^{--} \\ TFA \end{matrix}\right| < H_2O$$

Cr^{3+}-Verbindungen:

$$Dq: N_3^- > ONO^- > Cl^- > H_2O > NCS^- > Br^- > J^- > OH^-$$

$$\beta: N_3^- < ONO^- < OH^- < Cl^- < Br^- < NCS^- < H_2O$$

Wenn die berechneten Werte mit den entsprechenden Parametern der Grundverbindungen [19, 20] verglichen werden, findet man eine sich ändernde Übereinstimmung.

Der für $[Co(H_2O)_6]^{3+}$ berechnete $10Dq$ Wert von 20,650 cm^{-1} stimmt mit dem für $[Co(NH_3)_5H_2O]^{3+}$ erhaltenen fast vollständig überein, während derselbe im Falle von $[Co(NH_3)_5CN]^{2+}$ innerhalb von 6% zu liegen kommt. Die Abweichung ist z. B. bei den CO_3^{--}, NO_2^- und $C_2O_4^{--}$ enthaltenden Verbindungen bereits beträchtlicher (25, 23 bzw. 43%), was teilweise auch damit erklärt werden kann, daß CO_3^{--} und $C_2O_4^{--}$ als zweizähnige Liganden in den entsprechenden Grundverbindungen gebunden sind.

In den Co^{3+}-Komplexen der aliphatischen Monocarbonsäuren [21] ist der Polarisationsgrad der Co—O Bindungen nicht genau bekannt, doch ist

Tabelle II

Spektraldaten und berechnete Parameter der Komplexe vom Typ $[Co(NH_3)_4X_2]^{n+}$

No.	X^a	ν_1^*(I)	ν_1^*(II)	ν_2^*	Dq	Dt	Ds	B	β
19.	H_2O	19 530		28 000	1890	347	72,3	561	0,53
20.	Cl^-	15 880	21 050	24 950	1464	591	123,1	459	0,43
21.	NO_2^-	22 730		~28 850	3170	−384	−80,0	348	0,33
22.	N_3^-	17 650		~25 250	1138	777	161,9	546	0,51
23.	TFA	17 900	22 000	28 170	1868	360	75,0	576	0,54
24.	MClA	18 020	21 800	27 620	1892	346	72,1	537	0,50
25.	DClA	17 920	21 800	27 860	1872	358	74,6	556	0,52
26.	TClA	17 760	21 900	28 010	1840	376	78,3	572	0,54
27.	DBrA	17 950	21 800	27 780	1878	354	73,8	550	0,52

[a] TFA = Trifluoracetat; MClA = Monochloracetat; DClA = Dichloracetat; TClA = Trichloracetat; DBrA = Dibromacetat.

Tabelle III

Spektraldaten und berechnete Ligandenfeld-Parameter der Komplexe vom Typ trans-$[Co(en)_2X_2]$ *und* $-[Cr(en)_2X_2]$

a) Co^{3+}-Verbindungen

No.	X	ν_1^*(I)	ν_1^*(II)	ν_2^*	Dq	Dt	Ds	B	β
28.	Cl^-	16 200	22 480	25 850	1483	600	125,0	494	0,46
29.	H_2O	18 200	22 500	29 120	1883	371	77,3	615	0,58
30.	Br^-	15 250	21 720	26 120	1293	709	147,7	550	0,52
31.	NCS^-	19 730		29 720	1845	393	81,9	660	0,62
32.	F^-	17 200	22 640	27 620	1683	486	101,2	563	0,53
33.	OH^-	19 000		26 300	1553	560	116,7	507	0,48
34.	TFA	18 170	22 900	28 400	1877	375	78,1	571	0,54
35.	MClA	18 380	22 420	28 090	1919	351	73,1	543	0,51
36.	DClA	18 270	22 620	28 170	1897	363	75,6	552	0,52
37.	TClA	17 970	22 840	28 410	1837	398	82,9	580	0,54
38.	DBrA	18 260	22 570	28 170	1895	364	75,8	553	0,52

b) Cr^{3+}-Verbindungen

No.	X	ν^*(I)	ν_1^*(II)	ν_2^*(I)	ν_2^*(II)	Dq	Dt	Ds	B	β
39.	Cl^-	17 550	21 880	25 380	27 720	1329	486	491,0	664	0,70
40.	Br^-	16 780	21 790	24 850	26 980	1175	574	475,0	651	0,69
41.	OH^-	18 250	19 900	25 250	30 300	1469	406	926,0	765	0,81
42.	H_2O	19 700	22 780	27 700		1760	240	50,0	608	0,64

anzunehmen, daß er sich parallel mit der Polarität der H—O Bindungen in der entsprechenden Säure ändert, welche ihrerseits qualitativ in der Größe der pK-Werte zum Ausdruck kommt. Die im Einklang damit berechneten *Dq*-Werte ändern sich fast linear mit den pK-Werten der Säure [21]:

	TClA	DClA	MClA	MBrA	CHO_2^-	$CH_3CO_2^-$
pK_s	0,70	1,30	1,85	1,86	3,75	4,76
Dq	1610	1610	1594	1594	1578	1554

Es soll jedoch bemerkt werden, daß dieser Zusammenhang nicht verallgemeinert werden kann und z. B. für die komplexbildenden Anionen der starken Säuren nicht gültig ist.

Ein Vergleich der Daten von entsprechenden Co^{3+}- und Cr^{3+}-Verbindungen zeigt, daß die Richtung der Änderung der *Dq*-Werte im großen und ganzen gleich ist, doch sind die Werte für Cr^{3+}-Verbindungen stets kleiner. Die *Dq*(H_2O) und *Dq*(NCS) Werte unterscheiden sich kaum, was darauf schließen läßt, daß in den Komplexen Me—S Bindungen vorliegen, da im Falle einer Me—N Bindung ein bedeutend höherer *Dq*-Wert zu erwarten ist.

Auch bei den *trans*-Verbindungen ist fast ausnahmslos die Spaltung von ν_1^* zu beobachten. Die für *trans*-$[Co(NH_3)_4X_2]$- und *trans*-$[Co(en)_2X_2]$-Verbindungen aufstellbaren *Dq*- und β-Reihen sind wie folgt:
Tetraamin-Verbindungen:

$$Dq:\ N_3^- < Cl^- < TClA < TFA < DClA < DBrA < H_2O < MClA < < CH_3CO_2^- < NO_2^-$$

$$\beta:\ NO_2^- < Cl^- < CH_3CO_2^- < MClA < N_3^- < \left|\begin{matrix} DClA \\ DBrA \end{matrix}\right| < H_2O < \left|\begin{matrix} TFA \\ TClA \end{matrix}\right|$$

»en«-Verbindungen:

$$Dq:\ Br^- < Cl^- < OH^- < F^- < TClA < NCS^- < TFA < H_2O < DBrA < < DClA < MClA < CH_3CO_2^- < NH_3$$

$$\beta:\ Cl^- < OH^- < NH_3 < CH_3CO_2^- < MClA < \left|\begin{matrix} Br^- \\ DClA \\ DBrA \end{matrix}\right| < F^- < < \left|\begin{matrix} TFA \\ TClA \end{matrix}\right| < H_2O < NCS^-$$

Wie ersichtlich, stimmt die Reihenfolge der Liganden bei den beiden Gruppen in großen Zügen überein, und für die »en« Komplexe ist *Dq* um etwa 2% größer, ähnlich wie für die entsprechende Grundverbindung. Bei den *trans*-$[Cr(en)_2X_2]$-Verbindungen sind in einigen Fällen unzweifelhaft auch für ν_2^*

Tabelle IV

Spektraldaten und Ligandenfeld-Parameter der cis-Co^{3+}- und cis-Cr^{3+}-Komplexe

No.	X	ν_1^*	ν_2^*	Dt	Ds	Dq	B	β
			a) Komplexe vom Typ $[Co(NH_3)_4X_2]$					
43.	NO_2^-	22 500	—	−331	− 68,9	3341	—	—
44.	H_2O	20 000	28 000	+240	+ 50,0	1887	522	0,49
45.	N_3^-	18 570	—	567	118,1	1055	—	—
46.	F^-	19 100	27 300	446	92,9	1363	553	0,52
47.	NO_3^-	19 500	~28 530	354	73,8	1597	597	0,56
48.	TFA	19 500	27 830	354	73,8	1597	553	0,52
49.	TClA	19 460	27 700	363	75,6	1574	548	0,51
50.	DClA	19 310	27 620	398	82,9	1485	556	0,52
51.	DBrA	19 270	27 590	407	84,8	1462	557	0,52
52.	MBrA	19 160	27 550	432	90,0	1399	564	0,53
53.	MClA	19 120	27 550	441	91,9	1375	567	0,53
			b) Komplexe vom Typ $[Co(en)_2X_2]$					
54.	CN^-	24 730	32 370	−750	−156,2	4442	409	0,39
55.	NO_2^-	23 000	—	−354	−73,8	3434	—	—
56.	NCS^-	20 370	—	+247	+51,5	1904	—	—
57.	H_2O	20 200	28 170	286	59,6	1805	524	0,49
58.	TFA	20 200	28 400	286	59,6	1805	539	0,51
59.	TClA	20 090	27 700	311	64,8	1741	504	0,47
60.	DClA	20 060	27 700	318	66,3	1724	507	0,48
61.	DBrA	20 060	27 700	318	66,3	1724	507	0,48
62.	MClA	19 920	27 660	350	72,9	1642	516	0,48
63.	OH^-	19 330	27 000	485	101,0	1298	524	0,49

c) Komplexe vom Typ $[Cr(en)_2X_2]$

No.	X	ν_1^*(I)	ν_1^*(II)	ν_2^*	Dt	Ds	Dq	B	β
64.	Cl^-	18 970	21 850	24 950	323	67,3	1358	420	0,44
65.	Br^-	18 400	21 500	24 150	389	81,0	1190	385	0,41
66.	N_3^-	19 650	21 150	~25 150	246	51,3	1554	399	0,42
67.	NCS^-	20 620		~26 800	270	56,3	1493	548	0,58
68.	OH^-	19 080	21 900	26 550	311	64,8	1389	547	0,58
69.	H_2O	20 650		27 280	263	54,8	1511	585	0,62
70.	F^-	19 120	21 980	26 880	306	63,8	1401	572	0,60

Anzeichen eines zusammengesetzten Charakters zu beobachten. Die für diese Verbindungen berechneten *Ds*-Werte sind sehr hoch, und nähern die *Dq*-Werte an. Die Verzerrung, d. h. die Trennung der Zustände $^4A_{2g}$ und $^4E_g^-$ ist erheblich, was auch durch Berechnung der Einelektronen-Bahnenergien bestätigt wurde. Die Energiedifferenz $E(d_{x^2-y^2}) - E(d_{z^2})$ fällt bei diesen Verbindungen in den Bereich von 4000 bis 6000 cm^{-1}, während sie bei den übrigen Verbindungen — wo ν_2^* nicht aufgespaltet wird — 2000 cm^{-1} nicht überschreitet. *Dq* und β ändern sich nach der folgenden Reihenfolge:

$$Dq\text{: } H_2O > OH^- > Cl^- > Br^-$$

$$\beta\text{: } H_2O < Br^- < Cl^- < OH^-$$

Unter Verwendung der für Monoacido-Komplexe erhaltenen Parameter wurden auch die $Dq^{(X)}$ und $Dq^{(Y)}$ Werte der Verbindungen von *trans*-[Me(en)$_2$ XY]-Typ berechnet. Im überwiegenden Teil der Fälle ergaben sich auch hier *Dq*-Werten die die für Monoacido- bzw. *trans*-Diacido-($X = Y$)-Komplexe erhaltenen annäherten. Die *Dq*-Reihe für Co^{3+}-Komplexe ist wie folgt:

$$J^- < Br^- < Cl^- < NCS^- < H_2O < NH_3 < NO_2^-$$

Bei den *cis*-Verbindungen wird ν_2^* nicht aufgespaltet, und im allgemeinen auch ν_1^* nicht, doch kann bei einigen Cr^{3+}-Komplexen eine Verbreitung von ν_1^* beobachtet werden, und dies rechtfertigte die Trennung dieser Bande. Für die »en« Verbindungen sind die *Dt*- und *Ds*-Werte niedriger, hingegen die von *Dq*, *B* und demzufolge auch von β und $\delta\%$ in jedem der Fälle höher, als für die entsprechenden NH_3-Verbindungen. Auf Grund der von uns berechneten Daten können für *Dq* und β die folgenden Reihen aufgestellt werden:

cis-[$Co(NH_3)_4X_2$]-Verbindungen:

$$Dq\text{: } NO_2^- > en > H_2O > C_2O_4^{--} = NO_3^- = TFA > TClA > OCHO^- =$$
$$= glyH = l\text{-}\alpha\text{-}al > DClA > DBrA > MBrA > MClA > CH_3CO^- > =$$
$$= F^- > N_3^-$$

$$\beta\text{: } H_2O < \left|\begin{matrix}en,\ TClA,\\ OCHO^-,\ glyH,\\ l\text{-}\alpha\text{-}al\end{matrix}\right| < \left|\begin{matrix}TFA,\ DBrA,\\ DClA,\ F^-,\\ CH_3CO_2^-\end{matrix}\right| < \left|\begin{matrix}C_2O_4^{--},\ MClA\\ MBrA\end{matrix}\right| < NO_3^-$$

Nach unseren Berechnungen für *cis*-($X \neq Y$)-Verbindungen liegen die $Dq^{(X)}$- und $Dq^{(Y)}$-Werte in der Nähe der für die vorangehende Verbindungsgruppe ($X = Y$) berechneten; die *Dq*-Reihe ist:

$$NH_3 > Py > Eta > NCS^- > H_2O > Cl^- > Br^- > J^-$$

Tabelle V

Spektraldaten und Ligandenfeld-Parameter der Co^{3+}- *und* Cr^{3+}-*Diacidotetraamin-Komplexe vom Typ* $(Y \neq X)$

No.	X^a	Y	ν_1^*(I)	ν_1^*(II)	ν_2^*	*Dt*	*Ds*	$Dq(X)^b$	$Dq(Y)^c$	*B*	β
					a) Verbindungen vom Typ *trans*-$[Co(en)_2XY]$						
71.	Cl^-	NH_3	18 900	22 070	27 770	291	60,6	1549	2482	501	0,46
72.	Br^-	NH_3	18 370	22 130	—	352	73,3	1336	2466	—	—
73.	J^-	NH_3	17 400	21 870	—	463	96,5	948	2479	—	—
74.	Cl^-	H_2O	18 120	22 370	26 810	381	79,4	1675	2167	474	0,44
75.	H_2O	NH_3	20 750	22 370	29 330	80	16,7	2288	2728	522	0,49
76.	Cl^-	NO_2^-	20 830		—	142	29,6	1511	3003	—	—
77.	Br^-	NO_2^-	20 600		—	194	40,4	1329	3021	—	—
78.	NCS^-	NH_3	19 685	22 300	~31 450	202	42,1	1861	2221	699	0,65
79.	Cl^-	NCS^-	17 900	21 950	~31 350	406	84,6	1507	2079	767	0,72
					b) Verbindungen vom Typ *cis*-$[Co(en)_2XY]$						
80.	Cl^-	NH_3	18 970	21 870	27 400	283	59,0	1556	2470	475	0,45
81.	Cl^-	EtA	18 970	21 600	27 270	283	59,0	1556	2470	467	0,44
82.	Cl^-	Py	19 030	21 530	27 170	277	57,7	1577	2526	459	0,43
83.	H_2O	Cl^-	19 270	—	26 600	249	51,9	2024	1476	413	0,39
84.	NCS^-	Cl^-	20 530		~32 360	210	43,8	2161	1626	—	—
85.	Br^-	NH_3	18 530	21 700	27 250	334	69,6	1252	2528	484	0,45
86.	Br^-	EtA	18 370	21 350	—	352	73,3	1314	2359	—	—
87.	Br^-	Py	18 370	—	—	352	73,3	1314	2359	—	—
88.	Br^-	NCS^-	19 920		~31 850	350	72,9	1456	2378	—	—
89.	NH_3	H_2O	20 790	—	29 240	75	15,6	2449	1926	514	0,48
					c) Verbindungen vom Typ *trans*-$[Cr(en)_2XY]$						
90.	H_2O	NCS^-	19 920		~25 090	430	89,6	1626	1563	483	0,51
					d) Verbindungen vom Typ *cis*-$[Cr(en)_2XY]$						
91.	H_2O	NCS^-	20 040		~25 150	402	83,8	964	1106	475	0,50
92.	Cl^-	NCS^-	19 960		~25 090	421	87,7	789	1033	479	0,51

a) EtA = Äthylamin; Py = Pyridin; *b)* bei *cis*-Verbindungen mit Formel (23) und *c)* bei *cis*-Verbindungen mit Formel (22) berechnet.

Die *Dt*- und *Ds*-Werte, die im wesentlichen über die tetragonale Verzerrung Aufschluß geben, ändern sich gemäß der entsprechenden Formeln linear mit *Dq* (Abb. 3). Aus den für Monoacido-, *trans*- und *cis*-Diacido-Verbindungen berechneten Werte ist ersichtlich, daß ein und derselbe Ligand bei den *trans*-Verbindungen die größte Verzerrung und demzufolge die Aufspaltung des

Energieniveaus hervorruft, während diese Wirkung bei Monoacidoverbindungen die geringste ist. Bei Verbindungen vom Typ ($X \neq Y$) fällt auch das arithmetische Mittel von $Dq^{(X)}$ und $Dq^{(Y)}$ genau auf die Gerade $Dq-Dt$ der Glieder der entsprechenden Gruppe. Das Gesagte gilt auch für die Cr^{3+}-Verbindungen, stets ist die Reihenfolge

$$Dq(trans) < Dq(cis) < Dq(\text{Monoacido})$$

identisch in bezug auf $X(Y)$. Die zu $Dt = 0$ (keine Verzerrung, $X = Y = NH_3$) gehörigen Werte 2510 und 2160 cm^{-1} geben bei Co^{3+}- und Cr^{3+}-Verbindungen

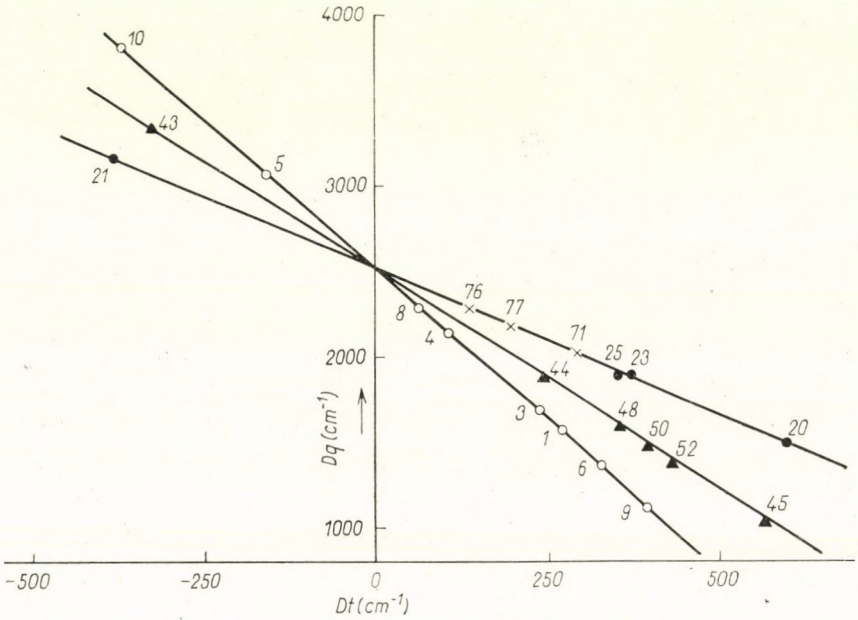

Abb. 3. Der *Dq—Ds*-Zusammenhang für Monoacidopentaamin-(-○-), *trans*-(-●-) und *cis*(-▲-) Diacido-Co^{3+}-Komplexe

mit guter Übereinstimmung die *Dq*-Werte der Hexaaminverbindungen (2498 und 2150 cm^{-1}).

Mit den Formeln (2a)—(2d) können die Einelektronenbahnenergien berechnet werden. Einige der für Co^{3+}-Monoacidoverbindungen erhaltenen charakteristischen Werte sind in Tabelle VI angeführt. Hier, wie auch bei allen übrigen Verbindungsgruppen, sind die Energiewerte

$$d_{x^2-y^2} > d_{z^2} > d_{xz,yz} > d_{xy}$$

doch ändert sich bei NO_2^-- und CN^--Verbindungen die Reihenfolge der Niveaus:

$$d_{z^2} > d_{x^2-y^2} > d_{xy} > d_{xz,yz}$$

Diese Änderung entspricht der relativen Feldstärkenänderung der planar und axial angeordneten Liganden.

Tabelle VI

Berechnete Einelektronen-Bahnenergien einiger Monoacidopentaamin-Co^{3+}-Komplexe (in cm^{-1})

X	$d_{x^2-y^2}$	d_{z^2}	$-d_{xy}$	$-d_{xz,yz}$
J^-	5 541	2 985	4 119	2 203
N_3^-	6 453	4 150	4 687	2 958
Br^-	8 008	6 123	5 652	4 239
ox	8 476	6 714	5 944	4 623
CO_3^{--}	9 685	8 249	6 695	5 619
Cl^-	9 241	7 689	6 419	5 255
OH^-	9 932	8 566	6 848	5 825
NO_3^-	10 425	9 194	7 155	6 232
F^-	11 041	9 974	7 539	6 738
H_2O	12 275	11 539	8 305	7 754
NCS^-	12 768	12 167	8 612	8 162
SO_3^{--}	13 631	13 264	9 149	8 873
NO_2^-	18 441	19 375	12 139	12 839
CN^-	23 138	25 327	15 052	16 702

ZUSAMMENFASSUNG

Es wird über die Elektronenanregungsvorgänge und die Elektronenanregungs-Absorptionsspektren von Monoacidopentaamin-, *trans*- und *cis*-Diacidotetraamin-Co^{3+}- und -Cr^{3+}-Komplexen berichtet und eine Berechnungsmethode der aus diesen ableitbaren Ligandenfeld-Parameter mitgeteilt. Auf Grund der berechneten *Dq*-, *B*-, β- und δ%-Werte wurden Schlüsse auf den Charakter den in diesen Komplexmolekülen zustande kommenden Bindungen gezogen.

LITERATUR

1. LINHARD, M., WEIGEL, M.: Z. anorg. allg. Chem. **264,** 321 (1951); **266,** 49, 73 (1951); **267,** 113, 121 (1951); **271,** 101 (1952)
2. (a) YAMADA, S., NAKAHARA, A., SHIMURA, Y., TSUCHIDA, R.: Bull. Chem. Soc. Japan **28,** 222 (1955); (b) TSUCHIDA, R. *et al.:* Bull. Chem. Soc. Japan **13,** 388, 436, 471, 476 (1938); **15,** 427 (1940)
3. FUJITA, J., SHIMURA, Y.: Bull. Chem. Soc. Japan **36,** 1281 (1963)
4. (a) BASOLO, F.: J. Am. Chem. Soc. **70,** 2634 (1948); **72,** 4393 (1950); (b) BASOLO, F., BALLHAUSEN, C. J., BJERRUM, J.: Acta Chem. Scand. **9,** 810 (1955)
5. BRIGANDO, J.: Bull. Soc. Chim. France **211** (1957)
6. LINHARD, M., WEIGEL, M.: Z. phys. Chem. N. F. **11,** 308 (1957)
7. (a) MCCLURE, D. S.: Advances in the Chemistry of Coordination Compounds. Ed. S. Kirschner. McMillan Co. New York 1961; (b) ORGEL, L. E.: J. Chem. Phys. **23,** 1004 (1955); (c) SHIMURA, Y.: Bull. Chem. Soc. Japan **25,** 49 (1952); **29,** 311 (1956)
8. (a) BALLHAUSEN, C. J., MOFFITT, W.: J. Inorg. Nucl. Chem. **3,** 178 (1956); (b) GRIFFITH, J. S., ORGEL, L. E.: J. Chem. Soc. (London) **1956,** 4981; (c) TANABE, Y., SUGANO, S.: J. Phys. Soc. Japan **9,** 766 (1954)

9. (a) YAMATERA, H.: Bull. Chem. Soc. Japan **31,** 95 (1958); (b) J. Inorg. Nucl. Chem. **15,** 50 (1960)
10. Vgl. z. B. HARTMANN, H., KRAUSE, H. R.: Z. Phys. Chem. N. F. **5,** 9 (1955)
11. BÁN, M., CSÁSZÁR, J.: Acta Chim. Acad. Sci. Hung. **54,** 133 (1967)
12. BALLHAUSEN, C. J.: Introduction to Ligand Field Theory. McGraw-Hill Co., London, 1962
13. BÁN, M.: Unveröffentliche Resultate
14. BÁN, M.: Acta Phys. Hung. (unter Druck)
15. BÁN, M.: Kandidaten-Dissertation. Szeged 1967
16. GRIFFITH, J. S.: The Theory of Transition Metal Ions. Univ. Press. Cambridge, 1961
17. JÖRGENSEN, C. K.: Absorption Spectra of Complexes with Unfilled d-Shells. Rept. to the Xth Solvay Council. Brussels, 1956
18. (a) LINHARD, M., WEIGEL, M.: Z. phys. Chem. N. F. **5,** 20 (1955); (b) BAKER, W. A., PHILLIPS, M. G.: Inorg. Chem. **5,** 1042 (1966)
19. BÁN, M., CSÁSZÁR, J.: Magy. Kém. Folyóirat, **73,** 318 (1967)
20. BÁN, M., CSÁSZÁR, J.: Magy. Kém. Folyóirat, **73,** 373 (1967)
21. KURODA, K., GENTILE, P. S.: J. Inorg. Nucl. Chem. **27,** 155 (1965)

Miklós BÁN
József CSÁSZÁR
Szeged, Rerrich Béla tér

Acta Chimica Academiae Scientiarum Hungaricae Tomus 57 (2), pp. 169—179 (1968)

INVESTIGATIONS ON THE KETO-ENOL TAUTOMERISM OF O-HYDROXYDIBENZOYLMETHANES BY NUCLEAR MAGNETIC RESONANCE

H. WAGNER,* O. SELIGMANN,* L. HÖRHAMMER,* M. NÓGRÁDI,** L. FARKAS,** J. STRELISKY*** and B. VERMES***

Received August 2, 1967

One of the most convenient methods for the preparation of flavones consists in the base-catalyzed rearrangement of an *o*-aroyloxyacetophenone (**I**) to an *o*-hydroxydibenzoylmethane (**III**), followed by acid-catalyzed cyclodehydratation to form the γ-pyrone ring (**V**) (BAKER—VENKATARAMAN synthesis [1—2]). As an intramolecular variant of the well-known CLAISEN condensation, the rearrangement clearly involves an intermediate of the 2-hydroxyflavanone type (**II**) and it has been assumed that a similar species (**IV**) is the intermediate in the acid-catalyzed ring closure of *o*-hydroxydibenzoylmethanes to flavones [3].

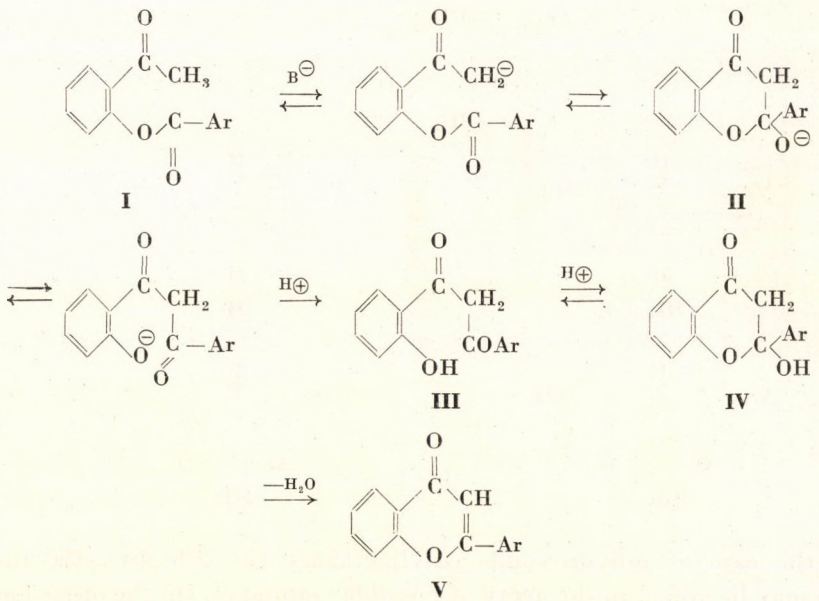

* *Institut für Pharmazeutische Arzneimittellehre der Universität München.*
** *Research Group for Alkaloidchemistry of the Hungarian Academy of Sciences.*
*** *Institute for Organic Chemistry, Technical University, Budapest.*

The keto-enol tautomerism of 1,3-diketones has been the subject of a very large number of both classical and recent studies [4], but no investigations have been reported on the tautomerism of the *o*-hydroxydibenzoylmethane system.

In 1952 OLLIS and WEIGHT [5] observed the existence of two forms of dibenzoylmethanes, a yellow and a colourless one, and suggested that the yellow form may correspond to the enol tautomer (**IIIe**) and the colourless one to a tautomer of either the keto (**IIIk**) or the 2-hydroxyflavone type (**IV**), but no experimental evidence has been published supporting their hypothesis.

In the course of our investigations on the synthesis of various flavones [6] we prepared a number of *o*-hydroxydibenzoylmethanes, and again observed the duality in their colour. A spectroscopic study was therefore initiated in order to elucidate the problem of tautomerism in this group of compounds.

Dibenzoylmethanes (and β-diketones in general) may exist in one keto- (**IIIk**) and four different enol-forms (**IIIe**$_1$, **IIIe**$_2$, **IIIe**$_3$, **IIIe**$_4$); however the existence of the geometrical isomers (**IIIe**$_3$, **IIIe**$_4$) where intramolecular hydrogen bonding is absent, is highly improbable. NMR studies have recently demonstrated that the unsubstituted dibenzoylmethane exists entirely in the hydrogen bonded enol form, whereas alkyl-aryl-1,3-diketones are present in solutions as an equilibrium mixture of the keto and enol forms [4].

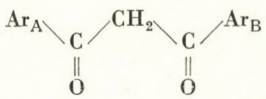

III$_k$

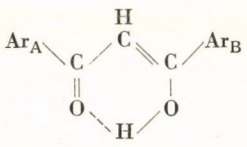

IIIe$_1$

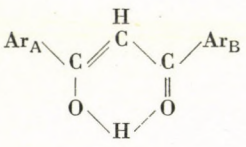

IIIe$_2$

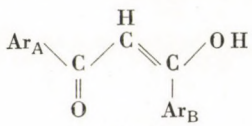

IIIe$_3$

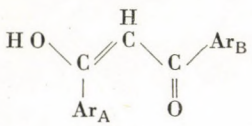

IIIe$_4$

In the case of *o*-hydroxydibenzoylmethanes the 2-hydroxyflavanone form (**IV**) may be added to the array of possible tautomers. On the other hand, of the enol forms, the tautomer having two carbonyl-hydroxyl hydrogen bonds (**IIIe'**$_1$) is supposed to be energetically favoured as compared to that having only one (**IIIe'**$_2$).

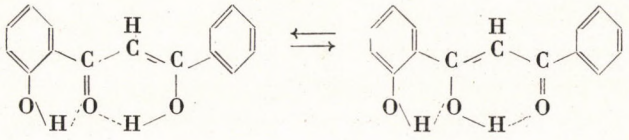

III′e$_1$ III′e$_2$

Ultraviolet spectroscopy can only distinguish between the conjugated enol tautomers on one hand, and the non-conjugated diketo- and/or 2-hydroxyflavanone intermediate, on the other. A further limitation is that, as a result of the rapid equilibration during dissolution, only the predominance of a certain tautomer can be established.

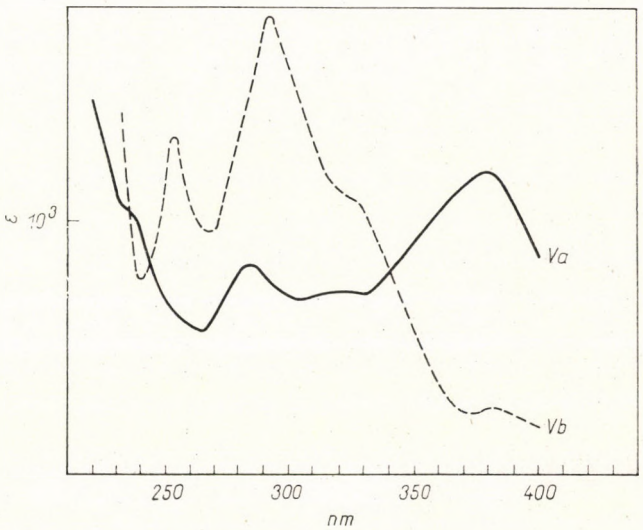

Fig. 1. Ultraviolet spectra of dibenzoylmethanes **Va** and **Vb**

A typical representative of the coloured type, 2-hydroxy-2',4,5,6-tetramethoxydibenzoylmethane (**Va**) (orange-yellow) shows a very intense long-wavelength band at 379 nm (Fig. 1), whereas the colourless 2,2'-dihydroxy-4,6-dimethoxydibenzoylmethane (**Vb**) has its main peak at 292 nm. If in **Va** the chelation has been destroyed by forming the phenolate, the UV spectrum reveals the predominance of the conjugated chromophore (main band at 385 nm) (Table I).

The composition of the equilibrium mixture cannot be assessed by this means as generally the UV spectra of the pure tautomers are not available.

In the case of compound **Vc**, however, we succeeded in isolating both forms, the white one melting at 125—126°, and the yellow one melting at 137—138°. As far as we know this is the first reported case of desmotropy ir

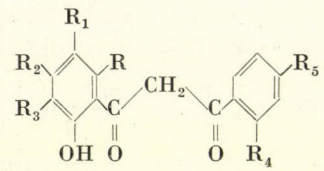

	R	R^1	R^2	R^3	R^4	R^5
Va	OCH_3	OCH_3	OCH_3	H	OCH_3	H
Vb	OCH_3	H	OCH_3	H	OH	H
Vc	OCH_3	H	OCH_2Ph	OCH_3	H	OCH_2Ph
Vd	OCH_3	H	OCH_3	H	OCH_2Ph	H
Ve	OCH_3	H	OCH_3	OCH_3	OCH_3	H
Vf	H	H	H	H	H	H
Vg	OCH_3	H	OCH_3	OCH_3	H	H
Vh	OCH_2Ph	H	OCH_3	OCH_3	H	H

the dibenzoylmethane group. Owing to rapid equilibration, both desmotrops exhibit the same UV spectrum in solution; in KBr pellets, however, they give rise to individual spectra (see Table I and Fig. 2).

Table I

Ultraviolet spectra of o-hydroxydibenzoylmethanes

Compound	$\lambda_{max.}$	log ε	$\lambda_{max.}$	log ε	$\lambda_{max.}$	log ε	$\lambda_{max.}$	log ε	Solvent
Va	236	3.95	284	3.95	318	3.90	379	4.10	EtOH
							368	4.19	0.002 *M* NaOEt
Vb	253	4.09	292	4.25			381	3.43	EtOH
			274	3.90			385	4.27	0.002 *M* NaOEt
Vc			289				379		EtOH
			274				370		0.002 *M* NaOEt
Vc m. p. 125—6°			292						KBr
Vc m. p. 137—8°					306		360		KBr
Vd	246	4.03	292	4.27			378	4.07	EtOH
			268	3.98			365	4.22	0.002 *M* NaOEt
Ve	236i	4.05	294	4.09			380	4.00	EtOH

NMR spectroscopy provides a very simple means to settle most of the problems concerning the tautomerism of *o*-hydroxydibenzoylmethanes (Table II).

A typical example is 2-hydroxy-2', 4, 5, 6-tetramethoxy-dibenzoylmethane (**Va**), an orange-yellow compound, to which, on basis of UV and IR spectroscopic evidence, the enol form can be assigned. If the NMR spectrum is measured immediately after dissolving the sample in deuterochloroform, the

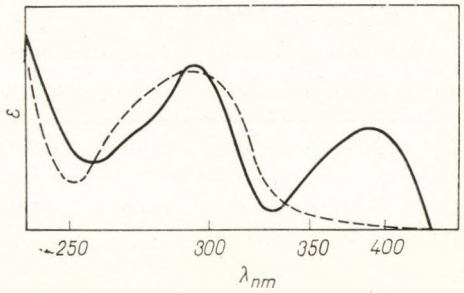

Fig. 2. Ultraviolet spectra of the desmotropic forms of dibenzoylmethane **Vc**. ——— enol form; - - - - - - keto form

spectrum of the pure enol tautomer is obtained (Fig. 3a). The four methoxyls are observed as three sharp singlets (δ 3.84, 3.91 and 3.95), and the isolated proton of ring *A* as a singlet at δ 6.33. The four protons of ring *B* give rise to a set of multiplets that, though inaccessible to simple first-order analysis, can be assigned with certainty to the individual protons.

The proton of the chelated *ortho* hydroxyl appears at δ 12.90. The characteristic features of the spectrum are the sharp singlet of the α-proton on the enolic double bond at δ 7.73 and the singlet of the extremely deshielded proton of enolic hydroxyl at δ 15.75.

If the spectrum is run again after an hour, small peaks indicating the presence of the keto tautomer emerge. Within 24 hours the establishment of the equlibrium is complete (Fig. 3b). Methoxyls appear as a set of singlets in the range of δ 3.79—4.00, and the peak of C_3—H is shifted slightly upfield. The intensity of the peak representing α-H is considerably reduced and two new singlets appear in the spectrum. The one at δ 4.67 can be assigned to the —$COCH_2$—CO-protons of the keto form, and the other at δ 13.20 to the chelated *o*-hydroxyl of the keto tautomer. No signals which could be attributed to a 2-hydroxyflavanone tautomer (multiplets of the ring-CH_2) could be detected in the spectrum.

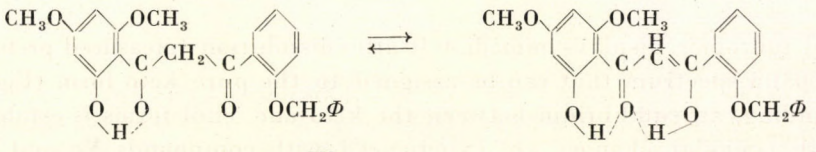

Vd

A counterpart of this phenomenon is experienced when running the spectra of 2'-benzyloxy-2-hydroxy-4,6-dimethoxydibenzoylmethane (**Vd**). The off-white compound, that according to the UV spectrum is a non-con-

Table II

NMR data of 2-hydroxydibenzoylmethanes

(δ values in p.p.m. relative to tetramethylsilane)

Compound	OCH_3	=CH—	$—COCH_2CO$	C_2—OH	=C—OH	C_3—H	C_5—H
Va (enol)	3.84 3.91 3.95	7.73	—	12.90	15.75	6.33	—
Va (keto)	4.00 3.82 3.78	—	4.63	13.16	—	6.29	—
Vb (keto)	3.83 3.53	—	4.63	13.61 11.93*	—	5.90d = 2.5 cps.	6.14d = 2.5 cps.
Vc (enol)	3.84 3.53	—	—	13.16	15.77	—	6.05
Vc (keto)	3.88 3.40	—	4.49	13.59	—	—	5.91
Vd (enol)	3.78 3.41	7.73	—	13.45	15.75	5.84d = 2.5 cps.	6.12d = 2.5 cps.
Vd (keto)	3.78 3.45	—	4.54	13.70 13.88	— (at —40°)	5.78d = 2.5 cps.	6.03d = 2.5 cps.
Ve (enol)	3.94 3.92 3.83	7.71	—	13.15	15.66	—	6.03
Ve (keto)	3.94 3.92 3.60	—	4.56	13.46	—	—	5.93

* C_2' — OH; d = doublet

jugated tautomer, displays immediately after dissolution (measured preferably at — 60°) a spectrum that can be assigned to the pure keto form (Fig. 4a). On standing, an equilibrium between the keto and enol forms is established (Fig. 4b). Similar changes are experienced with compounds **Vc** and **Ve**.

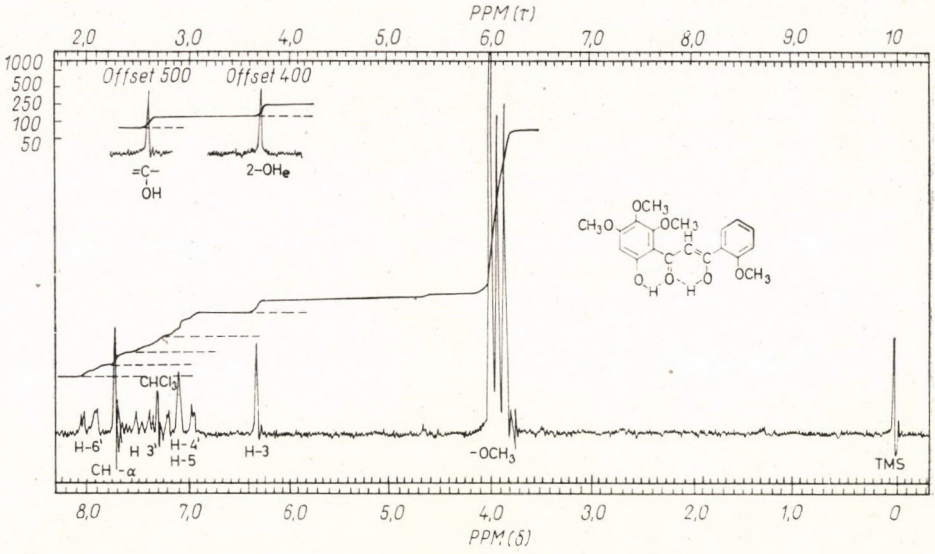

a

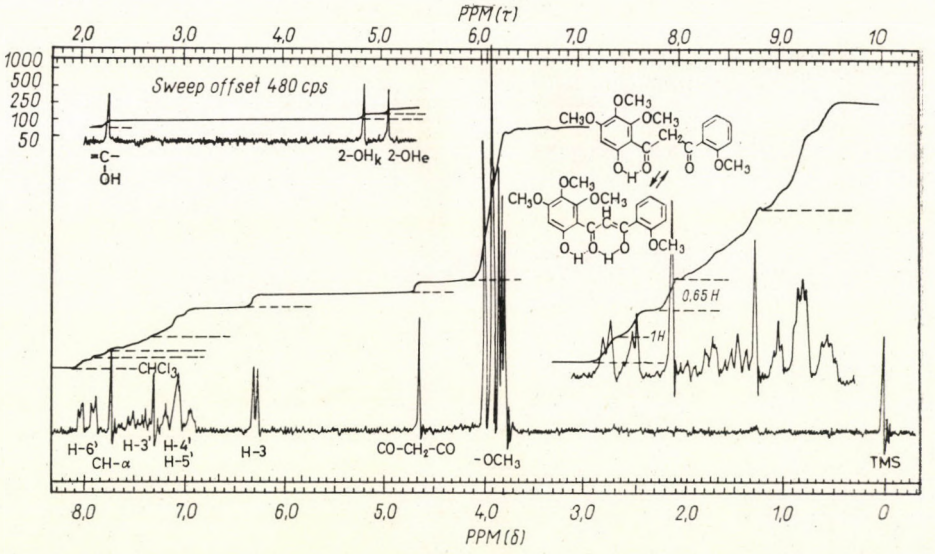

b

Fig. 3. NMR spectra of 2-hydroxy-2',4,5,6-tetramethoxy-dibenzoylmethane. 3*a*: 20 minutes after dissolution. 3*b*: 16 hours after dissolution

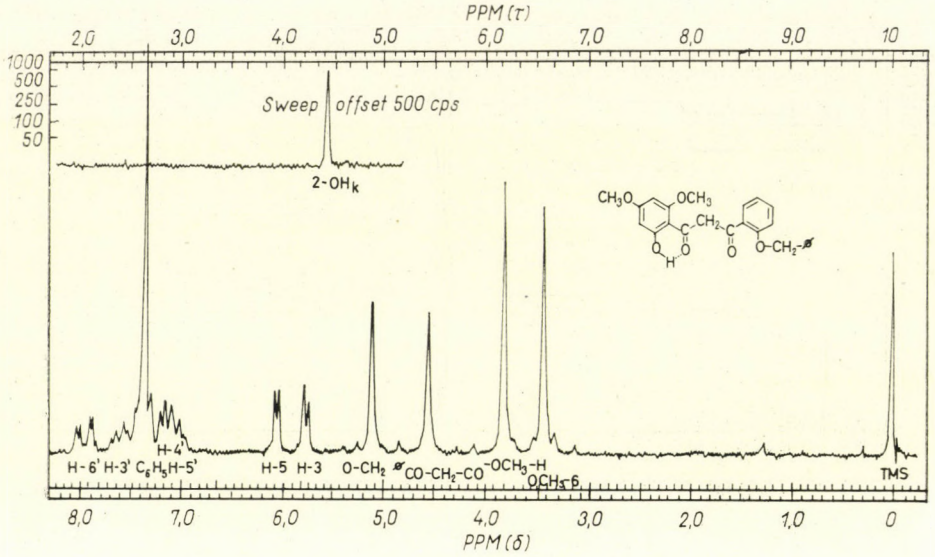

a

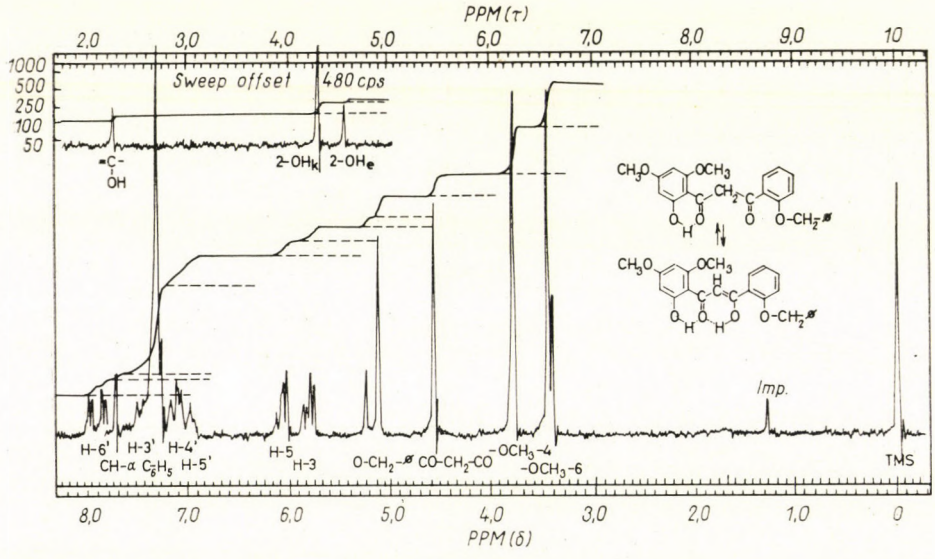

b

Fig. 4. NMR spectra of 2-hydroxy-2'-benzyloxy-4,6-dimethoxydibenzoylmethane. 4*a*: 5 minutes after dissolution. 4*b*: 20 hours after dissolution

2,2'-Dihydroxy-4,6-dimethoxydibenzoylmethane (**Vb**) in which both keto groups are stabilized by chelation, no conversion to the enol form can be observed.

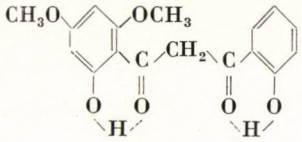

Vb

Based on the relative intensity of the $-COCH_2CO-$absorption in the keto form, the composition of the equilibrium mixture in $CDCl_3$ can be assessed (Table III).

Table III

Percentage of the keto tautomers of o-hydroxydibenzoylmethanes at 20°

	Solid	Equilibrium, $CDCl_3$ solution
Va	0%	43—50%
Vb	100%	100%
Vc m. p. 125—6°	100%	60—66%
Vc m. p. 137—8°	0%	
Vd	100%	68—75%
Ve	0%	65—69%

A considerable upfield shift (0.23—0.42 p. p. m.) of one of the methoxy peaks is experienced in the spectra of the keto tautomer of compounds **Vb, Vc** and **Ve**, as well as with both forms of **Vd**. Comparison of the substitution pattern of the compounds makes it possible to assign these singlets to the

Table IV

IR carbonyl absorption of o-hydroxydibenzoylmethanes in the solid state (KBr pellets)

	Chelated carbonyl		Free carbonyl
Va	1610		—
Vb		1600—1650	
Vc m. p. 125—6°	1605		1675
Vc m. p. 137—8°	1600		—
Vd	1630		1670
Ve	1615		—
Vf	1610		—
Vg	1610		1685
Vh	1600		—

C_6-OMe. As no similar effect is observed with either 2-hydroxy-3,4,6-trimethoxyacetophenone, or 2-hydroxy-4,5,6-trimethoxyacetophenone (methoxy-absorption in the range of δ 3.95—4.10), it may be inferred that the upfield shift of the C_6-OMe peak is caused by the anisotropic shielding effect of the other benzene-ring, Ar_B.

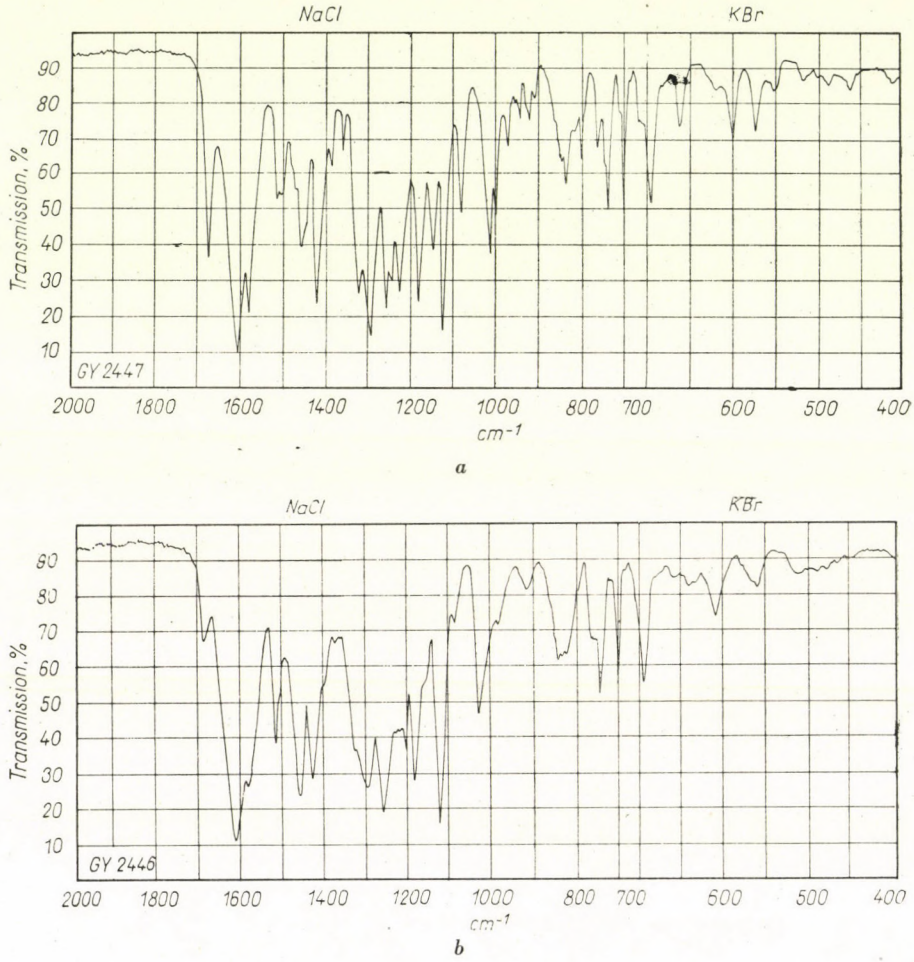

Fig. 5. Infrared spectra of the desmotropic forms of 2-hydroxy-4,4'-dibenzyloxy-3,6-dimethoxydibenzoylmethane. 5*a*: keto form; 5*b*: enol form

Having excluded the possibility of the 2-hydroxyflavanone tautomer, IR spectroscopy offers a very simple method of establishing whether a given dibenzoylmethane exists in the solid state in the keto or in the enol form. The IR spectrum of the enols (in KBr wafers) containing only one carbonyl group, exhibits a single carbonyl absorption which is shifted to lower wave

numbers by hydrogen bonding (Fig. 5a). In the keto form two bands can be observed in the carbonyl region, the absorption at higher wave numbers corresponding to the non-bonded group and the other one to that in chelation with the *ortho* hydroxyl (Fig. 5b).

Experimental

The NMR spectra were taken with a *Varian A60* instrument in $CDCl_3$ at 35°, unless stated otherwise. Chemical shifts are given as δ values in p. p. m. relative to tetramethylsilane as internal standard. The infrared spectra were taken on a *Perkin—Elmer* model *221G* instrument. The UV spectra were measured with a *Unicam SP 700* spectrophotometer.

2,2'-Dihydroxy-4,6-dimethoxydibenzoylmethane (Vb)

2'-Benzyloxy-2-hydroxy-4,6-dimethoxydibenzoylmethane **(Vd)** [6b] (2.5 g) was hydrogenated in the presence of palladium-on-carbon catalyst until the uptake of calculated amount of hydrogen. After filtration and evaporation, the crude product was purified by chromatography on silicic acid (eluant benzene-petroleum ether). On evaporation **Vb** was obtained as off-white crystals of m. p. 103—105°. Ferric reaction in methanol: green. Found: C 64.48; H 5.10. $C_{17}H_{16}O_6$ requires: C 64.55; H 5.10%.

The preparation of the other compounds is described in the literature: **Va** [6a], **Vb** [6b], **Vc** [7], **Vd** [6b], **Ve** [6a], **Vf** [8], **Vg** [9], **Vh** [9].

SUMMARY

The keto-enol tautomerism of *o*-hydroxydibenzoylmethanes has been investigated by NMR, IR and UV spectroscopy. In solution the compounds exist in equilibrium mixture of the keto and enol tautomers. The existence of a 2-hydroxyflavanone-type tautomer could not be demonstrated.

REFERENCES

1. Baker, W.: J. Chem. Soc. **1933,** 1381
2. Mahal, H. S., Venkataraman, K.: J. Chem. Soc. **1934,** 1767
3a. Gripenberg, J.: The Chemistry of Flavonoid Compounds (ed. Geissman, T. A.) Pergamon Press, Oxford, 1962. p. 411.
3b. Rao, A. V. R., Telang, S. A., Nair, P. M.: Indian J. Chem. **2,** 205 (1966)
4a. Jackman, L. M.: Application of Nuclear Magnetic Resonance Spectroscopy in Organic Chemistry. McMillan, New York, 1959. p. 71.
4b. Burdett, J. L., Rogers, M. T.: J. Am. Chem. Soc. **86,** 2105 (1964)
4c. Hay, R. W., Williams, P. P.: J. Chem. Soc. **1964,** 2270
4d. Allen, G., Dwek, R. A.: J. Chem. Soc. **1966B,** 161
5. Ollis, W. D., Weight, D.: J. Chem. Soc. **1952,** 3826
6a. Farkas, L., Nógrádi, M.: Chem. Ber. **98,** 164 (1965)
6b. Farkas, L., Vermes, B., Nógrádi, M.: Tetrahedron, **23,** 741 (1967)
6c. Farkas, L., Nógrádi, M., Sudarsanam, V., Herz, W.: J. Org. Chem. **31,** 3228 (1966)
7. Strelisky, J.: Unpublished results
8. Org. Synth. (Ed. N. Rabjohn) Coll. Vol. IV. John Wiley, New York, 1963. p. 479.
9. Farkas, L., Major, Á., Strelisky, J.: Chem. Ber. **96,** 1684 (1963)

Hildebert Wagner
Otto Seligmann
Ludwig Hörhammer
8 München 2, Karlstrasse 29. DBR

Mihály Nógrádi
Lóránd Farkas
János Strelisky
Borbála Vermes
Budapest XI., Gellért tér 4.

Acta Chimica Academiae Scientiarum Hungaricae Tomus 57 (2), pp. 181—189 (1968)

1,5-DIKETONES, IV*

SYNTHESIS OF SOME NEW ISOBENZOPYRYLIUM ANHYDROBASES

M. LEMPERT-SRÉTER and M. BÁRDY**

(Institute of Organic Chemistry, L. Eötvös University, Budapest)

Received September 7, 1967

It has recently been found that 2-(1-acetylpropyl)-4,3'-dimethoxy-5,4'-diacetoxybenzophenone (**Ia**), when heated a few hours with acetic acid at 240°, suffers total *O*-deacetylation and partial *O*-demethylation to yield an isobenzopyrylium anhydrobase, **IIa** [1].

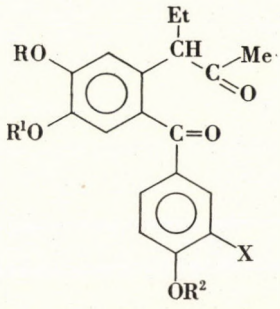

I

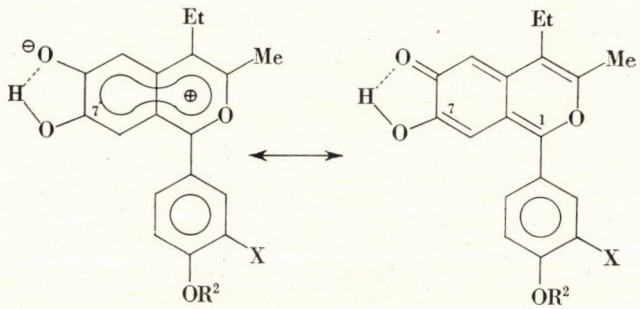

II

a: R=Me; R^1= R^2= Ac; X=MeO
b: R=R^1=R^2=Me; X=MeO
c: R=Me; R^1=Ac; R^2=Me; X=H
d: R=H; R^1=R^2=Me; X=OH

a : R^2=H; X = MeO
c : R^2=Me; X = H

IIa was characterized as an anhydrobase and, simultaneously, the structure of its skeleton proved by the following reactions: (a) addition of one mole of mineral acids gave isobenzopyrylium salts of type **IIIa**, whose free phenolic hydroxyl group could be methylated with diazomethane to yield **IIIb**, a well known [2] substance; (b) catalytic hydrogenation and subsequent methylation of the product furnished the chromane **IV**, another known [3] compound; (c) finally, treatment with ammonia transformed **IIa** into the isoquinoline **Va**. The site of partial demethylation in the course of the transformation of **Ia** into **IIa** followed clearly from the fact that ethylation of **IIa** in alkaline medium gave the naphthol **VIa** under skeletal rearrangement instead of the isomeric **VIb** [1].

* Part III: M. LEMPERT-SRÉTER and P. SOHÁR: Acta Chim. Acad. Sci. Hung. **54**, 203 (1967)

** Partly based on the thesis submitted by M. BÁRDY, L. Eötvös University, Budapest, 1966.

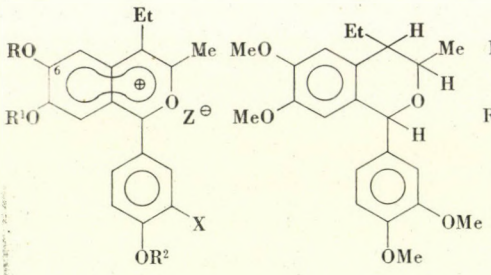

III

a: R=R¹=R²=H; X=MeO
b: R=R¹=R²=Me; X=MeO
c: R=R¹=H; R²=Me; X=H, Z=Cl
d: R=R¹=R²=Me; X=H
e: R=H; R¹=R²=Me; X=OH

IV

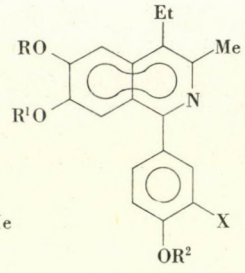

V

a: R=R¹=R²=H; X=MeO
c: R=R¹=H; R²=Me; X=H

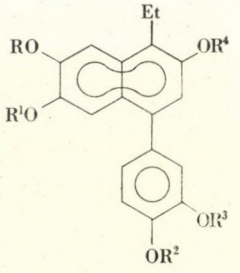

VI

a: R=R¹=R²=R⁴=Et; R³=Me
b: R=Me; R¹=R²=R³=R⁴=Et
c: R=R¹=R²=R³=R⁴=Me

All the above facts were, however, insufficient to exclude definitively the possibility that the anhydrobase exists, instead of the form **IIa** as assumed so far, in the tautomeric form **VIIa**. The clue to the determination of the position of the potential tautomeric equilibrium between **IIa** and **VIIa** was found during examination of an ethylation product of the anhydrobase, obtained under special conditions. If, namely, ethylation was performed in dry acetone solution in the presence of solid anhydrous potassium carbonate (instead of ethylating the anhydrobase, as usual, in an aqueous-alcoholic alkaline medium), the anhydrobase structure of the starting compound was, as clearly demonstrated by the UV spectrum of the product, retained, the surface basicity of the acid-binding agent being apparently insufficient to effect skeletal rearrangement into the naphthol **VIa**; the sole change was conse-

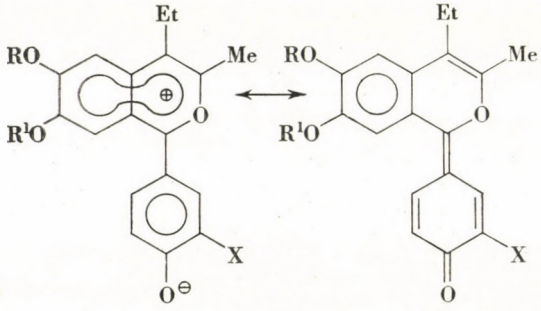

VII

a: R=R¹=H; X=MeO
b: R=R¹=Et; X=MeO
c: R=Me; R¹=X=H

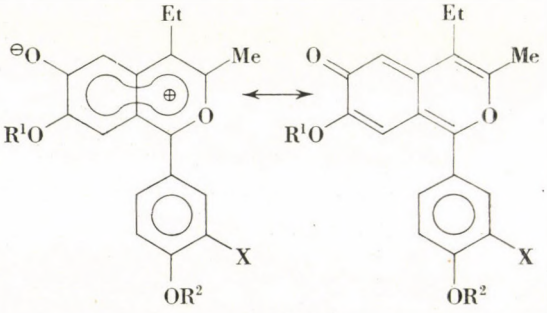

VIII

a: R¹=R²=Et; X=MeO
b: R¹=Me; R²=Me; X=H
c: R¹=R²=Me; X=OH

quently ethylation of the free phenolic hydroxyl groups of the starting compound. Depending whether the correct structure of the starting anhydrobase is **IIa** or **VIIa**, its diethylation product must possess structure **VIIIa** and **VIIb**, respectively.

While a considerable difference (with respect to the participation of the "quinone carbonyl" in a hydrogen bond) between structures **IIa** and **VIIIa** will readily be noticed, no such difference exists between structures **VIIa** and **b**

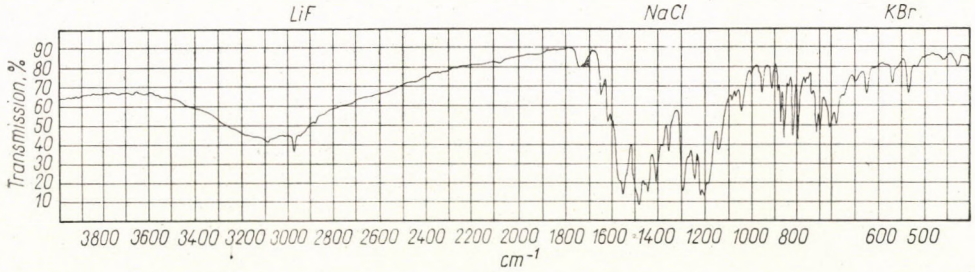

Fig. 1

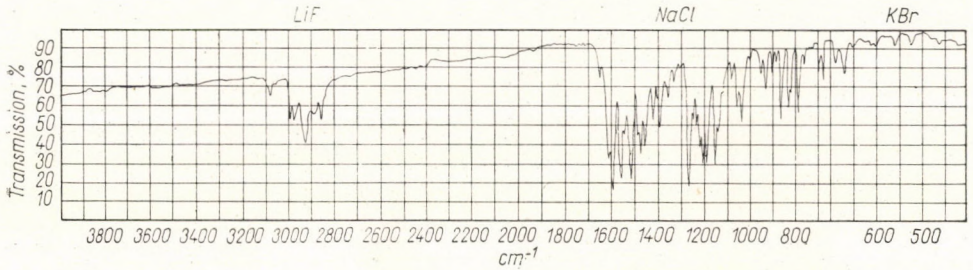

Fig. 2

IR spectra of the anhydrobase and its diethylation product are shown in Figs 1 and 2, respectively. Characteristic bands in the spectrum of the anhydrobase are, on the one hand, a very broad band extending from 3500 to 2800 cm^{-1}, indicating the presence of a chelate bond; and, on the other hand, four, partially merged bands in the double bond region (at 1642, 1560, 1542 and 1525 cm^{-1}). Bands, corresponding to the latter, are found in the spectrum of the diethyl derivative as well, shifted, however, somewhat to higher wave numbers (1642, 1584, 1551 and 1538 cm^{-1}). The band at 1642 cm^{-1} corresponds probably to the stretching vibration of the C=C bond in the hetero ring, while the other three bands belong to vibrations of the quinoid system and, especially that of the highest wave number among them, to the carbonyl stretching

vibration. The difference of 24 cm^{-1} between the carbonyl bands of the anhydrobase and its diethyl derivative again points to the participation of the carbonyl group in a hydrogen bond in the former compound. Consequently, the correct structure of the anhydrobase is **IIa** and not **VIIa**.

*

Hereafter we decided to investigate whether anhydrobases of type **II** could also be prepared from analogues of **Ia**. As the first analogue to be investigated we selected compound **Ib** [4] in which the acetoxy groups of **Ia** are replaced by methoxy groups. Heating an acetic acid solution of this compound, however, furnished only uncrystallizable tars.

Hence compound **Ic**, in which that part of the molecule of **Ia** which is involved in the formation of the isobenzopyrane nucleus is retained unchanged and which, therefore, could be expected to be a closer analogue of **Ia**, was next investigated.

Heating an acetic acid solution of **Ic** for a few hours at 240°, a yellow compound with properties similar to those of **IIa** was obtained, as expected. Structure **IIc**, presumed for the product by analogy, could be ascertained by analytical data, as well as by the IR and UV spectra which closely resembled those of **IIa**.*

Additional evidence in favour of structure **IIc** was furnished by the close similarity of the chemical properties of the new compound to those of **IIa**: *e.g.*, reaction with hydrochloric acid gave a 1 : 1 adduct (**IIIc**); methylation by diazomethane in the presence of mineral acids furnished **IIId**; in the course of catalytic hydrogenation two moles of hydrogen were added (from the reduction product, however, no crystalline derivatives could be prepared in this case); alcoholic ammonia transformed the compound into the isoquinoline **Vc**; and, finally, methylation by methyl iodide in the presence of sodium methylate gave **VIIIb**.

It may be assumed that formation of the anhydrobases **IIa** and **IIc** proceeds — similarly to the transformation of diketones of type **I** into isobenzopyrylium salts of type **III** by mineral acids [2] — *via* the corresponding 1H-isobenzopyran-1-ols, **IX**. However, while the hydroxyl group is readily cleaved from C—1 in anionic form by mineral acids, the acidity of acetic acid is insufficient to effect the same cleavage and, instead of the isobenzopyrylium cation (type **III**) an anhydrobase of type **II** is formed by 1,6-elimination of methanol.

* Structure **VIIc**, instead of **IIc**, cannot be excluded solely on the basis of the analytical data and the reactions of the product to be discussed later. However, if **VIIc** were the correct structure, the profund resemblance of the spectra to those of compound **IIa** could hardly be explained.

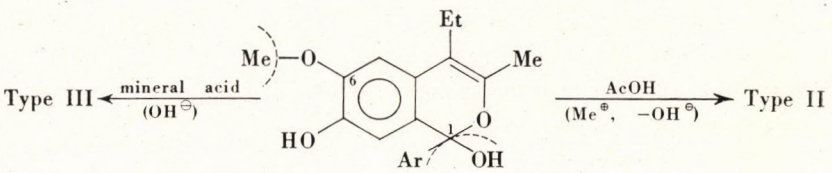

IX

Transformations **IIa**→**IIIa** and **IIc**→**IIIc** are reversible; the anhydrobases may be recovered from their 1 : 1 adducts with mineral acids by treatment of the latter with alkali. In the course of the latter reactions the isobenzopyrylium salts **III** are obviously attacked at their free phenolic hydroxyl group attached to C—6. A phenolic hydroxyl group of exactly the same kind is contained in the isobenzopyrylium salts **IIIe** obtainable from diisochavibetol [5]. It was, therefore, attempted to transform the latter salts into the corresponding anhydrobase **VIIIc**. Thus, a hot ethanolic solution of **IIIe** ($Z = ClO_4$) was treated with a buffer solution of pH = 7; on cooling, **VIIIc*** crystallized from the mixture. If the buffer solution was replaced by aqueous alkali, a product, shown by its IR spectrum to be a 1,5-diketone of type **I** (obviously **Id**) was formed rather than **VIIIc**, apparently by further decomposition of the latter.

Structure **VIIIc** was proved unambiguously by analysis and spectral studies. Further proof was gained by methylation of the product in alkaline medium, the resulting substance being identical in all respects with naphthol **VIc**, obtained under similar conditions also starting with **IIa** (or even **Ia**).

Striking differences are observed between the stabilities of the isobenzopyrylium anhydrobases **IIa**, **IIc** and **VIIIa**, **VIIIc**, respectively, in spite of the close similarity of their structures. Thus, while the anhydrobases **IIa** and **IIc** are recovered unchanged on passing carbon dioxide into their alkaline solutions, the anhydrobase **VIIId** is decomposed by alkalies, as already mentioned, to yield the diketone **Id**. Similarly, the anhydrobase **VIIIa** is also cleaved by alkalies. The latter reactions are obviously initiated by nucleophilic attack of hydroxyl ion at C—1 of the hetero ring (*cf.* [6]). In the case of anhydrobases **IIa** and **IIc**, however, another point of attack, *viz.* the phenolic hydroxyl group attached to C—7, presents itself to the hydroxyl ion, and as it is the more reactive site of the anhydrobase, only anionization, rather than cleavage of the hetero ring results.

* Transient formation of **VIIIc** in alkaline solutions of **IIIe** has been previously noticed by M. VAJDA on the basis of the temporary appearance of an UV spectrum very closely similar to that of **IIa** [5].

Experimental*

Anhydro-1-(3-methoxy-4-ethoxyphenyl)-3-methyl-4-ethyl-6-hydroxy-7-ethoxyisobenzopyrylium hydroxide (VIIIa)

IIa (1.0 g; 3.1 mmoles) was suspended in dry acetone (50 ml), anhydrous potassium carbonate (2.0 g) and ethyl iodide (1 ml; 12 mmoles) were added, and the mixture was refluxed for 24 hrs. under continuous stirring. The excess K_2CO_3 was removed by filtration and washed with chloroform, the washings being collected separately from the original filtrate. The latter was evaporated to dryness, the residue dissolved in the chloroform washings, the chloroform solution washed with water and evaporated to dryness. The oily red residue gave upon crystallization from ethanol lemon-yellow needles of VIIIa (0.65 g; 55%), m. p. 193—194°.
$C_{23}H_{26}O_5$ (382.4). Calcd. C 72.23; H 6.85. Found C 71.72, 72.28; H 6.84, 6.81%. For the UV spectrum, see Table I.

O(6)-Anhydro-1-(4-methoxyphenyl)-3-methyl-4-ethyl-6,7-dihydroxyisobenzopyrylium hydroxide (IIc)

1-(4-Methoxyphenyl)-2-methyl-3-ethyl-5-methoxy-6-acetoxyindane (3.5 g; 0.01 mole) was dissolved in acetic acid (35 ml). Under cooling and continuous stirring a solution of chromic acid (3.0 g; 0.03 moles) in acetic acid (15 ml) was added by drops. The oxidation mixture was allowed to stand for 24 hrs. and subsequently diluted with water and extracted with benzene. The benzene extract was washed with water, dried and evaporated to dryness.

The oily red residue of crude **Ic** (4.0 g) resisted all attempts of crystallization. Therefore, it was dissolved in acetic acid (8 ml) and heated for 20 hrs. at 240° in a sealed tube. The resulting dark brown solution was evaporated to dryness and the residue taken up in methanol. On standing yellow crystals of **IIc** (0.8 g; 25%) were deposited, m. p. 202—204° (from methanol). The product gave dark brown colour reaction with ferric chloride. $C_{19}H_{18}O_4$ (310.3). Calcd. C 73.54; H 5.83; OCH_3 10.23. Found C 73.42, 73.64; H 5.79, 5.90; OCH_3 10.30%. For the UV spectrum, see Table I.

Hydrochloric acid adduct (**IIIc**): **IIc** (0.4) g) was dissolved in acetic acid (2 ml). On the addition of cc. hydrochloric acid (0.5 ml) 1-(4-methoxyphenyl)-3-methyl-4-ethyl-6,7-dihydroxyisobenzopyrylium chloride (**IIIc**) was precipitated as a yellow crystalline powder (0.35 g), m. p. 248—250° (from a mixture of acetic and hydrochloric acids).
$C_{19}H_{19}O_4Cl$ (346.7). Calcd. Cl 10.21; Found Cl 10.23, 10.52%.

1-(4-Methoxyphenyl)-3-methyl-4-ethyl-6,7-dimethoxyisobenzopyrylium perchlorate (IIId, Z = ClO_4)

To a suspension of **IIc** (1.0 g) in ethanol (50 ml) containing hydrogen chloride (0.05 g) an ethereal solution of diazomethane, freshly prepared from nitrosomethylurea (4.0 g), was added under cooling. On shaking, the suspension gradually gave a clear solution. The solution was allowed to stand for 2 days, evaporated to dryness and the residue dissolved in aqueous acetic acid (5 ml). On the addition of a few drops of perchloric acid, yellow crystal of **IIId** (0.5 g; 40%) were deposited. M.p. and mixed m. p. with an authentic sample [7]: 251—253° (from acetic acid).

1-(4-Methoxyphenyl)-3-methyl-4-ethyl-6,7-dihydroxyisoquinoline (Vc)

IIc (0.5 g; 1.6 mmoles) was dissolved in 25% ethanolic ammonia solution (20 ml) under ice cooling. The solution was allowed to stand for 2 days in a refrigator and subsequently another day at room temperature. The originally red solution turned brown. After refluxing for 2 hrs., yellow crystals were deposited which, after recrystallization from ethanol, melted at 208—210°. Yield: 0.3 g (61%).
$C_{19}H_{19}O_3N$ (309.3) Calcd. C 3.787; H 6.19; O 15.53; OCH_3 10.03. Found C 74.11: H 5.87; O 15.45; OCH_3 10.21%.

* All m. p.-s are uncorrected.

Table I

UV spectra of isobenzopyrylium anhydrobases

Compound	Solvent	λ_{max} [nm] (log ε)			
IIa	BRITTON—ROBINSON buffer (pH = 7) in 50% aqueous methanol		242 (4.47);		393 (4.45)
IIc	,,			250 (4.47); 290 (4.00);	394 (4.42)
VIIIb	,,	232 (4.34) shoulder;	247 (4.78);	297 (3.95);	389 (4.40)
VIIIa	,,		243 (4.44);	252 (4.42) shoulder;	395 (4.40)
VIIIc	Ethanol		241 (4.42);	252 (4.37);	394 (4.38)
IIa	0.1N HCl		246 (4.41); 270 (4.37);	352 (3.97);	377 (4.13); 440 (4.26)
IIc	,,	226 (4.23); 238 (4.30);	244 (4.30); 272 (4.40);	335 (3.78);	372 (4.30); 428 (4.21)
VIIIb	,,	225 (4.25); 238 (4.33);	266 (4.41);	328 (3.76);	366 (4.32); 420 (4.24)
VIIIa	,,		247 (4.41); 271 (4.34);	352 (3.96) shoulder;	379 (4.13); 431 (4.18)
VIIIc	,,		246 (4.37); 269 (4.33);	353 (4.01);	377 (4.12); 429 (4.18)

Anhydro-1-(4-methoxyphenyl)-3-methyl-4-ethyl-6-hydroxy-7-methoxyisobenzopyrylium hydroxide (VIIIb)

IIc (0.31 g; 1 mmole) was suspended in methanol (10 ml) containing 3% sodium methoxide. Methyl iodide (0.1 ml; 1.6 mmoles) was added and the mixture refluxed for 8 hrs. During this period the solid material gradually dissolved. The red solution was evaporated to dryness and the partially solid residue rubbed with water. The yellow crystalline product obtained in this way was filtered off and thoroughly washed with ether to remove unchanged starting material (0.07 g; 22.5%). The ether-insoluble residue was recrystallized from methanol to yield 0.14 g (43.5%) of **VIIIb**, m. p. 199—200°.
$C_{20}H_{20}O_4$ (324.36); Calcd. C 74.05; H 6.22. Found C 74. 35, 74.18; H 6.00, 5.98%.

O(6)-Anhydro-1-(3-hydroxy-4-methoxyphenyl)-3-methyl-4-ethyl-6-hydroxy-7-methoxyisobenzopyrylium hydroxide (VIIIc)

1-(3-Hydroxy-4-methoxyphenyl)-3-methyl-4-ethyl-6-hydroxy-7-methoxyisobenzopyrylium perchlorate (**IIIe**, Z = ClO_4 [5]) (0.2 g; 0.53 mmoles) was boiled up with ethanol (2 ml). An aqueous methanolic phosphate buffer of pH 7 (1 ml) was added to the hot suspension, which caused immediate dissolution. On standing, yellow crystals (0.15 g; 83%) were deposited from the hot solution, m. p.: 267—270° (from DMF). $C_{20}H_{20}O_5$ (340.36).
Calcd. C 70.57; H 5.90. Found C 70.36, 70.28; H 5.67, 5.78%.
Hydrochloric acid adduct (**IIIe**, Z = Cl), yellow crystals, m. p. 240—242°.

1-(3,4-Dimethoxyphenyl)-3,6,7-trimethoxy-4-ethylnaphthalene (VIc)

VIIIc (0.06 g) was strirred with 20% aqueous NaOH (1 ml) and methyl sulphate (0.2 ml) for 4 hrs. at room temperature. The precipitate was extracted with ether and the extract recrystallized from methanol to yield 0.03 g of **VIc**, m. p. 146—147°, identified with an authentic sample [4] by mixed m. p. and IR spectra.

Reactions of isobenzopyrylium anhydrobases with alkali

(a) The addition of 1*N* aqueous NaOH to an aqueous suspension of **IIa**, brought about gradual dissolution of the compound; the colour of the solution turned through orange into light yellow. By passing carbon dioxide into this solution, **IIa** could be recovered unchanged.

(b) As **IIc** is insoluble in aqueous alkalies, it was dissolved in aqueous-ethanolic sodium hydroxide. On passing carbon dioxide into the solution, **IIc** was precipitated unchanged.

(c) On passing carbon dioxide into an aqueous-ethanolic alkaline solution of **VIIIc**, a precipitate different from the starting compound was obtained whose IR spectrum corresponded to that characteristic for compounds of type **I**.

(d) Since **VIIIa** is insoluble in aqueous alkalies, its ethanolic solution was treated with 1*N* NaOH. The IR spectrum of the precipitate, obtained on passing carbon dioxide into the solution, was found to be essentially identical with that of 1,5-diketones of type **I**.

*

The UV and IR spectra were taken by Dr. F. RUFF; the microanalyses were performed by the staff of the microanalytical laboratories (head: Dr. H. MEDZIHRADSZKY-SCHWEIGER) of this Institute. The authors wish to express their thanks to these colleagues for their valuable assistance.

SUMMARY

The tautomeric structure of a previously obtained isobenzopyrylium anhydrobase, O(6)-anhydro-1-(3-methoxy-4-hydroxyphenyl)-3-methyl-4-ethyl-6,7-dihydroxyisobenzopyrylium hydroxide (**IIa**), has been proved. Ethylation of **IIa** in the presence of solid potassium carbonate yields anhydro-1-(3-methoxy-4-ethoxyphenyl)-3-methyl-4-ethyl-6-hydroxy-7-ethoxyisobenzopyrylium hydroxide (**VIIIa**). A related anhydrobase, O(6)-anhydro-1-(4-methoxyphenyl)-3-methyl-4-ethyl-6,7-dihydroxyisobenzopyrylium hydroxide (**IIc**) was prepared similarly to **IIa**. The structure of the latter compound has been proved by spectroscopical and chemical methods.

By careful neutralization of the isobenzopyrylium salt **IIIe**, carrying a free phenolic hydroxyl group in position 6, 0(6)-anhydro-1-(3-methoxy-4-hydroxyphenyl)-3-methyl-4-ethyl-6-hydroxy-7-methoxyisobenzopyrylium hydroxide (**VIIIc**) can be obtained. The hetero ring of the anhydrobases **VIIIa** and **VIIIc** is cleaved — in contrast to that of their analogues **IIa** and **IIc** — by alkalies.

REFERENCES

1. MÜLLER, A., LEMPERT-SRÉTER, M.: Monatsh. **96,** 369 (1965)
2. MÜLLER, A., SZABÓ, L.: Chem. Ber. **77,** 6 (1944)
3. MÜLLER, A., LEMPERT-SRÉTER, M., KARCZAG-WILHELMS, A.: J. Org. Chem. **19,** 1533 (1954)
4. MÜLLER, A., HARTAY, M.: Chem. Ber. **75,** 891 (1942)
5. VAJDA, M.: Unpublished results.
6. LEMPERT-SRÉTER, M.: Cand. chem. Thesis, Budapest, 1965.
7. LEMPERT-SRÉTER, M., MÜLLER, A.: Acta Chim. Acad. Sci. Hung. **41,** 451 (1964)

Magda LEMPERT-SRÉTER
Margit BÁRDY
Budapest VIII., Múzeum krt. 4/b.

Acta Chimica Academiae Scientiarum Hungaricae Tomus 57 (2), pp. 191—203 (1968)

1,2,4-TRIAZINES AND CONDENSED DERIVATIVES, VI*

SYNTHESIS OF 6-METHYL-7*H*-THIAZOLO[3,2-b][1,2,4]THIAZINE-3(2*H*)-DIONE AND 2-METHYL-6,7-DIHYDRO-3*H*,8*H*-[1,3]THIAZINO[3,2-b][1,2,4]TRIAZINE-3,8-DIONE

G. DOLESCHALL, Gy. HORNYÁK, L. LÁNG,** K. LEMPERT and K. ZAUER

(Research Group for Alkaloid Chemistry of the Hungarian Academy of Sciences, and Department of Organic Chemistry of the Technical University, Budapest)

Received September 15, 1967

It has been shown in previous papers [1, 2] of the present series that 3-thio-1,2,4-triazine-3,5(2*H*,4*H*)-diones (**1**) may be transformed by treatment with appropriate bifunctional compounds, such as alkylene halides or α-halo-oxo compounds, into bicyclic compounds containing the thiazolo-[3,2-b]- (**2a, b**) or [1,3]thiazino[3,2-b][1,2,4]triazine skeleton (**3**).

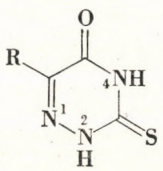

1

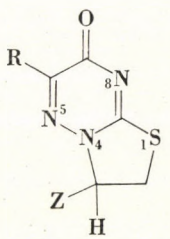

2

a: Z = H
b: Z = OH

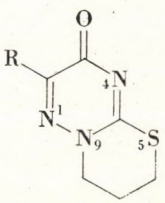

3

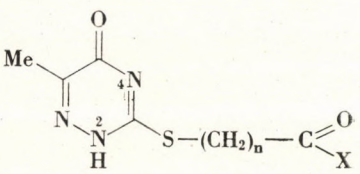

4

a: n = 1, X = OH
b: n = 1, X = OEt
c: n = 1, X = NH_2
d: n = 2, X = OH
e: n = 2, X = OEt

It was obvious to try to perform the above type of reaction by using halogen derivatives of carboxylic acids, or of carboxylic acid derivatives, as bifunctional reagents. It is known [3] that 3-thio-6-methyl-1,2,4-triazine-3,5(2*H*)-dione (**1**, R = CH_3) reacts with chloroacetic acid in alkaline solution to yield 3-(carboxymethylthio)-6-methyl-1,2,4-triazin-5(2*H*)-one (**4a**), while the reaction of the sodium salt of **1** (R = CH_3) with the same reagent in anhy-

* Part V: G. DOLESCHALL, M. HORNYÁK-HÁMORI, K. LEMPERT: Acta Chim. Acad. Sci. Hung. **55**, 319 (1968).

** Present address: *Spectroscopical Department of the Hungarian Optical Works, Budapest.*

drous ethanol gives the ethyl ester (**4b**) of **4a**.* We prepared compounds **4a** and **4b** by using bromoacetic acid and its ethyl ester, respectively, as reagents. It may be noted that the ester **4b** was found to be the reaction product instead of the expected **4c** even if **1** (R = CH_3) was reacted with chloroacet*amide* in ethanolic solution in the presence of sodium ethoxide.

By reacting the sodium salt of **1** (R = CH_3) with β-bromopropionic acid, **4d** similarly was obtained.

For preparing the desired bicyclic 1, 2, 4-triazine derivatives, the cyclization of carboxylic acids **4a** and **4d** had to be effected. On treatment in acetic anhydride with dry hydrogen chloride **4a** eliminates one molecule of water to yield 6-methyl-7*H*-thiazolo[3,2-b][1,2,4]triazine-3(2*H*),7-dione (**5**). **4d** may similarly be cyclized by acetic anhydride, either in the presence of pyridine or by passing dry hydrogen chloride into the reaction mixture, to yield 2-methyl-6,7-dihydro-3*H*,8*H*[1,3]thiazino[3,2-b][1,2,4]triazine-3,8-dione (**8**).

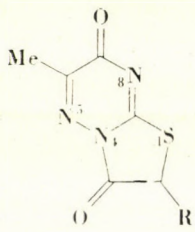

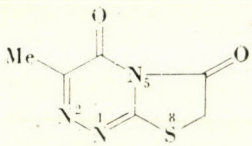

7

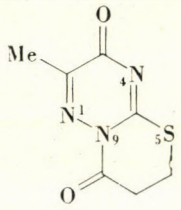

8

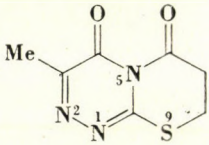

9

5: R = H

6: R = CH_2COOH

It will be noticed that the above syntheses are not structure proving, because the cyclizations performed in the final steps could also have furnished the isomerides containing the thiazolo[2,3-c]- (**7**) and [1,3]thiazino[2,3-c]-[1,2,4]triazine skeletons (**9**), respectively. The correctness of the assigned structures **5** and **8**, however, is proved unequivocally by the spectral properties of the products which will be discussed in some detail below.

*

5 and especially **8** proved to be very reactive compounds reacting easily with nucleophilic reagents under cleavage of the amide group incorporated into the thiazole and 1,3-thiazine rings, respectively, and thereby acylating the nucleophiles. Thus, although **5** may be recrystallized from ethanol, on prolonged standing in ethanolic solution it is converted into **4b**, and by treatment

* Compounds **4a**—**e** are potentially tautomeric but exist, as demonstrated by spectroscopical methods (see below and *cf.* [1, 4]), in the forms depicted above.

with ethanolic ammonia, **4c** [2] is obtained. **8**, on the other hand, does not survive even recrystallization from ethanol: it suffers alcoholysis to yield **4e**, while treatment with moist acetone gives the hydrolysis product **4d**.

*

The synthesis of **5** was achieved also by a "reversed" route, by constructing firstly the thiazole ring, and then, by the aid of properly selected substituents of the first ring, condensing the 1,2,4-triazine ring to it.

The starting compound **14a** [5], which already contained the thiazole skeleton, was prepared from acetone thiosemicarbazone (**10**) and ethyl chloroacetate.

As is well known [5, 6], the 4-thiazolidinone synthesis starting with thiosemicarbazones and α-halogenoacids or derivatives of the latter is general but, unfortunately, not structure proving. Thus *e. g.*, in the above case the structure of the condensation product could be besides **14a** also **15a** or **16a**. Moreover, according to WILSON and BURNS, it is just structure **14a** which should *not* be taken into consideration for the product, because its acid hydrolysis yields 2,4-thiazolinedione (**17**) [5]. Since, however,

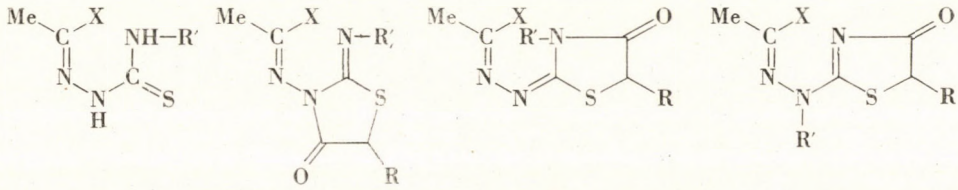

14 **15** **16**

10: X = Me; R′ = H
11: X = ; R′ = Me
12: X = COOH; R′ = H
13: X = COOH; R′ = Me

a: X = Me; R = R′ = H
b: X = R′ = Me; R = H
c: X = COOH; R = R′ = H
d: X = COOMe; R = H; R′ = Me
e: X = Me; R = CH_2COOH; R′ = H
f: X = R′ = Me; R = CH_2COOMe
g: X = COOH; R = CH_2COOH; R′ = H
h: X = COOH; R = CH_2COOMe; R′ = Me
i: X = COOMe; R = CH_2COOMe; R′ = Me

during acid hydrolysis preliminary isomerization of **14a** into **15a** (or **16a**) is not *a priori* excluded — in fact, rearrangements of this type have been observed by different authors [7—10] —, the formation of **17** by no means precludes the correctness of structure **14a**.

According to our spectroscopic studies, structure **16a** may undoubtedly be excluded for the condensation product. By starting with the 4-methyl-thiosemicarbazone (**11**) instead of the unsubstituted thiosemicarbazone of acetone, an analogous product could be obtained whose UV spectrum was found to be practically identical with that of the condensation product of acetone thiosemicarbazone, while the IR spectra of the two products proved to be identical in the double bond region being the most relevant to the present problem. For the condensation product obtained from acetone 4-methylthiosemicarbazone, however, only structures **14b** and **15b** are possible and structure **16b** is not.

From the remaining two alternative structures, **14a** and **15a** the former seems to be more probable for the condensation product obtained with acetone thiosemicarbazone. Structures **15a** and **16a**, the latter being precluded just above, should namely be mutually tautomeric, and tautomeric equilibria of this type are — according to different authors (*cf.*, *e.g.* [11—14]) — always strongly shifted, at the expense of the "imino forms" corresponding to **15a**, towards the "amino forms" corresponding to **16a**. It may therefore be assumed that, in our case, form **15a** is incapable of existing.

Considering the above facts, in the following only structure **14a** (and its analogues) will be taken into consideration.

*

By heating **14a** in aqueous methanol with pyruvic acid, its acetone moiety may be expelled and replaced by pyruvic acid to give **14c**. By refluxing **14c** with a mixture of acetic acid and acetic anhydride, a product, identical in all respects with **5** prepared by another route as already described above, was obtained.

Formation of **5** in the latter reaction may be explained most readily if structure **14c** is supposed for the starting compound. This structure, however, is not proved by the course of the cyclization — and the alternative structures **15c** and **16c** are thereby not precluded —, since transient opening and subsequent closure of the thiazole ring in the other possible direction during closure of the triazine cycle may not be precluded.

*

Experiments were also conducted with the aim to synthesize the carboxymethylated analogue **6** of **5**, analogously to the second synthesis of the latter. The starting compound **14e** [15] needed for this object is readily accessible by condensing maleic anhydride with **10**.

*

The 4-thiazolidinone synthesis used for the preparation of **14e** is, as well as the synthesis discussed above, quite general [6, 15—17] but, again not structure proving, permitting for the product structures **15e** and **16e** besides structure **14e**.

The acetone moiety in **14e** may be again, as in **14a**, replaced by pyruvic acid to yield **14g**. The latter could also be prepared — though in a lower yield — starting directly with pyruvic acid thiosemicarbazone (**12**) and maleic anhydride. In contrast to **14c**, **14g** could not be cyclized to the desired product **6**.

Attempts to prepare **6** directly by condensing **1** ($R = CH_3$) with maleic anhydride also failed because these two compounds did not react.

*

Spectroscopic investigations

An inspection of formulas **5** and **7** and **8** and **9**, respectively, readily reveals that the two alternative structures of the cyclization product of **4a** as well as of **4d** differ considerably. While the chromophoric system of **5** and **8** is cross-conjugated, the conjugation in **7** and **9** is seen to be continuous. According to previous experience [1, 2, 4] this difference should be sufficient to allow choice between the alternative structures of the products based on a study of their UV and IR spectra. A further important difference between the alternative structures is that, while a diacylamine-like partial structure, similar to that found in *N*-acyl-γ-lactams, is incorporated into **7** and **9**—perhaps it would be even more adequate to speak of an *N*,*N*-diacylamidine partial structure (**18**) —, in **5** and **8** no such structure is found. This difference should again, enable us to decide between the alternative structures, by means of the IR spectra.

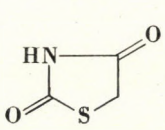

17

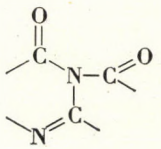

18

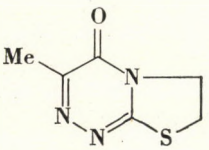

19

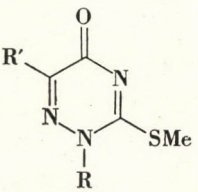

20

a: R = H; R′ = Me
b: R = Me; R′ = H
c: R = Ac; R′ = Me

In Fig. 1 the UV spectrum, recorded in dioxane,* of the cyclization product of **4a** is shown together with the spectra of **2a** (R = Me) [1] and **19** [1], taken in ethanol, for comparison. In Table I the spectral data of the same compounds are compiled together with those of the cyclization product of **4d** and the acetylation product of **20a**, as well as those of **3** (R = Me) [1], **20b** and **21**,** used as model compounds.

From the shapes of the curves shown in Fig. 1, as well as from the data presented in Table I, it may be unequivocally deduced that the structures of the cyclization products of **4a** and **4d** are analogous to those of the model compounds containing the cross-conjugated chromophoric system, their correct structures, therefore, being **5** and **8**, respectively, and not **7** and **9**. Thus, ring closure of **4a** and **4d** takes place under participation of *N*-2, not *N*-4 of the triazine ring, this conclusion being in agreement with the observation that the strongest nucleophilic center of compounds of types **4** and **20a** is *N*-2 [1, 18].

* The spectrum may not be recorded in ethanol because of the rapid alcoholysis of the compound, as a consequence of which the spectrum of **4b** would be obtained under these conditions.

** The latter two model compounds were kindly furnished by Dr. J. GUT, *Institute for Organic Chemistry and Biochemistry of the Czechoslovak Academy of Sciences, Prague.*

It is interesting to note that the absorption band in the vicinity of 250 nm is found to be split in the UV spectra of compounds **5** and **8**, and, as a consequence, broadened in the direction of higher wave lengths, as compared to the corresponding bands of the model compounds **2a**, **3** and **20b**. This splitting and broadening is also found in the spectrum of the monocyclic acetylation product (**20c**) of **20a**. Therefore, it must be a consequence of the fact that the ring nitrogen atom in position 2 of the triazine ring is acylated in the compounds discussed. Structure **20c** for the acetylation product has also been deduced from the UV spectrum.

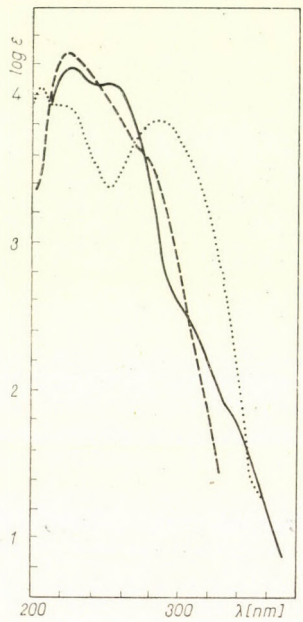

Fig. 1. Ultraviolet spectra
——— Cyclization product (**5**) of **4a** in anhydrous dioxane; - - - - - **2a** (R=Me), in ethanol; ..... **19**, in ethanol

The positions of the carbonyl bands of the cyclization product of **4a** are also shown in Table I. The wave numbers found seem to be much too low in comparison with those expected for structure **7**. The carbonyl bands, *e. g.*, of 1-acetyl-5-benzylidenehydantoins (**22**) which also contain the *N*-acylated γ-lactam-like partial structure, are found between 1800—1778, 1775—1742 and 1713—1712 cm^{-1}, respectively [19], while those of the imidazopyrimidinedione **23**, a compound even more closely related to **7**, are found at 1815, 1720 and 1695 cm^{-1} [20]. However, the

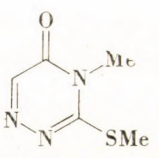

21

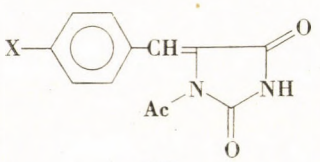

22

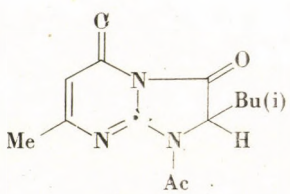

23

Table I

UV and IR spectra of some simple 1,2,4-triazine derivatives

Compound	Solvent	λ_{max} [nm] (log ε)	$\nu_{C=O}$ (cm^{-1}) (KBr-pellet)
Cyclization product **(5)** of **4a**	Dry dioxane	232 (4.18); 255 (4.06)	1760 and 1690
Cyclization product **(8)** of **4d**	,,	238 (4.14); 264 (4.24)	1765 and 1675
Acetylation product **(20c)** of **20a**	,,	242 (4.18); 264 (4.19)	1745 and 1685
2a (R = Me) [1]	Ethanol	232 (4.32)	1645
3 (R = Me) [1]	,,	238 (4.36)	1645
20b* [1]	Methanol	235 (4.38)	1670
19 [1]	Ethanol	212 (4.07); 225 (3.96), shoulder; 292 (3.83)	1685
21* [1]	Methanol	208 (4.11); 226 (3.76), shoulder; 298 (3.92)	1695

* These model compounds were kindly furnished by Dr. J. GUT *(Institute for Organic Chemistry and Biochemistry of the Czechoslovak Academy of Sciences, Prague)*

positions of the carbonyl bands of the cyclization product of **4a** agree well with structure **5** as shown, for example, by comparison with the positions of the carbonyl bands (1770 and 1660 cm^{-1}) of the imidazoquinazolinedione **24** [21].

*

Compounds **4a-e** are seen to be at least potentially tautomeric. The hydrogen atom shown in the above formulas at *N*-2 could, in principle, be attached either to *N*-4 (5(4*H*)-one form), or to the oxygen atom of the ring carbonyl group (aromatic form). The free acids are present in alcoholic solution, as shown by a comparison of their UV spectra with those of the model compounds **20b**, **21** and **25** [23] (*cf.* Tables I and II), undoubtedly in the forms **4a** and **4d**. At concentrations of and higher than 10^{-4} moles/lit. the esters, too, are existing in the corresponding tautomeric forms (**4b** and **4e**).

Table II

UV spectra of some 1,2,4-triazine derivatives (in ethanol)

Compound	λ_{max} [nm] (log ε)	Notes
4a	232 (4.27)	
4d	236 (4.30)	
4c	235 (4.26)	
4b	233.5 (4.28)	$c = 8.8 \cdot 10^{-5} - 8.9 \cdot 10^{-4}$ moles/lit.
4b	217 (4.18); 290 (3.77)	$c = 5.74 \cdot 10^{-6} - 5.7 \cdot 10^{-5}$ moles/lit.
4e	234 (4.26)	$c = 4.3 \cdot 10^{-4}$ moles/lit.
4e	225 (4.14); 288 (3.72)	$c = 4.3 \cdot 10^{-6}$ moles/lit.
26a [23]	228 (4.24); 300 (3.69)	in *N*/1000 aqueous NaOH
26b [23]	228 (4.21); 296 (3.76)	in *N*/1000 ethanolic NaOH

*

By reducing the concentration of their ethanolic solutions to or below 10^{-5} moles/lit., the shapes of the UV spectra of **4b** and **4e** are characteristically changed and become practically identical with that of model compound **25** containing an aromatic bond system.

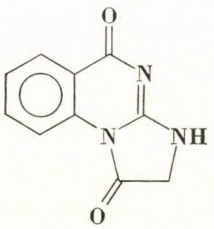

24

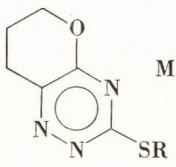

25

a: R = Me
b: R = Et

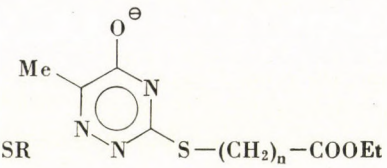

26

b: n = 1
e: n = 2

The concentration dependence of the latter spectra may be interpreted by assuming electrolytic dissociation of the hydrogen atoms attached to *N*—2 in **4b** and **4e**, and an actual electron distribution in the resulting mesomeric anions closely approaching that represented by formula **26**.*

The admissibility of the above assumptions is substantiated by the fact that in the case of compounds **4a** and **4d**, in which the presence of the free carboxyl group necessarily suppresses the heterolytic dissociation of the N(2)-H bond, no concentration dependence of the UV spectra could be observed, at least at dilutions up to 10^{-6} moles/lit.; furthermore, by the observation that changes of the UV spectra analogous to those brought about by dilution in the case of compounds **4b** and **4e**, may also be produced by adding alkalies to the solutions, and that not only with solutions of compounds **4b** and **4e**, but also of compounds **4a** and **4d** (*cf.* [24]).

Experimental**

3-(Ethoxycarbonylmethylthio)-6-methyl-1,2,4-triazin-5(2*H*)-one (4b)

Sodium (0.46 g; 20 mg-atoms) and then 3-thio-6-methyl-1,2,4-triazine-3,5(2*H*,4*H*)-dione (**1**, R=Me) (2.86 g; 20 mmoles) were dissolved in dry ethanol (40 ml); chloroacet*amide* (1.85 g; 20 mmoles) was added and the mixture refluxed for 1/2 hr. The oily residue obtained on evaporation of the solvent in vacuum was rubbed with water (15 ml), when it solidified. The product was filtered off and dried in air at 80° to yield 1.3 g (28%)*** of **4b**, m. p., after recrystallization from ethyl acetate, and mixed m. p. with an authentic sample prepared as described in literature [3, 22]: 173—4°; lit. m. p.: 165—6° (ethanol) [22].
$C_8H_{11}N_3O_3S$ (229.3) Calcd. N 18.75 S 14.31. Found N 18.51, 18.47; S 14.01, 14.02%.

3-(2-Carboxyethylthio)-6-methyl-1,2,4-triazin-5(2*H*)-one (4d)

A mixture consisting of **1** (R=Me) (5.0 g; 35 mmoles), sodium hydroxide (2.8 g; 70 mmoles), β-bromopropionic acid (6.15 g; 40 mmoles) and water (50 ml) was refluxed for 15 min. and, after cooling, acidified with conc. HCl. The crystalline product was washed with a small amount of water and dried in air at 80° to yield 2.1 g (28%) of **4d**, m. p. 186° (from nitromethane).
$C_7H_9N_3O_3S$ (215.2). Calcd. N 19.53; S 14.90. Found N 19.79, 19.53; S 14.52, 14.43%.

6-Methyl-7*H*-thiazolo[3,2-b][1,2,4]triazine-3(2*H*),7-dione (5)]

(*a*) To a dry ethanolic solution (80 ml) of metallic sodium (0.92 g; 40 mg-atoms) and **1** (2.86 g; 20 mmoles) bromoacetic acid (2.78 g; 20 mmoles) was added, the mixture refluxed for 1/2 hr. and concentrated to about 10 ml. After cooling, the sodium bromide containing crystals of the Na-salt of **4a** (4.9 g) were filtered off and dried in air. The product was suspended in acetic anhydride (50 ml) and a stream of dry hydrogen chloride was passed for 3/4 hours into the mixture, with stirring. A spontaneous rise of temperature (60—80°) was observed. For completing the reaction, the introduction of HCl gas was continued for another 10 min. under refluxing. Undissolved inorganic salts were removed by filtration of the hot solution, and, after cooling, the filtrate was kept overnight in a refrigerator whereby crystals of **5** (1.9 g; 52%) deposited in the form of yellow needles. The latter were filtered off by suction, washed with dry ether and dried in vacuum over paraffin shavings, m. p. 175° (from dioxane).
$C_6H_5N_3O_2S$ (183.2) Calcd. N 22.95; S 17.50. Found N 23.05; S 17.52%.

(*b*) A mixture of **14c** (see below) (8.0 g; 40 mmoles), acetic acid (150 ml) and acetic anhydride (40 ml) was refluxed for 3 hrs., the solution filtered and evaporated to dryness in vacuum. The residue was dissolved in acetone (10 ml) by gentle heating and the product precipitated by the addition of ether (30 ml) to obtain 4.6 g (63%) of **5**, m. p.: 178—9° (from dioxane). The product was shown by mixed m. p. and the IR spectrum to be identical with the product prepared according to (*a*).

* A similar concentration dependence of the UV spectra was found in the case of **20a** as well as of other related 1,2,4-triazines (*cf.* [24]).

** All m. p.'s are uncorrected.

*** From the aqueous mother liquor rather large additional amounts of a less pure product could be obtained.

2-Methyl-6,7-dihydro-3*H*,8*H*-[1,3]thiazino[3,2-b][1,2,4]triazine-3,8-dione (8)

(*a*) A mixture of **4d** (1.5 g; 7 mmoles), acetic anhydride and pyridine (15 ml each) was stirred for 15 min. at room temperature and the yellowish solution obtained, subsequently evaporated to dryness in vacuum. The yellowish crystalline residue was suspended in ether, filtered off by suction and dried over P_2O_5 in vacuum to yield 1.24 g (90%) of **8**, m. p. 155—6° (from acetic anhydride-ether).
$C_7H_7N_3O_2S$ (197.2) Calcd. C 42.63; H 3.58; N 21.31. Found C 42.90, 43.00; H 3.88, 3.40; N 21.31, 21.57%.

(*b*) Into a suspension of **4d** (0.5 g; 2.3 mmoles) in acetic anhydride (20 ml) a stream of dry hydrogen chloride was passed, with stirring. After approximately 10 min. a clear solution resulted from which, after another 10 min., colourless crystals began to deposite. After stirring for further 10 min. the product was filtered off and worked up as under (*a*) to yield 0.37 g (83%) of **8**, m. p. and mixed m. p. with the product prepared according to (*a*) 155—6°.

Ethanolysis

8 (1.0 g; 5 mmoles) was boiled up with dry ethanol (10 ml) and the solution evaporated to dryness in vacuum. By crystallization of the oily residue from acetone-petroleum ether 0.51 g (40%) of **4e**, m. p.: 108—9°, was obtained.
$C_9H_{13}N_3O_3S$ (243.3) Calcd. N 17.28; S 13.17. Found: N 17.48, 17.46; S 12.80, 13.06%.

The above product proved by m. p. and mixed m. p. determination to be identical with an authentic sample prepared from **4d** by direct esterification with ethanol in the presence of hydrochloric acid.

Hydrolysis

An aqueous suspension (5 ml) of **8** (0.1 g; 0.5 mmoles) was stirred 5 min. at room temperature, during which time hydrolysis to **4d** was complete, in spite of the heterogeneous system used. Yield: 87 mg (80%), m. p. and mixed m. p. with an authentic sample of **4d**: 186°.

Table III

UV spectra of some 2-imino-3-alkylideneamino-4-thiazolidinones (in ethanol)

Compound	λ_{max} [nm] (log ε)
14a	220 (4.21); 258 (4.17)
14b	226 (4.22); 258 (4.17)
14e	220 (4.19); 260 (4.18)
14f	228 (4.19); 258 (4.19)
14c	242 (4.09); 285 (4.22)
14d	248 (4.12); 284 (4.10)
14h	247 (4.14); 283 (4.15)
14i	248 (4.11); 286 (4.18)

2-Imino-3-(isopropylideneamino)-4-thiazolidinone (14a)

For the preparation of **14a** the method described in literature [5] was used with the only difference that the sodium salt of acetone thiosemicarbazone (**10**) was not isolated but, instead, *in situ* reacted with ethyl chloroacetate. Yield: 75.5%; m. p. 177—8° (lit. [5] m. p. 175—6°).

For the spectral data of **14a** and its analogues **14b**—i, see Table III.

By passing dry HCl into a solution of **14a** in dry dioxane, the hydrochloride was obtained in theoretical yield, m. p. 195° (dec.).
$C_6H_6N_4OS.HCl$ (207.5) Calcd. Cl 17.1; S 15.41. Found Cl 16.77; S 15.50%.

2-Methylimino-3-(isopropylideneamino)-4-thiazolidinone (14b)

(*a*) Acetone 4-methylthiosemicarbazone (**11**) [25] (3.0 g; 21 mmoles) was dissolved in a warm, dry methanolic solution (10 ml) of metallic sodium (0.50 g; 22 mg-atoms). After cooling, ethyl chloroacetate (2.66 g; 22 mmoles) was added by drops, and the resulting mixture refluxed for 1.5 hrs. on a steam bath. The product was finally precipitated by the addition of water, filtered off, and washed with water to yield 2.70 g (71%) of **14b**, m. p. 102—3° (after sublimation at 5—6 Torr, bath temperature: 90—110°).

(*b*) **14a** (1.2 g; 7 mmoles) was methylated in dioxane solution with diazomethane (ethereal solution). The oily residue obtained on evaporation solidified on rubbing with water (10 ml) to yield 0.9 g (70%) of a product which, after sublimation, proved by m. p. (102—3°) and mixed m. p. to be identical with the product prepared according to (*a*).

$C_7H_{11}N_3OS$ (185.2). Calcd. C 45.40; H 5.99; N 22.69. Found C 46.00, 46.02; H 5.99, 6.29; N 22.21, 22.63%.

2-Imino-3-(1-carboxyethylideneamino)-4-thiazolidinone (14c)

A mixture of **14a** (6.0 g; 35 mmoles), pyruvic acid (3.6 g; 42 mmoles), methanol (30 ml) and water (50 ml) was refluxed for 1.5 hrs. on a steam bath. The solution was then evaporated to approximately 4/5 parts of its original volume. After cooling, the crystalline product was filtered off and washed with water to yield 3.7 g (52%) of **14c**, m. p. 225° (dec.).

$C_6H_7N_3O_3S + 1/2\ H_2O$ (210.1) Calcd. C 35.83; H 3.51; S 15.92. Found C 35.86; H 3.81; S 16.03%.

2-Methylimino-3-(1-methoxycarbonylethylideneamino)-4-thiazolidinone (14d)

was prepared by methylation of **14c** (1.0 g; 5 mmoles) with diazomethane in a methanol-ether solution to obtain 0.9 g (82%) of a product melting at 160—1° (from aqueous ethanol).

$C_8H_{11}N_3O_3S$ (229.2). Calcd. N 18.34; S 13.96. Found N 18.25; S 14.05%.

[2-Imino-3-(isopropylideneamino)-4-oxo-5-thiazolidinyl]-acetic acid (14e)

According to the method described in literature [15] we could prepare **14e** in low yields only. The following modification proved to be advantageous.

A mixture of maleic anhydride (8.8 g; 90 mmoles), acetone thiosemicarbazone (**10**) (9.8 g; 90 mmoles) and dry dioxane (25 ml) was heated until a vigorous reaction started to give a brown solution which came spontaneously to boiling. After the reaction subsided, the mixture was refluxed for a few minutes more, and, after cooling, inoculated with a small crystal of **14e** and allowed to stand for 2 days. Crystallization finally was completed by the addition of gasoline (45 ml). The product was filtered off by suction, washed with gasoline and finally with ether to yield 17.6 g (95.2%) of **14e**, m. p. 218—9° (dec.), (lit. [15] m. p. 223° (dec.)).

Methyl [2-methylimino-3-(isopropylideneamino)-4-oxo-5-thiazolidinyl]-acetate (14f)

was prepared in essentially theoretical yield by the methylation of **14e** (1.2 g; 5.3 mmoles) with diazomethane. The product was purified by sublimation and subsequent recrystallization from methanol-petroleum ether. M. p. 122—3°.

$C_{10}H_{15}N_3O_3S$ (257.2). Calcd. C 46.69; H 5.88; N 16.34; S 12.56. Found C 46.61; H 5.75; N 16.42; S 12.50%.

[2-Imino-3-(1-carboxyethylideneamino)-4-oxo-5-thiazolidinyl]-acetic acid (14g)

(*a*) A mixture consisting of **14e** (15 g; 65 mmoles), pyruvic acid (6.1 g; 69 mmoles) and methanol (30 ml) was refluxed for 1 hr. and subsequently evaporated in vacuum; the residue was rubbed with 30 ml of petroleum ether and, after being allowed to stand for 1/2 hr., filtered off by suction and washed with petroleum ether to yield 16.7 g (98.5%) of **14g**, m. p.: 187—8° (dec.) (from 15 parts of water, preheated to boiling, or from acetone-petroleum ether).
$C_8H_9N_3O_5S$ (259.2) Calcd. C 37.07; H 3.50; N 16.21; S 12.36. Found C 36.86; H 3.69; N 15.95; S 12.24%.

(*b*) A mixture consisting of pyruvic acid thiosemicarbazone (**12**) (5.5 g; 34 mmoles), maleic anhydride (3.3 g; 34 mmoles) and dry dioxane (20 ml) was refluxed for 5 min. and subsequently evaporated to dryness in vacuum on a steam bath. The residue was rubbed with ether (30 ml) whereby it became crystalline to yield 3.1 g (35%) of a product which, by m. p., mixed m. p. and the IR spectra proved to be identical with the product prepared according to (*a*).

Methyl [2-methylimino-3-(1-carboxyethylideneamino)-4-oxo-5-thiazolidinyl]-acetate (14h)

was prepared essentially as **14g** according to method (*a*) but, of course, starting with **14f**; the yield was almost theoretical. M. p.: 144—5° (from aqueous methanol).
$C_{10}H_{13}N_3O_5S$ (287.1). Calcd. C 41.81; H 4.56; N 14.36. Found C 41.70; H 3.92; N 14.00%.

Methyl [2-methylimino-3-(1-methoxycarbonylethylideneamino)-4-oxo-5-thiazolidinyl]-acetat (14i)

was prepared by methylation of either **14g** or **14h** with diazomethane in ethereal solution; the yield was in both cases theoretical. The crude products were purified by sublimation (0.1 Torr, bath temperature: 150°) and subsequent recrystallization from aqueous methanol. M. p. 156—7°.
$C_{11}H_{15}N_3O_5S$ (301.2). Calcd. C 43.85; H 5.02; N 13.95; S 10.65. Found C 43.81; H 4.71; N 13.99; S 10.96%.

2-Acetyl-3-methylthio-6-methyl-1,2,4-triazin-5(2*H*)-one (20c)

A mixture of 3-methylthio-6-methyl-1,2,4-triazin-5(2*H*)-one (**20a**) (2.0 g; 12.8 mmoles), acetic anhydride and dry pyridine (20 ml each) was refluxed for 1.5 hrs. and subsequently evaporated to dryness in vacuum. The oily residue, which solidified on standing, was recrystallized from a mixture of a small amount of acetic anhydride and dry ether and dried over paraffin shavings in a vacuum desiccator to yield 1.4 g (55%) of **20c**; yellowish crystalline powder, m. p. 110—1°.
$C_7H_9N_3O_5S$ (199.2) Calcd. C 42. 20; H 4.55; S 16.10. Found C 42.02; H 4.44; S 15.94%.

*

The UV spectra were taken with a *Spectromom* instrument, *Type* 201 *(Hungarian Optical Works, Budapest)*.

The authors' thanks are due to Dr. P. Sohár for the IR, to Mr. M. Vörös for the UV spectra; to the head and co-workers, Dr. I. Balogh-Batta and Miss K. Ófalvi, Mrs. S. Viszt-Simon and Mrs. I. Zauer-Csüllög, of the *Microanalytical Laboratories* of the *Institute of Organic Chemistry of the Technical University, Budapest*, for the microanalyses; and to the *United Works of Pharmaceutical and Dietetic Products, Budapest*, for financial support.

SUMMARY

Cyclization of 3-(carboxymethylthio)-6-methyl- (**4a**) and 3-(2-carboxymethylthio)-6--methyl-1,2,4-triazin-5(2*H*)-one (**4d**) gave 6-methyl-7*H*-thiazolo[3,2-b][1,2,4]triazine-3(2*H*),7--dione (**5**) and 2-methyl-6,7-dihydro-3*H*,8*H*-[1,3]thiazino[3,2-b][1,2,4]triazine-3,8-dione (**8**), respectively. The structures of the products are proved by their UV and IR spectra.

Compound **5** was alternatively prepared by cyclization of 2-imino-3-(1-carboxyethylideneamino)-4-thiazolidinone (**14c**). In this connection the structures of the compounds prepared by condensation of thiosemicarbazones with both haloacetic acid derivatives and maleic anhydride were reinvestigated. It has been found that the products of these reactions are probably not compounds of the type of 2,4-thiazolidinedione-2-hydrazones (**15**), as hitherto assumed, but derivatives (**14**) of 2-imino-3-amino-4-thiazolidinone.

REFERENCES

1. NYITRAI, J., BÉKÁSSY, S., and LEMPERT, K.: Acta Chim. Acad. Sci. Hung. **53,** 311 (1967)
2. DOLESCHALL, G., HORNYÁK, GY., HORNYÁK-HÁMORI, M., LEMPERT, K. and WOLFNER, A.: Acta Chim. Acad. Sci. Hung. **53,** 385 (1967)
3. GUT, J. and PRYSTAŠ, M.: Collection Czechoslov. Chem. Commun. **24,** 2986 (1959)
4. JONAŠ, J. and GUT, J.: Collection Czechoslov. Chem. Commun. **27,** 1886 (1962)
5. WILSON, F. J. and BURNS, R.: J. chem. Soc. [London] **121,** 870 (1922)
6. BROWN, F. C.: Chem. Revs. **61,** 468 (1961)
7. BEYER, H. *et al.:* Chem. Ber. **87,** 1385, 1392 (1954)
8. TAYLOR, E. C. *et al.:* J. Amer. Chem. Soc. **76,** 1866 (1954)
9. SPRAGUE, J. M. and LAND, A. H. in *Heterocyclic Compounds* (ed.: R. C. Elderfield), John Wiley and Sons, Inc., New York, 1957. Vol. 5. p. 618 et sequ. Herein references to earlier literature.
10. OHTA, M. and UEDA, H.: J. chem. Soc. Japan, pure Chem. Sect. **82,** 1525, 1528, 1530 (1961); ref.: Chem. Zbl. **1966,** Nr. 50—1048, 1049, 1050
11. COMRIE, A. M.: J. chem. Soc. [London] **1964,** 3478; with references to earlier literature.
12. NAJER, H. *et al.:* Bull. Soc. chim. France **1961,** 1226, 1231; **1963,** 328, 1022
13. DURDEN, J. A. *et al.:* J. Amer. Chem. Soc. **81,** 1931 (1959)
14. HOWELL, CH. F., QUINONES, N. Q. and HARDY, R. A., Jr.: J. Org. Chem. **27,** 1686 (1962)
15. MCLEAN, J. and WILSON, J. F.: J. chem. Soc. [London] **1939,** 1048
16. TIŠLER, M.: Vestn. Sloven. Kem. Društva **4,** 91 (1957)
17. M. KRBAVČIČ *et al.:* J. Medicinal Chem. **9,** 430 (1966)
18. GUT, J. in *Advances in Heterocyclic Chemistry* (Edited by A. R. Katritzky), Academic Press, New York and London, 1963. Vol. 1. pp. 223—228.
19. DERKOSCH, J.: Monatsh Chem. **92,** 361 (1961)
20. HORNYÁK, GY.: Techn. D. Thesis, Technical University, Budapest, 1967.
21. DOLESCHALL, G., LÁNG, L. and LEMPERT, K.: Acta Chim. Acad. Sci. Hung. **47,** 405 (1966)
22. GUT, J., PRYSTAŠ, M., JONAŠ, J.: Collection Czechoslov. Chem. Commun **26,** 986 (1961)
23. DOLESCHALL, G., HORNYÁK-HÁMORI, M., LEMPERT, K.: Acta Chim. Acad. Sci. Hung. **55,** 319 (1968)
24. SZIVÓS, K.: Thesis, Eötvös Lóránd University, Budapest, 1967.
25. BOSE, P. K.: Quart. J. Ind. Chem. Soc. **2,** 112 (1926); Chem. Zbl. **1926, I,** 1199

Gábor DOLESCHALL
Gyula HORNYÁK
Károly LEMPERT
Károly ZAUER
Budapest XI., Gellért tér 4.

László LÁNG
Budapest XII., Csörsz u. 35/43.

Acta Chimica Academiae Scientiarum Hungaricae Tomus 57 (2), pp. 205—212 (1968)

BINDUNGSSYSTEM DER N-ACYL-SULFILIMINE, VI*

KONJUGATIVER EFFEKT DER S-METHYL-N-*p*-TOLYLSULFONYL-SULFILIMIN-GRUPPE

Á. KUCSMAN, F. RUFF, S. SÓLYOM und T. SZIRTES

(Institut für Organische Chemie der L. Eötvös Universität, Budapest)

Eingegangen am 13. Oktober 1967

Wichtigere Merkmale der Feinstruktur der N-Acyl-sulfilimine sind unlängst mit Hilfe IR- und UV-spektroskopischer [1—4] sowie röntgenographischer [5, 6] Untersuchungen aufgedeckt worden. Auf diese Weise konnte bewiesen werden, daß N-Sulfonyl-sulfilimine ($RR'S^{IV}NS^{VI}O_2Q$; R, R′ = aliphatische oder aromatische Gruppen; Q = z. B. CH_3 oder $C_6H_4CH_3$) im $S^{IV}NS^{VI}$ Molekülanteil ein delokalisiertes $d\pi$ Bindungssytem enthalten. Das S^{VI} Schwefelatom bildet das zentrale Atom eines kumulierten $d\pi$ Bindungssystems: zwischen den Elektronensystemen des $S^{IV}NS^{VI}$ Molekülanteils und der $S^{VI}O_2$ Gruppe besteht keine konjugative Wechselwirkung, hingegen zeigt sich eine derartige Wechselwirkung, wenn auch in geringerem Maße, zwischen dem S^{IV} Schwefelatom und aromatischen R, R′ Gruppen. Auf die letztere Wechselwirkung konnte u. a. daraus geschlossen werden, daß die Frequenz der für N-Sulfonyl-sulfilimine charakteristischen ν_{SN3} Bande um die Wellenzahl 5—18 cm^{-1} vermindert ist, hingegen sich die integrale Intensität ihrer Absorption vergrößert, wenn z. B. die R, R′ = Äthylgruppen gegen Phenylgruppen vertauscht werden; ein derartiger konjugativer Effekt ist bei den analog gebauten Sulfoxyden nicht nachweisbar. (Es ist bemerkenswert, daß in N-Sulfonyl-sulfiliminen, die eine S-Methylgruppe enthalten, eine prägnante $CH_3—S^{IV}$ Hyperkonjugation nachgewiesen werden konnte.) UV spektroskopische Untersuchungen [4] haben ergeben, daß das S^{IV}-Schwefelatom solcher N-Sulfonyl-sulfilimine, die als R eine *p*-substituierte Phenylgruppe enthalten, in angeregtem Zustand sich als Akzeptor verhält, wenn der *p*-Substituent Donorcharakter besitzt.

Zwecks weiterer Klärung der Wechselwirkung des S^{IV} Schwefelatoms und des aromatischen Systems schien es angezeigt, zu untersuchen, welche Wirkung die mit ihrem S^{IV} Schwefelatom an ein aromatisches System gebundene »Sulfilimingruppe« ($RS^{IV}NSO_2Q$) auf das Elektronensystem der aromatischen Gruppe im Grundzustand ausübt. Um die Wechselwirkung der »Sulfilimingruppe« und des aromatischen Systems auf quantitative Art

* V. Mitteilung: Acta Chim. Acad. Sci. Hung. **54**, 153 (1967).

charakterisieren zu können, haben wir mit der S-Methyl-N-*p*-tolylsulfonyl--sulfilimingruppe [$-S^{IV}(CH_3)NTs$] in *p*- und *m*-Stellung substituierte Derivate der Benzoesäure und des Phenols hergestellt (**I**—**IV**; Ts = *p*-$CH_3C_6H_4SO_2$):

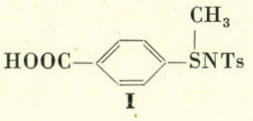

I

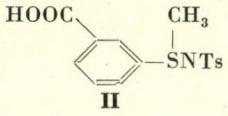

II

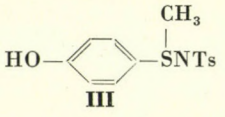

III

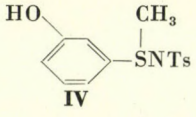

IV

Es wurden die Dissoziationsexponenten der Sulfilimine **I**—**IV** in 48%-igem wäßrigem Äthanol (vgl. [7, 8]) bestimmt (Tabelle I) und daraus die für die S-Methyl-N-*p*-tolylsulfonyl-sulfilimingruppe charakteristischen *Hammettschen* σ und σ' Konstanten berechnet; (Tabelle II; die σ bzw. σ' Werte

Tabelle I

Verbindung	pK_a*
S-Methyl-S-(4-carboxy-phenyl)-N-*p*-tolylsulfonyl-sulfilimin (**I**)	4,62
S-Methyl-S-(3-carboxy-phenyl)-N-*p*-tolylsulfonyl-sulfilimin (**II**)	4,70
S-Methyl-S-(4-hydroxy-phenyl)-N-*p*-tolylsulfonyl-sulfilimin (**III**)	8,79
S-Methyl-S-(3-hydroxy-phenyl)-N-*p*-tolylsulfonyl-sulfilimin (**IV**)	9,30
Benzoesäure	5,65**
Phenol	11,28**

* Die Bestimmung wurde in 48 Vol.% Alkohol enthaltendem wäßrigem Alkohol durchgeführt (s. im Versuchsteil).

** Die für Benzoesäure und Phenol bestimmten pK_0 Werte stimmen mit den Literaturangaben [7, 8] überein.

sind aus den Dissoziationsexponenten der entsprechenden Carbonsäuren bzw. Phenole berechnet worden). Zum Vergleich sind in der Tabelle II auch die *Hammetschen* σ und σ' Werte der CH_3S^{II}, $CH_3S^{IV}O$, $CH_3S^{VI}O_2$, CH_3O und NO_2 Gruppe verzeichnet.

Die Differenzwerte $\sigma_p - \sigma_m$ und $\sigma'_p - \sigma_p$ geben auf bekannte Weise Auskunft über den Typ der Konjugation. Hat die untersuchte Gruppe einen Donorcharakter (z. B. OCH_3), so ist die Differenz $\sigma_p - \sigma_m$ verhältnismäßig groß und hat ein negatives Vorzeichen, hingegen ist im Falle einer Akzeptorgruppe (z. B. NO_2) die Differenz $\sigma_p - \sigma_m$ unbedeutend gering und der Differenzwert $\sigma'_p - \sigma_p$ auffallend groß.

Ein Vergleich der in der Tabelle II zusammengefaßten Daten macht es ersichtlich, daß die S-Methyl-N-*p*-tolylsulfonyl-sulfilimingruppe einen typi-

schen Akzeptorcharakter hat und in dieser Hinsicht eher der Methylsulfonyl- als der Methylsulfinylgruppe nahe steht. Der starke Akzeptorcharakter der Sulfilimingruppe ist augenscheinlich darauf zurückzuführen, daß das S^{IV}

Tabelle II

Gruppe	σ_p	σ_m	σ'_p	σ'_m	$\sigma_p-\sigma_m$	$\sigma'_p-\sigma_p$	Literatur
$CH_3S^{IV}NTs$	+0,70	+0,65	+1,00	+0,80	+0,05	+0,30	*
CH_3S^{II}	−0,01	+0,14	+0,16	+0,16	−0,15	+0,17	[9]
$CH_3S^{IV}O$	+0,48	+0,51	+0,73	+0,53	−0,03	+0,25	[10]
$CH_3S^{VI}O_2$	+0,72	+0,65	+0,98	+0,70	+0,07	+0,26	[9]
CH_3O	−0,27	+0,28	−0,10		−0,55	+0,17	[11, 8]
NO_2	+0,78	+0,71	+1,27		+0,07	+0,39	[11]

* Die σ und σ' Werte wurden aus den in Tabelle I verzeichneten pK_a Werten nach der *Hammettschen* Gleichung ($\varrho\sigma = pK_0 - pK$) berechnet. Dabei wurde in Betracht gezogen, daß unter den angewandten Versuchsbedingungen für Carbonsäuren mit $\varrho = 1{,}46$, für Phenole mit $\varrho = 2{,}48$ gerechnet werden muß [7]. Die σ Werte sind aus den Dissoziationsexponenten der Carbonsäuren, die σ' Werte aus den Dissoziationsexponenten der Phenole berechnet worden.

Schwefelatom infolge seiner d-Bahnen zur Elektronenaufnahme befähigt ist, und die $S^{IV}N$ Bindung hier stärker polar ist als die $S^{IV}O$ Bindung (vgl. [1]). Die Fähigkeit zur Konjugation der Sulfilimingruppe äußert sich auf prägnante Art im Anion des Phenolderivates **III**, in welchem die Möglichkeit einer Donor-Akzeptor Wechselwirkung besteht; die Konjugation, in welche das S^{IV} Schwefelatom einbezogen ist, läßt sich mit den mesomeren Grenzstrukturen **V** und **VI** veranschaulichen:

V **VI**

Die Sulfilimine **I**—**IV** wurden in neutralem wäßrigem Medium oder wäßrigem Dioxan durch Umsetzen der entsprechenden Thioäther mit Chloramin-T hergestellt:

$$RR'S + TsNCl^{\ominus} \longrightarrow RR'SNTs + Cl^{\ominus}$$

Bei der Herstellung des Sulfilimins **I** richteten wir uns an unser bereits beschriebenes [12] Verfahren; die aus *p*-Aminobenzoesäure ausgehende Synthese [13, 14] des als Ausgangssubstanz für das Sulfilimin dienenden Methyl-(4-carboxy-phenyl)-sulfids ließ sich wesentlich vereinfachen.

Das Sulfilimin **II** wurde nach der Methode von CLARKE, KENYON und PHILLIPS [15] hergestellt.

Eine unmittelbare Herstellung des Sulfilimins **III** durch Einwirkung von Chloramin-T auf das Methyl-(4-hydroxy-phenyl)-sulfid war nicht möglich, da das Sulfid mit phenolischer Hydroxylgruppe eine Oxydation erlitt. Diese Schwierigkeit konnte durch vorübergehenden Schutz der Hydroxygruppe durch Acetylierung behoben werden: das Methyl-(4-acetoxy-phenyl)-sulfid ließ sich mit Chloramin-T glatt zum entsprechenden Sulfilimin (**IIIa**) umsetzen, und letzteres dann mit verdünnter Lauge zum Sulfilimin **III** entacetylieren. Die Benzylschutzgruppe hat sich hingegen nicht bewährt, da das aus dem Methyl-(4-benzyloxy-phenyl)-sulfid gewonnene Sulfilimin (**IIIb**) auf selektive Art nicht entbenzyliert werden konnte. Durch katalytische Hydrierung oder durch Essigsäure- bzw. Essigsäureanhydrid und Bromwasserstoff wird nämlich zuerst die $S^{IV}N$ Bindung aufgespalten.

Das Sulfilimin **IV** ließ sich unmittelbar aus Chloramin-T und Methyl-(3-hydroxy-phenyl)-sulfid herstellen, da letzteres unter den angewandten Versuchsbedingungen keine Oxydation erleidet.

Beschreibung der Versuche

Methyl-(4-carboxy-phenyl)-sulfid

In 163 ml Wasser wurden 5,75 g (0,144 *M*) Natriumhydroxyd, 18,7 g (0,136 *M*) *p*-Aminobenzoesäure und 9,38 g (0,136 *M*) Natriumnitrit gelöst, dann ließ man diese Lösung langsam zu einem mit Eis gekühlten und gerührten Gemisch von 37,5 ml konzentrierter (ungefähr 0,45 *M*) Salzsäure und 50 g Eis hinzutropfen. Nach 3stündigem Rühren neutralisierte man das eiskalte Gemisch mit einer konzentrierten, kalten Natriumacetatlösung, filtrierte es nachher ab, wobei man das Filtrat gleich in eine Lösung von 62,5 g Kaliumäthylxanthogenat in 200 ml Wasser rinnen ließ. Das so gewonnene Gemisch wurde nebst Rühren 1 Stunde auf 80° erwärmt. Es entstand eine braune Lösung, die nach dem Abkühlen mit konzentrierter Salzsäure auf pH = 3 eingestellt wurde. Nun filtrierte man den entstandenen Niederschlag ab und erwärmte ihn mit 100 ml 10%iger Natronlauge 2 Stunden am Wasserbade, versetzte dann das Gemisch mit 12,5 g Natriumdithionit und hielt seine Temperatur noch 10 Minuten bei 90°. Jetzt wurde die entstandene braune Lösung filtriert und das Filtrat mit konzentrierter Salzsäure auf pH = 4 eingestellt, wodurch sich die entstandene 4-Mercaptobenzoesäure in Form weißer Kristalle ausschied; sie wurde schnell abfiltriert, mit Wasser gewaschen und noch in nassem Zustand sofort weiter verarbeitet. Der gewaschene und abgepreßte nasse Niederschlag, der ungefähr 16 g (ca. 0,1 *M*) wog, wurde in einer Lösung von 24 g (0,6 *M*) Natriumhydroxyd in 450 ml Wasser aufgelöst, dann diese Lösung nach Zusatz von 25,2 g (18,5 ml; 0,2 *M*) Dimethylsulfat 7 Stunden geschüttelt, nachher das Gemisch mit Äther ausgeschüttelt und die abgetrennte wäßrige Schicht mit Salzsäure angesäuert. Das ausgeschiedene, weiße Rohprodukt konnte durch einmaliges Umlösen aus einem 7 : 3 Gemisch von Wasser und Alkohol unter Anwendung von Tierkohle in reinen Zustand gebracht werden. Ausbeute 7.3 g (32% d. Th.); Schmp. 191—193°.

Methyl-(4-acetoxy-phenyl)-sulfid

Eine Lösung von 2.8 g (0,02 *M*) Methyl-(4-hydroxy-phenyl)-sulfid, das nach dem vorzüglichen Verfahren von GOETHALS und RADZITZKY [16] hergestellt worden war, in einem Gemisch von 10 ml (0,1 *M*) Essigsäureanhydrid und 8 ml (0,1 *M*) Pyridin wurde nach 2 stündigem Erwärmen am Wasserbad mit 300 g Eis vermischt. Die ausgeschiedene Ölschicht erstarrte während des Stehens über Nacht. Das abgesonderte Produkt wurde in 500 ml Wasser aufgeschlämmt, nachher filtriert und scharf abgepreßt. Das so gewonnene Rohprodukt wog trocken 2,8 g (77% d. Th.), Schmp. 43—44°, mit der Literaturangabe [17] übereinstimmend.

S-Methyl-S-(4-acetoxy-phenyl)-N-p-tolylsulfonyl-sulfilimin (IIIa)

In je 20 ml eines 4 : 1 Gemisches von Dioxan und Wasser wurden 1,8 g (0,01 *M*) Methyl-(4-acetoxy-phenyl)-sulfid und 2,8 g (0,01 *M*) Chloramin-T gelöst, dann die beiden Lösungen vermischt und 2 Stunden am Wasserbad erwärmt. Man trieb das Lösungsmittel bei Unterdruck ab und nahm den Rückstand in einem Gemisch von 40 ml Äthylacetat und 30 ml Wasser auf. Die abgetrennte organische Phase wurde mit 10 ml 5%iger Natronlauge durchgeschüttelt (starke Selbsterwärmung!), schnell von der Lauge getrennt, nachher noch zweimal mit je 30 ml Wasser gewaschen, über Magnesiumsulfat getrocknet und eingedampft. Es blieb ein mit Kristallen durchsetztes Öl (3,1 g) zurück. Das abgesonderte kristalline Rohprodukt (1,5 g) lieferte nach dem Umkristallisieren aus 3 ml Alkohol 1,2 g (34% d.Th.) schneeweiße Kristalle von Schmp. 101—102°. Zur Analyse wurde eine kleine Probe aus Alkohol noch viermal umkristallisiert, wodurch sich der konstante Schmp. von 103—104° erreichen ließ.

$C_{16}H_{17}NO_4S_2$ (351,5) Ber. C 54,7 H 4,9 S 18,3%
Gef. C 54,7 H 5,2 S 18,4%.

Charakteristische Banden des IR-Spektrums (KBr-Tablette): ν_{CO} (Phenolester): 1760 cm^{-1}; ν_{SO_2} (asymm.): 1282 cm^{-1}; ν_{SO_2} (symm.): 1140 cm^{-1}; ν_{SNS}: 962 cm^{-1}.

S-Methyl-S-(4-hydroxy-phenyl)-N-p-tolylsulfonyl-sulfilimin (III)

Eine Lösung von 7,0 g (0,02 *M*) des Sulfilimins **IIIa** in 30 ml Äthylacetat wurde zuerst 1/2 Minute mit 20 ml, dann je 10 Minuten zweimal mit je 40 ml, schließlich je 15 Minuten zweimal mit je 40 ml 5%iger Natronlauge geschüttelt, die wäßrigen Phasen jeweils abgetrennt und vor jeder Ausschüttelung die organische Phase mit Äthylacetat auf das ursprüngliche Volumen gebracht. Die gesondert abgetrennten alkalischen Lösungen wurden der Reihe nach mit 6, 24 und abermals 24 ml konz. Salzsäure angesäuert und die ausgeschiedenen weißen Kristalle (0,85 + 2,45 + 0,5 g = 3,8 g) aus 20, 40 bzw. 12 ml Alkohol umkristallisiert. Auf diese Art konnten 0,64 g (Schmp. 192—193°), 2,0 g (Schmp. 188—190°) und 0,46 g (Schmp. 193—194°), d.h. insgesamt 3,1 g (50% d.Th.) des einmal umkristallisierten desacetylierten Produktes **III** gewonnen werden. Der Schmelzpunkt der zweiten Fraktion (2,0 g) erhöhte sich nach einer zweiten Kristallisation auf 192—193°. Zur Analyse und spektralen Untersuchung wurde die dritte Fraktion (Schmp. 193—194°) herangezogen.

$C_{14}H_{15}NO_3S_2$ (309,4) Ber. C 54,3; H 4,9; O 15,5; S 20,7%
Gef. C 54,6; H 4,8; O 15,5; S 20,2%.

Charakteristische Banden des IR-Spektrums (KBr-Tablette): ν_{OH}: 2400—3300 cm^{-1}; ν_{SO_2} (asymm.): 1300 cm^{-1}; ν_{SO_2} (symm.): 1145 cm^{-1}; ν_{SNS}: 950 cm^{-1}.

Methyl-(4-benzyloxy-phenyl)-sulfid

Eine gerührte Lösung von 7 g (0,05 *M*) Methyl-(4-hydroxy-phenyl)-sulfid und 7 g (0,055 *M*) Benzylchlorid in 50 ml absol. Aceton wurde nach Zusatz von 13,8 g (0,1 *M*) frisch geglühtem Kaliumcarbonat und 0,5 g Kaliumjodid 20 Stunden rückfließend gekocht, dann abfiltriert und das ungelöste Salz mit 30 ml Aceton nachgewaschen. Nach Eindampfen des Filtrats blieb ein gelblicher fester Rückstand (11,2 g) zurück, dessen Lösung in 100 ml Benzol in zwei Ansätzen mit insgesamt 100 ml 5%iger Natronlauge ausgeschüttelt und nachher über Magnesiumsulfat getrocknet wurde. Durch Abdampfen des Lösungsmittels ließ sich ein gelbliches Kristallprodukt (9,5 g) gewinnen, das nach einmaligem Umlösen aus 40 ml Alkohol (Tierkohle) 7,1 g (62% d.Th.) schneeweiße, blättrige Kristalle vom Schmp. 82—83° lieferte. Literaturangabe [18]: Schmp. 78—79,5°.

$C_{14}H_{14}OS$ (230,3) Ber. S 13,9% Gef. S 14,1%.

Charakteristische Banden des IR-Spektrums (KBr-Tablette): γ_{CH}(1,4-Disubstitution): 813 cm^{-1}; die für monosubstituierte aromatische Ringe charakteristischen Banden: 695, 748 cm^{-1}.

S-Methyl-S-(4-benzyloxy-phenyl)-N-p-tolylsulfonyl-sulfilimin (IIIb)

In je 75 ml eines 4 : 1 Dioxan-Wasser Gemisches wurden 5 g (0,022 *M*) Methyl-(4-benzyloxy-phenyl)-sulfid, ferner 6,2 g (0,022 *M*) Chloramin-T gelöst, die beiden Lösungen vereinigt und nachher 2 Stunden am Wasserbade erwärmt. Nach dem Eindampfen des Reaktionsgemisches blieb ein weißes Kristallprodukt zurück, das in 350 ml Äthylacetat gelöst wurde. Die mit 100 ml 5%iger Natronlauge, nachher mit Wasser gewaschene und schließlich getrocknete ($MgSO_4$) Lösung hinterließ nach dem Eindampfen 7,7 g eines Rohproduktes, das nach einmaligem Umlösen aus 25 ml Alkohol 6 g (68% d.Th.) des analysenreinen Sulfilimins **IIIb** lieferte. Schmp. 124—125°.

$C_{21}H_{21}NO_3S_2$ (399,5)	Ber.	C 63,1;	H 5,3;	N 3,5;	S 16,1%
	Gef.	C 62,8;	H 5,6;	N 3,6;	S 15,9%.

Charakteristische Banden des IR-Spektrums (KBr-Tablette): ν_{SO_2} (asymm.): 1278 cm^{-1}; ν_{SO_2} (symm.): 1138 cm^{-1}; ν_{SNS}: 958 cm^{-1}; γ_{CH} (1,4-Disubstitution): 815 cm^{-1}; die für monosubstituierte aromatische Ringe charakteristischen Banden: 704, 756 cm^{-1}.

Katalytische Hydrierung des S-Methyl-S-(4-benzyloxy-phenyl)-N-p-tolylsulfonyl-sulfilimins (IIIb)

Eine Lösung von 0,4 g (1 *mM*) des Sulfilimins **IIIb** in 20 ml Dimethylformamid wurde in Gegenwart von 0,2 g 10%iger Pd-Tierkohle hydriert. Die Wasserstoffaufnahme, die in 30 Minuten beendet war, betrug 24,4 ml (760 mm, 24 °C), d.h. 1 *mM*. Das bei Unterdruck eingedampfte Filtrat lieferte einen aus Alkohol in weißen Blättchen (0,1 g) kristallisierenden Rückstand. Das Produkt, das bei 82° schmolz, erwies sich als Methyl-(4-benzyloxy-phenyl)-sulfid. Identifizierung: Schmp. und Misch-Schmp., ferner IR-Spektrum.

Reaktion des S-Methyl-S-(4-benzyloxy-phenyl)-N-p-tolylsulfonyl-sulfilimins (IIIb) mit einer Lösung von Bromwasserstoff in Eisessig

Eine Lösung von 1 g (2,5 *mM*) des Sulfilimins **IIIb** in 20 ml Eisessig wurde mit 7 ml 3,1 Gew.%igen Bromwasserstoff-Eisessig (2,7 *mM* HBr) versetzt. Die Lösung färbte sich allmählich gelblichbraun, wobei ein Kristallprodukt ausgeschieden wurde, das sich als Methyl-(4-benzyloxy-phenyl)-sulfid erwies. Identifizierung: Schmp. und Misch-Schmp., ferner IR-Spektrum.

Reaktion des S-Methyl-S-(4-benzyloxy-phenyl)-N-p-tolylsulfonyl-sulfilimins (IIIb) mit einer Lösung von Bromwasserstoff in Essigsäureanhydrid

Eine Lösung von 1,15 g (2,9 *mM*) des Sulfilimins **IIIb** in 7 ml 11,3 Gew.%igem Bromwasserstoff-Essigsäureanhydrid (9,8 *mM* HBr) wurde einige Tage stehen gelassen, wobei das anfangs ausgeschiedene rötliche Kristallprodukt wieder in Lösung ging. Das nach dem Eindampfen der Lösung gewonnene Produkt ließ sich aus 3 ml absol. Benzol umkristallisieren. Das farblose Kristallprodukt (0,4 g) erwies sich nach seinem Schmp. von 137—139° und IR-Spektrum als N-Acetyl-*p*-toluolsulfonamid [19]. Eine Mischprobe mit p-Toluolsulfonamid zeigte eine erhebliche Schmp.-Depression.

Charakteristische Banden des IR-Spektrums (KBr-Tablette): ν_{NH}: 3295 cm^{-1}; ν_{CO}: 1725 cm^{-1}; ν_{SO_2} (asymm.): 1335 cm^{-1}; ν_{SO_2} (symm.): 1168 cm^{-1}.

S-Methyl-S-(3-hydroxy-phenyl)-N-p-tolylsulfonyl-sulfilimin (IV)

Eine Lösung von 2 g (14,3 *mM*) Methyl-(3-hydroxy-phenyl)-sulfid ([10], vgl. [20, 21]) in einem Gemisch von 25 ml Dioxan und 8 ml Wasser wurde nach Zusatz einer Lösung von 4 g (14,3 *mM*) Chloramin-T in 30 ml Dioxan und 10 ml Wasser am Wasserbade 2 Stunden erwärmt, nachher bei Unterdruck eingedampft. Der ölige Rückstand erstarrte nach einigem Stehen. Das so gewonnene Kristallgut, das am Filter mit 5%iger Natronlauge und hierauf

mit Wasser gewaschen wurde, wog nach dem Trocknen im Vakuumexsiccator 3,6 g (65% d.Th.). Das Rohprodukt lieferte aus sehr verdünntem, etwa 10%igem Alkohol umgelöst (Tierkohle) 2 g eines Kristallproduktes vom Schmp. 155—156°. Durch wiederholtes Umlösen aus Alkohol ließ sich der Schmp. von 158° erreichen.

$C_{14}H_{15}NO_3S_2$ (309,4)	Ber.	C 54,3;	H 4,9;	N 4,5;	S 20,7%
	Gef.	C 54,1;	H 5,2;	N 4,5;	S 20,0%.

Charakteristische Banden des IR-Spektrums (KBr-Tablette): ν_{OH}: 2400—3300 cm^{-1}; ν_{SO_2} (asymm.): 1290 cm^{-1}; ν_{SO_2} (symm.): 1143 cm^{-1}; ν_{SNS}: 950 cm^{-1}.

Aciditätsmessungen

Die in Tabelle I angegebenen Dissoziationskonstanten wurden in 48 Vol.% Äthanol enthaltendem, wäßrigem Äthanol nach der Methode von SZMANT und SULD [7] bestimmt. Zur Bereitung des Lösungsmittels wurde durch Kochen vom gelösten Kohlendioxyd befreites destilliertes Wasser angewendet, ferner Alkohol (95,6%), der vorerst 10 Stunden mit Kaliumhydroxyd gekocht, dann durch Anwendung einer Kolonne destilliert wurde. Als Meßlösung diente aus *Sörensenscher* Lauge bereitete, 48 Vol.% Alkohol enthaltende 0,02n Natronlauge. Die Einwaage betrug ungefähr 10^{-4} Mol Sulfilimin; dieses wurde in Alkohol gelöst, dann die Lösung mit der nötigen Menge Wasser versetzt. Die Bestimmungen wurden bei 25 $\pm$0,2° durchgeführt, wobei man einen Stickstoffstrom durch die Lösung streichen ließ. Die Titrierungen wurden unter Anwendung des pH Meßgeräts *Radelkisz OP* 204 durchgeführt. Vor jeder Bestimmung wurde das Meßgerät mit Standardpufferlösungen von pH 4,01, 6,99 und 9,15 geeicht.

Die Dissoziationskonstanten wurden einerseits aus den Titrierungskurven graphisch ermittelt, andererseits aus den bei 20-, 40- und 60%iger Neutralisierung gefundenen pH-Werten berechnet; im letzteren Fall wurde der Durchschnitt der drei berechneten pK_a-Werte als pK_a-Wert angenommen; (von den so berechneten Durchschnittswerten, die in der Tabelle I verzeichnet sind, weichen die drei berechneten pK_a-Werte um $\pm$0,03 ab). Die auf zwei verschiedenen Arten ermittelten pK_a-Werte zeigen eine sehr gute Übereinstimmung. Da das S-Methyl-S-(3-hydroxy-phenyl)-N-*p*-tolylsulfonyl-sulfilimin (**IV**) eine sehr schwache Säure ist, konnte der Endpunkt der Titrierung nur ungenau festgestellt werden. Deshalb ließ sich in diesem Fall die graphische Methode nicht anwenden.

*

Wir danken Herrn Prof. V. BRUCKNER für die Anregung dieser Arbeit.

Die Mikroanalysen wurden in unserem Institut von Frau H. SCHWEIGER, Frau J. KAJTÁR und Frau S. KUTASSY durchgeführt, wofür wir auch an dieser Stelle bestens danken.

ZUSAMMENFASSUNG

Es wurden die Dissoziationsexponenten einiger Sulfilimine vom Typ $XC_6H_4S(CH_3)NTs$ (X = *p*-COOH, *m*-COOH, *p*-OH und *m*-OH) bestimmt und aus diesen die *Hammettschen* Konstanten der Gruppe $CH_3S^{IV}NTs$ berechnet. Die Werte σ_p: +0,70, σ_m: +0,65, σ'_p: +1,00 und σ'_m: +0,80 zeigen, daß die $CH_3S^{IV}NTs$ Gruppe einen starken Akzeptorcharakter hat und in dieser Beziehung der CH_3SO_2 Gruppe mehr ähnelt als der CH_3SO Gruppe. Dies dürfte als eine Folge der verhältnismäßig starken positiven Polarität des S^{IV} Schwefelatoms der Sulfilimine betrachtet werden.

LITERATUR

1. KUCSMAN, Á., RUFF, F., KAPOVITS, I.: Tetrahedron **22,** 1575 (1966)
2. KUCSMAN, Á., RUFF, F., KAPOVITS, I., FISCHER, J. G.: Tetrahedron **22,** 1873 (1966)
3. KUCSMAN, Á., KAPOVITS, I., RUFF, F.: Acta Chim. Acad. Sci. Hung. **54,** 153 (1967)
4. KUCSMAN, Á., RUFF, F., KAPOVITS, I.: Acta Chim. Acad. Sci. Hung. **50,** 325 (1967)
5. KÁLMÁN, A.: Acta Cryst. **22,** 501 (1967)
6. KUCSMAN, Á., KÁLMÁN, A., KAPOVITS, I.: Acta Chim. Acad. Sci. Hung. **53,** 97 (1967)
7. SZMANT, H. H., SULD, G.: J. Am. Chem. Soc. **78,** 3400 (1956)

8. SCHWARZENBACH, G., RUDIN, E.: Helv. Chim. Acta **22,** 360 (1939)
9. BORDWELL, F. G., COOPER, G. D.: J. Am. Chem. Soc. **74,** 1058 (1952)
10. BORDWELL, F. G., BOUTAN, P. J.: J. Am. Chem. Soc. **79,** 717 (1957)
11. STAAB, H. A.: Einführung in die theoretische organische Chemie. Verlag Chemie, Weinheim, 1959. S. 584—585.
12. KUCSMAN, Á., KAPOVITS, I., TANÁCS, B.: Tetrahedron **18,** 79 (1964)
13. KATZ, L., KARGER, L. S., SCHROEDER, W., COHEN, M. S.: J. Org. Chem. **18,** 1380 (1953)
14. KUCSMAN, Á.: Kandidatsarbeit, S. 125, Budapest, 1965.
15. CLARKE, S. G., KENYON, J., PHILLIPS, H.: J. Chem. Soc. **1927,** 193
16. GOETHALS, E., RADZITZKY, P. DE: Bull. Soc. Chim. Belges **73,** 546 (1964)
17. ZINCKE, T., EBEL, C.: Ber. **47,** 1100 (1914)
18. REIFSCHNEIDER, W.: Chem. Abstr. **60,** 13 189 (1964)
19. LOGEMANN, W., ARTINI, D., TOSOLINI, G., PICCININI, F.: Chem. Ber. **91,** 951 (1958)
20. NATELSON, S., GOTTFRIED, S. P.: J. Am. Chem. Soc. **61,** 1001 (1939)
21. BLACKBURN, S., CHALLENGER, F.: J. Chem. Soc. **1938,** 1872

Árpád KUCSMAN
Ferenc RUFF
Sándor SÓLYOM
Tamás SZIRTES

Budapest VIII., Múzeum-krt 4/b.

Acta Chimica Academiae Scientiarum Hungaricae Tomus 57 (2), pp. 213—217 (1968)

BENZAZEPINES, III*

PREPARATION OF 1H,-2,3-DIHYDRO-6,7-BENZO[1,5]-DIAZEPINES AND THEIR REDUCTION TO 1H,-2,3,4,5-TETRAHYDRO-6,7-BENZO-[1,5]-DIAZEPINES

K. HIDEG and O. H. HANKOVSZKY

(Institute of Pharmacology, University Medical School, Pécs)

Received October 17, 1967

In previous publications of this series [1, 2] a new method has been reported for the synthesis of 2,3-dihydro-6,7-benzo-[1,5]-thiazepines. Now this method has been extended to diazepines.

When *o*-phenylenediamine or its ring-substituted derivatives are refluxed with a salt of β-aminoketones (readily prepared from alicyclic or arylalkyl ketones by MANNICH reaction) in some organic solvent, *e.g.* alcohols, benzene, toluene, xylene, etc., the following β-elimination-addition and condensation reactions take place:

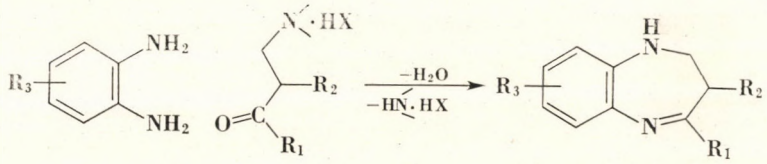

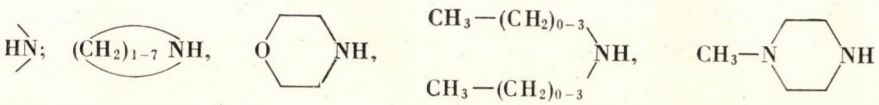

HX; HCl, HBr.

The meaning of substituents R_1, R_2 and R_3 are given in the Tables.

A secondary amine salt and water are formed in the reaction as by-products. If some apolar solvent is applied, and the water formed in the reaction

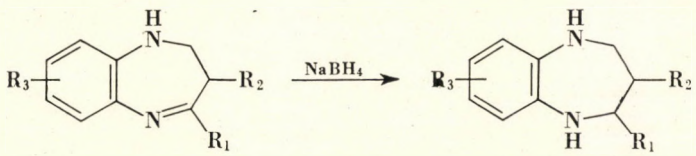

is continuously removed by azeotropic distillation (also removing the secondary amine salt), the progress of the reaction can be followed.

* Part II: Acta Chim. Acad. Sci. Hung. **56**, 405 (1968)

Table 1

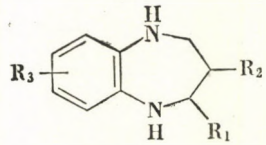

No.	R_1	R_2	R_3	Yield %	M. p., °C or B. p., °C/mm	Formula (Molecular weight)	Analyses, %		
							C	H	N
							Calcd./Found		
1		H	H	60	42—43	$C_{15}H_{14}N_2$ (222.30)	81.04 80.90	6.35 6.45	12.61 12.33
2		H	7(8)Cl	48	45—46 250—253/0.2	$C_{15}H_{13}ClN_2$ (256.75)	70.17 70.11	5.10 5.25	10.92 10.80
3	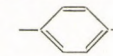	CH_3	H	76	36—39	$C_{17}H_{18}N_2$ (250.35)	81.56 81.78	7.25 7.40	11.19 10.98
4	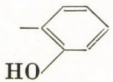	H	H	90	119—120	$C_{15}H_{13}N_2O$ (238.29)	75.61 75.70	5.92 6.11	11.76 11.50
5	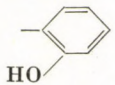	H	$7.8(CH_3)_2$	87	134—136	$C_{17}H_{18}N_2O$ (266.34)	76.67 76.97	6.81 6.78	10.52 10.71
6	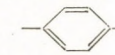	H	$7.8(CH_3)_2$	92	173—174	$C_{18}H_{20}N_2O$ (280.37)	77.11 77.14	7.19 7.42	9.99 9.87

Continued **Table I**

No.	R_1	R_2	R_3	Yield %	M. p., °C or B. p., °C/mm	Formula (Molecular weight)	Analyses, %		
							C	H	N
							Calcd./Found		
7	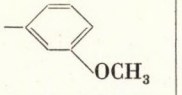	H	7.8(CH_3)$_2$	65	47—48	$C_{18}H_{20}N_2O$ (280.37)	77.11 76.90	7.19 7.32	9.99 9.62
8	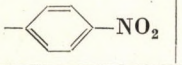	H	7.8(CH_3)$_2$	28	279—282	$C_{17}H_{17}N_3O_2$.HCl (331.80)	61.54 61.48	5.46 5.23	12.67 12.63
9	—CH_2—CH_2—CH_2—CH_2—		H	69	40—44	$C_{13}H_{16}N_2$ (200.29)	77.96 77.86	8.05 8.13	13.99 13.75
10	—CH_2—CH_2—CH_2—CH_2—		7(8)CH_3	75	175/0.15 222—225	$C_{14}H_{18}N_2$ (214.31) $C_{14}H_{18}N_2$.HCl (250.77)	78.47 78.29 67.06 67.12	8.46 8.28 7.63 7.67	13.07 13.17 11.17 11.37
11	—CH_2—CH_2—CH_2—CH_2—		7.8(CH_3)$_2$	68	53—54	$C_{15}H_{20}N_2$ (228.34)	78.90 78.70	8.83 8.62	12.27 12.57

Acta Chim. Acad. Sci. Hung. 57, 1968

Table II

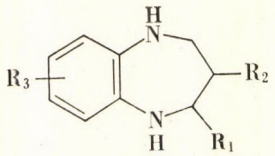

No.	R_1	R_2	R_3	Yield %	M. p., °C or B. p., °C/mm	Formula (Molecular weight)	Analyses, %		
							C	H	N
							Calcd./Found		
12	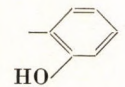	H	7.8(CH_3)$_2$	85	128—129	$C_{17}H_{20}N_2O$ (268.36)	76.09 75.84	7.51 7.44	10.44 10.60
13	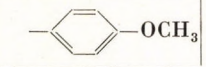	H	7.8(CH_3)$_2$	70	127—128	$C_{18}H_{22}N_2O$ (282.39)	76.56 76.76	7.85 7.80	9.92 10.09
14	—CH_2—CH_2—CH_2—CH_2—		7.(8)CH_3	65	160/0.1	$C_{14}H_{20}N_2$ (216.33)	77.73 77.77	9.32 9.52	12.95 12.80

The C = N bond of the dihydro derivative is slightly basic; a salt is obtained with hydrochloric acid in alcoholic medium.

The C = N double bond can be reduced with sodium borohydride in alcoholic solution to obtain the tetrahydro derivative in high yields.

The reduction is accompanied by vanishing of the yellow colour of the dihydro derivative, together with the higher wave length maximum in the UV spectrum.

The compounds prepared are listed in Tables I and II.

Experimental

1H,-2,3-Dihydro-4-(4'-methoxyphenyl)-6,7-benzo-(7,8-dimethyl)-[1,5]-diazepine (No. 6)

A suspension of 13.4 g (0.1 mole) of 4.5-dimethyl o-phenylenediamide and 28.3 g (0.1 mole) of β-piperidino-p-methoxypropiophenone hydrochloride in 100 ml of xylene were refluxed for 2 hrs. in an apparatus equipped with a MARCUSSON water separatory adapter. During this period 1.8 ml (0.1 mole) of water collected in the adapter. The reaction mixture was filtered still hot to separate piperidine hydrochloride (12 g). On cooling, the filtrate deposited orange crystals (92%). Recrystallization from xylene gave a product of m.p. 173—4°.

EtOH c, $0.5 \cdot 10^4$ mole
λ_{max} (log ε) mμ 276 (3.01), 360 (2.58).

1H,-2,3,4,5-Tetrahydro-4-(4'-methoxyphenyl)-6,7-benzo-(7,8-dimethyl)-[1,5]-diazepine (No. 13)

28.0 g (0.1 mole) of 1H,-2,3-dihydro-4-(4'-methoxyphenyl)-6,7-benzo-(7,8-dimethyl)-[1,5]-diazepine (No. 6) was dissolved in 250 ml of abs. EtOH, 12 g of sodium borohydride was added, and the mixture refluxed for 3 hrs. The complex was decomposed by the addition of water, the alcohol was removed by distillation, and the residue extracted three times with 50 ml of chloroform each. The organic extracts were combined, dried over anhydrous Na_2SO_4 and filtered. The solvent was evaporated and the residue crystallized from 70% EtOH to yield 85% product, m.p. 127—8°.

EtOH c, $0.5 \cdot 10^{-4}$ mole
λ_{max} (log ε) mμ 284 (2.24), 302 (2.32).

The authors express their thanks to Mrs. M. OTT and Miss T. HUSZÁR for the microanalyses and for technical assistance.

SUMMARY

The new method for the synthesis of benzthiazepines described in our earlier publications has been extended to benzdiazepines. *o*-Phenylenediamine or its ring-substituted derivatives were reacted with β-aminoketone salts; an amine salt and water were eliminated and substituted 1H,-2,3-dihydro-6,7-benzo-[1,5]-diazepines were obtained. The 4,5—C=N group was reduced with sodium borohydride to obtain the corresponding 1H,-2,3,4,5-tetrahydro-6,7-benzo-[1,5]-diazepines in high yields.

REFERENCES

1. HIDEG, K., HANKOVSZKY, H. O.: Acta Chim. Acad. Sci. Hung. **50,** 403 (1966)
2. HIDEG, K., HANKOVSZKY, H. O.: Acta Chim. Acad. Sci. Hung. **56,** 405 (1968)

Kálmán HIDEG
Olga H.-HANKOVSZKY } Pécs, Rákóczi út 2.

Acta Chimica Academiae Scientiarum Hungaricae Tomus 57 (2), pp. 219—223 (1968)

BENZAZOLES, VI*

O-ALKYLATION OF 2-(HYDROXYPHENYL)- AND 2-(HYDROXY-BENZYL) BENZAZOLES

O. H. HANKOVSZKY and K. HIDEG

(Institute of Pharmacology, University Medical School, Pécs)

Received October 17, 1967

In an earlier publication (Part III**) of this series, the alkylation of the imino group of benzimidazoles by means of alkyl halides or halogen acetamides, respectively, was reported.

In the present paper, we report that 2-hydroxy-phenyl or 2-hydroxy-benzyl-substituted benzimidazoles are selectively alkylated at the phenolic hydroxyl group on treatment with an equivalent amount of halogen alkylamines or halogen acetamide.

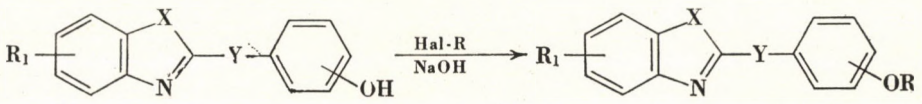

Evidently, 2-(hydroxyphenyl)benzoxazole and benzthiazole can be O-alkylated in this way.

The fact that in the case of benzimidazole the NH group has remained intact during the alkylation reaction is clearly demonstrated by the appearance of a stretching vibration band in the infrared spectrum of the alkylated derivative at 2.9—3.0 μ, indicating the presence of an NH group, as well as by intense bands at 9.2—9.4 μ characteristic of aryl-alkyl ethers.

Biological activity

Biogical tests revealed the physiological activity of these derivatives. Some characteristics of the relationship between chemical constitution and pharmacological action are as follows:

1. Particulary the benzimidazole derivatives exhibit selective coronary dilatatory effect.

* Part V.: HANKOVSZKY, H. O., HIDEG, K.: Acta Chim. Acad. Sci. Hung. **53**, 405 (1967)

** HIDEG, K., HANKOVSZKY, H. O.: Acta Chim. Acad. Sci. Hung. **49**, 303 (1966)

Table I

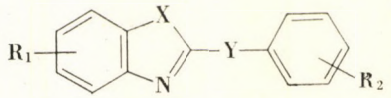

No.	R_1	R_2	X	Y	Yield, %	M. p., °C	Formula (Molecular weight)	Analyses, % C (Calcd./Found)	Analyses, % H (Calcd./Found)	Analyses, % N (Calcd./Found)	*
1	H	4'—OCH_2—	NH	CH_2	70	201—202 207—210	$C_{20}H_{17}N_3O$ (315.38) $C_{20}H_{17}N_3O.2HCl$ (388.31)	76.16 76.34 61.87 61.57	5.43 6.08 4.93 5.12	13.33 13.57 10.82 10.46	
2	H	4'—OCH_2—CH_2—N(CH_2—CH_3)(CH_2—CH_3)	NH	CH_2	78	35—36 197—200	$C_{20}H_{25}N_3O$ (323.44) $C_{20}H_{25}N_3O.2HCl$ (396.37)	74.27 74.50 60.61 60.34	7.79 7.89 6.86 6.78	12.99 12.40 10.60 10.20	
3	H	4'—OCH_2—C(=O)—N(CH_2—CH_3)(CH_2—CH_3)	NH	CH_2	90	130—131 159—161	$C_{20}H_{23}N_3O_2$ (337.43) $C_{20}H_{23}N_3O_2.HCl$ (373.89)	71.20 71.20 64.25 64.27	6.87 6.87 6.47 6.47	12.46 12.47 11.24 11.31	28 130** 28 131
4	H	4'—OCH_2—C(=O)—N($(CH_2)_2$—CH_3)($(CH_2)_2$—CH_3)	NH	CH_2	65	126—128	$C_{22}H_{27}N_3O_2.HCl$ (401.94)	65.75 66.08	7.02 7.00	10.45 10.41	

Continued **Table I**

No.	R_1	R_2	X	Y	Yield, %	M. p., °C	Formula (Molecular weight)	Analyses, % C	Analyses, % H	Analyses, % N	*
								Calcd./Found			
5	H	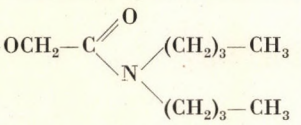	NH	CH_2	70	134—136	$C_{24}H_{31}N_3O_2.HCl$ (430.00)	67.04 67.34	7.50 7.67	9.77 9.56	
6	5(6)Cl	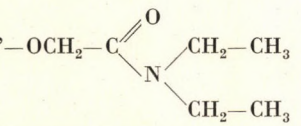	NH	CH_2	75	92—93	$C_{20}H_{22}ClN_3O_2.HCl$ (408.34)	58.83 58.50	5.67 5.47	10.29 9.93	
7	H	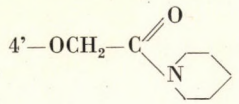	NH	CH_2	52	86—89 195—198	$C_{21}H_{23}N_3O_2$ (349.44) $C_{21}H_{23}N_3O_2.HCl$ (385.90)	71.62 71.32 65.36 65.30	6.31 6.21 6.27 6.65	12.53 12.73 10.89 11.20	
8	H	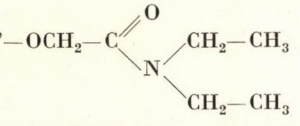	NH	—	74	122—125 204—206	$C_{19}H_{21}N_3O_2$ (323.40) $C_{19}H_{21}N_3O_2.HCl$ (359.87)	70.57 70.26 63.42 62.97	6.54 6.80 6.16 6.10	12.99 13.00 11.68 11.67	28 132 28 133
9	H	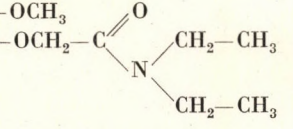	NH	—	90	115—116 179—180	$C_{20}H_{23}N_3O_3$ (353.43) $C_{20}H_{23}N_3O_3.HCl$ (389.89)	67.97 67.89 61.61 61.50	6.56 6.67 6.21 6.32	11.89 11.70 10.78 10.55	

Continued **Table I**

No.	R_1	R_2	X	Y	Yield, %	M. p., °C	Formula (Molecular weight)	Analyses, % C (Calcd./Found)	Analyses, % H (Calcd./Found)	Analyses, % N (Calcd./Found)	*
10	H	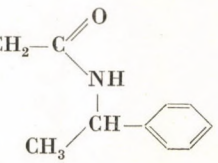	NH	—	72	180—182	$C_{23}H_{21}N_3O_2 . HCl$ (407.91)	67.73 67.85	5.44 5.20	10.30 10.16	
11	H	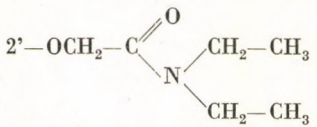	O	—	60	100—102	$C_{19}H_{20}N_2O_3 . HCl$ (360.85)	63.24 63.50	5.86 5.90	7.76 7.80	28 147
12	H	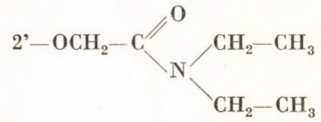	S	—	65	46—49 76—79	$C_{19}H_{20}N_2O_2S$ (340.45) $C_{19}H_{20}N_2O_2S . HCl$ (377.10)	67.04 67.15 60.52 60.70	5.92 6.00 5.61 5.68	8.23 8.33 7.43 7.60	

* *Sadtler Standard Spectra* Collection
** NMR Collection, No. 1832M

2. The effectiveness depends on the position of substituent R_2, position 4' being more favourable than position 2'.

3. The effectiveness also depends on the carboxamide group. In the case of an aliphatic carboxamide the activity is higher than in case of alicyclic amides.

The compounds prepared are summarized in Table I.

The IR and NMR spectroscopical measurements were made by *Sadtler Research Laboratories (Philadelphia)* and the spectra have been published in the proceedings of that *Laboratory (Sadtler Standard Spectra Collection)*, for which the authors wish to express their thanks.

The biological experiments were accomplished in our Institute by Prof. Dr. MÉHES, Prof. Dr. SZEKERES and Dr. PAPP. The results are to be published in detail elsewhere.

The authors thank Mrs. M. OTT and Miss T. HUSZÁR for the microanalyses and for technical assistance.

Experimental

2-[ortho-(2-Benzimidazoyl)phenoxy]-N,N-diethylacetamide (No. 8)

21.0 g (0.1 mole) of 2-(2'-hydroxyphenyl) benzimidazole was dissolved in ethanol (200 ml) and a solution containing 4 g (0.1 mole) of NaOH in about 10 ml of water was added. 14.9 g (0.1 mole) of N,N-diethyl-chloroacetamide was added, and the reaction mixture refluxed for 2 hrs. The NaCl which separated was filtered off and the filtrate concentrated. The residue was crystallized from 50% aqueous EtOH to yield 24.0 g (74%) of the product, m.p. 122—5°.

Hydrochloride. Dry HCl gas was passed into a solution of the base in acetone to precipitate the hydrochloride, which was recrystallized from EtOH, m.p. 204—6°.

SUMMARY

2-(Hydroxyphenyl)- and 2-(hydroxybenzyl) benzazoles (benzimidazole, benzoxazole, benzthiazole) can be O-alkylated in good yields with halogen alkylamines or halogen acetamides. In the case of benzimidazole derivatives alkylation proceeds selectively at the phenolic hydroxyl group. The compounds exhibit coronary dilatory effect.

Kálmán HIDEG
Olga H.-HANKOVSZKY
Pécs, Rákóczi út 2.

Acta Chimica Academiae Scientiarum Hungaricae Tomus 57 (2), pp. 225—240 (1968)

DETERMINATION OF MASS TRANSFER COEFFICIENTS IN THE EXTRACTION OF MEDICINAL PLANTS WITH AN ORGANIC SOLVENT

K. Szász

(Chemical Works of Gedeon Richter Ltd. Budapest)

Received August 8, 1967

The importance of pharmaceuticals of vegetable origin seems to have grown steadily in the last decades. Research in the field of plant chemistry has led to the discovery of a number of remarkable products, *e.g.* hypotensives and sedatives as reserpine and vincamine; carcinostatic agents as vinblastine and vincristine; and starting materials for partial syntheses of steroid hormones, such as diosgenin, solasodine, funtumine, funtumidine, etc.

The extraction of medicinal herbs with organic solvents is a problem which has been little studied. The majority of publications in the field of the extraction of vegetable matter deals with the extraction of sugar from sugar beet [1—6], while a few others are concerned with the production of vegetable fatty oils [7—9]. Because of the specific properties of the materials, the physical-chemical character of these processes markedly differs from the solvent extraction of medicinal herbs; only a few general conclusions can be utilized in the latter case. The cellular tissue of medicinal plants and the chemistry of their active principles are so diverse that the problem of their extraction with any one solvent cannot be treated generally. However, the intensive study of one particular solvent extraction process seemed to be a promising approach, and we hope that we have found by the results of this study some experimental techniques and correlations which can also be used in other cases.

The model we employed was the extraction of the alkaloids of the periwinkle (*Vinca minor* L.) [10], with toluene.

Mass transfer area

The equilibrium distribution, attained by diffusion of the active principle between the extracting solvent and the cell sap, is a function of several factors, such as the mass transfer area, ratio of solvent to solid, agitation, temperature. In this paper we propose to investigate (within the scope of the extraction, with toluene, of the alkaloids of the periwinkle) the role of the mass transfer area alone.

Preparation of a solid with a known ratio of intact and crushed mass transfer areas

When plant material is comminuted, some surfaces will be left intact, while others will be crushed. The extraction of the alkaloids across the surfaces left intact will proceed, by inhibited diffusion, more slowly than the uninhibited diffusion across surfaces consisting of crushed cells. To accelerate the extraction process it would seem the most expedient, to comminute to produce

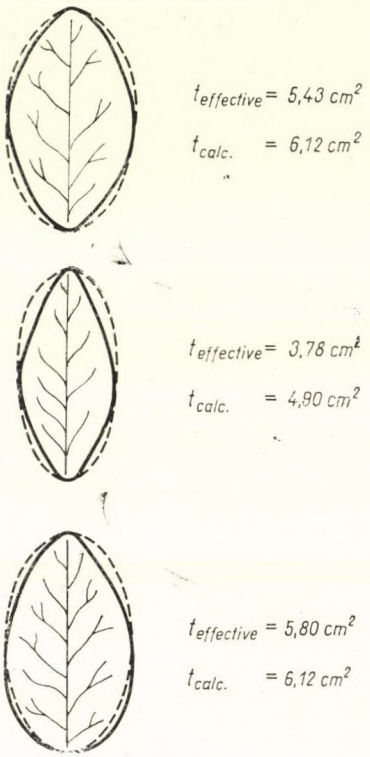

Fig. 1. Leaves of *Vinca minor* L., and the calculation of the surface area

as many fine particles as possible, thus ensuring the greatest possible proportion of crushed mass transfer area. However, in commercial operations this degree of comminution would encounter technological difficulties. Therefore, in our experimental studies of the principles of extraction, we used a comminution method whereby intact and crushed mass transfer areas of various dimensions could be obtained in a known ratio. For this purpose, the leaves of our model plant, periwinkle, proved suitable. The shape, size and smoothness of the surface of these leaves made the preparation of particles of known dimensions possible. These leaves are from 1.5 to 2.0 cm across, and from 3.0 to 5.0 cm long.

Intact leaves can be considered those with undamaged cell walls where in extraction mass transfer proceeds entirely by inhibited diffusion. Mention must be made of the fact that in order to simplify the picture, in all our experiments we assumed the top and the underside of the leaves to be equivalent from the point of view of mass transfer, though these two sides are different anatomically. (This experimental material is marked No. 0.)

Suitable length and breadth of the leaves allow regular square parallelepipeds to be cut out of them. If the thickness of the leaf is measured, the area of the four sides of the parallelepipeds can also be calculated; this area represents the crushed area, whereas the upper and lower planes of the parallelepipeds, *i.e.* the intact original exterior of the leaves, is the *surface formed by undamaged cells.*

Thus solid bodies are obtained for which the ratio of the mass transfer areas furnished by crushed and by undamaged cells can be calculated according to simple rules of geometry. Accordingly, square parallelepipeds measuring 1.00 by 1.00, or 0.50 by 0.50, or 0.25 by 0.25 cm were cut from the leaf blades. (This experimental material was marked No. 1, No. 2, and No. 3.)

Finally, from the same stock of leaves, experimental material was prepared by colloidal *milling*; this gave mainly crushed, mechanically opened cells (coarse and fine powder, marked No. 4 and No. 5).

Experimental extractions and their mathematical evaluation

With the experimental materials Nos 0 to 5, simple extractions were carried out under uniform standard conditions, and for each of the materials the alkaloid concentration of the extract as a function of time was determined.

When intact leaves are extracted, the quantity of alkaloids found in the extract is considered to be obtained entirely by inhibited diffusion. If the total surface area of the batches of intact leaves used is measured and calculated, the quantity of alkaloids extracted can be referred to unit mass transfer areas that consist of undamaged cells. Of course, from the same quantity of a *comminuted* solid substance, a greater quantity of the alkaloids is transferred into the solution during the same time. With *regularly comminuted* batches, the mass transfer area supplied by the undamaged cells being known, the quantity of alkaloids extracted across the crushed mass transfer surface area can be readily calculated. In our experiments we were careful that the well defined particles obtained in the preparatory operations of cutting or milling should not be further disintegrated; to prevent this, a so-called "stationary system" of extraction was adopted, *i.e.* the extracting solvent, toluene, was circulated through the loosely packed particles. In this case the material balance of the process can be written as follows:

$$-dx = f \cdot dy \tag{1}$$

where dx is the concentration change in the solid of the substance to be extracted (μg of the active principle per g of "cells"), dy is the concentration change in the extract of the substance to be extracted (μg of active substance per g of toluene extract), and f is the liquid ratio (g of toluene extract per g of "cells").

The expression "cells", in this context, indicates the insoluble dry matter of the leaves plus the solvent retained by it, the total quantity of the so-called "swell liquor" or "artificial cell liquor".

In the case of finite changes, Eq. (1) takes the form:

$$x = x_0 - f(y - y_0) \tag{2}$$

Based on FICK's First Law, mass transfer can be represented by

$$\frac{dx}{di} = - A \Phi (x - y) \tag{3}$$

where di is the time of extraction, A is a proportionality factor, and Φ is the mass transfer area of one unit mass of solids.

From Eq. (1) and Eq. (3) it follows that

$$-f\frac{dy}{di} = - A \Phi (x - y)$$

Substituting Eq. (2), when $y_0 = 0$, for x in this equation, separating the variables, after integration, and arranging the terms, we get

$$\frac{y_\infty - y}{y_\infty} = e \left(\text{exp.} - A \Phi \frac{f+1}{f} i \right) \tag{4}$$

In this equation y_∞ is the equilibrium concentration of the extract, determined by the correlation $\frac{x_0}{f+1} = y_\infty$; y is the actual concentration of the extract at time i; A is the proportionality factor; Φ is the mass transfer area of one unit mass of solids; and f denotes the liquid ratio.

Using common logarithms, Eq. (4) takes the following form:

$$\log \frac{y_\infty - y}{y_\infty} = - A \Phi \frac{f+1}{2 \cdot 3 f} i \tag{5}$$

If y changes as a function of time, and its values are known from experiments, the values of the term $\log \frac{y_\infty - y}{y_\infty}$ plotted as a function of time give a straight

line, when $A\Phi\frac{f\pm 1}{2\cdot 3f}$ is constant, this being the slope of the straight line so plotted.

In Eq. (5), y can be determined experimentally, and the values f, Φ, and y_∞ can be calculated from experimental data, respectively. The mass transfer coefficient A can then be calculated with the data thus obtained.

It is to be noted that the application of FICK's First Law for a diffusion process is allowed if we assume that the concentrations x and y are invariant to space co-ordinates, *i. e.* if the diffusion process is thought to be confined to the boundary layer (film) formed at the contact surface of drug extract; further if it is assumed that a convective equalization, which has a rate by several orders of magnitude higher than the diffusion process, is taking place in the cell liquor as well as in the fluid extract. If these conditions do not hold, then, strictly, FICK's Second Law only is applicable. In our experiments the assumption holds only for y: the recirculation of the extractive fluid assures the spatial equalization of concentration y by convection within the extractor. Our simplifying assumption cannot thus be maintained for concentration x within the cells. The independence of this value from the spatial co-ordinates cannot be assured by convection. Therefore, our following discussions have only an approximate character; we start with the assumption that the difference between uninhibited and inhibited diffusions is high enough to manifest itself clearly in the shape of the curves even when this simplified calculation is used.

An exact discussion of the problem, on the basis of FICK's Second Law will be given in a further communication.

Experimental

A sufficient quantity of experimental material, consisting of leaf blades only, had been harvested from one place and dried in a current of air.

In preliminary experiments we found that in order to achieve measurable effects, not less than 1.5 g of the air-dried drug had to be taken for one extraction experiment. To be able to calculate the specific mass transfer area, the surface area of a 1.5 g batch of intact leaves must be determined.

From a mass of leaves of apparently of the same size, 1.5 batches were weighed with 0.01 g accuracy, then the number of leaves in each batch was counted.

Table I

Number of leaf blades in a batch weighing 1.5 g

Number of leaves
49
51
48
47
50
Average 49 leaves

The average form of periwinkle leaves is nearly elliptic (Fig. 1). Therefore, to calculate the surface area of the two sides of the leaves in a 1.5 g batch, the formula $T = 2\,a.b.\pi$ for the area of an ellipse was used. For such a batch of intact leaves 460 cm² was found as the mass transfer area. However, since the outline of the leaves is not an exact ellipse, this method of calculation needs some correction. A number of leaves, selected to correspond as far as possible to the average form of leaves, was divided into two groups, one for most elliptical leaves, and one for leaves with the greatest deviations from an ellipse. The surface areas of these were then

(a) calculated on the basis of ellipses of the best fit (t_s) and

(b) measured with a planimeter (t_t).

In this way we found that the calculated area was somewhat greater than that actually measured, but the two values were not too different, so that the calculated area multiplied by a correction factor gave the actual value.

The applicability of the correction factor was checked as follows. From 1 cm pieces cut out of the leaves in the way described below, a batch of 1.5 g was found to have 191 pieces. The sum total of the surface area of the upper and lower surfaces is, of course, $2 \cdot 191 = 382$ cm², whereas the calculated area corrected by the factor mentioned above was 460.0.824 = 379 cm²; the error is less than 1%.

Table II

Determination of the correction factor to the calculated area of leaf surface

No.	Leaf surface area, mm²		t_t/t_s
	Calcd. (t_s)	Found (t_t)	
1	684	521	0.762
2	500	479	0.958
3	766	643	0.840
4	706	531	0.752
5	566	458	0.810
(Average) correction factor			0.824

Preparation of solid particles with intact and crushed mass transfer areas in known proportion

Three hollow steel punches were made, each with a square cutting edge of 1 cm, 0.5 cm and 0.25 cm, respectively, per side, so that with these 1.00 × 1.00, 0.50 × 0.50, and 0.25 × × 0.25 cm squares could be cut out of the leaves to furnish experimental material Nos 1, 2, and 3.

In order to be able to calculate the area of the sides of the parallelepipeds cut out of the leaves, the thickness of the leave blades was measured with a pair of micrometer callipers. The arithmetic mean of 150 such measurements gave 0.0136 cm as the height of the paralellepipeds. The probable error,

$$\sigma = \sqrt{\frac{\Sigma(d^2)}{n-1}}$$

(where σ = limes, d = deviation of a single measurement from the average value, n = number of measurements) was found to fall within $\pm 15\%$; thus the height h of the parallelepipeds was 0.0136 ± 0.0020 cm, or approximately $h = 0.014$ cm. A 1.5 g batch of the square parallelepipeds has a mass transfer area of 380 cm² of intact cells, and its mass transfer area r of crushed cells can be calculated by a simple geometrical operation using height $h = 0.014$ cm. Thus r (in cm²) $= 4.l.h$; expressed as per cents,

$$r_x = \frac{2h}{1+2h}\,100\,.$$

Besides the samples with a mass transfer area given by intact cells only (whole leaves, sample No. 0), and the samples with a known proportion of mass transfer area given by crushed cells (samples No. 1, 2, and 3), samples of *coarse powder*, from comminution in a hammer mill (sample No. 4) and samples of *fine powder* prepared with the help of a high speed rotary blade (coffee) mill (sample No. 5) were also subjected to extraction experiments. Thus the samples of solids prepared were the following:

Table III

Solid particles, with intact and crushed mass transfer surface areas of definite ratio

No.	Particle size	Percentage intact surface area $(100 - r_x)$	Percentage crushed surface area (r_x)
0	Intact leaves	100	—
1	1.00 by 1.00 cm	97.3	2.7
2	0.50 by 0.50 cm	94.7	5.3
3	0.25 by 0.25 cm	90.0	10.0
4	Coarse powder	81.3*	18.7*
5	Fine powder	22.0*	78.0*

*The surface area ratios for coarse and fine powders result from the slopes of the respective velocity curves.

Determination of the alkaloid contents of the solid substance

The alkaloid contents of the samples were determined by our method developed earlier [11].

Finely comminuted leaf powder (3 g) is kneaded with a 10% solution of ammonia (3 ml). The wet mass is extracted with benzene (first 20 ml, then twice with 10 ml). The filtered extracts are combined and made up with benzene to 100 ml.

A 20-ml aliquot of this stock solution is shaken with a 2% solution of sulphuric acid (three times 10 ml portions). The filtered acid extracts are combined, and from this a 20-ml aliquot is taken and made alkaline ($p_H 8$) with a solution of sodium hydroxide. The alkaline mixture is shaken with chloroform (4 times 5 ml portions). The chloroform extracts are filtered through anhydrous sodium sulphate, and combined. To 10 ml of the solution in chloroform, 5 ml of glacial acetic acid is added, and this mixture is titrated with a 0.01 *N* solution of perchloric acid in glacial acetic acid and carbon tetrachloride, in the presence of Crystal Violet indicator. One ml of the reagent is equivalent to 3.544 mg alkaloid, expressed as vincamine.

If the quantity of the alkaloids to be expected was less than 100 μg especially in cases of extractions of short duration, the determinations were carried out colorimetrically according to our amphi-indicator method [12]. In this case the organic solvent extract (in benzene or in toluene) is shaken with sulphuric acid (2% solution); amphi-indicator is added to an aliquot portion of the sulphuric acid solution, and this aqueous acidic mixture that contains the alkaloids and the indicator, is extracted with chloroform; finally the separated chloroform phase is tested colorimetrically.

According to the titrimetric, or amphi-indicator method described above, the overall alkaloid content of the leaf mass used as the starting material in all our experiments was determined in repeated tests. The deviation between the mean values obtained by titration and colorimetry was less than 5%; thus the mean of these was accepted as the alkaloid content, expressed as vincamine. Accordingly,

$$x_0 = 2250 \frac{\mu g}{g}$$

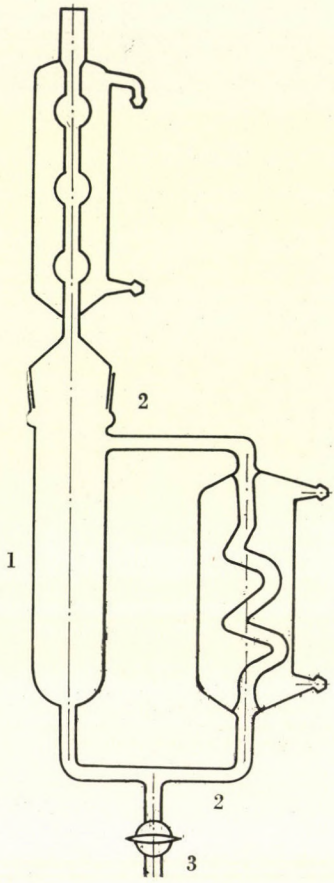

Fig. 2. Solid/liquid recirculation extractor

Alkaline digestion without crushing of the solid particles

The decomposition of the natural salts of the alkaloids, in order to obtain the bases which are soluble in organic solvents, cannot be achieved by a "kneading" with alkali of the vegetable substance, because this would further disintegrate the particles in an uncontrollable degree, and so the determination of the mass transfer area would become impossible.

The best way found for digestion without mechanical treatment is keeping the mass to be extracted in a closed space saturated with ammonia and water vapour, for a fixed time.

Some 25% aqueous ammonia solution is placed into the lower receptacle of a desiccator. The weighed mass of the solid to be extracted is distributed over the grid above and the desiccator is closed hermetically

Before using this method, the effectiveness of the digestion by water vapour saturated with ammonia had to be assessed. The knowledge of the conditions applicable to the decomposition of alkaloid salts in whole intact leaves is especially important. For this purpose, one part of a mass of leaves was finely powdered. The alkaloid content of a portion of this powder was determined in the way described above. Another portion of the whole leaves was placed into the ammonia atmosphere. The alkaloid content of this second part of the leaves was determined after exposure to the action of the ammoniacal atmosphere for 0.5, 1.0 and 2.0 hrs., respectively. With a powdered sample the effect of such an ammoniacal treatment for 0.5 to 1.0 hr. gave the same result as the kneading treatment.

Weighed batches of intact, whole leaves were kept in ammonia atmosphere from 1 to 10 hrs. It was found that full digestion could be achieved within 5 hrs. even when intact leaves were treated in this way. Accordingly, in every extraction test the alkaline digestion of the sample was carried out by keeping it for 5 hrs. in water vapour saturated with ammonia.

Extraction without crushing the solid particles

In order to accelerate the tests, and to keep the value of y independent of spatial coordinates, the method of mixing must be such that during the process of extraction no crushing of the particles of given size should occur owing to mechanical or hydrodynamical effects. For this purpose an apparatus was designed (*cf.* Fig. 2) wherein the continuous exchange of the cell fluid and feed fluid respectively the continuous mixing was realized by convective recirculation, produced by differences of density brought about by a thermal gradient.

The parts of the apparatus are:

(a) extraction chamber
(b) convector
(c) extract drain tap.

The extraction chamber (1) is made to accommodate a 35 mm o. d. Soxhlet tube. At top and bottom the extraction chamber is connected to a jacketed spiral tube, the convector (2). Water at a temperature higher than ambient is circulated in the jacket. This water warms the solvent in the spiral tube, and this part of the solvent rises and flows into the extraction chamber. At the same time, naturally, fresh solvent is sucked into the spiral tube at its lower end. Of course, enough solvent should be present in the system to flood the chamber above the level where the upper end of the spiral is connected. Thus the solvent is allowed to circulate freely in the system, and the leaf mass of a given particle size filled into the Soxhlet tube in a matrix of an indifferent material, *e.g.* glass beads, is extracted without being disintegrated.

For each test a 1.5 g portion of the leaf mass was used, weighed to 0.01 g accuracy. Digestion was achieved by keeping this sample for 5 hrs. in an atmosphere of water vapour saturated with ammonia. The digested mass was transferred into the Soxhlet tube, where it was embedded among glass beads, so that its particles were freely accessible to the circulating liquid phase. After the Soxhlet tube had been placed into the extraction chamber, the system was filled with the same amount of toluene (200 g) in each test. The convector was heated by circulating water of 45°, from a thermostat. Heating was started prior to filling in the solvent, in order to start convection in the same way in each test as soon as the liquid level reached the upper inflow aperture of the extraction chamber.

Determination of the mass of the extract (E) and raffinate (R), and of the concentration of the extracts

In the case of each particle size (samples No. 0 to No. 5) repeated extraction tests were carried out, in the apparatus described for 0.167, 0.5, 1.0 3.0 and 5.0 hrs., using air-dry batches of 1.5 g each, previously exposed to an ammonia atmosphere for 5 hrs., with a 200-g portion of toluene as the solvent. After extraction, the extract was drained from the apparatus. On the average, 196 g extract ($E = 196$) was recovered.

In order to determine the amount of raffinate, 1.5 g portions from the air-dry samples were weighed to 0.01 g accuracy. These were kept for 5 hrs. in the ammonia atmosphere as described above, placed into toluene (100 g), and allowed to soak there for several hours. The solid part was then collected on a filter of known weight, and weighed rapidly. In this way the weight was found of the 1.5 g batches of leaf mass with the toluene retained in them (*cf.* Table IV).

(The original air-dry material contained about 6 to 10% moisture; during exposure to the ammonia atmosphere this increased by 3% only. Thus, when 1.5 g of air-dry solid is taken, about 1.4 g is the vegetable substance M, and about 0.15 g is its moisture content after treatment. At 37.8°C, toluene dissolves 0.076% (w/w) of water; thus 200 g of toluene is just enough to keep the above amount of water in solution.)

Table IV

Total weight of 1.5 g solid matter and the liquid phase retained by it (raffinate R)

Particle size	Weight of raffinate g
1.00 by 1.00 cm	3.60
	4.05
	3.82
0.50 by 0.50 cm	3.75
	4.00
	4.05
0.25 by 0.25 cm	3.90
	3.90
Coarse powder	4.35
	4.13
Fine powder	4.13
Average	$3.97 \simeq 4 = R$

The probable error of one measurement is 5.2%.

Note. In our calculations the term raffinate R does not mean only the so-called "artificial cell liquor" (a little water and mainly toluene; about 4.0 — 1.4 = 2.6 g) but the sum $R = 4.0$ g of the vegetable substance ($M = 1.4$ g) plus the cell liquor ($S = 2.6$ g) Accordingly, the liquid ratio is defined here, instead of the usual expression $f = \frac{E}{S}$, by $f = \frac{E}{S + M}$ the apparent liquid ratio.

The alkaloid concentration μg/ml of the extracts obtained in the way described was determined by the methods discussed. In Table V the mean values of repeatedly determined alkaloid concentrations, are summarized which express the extraction velocities. (Every figure in this Table is the average of five parallel measurements; the deviation of these is $\pm 5\%$.)

Table V

Extraction velocity as a function of the ratio of intact to crushed mass transfer areas
Alkaloid concentration of the extract in μg/ml

Particle size	0.167 hr.	0.5 hr.	1 hr.	3 hrs.	5 hrs.
Intact leaves	—	—	3.0	8.0	12.0
1.00 by 1.00 cm	—	4.0	7.2	11.6	15.4
0.50 by 0.50 cm	—	6.2	11.0	15.6	19.1
0.25 by 0.25 cm	3.6	10.3	13.2	17.3	20.3
Coarse powder	6.4	15.4	18.6	21.4	24.0
Fine powder	20.3	26.3	29.7	34.5	36.0

Note. No measurable amount of alkaloids was extracted during 0.167 hrs. from intact leaves (1.00 by 1.00 cm, and 0.50 by 0.50 cm size parallelepipeds), and during 0.5 hr. from intact leaves.

Interpretation of the experimental results

Mathematical formulation of the extraction across a given mass transfer surface area

From the experiments, we have the following values:

$$x_0 = 2250\ \mu g \left(\frac{\mu g}{g \text{ of air-dry drug}} \right)$$

$$f = \frac{E}{R} = \frac{196}{4} = 49$$

$$y = \frac{x_0}{f+1} = 45\ \mu g \left(\frac{\mu g}{g \text{ of extract}} \right)$$

When, on the basis of the experimental y values listed in Table V, the values of the term $\log \frac{y_\infty - y}{y_\infty}$ are calculated, the data shown in Table VI are obtained.

Table VI

The values of the term $\frac{y_\infty - y}{y_\infty}$ *for solids of various particle size*

Particle size	0.167 hr.	0.5 hr.	1 hr.	3 hrs.	5 hrs.
Intact leaves	—	—	—0.028	—0 084	—0.135
1.00 by 1.00 cm	—	—0.040	—0.075	—0.120	—0.180
0.50 by 0.50 cm	—	—0.065	—0.120	—0.184	—0.240
0.25 by 0.25 cm	—0.036	—0.112	—0.150	—0.210	—0.260
Coarse powder	—0.066	—0.180	—0.232	—0.280	—0.330
Fine powder	—0.260	—0.380	—0.468	—0.638	—0.700

See Note to Table V.

When these are plotted as a function of time (Fig. 3) a straight line presents itself only in the case of test with intact whole leaves.

The slope m_0 of this line is

$$\operatorname{tg} \alpha_0 = m_0 = 0.028$$

Therefore, in Eq. (5) the coefficient of i is constant and equal to the slope of the straight line:

$$m_0 = -A\Phi \frac{f+1}{2 \cdot 3f} = -0.028$$

where

$$\frac{f+1}{2 \cdot 3f} = 0.443,$$

consequently

$$m_0 = -A \Phi 0.443 \tag{6}$$

Since $\Phi = \frac{F}{R}$ and $F = 380$ cm², and $R=4$, the unit mass transfer surface area Φ in the case of intact leaves is

$$\Phi = \frac{380}{4} = 95 \frac{\text{cm}^2}{g}$$

From Eq. (6) it follows that

$$A_0 = 6.68 \cdot 10^{-4} \frac{g}{\text{cm}^2 \text{ hour}}$$

In this way the mass transfer coefficient is expressed numerically, as a quantity of alkaloid, and as a function of time and surface area of intact periwinkle leaves.

Relation between the extraction velocity and the ratio of intact to crushed mass transfer areas

In the case of comminuted solids the mass transfer area F is the sum of the intact surface area a and the crushed surface area r:

$$F = a + r \tag{7}$$

From the diagram in Fig. 3 it is to be seen that, in the course of the extraction, after the lapse of time i, where zero time is one hour, the mass transfer coefficient will become equal to that found for intact leaves ($A_0 = 6.68 \cdot 10^{-4}$ g/cm² hour), because the curves that represent the extraction velocities will turn after a certain time i, about one hour, into straight lines of the same slope that characterizes the line of the extraction process of intact leaves. This indicates that, in samples which also have crushed surfaces, diffusion across these surfaces is completed in the initial period, and from then on extraction proceeds across the surface formed by intact cells.

The value of slope m in the interval between time 0 and time i varies according to the proportion of the crushed surface area. The values of these slopes can be calculated with the help of graphs in Fig. 3, from the curvatures that correspond to the initial period of the extraction process (from data given

for that period). In this way the values shown in Table VII are obtained, where

$$r_x = \frac{r}{a + r} .$$

Since in every case of regular comminution $a = 380$ cm^2,

$$r_x = \frac{r}{380 + r} ;$$

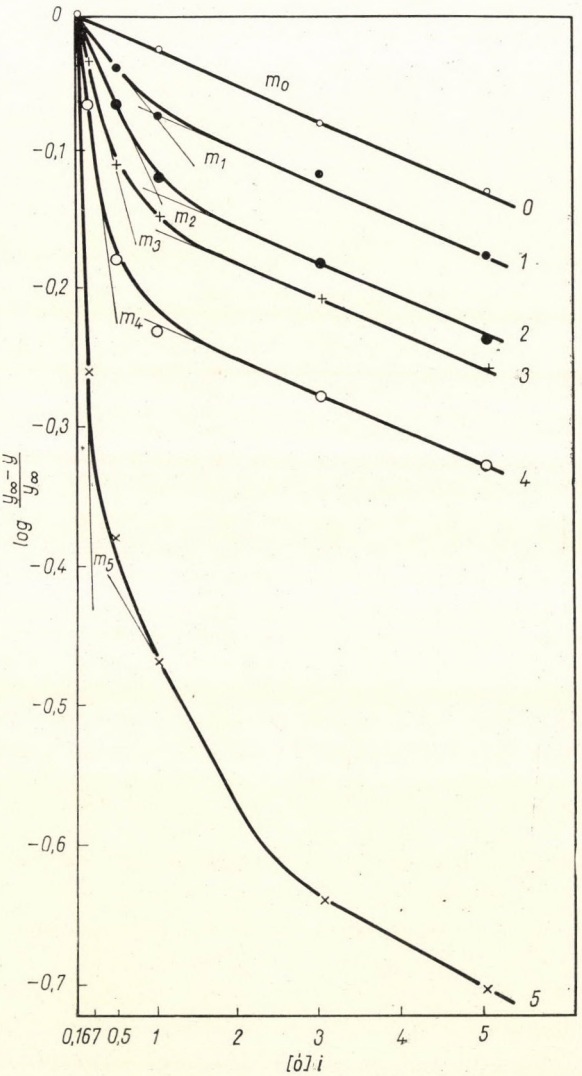

Fig. 3. Extraction velocities for various particles of a drug — 0 = Intact leaves — 1 = 1.0 by 1.0 cm — 2 = 0.5 by 0.5 cm — 3 = 0.25 by 0.25 cm — 4 = Coarse powder — 5 = Fine powder

from this

$$r = \frac{380 r_x}{1 - r_x}$$

Substituting this in Eq. (7), the mass transfer area can be written as

$$f = 380 + \frac{380 r_x}{1 - r_x}$$

and the specific mass transfer area is calculated as follows:

$$\Phi = \frac{F}{R} = \frac{380 + \dfrac{380 r_x}{1 - r_x}}{4}$$

Table VII

Variation of the slope m of the extraction curves as a function of the proportion of crushed mass transfer area

Particle size	r_x (ratio of crushed area)	Slope, m
Intact leaves	0	−0.028 0 to 1 hr.
1.00 by 1.00 cm	0.027	−0.080 0 to 0.5 hr.
0.50 by 0.50 cm	0.053	−0.130 0 to 0.5 hr.
0.25 by 0.25 cm	0.100	−0.216 0 to 0.167 hr.
Coarse powder	0.187*	−0.395 0 to 0.167 hr.
Fine powder	0.780*	−1.560 0 to 0.167 hr.

* The ratios of the crushed mass transfer areas of the coarse and fine powders are calculated values (see later on).

From this, we get:

$$\Phi = \frac{95}{1 - r_x} \tag{8}$$

On the other hand, when the values of Table VII, *i.e.* the slopes of the extraction curves, are plotted as a function of the ratios of crushed mass transfer area, the straight line shown in Fig. 4 will result,

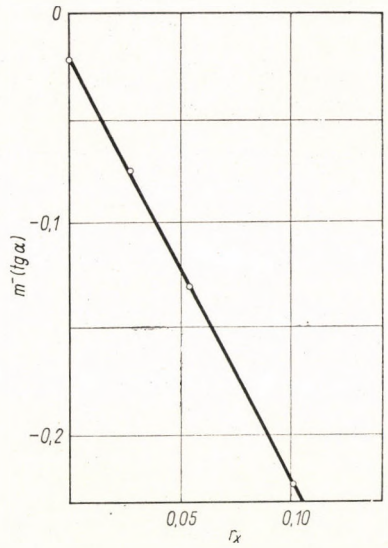

Fig. 4. Slopes of the extraction velocity curves as a function of the ratio of crushed surface area

of which the equation will be:

$$m = 1.96 r_x - 0.028 \tag{9}$$

wherefrom

$$r_x = -0.51\ \mathrm{m} - 1.43 \cdot 10^{-2} \tag{10}$$

In this manner the proportion of the crushed mass transfer area is correlated to the slope of the extraction curve. On this basis — using the slopes calculated from curves that characterize the extraction of both coarse and fine irregular particles obtained by milling — we find that 18.7% of the mass transfer area of our coarse sample, and 78.0% of that of our fine sample, consists of crushed cells.

Calculation of the mass transfer coefficient for comminuted solid matter

Having found a correlation between the proportion of the crushed mass transfer area r_x of our comminuted solid samples and the extraction velocity m, on the basis of Eq. (6) and Eq. (8) we can write:

$$m = -A \frac{95}{1 - r_x} 0.443 \tag{11}$$

On the other hand, from Eq. (10) and Eq. (11) it follows that

$$m = -A \frac{95 \cdot 0.433}{1-(-0.51m - 1.43 \cdot 10^{-2})}$$

and then

$$A = (1.215\, m^2 + 2.41\, m)10^{-2} \qquad (12)$$

From Eq. (12), and using the slopes, m, calculated from the graphs in Fig. 3, the mass transfer coefficient A can be calculated for a solid made up of particles of given size distribution.

When this calculation is made according to Eq. (12), the values listed in Table VIII result for all the samples we have tested.

Table VIII

Mass transfer coefficient of solids of various particle sizes

Particle size	Crushed surface area, %	Slope of the curve $\log \frac{y_\infty - y}{y_\infty}$ (between 0 and 1 hr.)	Mass transfer coefficient $\frac{g}{cm^2 \cdot hr.}$
Intact leaves	0	$m_0 = -0.028$	$A_0 = 6.65 \cdot 10^{-4}$
1.00 by 1.00 cm	2.7	$m_1 = -0.081$	$A_1 = 18.7 \cdot 10^{-4}$
0.50 by 0.50 cm	5.3	$m_2 = -0.129$	$A_2 = 29.1 \cdot 10^{-4}$
0.25 by 0.25 cm	10.0	$m_3 = -0.224$	$A_3 = 41.9 \cdot 10^{-4}$
Coarse powder	18.7	$m_4 = -0.395$	$A_4 = 76.1 \cdot 10^{-4}$
Fine powder	78.0	$m_5 = -1.560$	$A_5 = 80.4 \cdot 10^{-4}$

SUMMARY

An experimental method has been devised for the measurement of the diffusion of the active principle (the alkaloids) of periwinkle (*Vinca minor* L.) leaves when extracted with toluene. In the course of these experiments comminution was carried out so that intact (natural) and crushed mass transfer areas resulted in a known ratio. In this way the mass transfer coefficients both for inhibited and uninhibited diffusion have been determined. It has been found that there is a difference of an order of magnitude between the velocities of these two types of diffusion. This difference is also shown in the time graphs plotted on the basis of FICK's First Law. Further, it has been found that in the extraction of solid particles, where the mass transfer area also includes crushed surfaces, uninhibited diffusion is complete within a specified time, and then the extraction velocity is determined by inhibited diffusion across surfaces composed of intact cells. From the correlation between the extraction velocity and the ratio of intact to crushed mass transfer areas, it is possible to calculate this ratio, and the mass transfer coefficient, for irregularly comminuted particles, *e.g.* for such obtained by milling.

Kálmán Szász; Budapest X., Gyömrői út 19/21.

INDEX

PHYSICAL CHEMISTRY — PHYSIKALISCHE CHEMIE — ФИЗИЧЕСКАЯ ХИМИЯ

SZŐKE, S. and BAITZ, E.: The Potential Energy Functions of Diatomic Molecules (Halides and Hydrides of the Groups Ia and IIa) 129

TÖRÖK, F.: On the Parameter Form of Force Constant Matrix, VI. On the Common Force Constant Matrices of Isotopic Molecules 141

Чордаш Л.: Программирование для ЭВМ типа «Урал-2» для рентгеноструктурного анализа I. Суммирование двухмерных рядов Фурье 147

BÁN, M. und CSÁSZÁR, J.: Untersuchung der Elektronenanregungsvorgänge und der Bindungsverhältnisse der Komplexe von $3d^n$ Elementen mit der Ligandenfeldmethode, III. Monoacido-, trans-Diacido- und cis-Diacido-Kobalt(III)- und Chrom(III)-Komplexe 153

ORGANIC CHEMISTRY — ORGANISCHE CHEMIE — ОРГАНИЧЕСКАЯ ХИМИЯ

WAGNER, H., SELIGMANN, O., HÖRHAMMER, L., NÓGRÁDI, M., FARKAS, L., STRELISKY, J. and VERMES, B.: Investigations on the Keto-Enol Tautomerism of O-Hydroxy-Dibenzoylmethanes by Nuclear Magnetic Resonance 169

LEMPERT-SRÉTER, M. and BÁRDY, M.: 1,5-Diketones, IV. Synthesis of Some New Isobenzopyrylium Anhydrobases 181

DOLESCHALL, G., HORNYÁK, Gy., LÁNG, L., LEMPERT, K. and ZAUER, K.: 1,2,4-Triazines and Condensed Derivatives, VI. Synthesis of 6-methyl-7*H*-thiazolo [3,2-b] [1,2,4] thiazine-3 (2*H*)-dione and 2-methyl-6,7-dihydro-3*H*, 8*H*-[1,3] thiazino [3,2-b] [1,2,4] triazine-3,8-dione 191

KUCSMAN, Á., RUFF, F. SÓLYOM, S. und SZIRTES, T.: Bindungssystem der N-Acyl-sulfilimine, VI. Konjugativer Effekt der S-Methyl-N-p-tolylsulfonyl-sulfilimingruppe 205

HIDEG, K. and HANKOVSZKY, O. H.: Benzazepines, III. Preparation of 1H,-2,3-Dihydro-6, 7-Benzo [1,5]-Diazepines and their Reduction to 1H,-2,3,4,5-Tetrahydro-6, 7-Benzo-[1,5] Diazepines 213

HANKOVSZKY, O. H. and HIDEG, K.: Benzazoles, VI. O-Alkylation of 2-(Hydroxyphenyl)- and 2-(Hydroxy-Benzyl) Benzazoles 219

CHEMICAL TECHNOLOGY — CHEMISCHE TECHNOLOGIE — ХИМИЧЕСКАЯ ТЕХНОЛОГИЯ

SZÁSZ, K.: Determination of Mass Transfer Coefficients in the Extraction of Medicinal Plants with an Organic Solvent 225

Printed in Hungary

A kiadásért felel az Akadémiai Kiadó igazgatója — Műszaki szerkesztő: Farkas Sándor

A kézirat nyomdába érkezett: 1968. V. 14. — Terjedelem: 10 (A/5) ív, 33 ábra

68.65638 Akadémiai Nyomda, Budapest — Felelős vezető: Bernát György

ACTA CHIMICA

ТОМ 57 — ВЫП. 2

РЕЗЮМЕ

Функция потенциальной энергии для двухатомных молекул

(Гидридные и галоидные соединения элементов групп Ia и IIa.)

Ш. СЁКЕ и Э. БАЙТЦ

Для молекул щелочных и щелочноземельных металлов были определены значения величин $d=k_e r_e (e_1 e_2 D_e)^{1/2}$ применяемых в расчетах потенциальной энергии. Были определены и значения a и ab параметров Леннард-Джонса, которые в пределах средних отклонений 4,6 и 3,9% можно считать постоянными в отдельных типах связи. Было доказано то предположение, что параметр b является постоянным независимо от типа связи. Проводилось сравнение между функциями потенциальной энергии с различными основными принципами и было установлено, что выражения типа Липпинкотта приводят к результатам удовлетворительной точности и в ионной области.

Параметрическое построение матрицы F силовых постоянных, VI. Свойства общей матрицы силовых постоянных молекул одинаковой симметрии с различными изотопными заместителями

Ф. ТЁРЁК

Доказывается, что те F матрицы, которые одновременно удовлетворяют двум вековым уравнениям n-измерений для молекул одинаковой симметрии с изотопными заместителями, являются функциями $\binom{n}{2}$ числа параметров. Приводится система уравнений для определения независимо изменяющихся параметров. Приводимая зависимость позволяет рассчитать общие F матрицы, относящиеся к систематически изменяемым величинам независимо изменяющихся параметров, а также определить крайние значения элементов общих F матриц.

Обсуждение процессов электронного возбуждения и характера связей в комплексах металлов с электронной структурой $3d^n$ с помощью метода лигандного поля, III. Моноацидо-, транс-диацидо- и цис-диацидо-комплексы кобальта (III) и хрома(III)

М. БАН и Й. ЧАСАР

Авторами описывается метод расчета параметров лигандного поля, связанных с процессами электронного возбуждения и с электронными спектрами поглощения, для моноацидо-пентамин-, транс- и цис-диацидо-тетрамин-комплексов Co^{3+} и Cr^{3+}. На основе вычисленных значений Dg, B, β, δ % делаются заключения о характере связей в молекуле комплекса.

Исследование кето-энольной таутомерии о-гидрокси-дибензоилметанов с помощью метода ЯМР

Х. ВАГНЕР, О. ЗЕЛИГМАНН, Л. ХЁРХАММЕР, М. НОГРАДИ, Л. ФАРКАШ, Й. ШТРЕЛИСКИЙ и Б. ВЕРМЕШ

Кето-энольная таутомерия о-гидрокси-дибензоил-метанов изучалась с помощью ЯМР, ИК- и УФ-спектроскопии. В растворе они присутствуют в виде равновесной смеси кетонных и энольных таутомеров. Существование таутомера типа 2-гидрокси-флавона не удалось обнаружить.

1,5-Дикетоны, IV. Получение новых ангидро-оснований изобензпирилия

М. ЛЕМПЕРТ-ШРЕТЕР и М. БАРДИ

Было доказано таутомерное строение ранее полученного ангидро-основания изобензпирилия, а именно *о*(6)-ангидро-1(3-метокси-4-гидроксифенил)-4-метил-4-этил-6,7-дигидрокси-изобензпирилиюм гидроксида (IIa). Соединение (IIa) этилировалось до ангидро-1-(3-метокси-4-этоксифенил)-3-метил-4-этил-6-гидрокси-7-этокси-изобензпирилиюм гидроксида (VIIIa). Подобно IIa был получен *о*(6)-ангидро-1-(4-метоксифенил-3-метил-4-этил-6,7-дигидрокси-изобензпирилиюм гидроксида (IIc), строение которого подтверждалось химическими и спекстроскопическими методами. С помощью острожной нейтрализации изобензпирилиевой соли, содержащей свободный фенольный гидроксил в положении 6 (IIIe), был получен *о*(6)-ангидро-1-(3-метокси-4-гидроксифенил)-3-метил-4-этил-6-гидрокси-7-метокси-1*H*-изобензпирилиюм гидроксида (VIIIc). Изобензпирилиевые ангидро-основнаяи VIIIa и VIIIc — в противоположность их аналогам IIa и IIc — претерпевают глубокие изменения с размыканием гетероцикла под действием щелочи.

1,2,4-Триазины и их конденсированные производные, VI. Синтез 6-метил-7H-тиазоло[3,2-в] [1,2,4]гриазин-3(2H), 7-диона и 2-метил-6-,7-дигидро-3H,8H-[1,3]тиазино[3,2-в]-[1,2,4]гриазин-3,8-диона

Г. ДОЛЕШАЛ, ДЬ. ХОРНЯК, Л. ЛАНГ, К. ЛЕМПЕРТ и К. ЗАУЭР

С помощью замыкания кольца были получены 6-метил-7*H*-тиазоло[3,2-b] [1,2,4 триазин-3(2*H*),7-дион (5) и 2-метил-6,7-дигидро-3*H*,8*H*-[1,3]тиазино[3,2-b] [1,2,4]-триазин-3,8-дион (8) из 3-(карбоксиметил-тио)-6-метил- и 3-(2-карбоксиэтил-тио)-6-метил-1,2,4-триазин-5(2*H*)-онов (**4a** и **d**). Строение полученных соединений подтверждалось на основе их ультрафиолетовых и инфракрасных спектров.

Соединение **5** было получено также с помощью замыкания кольца из 2-имино-3-(1-карбоксиэтилиден-амино)-4-тиазолидинона (**14c**). В связи с этим вновь исследовалось строение соединений, получаемых в реакции тиосемикарбазонов с производными галогеноуксусной кислоты или с ангидридом малеиновой кислоты. Полагалось, что в этих реакциях образуются не соединения типа 2,4-тиазолидин-дион-2-гидразона (**15**), но производные 2-имино-3-амино-4-тиазолидинона (**14**).

Система связей N-ацил-сульфилиминов, VI. Эффект сопряжения S-метил-N-п-толилсульфонил-сульфилиминовой группы

А. КУЧМАН, Ф. РУФФ, Ш. ШОЙОМ и Т. СИРТЕШ

Были определены диссоциационные экспоненты нескольких соединений типа $XC_6H_4S(CH_3)NTs$ (где X = *п*-COOH, *м*-COOH, *п*-OH, *м*-OH) и на основе этого также Гаммета конста нты σ группы $CH_3S^{IV}NTs$. Полученные значения ($\sigma_п = +0{,}70$, $\sigma_M = +0{,}65$, $б'_п + 1{,}00$, $б'_M + 0{,}80$) показывают, что группа $CH_3S^{IV}NTs$ является сильным акцептором, и что по ее поведению она стоит ближе к группе CH_3SO_2, чем к группе CH_3SO. Это, вероятно, связано с относительно сильной положительной поляризованностью атома серы S^{IV} в сульфилиминовой группе.

Бензазепины, III. Получение 1H,-2,3-дигидро-6,7-бензо-[1,5] диазепинов и восстановление их до 1H,-2,3,4,5-тетрагидро-6,7-бензо-[1,5] диазепинов

К. ХИДЕГ и О. Х. ХАНКОВСКИЙ

Уже описанный нами ранее метод получения бензтиазепинов распространялся для получения бенздиазепинов. *о*-Фенилендиамин и его производные, замещенные в ядре, подвергались взаимодействию с солями *β*-амино-кетонов; при выделении аминовой соли и воды образуются 1*H*,-2,3-дигидро-6,7-бензо-[1,5]-диазепины. Группа C = N в положении 4,5 восстанавливалась с помощью $NaBH_4$, в результате чего с хорошим выходом получали 1*H*,-2,3,4,5-тетрагидро-6,7-бензо-[1,5]-диазепины.

Бензазолы, VI. Алкилирование по кислороду 2-(гидроксифенил)- и 2-(гидроксибензил) бензазолов

О. Х. ХАНКОВСКИЙ и К. ХИДЕГ

Алкилирование по кислороду 2-(гидроксифенил)- и 2-(гидроксибензил) бензазолов (бензимидазола, бензоксазола, бензтиазола) происходит с хорошим выходом под действием галогенированных алкиламинов и ацетамидов. В случае производных бензимидазола селективно алкилируется только фенольный гидроксил. Соединения обладают, в терапийной степени, расширяющим влиянием на венечную артерию.

Определение коэффициента передачи вещества в экстракции лекарственных растений органическими растворителями

К. САС

Был разработан экспериментальный метод измерения диффузии активного вещества при толуольной экстракции алкалоидов из растения «Vinca minor L.». Применялось такое правильное измельчение, чтобы образовывалось известное отношение невредимой (естественной) к разрушенной поверхности передачи вещества. На основе этого определялся коэффициент передачи вещества при затрудненной и свободной диффузии. Было установлено, что скорости этих двух диффузий различаются по порядку, что проявляется и на диаграммах по времени, построенных на основе интерпретации процесса по 1-ому закону Фика. Также было установлено, что при экстракции материала, обладающего и разрушенной поверхностью, свободная диффузия через некоторое время прекращается, и по истечении этого периода скорость экстракции определяется скоростью диффузии, происходящей через поверхность невредимых клеток.

На основе зависимости скорости экстракции от отношения невредимой к разрушенной поверхности, последняя величина и коэффициент передачи вещества могут быть рассчитаны и для твердых материалов с неровным размельчением — например, для производственного помола.

The Acta Chimica publish papers on chemistry in English, German, French and Russian.

The Acta Chimica appear in volumes consisting of four parts of varying size, 4 volumes being published a year.

Manuscripts should be addressed to

Acta Chimica
Budapest 112/91 Műegyetem

Correspondence with the editors should be sent to the same address.

The rate of subscription is 165 forints a volume. Orders may be placed with "*Kultúra*" Foreign Trade Company for Books and Newspapers (Budapest I., Fő utca 32. Account No. 43-790-057-181) or with representatives abroad.

Les Acta Chimica paraissent en français, allemand, anglais et russe et publient des mémoires du domaine des sciences chimiques.

Les Acta Chimica sont publiés sous forme de fascicules. Quatre fascicules seront réunis en un volume (4 volumes par an).

On est prié d'envoyer les manuscrits destinés à la rédaction à l'adresse suivante:

Acta Chimica
Budapest 112/91 Műegyetem

Toute correspondance doit être envoyée à cette même adresse.

Le prix de l'abonnement est de 165 forints par volume.

On peut s'abonner à l'Entreprise pour le Commerce Extérieur de Livres et Journaux «*Kultúra*» (Budapest I., Fő utca 32. Compte-courant No. 43-790-057-181) ou à l'étranger chez tous les représentants ou dépositaires.

«*Acta Chimica*» издают трактаты из области химической науки на русском, французском, английском и немецком языках.

«*Acta Chimica*» выходят отдельными выпусками разногообъема. 4 выпуска составляют один том. 4 тома публикуются в год.

Предназначенные для публикации рукописи следует направлять по адресу:

Acta Chimica
Budapest 112/91 Műegyetem

По этому же адресу направлять всякую корреспонденцию для редакции.

Подписная цена «*Acta Chimica*» — 165 форинтов за том. Заказы принимает предприятие по внешней торговле книг и газет «*Kultúra*» (Budapest I., Fő utca 32. Текущий счет № 43-790-057-181) или его заграничные представительства и уполномоченные.

44,— Ft

Reviews of the Hungarian Academy of Sciences are obtainable at the following addresses:

ALBANIA

Ndermarja Shtetnore e Botimeve
Tirana

AUSTRALIA

A. Keessing
Box 4886, GPO
Sydney

AUSTRIA

Globus Buchvertrieb
Salzgries 16
Wien I

BELGIUM

Office International de Librairie
30, Avenue Marnix
Bruxelles 5
Du Monde Entier
5, Place St. Jean
Bruxelles

BULGARIA

Raznoiznos
1, Tzar Assen
Sofia

CANADA

Pannonia Books
2. Spadina Road
Toronto 4, Ont.

CHINA

Waiwen Shudian
Peking
P. O. B. 88

CZECHOSLOVAKIA

Artia
Ve Smečkách 30
Praha 2
Poštovná Novinová Služba
Dovoz tisku
Vinohradská 46
Praha 2
Mad'arská Kultura
Václavské nám. 2
Praha I
Poštová Novinová Služba
Dovoz tlače
Leningradská 14
Bratislava

DENMARK

Ejnar Munksgaard
Nörregade 6
Copenhagen

FINLAND

Akateeminen Kirjakauppa
Keskuskatu 2
Helsinki

FRANCE

Office International de Documentation et Librairie
48, rue Gay Lussac
Paris 5

GERMAN DEMOCRATIC REPUBLIC

Deutscher Buch-Export und Import
Leninstraße 16
Leipzig 701
Zeitungsvertriebsamt
Clara Zetkin Straße 62
Berlin N. W.

GERMAN FEDERAL REPUBLIC

Kunst und Wissen
Erich Bieber
Postfach 46
7 Stuttgart S.

GREAT BRITAIN

Collet's Holdings Ltd.
Dennington Estate
London Rd.
Wellingborough, Northants.
Robert Maxwell and Co. Ltd.
Waynflete Bldg. The Plain
Oxford

HOLLAND

Swetz and Zeitlinger
Keizersgracht 471—487
Amsterdam C
Martinus Nijhof
Lange Voorhout 9
The Hague

INDIA

Current Technical Literature
Co. Private Ltd.
India House OPP
GPO Post Box 1374
Bombay I

ITALY

Santo Vanasia
Via M. Macchi 71
Milano
Libreria Commissionaria Sansoni
Via La Marmora 45
Firenze

JAPAN

Nauka Ltd.
92, Ikebukur O-Higashi 1-chome
Toshima-ku
Tokyo
Maruzen and Co. Ltd.
P. O. Box 605
Tokyo-Central
Far Eastern Booksellers
Kanda P. O. Box 72
Tokyo

KOREA

Chulpanmul
Phenjan

NORWAY

Johan Grundt Tanum
Karl Johansgatan 43
Oslo

POLAND

Ruch
ul. Wronia 23
Warszawa

ROUMANIA

Cartimex
Str. Aristide Briand 14—18
Bucureşti

SOVIET UNION

Mezhdunarodnaya Kniga
Moscow G—200

SWEDEN

Almquist and Wiksell
Gamla Brogatan 26
Stockholm

USA

Stechert Hafner Inc.
31, East 10th Street
New York, N. Y. 10003
Walter J. Johnson
111, Fifth Avenue
New York, N. Y. 10003

VIETNAM

Xunhasaba
19, Tran Quoc Toan
Hanoi

YUGOSLAVIA

Forum
Vojvode Mišića broj 1
Novi Sad
Jugoslovenska Knjiga
Terazije 27
Beograd

24. IX. 1968. Index: 26.007

ACTA CHIMICA

ACADEMIAE SCIENTIARUM HUNGARICAE

ADIUVANTIBUS

L. ERDEY, K. POLINSZKY, G. SCHAY

AC

R. BOGNÁR, GY. BRUCKNER, Z. CSŰRÖS, T. ERDEY-GRÚZ, Z. FÖLDI, M. FREUND, Á. GERECS, GY. HARDY, J. HOLLÓ, Á. KISS, M. KORACH, F. MÁRTA, F. NAGY, E. PUNGOR, Z. SZABÓ, P. TÉTÉNYI, L. VARGHA, K. VAS

REDIGIT

B. LENGYEL

TOMUS 57 FASCICULUS 3

AKADÉMIAI KIADÓ, BUDAPEST

1968

ACTA CHIM. ACAD. SCI. HUNG.

ACTA CHIMICA

A MAGYAR TUDOMÁNYOS AKADÉMIA KÉMIAI TUDOMÁNYOK OSZTÁLYÁNAK IDEGEN NYELVŰ KÖZLEMÉNYEI

SZERKESZTI

LENGYEL BÉLA

TECHNIKAI SZERKESZTŐK

DEÁK GYULA és HARASZTHY-PAPP MELINDA

Az Acta Chimica német, angol, francia és orosz nyelven közöl értekezéseket a kémiai tudományok köréből.

Az Acta Chimica változó terjedelmű füzetekben jelenik meg, egy-egy kötet négy füzetből áll. Évente átlag négy kötet jelenik meg.

A közlésre szánt kéziratok a szerkesztőség címére (Budapest 112/91 Műegyetem) küldendők.

Ugyanerre a címre küldendő minden szerkesztőségi levelezés. A szerkesztőség kéziratokat nem ad vissza.

Az Acta Chimica előfizetési ára kötetenként belföldre 120 Ft, külföldre 165 Ft. Megrendelhető a belföld számára az „Akadémiai Kiadó"-nál (Budapest V., Alkotmány utca 21. Bankszámla 05-915-111-46), a külföld számára pedig a „Kultúra" Könyv- és Hírlap Külkereskedelmi Vállalatnál (Budapest I., Fő utca 32. Bankszámla: 43-790-057-181) vagy annak külföldi képviseleteinél és bizományosainál.

Die Acta Chimica veröffentlichen Abhandlungen aus dem Bereiche der chemischen Wissenschaften in deutscher, englischer, französischer und russischer Sprache.

Die Acta Chimica erscheinen in Heften wechselnden Umfanges. Vier Hefte bilden einen Band. Jährlich erscheinen 4 Bände.

Die zur Veröffentlichung bestimmten Manuskripte sind an folgende Adresse zu senden:

Acta Chimica
Budapest 112/91 Műegyetem

An die gleiche Anschrift ist auch jede für die Redaktion bestimmte Korrespondenz zu richten.

Abonnementspreis pro Band: 165 Forint. Bestellbar bei dem Buch- und Zeitungs-Außenhandels-Unternehmen »*Kultúra*« (Budapest I., Fő utca 32. Bankkonto No. 43-790-057-181) oder bei seinen Auslandsvertretungen und Kommissionären.

Acta Chimica Academiae Scientiarum Hungaricae Tomus 57 (3), pp. 241—245 (1968)

MECHANISM OF ADSORPTION INDICATION, III

4-(4'-NITROPHENYLAZO)-1-NAPHTHOL, A NEW ADSORPTION INDICATOR

L. LÉGRÁDI

(Nitrokémia Industrial Plants, Fűzfőgyártelep)

Received May 19, 1967

In previous communications we described a nitron type adsorption indicator prepared by the diazotization of *p*-nitroaniline and subsequent coupling with α-naphthylamine [1], and also an amphoteric adsorption indicator [2] made by the introduction of an additional basic substituent. The present paper describes an adsorption indicator in which the basic amino group is absent, its place being taken by a phenolic hydroxyl group of acid character. The indicator has been prepared by the diazotization of *p*-nitroaniline and subsequent coupling with α-naphthol:

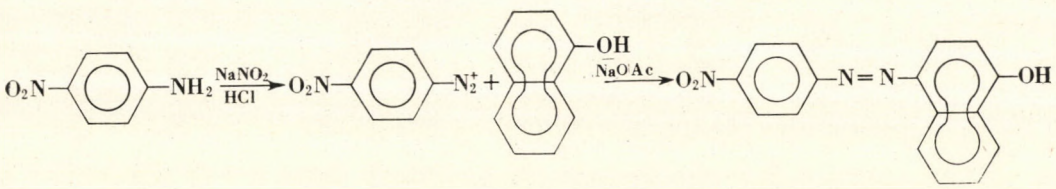

This compound has been found suitable for indicating the end-point in all argentometric titrations, so it may be regarded as universal argentometric indicator.

Experimental

4-(4'-Nitrophenylazo)-1-naphthol is an indicator acid; its acid colour is yellow, its basic colour violet. The colour change occurs in the pH range 9.10—10.2, with $p_i = 9.6$. Fig. 1 shows the adsorption spectrum of the indicator. This indicator was used in argentometric titrations, and the results are shown in Table I. The data represent the means of three measurements. The titrations were made with solutions of 50 ml initial volume to which 0.3 ml of a 0.2% alcoholic solution of the indicator had been added. The solution was adjusted to pH 8—9, as more alkaline pH values result in higher than the correct consumption of the titrant. Reversed titration (the titration of silver ion with a halide ion) may also be carried out, but in this case the alkali should be added to the solution near the end of the titration. The relative error in the titration of anions with 0.1 *N* $AgNO_3$ is $\pm 0.12\%$.

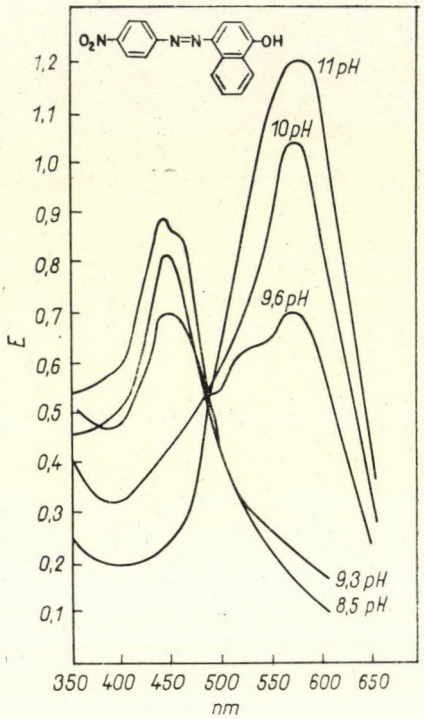

Fig. 1. Absorption spectrum of 4-(4'-nitrophenylazo)-1-naphthol in water

Table I

Titration of anions with silver nitrate in the presence of 4—(4'-nitrophenylazo)-1-naphthol indicator

Ion	$AgNO_3$ standard solution	Medium	Colour change	$AgNO_3$ used, ml Potentiometric titration	With indicator	Difference	
						ml	%
Chloride	0.1 *N*	1 drop 0.1 *N* NaOH	violet-grey to blue	5.06	5.09	0.03	0.6
Bromide	0.01 *N*	2 drops 0.1 *N* NaOH	violet-red to blue	10.20	10.20	0.00	0.0
Iodide	0.01 *N*	2 drops 0.1 *N* NaOH	orange to greenish-blue	10.24	10.27	0.03	0.3
Thiocyanate	0.01 *N*	2 drops 0.1 *N* NaOH	violet-red to blue	9.92	10.00	0.08	0.8
Cyanide	0.1 *N*	2 drops 0.1 *N* NaOH	violet to violet-blue	4.92	4.94	0.02	0.4

The mechanism of indication

The investigation of the adsorption indication mechanism of 4-(4'-nitrophenylazo)-1-naphthol represented an example when the azo-dye contained nitro and phenolic hydroxyl groups only. In order to learn more about the mechanism, the pH was measured during titration, and the changes in the dissociation constant of the dye adsorbate under the influence of an excess of its own ions were assessed.

1. pH changes during titration

To 5 ml of a 0.1 *N* anion solution, 45 ml of water, one drop (or in the case of iodide ion two drops) of 0.1 *N* NaOH solution, and 0.3 ml of a 0.2% alcoholic solution of the indicator were added. The solution was titrated with 0.1 *N* $AgNO_3$. The pH of the solution was continuously measured using glass and calomel electrodes. At the point of equivalence the pH decreased by 0.2—0.5. This change, which indicates the loss of a proton due to the presence of excess silver ions, is similar to the change observed with basic dyes.

Table II

Dye adsorbate as an acid-base indicator adsorptive: 4—(4'-nitrophenylazo)-1-naphthol

Adsorbent	Excess of own ion, equ.	pH Range of colour change	Dissociation constant, K	Colour change
Silver chloride	50% Ag^+	6.4— 8.0	$6.31 \cdot 10^{-8}$	orange to bluish-grey
	10% Ag^+	7.0— 8.6	$1.59 \cdot 10^{-8}$	orange to violet-blue
	equ. point	8.2—10.4	$5.01 \cdot 10^{-10}$	orange to violet-blue
	10% Cl^-	8.6—10.8	$2.00 \cdot 10^{-10}$	orange to blue
	50% Cl^-	8.8—10.8	$1.59 \cdot 10^{-10}$	orange to blue
Silver bromide	50% Ag^+	5.5— 7.7	$2.51 \cdot 10^{-7}$	orange to greyish-blue
	10% Ag^+	6.0— 7.6	$1.59 \cdot 10^{-7}$	orange to greyish-blue
	equ. point	6.8— 9.4	$7.94 \cdot 10^{-9}$	orange to greyish-blue
	10% Br^-	8.8—10.2	$3.16 \cdot 10^{-10}$	orange to violet-blue
	50% Br^-	9.2—10.8	$1.00 \cdot 10^{-10}$	orange to violet-blue
Silver iodide	50% Ag^+	6.2— 8.2	$6.31 \cdot 10^{-8}$	orange to greenish-blue
	10% Ag^+	6.9— 8.7	$1.59 \cdot 10^{-8}$	orange to greenish-blue
	equ. point	9.0—10.5	$2.00 \cdot 10^{-10}$	orange to green
	10% I^-	9.5—11.1	$5.01 \cdot 10^{-11}$	orange to bluish-grey
	50% I^-	9.8—11.4	$2.51 \cdot 10^{-11}$	orange to bluish-grey
Silver thiocyanate	50% Ag^+	7.0— 8.6	$1.59 \cdot 10^{-8}$	orange to bluish-grey
	10% Ag^+	8.4— 9.6	$1.00 \cdot 10^{-9}$	orange to bluish-grey
	equ. point	9.9—11.1	$3.16 \cdot 10^{-11}$	orange to bluish-grey
	10% CSN^-	11.0—12.6	$1.59 \cdot 10^{-12}$	orange to violet
	50% CSN^-	11.6—12.8	$6.31 \cdot 10^{-13}$	orange to violet
Silver cyanide	50% Ag^+	8.0— 9.2	$2.51 \cdot 10^{-9}$	orange to violet
	10% Ag^+	8.1— 9.9	$1.00 \cdot 10^{-9}$	orange to violet-blue
	equ. point	8.8—10.2	$3.16 \cdot 10^{-10}$	orange to violet
	10% CN^-	9.0—10.8	$1.26 \cdot 10^{-10}$	orange to violet-blue
	50% CN^-	9.4—10.8	$7.94 \cdot 10^{-11}$	orange to violet-blue

2. Determination of the change of the dissociation constant of dye adsorbates

The measurements were carried out according to the method described in our previous paper [1], and the experimental results are summed up in Table II. These indicate an increase in the dissociation constant of the dye adsorbate in the presence of cation excess and a decrease in the presence of anion excess, with a jump in the values at the point of equivalence. This behaviour is characteristic of all precipitate indicators which function on the acid-base principle [3]. The colour change occurs on precipitates which carry no charge only in rather alkaline medium; this necessitates adjustment of an alkaline pH before titration.

Discussion

The mechanism of the adsorption indication of 4-(4'-nitrophenylazo)-1--naphthol will be illustrated here using the iodide ion as an example. In the range of the colour change, the solution contains both undissociated and dissociated molecules:

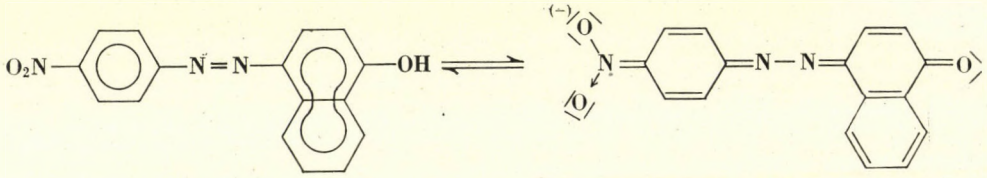

On the addition of silver nitrate to the iodide ion, silver iodide precipitates, and in the presence of an excess of iodide ions the precipitate will adsorb the undissociated indicator, while in the presence of excess silver ion the adsorbed indicator will lose a proton under the action of the positively charged precipitate. This proton loss was experimentally demonstrated. The process is the following:

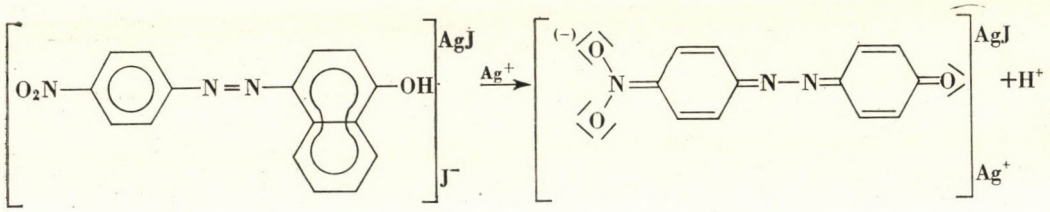

The colour which has turned bluish-green in the presence of silver nitrate, turns again orange when potassium iodide is added. As the medium is alkaline this last change is probably accompanied by a potassium ion uptake:

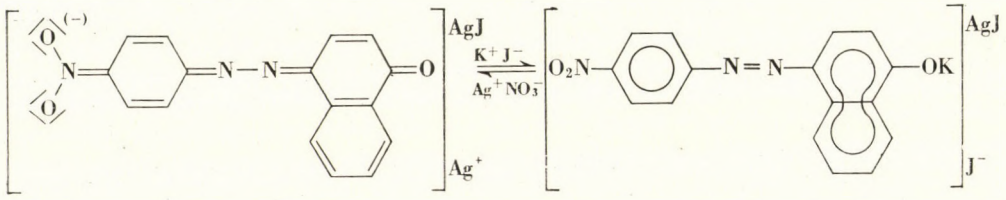

When the iodide ion is titrated in a strongly alkaline medium (at about pH 10), the indicator is completely dissociated in the solution. This dye anion is not adsorbed by the negatively charged precipitate, and adsorption will take place only on the addition of the first drop of excess silver ion. Proton loss is not involved in the adsorption process as the dye has already lost a proton while in solution. The colour change is due to the adsorption of the violet dye anion on the positively charged yellow silver iodide precipitate, giving bluish-green nitronic acid, or to the formation of the silver salt of this acid.

SUMMARY

A universal argentometric indicator, 4-(4'-nitrophenylazo)-1-naphthol, is described which is suitable for the titration of chloride, bromide, iodide, thiocyanate and cyanide ions. Titration should be carried out at pH 9—10. The indicator functions on the acid-base principle, as shown by the changes of the dissociation constant of the dye adsorbate in the presence of an excess of its own ions. The mechanism of indication is discussed in detail.

REFERENCES

1. LÉGRÁDI, L.: Magy. Kém. Foly. **73,** 525 (1967)
2. LÉGRÁDI, L. Magy. Kém. Foly. **74,** 56 (1968)
3. PUNGOR, E., SCHULEK, E.: Z. anal. Chem. **150,** 116 (1956)

László LÉGRÁDI; Füzfőgyártelep. Hungary

Acta Chimica Academiae Scientiarum Hungaricae Tomus 57 (3), pp. 247—255 (1968)

MECHANISM OF ADSORPTION INDICATION, IV

COMBINATION OF THE FAJANS INDICATION WITH THE ACID—BASE PRINCIPLE

L. LÉGRÁDI

(Nitrokémia Industrial Plants, Fűzfőgyártelep)

Received June 19, 1967

In our previous communication [1] was described an adsorption indicator, useful for argentometric titrations, which was obtained by the diazotization of *p*-nitroaniline and subsequent coupling with α-naphthol. In this paper are reported on adsorption indicators which contain a sulphonic acid group in addition to the nitro and phenolic hydroxyl groups. *Ortho-*, *meta-*, and *para*-nitroaniline, and 2, 4- and 3, 5-dinitroaniline were diazotized and coupled with 1-naphthol-4-sulphonic acid to obtain the following indicators:

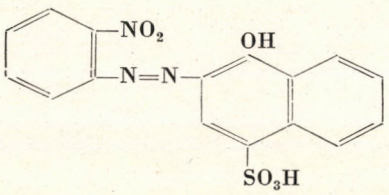

2-(2'-nitrophenylazo)-1-naphthol-4-sulphonic acid

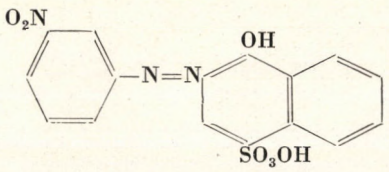

2-(3'-nitrophenylazo)-1-naphthol-4-sulphonic acid

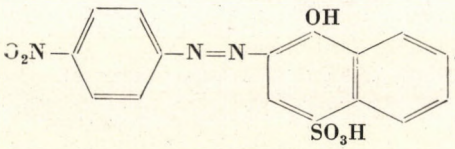

2-(4'-nitrophenylazo)-1-naphthol-4-sulphonic acid

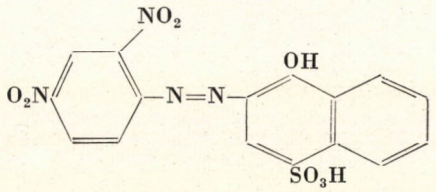

2-(2',4'-dinitrophenylazo)-1-naphthol--4-sulphonic acid

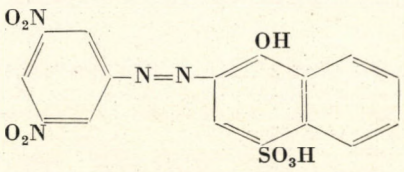

2-(3',5'-dinitrophenylazo)-1-naphthol--4-sulphonic acid

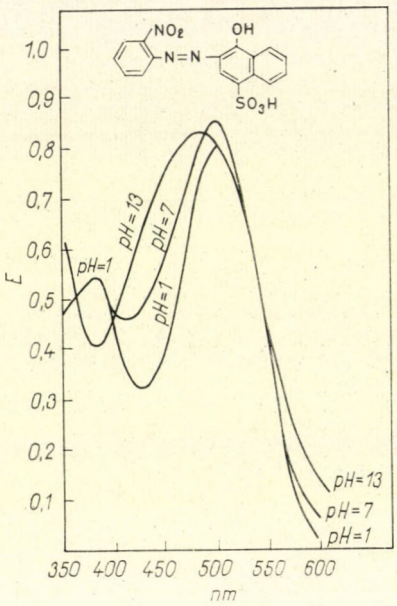

Fig. 1. Absorption spectrum of 2-(2'-nitrophenylazo)-1-naphthol-4-sulphonic acid in water

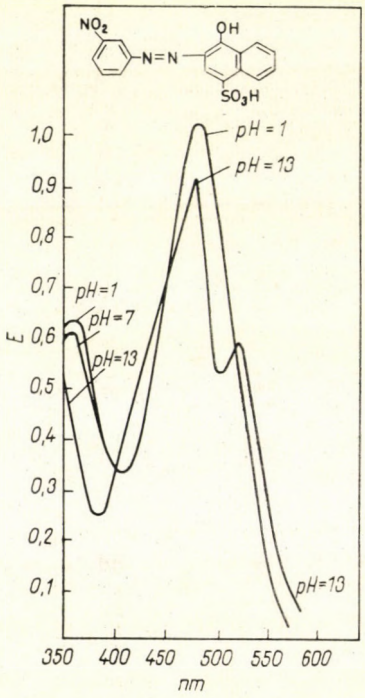

Fig. 2. Absorption spectrum of 2-(3'-nitrophenylazo)-1-naphthol-4-sulphonic acid in water

Experimental

Figs 1—3 show the absorption spectra of compounds 1, 2 and 3. It appears that only compound 3 has an acid-base indicator character, its colour in the acidic form being orange and in the alkaline form violet. The colour change occurs in the pH range 6.8—8.4, with p_i = = 7.6. Compounds 4 and 5 are also acid-base indicators; their properties have already been reported [2].

Table I shows the use of the compounds in argentometric titrations. The measurements were carried out by adding 1 drop of a 2 *N* NaOH solution to 50 ml of the solution to be titrated. The highest accuracy was achieved by titrations in the presence of compound 3; the results are given in Table II. The values represent the means of three measurements. The percentage relative error is $\pm 0.13\%$. The indicator was dissolved in 60% alcohol and for each titration 0.5 ml of the 0.1% solution was used. The solution should not be strongly alkaline, or the titration results will be too high. For each titration 50 ml of the initial solution was used. Iodide ion alone could be titrated with 0.01 *N* $AgNO_3$. When $AgNO_3$ is titrated with KI, the colour change is less pronounced than in the titration of the anion.

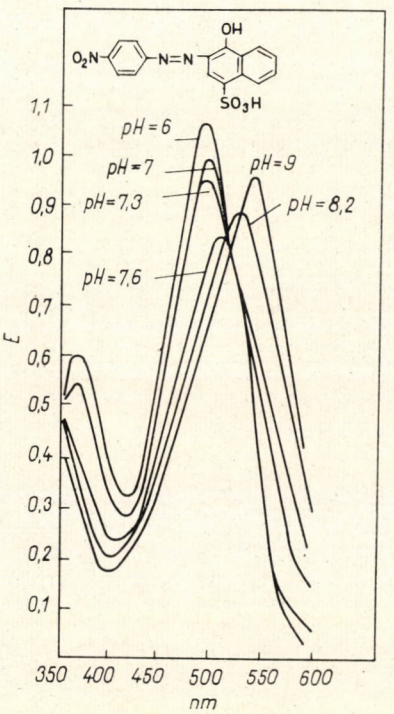

Fig. 3. Absorption spectrum of 2-(4'-nitrophenylazo)-1-naphthol-4-sulphonic acid in water

The mechanism of indication

The mechanism of the adsorption indication of azo dyes containing phenolic hydroxyl and sulphonic acid groups in addition to the nitro group, was studied taking 2-(4'-nitrophenylazo)-1-naphthol-4-sulphonic acid as the example. To clarify the mechanism, the following physical measurements were carried out: *(1)* measurement of the pH of the solution during titration; *(2)* determination of the changes in the dissociation constant of the dye adsorbate due to an excess of its own ions; and *(3)* adsorption measurements.

Table I

Use of indicators in argentometric titrations

Indicator	Ion titrated	Medium	Colour change	Note
1.	J^-	alkaline	yellow to greenish-yellow	poor change of colour
1.	CSN^-	alkaline	orange to grey	
2.	Cl^-	neutral	yellow to red	
2.	Br^-	neutral and alkaline	yellow to violet	
2.	I^-	neutral	yellow to pink	
2.	CSN^-	neutral and alkaline	yellow to pink or violet	
2.	CN^-	NaCN without additional alkali	orange to red	
4.	Cl^-	alkaline	blue to grey	poor change of colour
4.	Br^-	alkaline	blue to grey	
4.	I^-	alkaline	green to greenish-yellow	
4.	CN^-	NaCN without additional alkali	red to blue	
5.	Cl^-	neutral	yellow to pale violet	poor change of colour
5.	Cl^-	alkaline	red to grey	
5.	Br^-	neutral	yellow to violet-grey	
5.	Br^-	alkaline	orange to grey;	
5.	I^-	alkaline	yellow to green	
5.	CSN^-	neutral	yellow to orange	

Table II

Titration of anions with silver nitrate in the presence of 2-(4'-nitrophenylazo)-1-naphthol-4-sulphonic acid

Ion	$AgNO_3$ titrating solution	Medium	Colour change	$AgNO_3$ used, ml with Potentiometric indicator	titr.	Difference, ml	Difference, %
Cyanide	0.1 *N*	NaCN solution	red to violet	4.00	4.03	0.03	0.75
Iodide	0.1 *N*	neutral	yellow to pink	5.16	5.16	0.00	0.00
Iodide	0.01 *N*	1 drop 1 *N* NaOH	red to greyish-green	10.32	10.37	0.05	0.50
Bromide	0.1 *N*	neutral	orange to violet	5.10	5.11	0.01	0.20
Bromide	0.1 *N*	1 drop 1 *N* NaOH	red to bluish-grey	5.10	5.10	0.00	0.00
Thiocyanate	0.1 *N*	neutral	orange to pink	5.16	5.18	0.02	0.40
Thiocyanate	0.1 *N*	1 drop 0.5 *N* NaOH	red to violet-blue	5.16	5.16	0.00	0.00
Chloride	0.1 *N*	neutral	yellow to red	4.90	4.93	0.03	0.60
Chloride	0.1 *N*	1 drop 1 *N* NaOH	red to bluish-violet	4.90	4.87	0.03	0.60

Table III

Dye adsorbate as acid-base indicator

Adsorptive: 2-(4'-nitrophenylazo)-1-naphthol-4-sulphonic-acid

Adsorbent	Excess of own ion, equ.	pH Range of colour change	Dissociation constant, K	Colour change
Silver chloride	50% Ag^+	4.9—6.9	$1.26 \cdot 10^{-6}$	orange-red to violet
	10% Ag^+	5.2—7.0	$7.94 \cdot 10^{-7}$	red to blue
	equ. point	5.3—7.7	$3.16 \cdot 10^{-7}$	red to violet
	10% Cl^-	6.6—8.0	$5.01 \cdot 10^{-8}$	orange to violet
	50% Cl^-	6.6—8.2	$3.98 \cdot 10^{-8}$	orange to violet
Silver bromide	50% Ag^+	3.6—5.6	$2.51 \cdot 10^{-5}$	orange to greyish-blue
	10% Ag^+	4.2—6.8	$3.16 \cdot 10^{-6}$	orange-red to blue
	equ. point	4.5—7.5	$1.00 \cdot 10^{-6}$	orange-red to blue
	10% Br^-	5.0—8.0	$3.16 \cdot 10^{-7}$	orange to violet-red
	50% Br^-	6.1—8.1	$7.94 \cdot 10^{-8}$	orange to violet-red
Silver iodide	50% Ag^+	4.0—6.0	$1.00 \cdot 10^{-5}$	orange-red to bluish-grey
	10% Ag^+	4.6—6.4	$3.16 \cdot 10^{-6}$	orange-red to violet-grey
	equ. point	6.8—8.3	$2.82 \cdot 10^{-8}$	orange to violet
	10% I^-	6.6—8.6	$2.51 \cdot 10^{-8}$	yellow to violet-red
	50% I^-	6.6—8.4	$3.16 \cdot 10^{-8}$	yellow to violet-red
Silver cyanide	50% Ag^+	6.5—7.5	$1.00 \cdot 10^{-7}$	violet-red to violet
	10% Ag^+	6.8—8.4	$2.51 \cdot 10^{-8}$	claret red to dark violet
	equi. point	8.3—9.5	$1.26 \cdot 10^{-9}$	red to dark violet
	10% CN^-	7.6—9.6	$2.51 \cdot 10^{-9}$	orange to violet-red
	50% CN^-	7.0—9.4	$6.31 \cdot 10^{-9}$	orange to violet-red
Silver thiocyanate	50% Ag^+	4.0—5.6	$1.59 \cdot 10^{-5}$	pink to violet
	10% Ag^+	4.5—6.5	$3.16 \cdot 10^{-6}$	pink to violet
	equ. point	5.5—8.3	$1.26 \cdot 10^{-7}$	pink to violet
	10% CSN^-	5.8—8.2	$1.00 \cdot 10^{-7}$	orange to violet-red
	50% CSN^-	6.0—8.2	$7.94 \cdot 10^{-8}$	orange to violet-red

1. pH changes during titration

50 ml of water and 0.5 ml of a 0.1% indicator solution were added to 10 ml of 0.1 N anion solution, and the mixture was then titrated with 0.1 N $AgNO_3$. The pH was measured during titration using glass calomel electrodes. A pH decrease of 0.3—0.5 was observed at the equivalence point during the titration of anions; when silver ion was titrated, the pH decreased until the middle of the titration and then rose by 0.2—0.5 at the equivalence point. This pH change is the same as in the case of indicators containing basic groups, when the indicator loses a proton at the equivalence point in the titration of anions and takes up a proton in the titration of cations.

2. Determination of the change of the dissociation constant of dye adsorbates

The measurements were carried out according to the method described in our earlier papers [3]. The results (Table III) show that there is no change in the dissociation constant of the 2-(4'-nitrophenylazo)-1-naphthol-4-sulphonic acid on silver iodide, silver thiocyanate, or no silver cyanide in the presence of an excess of anions. On the basis of former experiments, this would mean that the anion cannot bring about a colour change; in other words, the solution which has been titrated with silver ion should not change its colour when anions are added. In reality, this is not so; a colour change will also occur with the addition of anions, though this may be less intensive than with silver ions. The dissociation constant of the indicator remains unchanged in the presence of an excess of anions, because partial or total desorption has already taken place. With silver chloride and silver bromide, desorption is slower resulting in a slight change in the dissociation constant in the presence of anion excess.

3. Adsorption measurements

The experiments were carried out in each case with 10^{-4} mole silver iodide adsorbent. 0.6 ml of the 0.1% indicator solution and 20—10 ml of a 0.01 *N* $AgNO_3$ solution were added to 10—20 ml of a 0.01 *N* KI solution, and the mixture was made up to 100 ml. The light absorption of the non-adsorbed dye was measured spectrophotometrically at 480 nm in the presence of 0, 1, 3, 5 and 10 ml of 0.1 *N* iodide and silver ions, respectively. The spectrophotometric measurements were performed in neutral and acid (pH 1) medium in accordance with a preliminary experiment (4). The results are shown in Fig. 4, where the quantity of the adsorbed dye expressed in percentage of the total dye applied is plotted against the concentration of the iodide and silver ions, respectively. This Figure shows that in the presence of iodide ions the dye is not adsorbed, while in the presence of silver ions adsorption is nearly complete (for the small quantities of dye applied). In acidic medium dye adsorption is considerable even at low silver concentrations and a sudden rise is observed when the quantity of silver ions is slightly raised. In neutral media the rise in the quantity of adsorbed dye under the influence of silver ions is slower, but reaches a higher value. The less favourable results obtained in neutral medium are due to the formation of a precipitate in the presence

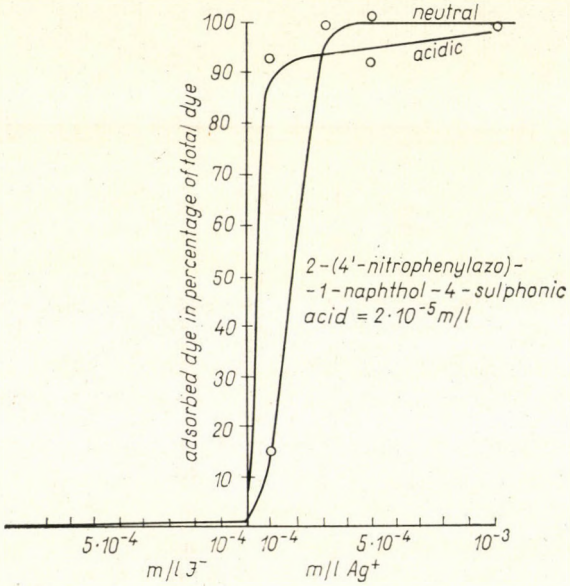

Fig. 4. Adsorption of 2-(4'-nitrophenylazo)-1-naphthol-4-sulphonic acid on silver iodide in the presence of iodide (I^-) and silver (Ag^+) ions, respectively

of higher silver ion quantities; in the presence of the colloidal component the solution will darken after a certain period of time, thus the light absorption of the dye in the solution will be higher. It follows, therefore, from the adsorption measurements that in the presence of an excess of the anion the mechanism of indication is associated with a desorption process, while in the presence of an excess of silver ion with an adsorption process.

Discussion

The mechanism of indication. The indication mechanism of 2-(4'-nitrophenylazo)-1-naphthol-4-sulphonic acid can be discussed using the example of the iodide ion. When iodide ion is titrated with silver nitrate in a neutral solution, the colour of the indicator in the initial solution is yellow. At the equivalence point the indicator is adsorbed with an orange colour producing a detectable colour change. The process is associated with the loss or uptake, of a proton which could be observed experimentally:

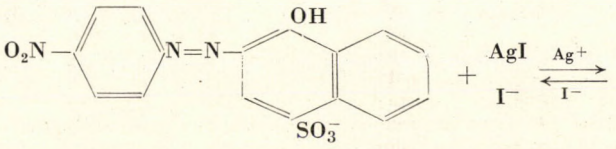

yellow solution

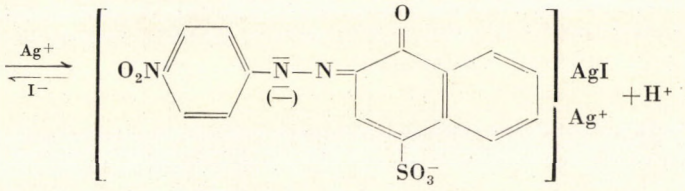

orange precipitate

On back titration the indicator is desorbed and goes into solution. When the titration is carried out under alkaline conditions, indication will proceed by an other mechanism. Alkalinity must be of such a degree that the indicator should display the alkaline or faintly alkaline colour in solution. In alkaline solutions the indicator is red; when titrated with silver nitrate, into greyish-green the colour will change at the equivalence point. This is not accompanied by the loss or uptake of a proton. The colour change is due in the presence of an excess of silver ions to adsorption and to the formation of the silver salt, and in the presence of an excess of anions to desorption and decomposition of the silver compound. On back titration the greyish-green colour of the precipitate turns yellow and the colourless solution becomes red:

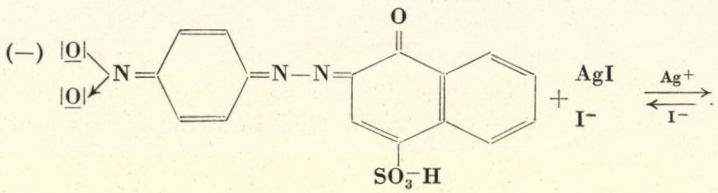

red solution

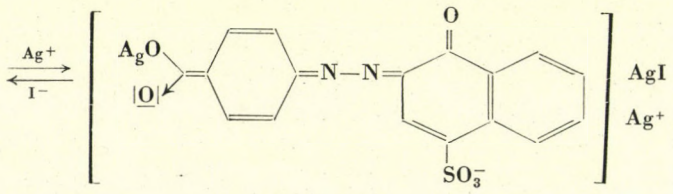

greyish-green precipitate

Desorption in the presence of anion excess and adsorption in the presence of silver ion excess were confirmed by the adsorption measurements described in the foregoing paragraph.

Fajans indication. According to Fajans' original theory, the dye anion or cation is bound by secondary adsorption forces to the oppositely charged precipitate after the precipitate has bound cations or anions from the solution by primary adsorption forces. Fajans suggested that the colour change was due to electron deformation associated with the adsorption process. Later experiments have, however, shown that fluorescein, eosin and its derivatives, on whose behaviour Fajans founded his indicator theory, are surface precipitate indicators, that is to say, they form a precipitate with the silver ion[5].

Comparison of the investigated indication mechanism and Fajans indication. The adsorption indication of 2-(4'-nitrophenylazo)-1-naphthol-4-sulphonic acid resembles the indication mechanism of fluoroscein in that the first is also a negatively charged dye which cannot be adsorbed on negatively charged precipitates but will remain in solution. Thus, the adsorption-desorption process is the same. The difference between the two indicators is that 2-(4'-nitrophenylazo)-1-naphthol-4-sulphonic acid, although it contains a sulphonic acid group, forms no precipitate with silver ion in solution, and no surface precipitate indication takes place.

Comparison of the indication mechanism of the indicator and of basic dyes. The particular adsorption-desorption process cannot be observed with basic dyes. The dye is positively charged, or has no charge, and not even the dye cation is desorbed from the positively charged precipitate. In the case of negatively charged dyes, desorption occurs only when the charge is strongly negative, that is to say, when the dye contains several acid groups, primarily strongly acidic sulphonic acid groups. Without this latter group, 2-(4'-nitrophenylazo)-

1-naphthol-4-sulphonic acid would not be desorbed from the negatively charged precipitate. Thus, in the case under discussion, the sulpho group plays an active part in the production of colour change, though it gives rise to no structural change or precipitation during the indication process; such a colour change may in certain cases be advantageous.

Demonstration of the indication. The adsorption indication mechanism presented in the preceding paragraphs may be confirmed by pH measurements during titration as these will indicate the loss or uptake of a proton. The dissociation constant of the dye adsorbate increases under the effect of cation excess, while in the presence of anion excess the dissociation constant remains unchanged or changes only slightly. This distinguishes the new indicator from azo which contain only nitro and amino groups, and whose dissociation constants decrease markedly in the presence of an excess of anions. Indication can also be demonstrated by the measurement of adsorption: on negatively charged precipitates the indicator is desorbed, and on positively charged precipitates it is adsorbed.

SUMMARY

A new adsorption indicator, 2-(4'-nitrophenylazo)-1-naphthol-4-sulphonic acid, suitable for the argentometric titration of chloride, bromide, iodide, thiocyanate and cyanide ions, is presented.

The mechanism of indication is a combination of an adsorption–desorption process and the acid–base principle. The colour change is due to the formation of a nitric acid structure in the presence of silver ion or of alkali. This type of indication can be demonstrated by the following physical measurements: (a) determination of pH changes during titration; (b) demonstration of a practically unchanged dissociation constants of the dye adsorbate in the presence of anion excess; (c) adsorption measurements.

REFERENCES

1. LÉGRÁDI, L.: Magy. Kém. Foly. **74,** 61 (1968)
2. LÉGRÁDI, L.: Magy. Kém. Foly. **72,** 26 (1966)
3. LÉGRÁDI, L.: Magy. Kém. Foly. **70,** 27, 404 (1964)
4. PUNGOR, E., H-ROKOSINYI, E.: Magy. Kém. Foly. **63,** 28 (1957)
5. PUNGOR, E., KONKOLY-THEGE, I.: Talanta, **10,** 1211 (1963)

László LÉGRÁDI; Füzfőgyártelep. Hungary

Acta Chimica Academiae Scientiarum Hungaricae Tomus 57 (3), pp. 257—263 (1968)

THE NEPHELAUXETIC SERIES AND THE ORDER OF THE MÖSSBAUER PARAMETERS OF IRON COMPLEXES

K. BURGER, A. VÉRTES and E. PAPP-MOLNÁR

(Institute of Inorganic and Analytical Chemistry and Institute of Physical Chemistry and Radiology of the L. Eötvös University, Budapest)

Received November 16, 1967

It is known that the electron cloud of the central atom of transition metal complexes is expanded by ligands, which change the degree of repulsion between the electrons of the central atom. This is called the nephelauxetic effect [1—3] of the ligands, which is the more pronounced, the stronger is the covalent character of the bond between the metal and the donor atom. By arranging the ligands in the order of the magnitude of their nephelauxetic effects JØRGENSEN [4, 5] established the following nephelauxetic series*: $F < H_2O < (CH_3)_2SO < CH_3CONH_2 < NH_2-CO-NH_2 < NH_3 < en < (COO)_2^{2-} < NCS^- < Cl^- < CN^- < Br^- < I^- < S^{2-} \sim dtp < dtc < dsp$

where *en* = ethylenediamine; *dtp* = diethyldithiophosphate; *dtc* = diethyldithiocarbamate; *dsp* = diethyldiselenophosphate.

Accordingly, the nephelauxetic series of the donor atoms is:

$$F < O < N < Cl < Br < I < S < Se.$$

Experiments have shown that the nephelauxetic series well represents the order of covalency of the complexes.

Of the Mössbauer parameters, particularly the values of the isomer shift, but in the case of high spin iron(II) complexes indirectly also the values of quadrupole splitting depend to a considerable extent on the covalency of the bond between the metal and donor atom. An increase in covalent character results in an increase of the *s* electron density, and occasionally in a decrease of *d* electron density, on the central atom. Both changes will increase the electron density at the nucleus.**

* The order was established on the basis of spectroscopic measurements, according to the $(1-\beta)$ values of the ligands, where $\beta = B_0/B_c$, B_0 being the parameter characteristic of the repulsion of the electrons of the ion in the gaseous state, and B_c that of the electrons in the complex formed with the investigated ligand. $(1-\beta)$ can be written as a product of a function h of the ligand and k of the central atom: $(1-\beta) = hk$.

** In first approximation, only the *s* electrons have a finite density at the nucleus. Thus, an increase of the *s* electron density on the central atom obviously will increase the electron density at the nucleus. 3*d* electrons, due to their shielding effect on 3*s* and even 4*s* electrons, decrease the electron density at the nucleus [6, 7]. Therefore, both a decrease in *d* electron density and an increase in *s* electron density will increase the electron density at the nucleus.

The value of the Mössbauer isomer shift (δ) is a measure of the change in electron density at the nucleus.* With iron compounds, the value of the isomer shift is reduced by an increase in electron density at the nucleus.

Therefore, it is to be expected that the decreasing order of the isomer shifts for iron complexes with various ligands will be approximately the same as the increasing order of the covalency of the bond between the metal and donor atom, *i. e.* as the nephelauxetic series of the ligands. Indeed, DANON [8] did mention this trend, though it is not very apparent in the systems investigated by him.

In the iron (II) complexes of the more or less strongly π-acceptor ligands, the increase of the covalent character of the bond between the metal and donor atom furthers the transfer of *d* electrons from the non σ-bonding orbitals of the central atom to the π-acceptor orbitals of the ligand[9]. In high-spin iron (II) complexes, this electron transfer results in an increase of the symmetry of the *d* shell. The $d^6(t_{2g}^4 e_g^2)$ electron structure of the iron (II) central atom approaches gradually the $d^5\,(t_{2g}^3 e_g^2)$ spherical symmetric electron structure, which is characteristic of the high-spin iron (III) atom [10, 11]. Thus, a transfer of *d*-electrons, furthered by the increase in covalency, will increase the symmetry of charge distribution about the iron nucleus, decreasing hereby the value of the electric field gradient, which is manifested by a decrease in the magnitude of the Mössbauer quadrupole splitting (ΔE).

Therefore, it is to be expected that for high-spin iron (II) complexes having about similar coordination spheres, where the symmetry of charge distribution depends largely on the above-mentioned electron transfer, *i. e.* on the covalent character of the coordinative bond which decides this transfer, the decreasing order of the values of quadrupole splitting (ΔE) will run approximately parallel with the increasing order of covalency, *i. e.* with the nephelauxetic series.

It was thought, therefore, reasonable to set the Mössbauer data of iron complexes in order on the basis of the above considerations. The following compounds were prepared, analyzed, and their Mössbauer spectra recorded: $FeI_2 \cdot 4H_2O$, $FeBr_2 \cdot 4H_2O$, FeS of stoichiometric composition, $Fe(H_2PO_2)_2$, Fe(II) diethyldithiocarbamate and Fe(II) anthranilat (Figs 1—5). Our data were supplemented with the Mössbauer parameters of a few iron(II) compounds reported in literature.

* The value of the isomer shift (δ) is:

$$\delta \approx KZe^2\,[|\psi(0)|_a^2 - |\psi(0)|_s^2]\,[R_e^2 - R_g^2]$$

where K is a material constant, Z is the atomic number, $e\,|\,\psi(0)\,|_a^2$ and $e\,|\,\psi(0)\,|_s^2$ are the electron densities at the Mössbauer nucleus of the absorbent and the source, respectively, and R_e and R_g denote the radius of the nucleus in the excited and ground state, respectively.

Experimental

The Mössbauer spectra were recorded with an instrument constructed by the Physical-Chemical and Radiological Institute of the L. Eötvös University, at modular operation. The source was ^{57}Co isotope diffused into a stainless steel plate, having an activity of ~ 1 mC. An ND-204 scintillation counter was used for the detection of γ-radiation, and an NTA-256 analyser for the recording of the spectra. Measured with a $K_4Fe(CN)_6$-absorber, the width of the line emitted by the source was 0.4 mm/s. The instrument was calibrated with a natural iron foil of 20 mg/cm^2 thickness and a $FeSO_4 \cdot 7\ H_2O$ absorber of ~ 30 mg/cm^2 thickness at room temperature: $\Delta E = 3.20$ mm/s. $\delta = 1.4$ mm/s.

A cryostat with "Hungarocell" plastic foam insulation was used for the measurements carried out at liquid air temperature. The sample holder was placed to the bottom of the cryostat.

The thickness of the absorbers was selected such as to have an iron content of 10—20 mg/cm^2.

The iron compounds investigated were of analytical purity. The state of oxidation of the central atoms was checked by oxidimetric titration methods.

Results and discussion

The Mössbauer parameters determined by us and those taken from literature are summarized in Tables I and II. In each case the radiation source was ^{57}Co diffused into stainless steel. A short summary of the conclusions drawn from these data is given in the following:

Table I

The Mössbauer parameters of highs-spin iron compounds

Compound	Isomer shift, mm/sec	Quadrupole splitting, mm/sec	Temperature, °K	l/h	Ref.
FeF_2	1.4±0.05	2.68	299		13
FeF_2	1.4 ±0.05	2.68	85	1.25	13
$Fe(H_2PO_2)_2$	1.29±0.05	2.62±0.05	room temperature		present work
$Fe(H_2PO_2)_2$	1.38±0.05	2.70±0.05	liquid air		present work
Fe(II)anthr$_2$	1.28±0.05	2.68±0.05	liquid air		present work
Fe(III)anthr$_3$	0.47±0.05	0.64±0.08	liquid air		present work
$FeCl_2$	1.01±0.05	0.70±0.05	room temperature		present work
$FeCl_2$	1.23±0.07	1.10±0.05	liquid air	0.5	present work
FeI_2	1.01±0.1	0.66±0.03	290		14
FeI_2	1.12±0.1	0.87±0.03	77	0.38	14
FeS	0.59±0.05	0.48±0.1	liquid air		present work
Fe(II)dtc$_2$	0.59±0.05	0.4 ±0.05	liquid air		present work
Fe(III)dtc$_3$	0.53±0.05	0.5 ±0.08	liquid air		present work

1. Both the isomer shift and quadrupole splitting values of the anhydrous iron (II) halides, shown in Table I., present an order which corresponds to the nephelauxetic series, in accordance with the considerations discussed in the

introductory part. Of the investigated iron salts, iron (II) fluoride, having the strongest ionic character, gave the greatest isomer shift, indicative of the lowest electron density at the nucleus, as well as the greatest quadrupole splitting, indicating the greatest field gradient at the nucleus. Both the isomer shift and quadrupole splitting decreases according to the ligand order: fluoride > chloride > iodide. This order actually corresponds to the nephelauxetic series of the halide ligands, and to the order of increasing covalent character of the iron halides. Moreover, the quadrupole splitting values of the iron (II) halides show a linear correlation with the reciprocal h values characteristic for the nephelauxetic effect of the ligands.

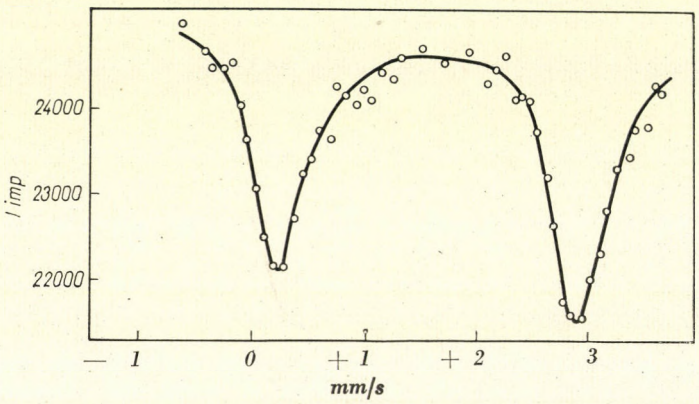

Fig. 1. Mössbauer spectrum of $Fe(H_2PO_2)_2$ at the temperature of liquid air

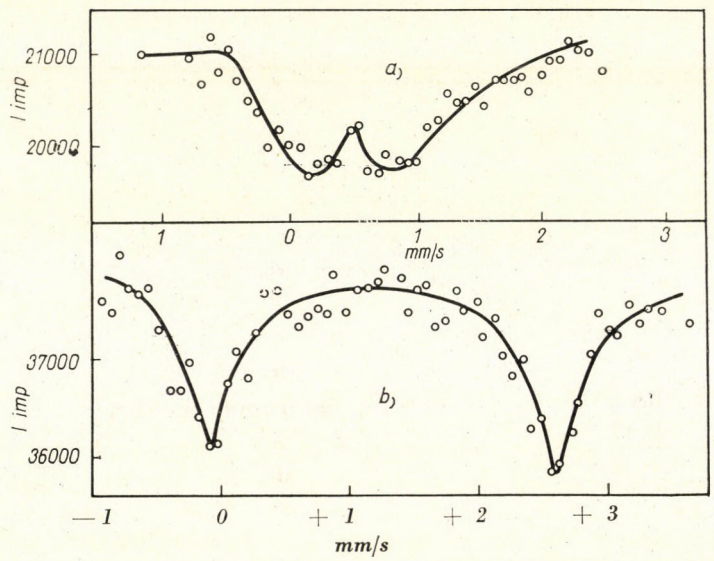

Fig. 2. Mössbauer spectra of Fe(III) anthranilate (a) and Fe(II) anthranilate (b) at the temperature of liquid air

The isomer shift and quadrupole splitting values of $Fe(H_2PO_2)_2$ (donor atoms O), Fe *anthr*$_2^*$ (donor atoms O and N), Fe *dtc*$_2$ (donor atoms S) and FeS (donor atom S) also readily fit into an order which corresponds to the nephe-

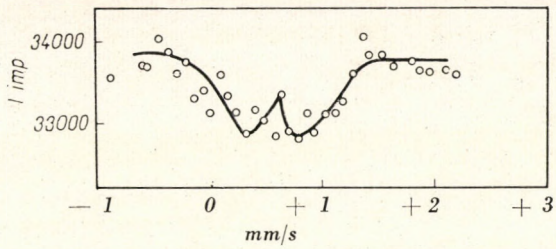

Fig. 3. Mössbauer spectrum of FeS at the temperature of liquid air

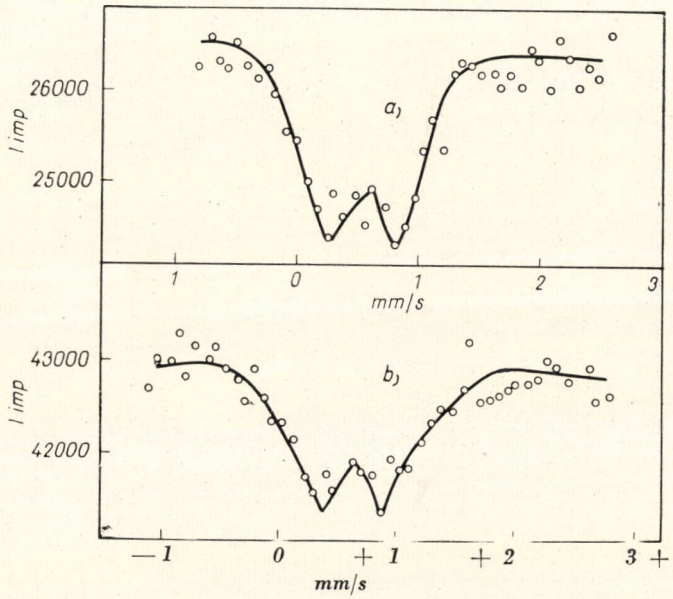

Fig. 4. Mössbauer spectra of Fe(III) diethyldithiocarbamate (a) and Fe(II) diethyldithiocarbamate (b) at the temperature of liquid air

lauxetic series of the ligands. Complexes with the strongest covalent character presented the lowest isomer shift and quadrupole splitting values.

As contrary to this, the data in Table II show that the Mössbauer spectra of iron(II) halides containing water of crystallization do not reflect a nephelauxetic effect. The Mössbauer parameters of the three substances investigated are similar.

* *anthr* = anthranilate

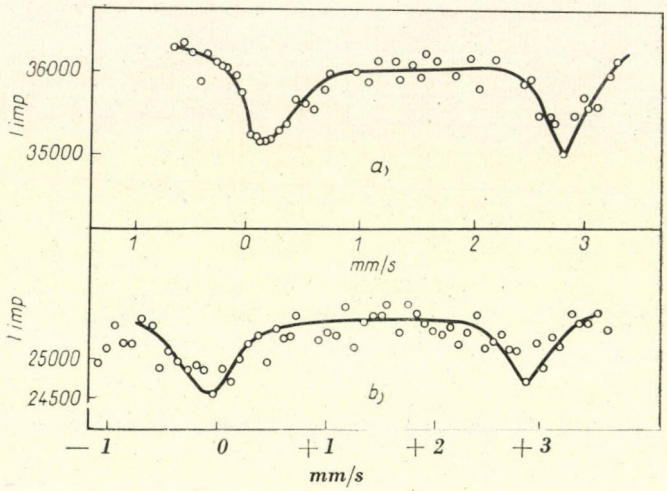

Fig. 5. Mössbauer spectra of $FeBr_2 \cdot 4H_2O$ (a) and $FeI_2 \cdot 4H_2O$ (b) at the temperature of liquid air

Table II

The Mössbauer parameters of iron halides containing water of crystallization, at the temperature of liquid air

Compound	Isomer shift, mm/sec	Qadrupole splitting, mm/sec	Ref.
$FeCl_2 \cdot 4H_2O$	1.35±0.05	3.0 ±0.05	15
$FeBr_2 \cdot 4H_2O$	1.47±0.05	2.75±0.05	present work
$FeI_2 \cdot 4H_2O$	1.41±0.05	3.0 ±0.05	present work

The behaviour of these compounds, inconsistent with the regularities discussed before, can be explained by the fact that in each of them the predominant part of the coordination sphere of iron (II) is occupied by water molecules. Thus, the electron structure of the central atom is determined primarily by these molecules, and the halides have almost no influence. Moreover, the Mössbauer spectrum is similar to that of $FeSO_4 \cdot 4H_2O$ ($\Delta E = 3.5$ mm/s, $\delta = 1.48$ mm/s), having an analogous coordination sphere (containing likewise four molecules of water of crystallization). The effect on the Mössbauer spectrum of the number of water molecules attached directly to the central atom has been proved unequivocally by our recent investigations. The values of quadrupole splitting of iron (II) sulphate samples, containing different amounts of water of crystallization, differ considerably [12].

2. A comparison of the Mössbauer parameters of analogous iron (II) and iron (III) complexes clearly shows that with the increase of the π-acceptor ability of the ligand consequently with an increase of the covalent character

of the complex, the Mössbauer spectrum of the iron (II) atom shows gradually increasing similarity to the picture characteristic of the iron (III) atom. The Mössbauer spectra of the iron (II) and iron (III) complexes of anthranilic acid, containing O and N donor atoms and having thus, according to the nephelauxetic series, relatively ionic character, still differ substantially (Fig. 2). The difference between the values of isomer shifts is about 1 mm/s, and that between the values of quadrupole splitting about 2 mm/s. Conversely, the Mössbauer spectra of the iron (II) and iron (III) complexes of diethyldithiocarbamate of high π-acceptor ability, found at the end of the nephelauxetic series, are similar (Fig. 4). The difference between the corresponding Mössbauer parameters only slightly exceeds the limit of error of the measurements. This fact shows that the more pronounced metal → ligand electron transfer in the iron (II) complex gives rise to an electron structure nearly similar to that of the iron (III) atom.

The authors wish to thank Mr. J. Soós, electric engineer, for his help in developing the measuring instrument, and Mrs. L. Suba for her careful work in recording the Mössbauer spectra.

SUMMARY

The connection between the nephelauxetic effect of ligands and the Mössbauer parameters of their iron complexes is discussed. The measurements of the authors and those published in literature show that the Mössbauer parameters of anhydrous iron(II) halides, anthranilate, hypophosphite, sulphide and diethyldithiocarbamate follow the order of the nephelauxetic series.

REFERENCES

1. Jørgensen, C. K.: Mat. Fys. Medd. Dan. Vid. Selsk. **30,** 22 (1956)
2. Jørgensen, C. K.: Acta Chem. Scand. **11,** 53 (1957)
3. Jørgensen, C. K.: Discuss. Faraday Soc. **26,** 110 (1958)
4. Jørgensen, C. K.: Absorption Spectra and Chemical Bonding in Complexes. Pergamon Press, Oxford, 1962
5. Jørgensen, C. K.: Structure and Bonding **1,** 3 (1966)
6. Watson, R. E., Freemann, A. J.: J. Phys. Rev. **123,** 2027 (1961)
7. Walker, R. L., Wertheim, G. K., Jaccarino, V.: Phys. Rev. Letters **6,** 98 (1961)
8. Danon, J.: Rev. Mod. Phys. **36,** 459 (1964)
9. Orgel, L. E.: An Introduction to Transition-Metal Chemistry. Methuen, London, 1960.
10. Burger, K., Korecz, L., Manuaba, I. B. A., Mag, P.: J. Inorg. Nucl. Chem. **28,** 1673 (1966)
11. Burger, K., Korecz, L., Tóth, A.: Magyar Kém. Foly. **73,** 455 (1967)
12. Vértes, A.: Unpublished results.
13. Wertheim, G. K.: Phys. Rev. **121,** 63 (1961)
14. Fujita, T., Ito, A., Ono, K.: J. Phys. Soc. Japan **21,** 1734 (1966)
15. Dézsi, I., Keszthelyi, L., Molnár, B., Pócs, L.: Investigation of condensed aqueous systems by Mössbauer effect. Central Research Institute for Physics Rept. 9/1967. Budapest

Kálmán Burger
Attila Vértes
Etelka Papp-Molnár

Budapest, VIII. Múzeum krt 4/b

Acta Chimica Academiae Scientiarum Hungaricae Tomus 57 (3), pp. 265—274 (1968)

SOME PROBLEMS CONCERNING THE THEORY OF THE APPLICATION OF RADIOACTIVE KRYPTONATES AS COMPLEXOMETRIC INDICATORS*

J. TÖLGYESSY, T. BRAUN and S. VARGA

(Department of Radiochemistry and Radiation Chemistry, Slovak Technical University, Bratislava
and
Institute of Inorganic and Analytical Chemistry, L. Eötvös University, Budapest)

Received November 20, 1967

In former communications we discussed the essential features of the use of "radioactive kryptonates" as complexometric indicators, and the preparation, by a diffusion technique or by bombardment with accelerated ^{85}Kr ions, of radioactive inclusion indicators. We also studied their characteristics [1], and finally, discussed the determination of calcium ions [2] and of iron [3] with EDTA, and of nickel [4] with KCN. In these determinations $AgIO_3$ [^{85}Kr], $Y_2(C_2O_4)_3$[^{85}Kr], and AgI [^{85}Kr] radioactive kryptonates were employed as indicators using discontinuous titration techniques.

In this paper some theoretical questions of the application of radioactive kryptonates as complexometric indicators will be dealt with.

Fundamentals of the use of radioactive kryptonates as complexometric indicators

In developing the use of radioactive kryptonates in titrimetry, we proceeded from the work of BRAUN *et al.* [5, 6], who used a precipitate labelled with ^{110m}Ag as solid indicator. The advantages of radioactive kryptonates compared to a precipitate labelled with ^{110m}Ag have been explained in a former communication [1].

In a titration based upon the complexing reaction

$$M + C \rightleftharpoons MC^{**}, \qquad (1)$$

the end-point is detected adding a sparingly soluble AB[^{85}Kr] inclusion compound to the solution of the component M to be determined.

A prerequisite for the end-point detection is that, in the course of the titration, component A should react with the complexing agent C only when

* Radioactive kryptonates in volumetric analysis. V.
** For a simpler presentation, charges will not be shown in the general equations.

the entire quantity of M to be determined has already reacted. Complexation of component A may be described by the following dissolution reaction:

$$AB\,[^{85}Kr] + C \rightleftarrows AC + B + {}^{85}Kr\,. \tag{2}$$

The excess titrant reacts with the solid kryptonated precipitate breaking down the order structure of its surface layers, thus liberating radioactive krypton. Since the reaction product is a gas (^{85}Kr), it can readily be separated from the other components of the system, which are solids (kryptonate indicator) or liquids (test solution and titrant).

In a first approximation, the conditions of the success of such a titration are the following:

1. The inequality

$$pK_{MC} < pK_{AC} \tag{3}$$

should hold between the stability constants of the complexes MC and AC.

2. The ratio of the stability constant of the complex AC to the solubility product of the radioactive krypton inclusion compound AB[^{85}Kr] should be chosen correctly: this ratio must effect the dissolution of the kryptonate only when there is an excess of the complexing agent present.

If a solution of component M, also containing the radioactive kryptonate indicator AB[^{85}Kr], is titrated with complexing agent C, measurement of the activity of the kryptonate during titration will show this to be constant up to the point where free M is still available in the solution. Following the quantitative complexing of M, the excess of the complexing agent will begin to react with component A, causing the dissolution of the radioactive kryptonate AB [^{85}Kr]. Accordingly, the radioactivity of the latter will be diminished in propor-

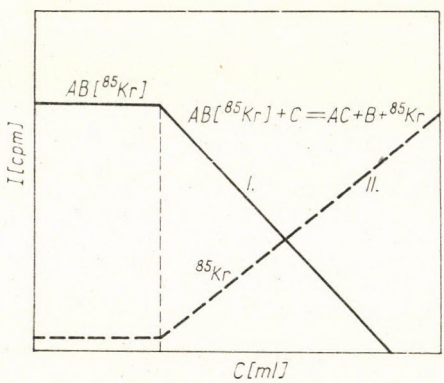

Fig. 1. Theoretical curves of complexometric titrations in the presence of a radioactive kryptonate indicator. (I — measurement of the activity of the indicator) (II — measurement of the activity of the ^{85}Kr liberated)

tion to any excess of C. The activity of the liberated radioactive krypton ^{85}Kr can be measured: nitrogen is bubbled through the solution, which carries the ^{85}Kr gas into a detector, where the activity can be measured continuously. The theoretical titration curves are shown in Fig. 1.

Fig. 2 presents the titration curve for the determination of Ca^{2+} with a 10^{-2} *M* solution of EDTA in the presence of the $AgIO_3[^{85}Kr]$ kryptonate in-

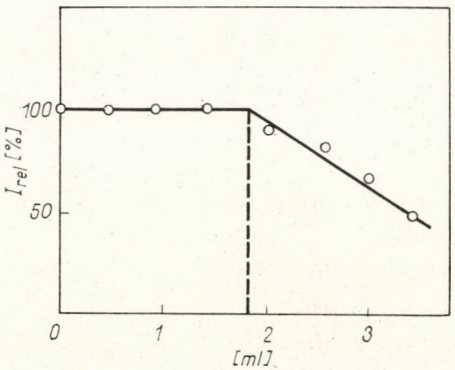

Fig. 2. Titration of Ca^{2+} with a 10^{-2} M solution of EDTA; indicator: $AgIO_3[^{85}Kr]$

dicator. In this case discontinuous titration was used. Up to the end-point, the reaction is

$$Ca^{2+} + Y^{4-} \rightleftarrows CaY^{2-} . \tag{4}$$

After the end-point, the excess of EDTA dissolves the kryptonate:

$$AgIO_3[^{85}Kr] + Y^{4-} \rightleftarrows AgY^{3-} + IO_3^- + {}^{85}Kr \tag{5}$$

causing its activity to decrease in proportion to the addition of the titrant.

Fig. 3 is the titration curve of a determination of Ni^{2+} with a 0.1 *M* solution of KCN in the presence of $AgI[^{85}Kr]$ indicator. Here the titration curve was recorded in a continuous process.

Up to the end-point the reaction is:

$$Ni^{2+} + 4\,CN^- \rightleftarrows Ni(CN)_4^{2-} \tag{6}$$

and after the end-point has been reached the reaction

$$AgI[^{85}Kr] + 2CN^- \rightleftarrows Ag(CN)_2^- + I^- + {}^{85}Kr \tag{7}$$

occurs.

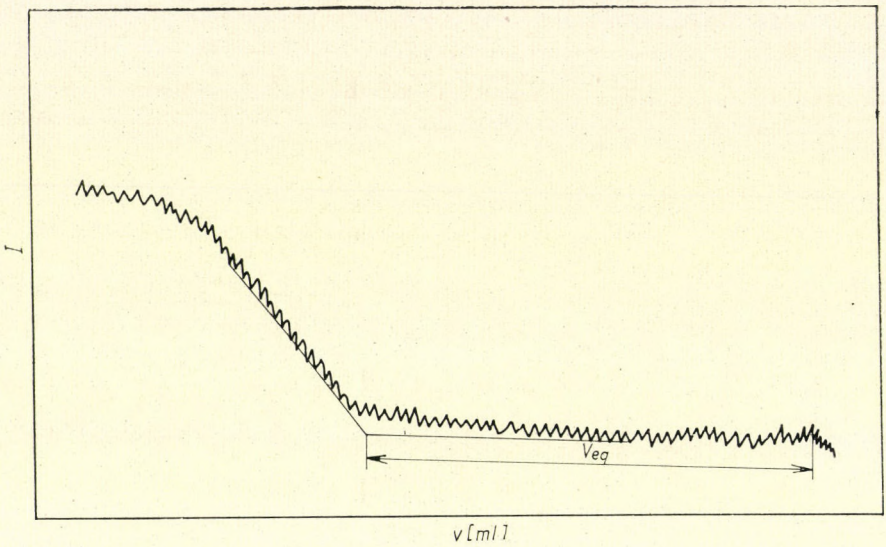

Fig. 3. Titration of Ni^{2+} with a 10^{-1} M solution of KCN; indicator: AgI[^{85}Kr]; automatic addition of the titrant; continuous measuring of activity

The functioning of the radioactive kryptonate indicator

The competition of the metal ion of the radioactive kryptonate indicator with the ion to be determined for the ligand of the titrant is analogous to the successive titration of two metall ions. It has been shown by FLASCHKA [7] that, provided there is a difference of one order of magnitude between the stability constants of the two complexes, the end-point can still be evaluated, though not quite accurately.

In choosing the radioactive kryptonate indicator, or the solid carrier to be labelled with radioactive krypton, account must be taken of the equilibria attained both in and after the end-point. The equilibrium in the end-point is given by the equation:

$$AB[^{85}Kr] + MC \rightleftarrows AC + M + B + {}^{85}Kr. \qquad (8)$$

(For the sake of simplicity, the radioactive kryptonate, AB[^{85}Kr], will be denoted in the following equations by AB.)

In the calculations, account is taken of the side reaction of M with some other anion X, possibly present in the system, and also of the side reaction of C with a cation, Z, possibly present in the system. (In practical instances of titrations at various pH values described up to now, mainly hydroxyl ions were dealt with as X, and hydrogen ions as Z.)

The equilibrium constant is

$$K_I = \frac{[AC][M][B]}{[MC]} = \frac{K_2' \cdot K_S}{K_1'} . \tag{9}$$

K_I can be calculated from the values of K_1' K_S and K_2'.

These are the stability constants and solubility product of the following complexes and precipitate, respectively:

$$MC \rightleftarrows M + C; \quad K_1' = \frac{[MC]}{[M'][C']} = \frac{K_1}{\alpha_{M(X)} \cdot \alpha_{C(Z)}} \tag{10}$$

$$AC \rightleftarrows A + C; \quad K_2' = \frac{[AC]}{[A'][C']} = \frac{K_2}{\alpha_{A(X)} \cdot \alpha_{C(Z)}} \tag{11}$$

and

$$\downarrow AB \rightleftarrows A + B; \quad K_S = [A][B] . \tag{12}$$

For the complexes formed, the apparent stability constants are taken into consideration.

In the preceding Equations

$$[M'] = [M] + [MX] + \ldots [MX_n] \tag{13}$$

$$\alpha_{M(X)} = \frac{[M']}{[M]} \tag{14}$$

$$\beta_n = \frac{[MX]}{[M][X]^n} \tag{15}$$

$$\alpha_{M(X)} = 1 + [X]\beta_1 + [X]^2\beta_2 + \ldots + [X]^n\beta_n \tag{16}$$

$$\alpha_{C(Z)} = 1 + [Z]\beta_1 + [Z]^2\beta_2 + \ldots + [Z]^m\beta_m \tag{17}$$

$$\beta_m = \frac{1}{k_1 \cdot k_2 \ldots k_m}; \quad K_1 = \frac{[C][Z]}{[CZ]} . \tag{18}$$

(If $Z = H^+$, then β_m is the stability constant of the proton ligand, *i.e.* the reciprocal of the dissociation constant.)

In order to carry out such titrations, the value of K_1 must be as small as possible, so that in the end-point Reaction (8) in the direction of the upper arrow should be negligible.

After the end-point, Equilibrium (2) must be considered. The equilibrium constant of this reaction is:

$$K_{II} = \frac{[AC][B]}{[C]} = K_S \cdot K_2'. \tag{19}$$

For the correct performance of titrations it is necessary that constant K_{II} should be a value as high as possible, in order that Reaction (2) should be complete with the excess of C.

The functioning of the AB[^{85}Kr] indicator can also be studied on the basis of its solubility product.

The apparent solubility product of the indicator is:

$$K_S' = [A'][B'] = \alpha_{A(C)} \cdot \alpha_{B(H)} \cdot K_S, \tag{20}$$

where K_S is the original solubility product of the indicator AB; [A'], [B'] and $\alpha_{A(C)}$, $\alpha_{B(H)}$ are as given previously.

Accordingly, in a calculation of the apparent solubility product of indicator AB, the functioning of the indicator is interpreted as the side reaction of ion A in the presence of complexing agent C. Increased solubility and the higher value of the apparent solubility product are due to the fact that the component (titrant) reacts with one of the components of the precipitate. The more stable the complex thus formed, the higher the solubility of the indicator.

The functioning of the indicator is satisfactory when the solubility of the precipitate is enhanced abruptly. Perceptibility of a change in the solubility is a function of the decrease of the activity of the indicator AB[^{85}Kr].

The selection and application of radioactive kryptonate indicators

The practical application of the theoretical relations discussed will be demonstrated on the example of the radiochelatometric determination of the ions Ca^{2+}, Mg^{2+}, and Sr^{2+}.

For the radiometric titration of Ca^{2+}, Mg^{2+}, and Sr^{2+} ions, insoluble compounds of such metal ions which give complexes of a lower stability with EDTA might be considered suitable. Taking account of the stability constants of the EDTA complexes of the three ions (log K for CaY^{2-} is 10.7, for MgY^{2-} it is 8.7, and for SrY^{2-} 8.6), only Ag^{+} and Ba^{++} ions are suitable as the metal component of the indicator (log K for AgY^{3-} is 7.3, for BaY^{2-} it is 7.7). Of these, silver is the choice, in the form of silver iodate precipitate, for the following reasons:

— the solubility exponent of silver iodate is 7.3, as required on the basis of what has been stated above;

— an $AgIO_3[^{85}Kr]$ kryptonate of relatively high specific activity can be prepared by the diffusion method [1];
— the stability in water of the $AgIO_3[^{85}Kr]$ inclusion compound is high (its activity does not decrease).

For a titration of Ca^{2+}, Mg^{2+}, and Sr^{2+} ions in the presence of $AgIO_3$ $[^{85}Kr]$ kryptonate indicator the determination of the optimum pH is absolutely necessary. Therefore, we have calculated the apparent stability constants as

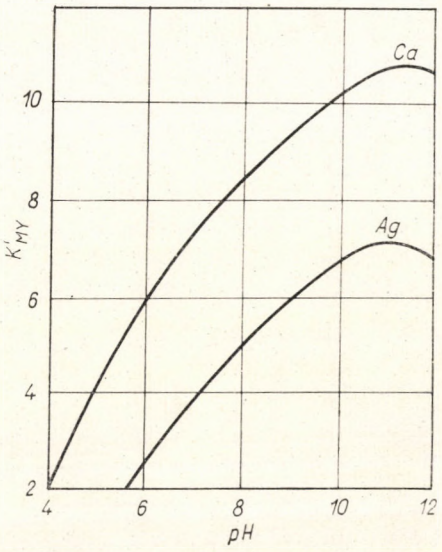

Fig. 4. Logarithms of the apparent stability constants of the EDTA complexes of Ca^{2+} and Ag^{+}, as a function of the pH

a function of the pH for the EDTA complexes of Ca^{2+}, Sr^{2+}, Mg^{2+}, and Ag^{+} ions [6] (*cf.* Fig. 4).

As compared with Ag^{+} ions, it is mainly in the case of Ca^{+2} ions that a relatively large difference is found in the stability constants at pH values 9.5 to 10. In the case of Mg^{2+} and Sr^{2+} ions the situation is not quite so advantageous, nevertheless the stability differences found here still allow titrations to be carried out [7].

The functioning of the $AgIO_3$ $[^{85}Kr]$ indicator in the end-point is determined by the equilibrium

$$AgIO_3\,[^{85}Kr] + CaY^{2+} \rightleftharpoons AgY^{3-} + Ca^{2+} + IO_3^- + {}^{85}Kr \qquad (21)$$

of which the equilibrium constant is

$$K_I = \frac{[AgY^{3-}]\,[Ca^{2+}]\,[IO_3^-]}{[CaY^{2-}]} = \frac{K'_{AgY} \cdot K'_{S(AgIO_3)}}{K'_{CaY}} \qquad (22)$$

where

$$K_{S(AgIO_3)} = [Ag^+]\,[IO_3^-] = 10^{-7.3} \tag{23}$$

$$K'_{AgY} = \frac{K_{AgY}}{\alpha_{Ag(OH)} \cdot \alpha_{Y(H)}} \text{ and } K'_{CaY} = \frac{K_{CaY}}{\alpha_{Ca(OH)} \cdot \alpha_{Y(H)}} . \tag{24}$$

If the values at pH = 10 (from Fig. 4) of K'_{AgY} and K'_{CaY} are introduced into the expression for constant K_I, we get: $K_I \approx 10^{-10}$.

The value calculated shows that at pH = 10 the shift of Equilibrium (21) in the direction of the upper arrow is negligible and, accordingly, during a

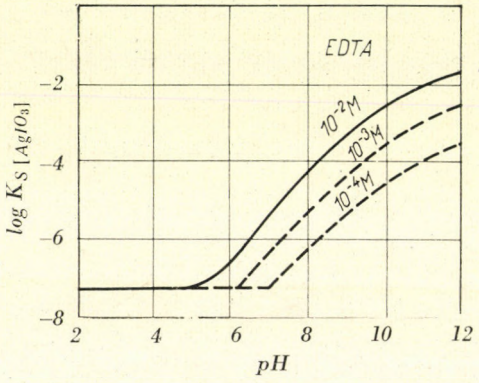

Fig. 5. Apparent solubility products of $AgIO_3$ in EDTA solutions of various concentrations, as a function of the pH

titration with EDTA the indicator $AgIO_3$ [^{85}Kr] does not begin to dissolve to any significant degree, if there are titratable Ca^{2+} ions still present in the solution. After the end-point, Reaction (5) becomes predominant, whose equilibrium constant is

$$K_{II} = \frac{[AgY^{3-}]\,[IO_3^-]}{[Y^{4-}]} = K_S \cdot K'_{AgY} . \tag{25}$$

If the value at pH = 10 of K'_{AgY} (from Fig. 4) is substituted into Equation (25) then $K_{II} \approx 1$. This shows that at pH = 10 Equilibrium (5) is completely shifted in the direction of the upper arrow, *i.e.* the $AgIO_3$ precipitate will completely be dissolved in the excess of EDTA.

In order to find out the pH value most suitable for the functioning of the indicator, and to see how this is influenced by the concentration of the titrant, we have calculated the apparent solubility product of $AgIO_3$ for various concentrations of EDTA as a function of the pH [6]:

$$K'_{S(AgIO_3)} = 10^{-7.3}\,\alpha_{Ag(Y)} \cdot \alpha_{IO_3(H)} \tag{26}$$

where

$$\alpha_{Ag(Y)} = 1 + [Y]\,K_{AgY} = 1 + \left(\frac{[Y']}{\alpha_{Y(H)}}\right) \cdot K_{AgY} \,. \qquad (27)$$

The calculations have been carried out for $[Y'] = 10^{-2}$, 10^{-3}, and 10^{-4} M concentrations of the EDTA solution; the results are listed in Fig. 5.

This figure shows that at pH = 10 chosen for the titration, the solubility product changes by several orders of magnitude in the case of all the three concentrations of EDTA. Fig. 5 also shows that at lower concentrations of EDTA the initial pH of the solution is higher. When the conditions of a titration are selected, this must definitely be taken into account.

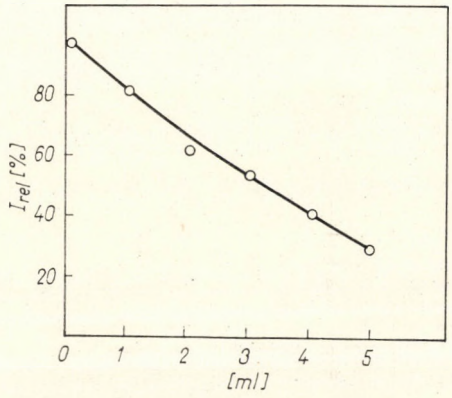

Fig. 6. Change of activity of the $AgIO_3[^{85}Kr]$ kryptonate indicator during the addition of a 10^{-2} M solution of EDTA

By way of illustration, Fig. 6 shows the decrease of activity of $AgIO_3$ $[^{85}Kr]$ as a function of the quantity added of a 10^{-2} M solution of EDTA.

In the manner described, a study has been made of the feasibility of estimations of Fe^{3+} and Ni^{2+}. Fe^{3+} was determined [3] with EDTA in the presence of the kryptonate indicator $Y_2(C_2O_4)_3[^{85}Kr]$, and Ni^{2+} was titrated with KCN [4] in the presence of $AgI[^{85}Kr]$.

SUMMARY

The application of radioactive kryptonates as complexometric indicators is discussed. Factors governing the suitability of a radioactive kryptonate indicator are mentioned. The equilibria obtained both in and after the end-point, which are characterized by the apparent stability constants and the solubility product, respectively, of the complexes and the indicator present in the system, must be taken into account when selecting the indicator for use. The application of the theoretical relations is illustrated on a practical example, using $AgIO_3[^{85}Kr]$ indicator and studying its functioning. The determination of Ca^{2+} ions with EDTA in the presence of $AgIO_3[^{85}Kr]$ is described.

REFERENCES

1. TÖLGYESSY, J., VARGA, S., JESENÁK, V., HRONCOVÁ, D.: Chem. zvesti (In the press)
2. TÖLGYESSY, J., JESENÁK, V., VARGA, S., HRONCOVÁ, D.: Chem. zvesti (In the press)
3. TÖLGYESSY, J., JESENÁK, V., VARGA, S., SILES, B.: Isotopentechnik (In the press)
4. TÖLGYESSY, J., VARGA, S., JESENÁK, V.: Isotopentechnik (In the press)
5. BRAUN, T., MAXIM, I., GALATENAU, I.: Nature, **182,** 936 (1958)
6. BRAUN, T.: Thesis, Budapest, 1966
7. FLASCHKA, H.: Talanta **8,** 381 (1961)

Juraj TÖLGYESSY
Tibor BRAUN
Stefan VARGA

Budapest, VIII. Múzeum krt. 4/b

Acta Chimica Academiae Scientiarum Hungaricae Tomus 57 (3), pp. 275—289 (1968)

FORMATION, THERMAL DECOMPOSITION AND STRUCTURE OF THE SYSTEM UO_3–H_2O, III

THERMAL DECOMPOSITION OF β-$UO_3 \cdot 2H_2O$ PRODUCED FROM γ-UO_3

Z. Pokó, M. Fodor and E. Szabó

(Central Research Institute for Physics, Budapest)

Received June 9, 1967

Introduction

Investigations of the system UO_3–H_2O have led to the preparation of uranium trioxide hydrates differing from one another in composition and modification. The differences have been attributed to both the starting compound and the conditions used in the experiments. A special problem in the study of this system is that the one amorphous and six crystalline (α-, β-, γ-, δ-, ε and ζ) modifications of uranium trioxide have been observed to the present time, which are different, even in their behaviour on hydration. One of the most interesting of these modifications is the γ-UO_3 modification.

γ-UO_3 can be produced from uranyl nitrate hexahydrate by thermal decomposition [1—11], or from U_3O_8 and amorphous or other crystalline forms of uranium trioxide [2, 12, 13] heated under pressure in oxygen. The composition, colour and form of the product was found to vary with the different experimental conditions.

The thermal stability and the decomposition in air of various modifications of uranium trioxide were first studied by Hoekstra and Siegel [2]. It was the γ-UO_3-type that in these experiments needed the highest temperature ($\sim$690°C) to become converted into U_3O_8. Consequently, γ-UO_3 was supposed to be the most stable of the UO_3 modifications [7, 8]. There is, however, a slight difference between the reported values of the transformation temperature.

Complete investigations of the structure have been reported only for the α- [14], δ- [21] and γ-UO_3-types, in which the positions of the oxygen atoms, however, are given only on the basis of spatial considerations. The interpretation of the X-ray diffraction data for γ-UO_3 is far from being uniform, and orthorhombic [22, 26], monoclinic [6, 23] pseudotetragonal [24] and tetragonal [25] structures have been suggested as alternatives. The variety of these suggestions is considered by some authors [26] to be due to the different techniques applied for the production of γ-UO_3.

In most of the uranium compounds hexavalent uranium is present as a constituent of an uranyl group. Though the structure of uranyl compounds

has already been extensively investigated [2, 14—20], the type of bonding in U(VI) oxides is not yet fully known. The existence of uranyl groups is difficult to recognize from the IR spectra, and full interpretation of the different bands

Table I

Review of the compositions and modifications of $UO_3 \cdot 2H_2O$ *proposed by different authors*

Authors	Technique	Modification	Composition
HÜTTIG, SCHROEDER [29]	chemical	$UO_3 \cdot 2H_2O$	$H_2UO_4 \cdot H_2O$
VIER [27]	microscopic (X-ray diffraction)	α-$UO_3 \cdot 2H_2O$ β-$UO_3 \cdot 2H_2O$	—
DAWSON, WAIT, ALCOCK, CHILTON [6]	thermogravimetric X-ray diffraction	$UO_3 \cdot 2H_2O$	—
PROTAS [34]	thermogravimetric diff. thermoanalytical	schoepite I $UO_3 \cdot 2H_2O$	$U_4O_9(OH)_6 \cdot 5H_2O$
GENTILE, TALLEY, COLLOPY [35]	chemical	$UO_3 \cdot 2H_2O$	$H_2UO_4 \cdot H_2O$
CHRIST, CLARK [37]	X-ray diffraction	schoepite I [β-$UO_3 \cdot 2H_2O$]	$UO_2(OH)_2 \cdot H_2O$
DEANE [39]	IR spectroscopy	$UO_3 \cdot 2H_2O$	$UO_2(OH)_2 \cdot H_2O$
PORTE, GUTOWSKY, BOGGS [28]	X-ray diffraction proton magnetic resonance	α-$UO_3 \cdot 2H_2O$ β-$UO_3 \cdot 2H_2O$	$U_2O_5(OH)_2 \cdot 3H_2O$
SCHWARZMANN, GLEMSER [40]	IR spectroscopy proton magnetic resonance	$UO_3 \cdot 2H_2O$	$UO_2(OH)_2 \cdot H_2O$
RODE, GOLOVLEVA KUZNETSOV, KOZMIN [30]	X-ray diffraction thermogravimetric	β-$UO_3 \cdot 2H_2O$	[β-$UO_2(OH)_2 \cdot H_2O$]
WHEELER, DELL, WAIT [10]	diff. thermoanalytical (X-ray diffraction)	α-$UO_3 \cdot 2H_2O$ β-$UO_3 \cdot 2H_2O$	—
DEBETS, LOOPSTRA [36]	X-ray diffraction	β-$UO_3 \cdot 2H_2O$	$H_2UO_4 \cdot H_2O$
LONADIER, BOGGS [38]	isotopic exchange X-ray diffraction proton magnetic resonance	α-$UO_3 \cdot 2H_2O$ β-$UO_3 \cdot 2H_2O$	$UO(OH)_4$? $U_2O_5(OH)_2 \cdot 3H_2O$
FODOR, POKÓ, SZABÓ [32] FODOR, POKÓ, MINK [33]	derivatography IR spectroscopy	α-$UO_3 \cdot 2H_2O$	$[U_3O_7(OH)_4 \cdot 2H_2O]2H_2O$

has not yet been attempted. Nevertheless, the spectra are useful for the identification of the different phases.

Similarly to the complexity of the uranium trioxide phases, the system UO_3–H_2O also presents a number of problems. Depending on the starting material and the given experimental conditions (temperature, pressure, etc.), the composition and structure of the "hydrate" phase may vary from product to product. Among the modifications observed to date, there are two types of uranium trioxide dihydrates (α- and β-) at least five types of monohydrates, $UO_3 \cdot 0.8H_2O$, (α-, β-, γ-, δ and ε-), and a hemihydrate of the composition $UO_3 \cdot 0.5H_2O$.

The hydration of uranium trioxides in water or water vapour at room temperature usually yields a compound that can be described by the formula $UO_3 \cdot 2\,H_2O$. The dihydrates obtained from different types of uranium trioxide are seen to have differing properties.

The data listed in Table I show that the numerous investigations of uranium trioxide dihydrate performed by various physico-chemical methods resulted in different formulas for the description of the composition and structure of the dihydrate. The majority of the results indicates, however, the presence of hydroxyl groups besides the water molecules, and even possible hydrogen bond formation. The compound is considered by some authors as uranic acid monohydrate, or uranyl hydroxide monohydrate, while others suggest a dimeric, or even polymeric complex structure.

Proper evaluation of the experimental data is difficult because a complete structural analysis of $UO_3 \cdot 2H_2O$ has not yet been reported. Apart from PORTE *et. al.* [28], authors [6, 9, 10, 30, 34, 37] have been unable to identify two forms from the X-ray diffraction patterns, since the scattering power of oxygen atoms is masked by that of the much heavier uranium atoms. This fact, combined with large radiation absorption and poor crystallization, causes a substantial error in the determination of the positions of the oxygen atoms. The unit cell is usually taken to be orthorhombic which corresponds to β-$UO_3 \cdot \cdot 2H_2O$ according to VIER's crystallographic determination.

The results obtained by other experimental methods indicate the formation of two types of dihydrate [10, 27, 38]. The dihydrate obtained from γ-UO_3 is generally considered to be the β-$UO_3 \cdot 2H_2O$-type described by VIER, while the other is regarded as α-$UO_3 \cdot 2H_2O$.

Thermogravimetry and differential thermoanalysis of uranium trioxide dihydrate has been reported by various authors, but with discrepant results on the process of decomposition. DAWSON *et al.* [6] observed that the removal of the water content from the dihydrate occurred in two steps involving the formation of an intermediate phase described as $UO_3 \cdot 0.8H_2O$, whereas PROTAS [34] concluded from the relative water losses the existence of a $U_4O_9(OH)_6 \cdot \cdot 5H_2O$ phase. WHEELER *et al.* [10] observed that β-$UO_3 \cdot 2H_2O$ produced

from γ-UO_3 decomposed at lower temperatures than the α-modification, which seems to be more stable. This is confirmed by the fact that the β-modification is converted into α-$UO_3 \cdot 2H_2O$ by boiling for 15 minutes in water at 100° C.

Experimental results

The properties of the system UO_3–H_2O were investigated by analyzing first the thermal decomposition of different uranium trioxide modifications produced by various methods, then the hydration and hydrolysis processes of the same products, and finally by studying the thermal decomposition of the hydrolysis products. Parallel with the thermogravimetric measurements, the infrared spectra of the oxides, hydrates and thermal decomposition products obtained in the experiments were also studied.

It has been shown by our earlier derivatographic and IR spectroscopic experiments [31—33] that from both the amorphous and the β-type UO_3 the same α-$UO_3 \cdot 2H_2O$ product is obtained. The properties and structure of this dihydrate, as inferred from the experimental data, are different from those reported in the literature.

In the present paper the results of the experiments on the system γ-UO_3–H_2O are summarized. On the hydration of γ-UO_3 a dihydrate of β-$UO_3 \cdot 2H_2O$ type is formed. The existence of this modification has not yet been definitely proved, and little is known about its properties. The derivatographic experiments reported here clearly show the differences between the two dihydrate modifications, and yield more accurate information about the particular features of the β-$UO_3 \cdot 2H_2O$-type dihydrate.

The thermogravimetric investigations were performed with the use of a Derivatograph developed by F. PAULIK, J. PAULIK and L. ERDEY [41]. The simultaneously plotted differential thermogravimetric (DTG), thermogravimetric (TG) and differential thermoanalytic (DTA) data obtainable from the derivatograph permit the analysis of the overlapping process; this affords a better insight into the processes involved in the thermal decomposition of the uranium trioxides and their hydrates.

Before thermogravimetric analysis, the composition of each product was established by determining the ignition losses, using the conventional technique of heating the sample at 800° C in air for 2 hours to yield U_3O_8. For thermogravimetry, samples of the same uranium content (2 mmole $UO_3 \cdot xH_2O$ = = 0,57 — 0,64 g) were used. A heating rate of 4.5° C/min. was applied in the experiments.

Preparation and thermal decomposition of γ-UO_3

The γ-UO_3 samples used for the study of the system γ-UO_3–H_2O were prepared by simultaneous thermal dehydration and denitration of uranyl nitrate hexahydrate.

The uranyl nitrate hexahydrate was first purified by tributyl phosphate extraction and recrystallization [42]. For thermal decomposition the quartz cylinder shown in Fig. 1 was used. The dismountable quartz cylinder is entirely closed at one end and has a ground head with two holes, one for the tube protruding into the denitrating volume, the other for the outlet tube provided for the circulation and exhaust of the vapours and gases, respectively. The device is suitable for the simultaneous production of two UO_3 modifications. Parallel with the production of γ-UO_3 one can obtain from U_3O_8 an ε-type uranium trioxide which is formed due to the presence of the nitrogen oxides

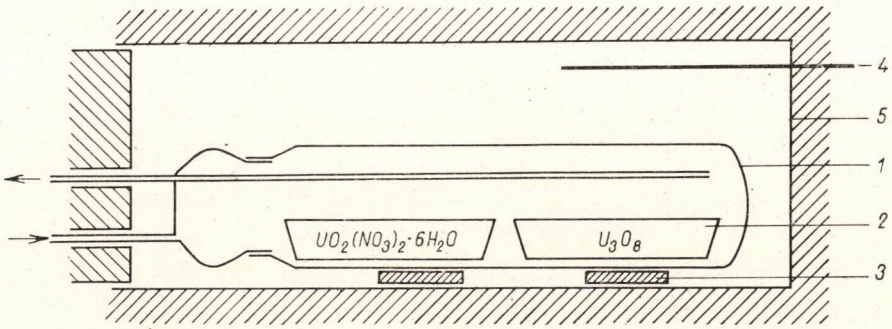

Fig. 1. De-nitrating device. 1. Quartz cylinder. 2. Quartz vessel. 3. Ceramic support. 4. Thermoelement. 5. Furnace

produced during the process. The crystalline uranyl nitrate hexahydrate and the U_3O_8 were placed in two quartz vessels introduced into the cylinder in adjacent positions. The whole assembly was then heated in a furnace at controlled temperature.

The rate of heating from 200° to 350° C was about 1° C/min. The γ-UO_3 thus obtained was pulverized. Both modifications were kept for 1 hour at 400° C to remove any possible moisture or nitrate contamination, and were finally stored in an exsiccator over silicagel.

The nitrogen content, ignition loss, infrared spectrum and derivatogram were determined for each product. The nitrogen content of the γ-UO_3 product was determined as $\sim$0.03% by the modified semi-microanalytical method of Kjeldahl. The infrared spectrum of the sample agreed with that reported by HOEKSTRA for the γ-UO_3 modification [2].

The derivatographic investigation showed that γ-UO_3 transforms to U_3O_8 in a single step. The complete derivatogram of γ-UO_3 is to be seen in Fig. 2. The DTG curve shows that one oxygen loss starts at 665°, there rate of weight loss being highest at 685°, and oxygen is fully removed at about 715° C. The DTA curve proves this oxygen loss to be an endothermic process. The characteristic temperature of the DTA peak coincides with that of the DTG

peak. By analyzing the derivatogram it can be established that the γ-UO_3-type is less hygroscopic than the β-type and amorphous UO_3, but becomes stoichiometric only immediately before transformation. γ-UO_3 was found to require

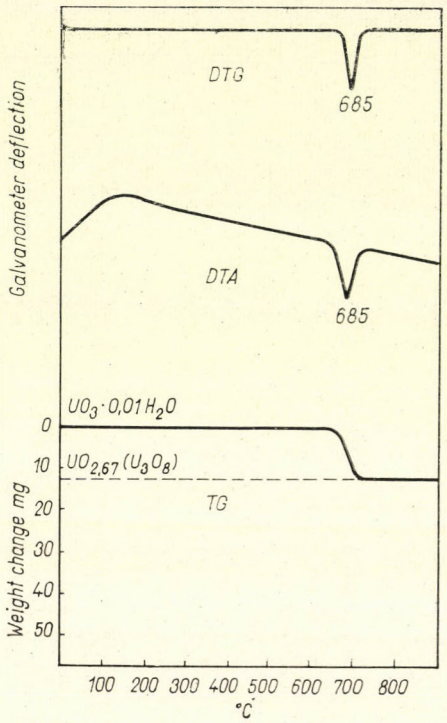

Fig. 2. Derivatogram of γ-UO_3

the highest temperature for transforming to U_3O_8, compared with the other types used in the present investigations. This is in agreement with the literary data showing γ-UO_3 to be of the highest thermal stability among the uranium trioxides.

Thermal decomposition of the hydrolysis products of γ-UO_3

When γ-UO_3 produced from uranyl nitrate hexahydrate is hydrated or hydrolyzed in water, systematic changes are observed in the derivatograms of the samples. These changes differ to some extent from the phenomena observed with the hydrates obtained from amorphous and β-UO_3 [33].

Equal aliquots of γ-UO_3 were placed into weighing bottles with a ground lid, and hydrolyzed in distilled water at room temperature, under constant agitation, for varying periods. In contrast with the β-, or the amorphous

variety, the complete hydrolysis of γ-UO_3 takes a long time (about 3 days), probably because of the smaller specific surface ($\sim 3 m^2/g$) of this type.

The ignition loss, the derivatogram and the infrared spectrum were determined for each product.

The DTG curves shown in Fig. 3 were plotted for the hydrates obtained after different periods of hydrolysis.

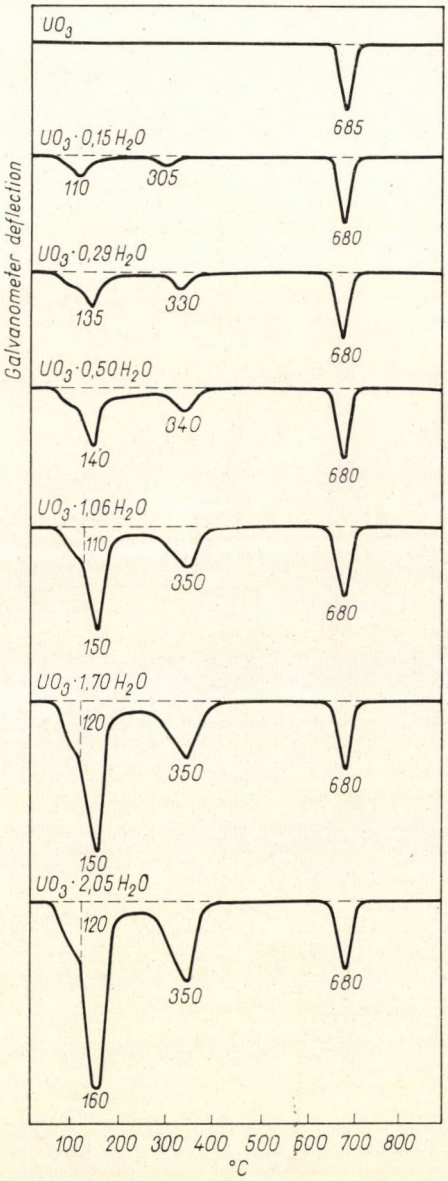

Fig. 3. Differential thermogravimetric curves for γ-UO_3 and its hydrolysis products

The analysis of the DTG curves shows that, contrary to the observations made on the hydrates of β- and amorphous UO_3, three types of water loss occur in any γ-UO_3 hydrate, even in that containing the minimum quantity of water. These processes are similar in nature to the water removal, on thermal decomposition, from the products of higher water contents. The different processes, however, overlap in time. The shape of the DTG curves, for increasingly hydrated products, indicate that the first water loss starts at 40°, attains its maximum gravimetric rate at 120°, and it is completed only at 400°C. The second water loss starts before the termination of the first one, and is manifested therefore only by an inflexion on the DTG curve. The DTG peaks appearing at 160° and 350°C correspond to the second and third dehydration processes which occur in the temperature ranges from 110° to 220°, and 290 to 420C°, respectively. Each of the three types of water removal is an endothermic process.

The derivatographic analysis of products, obtained by partial hydration shows that the dehydration involves three different processes in both the initial and the increasingly hydrated products.

Thermal decomposition of β-$UO_3 \cdot 2H_2O$

Previous investigations have shown that the hydration of amorphous and β-UO_3 led to the same α-$UO_3 \cdot 2H_2O$ modification of identical properties [32, 33]. The derivatograms of γ-UO_3 samples hydrated to various degrees already exhibit some differences from those of the corresponding hydration products of amorphous and β-UO_3. A thorough comparison of the $UO_3 \cdot 2H_2O$ hydrolysis end products of different origins provides conclusive evidence concerning the different thermal properties of the two kinds of dihydrates.

In order to achieve complete hydration and hydrolysis, the amorphous and the β-UO_3 samples were left for a week, and the γ-UO_3 sample for a whole month, to hydrolyze in water at room temperature. They were subsequently processed as described above; the α-type dihydrate was found to be light yellow, and the β-type of greenish yellow colour.

The complete derivatogram of β-$UO_3 \cdot 2H_2O$ produced from the γ-UO_3 modification is shown in Fig. 4, and that of the α-type dihydrate is given for comparison in Fig. 5.

It is apparent from the two derivatograms that, as the temperature increases, two water molecules are lost, in three different steps from both the β-and α-type dihydrates. The first dehydration step is manifested by a mere inflexion at 120°, while the two further steps are marked by definite peaks at 160° and 350°C on the DTG curves. Considering only the changes in weight at the inflexion and the minima on the DTG curve, the dehydration should occur by the successive loss of 0.33, 1.0 and 0.66 moles of water. The analysis of the DTG

curves for the γ-UO_3 products hydrated to different degrees, and also the shape of the DTG curve for β-$UO_3 \cdot 2H_2O$, indicate an overlapping of the dehydration processes. It can be seen from the graphical analysis of the DTG curve, shown in Fig. 6, that the areas below the different peaks are equal. This means that in each dehydration step 0.66 mole of water is lost per U atom. Each of these processes is endothermic. These observations suggest that, like

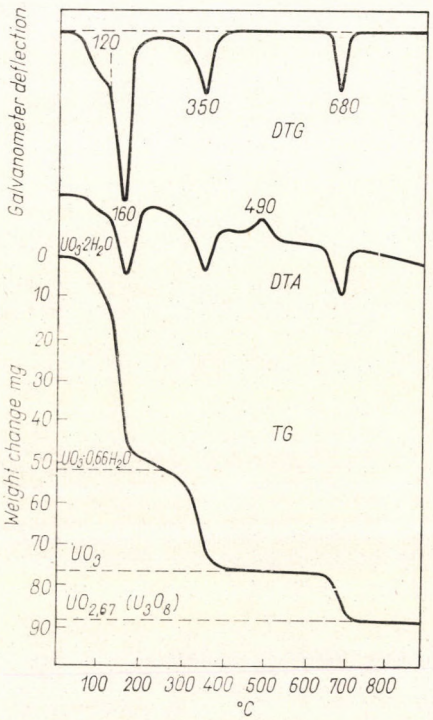

Fig. 4. Derivatogram of β-$UO_3 \cdot 2H_2O$

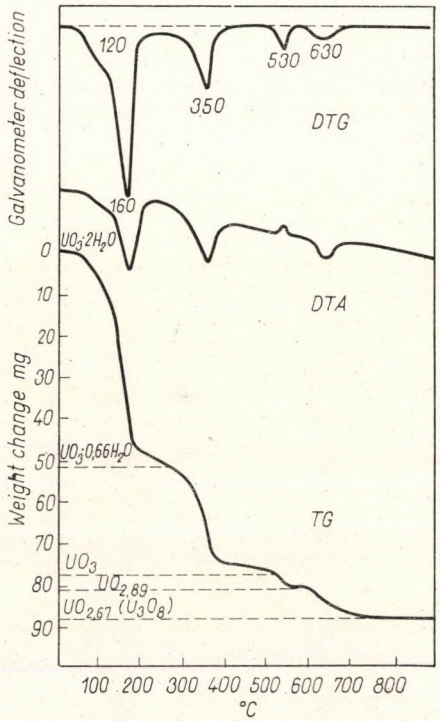

Fig. 5. Derivatogram of α-$UO_3 \cdot 2H_2O$

the α-type, β-$UO_3 \cdot 2H_2O$ is not of a monomeric, but of a trimeric or polytrimeric structure. If the structure is trimeric, the water loss is thought to be two molecules per step; these water molecules are present, however, in different bonding forms and they are unlike in bond energy.

The two dihydrate modifications show a quite different thermal decomposition after complete dehydration.

The α-$UO_3 \cdot 2H_2O$-type product was seen to transform to amorphous UO_3 at 500°C and finally to decompose in two steps to U_3O_8. The first oxygen loss, occurring at 530°C and resulting in an intermediate $UO_{2.89}$ form, is an exothermic, and the second at 630°C an endothermic process. The first step involves 1/3, and the second 2/3 of the total oxygen loss.

The derivatogram of the β-$UO_3 \cdot 2H_2O$ modification indicates the formation of an UO_3 phase at 400°C which persists to 650°C. The DTA curve on the other hand, reveals a protracted exothermic process in this temperature with a peak at 490°C, but involving no change of weight. The initially orange-red UO_3-type product turns to olive-green during the exothermic process.

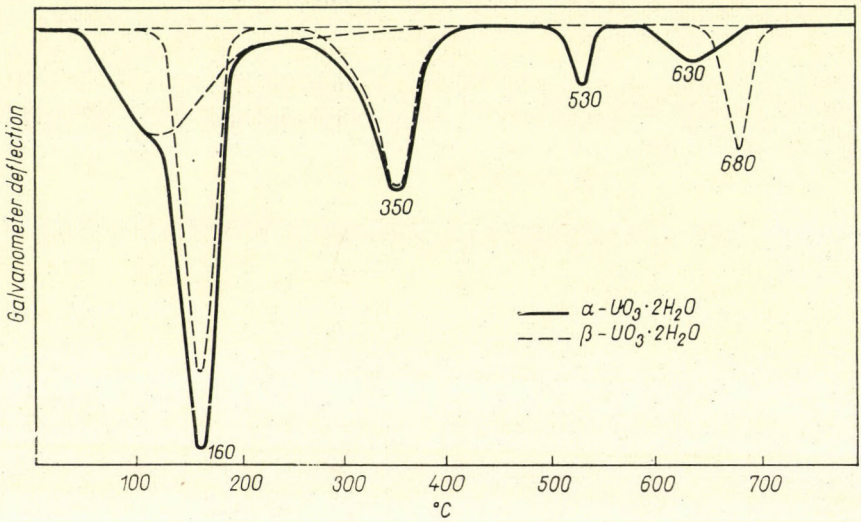

Fig. 6. Graphical analysis of the differential thermogravimetric curves for α- and β-$UO_3 \cdot 2H_2O$ samples

These observations suggest a phase transformation occurring in the UO_3 produced by the thermal decomposition of the β-type dihydrate. On continued heating the UO_3 obtained at the higher temperature is converted into U_3O_8 in a single endothermic step, in the range 650—710°, with a DTG peak at 680° C.

The thermal decomposition processes of the two dihydrates can be described as follows:

$$(\alpha,\beta)UO_3 \cdot 2H_2O \xrightarrow[-0.66H_2O]{120°C\ (40—400°C)} UO_3 \cdot 1.33H_2O \xrightarrow[-0.66H_2O]{160°C\ (110—220°C)} UO_3 \cdot 0.66H_2O \xrightarrow[-0.66H_2O]{350°C\ (290—420°C)} \begin{matrix}(\alpha)\\(\beta)\end{matrix}$$

$$(\alpha)\ UO_3 \xrightarrow[\text{0.11 atom oxygen}]{530°C\ (500—550°C)} UO_{2.89} \xrightarrow[\text{0.22 atom oxygen}]{630°C\ (580—690°C)} UO_{2.67}(U_3O_8)$$

$$(\beta)\ UO_3 \xrightarrow[\text{exothermic process}]{490°C\ (460—520°C)} UO_3 \xrightarrow[\text{0.33 atom oxygen}]{680°C\ (650—710°C)} UO_{2.67}(U_3O_8)$$

The observed phenomena suggest that the different properties of the α- and β-type dihydrates are due to the presence of different uranium-oxygen bonds. Since this fact cannot be discerned by X-ray diffraction, analysis, other experimental evidence is required.

Hydration of the two UO_3 phases produced from β-$UO_3.2H_2O$

We have already seen that the UO_3, obtained by thermal decomposition from β-$UO_3 \cdot 2H_2O$, undergoes a phase transformation at elevated temperatures. The two UO_3 phases behave differently on hydration and give hydrolysis end-products of different properties.

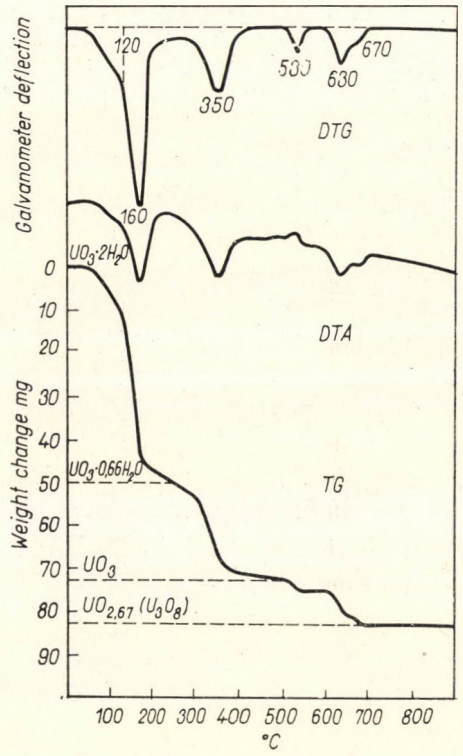

Fig. 7. Derivatogram for the hydrolysis product of the UO_3 phase produced at 420° C from β-$UO_3 \cdot 2H_2O$

To study the hydration of the two UO_3 modifications, the β-type dihydrate was heated in air for an hour at 420°C to obtain the first, then at 620°C to obtain the second UO_3 phase. Both products were hydrolyzed in water at room temperature for two weeks, and the hydrolysis products were processed and analyzed in the usual way.

The derivatogram of the $UO_3 \cdot 2H_2O$ hydrolysis product, obtained from the 420° C-UO_3, is shown in Fig. 7. The dehydration occurs in the same way as observed for the thermal decomposition of the α- and β-type dihydrates. The thermal decomposition of the oxide phases, produced after complete dehydration, however, seems to be a more complex process: the derivatograms exhibit all of the deoxidation peaks which characterize specifically either the α- or

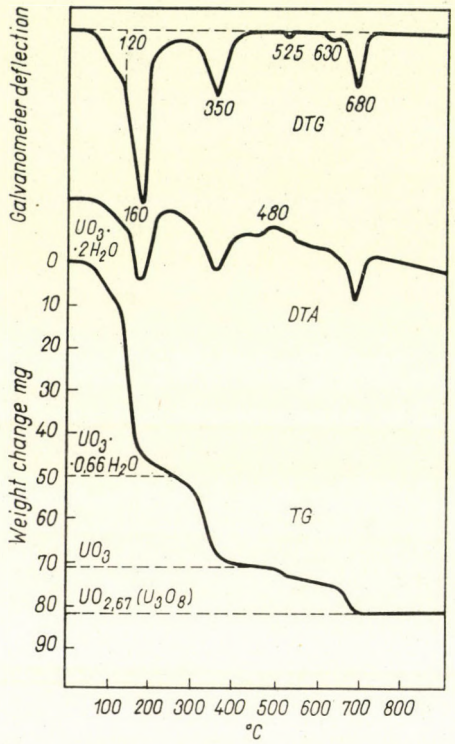

Fig. 8. Derivatogram for the hydrolysis product of the UO_3 phase produced at 620° C from β-$UO_3 \cdot 2H_2O$

the β-type dihydrates. This dihydrate thus seems to be a mixture of the α- and β-modifications. The relative contributions of the two modifications can be evaluated from the thermogravimetric curve. This shows that the dihydrate obtained on hydrolysis from the 420° C-UO_3 is predominantly of the α-$UO_3 \cdot 2H_2O$ type.

The hydrolysis of all but the γ-type uranium trioxide modifications was found to lead to an α-$UO_3 \cdot 2H_2O$-type product. These results indicate that the α-$UO_3 \cdot 2H_2O$ is the most stable dihydrate modification. This is why even the UO_3 produced from β-$UO_3 \cdot 2H_2O$ by thermal decomposition at 420° C is converted by hydration into the α-type dihydrate.

The hydrolysis product, obtained from the olive-green UO_3 produced by thermal decomposition of β-$UO_3 \cdot 2H_2O$ at 620° C, has also the composition $UO_3 \cdot 2H_2O$. It is apparent from the derivatogram shown in Fig. 8 that the thermal dehydration of the 620° C variety is similar to that observed for the other dihydrates. The thermal decomposition, however, differs from that of the other dihydrate modifications. We have again the deoxidation peaks of both the α- and β-types of dihydrate, but the thermogravimetric evaluation now shows the preponderance of the β-type. Thus the UO_3 obtained from β-$UO_3 \cdot 2H_2O$ at 620° C, re-transforms on re-hydration to the initial β-type dihydrate.

Conclusions

It has been established from the experimental evidence that the hydrates produced by the hydrolysis of γ-UO_3 are different from the hydrolysis products of the other uranium trioxide modifications studied earlier. The distinct properties of the α- and β-type dihydrates are well apparent from the difference in the thermal decomposition of the hydrolysis products obtained at room temperature.

The hydrolysis products of γ-UO_3 are dehydrated, even in the initial stage of hydrolysis, by three thermally different processes. This distinguishes the β-$UO_3 \cdot 2H_2O$ produced from γ-UO_3, even in the stage of its formation, from the α-type dihydrate.

The derivatographic analysis of β-$UO_3 \cdot 2H_2O$ produced from γ-UO_3 led to the following conclusions:

(a) The dehydration occurs, similarly to α-$UO_3 \cdot 2H_2O$, in three steps and the gravimetric evaluation of the curves again suggests a trimeric or polymeric formula for the description of β-$UO_3 \cdot 2H_2O$.

(b) The thermal decomposition of the oxide modifications obtained on complete dehydration is strikingly different. The UO_3 phase produced from the β-type dihydrate at 420° C undergoes ot 485° C a phase transformation in an exothermic process without any change of weight. The second UO_3 phase thus formed is converted in a single step to U_3O_8 by an endothermic process, setting in at 690°C. In contrast with these observations, the amorphous UO_3 obtained from the α-type dihydrate is converted into U_3O_8 through an intermediate $UO_{2.89}$ form, in two steps; the first, setting in at 530° C, is a slightly exothermic, the second, at 630° C, an endothermic process.

The difference between the two types of dihydrate is manifested also by the behaviour of their thermal decomposition products on re-hydrolysis.

The re-hydrolysis of amorphous UO_3 produced from α-$UO_3 \cdot 2H_2O$ by thermal decomposition gives only α-type dihydrate. The two UO_3 phases produced from β-$UO_3 \cdot 2H_2O$, the first at 420° C and of orange-red colour, the

second at 620° C and of olive-green colour, yield on re-hydrolysis a mixture of α- and β-type dihydrates, the α-type predominating in the former, the β-type in the latter case.

The authors thanks are due to Mrs. Zs. BUZÁSSY and Mr. B. SZLOVÁK for their assistance in the experiments.

SUMMARY

The properties of the system UO_3–H_2O have been studied by the analysis of the thermal decomposition of uranium trioxide hydration products of different origins. The results obtained on the system, γ-UO_3–H_2O, and in particular observations concerning the thermal decomposition of the β-$UO_3 \cdot 2H_2O$-type dihydrate, produced from γ-UO_3, are reported. The derivatographic results show the difference between γ-UO_3 and the other uranium oxide hydration products. The distinct properties of the α- and β-type dihydrates become well apparent from an analysis of the thermal behaviour of the UO_3 hydrolysis products obtained at room temperature.

REFERENCES

1. KATZ, J. J., RABINOWITCH, E.: The Chemistry of Uranium, National Nuclear Energy Series, Div. VIII., Vol. 5. McGraw-Hill, New York, 1951
2. HOEKSTRA, H. R., SIEGEL, S.: J. Inorg. Nucl. Chem. **18,** 154 (1961)
3. BRIDGE, J. R., MELTON, C. W., SCHWARTZ, C. M., VAUGHAN, D. A.: BMI—1110, July 12, 1965
4. VAUGHAN, D. A., BRIDGE, J. R. and SCHWARTZ, C. M.: BMI Report, 1205 (1957)
5. ONDREJCIN, R. S., GARRETT, T. P., Jr.: Phys. Chem. **65,** 471 (1961)
6. DAWSON, J. K., WAIT, E., ALCOCK, K., CHILTON, D. R.: J. Chem. Soc. **683,** 3531 (1956)
7. CORNMAN, W. R.: USA E. C. Report, DP-749 (1962)
8. DELL, R. M., WHEELER, V. J.: Trans, Faraday Soc. **58,** 1590 (1962)
9. DELL, R. M., WHEELER, V. J.: Trans. Faraday Soc. **59,** 485 (1963)
10. WHEELER, V. J., DELL, R. M., WAIT, E.: J. Inorg. Nucl. Chem., **86,** 1829 (1964)
11. JONKE, A. A., PETKUS, E. J., LOEDING, J. W., LAWROWSKI, S.: Nucl. Sci. Eng. **2,** 303 (1957)
12. SHEFT, I., FRIED, S., DAVIDSON, N.: J. Am. Chem. Soc. **72,** 2172 (1950)
13. VIDAVSKII, L. M., LAVUT, E. G., KOVBA, L. M., IPPOLITOVA, E. A.: Dokl. Akad. Nauk SSSR. **154,** 1371 (1964)
14. ZACHARIASEN, W. H.: Acta Cryst. **1,** 265 (1948)
15. ZACHARIASEN, W. H.: Acta Cryst. **7,** 795 (1954)
16. ZACHARIASEN, W. H., PLETTINGER, H. A.: Acta Cryst. **12,** 526 (1959)
17. JONES, L. H.: Spectrochim. Acta **10,** 395 (1958)
18. JONES, L. H.: Spectrochim. Acta **11,** 409 (1959)
19. MCGLYNN, S. P., SMITH, J. K., NEELY, W. C.: J. Chem. Phys. **35,** 105 (1961)
20. DYATKINA, M. E., MIKHAILOV, Yu. N.: Zh. Strukt. Khim. **3,** 724 (1962)
21. WAIT, E.: J. Inorg. Nucl. Chem. **1,** 309 (1955)
22. PERIO, P.: Bull. soc. chim. France, **1953,** 776
23. CONOLLY, D. E.: Acta Cryst. **12,** 949 (1959)
24. WOLFF, P. M.: Acta Cryst. **14,** 322 (1961)
25. ENGMANN, R., WOLFF, P. M.: Acta Cryst. **16,** 993 (1963)
26. BEKETOV, A. R., STREKALOVSKII, V. N., VLASOV, V. G.: Zh. Strukt. Khim. **6,** 164 (1965)
27. VIER, D. T.: USA E. C. Report, A-1277 (1944)
28. PORTE, A. L., GUTOWSKY, H. S., BOGGS, J. E.: J. Chem. Phys. **36,** 1695 (1962)
29. HÜTTIG, G. F., SCHROEDER, E.: Z. Anorg. Chem. **121,** 234 (1922)
30. RODE, E. A., GOLOVLEVA, Z. S., KUZNETSOV, V. G., KOZMIN, P. A.: Zh. Neorgan. Khim. **8,** 2751 (1963)
31. SZABÓ, E., BAKOS, L., CZEGLÉDI, B., FODOR, M., MÜLLER, P.: Proc. of the 3-rd Internat. Conf. of Peaceful Uses of Atomic Energy, Geneva, 1964. A (Conf. 28) PI 450
32. FODOR, M., POKÓ, Z., SZABÓ, E.: Magyar Kém. Foly. **71,** 104 (1965)

33. FODOR, M., POKÓ, Z., MINK, J.: Mikrochim. Acta **4—5,** 865 (1966)
34. PROTAS, J.: Bull. soc. Franc. Miner. Crist. LXXXII, 239 (1959)
35. GENTILE, P. S., TALLEY, L. H., COLLOPY, T. J.: J. Inorg. Nucl. Chem. **10,** 114 (1959)
36. DEBETS, P. C., LOOPSTRA, B. O.: J. Inorg. Nucl. Chem. **25,** 945 (1963)
37. CHRIST, C. L., CLARK, Joan R.: Amer. Mineralogist **45,** 1026 (1960)
38. LONADIER, F. D., BOGGS, J. E.: J. Less-Common Metals **5,** 112 (1963)
39. DEANE, A. M.: J. Inorg. Nucl. Chem. **21,** 238 (1961)
40. SCHWARZMANN, E., GLEMSER, O.: Z. Anorg. Allg. Chem. **315,** 305 (1962)
41. PAULIK, F., PAULIK, J., ERDEY, L.: Z. Anal. Chem. **160,** 241 (1958)
42. BAKOS, L., SZABÓ, E.: Magyar Kémikusok Lapja **8,** 433 (1964)

Zoltán POKÓ
Miklós FODOR
Elek SZABÓ

Budapest, XII. Konkoly Thege út

Acta Chimica Academiae Scientiarum Hungaricae Tomus 57 (3), pp. 291—299 (1968)

INVESTIGATIONS ON ION EXCHANGE EQUILIBRIA WITH RADIOACTIVE TRACER METHOD, XII

DETERMINATION OF THE SUCCESSIVE FORMATION CONSTANTS OF α-HYDROXY-ISOBUTYRATE COMPLEXES OF EUROPIUM

T. LENGYEL

(Institute of Isotopes, Hungarian Academy of Sciences, Budapest)

Received October 18, 1967

Introduction

In a previous paper [1] the advantages of liquid ion exchangers for investigating the formation and structure of complex species were discussed. However, in the course of the measurements, the conditions chosen made it possible to determine only the stability constant of the 1 : 1 complex. In order to obtain exact data on further species, measurements in a rather wide range of ligand concentration must be performed. At the same time, the treatment of experimental data by the arduous though well-established method developed by FRONAEUS [2, 3] and by a new method of computation, which will be discussed later, seemed to be necessary.

Extensive investigations with α-hydroxyisobutyrates have recently been performed [4], but the comparatively poor agreement with potentiometric determinations [5, 6] regarding the second and third stability constants made it necessary to slightly alter the experimental conditions.

At the same time, comparison of the results obtained by the two different ways of computations seemed to be reasonable in order to mutually prove the reliabilities of the methods.

The Fronaeus method

This method of graphical computation is perhaps the most reliable one reported in the literature. The presentation excellently summarized by ROSSOTTI and ROSSOTTI [7] has been employed in this work without any significant modifications. The method of calculation is given here without detailed comments, and —with a few exceptions — the notations of the handbook cited are used throughout.

First of all the function

$$\Phi = \frac{D^0/D - 1}{[L]} \qquad (1)$$

is introduced. Plotting Φ against [L] and extrapolating to [L] = 0, the value

$$\Phi_0 = (\beta_1 - \gamma_1) \tag{2}$$

is obtained. This is used to calculate a further function

$$f = \frac{D^0/D\,\{(\beta_1 - \gamma_1)\,[L] - 1\} + 1}{[L]^2} = \beta_1 \Phi - F_2 + \gamma_2 (\Phi[L] + 1) \tag{3}$$

whence

$$f_0 = \lim_{[L]\to 0} f = \beta_1 (\beta_1 - \gamma_1) - (\beta_2 - \gamma_2) \tag{4}$$

can be determined as the intersection by extrapolating the curve of the diagram f *vs.* [L].

$$\text{Plotting } \frac{f - f_0}{[L]} \text{ against } \frac{\Phi - \Phi_0}{[L]},$$

a straight line of slope β_1 is obtained, according to the equation

$$\frac{f - f_0}{[L]} = \frac{\Phi - \Phi_0}{[L]} \beta_1 + \gamma_2 \Phi - F_3 \tag{5}$$

substituting the β_1 value thus obtained into Eq. (4) the term $(\beta_2 - \gamma_2)$ can be determined.

Combining Eqs (1) and (3), we get:

$$\vartheta = f - \beta_1 \Phi + \frac{D^0 (\beta_2 - \gamma_2)}{D[L]} = \beta_2 \Phi - F_3 . \tag{6}$$

Therefore, the limiting slope yields

$$\lim_{\Phi\to 0} \frac{d\vartheta}{d\Phi} = \beta_2 . \tag{7}$$

The further steps of the calculation are based on the relation

$$F_t = \sum_{n=t}^{n=N} \beta_n [L]^{n-t}, \tag{8}$$

according to which β_3 is obtained as the intersection of the plot F_3 against [L], where the values of F_3 obtained with the aid of Eq. (6) are used.

The new method

The other method chosen for the computation of the successive formation constants is based on the relations developed previously [1]; it excels in the relatively simple treatment of the experimental data.

In the uncomplexed system, the distribution ratio (neglecting symbols of charge) is determined as

$$D^0 = \frac{{}_0[M]}{{}_w[M]} \tag{9}$$

while in the presence of a complexing agent, presuming that charged complexes do not undergo partition (an assumption proved previously [1]), we have:

$$D = \frac{{}_0[M]}{{}_w[M] + \sum_{i=1}^{N} {}_w[ML_i]}. \tag{10}$$

Taking into account the basic relation

$${}_w[M] + i\,{}_w[HL] = {}_w[ML] + i\,{}_w[H], \tag{11}$$

the mass action law yields

$$K_e = \frac{{}_w[ML_i]\,{}_w[H]^i}{{}_w[M]\,{}_w[HL^i]}. \tag{12}$$

The combination of Eqs (9), (10) and (12) results in

$$D = \frac{{}_0[M]}{{}_w[M] + \dfrac{K_e\,{}_w[M]\,{}_w[HL]^i}{{}_w[H]^i}} = \frac{D^0}{1 + \sum_{i=1}^{N} \dfrac{K_e\,{}_w[HL]^i}{{}_w[H]^i}}, \tag{13}$$

which on rearranging and taking the logarithms gives:

$$\log\left(\frac{D^0}{D} - 1\right) = i\left\{{}_w(pH) + \log {}_w[HL]\right\} + \log K_e. \tag{14}$$

Eq. (14) is valid with the assumption that, within given concentration ranges of the complexing agent and at given pH, only one of the complex species prevails, *i.e.* when plotting the left hand side of Eq. (14) against $\{{}_w(pH) + {} + \log_w[HL]\}$, linear sections corresponding to $i = 1, 2 \ldots N$ can be distinguished.

Introducing the overall formation constants of the species $[ML_i]$

$$\beta_i = \frac{{}_w[ML_i]}{{}_w[M]\,{}_w[L]^i}, \tag{15}$$

Eq. (15) can be rearranged as

$$\frac{\beta_i}{K_e} = \frac{{}_w[HL]^i}{{}_w[H]^i\,{}_w[L]^i}. \tag{16}$$

In the knowledge of (or by determining experimentally) the acid dissociation constant K_d for the reaction

$$[HL] \rightleftarrows [H] + [L] \tag{17}$$

and taking the logarithms, Eq. (16) can be rewritten as

$$\log \beta_i = \log K_e + i\,pK_d. \tag{18}$$

Summarizing the method outlined above, the first task is to plot the values $\log(D^\circ/D - 1)$ as a function of $\{{}_w(pH) + \log {}_w[HL]\}$. The curve obtained can be divided into linear parts characterized by the slopes $i = 1, 2 \ldots . N$, according to the species (ML_i) prevailing under the given conditions. By extrapolation of the linear parts of the curves, the intersections give the corresponding $\log K_e$ values from which the β_i values can be calculated with the aid of Eq. (18).

The main advantage of this type of calculation is that the errors involved in the determination of each of the β_i values are not cumulated, an achievment which can hardly be attained in most of the methods commonly used. The experimental procedure is also simple and has the additional advantage that the adjustment of a constant pH is unnecessary.

Experimental

Static equilibrium measurements were carried out at 25° in the same way as described previously [1]. $^{152-154}$Eu tracer was produced by the conventional (n, γ) reaction; owing to the high activation cross section considerable specific activity could be attained, thus the precision of the measurements was increased in spite of the relatively low metal concentration (10^{-6} M as $Eu(ClO_4)_3$ used.

Stock solutions of α-hydroxyisobutyric acid were prepared from the c.p. reagent so that the ionic strength made up with sodium perchlorate was 0.1 M, the pH being adjusted as quoted in each of the series of measurements.

The free ligand concentrations were calculated on the basis of the dissociation constant value ($pK_d = 3.94$) obtained by potentiometric measurements, titrating the complexing agent in 0.1 M perchlorate medium. This result confirms the data published by SMITH and HOFFMAN [8].

Di-2-ethylhexyl-phosphoric acid dissolved in toluene (10^{-2} F) was chosen as the liquid ion exchanger, as before.

The concentration of europium was determined radiometrically, by a well-type scintillation detector. The pH values in the aqueous phase were measured by a Radiometer PH-4 instrument, using a glass-calomel electrode pair. The errors of the determinations did not exceed ± 0.01 pH units.

When adopting the Fronaeus method, the ligand concentration was corrected for smaller deviations in the pH; when large changes were found, the measurement was discarded and repeated.

Results and discussions

In order to check the valency state of the uncomplexed species and to determine the D° values, the dependence of the distribution ratio on the pH of the aqueous phase was investigated. The experimental data (presented in

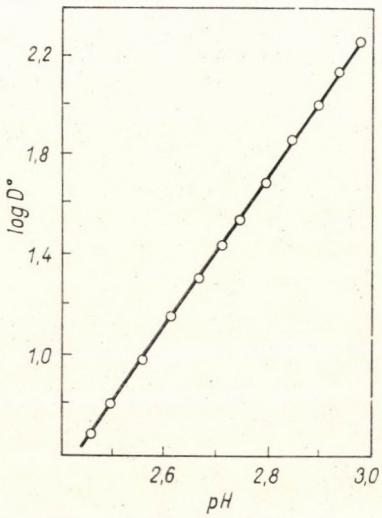

Fig. 1. Distribution ratio as a function of the pH $[Eu^{3+}] = 10^{-6}$ *M*; [DEHPA] $= 10^{-2}$ *F*; $[ClO_4^-] = 0.1$ *M*

Fig. 1) show a third power dependence, indicating the partition of trivalent Eu^{3+} species.

In Tables I and II, the results of equilibrium measurements performed in the presence of the ligand investigated are compiled as a function of the free ligand and analytical butyrate concentrations, respectively. Based on these measurements, the successive (stepwise) formation constants were determined using the two methods outlined above.

From the data of Fig. 1 and Table I, the curve given in Fig. 2 was constructed, according to which Φ_0 is equal to 196. Using Eq. (3), the data plotted in Fig. 3 were obtained, from which $f_0 = -2.55 \cdot 10^{-5}$ could be determined.

In accordance with Eq. (5), from the $f - f_0/[L]$ *vs.* $\Phi - \Phi_0/[L]$ plot shown in Fig. 4 (neglecting some points scattering) a curve with an initial slope $\beta_1 =$

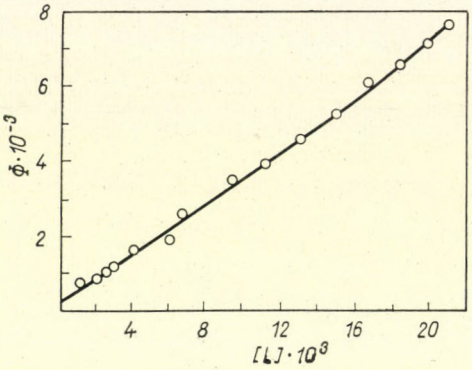

Fig. 2. Φ as a function of the ligand concentration, calculated according to Eq. (1), using the data of Table I. $[Eu^{3+}] = 10^{-6} M$; [DEHPA] $= 10^{-2}$ *F*; $[ClO_4^-] = 0.1$ *M*

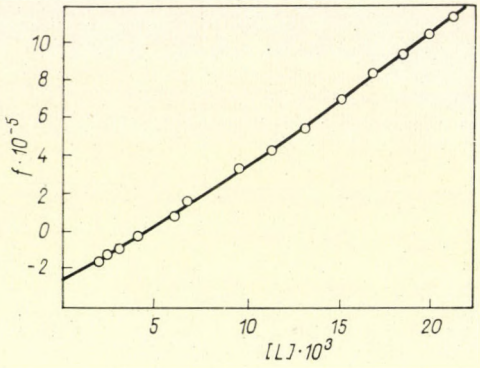

Fig. 3. f as a function of the free ligand concentration, calculated according to Eq. (3), using the data of Table I

$= K_1 = 501$ was obtained. By substitution into Eq. (4), the value of $(\beta_2 - \gamma_2)$ was obtained from which $\beta_2 = 9.60 \cdot 10^4$ was determined as the slope of the curve ϑ *vs.* Φ shown in Fig. 5, constructed with the aid of Eq. (6).

Table I

Experimental results of equilibrium measurements
(Fronaeus method)

[L] · 10³ *M*	pH	*D*
1.097	2.68	$1.24 \cdot 10^{1}$
2.010	2.64	$6.10 \cdot 10^{0}$
2.502	2.64	$4.62 \cdot 10^{0}$
3.006	2.64	$3.72 \cdot 10^{0}$
4.117	2.555	$1.22 \cdot 10^{0}$
6.105	2.58	$7.89 \cdot 10^{-1}$
6.756	2.565	$5.40 \cdot 10^{-1}$
7.942	2.57	$4.65 \cdot 10^{-1}$
9.447	2.57	$3.04 \cdot 10^{-1}$
11.203	2.565	$2.22 \cdot 10^{-1}$
13.079	2.575	$1.78 \cdot 10^{-1}$
15.080	2.58	$1.39 \cdot 10^{-1}$
16.824	2.58	$1.08 \cdot 10^{-1}$
18.600	2.565	$8.11 \cdot 10^{-2}$
19.952	2.58	$7.73 \cdot 10^{-2}$
21.114	2.565	$6.14 \cdot 10^{-2}$

Table II

Experimental results of equilibrium measurements
(new method)

$[HL] \cdot 10^2 F$	pH	D
1	2.96	$1.00 \cdot 10^2$
2	2.80	$2.97 \cdot 10^1$
3	2.72	$1.56 \cdot 10^2$
4	2.68	$1.05 \cdot 10^1$
6.5	2.67	$7.31 \cdot 10^0$
10	2.66	$5.50 \cdot 10^0$
18	2.58	$1.66 \cdot 10^0$
25	2.55	$8.64 \cdot 10^{-1}$
37	2.54	$3.75 \cdot 10^{-1}$
63	2.53	$1.36 \cdot 10^{-1}$
87	2.52	$5.40 \cdot 10^{-2}$
117	2.50	$2.51 \cdot 10^{-2}$
143	2.49	$1.29 \cdot 10^{-2}$
195	2.48	$5.35 \cdot 10^{-3}$
300	2.46	$1.26 \cdot 10^{-3}$

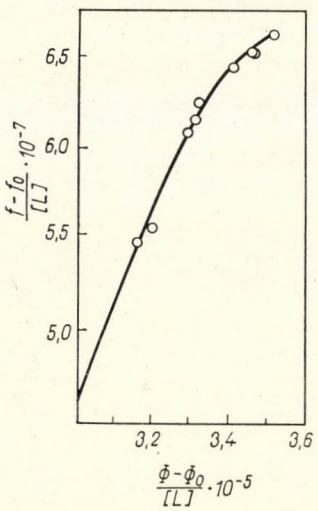

Fig. 4. $\frac{f - f_0}{[L]}$ as a function of $\frac{\Phi - \Phi_0}{[L]}$ calculated according to Eq. (5), using the data of Table I

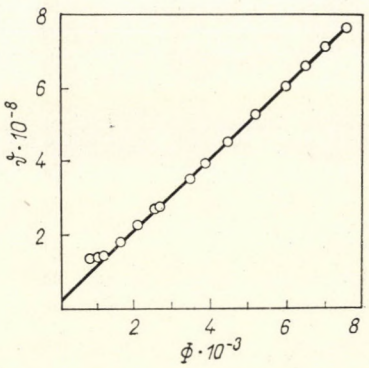

Fig. 5. ϑ as a function of Φ, calculated according to Eq. (6), using the data of Table I

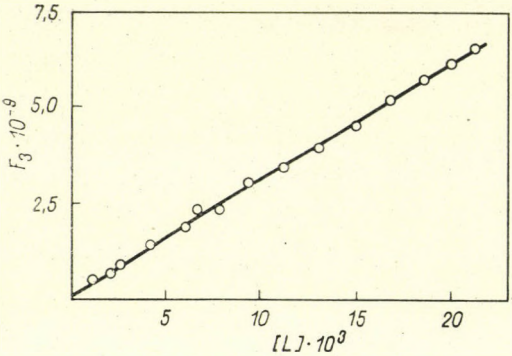

Fig. 6. F_3 as a function of the free ligand concentration, calculated according to Eqs (6) and (8), using the data of Table I

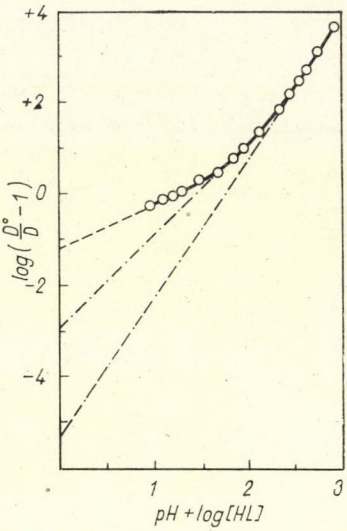

Fig. 7. $\log\left(\frac{D^\circ}{D}-1\right)$ as a function of $\{pH + \log w[HL]\}$, calculated according to Eq. (14), using the data of Table II

Finally, using Eq. (8), form the straight line drawn in Fig. 6, β_3 was found to be $3.47 \cdot 10^8$.

When the other method of calculation was employed, the graphic representation of Eq. (14) directly resulted in Fig. 7, from which the interactions referring to slopes 1, 2 and 3 yielded $\log K_{e1} = -1.24$, $\log K_{e2} = -2.91$ and $\log K_{e3} = -5.31$; substituting these into Eq. (18), the values $\log \beta_1 = 2.70$, $\log \beta_2 = 4.97$ and $\log \beta_3 = 6.51$ were obtained.

The results of the two methods and those published by different authors are summarized in Table III. The best agreement was found with the data of CHOPPIN and CHOPOORIAN [6]; the discrepancies among the present results

Table III

Formation constants of α-hydroxyisobutyrate complexes of europium

$\log K_1$	$\log K_2$	$\log K_3$	Experimental (calculation) method	Reference
2.72	2.36	1.32	ion exchange	[4]
2.71	2.22	0.98	pot. metr. titr.	[5]
2.70	2.24	1.58	pot. metr. titr.	[6]
2.70	2.28	1.56	ion exchange, Fronaeus method	present work
2.70	2.27	1.54	ion exchange, new method	present work

and other data of the literature (with the exception of log K_3 values) are also slight.

The present work has shown that liquid ion exchangers can be conveniently used for the precise determination of successive formation constants.

Main symbols used

D°	Distribution ratio in the absence of complexing agent
D	Distribution ratio in the presence of complexing agent
[HL]	Analytical concentration of the complexing agent (α-hydroxyisobutyric acid
i	Stoichiometric coefficient
K_i	Successive formation constant of the species $[ML_i]$
K_e	Stoichiometric equilibrium constant as defined in Eq. (11)
[L]	Ligand (free ligand) concentration
M	Metal
N	Maximum coordination number
pK_d	Negative logarithm of the dissociation constant of the complexing agent
β_i	Overall formation constant of the species $[ML_i]$
	Indices
w	Aqueous phase
o	Organic phase

SUMMARY

Using the liquid ion exchanger di-2-ethylhexyl-phosphoric acid, the successive formation constants for the α-hydroxyisobutyrate complexes of europium have been determined. The Fronaeus method and another type of calculation yielded the values $\log K_1 = 2.70$, $\log K_2 = 2.27$ and $\log K_3 = 1.55$, in reasonably good agreement with the literature data.

REFERENCES

1. Lengyel, T., Törkő, J.: Acta Chim. Acad. Sci. Hung. **54,** 27 (1967)
2. Fronaeus, S.: Acta Chem. Scand. **5,** 859 (1951)
3. Fronaeus, S.: Svensk. Kem. Tidskr. **65,** 19 (1953)
4. Lyle, S. J., Naqvi, S. J.: J. Inorg. Nucl. Chem. **28,** 2993 (1966)
5. Stagg, W. R., Powell, J. E.: USAEC Rep. IS-727 (Washington) 1963
6. Choppin, G. R., Chopoorian, J. A.: J. Inorg. Nucl. Chem. **22,** 97 (1961)
7. Rossotti, F. J. C., Rossotti, H.: The Determination of Stability Contants. McGraw-Hill, New York, 1961
8. Smith, H. L., Hoffman, D. C.: J. Inorg. Nucl. Chem. **3,** 243 (1956)

Tamás Lengyel; Budapest, XII. Konkoly Thege u.

Acta Chimica Academiae Scientiarum Hungaricae Tomus 57 (3), pp. 301—311 (1968)

ÜBER DEN WANDERUNGSMECHANISMUS VON WASSERSTOFF- UND HYDROXYLIONEN, VIII

EINFLUß DER ZUSAMMENSETZUNG VON GLYCERIN–WASSER-GEMISCHEN AUF DIE ELEKTRISCHE LEITFÄHIGKEIT UND VISKOSITÄT VON GELÖSTEM HCl, KOH, KF UND KCl BEI 5 UND 25 °C

T. ERDEY-GRÚZ and E. KUGLER

(Institut für Physikalische Chemie und Radiologie der Eötvös Loránd Universität, Budapest)

Eingegangen am 16. Oktober 1967

Im Rahmen unserer Studien über den Ionenwanderungsmechanismus soll nun im Anschluß an unsere Untersuchungen über die Leitfähigkeit einiger Elektrolyte in Gemischen von ein- und zweiwertigen Alkoholen und Wasser [1—3] über unsere Messungen in Gemischen von Wasser und Glycerin als dreiwertiger Alkohol berichtet werden.

Die Leitfähigkeit der Lösungen von HCl in Glycerin–Wasser-Gemischen wurde bis zu einem Glyceringehalt von etwa 35 Mol% von DNEPROW [4], CONWAY und Mitarbeitern [5] sowie von WOOLF [6] untersucht. Die Leitfähigkeit von KCl in Glycerin und Glycerin–Wasser-Gemischen haben ACCASCINA und D'APRANO [7] bestimmt. Diese Daten sind jedoch zum systematischen Studium des prototropen Wanderungsmechanismus unzulänglich, und demzufolge wurden auf Grund der in unseren früheren Mitteilungen dargelegten Gesichtspunkte die Leitfähigkeit und die Viskosität von in Glycerin–Wasser-Gemischen gelöstem HCl, KOH, KCl und KF, bei einer Konzentration von 0,01 *n*, bei 5 und 25 °C, bestimmt.

Experimenteller Teil

Zur Messung der Leitfähigkeit und der Viskosität der Lösungen wurden die in den vorangehenden Mitteilungen beschriebenen Einrichtungen benützt. Die gelösten Stoffe wurden auf die beschriebene Weise gereinigt [1, 2].

Die Reinigung des Glycerins erfolgte durch wiederholte fraktionierte Destillation des analytisch reinen Ausgangstoffes im Vakuum. Die spezifische Leitfähigkeit des so erhaltenen Glycerins betrug $8—10 \cdot 10^{-9}$ ohm^{-1} cm^{-1}. Sein Wassergehalt wurde mit dem Fischer-Reagens bestimmt.

Die Versuchsergebnisse

Leitfähigkeit

Die Ergebnisse der Leitfähigkeitsmessungen sind in Abb. 1 zusammengefaßt.

Die Äquivalentleitfähigkeit des in Glycerin gelösten HCl wird durch Zugabe von geringen Wassermengen wesentlich herabgesetzt und durchläuft bei etwa 8 Mol% Wassergehalt bei beiden untersuchten Temperaturen ein Minimum. In Lösungen die mehr als 40 Mol% Wasser enthalten, nimmt die Leitfähigkeit bis zur Erreichung des der wäßrigen Lösung entsprechenden Wertes steil zu.

Die Leitfähigkeiten der KOH-, KCl- und KF-Lösungen nehmen in Gemischen mit niedrigem Wassergehalt mit steigenden Wassergehalten in der

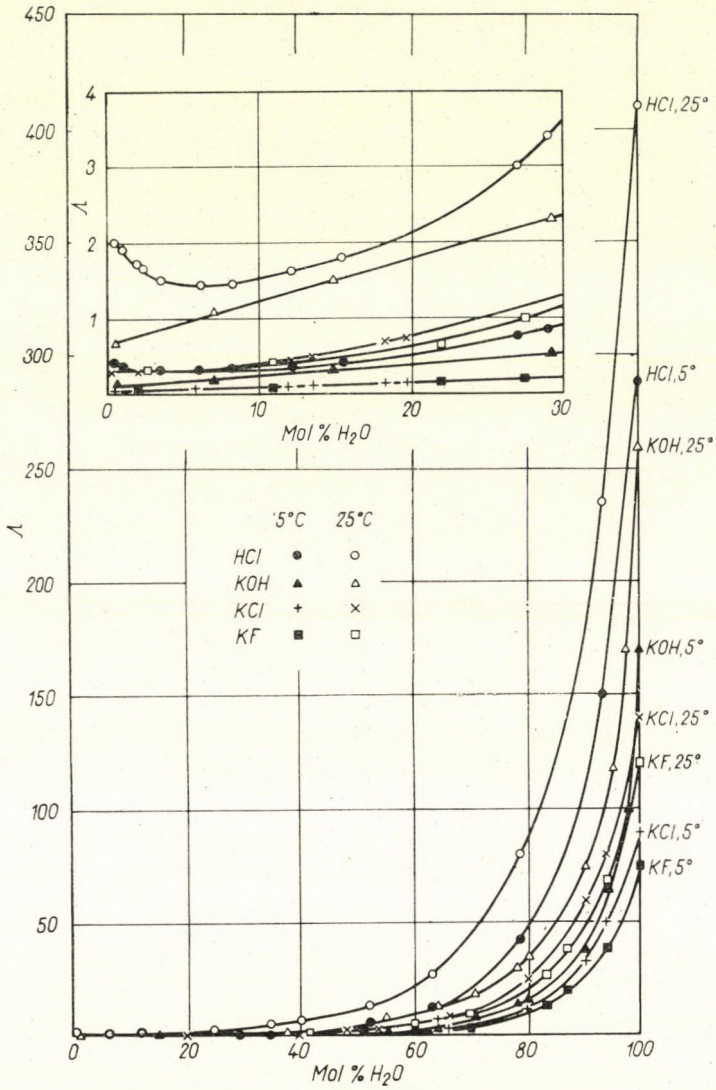

Abb. 1. Äquivalentleitfähigkeit von 0,01 *n* HCl-, KOH-, KCl- und KF-Lösungen in Glycerin–Wasser-Gemischen bei 5 und 25 °C in Abhängigkeit vom Wassergehalt

Reihenfolge der in wäßriger Lösung gemessenen Leitfähigkeiten langsam zu. Diese Zunahme der Leitfähigkeit wird bei KOH-Lösungen von einem Wassergehalt von etwa 40 und KCl- und KF-Lösungen von einem Wassergehalt von

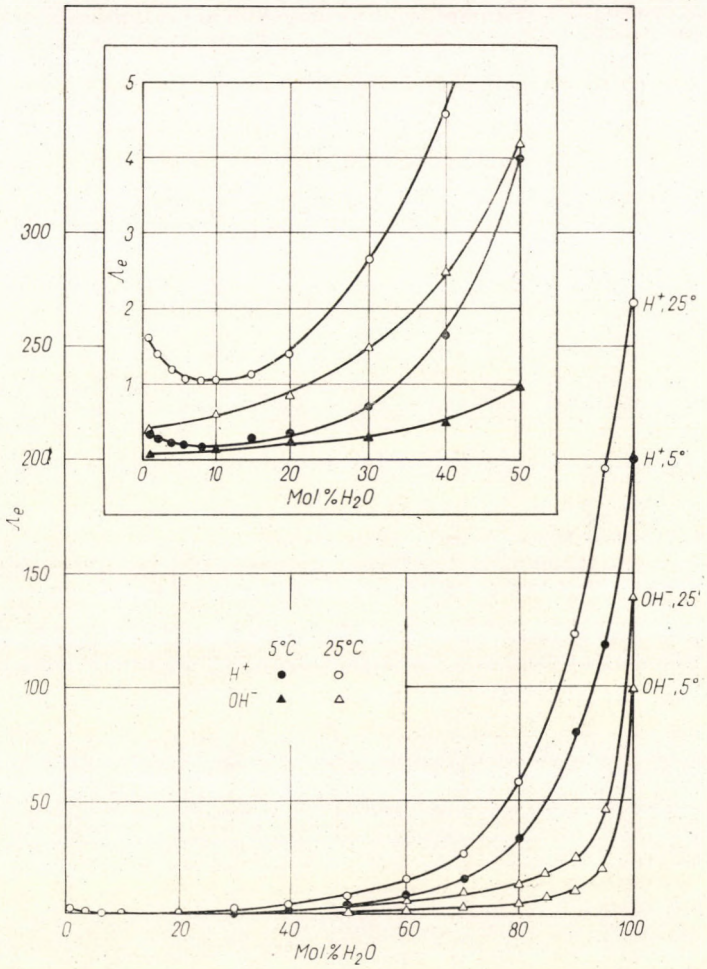

Abb. 2. Extraleitfähigkeit von Wasserstoff- und Hydroxylionen in Glycerin–Wasser-Gemischen bei 5 und 25 °C in Abhängigkeit vom Wassergehalt

etwa 60 Mol% angefangen bis zum Erreichen des Wertes für wäßrige Lösungen steiler.

Auf Grund der gemessenen Leitfähigkeitswerte durchläuft der vom Protonenübergang stammende Teil der Leitfähigkeit der Wasserstoffionen, die Extraleitfähigkeit, ($\Lambda_{e,H^+} = \Lambda_{HCl} - \Lambda_{KCl}$) bei beiden untersuchten Temperaturen in Lösungen von etwa 10 Mol% Wassergehalt ein flaches Minimum (Abb. 2).

Die Extraleitfähigkeit des Hydroxylions ($\Lambda_{e,OH^-} = \Lambda_{KOH} - \Lambda_{KF}$) steigt bis zu einem Wassergehalt von etwa 30 Mol% nur gering an, und von 70 Mol% Wassergehalt angefangen steil bis zu dem der wäßrigen Lösung entsprechenden Wert (Abb. 2.)

Die Temperaturkoeffizienten* der gemessenen Leitfähigkeit sind in Abb. 3 dargestellt.

Der Temperaturkoeffizient der Leitfähigkeit von HCl-Lösungen weist in Gemischen von etwa 4 Mol% Wassergehalt ein ziemlich scharfes Maximum auf. Der Temperaturkoeffizient der KOH-Lösungen nimmt mit steigendem Wassergehalt monoton ab. Der KOH-Koeffizient weicht bei einer Gemischzusammensetzung bei welcher der Tempereturkoeffizient der HCl-Lösungen ein Maximum aufweist, kaum von dem des HCl ab. In Lösungen mit einem Wassergehalt von weniger als etwa 66 Mol% ist der Temperaturkoeffizient der Leitfähigkeit der KOH-Lösungen kleiner, in Lösungen mit höherem Wassergehalt hingegen größer, als der der KCl- und KF-Lösungen. In Gemischen von mehr als etwa 95 Mol% Wassergehalt nimmt der Temperaturkoeffizient der KOH-Leitfähigkeit bis zu dem in wäßriger gemessenen Wert steil ab.

Der Temperaturkoeffizient der Leitfähigkeit von KCl- bzw. KF-Lösungen nimmt mit steigendem Wassergehalt monoton ab.

In Abb. 4 sind, auf Grund des Zusammenhangs $\Lambda = Ae^{-E/RT}$ berechnet, die Aktivierungsenergien der Leitfähigkeit der untersuchten Elektrolyten in Abhängigkeit vom Wassergehalt dargestellt. Im Falle von HCl besitzt die Aktivierungsenergie bei 4 Mol% Wassergehalt einen Höchstwert, um dann bis zu dem der wäßrigen Lösung entsprechenden Wert monoton abzunehmen. Die Aktivierungsenergie der Leitfähigkeit von KOH, KCl und KF nimmt mit steigendem Wassergehalt monoton ab. Die Aktivierungsenergie von KOH ist unterhalb eines Wassergehalts von 66 Mol% und über einem Wassergehalt von 95 Mol% kleiner, in Lösungen mit Wassergehalten zwischen diesen beiden Werten hingegen größer, als die Aktivierungsenergie von KCl und KF.

Viskosität

Die Viskositäten der Glycerin–Wasser-Gemische sowie der Lösungen der untersuchten Elektrolyten in diesen Gemischen nehmen vom Wert des reinen Glycerins bis zum Wert des Wassers monoton ab. Aus den bei 5 und 25 °C gemessenen Werten berechnet, nimmt der Temperaturkoeffizient der Viskosität mit steigendem Wassergehalt monoton ab, und ist größer, als der Temperaturkoeffizient der Leitfähigkeit der untersuchten Elektrolyte in den entsprechenden Gemischen (Abb. 3).

* $\alpha_\Lambda = \frac{1}{\Lambda_k} \frac{\Delta\Lambda}{\Delta T} 100$, wo $\Lambda_k = \frac{\Lambda_{25°} - \Lambda_{5°}}{2}$

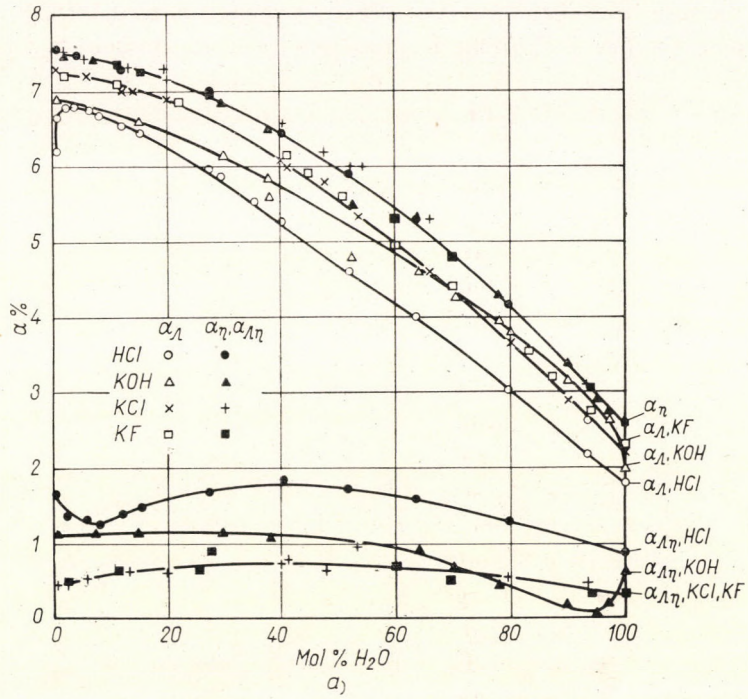

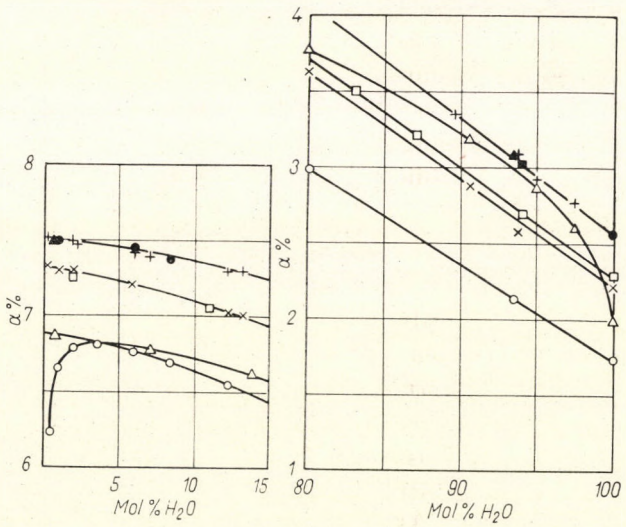

Abb. 3. Temperaturkoeffizient der in Glycerin–Wasser-Gemischen bei 5 und 25 °C gemessenen Äquivalentleitfähigkeit, Viskosität und des $\Lambda\eta$-Produktes in Abhängigkeit vom Wassergehalt

Die auf Grund des Zusammenhangs $\eta = Be^{E/RT}$ berechnete Aktivierungsenergie nimmt mit steigendem Wassergehalt monoton ab (Abb. 4). Die Aktivierungsenergie der Viskosität ist für jedes der untersuchten Elektrolyte größer als die Aktivierungsenergien der Leitfähigkeit.

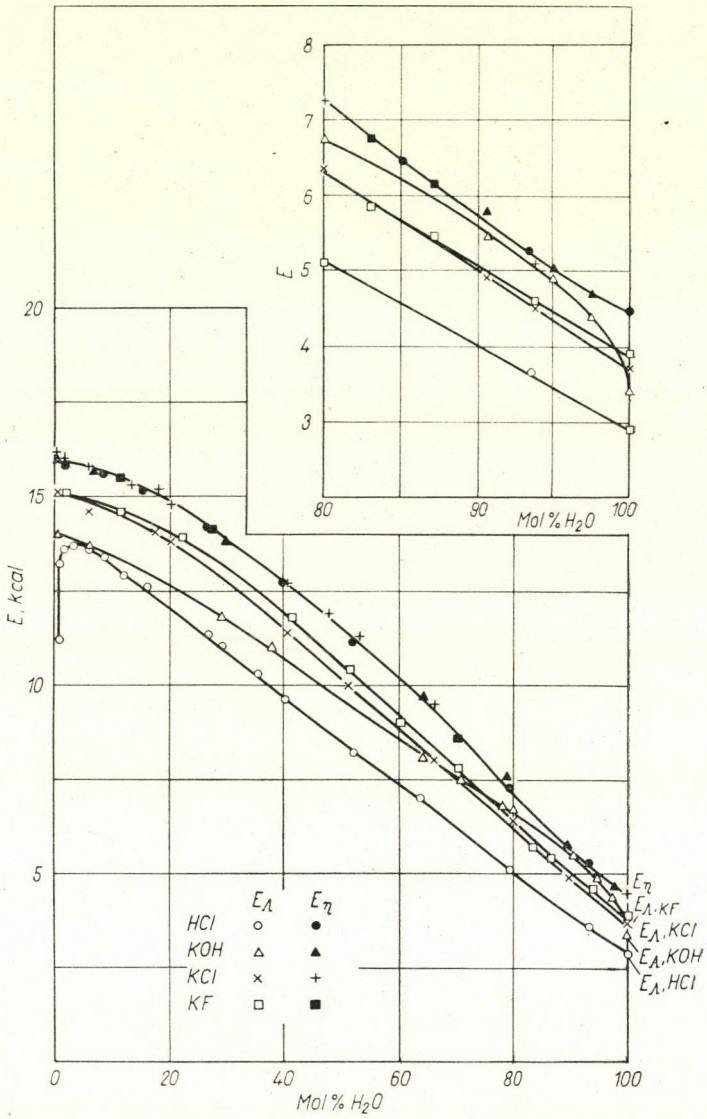

Abb. 4. Änderung der Aktivierungsenergien der Leitfähigkeit und der Viskosität in Glycerin–Wasser-Lösungen von HCl, KOH, KCl und KF mit dem Wassergehalt

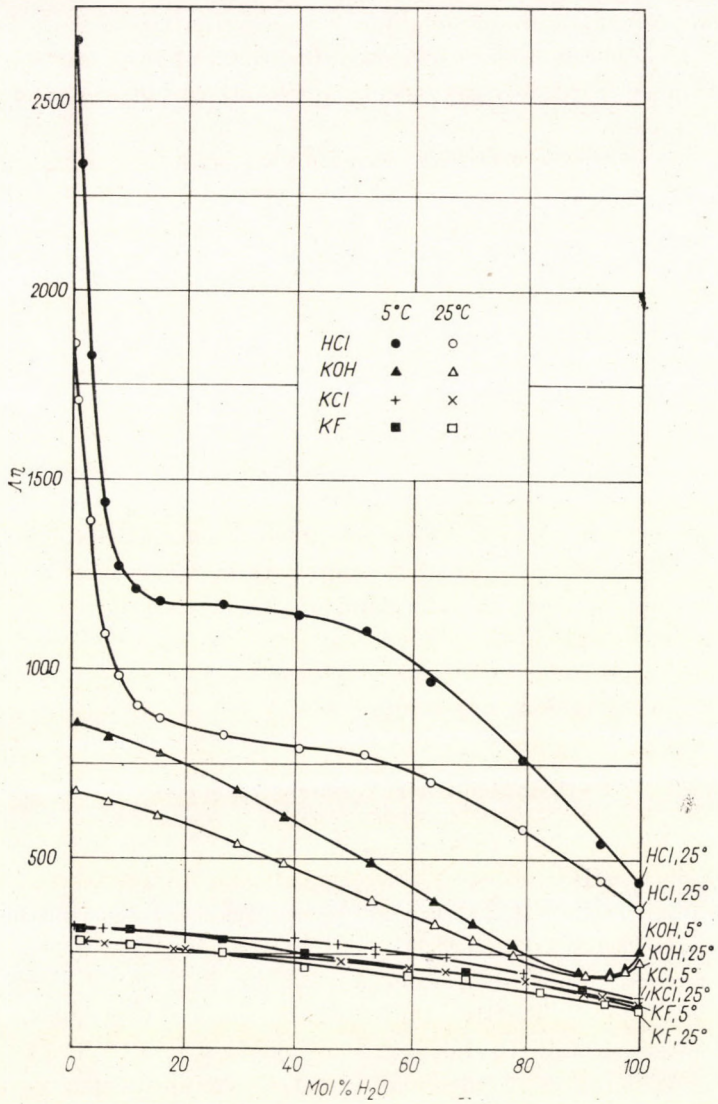

Abb. 5. Die Änderung des $\Lambda\eta$-Produktes von HCl, KOH KCl und KF in Glycerin–Wasser-Gemischen in Abhängigkeit vom Wassergehalt, bei 5 und 25 °C

Λη-Produkt

Das Produkt der Äquivalentleitfähigkeit und der Viskosität der untersuchten Elektrolyte ist als Funktion des Wassergehaltes bei 5 und 25 °C in Abb. 5. gezeigt.

Das $\Lambda\eta$-Produkt der Lösungen von HCl in Glycerin ist bei beiden Temperaturen bedeutend größer, als in wäßrigen Lösungen. In Gemischen mit

niedrigem Wassergehalt nimmt sein Wert steil ab. Im Bereich zwischen 15 und 50 Mol% Wassergehalt ändert sich das $\Lambda\eta$-Produkt kaum, um dann von 50 Mol% angefangen fast linear bis zu dem der wäßrigen Lösung entsprechenden Wert abzunehmen.

Das $\Lambda\eta$-Produkt des KOH ist wesentlich höher im Glycerin als im Wasser. Mit ansteigendem Wassergehalt nimmt das $\Lambda\eta$-Produkt ab und erreicht bei 95 Mol% Wassergehalt bei beiden untersuchten Temperaturen ein deutliches Minimum. Beim Minimum weichen die Werte der $\Lambda\eta$-Produkte für die beiden Temperaturen kaum voneinander ab.

In KCl- und KF-Lösungen nimmt das $\Lambda\eta$-Produkt von dem der Glycerinlösung entsprechenden Wert mit steigendem Wassergehalt langsam monoton, bis zu dem der wäßrigen Lösung entsprechenden Wert ab.

In sämtlichen untersuchten Elektrolytlösungen ist das $\Lambda\eta$-Produkt bei 5 °C größer als bei 25 °C. Bei HCl-Lösungen durchläuft der Temperaturkoeffizient des $\Lambda\eta$-Produkts in Lösungen mit 4 Mol% Wassergehalt ein Minimum, in Lösungen mit etwa 40 Mol% Wassergehalt hingegen ein Maximum (Abb. 3). Im Falle von KOH ändert sich der Temperaturkoeffizient in Lösungen von weniger als 50 Mol% Wassergehalt kaum; in Lösungen von 92 Mol% Wassergehalt weist der Temperaturkoeffizient ein Minimum mit sehr niedrigem Wert auf. Der Temperaturkoeffizient des $\Lambda\eta$-Produkts von KCl und KF ändert sich mit dem Wassergehalt nur wenig.

Diskussion der Versuchsergebnisse

Die Änderung der Äquivalentleitfähigkeit des in Glycerin–Wasser-Gemischen gelösten HCl mit dem Wassergehalt läßt darauf schließen, daß die in Lösungen mit hohem Glyceringehalt vorliegenden Glycerinoxoniumionen ($CH_2OH-CHOH-CH_2OH_2^+$, $CH_2OH_2^+-CHOH-CH_2OH_2^+$) den Strom nicht nur durch hydrodynamische Wanderung, sondern auch durch Protonenübergang leiten, ähnlich wie die OH_3^+-Ionen in wäßriger Lösung oder in Lösungen mit hohem Wassergehalt. In Lösungen mit minimaler Leitfähigkeit sind die Umstände sowohl für die Hydroxonium- als auch für die Glycerinoxoniumionen am ungünstigsten, und der prototrope Wanderungsmechanismus spielt hier im Stromtransport die geringste Rolle.

Der Wert des $\Lambda\eta$-Produktes ist in Glycerin wesentlich höher als in Wasser. Sein steiler Anstieg in Lösungen mit niedrigem Wassergehalt weist darauf hin, daß die Wasserstoffionen in solchen Lösungen überwiegend in Form von Glycerinoxoniumionen vorliegen, und die Beteiligung dieser Ionen an der Leitung viel größer ist, als in wäßrigen Lösungen. Dies wird auch durch die Tatsache bestätigt, daß die Überführungszahl der Wasserstoffionen in Glycerin höher ist, als in Wasser [8]. Die starke prototrope Leitung kann damit erklärt werden, daß im Glycerinoxoniumion mehr Protonen austauschfähig sind, als

im Hydroxoniumion, wodurch die auf die Leitfähigkeit in entgegengesetzter Richtung wirkende hohe Viskosität überkompensiert wird.

Das $\Lambda\eta$-Produkt ist auch für KCl und KF in Glycerinlösungen größer als in Wasser (Abb. 5). Hieraus kann auf die Auflockerung der Flüssigkeitsstruktur durch die Ionenkraftfelder geschlossen werden. Diese Wirkung gelangt jedoch mit steigendem Glyceringehalt nur allmählich zu Geltung, so daß sie keine plötzliche große Änderung hervorruft.

Offensichtlich tritt die in der unmittelbaren Umgebung der Ionen zustandekommende strukturlockernde Wirkung auch im Falle der Wasserstoffionen auf, was nach je einem Protonenübergang die für den nächsten Übergang günstige Drehung des Lösungsmittelmoleküls erleichtern würde, deren Geschwindigkeit nach der Theorie von CONWAY, BOCKRIS und LINTON [6] für die prototrope Leitung determinierend ist. Es ist jedoch kaum anzunehmen, daß dieser Drehung im Falle der nicht kugelsymmetrischen Glycerinmoleküle eine bedeutende Rolle zukommt. Es dürfte wahrscheinlicher sein, daß die Struktur des Glycerins einen sich fortpflanzenden Protonenübergang ohne Drehung der Moleküle zuläßt. Damit wäre es zu erklären, daß die Leitfähigkeit von Wasserstoffionen in Glycerin relative größer ist, als dies auf Grund der hohen Viskosität im Vergleich zu der in Äthylenglykol gemessenen Leitfähigkeit [3] zu erwarten wäre.

Das $\Lambda\eta$-Produkt von KOH ist in Glycerin bedeutend größer als in wäßriger Lösung. Wenn man dazu noch bedenkt, daß auch die Überführungszahl der Hydroxylionen in Glycerinlösung erfahrungsgemäß [8] höher als in Wasser ist, liegt es auf der Hand, daß in Glycerin auch ein Protonenübergang nach dem Schema

$$RO^- + ROH \rightleftharpoons ROH + RO^-$$

möglich ist. Es scheint daher wahrscheinlich zu sein, daß in Glycerin sowohl die ROH_2^+ — als auch die RO^--Ionen zu einem Protonenaustausch fähig sind, ähnlich wie OH_3^+ — und OH^--Ionen in wäßriger Lösung. Diese Folgerung wird auch durch unsere Untersuchungen im zweiwertigen Alkohol Äthylenglykol [3] bestätigt, bei denen für das $\Lambda\eta$-Produkt von KOH und für die Überführungszahl des Hydroxylions annähernd der gleiche Wert gefunden wurde, wie in wäßriger Lösung. Wenn wir diese Annahme mit den Ergebnissen der in einwertigen Alkoholen durchgeführten Untersuchungen vergleichen [1, 2] — bei denen wir im Einklang mit Resultaten anderer Forscher [9] zu der Feststellung gelangten, daß die Hydroxylionen in KOH-Lösungen hydrodynamisch leiten —, erscheint es wahrscheinlich zu sein, daß die größere Zahl der Hydroxylgruppen und infolgedessen die einen rotationsfreien Protonenübergang ermöglichende Flüssigkeitsstruktur günstige Verhältnisse für den Protonenübergang und für das Zustandekommen von RO^--Ionen schafft.

Wenn zu einer Lösung von KOH in Glycerin Wasser gegeben wird, so nimmt das $\Lambda\eta$-Produkt monoton ab, was darauf hinweist, daß sich das Gleichgewicht

$$RO^- + H_2O \rightleftarrows ROH + OH^-$$

mit steigendem Wassergehalt nur allmählich nach rechts verschiebt, da die Protonenaffinität des Wassers größer ist als die des Alkohols. Die RO^--Ionen leiten jedoch auch bei der gestörten Alkoholstruktur nach einem prototropen Mechanismus, während die Hydroxylionen überwiegend hydrodynamisch wandern. Mit steigender Wasserkonzentration ändert sich — der Änderung der Flüssigkeitsstruktur und der Verschiebung des Gleichgewichts entsprechend — auch die Beteiligung der RO^-- und OH^--Ionen an der prototropen Leitung, die dann bei einem Wassergehalt von etwa 95 Mol% ein Minimum erreicht. Eine weitere Erhöhung des Wassergehaltes schafft für die prototrope Leitung der Hydroxylionen günstige Verhältnisse, und dementsprechend steigt der Wert des $\Lambda\eta$-Produktes bis zu dem der wäßrigen Lösung entsprechenden Wert an.

Wie aus Abb. 5 ersichtlich ist, nimmt das Produkt $\Lambda\eta$ der KOH-Lösungen selbst in Gemischen, die dem Minimum der prototropen Leitung entsprechen, nicht bis zu den in KCl- bzw. KF-Lösungen gefundenen Werten ab. Dies läßt auf eine die Flüssigkeitsstruktur lockernde Wirkung der Hydroxylionen schließen. In der Umgebung der Hydroxylionen nimmt die Mikroviskosität der Lösung ab, und demzufolge wird die hydrodynamische Beweglichkeit größer, als dies der Makroviskosität der Lösung entsprechen würde.

Der Unterschied zwischen der strukturlockernden Wirkung von Hydroxylionen und Fluorid- bzw. Chloridionen ist offenbar jener Tatsache zuzuschreiben, daß die Ladungsverteilung bzw. das Kraftfeld der Fluorid- bzw. Chloridionen kugelsymmetrisch ist, das des Hydroxylions hingegen wahrscheinlich nicht. Es kann daher angenommen werden, daß die aufspaltende Wirkung der Hydroxylionen auf die Wasserstoffbrücken und die Dipol-Dipol-Bindungen — die in der Gestaltung der Flüssigkeitsstruktur eine Rolle spielen — in Glycerin wesentlich stärker ist, als die der kugelsymmetrischen Fluorid- und Chloridionen.

ZUSAMMENFASSUNG

Die Äquivalentleitfähigkeit des in Glycerin gelösten HCl nimmt bei Zugabe von wenig Wasser ab, durchläuft bei 8 Mol% Wassergehalt ein Minimum, um dann wieder anzusteigen. Die Äquivalentleitfähigkeit von KOH-Lösungen ändert sich bis zu einem Wassergehalt von etwa 40 Mol%, die der KCl- und KF-Lösungen bis zu etwa 60 Mol% nur wenig, und steigt dann steiler bis zu den den wäßrigen Lösungen entsprechenden Werten an.

Das Produkt der Äquivalentleitfähigkeit und der Viskosität von in Glycerin gelöstem HCl, nimmt von einem Wert, der bedeutend größer ist als der für wäßrige Lösung, mit steigendem Wassergehalt steil ab, ändert sich im Bereich von 15 bis 50 Mol% Wassergehalt kaum und nimmt über diesem Wert fast linear ab. In KOH-Lösungen weist das $\Lambda\eta$-Produkt bei einem Wassergehalt von 95 Mol% ein Minimum auf.

Die Aktivierungsenergie der Leitfähigkeit von HCl besitzt in einer Lösung von 4 Mol% Wassergehalt ein Maximum, um dann von dem Wert von 13,8 kcal/Mol fast linear bis zu dem der wäßrigen Lösung entsprechenden Wert abzunehmen. Die Aktivierungsenergien der Leitfähigkeiten von KOH, KCl, und KF nehmen mit steigendem Wassergehalt monoton ab.

Auf Grund der Versuchsergebnisse kann festgestellt werden, daß die Glycerinoxoniumionen in Lösungen mit hohem Glyceringehalt den Strom nicht nur durch hydrodynamische Wanderung, sondern in einem bedeutenden Maße auch durch Protonenübergang leiten.

Es scheint wahrscheinlich zu sein, daß in Glycerin auch die Glycerationen zu Protonenaustausch fähig sind, ähnlich wie die Hydroxylionen in wäßriger Lösung. In der relativ starken Beweglichkeit der Hydroxylionen kommt ihrem nicht-kugelsymmetrischen Kraftfeld eine Rolle zu, sie üben eine stärkere strukturlockernde Wirkung aus, als die kugelsymmetrischen F^-- und Cl^--Ionen.

LITERATUR

1. Erdey-Grúz, T., Kugler, E. und Reich A.: Acta Chim. Acad. Sci. Hung. **13,** 428 (1958).
2. Erdey-Grúz, T., Kugler, E. und Hidvégi, J.: Acta Chim. Acad. Sci. Hung. **19,** 89 (1959).
3. Erdey-Grúz, T., Kugler, E. und Hidvégi, J.: Acta Chim. Acad.Sci.Hung. **19,** 363 (1959).
4. Dneprow, A. F.: Ucenie Zapiski, LGU, **40,** 19 (1939).
5. Conway, B. E., Bockriss, J. O'M and Linton, H.: J. Chem. Phys. **24,** 834 (1956).
6. Woolf, L. A.: J. Phys. Chem. **64,** 500 (1960).
7. Accascina, F., D'Aprano, A. und Goffredi, M.: Ricerca sci. **34,** (II-A) 443 (1964).
8. Erdey-Grúz, T., Majthényi, L. und Czakó-Nagy, I.: Acta. Chim. Acad. Sci. Hung. **53,** 28 (1967).
9. Jones, G. E. M. and Hughes, O. L.: J. Chem. Soc **1934,** 1197.
10. Barthel, J. und Schwitzgebel, G.: Z. Phys. Che'm. N. F. **54,** 181 (1967)

Tibor Erdey-Grúz
Elvira Kugler
} Budapest, VIII. Puskin u. 11/13

Acta Chimica Academiae Scientiarum Hungaricae Tomus 57 (3), pp. 313—321 (1968)

DIE KATALYTISCH KINETISCHE DEUTUNG DER SCHEINBAR REVERSIBLEN DREIECKREAKTION ERSTER ORDNUNG DER *n*-BUTENISOMERISIERUNG

D. KALLÓ

(Zentralforschungsinstitut für Chemie der Ungarischen Akademie der Wissenschaften, Budapest)

Eingegangen am 22. November 1967

1. Die formelle Dreieckreaktion

Unsere früheren Untersuchungen haben bewiesen, daß die Umwandlungen der drei *n*-Butenisomeren ineinander auf sauren Oxidkatalysatoren mit einem Dreieckreaktionsschema charakterisiert werden können, in dem die einzelnen Schritte reversibel sind [1]. Neuerdings haben wir die Umisomerisierung von *n*-Butenen auch an Kationenaustauschharzen durchgeführt [2]. Aus dem Verlauf der Konversionskurven konnten hinsichtlich der Dreieckreaktion die gleichen Schlüsse gezogen werden.

Auch bei diesen Untersuchungen haben wir eine ständige Aktivitätsabnahme des Katalysators beobachtet. Die Versuche wurden in einer statischen Gaszirkulationsapparatur [3] durchgeführt, und die Zusammensetzung des Gasgemisches von *n*-Butenen wurde von Zeit zu Zeit bestimmt. Nach etwa einer halben Stunde war die Konzentration der praktisch reinen Ausgangskomponente 1-Buten auf ca. 20% gesunken. Nach Evakuieren und Wiederauffüllen des Systems wurden die zu reproduzierenden Konversionskurven

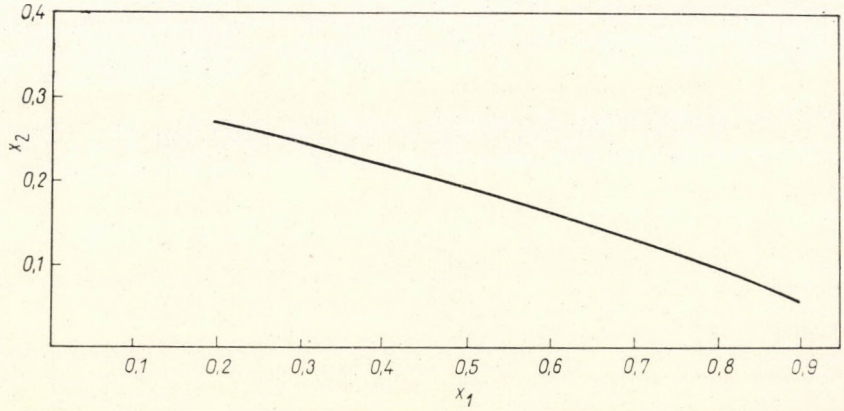

Abb. 1. Die Selektivitätskurve der *n*-Butenisomerisierung auf saurem Kationenaustauschharz »Amberlyst 15« bei 30—750 Torr und 100 °C; x_1: Molenbruch von 1-Buten, x_2: Molenbruch von *cis*-2-Buten

bestimmt. Die Neigungswinkel der einander folgenden Kurven wurden immer kleiner, weil die Aktivität des Katalysators ständig abnahm. Wenn aber die Konzentration der einen Komponente als Funktion der Konzentration der anderen, d. h. also, eine Selektivitätskurve aufgenommen wird, wie z. B. auf Abb. 1 $x_2 = f_2(x_1)$, wobei x_2 der Molenbruch der Komponente cis-2-Buten und x_1 der von 1-Buten ist, so erhält man unabhängig vom Aktivitätszustand des Katalysators den gleichen Zusammenhang zwischen diesen Größen. Es wurde ferner gefunden, daß die Änderung des Druckes (von 30 bis 750 Torr) den Verlauf der Selektivitätskurve nicht beeinflußt. Die für diesen Kontakt erhaltene Kurve läßt sich auf Grund der reversiblen Dreieckreaktion erster Ordnung folgenderweise deuten:

Die Reaktion läuft nach dem Schema 1 ab.

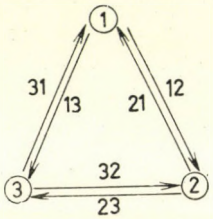

Schema 1,

wobei ① 1-Buten,
② *cis*-2-Buten und
③ *trans*-2-Buten
im gasförmigen Zustand bedeutet.

Die entsprechenden Reaktionsgeschwindigkeitsgleichungen sind:

$$-\frac{dn_1}{d\tau} = (k_{13} + k_{12})\,p_1 - k_{21}\,p_2 - k_{31}\,p_3\,, \tag{1}$$

$$-\frac{dn_2}{d\tau} = (k_{21} + k_{23})\,p_2 - k_{32}\,p_3 - k_{12}\,p_1\,, \tag{2}$$

$$-\frac{dn_3}{d\tau} = (k_{32} + k_{31})\,p_3 - k_{13}\,p_1 - k_{23}\,p_2\,, \tag{3}$$

n = Molenzahl in der Gasphase, in Mol,
τ = Kontaktzeit, in g_{Kat} s,
k = Geschwindigkeitskonstante, in Mol $Torr^{-1}$ g_{Kat}^{-1} s^{-1},
1, 2, 3 = auf 1-Buten, *cis*-2-Buten und *trans*-2-Buten hinweisende Indizes,
12, 21, 23, 32, 31, 13 = Übergänge nach dem Schema 1.

Nach Dividieren von Gl. (2) durch Gl. (1) ergibt sich:

$$\frac{dn_2}{dn_1} = \frac{(k_{21} + k_{23})\, p_2 - k_{32}\, p_3 - k_{12}\, p_1}{(k_{13} + k_{12})\, p_1 - k_{21}\, p_2 - k_{31}\, p_3} \,. \tag{4}$$

Da die Molenzahl n, der Partialdruck p bzw. der Molenbruch x während der Umwandlungen proportionale Größen sind, kann statt Gl. (4) stehen:

$$\frac{dx_2}{dx_1} = \frac{(k_{21} + k_{23})\, x_2 - k_{32}\, x_3 - k_{12}\, x_1}{(k_{13} + k_{12})\, x_1 - k_{21}\, x_2 - k_{31}\, x_3} \,. \tag{5}$$

Da alle Geschwindigkeitskonstanten (k) in Gl. (5) gleiche Dimensionen haben, läßt sich die rechte Seite der Gleichung dadurch vereinfachen, und man erhält die Differentialgleichung der Selektivitätskurve $x_2 = f_2(x_1)$ mit dimensionslosen Geschwindigkeitskonstanten (k'):

$$\frac{dx_2}{dx_1} = \frac{(k'_{21} + k'_{23})\, x_2 - k'_{32}\, x_3 - k'_{12}\, x_1}{(k'_{13} + k'_{12})\, x_1 - k'_{22}\, x_2 - k'_{31}\, x_3} \,. \tag{6}$$

Nach Dividieren des Zählers und des Nenners auf der rechten Seite der Gl. (6) durch k'_{12} erhält man die auf k'_{12} bezogenen relativen Werte der Geschwindigkeitskonstanten:

$$k''_{12} \equiv 1 \,,$$
$$k''_{23} \equiv k'_{23}/k'_{12} \text{ usw.}$$

Mit verschiedenen k''-Werten wurde Gl. (6) numerisch integriert, und letzten Endes wurden jene k''-Werte bestimmt, mit denen rechnerisch eine Kurve erhalten wird, die sich der auf Abb. 1 dargestellten experimentellen Kurve am besten annähert. Die völlig unregelmäßigen Abweichungen der Molenbrüche betrugen durchschnittlich 0,003 entlang der Selektivitätskurve $x_2 = f_2(x_1)$ im Bereich von $x_1 = 0{,}20 - 0{,}90$. Die entsprechenden relativen Geschwindigkeitskonstanten sind:

$$\begin{aligned} k''_{12} &\equiv 1 & k''_{21} &= 0{,}23 \pm 0{,}02 \\ k''_{23} &= 1{,}5 \pm 0{,}1 & k''_{32} &= 0{,}7 \pm 0{,}02 \\ k''_{31} &= 0{,}17 \pm 0{,}02 & k''_{13} &= 1{,}5 \pm 0{,}1 \end{aligned} \tag{7}$$

die — wie gezeigt wurde — im ganzen Konversionsbereich gültig sind. (Trotz der guten Übereinstimmung der gemessenen und berechneten Kurven sind die erhaltenen Geschwindigkeitskonstanten mit beträchtlichen Ungewißheiten behaftet, weil die Selektivitätskurve ziemlich charakterlos ist.) Das weist darauf hin, daß die Gültigkeit der formellen Dreieckreation für diese Isomerisierung hinsichtlich der Selektivität als bewiesen betrachtet werden kann.

2. Sternschema der katalytischen Reaktion

Alldiese Behauptungen sind selbstverständlich nur gültig, wenn die Kinetik der *n*-Butenisomerisierung phänomenologisch betrachtet wird. Die Umsetzungen sind aber Ergebnisse katalytischer Vorgänge, bei denen bekanntlich drei Teilprozesse nacheinander ablaufen: die Absorption, die Oberflächenreaktion und die Desorption.

Das würde auf Grund des phänomenologischen Dreieckschema folgendes bedeuten:

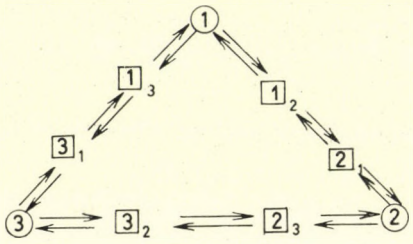

Schema 2,

wobei □ auf den adsorbierten Zustand hinweist.

Nach diesem Schema sollte also jedes einzelne Isomere in zwei adsorbierten Zuständen vorkommen bzw. sollte zwischen sechserlei Formen von adsorbierten *n*-Buten unterschieden werden können. Diese Annahme scheint kaum haltbar zu sein, weil die an Brönstedschen sauren Zentren adsorbierten *n*-Butenisomeren als *n*-Butylcarboniumionen mit der gleichen chemischen Formel zu betrachten sind [4]:

$$\left.\begin{array}{l} CH_2{=}CH{-}CH_2{-}CH_3 \\ CH_3{\diagdown}CH{=}CH{\diagup}CH_3 \\ CH_3{\diagdown}CH{=}CH{\diagdown}CH_3 \end{array}\right\} + H^+\,Kat^- \rightleftarrows CH_3{-}{}^+CH{-}CH_2{-}CH_3 \cdot Kat^- .$$

Nach dieser Formulierung sind nur Einzelbindungen vorhanden, und deshalb ist es sehr unwahrscheinlich, daß sich die aus den verschiedenen Isomeren gebildeten *n*-Butylcarboniumionen im stabilen, nicht aktivierten Zustand voneinander unterscheiden. Diese ursprüngliche Vorstellung von PINES und HAAG [4] über die Struktur von einem einheitlichen *sec*-Butylcarboniumion hat BROUWER abgelehnt [5], seine Versuchsdaten, auf die er sich gestützt hat, sind aber zu ungenau.

Wenn die drei *n*-Butenisomeren im adsorbierten Zustand die gleichen sind, ist das phänomenologische Dreieckschema durch ein der katalytischen Umwandlung angepaßtes »Stern«- oder Y-Schema zu ersetzen, nach dem die

katalytische *n*-Butenisomerisierung über das *sec*-Butylcarboniumion als gemeinsames Zwischenprodukt vor sich gehen kann:

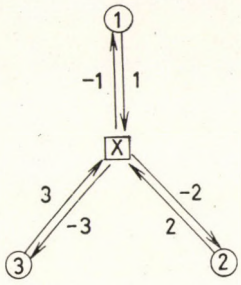

Schema 3,

wobei $\boxed{X}$ das gemeinsame Zwischenprodukt auf der Katalysatoroberfläche ist.

Der Ersatz des Schemas 2 durch das einfachere Schema 3 ergibt, daß die sog. Oberflächenreaktion völlig wegfällt, die Umwandlungen also mit der Ad- bzw. Desorption gleichzeitig stattfinden.

3. Kinetische Gleichungen der katalytischen *n*-Butenisomerisierung

Auf Grund der Gültigkeit der für das Schema 1 aufgestellten Selektivitätsgleichung (6) ist die Isomerisierung in praktisch vollen Einklang mit den Erfahrungen phänomenologisch zu deuten. Daher soll gezeigt werden, daß die formell nach dem Schema 1 ablaufende Isomerisierung kinetisch auch durch das Schema 3 widerspruchslos beschrieben werden kann.

In diesem Sinne können die Umwandlungsgeschwindigkeiten der einzelnen Isomeren wie folgt angegeben werden:

$$-\frac{dn_1}{d\tau} = k_1 (c_0 - c_X) p_1 - k_{-1} c_X , \tag{8}$$

$$-\frac{dn_2}{d\tau} = k_2 (c_0 - c_X) p_2 - k_{-2} c_X , \tag{9}$$

$$-\frac{dn_3}{d\tau} = k_3 (c_0 - c_X) p_3 - k_{-3} c_X , \tag{10}$$

n = Molenzahl in der Gasphase, in Mol,
τ = Kontaktzeit, in g_{Kat} s,
k_1, k_2, k_3 = Geschwindigkeitskonstanten, in $Torr^{-1}\ s^{-1}$,
k_{-1}, k_{-2}, k_{-3} = Geschwindigkeitskonstanten, in s^{-1},
c_0 = Anzahl der aktiven Zentren, in Mol g_{Kat}^{-1},
c_X = Oberflächenkonzentration des Zwischenprodukts X, in Mol g_{Kat}^{-1},
1, 2, 3, −1, −2, −3 = Übergänge nach dem Schema 3.

Aus der Stöchiometrie des Prozesses folgt ferner, daß

$$\frac{dn_X}{d\tau} = -\left(\frac{dn_1}{d\tau} + \frac{dn_2}{d\tau} + \frac{dn_3}{d\tau}\right) = -\frac{dn_g}{d\tau} \tag{11}$$

ist, wobei n_X die Molenzahl von X, in Mol und n_g die Molenzahl in der Gasphase, in Mol, bedeutet. Aus den Gl.-en (8), (9), (10), (11) ist c_X auszudrücken:

$$c_X = \frac{(k_1 p_1 + k_2 p_2 + k_3 p_3)\, c_0 - \dfrac{dn_X}{d\tau}}{k_1 p_1 + k_2 p_2 + k_3 p_3 + k_{-1} + k_{-2} + k_{-3}} \tag{12}$$

und als nicht gemessene Größe zu eliminieren. So erhält man nach gewisser Umordnung die Geschwindigkeitsgleichungen wie folgt:

$$-\frac{dn_1}{d\tau} = \left[(k_1 k^*_{-3} + k_1 k^*_{-2})\, c_0 p_1 - k_2 k^*_{-1} c_0 p_2 - k_3 k^*_{-1} c_0 p_3\right] \times$$
$$\times \left(1 - \frac{k_1 p_1 + k_2 p_2 + k_3 p_3}{k_1 p_1 + k_2 p_2 + k_3 p_3 + k_{-1} + k_{-2} + k_{-3}}\right) +$$
$$+ \frac{k_1 p_1 + k_{-1}}{k_1 p_1 + k_2 p_2 + k_3 p_3 + k_{-1} + k_{-2} + k_{-3}} \frac{dn_X}{d\tau}, \tag{13}$$

$$-\frac{dn_2}{d\tau} = \left[(k_2 k^*_{-1} + k_2 k^*_{-3})\, c_0 p_2 - k_3 k^*_{-2} c_0 p_3 - k_1 k^*_{-2} c_0 p_1\right] \times$$
$$\times \left(1 - \frac{k_1 p_1 + k_2 p_2 + k_3 p_3}{k_1 p_1 + k_2 p_2 + k_3 p_3 + k_{-1} + k_{-2} + k_{-3}}\right) +$$
$$+ \frac{k_2 p_2 + k_{-2}}{k_1 p_1 + k_2 p_2 + k_3 p_3 + k_{-1} + k_{-2} + k_{-3}} \frac{dn_X}{d\tau}, \tag{14}$$

$$-\frac{dn_3}{d\tau} = \left[(k_3 k^*_{-2} + k_3 k^*_{-1})\, c_0 p_3 - k_1 k^*_{-3} c_0 p_1 - k_2 k^*_{-3} c_0 p_2\right] \times$$
$$\times \left(1 - \frac{k_1 p_1 + k_2 p_2 + k_3 p_3}{k_1 p_1 + k_2 p_2 + k_3 p_3 + k_{-1} + k_{-2} + k_{-3}}\right) +$$
$$+ \frac{k_3 p_3 + k_{-3}}{k_1 p_1 + k_2 p_2 + k_3 p_3 + k_{-1} + k_{-2} + k_{-3}} \frac{dn_X}{d\tau}, \tag{15}$$

wobei

$$k^*_{-1} = \frac{k_{-1}}{k_{-1} + k_{-2} + k_{-3}} \qquad \text{ohne Dimension,}$$

$$k^*_{-2} = \frac{k_{-2}}{k_{-1} + k_{-2} + k_{-3}} \qquad \text{ohne Dimension,}$$

$$k^*_{-3} = \frac{k_{-3}}{k_{-1} + k_{-2} + k_{-3}} \qquad \text{ohne Dimension,}$$

die Desorptionswahrscheinlichkeiten von X in 1, 2 und 3 sind.

Den Erfahrungen nach können die zweiten Glieder der rechten Seite der Gl.-en (13), (14) und (15) vernachlässigt werden. Die Versuche wurden in einer statischen, geschlossenen Gaszirkulationsapparatur (s. unter 1) durchgeführt, in der die Molenzahländerungen der einzelnen Isomeren in der Gasphase den Änderungen der betreffenden Partialdrücke bzw. die Gesamtmolenzahländerung $[-dn_g = dn_\times$, s. Gl. (11)] der Gesamtdruckänderung entsprechen. Der Gesamtdruck blieb in der Versuchszeit innerhalb der Meßgenauigkeit (± 1 Torr) konstant, während sich die Partialdrücke in der Größenordnung von 100 Torr änderten. Wenn demnach Gl. (14) durch Gl. (13) dividiert wird, und die zur Gl. (5) benötigten Voraussetzungen angenommen werden, so erhält man:

$$\frac{dx_2}{dx_1} = \frac{(k_2 k^*_{-1} + k_2 k^*_{-3})\, x_2 - k_3 k^*_{-2}\, x_3 - k_1 k^*_{-2}\, x_1}{(k_1 k^*_{-3} + k_1 k^*_{-2})\, x_1 - k_2 k^*_{-1}\, x_2 - k_3 k^*_{-1}\, x_3} \,. \tag{16}$$

Auf der rechten Seite der Gl. (16) ist die Vereinfachung durch die Dimension von k_1, k_2 bzw. k_3 ermöglicht, und so ergibt sich die Differentialgleichung der Selektivitätskurve $x_2 = f_2(x_1)$:

$$\frac{dx_2}{dx_1} = \frac{(k'_2 k^*_{-1} + k'_2 k^*_{-3})\, x_2 - k'_3 k^*_{-2}\, x_3 - k'_1 k^*_{-2}\, x_1}{(k'_1 k^*_{-3} + k'_1 k^*_{-2})\, x_1 - k'_2 k^*_{-2}\, x_2 - k'_3 k^*_{-1}\, x_3} \,. \tag{17}$$

Die vollkommene Übereinstimmung der phänomenologisch erhaltenen Gl. (6) mit der auf Grund des Mechanismus der katalytischen Isomerisierung abgeleiteten Gl. (17) ist offensichtlich. Die dimensionslosen Geschwindigkeitskonstanten entsprechen einander auf folgende Weise:

$$\begin{aligned} k'_{12} &= k'_1 k^*_{-1} & k'_{21} &= k'_2 k^*_{-1} \\ k'_{23} &= k'_2 k^*_{-3} & k'_{32} &= k'_3 k^*_{-2} \\ k'_{31} &= k'_3 k^*_{-1} & k'_{13} &= k'_1 k^*_{-3} \,. \end{aligned} \tag{18}$$

Es ist bemerkenswert, daß immer Produkte der Geschwindigkeitskonstanten in bestimmter Kombination vorkommen. Diese Produkte wiederspiegeln in jedem Falle die kinetischen Konsequenzen des vorausgesetzten Sternmechanismus:

Um die Geschwindigkeiten der Umwandlung einer allein anwesenden Komponente (z.B. $x_1 = 1$) in die weiteren zwei Komponenten (2 und 3) ausdrücken zu können, muß die Adsorptionsgeschwindigkeit (k'_1) mit den den zwei Umsetzungsprodukten entsprechenden Desorptionswahrscheinlichkeiten (k^*_{-2}, k^*_{-3}) multipliziert werden. Das Produkt mit der eigenen Desorptionswahrscheinlichkeit der Komponente 1 (k^*_{-1}) würde deren Rückbildungsgeschwindigkeit ($k'_1 k^*_{-1}$) angeben, die aber eine experimentell nicht zu bestimmende Umwandlung ist.

4. Anwendung der kinetischen Gleichungen

Beim Vergleich der Gl.-en (6) und (17) zeigt sich, daß die Bestimmung der relativen Geschwindigkeitskonstanten auf Grund des Dreieckschemas 1 viel leichter ist, als auf Grund des Stern- oder Y-Schemas 3. Aus Gl.-en (18) könnten die sechs Unbekannten k'_1, k'_2, k'_3, k^*_{-1}, k^*_{-2}, k^*_{-3} in Kenntnis von k'_{12}, k'_{23}, k'_{31}, k'_{21}, k'_{32}, k'_{13} nur dann berechnet werden, wenn die sechs Gl.-en (18) unabhängig wären. Das ist aber nicht der Fall: jede der ersten fünf Gleichungen determiniert die sechste:

$$\frac{k'_1/k^*_{-1}}{k'_2/k^*_{-2}}\,\frac{k'_2/k^*_{-2}}{k'_3/k^*_{-3}}\,\frac{k'_3/k^*_{-3}}{k'_1/k^*_{-1}} = \frac{K_1}{K_2}\,\frac{K_2}{K_3}\,\frac{K_3}{K_1} =$$

$$= \frac{k'_{12}}{k'_{21}}\,\frac{k'_{23}}{k'_{32}}\,\frac{k'_{31}}{k'_{13}} = K_{12}\,K_{23}\,K_{31} = \frac{\bar{x}_2}{\bar{x}_1}\,\frac{\bar{x}_3}{\bar{x}_2}\,\frac{\bar{x}_1}{\bar{x}_3} = 1\,, \tag{19}$$

K = Gleichgewichtskonstante,
$\bar{x}$ = Molenbruch im Gleichgewicht.

Die sechste unabhängige Gleichung ist [s. die Symbole in Gl. (15)]:

$$k^*_{-1} + k^*_{-1} + k^*_{-3} = 1\,. \tag{20}$$

So können die Geschwindigkeitskonstanten für das Y-Schema mit denen für das Dreieckschema wie folgt angegeben werden:

$$\begin{aligned} k'_1 &= k'_{12} + \frac{k'_{12}\,k'_{31}}{k'_{32}} + k'_{13} \\ k'_2 &= k'_{23} + \frac{k'_{23}\,k'_{12}}{k'_{13}} + k'_{21} \\ k'_3 &= k'_{31} + \frac{k'_{31}\,k'_{23}}{k'_{21}} + k'_{32}\,. \end{aligned} \tag{21}$$

Die auf das Y-Schema gültigen Desorptionswahrscheinlichkeiten aus den auf das Dreieckschema gültigen Geschwindigkeitskonstanten zu berechnen, ist sehr kompliziert und um das zu vermeiden, werden die Ausdrücke der Desorptionswahrscheinlichkeiten in den folgenden einfacheren Formen angegeben:

$$\begin{aligned} k^*_{-1} &= \frac{k'_{31}}{k'_3} = \frac{k'_{21}}{k'_2} \\ k^*_{-2} &= \frac{k'_{12}}{k'_1} = \frac{k'_{32}}{k'_3} \\ k^*_{-3} &= \frac{k'_{23}}{k'_2} = \frac{k'_{13}}{k'_1} \end{aligned} \tag{22}$$

Die mit den in Gl-en (7) angegebenen dimensionslosen relativen Geschwindigkeitskonstanten berechneten, gleichfalls auf k'_{12} bezogenen Werte sind:

$$k''_1 = 2{,}8 \pm 0{,}2 \qquad k^*_{-1} = 0{,}085 \pm 0{,}01$$
$$k''_2 = 2{,}6 \pm 0{,}2 \qquad k^*_{-2} = 0{,}36 \pm 0{,}04$$
$$k''_3 = 1{,}9 \pm 0{,}2 \qquad k^*_{-3} = 0{,}56 \pm 0{,}06$$

Viel aussagekräftiger sind aber die — wie auf Grund der Gl. (17) gestattet — auf k''_1 bezogenen relativen Adsorptionsgeschwindigkeitskonstanten:

$$k'''_1 \equiv 1$$
$$k'''_2 = 0{,}9 \pm 0{,}1$$
$$k'''_3 = 0{,}7 \pm 0{,}1\,.$$

Auf solche Weise können die relativen Adsorptionsgeschwindigkeitskonstanten der drei *n*-Butenisomeren berechnet werden, die auf einem Ionenaustauschharz vom Typ »Amberlyst 15« die folgende Reihenfolge zeigen: 1-Buten $>$ $>$ *cis*-2-Buten $>$ *trans*-2-Buten, und die für die Desorption: 1-Buten $\ll$ *cis*-2-Buten $<$ *trans*-2-Buten.

Die geschilderte kinetische Methode ermöglicht demnach eine eingehendere Untersuchung des Isomerisationsmechanismus.

ZUSAMMENFASSUNG

Die Kinetik der *n*-Butenisomerisierung auf sauren Katalysatoren läßt sich *phänomenologisch* auf Grund einer reversiblen Dreieckreaktion erster Ordnung beschreiben, kann aber auch als ein katalytischer Vorgang gedeutet werden, bei dem die Bildung des sec-Butylcarboniumions als ein gemeinsames Zwischenprodukt angenommen wird. Dementsprechend spielt sich die Kontaktreaktion nach dem Schema

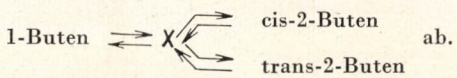

Die für dieses Schema abgeleiteten Selektivitätsgleichungen können formell in die für das phänomenologische Dreieckschema aufgestellten Gleichungen übergeführt und die relativen Adsorptionsgeschwindigkeiten und Desorptionswahrscheinlichkeiten der einzelnen Isomeren berechnet werden.

LITERATUR

1. KALLÓ, D.—SCHAY, G.: Acta Chim. Acad. Sci. Hung. **39,** 183 (1963)
2. KALLÓ, D.—PRESZLER, I.: Institutsbericht von KKKI 1967
3. NAGY F.: Kontakt katalitikus reakciók kinetikája. Kontakt katalízis (Kinetik kontaktkatalytischer Reaktionen. Kontakt Katalyse; ungarisch). Akadémiai Kiadó, Budapest 1966. S. 430—3.
4. HAAG, W. O.—PINES, H.: J. Am. Chem. Soc. **82,** 2488 (1960)
   LEFTIN, H. P.—HABSON, M.C.: Advances in Catalysis. Bd. 14. Academic Press, New York — London 1963.
5. BROUWER, D. M.: J. Cat. **1,** 22 (1962)

Dénes KALLÓ; Budapest, II. Pusztaszeri út 57/69

Acta Chimica Academiae Scientiarum Hungaricae Tomus 57 (3), pp. 323—333 (1968)

ÜBER DIE QUANTITATIVE POLAROGRAPHISCHE BESTIMMUNG DES MORPHINGEHALTS VON MOHNKAPSELN

B. ZSADON und T. PAÁL

(Chemisch-Technologischer Lehrstuhl der Eötvös Loránd Universität, Budapest)

Eingegangen am 8. September 1967

Die Methode von BAGGESGAARD-RASMUSSEN, nach der Morphin in salzsaurem Medium mit Kaliumnitrit behandelt (im folgenden »nitrosiert«) und nach Alkalisierung polarographisch bestimmt wird, ist auch zur Bestimmung des Morphingehalts von Mohnkapseln allgemein angewandt [1]. Wie dies bereits in unseren früheren Mitteilungen eingehend diskutiert wurde, haben wir mit dieser Methode im Falle von Mohnkapsel-Extrakten deformierte polarographische (Diffusions-) Stufen, und auf Grund dieser berechnet, höhere Werte als die echten Morphingehalte erhalten [2, 3, 4]. (Diese Abweichung war von der Herkunft der Mohnkapseln abhängig verschieden: im allgemeinen betrug sie 15—30%, doch ergaben sich in einigen Fällen auch Abweichungen von 35—45%.) Dieses Ergebnis steht mit den Erfahrungen anderer Authoren in Einklang [5, 6, 7], und seine Richtigkeit wurde von uns durch systematische präparative Untersuchungen auch quantitativ bestätigt [4].

Nach der übereinstimmenden Feststellung der zitierten eigenen Mitteilungen, sowie der Arbeiten anderer Autoren, solle diese Abweichung durch gewisse wasserlöslichen, das Morphin begleitenden Stoffe phenolischen Charakters verursacht werden, weil auch diese Stoffe nach Nitrosierung dem Morphin gleich eine polarographische Aktivität aufweisen. Diese »Störstoffe« sind anwesend unabhängig davon ob der Auszug durch wäßrige, wäßrig-saure, wäßrig-alkalische Extraktion oder ohne vorangehende Neutralisation (Aufschluß) durch Extraktion mit einem organischen Lösungsmittel (z.B. mit Alkohol oder Aceton) erhalten wurde. Falls das Morphin vor der Nitrosierung mit einer geeigneten Methode (z. B. Extraktion bei pH 8—9 mit organischen Lösungsmitteln) von den Störstoffen getrennt wird, können auch im Falle von Extrakten verläßliche Ergebnisse (mit der präparierbaren Menge gleiche oder nahezu gleiche Resultate) mit der polarographischen Methode erhalten werden.

Die vorliegende Mitteilung befaßt sich mit jenen Untersuchungen, die dazu bestimmt waren, unter den Umständen der polarographischen Bestimmung einen Unterschied zwischen dem Verhalten des Morphins und der Störstoffe zu finden, um dadurch ohne eine tatsächliche Trennung der Störstoffe ihre Störwirkung bei der polarographischen Bestimmung des Morphingehalts von Mohnkapseln bzw. Mohnkapsel-Extrakten auswerten zu können.

Abhängigkeit der polarographischen Stufenhöhe des Morphins von der Dauer und Temperatur der Nitrosierung

Nach den ursprünglichen Vorschriften von H. BAGGESGAARD-RASMUSSEN soll das Morphin vor der Aufnahme des Polarogramms in 1 *n* salzsaurem Medium bei Zimmertemperatur 5 Minuten lang mit Kaliumnitrit behandelt und die »Nitrosierung« dann durch Zugabe von Kaliumhydroxyd (Alkalisieren) unterbrochen werden [1]. Wenn wir die Dauer und die Temperatur der Nitrosierung änderten, zeigte sich eine gut reproduzierbare Änderung der Stufenhöhe. Wenn die Nitrosierung länger als 5 Minuten dauerte, so verringerte sich die Stufenhöhe, und zwar in um so größerem Maße, je höher die Temperatur war. Unsere Nitrosierungsversuche wurden in einem Ultrathermostat mit einer Dauer von 5 bis 50 Minuten vorgenommen.

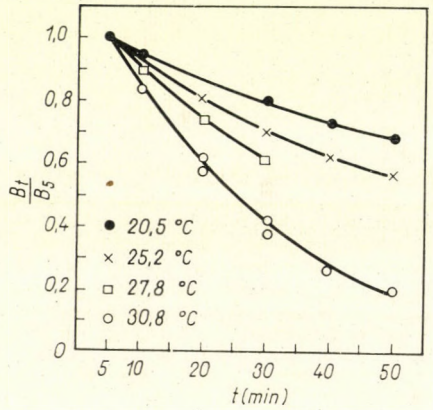

Abb. 1. Änderung der polarographischen Stufenhöhe des Morphins als Funktion der Nitrosierungsdauer ($t \geq 5$ Minuten)

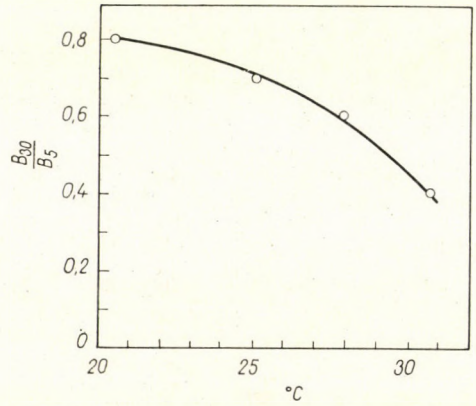

Abb. 2. Änderung des Verhältnisses der 30 und 5 Minuten dauernden Nitrosierung entsprechenden Stufenhöhen als Funktion der Nitrosierungstemperatur

Abb. 1 zeigt die Änderung des Quotienten der nach t Minuten dauernder Nitrosierung (Bt) und nach 5 Minuten dauernder Nitrosierung gemessenen Stufenhöhe (B_5) — d. h. der relativen Stufenhöhe als Funktion der Dauer (t) der Nitrosierung, bei 20,5, 25,2 27,8 und 30,8 °C.

In Abb. 2 ist das Verhältnis der nach 30 Minuten dauernder und der nach 5 Minuten dauernder Nitrosierung gemessenen Stufenhöhe, B_{30}/B_5, als Funktion der Nitrosierungstemperatur dargestellt.

Aus den Diagrammen in Abb. 1 und 2 geht hervor, daß die Abnahme der Stufenhöhe einer chemischen Reaktion zuzuschreiben ist, bei der das die polarographische Stufe liefernde »aktive« Morphinderivat* in ein »inakti-

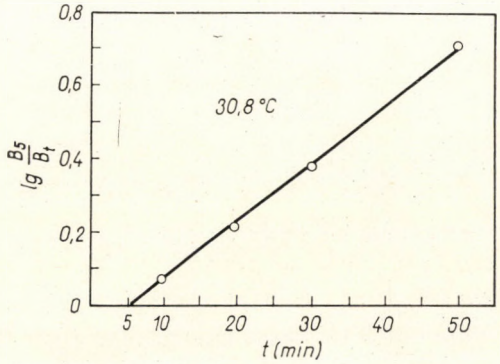

Abb. 3. Kinetische Analyse der Änderung der Stufenhöhen

ves« Produkt umgewandelt wird. Auf Grund der Meßergebnisse war diese Abnahme von erster kinetischer Ordnung. Dies wird auch durch Abb. 3 bestätigt, wo als Beispiel für bei 30,8 °C durchgeführte Messungen lg B_5/B_t als Funktion der Nitrosierungsdauer (t) dargestellt und der kinetischen ersten Ordnung entsprechend eine Gerade erhalten wurde.

Die Änderung der polarographischen Stufenhöhe von salzsauren Mohnkapsel-Extrakten als Funktion der Nitrosierungsdauer

Die oben beschriebenen Untersuchungen wurden auch mit salzsauren Extrakten von Mohnkapseln von sechs verschiedener Herkunft durchgeführt. Zu diesem Zweck wurden deshalb salzsaure Extrakte gewählt, weil zur vollständigen Extraktion des Morphins die Extraktion mit Salzsäure als eine der wirksamsten Methoden angesehen und auch für Serienanalysen ziemlich ausgedehnt verwendet ist [12].

* Es wurde von verschiedenen Autoren bewiesen, daß das Hauptprodukt in der schnellen Reaktion des Morphins mit Überschuß von Salpetrigersäure bzw. nitrosen Gasen 2-Nitromorphin ist [8, 9, 10, 11].

Die Daten über die Herkunft der zur Untersuchung verwendeten Mohnkapseln sind in Tabelle I zusammengefaßt. Die einzelnen Muster werden in der Folge mit den Serienummern der Tabelle I bezeichnet.

Tabelle I

Daten über die Herkunft der untersuchten Mohnkapseln

No.	Benennung der Mohnkapseln	Jahr des Züchtens
I.	SB	1965
II.	SC	1965
III.	Kompolt	1965
IV.	Budakalász	1965
V.	Budakalász	1966
VI.	BC	1966

Die Muster wurden vorangehend mit drei verschiedenen Methoden *(A, B* und *C)* analysiert.

Methode »A«: Das Muster wurde mit Salzsäure extrahiert, der Extrakt auf die übliche Weise (5 Minuten lang) nitrosiert und dann polarographiert. Auf diese Weise wurden zusammen mit dem Morphin auch die im Extrakt anwesenden Störstoffe gemessen, und demzufolge erhielten wir stets einen höheren Wert als der echte Morphingehalt.

Methode »B«: Es wurde mit salzsaurem, 80%igem Äthanol extrahiert, sodann nach Konzentrierung und Reinigung des Extrakts das Morphin bei pH 8—9 mit einem Benzol-Butanol-Gemisch durch Extraktion von den Störstoffen getrennt und nachher bestimmt. Unsere früheren Untersuchungen [4] bestätigen, daß auf diese Weise der echte, von Störstoffen freie Morphingehalt gemessen werden kann.

Methode »C«: Mit 80%igem Äthanol wurden 300—300 g der Muster extrahiert und das Morphin nach Isolierung in kristalliner Form bestimmt.

Die Analysenergebnisse sind in Tabelle II zusammengefaßt.

Nach der obengenannten Analyse der Mohnkapsel-Muster wurden die salzsauren Extrakte auch nach 30 Minuten dauernder Nitrosierung polarographiert. Ähnlich, wie bei Versuchen mit reinem Morphin, fanden wir auch hier eine Abnahme der Stufenhöhe, diese Abnahme war aber stets geringer, als im Falle des reinen Morphins. Auch war das Maß der Abnahme bei den einzelnen Mohnkapsel-Proben verschieden. Um dies zu veranschaulichen, sind in Tabelle III die Quotienten der Stufenhöhen der nach 30 Minuten und nach 5 Minuten dauernder Nitrosierung für reines Morphin bzw. für die verschiedenen Extrakte aufgenommen Polarogramme angegeben. Ein Teil der

Muster wurde in einem Ultrathermostate bei 27,8 °C, ein anderer Teil bei 30 °C nitrosiert.

In der Spalte *A* der folgenden Tabelle IV sind die konkreten Werte der in der einer Versuchsserie mit den salzsauren Extrakten erhaltenen Stufen-

Tabelle II

Der mit verschiedenen Methoden bestimmte Morphingehalt der untersuchten Mohnkapseln

No.	Morphingehalt g/100 g		
	A	*B*	*C*
I.	0.60	0,46	0,45
II.	0,54	0,32	0,31
III.	0,64	0,47	0,45
IV	0,44	0,27	0,25
V.	0,45	0,30	0,28
VI.	0,41	0,28	—

A: aus salzsaurem Extrakt polarographisch bestimmtes Morphin;
B: aus dem äthanolischen Extrakt nach Extraktion mit Benzol-Butanol bestimmtes Morphin;
C: aus dem äthanolischen Extrakt in kristalliner Form isoliertes Morphin

Tabelle III

Verhältnis der nach 30 Minuten und 5 Minuten dauernder Nitrosierung gemessenen Stufenhöhen

Bezeichnung	No.	Verhältnis der durchgeführten Nitrosierung gemessenen Stufenhöhen	
		bei 27,8 °C	bei 30 °C
b_{30}	Standard-Morphin	0,62	0,45
a_{30}	I.	0,71	—
	II.	0,78	—
	III.	0,72	—
	IV.	0,76	—
	V.	—	0,63
	VI.	—	0,65

$$a_{30} = \frac{A_{30}}{A_5} \quad \text{und} \quad b_{30} = \frac{B_{30}}{B_5},$$

A_5 und A_{30}: die nach 5 bzw. 30 Minuten dauernder Nitrosierung des salzsauren Extrakts gemessenen Stufenhöhen,
B_5 und B_{30}: die nach 5 bzw. 30 Minuten dauernder Nitrosierung des Standard-Morphins gemessenen Stufenhöhen

höhen angegeben. Die Daten in der Spalte *B* wurden hingegen auf Grund der Daten in Spalte *B* der Tabelle II berechnet. Sie geben an, wie hoch die dem echten Morphingehalt entsprechenden Stufen nach 5 bzw. 30 Minuten dauernder Nitrosierung wären. Diese Berechnung wird dadurch ermöglicht, daß nach der Extraktion bei pH 8—9 der echte Morphingehalt, ohne Verlust und störende Stoffe gemessen wurde. Dabei wird angenommen, daß sich die Stufenhöhe des Morphins, unabhängig von den Störstoffen, auch in deren Gegenwart (also in den Extrakten) in gleichem Verhältnis ändert.

Tabelle IV

Vergleich der gemessenen und berechneten Stufenhöhen

No.	Nitrosierungs-dauer, Min	Stufenhöhe, mm		
		A	*B*	*A*—*B*
Bei 27,8 °C gemessene Daten:				
Standard-Morphin, 1 mg	5	178		
	30	110		
I.	5	133	102	31
	30	95	63	32
II.	5	120	71	49
	30	94	44	50
III.	5	142	104	38
	30	102	64	38
IV.	5	98	60	38
	30	75	37	38
Bei 30 °C gemessene Daten:				
Standard-Morphin, 1 mg	5	175		
	30	79		
V.	5	98	65	33
	30	62	29	33
VI.	5	90	61	29
	30	58	27	31

A: im salzsauren Extrakt polarographisch gemessene Daten,

B: die dem echten Morphingehalt entsprechenden Stufenhöhen (aus Spalte »*B*« der Tabelle II berechnete Daten).

Bemerkung: die Messungen wurden in der im experimentellen Teil beschriebenen Weise ausgeführt. Sämtliche Daten sind auf Empfindlichkeit 4×10^{-8} Amper/Teilung umgerechnet angegeben.

Folgerungen und die Berechnung des Morphingehaltes auf Grund der Versuchsergebnisse

Auf Grund der obigen Ausführungen vergibt die Differenz der zusammengehörigen Werte der Spalten A und B $(A - B)$ stets die den Störstoffen entsprechende Stufenhöhe an. Aus der Tatsache, daß die der 5 und 30 Minuten dauernden Nitrosierung entsprechenden Unterschiede $(A - B)$ für das gleiche Muster stets gleich oder nahezu gleich waren, folgt, daß die den Störstoffen entsprechende Stufenhöhe unter den gegebenen Versuchsbedingungen mit zunehmender Nitrosierungsdauer nicht abnahm oder zumindest keine signifikante Änderung zeigte.

Diese Schlußfolgerung konnte noch durch eine weitere, in Verbindung mit den derivierten Polarogrammen gemachte Beobachtung bestätigt werden. Wie aus dem Schema in Abb. 4 ersichtlich ist, besteht ein wesentlicher Unter-

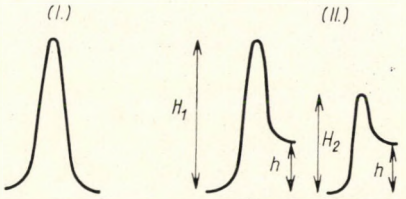

Abb. 4. Schema der derivierten Polarogramme von Morphin (I) und Mohnkapsel-Extrakt (II)

schied zwischen den derivierten Polarogrammen des reinen Morphins (I) und des auch Störstoffe enthaltenden Extraktes (II). Der absteigende Ast der in Gegenwart von Störstoffen aufgenommenen derivierten Kurven (II) kehrt nämlich nicht bis zu dem Niveau des Grundstromes (im Gegensatz zum reinen Morphin) zurück, sondern biegt in einer vom Grundstrom gemessenen Höhe h von diesem ab. Nach unseren Beobachtungen ist diese Höhe h der Menge der anwesenden Störstoffe proportional und ändert sich mit steigender Nitrosierungsdauer praktisch nicht, im Gegensatz zu der Gesamthöhe der Stufe (H), welche gut meßbar abnimmt $(H_1 > H_2)$.

Diese Resultate geben einerseits Antwort auf jene Frage, weshalb die relative Abnahme der Stufenhöhe im Falle von Extrakten, die auch Störstoffe enthalten, geringer ist und gestatten anderseits in Kenntnis der zu zwei verschiedenen Nitrosierungszeiten gehörenden Stufenhöhen die Berechnung des echten Morphingehaltes (oder die diesem entsprechende korrigierte Stufenhöhe), ohne Trennung der Störstoffe.

Im Falle von Extrakten wird das Morphin zusammen mit den Störstoffen bestimmt, d. h.

$$A = B + Z \qquad (1)$$

wo A die gemessene Stufenhöhe des Extraktes, B die dem anwesenden Morphin entsprechende Stufenhöhe, und Z die durch die Störstoffe verursachte Zunahme der Stufenhöhe bedeutet. Die Werte von A und B sind von der Nitrosierungsdauer abhängig, während nach unseren Beobachtungen der Wert von Z unter den gegebenen Versuchsbedingungen konstant ist.

Das Verhältnis der zwei verschiedenen Nitrosierungszeiten (z. B. bei 5 und 30 Minuten) entsprechenden Stufenhöhen des im Extrakt anwesenden Morphins kann folgend angegeben werden:

$$\frac{B_{30}}{B_5} = \frac{A_{30} - Z}{A_5 - Z} \tag{2}$$

wo A_5 und B_5 die zu 5 Minuten dauernder Nitrosierung und A_{30} und B_{30} die zu 30 Minuten dauernder Nitrosierung gehörenden Stufenhöhen bedeuten.

Die zu den Nitrosierungszeiten von 5 un 30 Minuten gehörende relative Abnahme der Stufenhöhe des reinen Morphins ist aus früheren Versuchen bekannt (siehe Abb. 2), und deshalb kann bei der Berechnung des Morphingehaltes die folgende Substitution eingeführt werden:

$$b_{30} = \frac{B_{30}}{B_5} . \tag{3}$$

Dies ergibt für Z die folgende Gleichung:

$$Z = \frac{A_{30} - A_5 - b_{30}}{1 - b_{30}} \tag{4}$$

Die dem echten Morphingehalt entsprechende Stufenhöhe kann also aus dem folgenden Zusammenhang erhalten werden:

$$B_5 = A_5 - \frac{A_{30} - A_5 - b_{30}}{1 - b_{30}} . \tag{5}$$

In der Spalte A der Tabelle II wurde der mit den Störstoffen zusammen gemessene »Morphingehalt« (»Morphin«) angegeben. Aus diesen Daten kann unter Verwendung der in Tabelle III zusammengefaßten Daten der echte Morphingehalt mit der folgenden Formel berechnet werden:

$$\text{Morphin} = \text{»Morphin«} \cdot \frac{1 - a_{30}}{1 - b_{30}} \tag{6}$$

wo a_{30} und b_{30} die entsprechenden Daten der Tabelle III bedeuten, bzw.

$$a_{30} = \frac{A_{30}}{A_5}$$

ist.

Die mit Formel (6) berechneten Werte wurden in Tab. V zusammengefaßt, wo zum Vergleich auch die Abweichungen von den Werten in den Spalten *A*, *B* und *C* der Tabelle II angegeben sind.

Tabelle V

Morphingehalt der Mohnkapsel-Muster, nach (6) berechnet

No.	Berechneter Morphingehalt g/100 g	Prozentuelle Abweichung von den Werten in Spalten der Tabelle II		
		A	*B*	*C*
I.	0,46	—27	0	+2
II.	0,31	—42	—3	0
III.	0,47	—26	0	+4
IV.	0,27	—38	0	+8
V.	0,30	—33	0	+7
VI.	0,27	—36	—3	—

Die gute Übereinstimmung der berechneten Werte mit dem nach der Methode *B* bestimmten Morphingehalt sowie ihre geringe Abweichung von der in kristalliner Form erhaltenen Morphinmenge rechtfertigt unsere Annahme und bestätigt die Richtigkeit der Berechnungsmethode. Auf Grund der diskutierten Ergebnisse ist zu hoffen, daß unsere Beobachtungen die Basis einer neuen polarographischen Morphin-Bestimmungsmethode bilden können, die auch dazu geeignet sein wird, das Morphin is solchen Mohnkapsel-Extrakten genau zu bestimmen, die Begleitstoffe enthalten, welche die Bestimmung sonst stören würden. Die Ausarbeitung einer solchen Methode ist im Gange, und im Rahmen dieser Arbeit werden weitere Messungen zur Bestimmung der Reproduzierbarkeit der Daten durchgeführt.

Experimenteller Teil

Polarographie der Standard-Morphinlösung

Aus gereinigter, kristalliner Morphinbase wurde mit 1 *n* Salzsäure eine Standard-Lösung von 0,2 mg/ml Konzentration hergestellt. Aus dieser Lösung wurden 5 ml (1 mg Morphin) in eine für 15 ml Volumen kalibrierte, mit ein geschliffenem Glasstopfen versehene Proberöhre pipettiert, die dann in einen Ultrathermostat gestellt und 15 Minuten stehen gelassen wurde. Sodann wurden 2 ml einer molaren Kaliumnitritlösung zugegeben, und die Proberöhre wurde verschlossen. Nach Verlauf der vorgeschriebenen Nitrosierungszeit wurde die Reaktion durch Zugabe von 3 ml 20%iger Kaliumhydroxydlösung unterbrochen. Die alkalische Lösung wurde mit 1 ml 1%iger Gelatinelösung versetzt, das Volumen der Lösung mit destilliertem Wasser auf 15 ml ergänzt, sodann wurde polarographiert. (Polarograph: Radelkisz Type OH 102, Tropfzeit 2,2 sec.)

Extraktion der Mohnkapseln mit Salzsäure (Methode A)

2,5 g fein gemahlte, lufttrockene Mohnkapseln wurden mit 40 + 3×20 ml 1 *n* Salzsäure durch je einstündiges Schütteln erschöpfend extrahiert. Der filtrierte Extrakt wurde auf 100 ml aufgefüllt. Aus diesem Extrakt wurden zur Analyse Muster von 5 ml entnommen und auf die gleiche Weise wie das Standard-Morphin, nitrosiert und polarographiert.

Bestimmung des Morphingehalts nach Trennung der Störstoffe (Methode B)

10 g fein gemahlte, lufttrockene Mohnkapseln wurden mit 200 + 3×100 ml salzsaurem 80%igem Äthanol durch je einstündiges Schütteln erschöpfend extrahiert (auf Salzsäure bezogen war das 80%ige Äthanol 0.1 normal). Das Volumen der vereinigten Extrakte wurde im Vakuum auf 30 ml eingeengt. Die wäßrige Lösung wurde filtriert, der pH des Filtrats auf 5,5 eingestellt und zur Reinigung wurde mit 5×20 ml eines Benzol-Butanol-Gemisches (7 : 3 Volumenteile) ausgeschüttelt. Die organische Phase wurde dann mit 2×10 ml wäßriger Pufferlösung (pH = 5,5) ausgeschüttelt. Die wäßrigen Extrakte wurden kombiniert, und im Vakuum wieder bis auf ein Volumen von 25–30 ml eingedampft. Nun wurde der pH der gereinigten, konzentrierten wäßrigen Lösung bis pH 8—9 alkalisiert und mit 5×30 ml eines Benzol-Butanol-Gemisches (7 : 3 Volumenteile) wurde extrahiert. Die organischen Phasen wurden mit 20 ml destilliertem Wasser, danach mit 5×10 ml 1 *n* Salzsäure extrahiert. Aus diesem salzsauren Extrakt wurde das Lösungsmittel in Vakuum abgetrieben und das Volumen der Lösung auf 50 ml ergänzt. 2 ml Teile dieser Lösung wurden ähnlich wie das Standard-Morphin polarographiert.

Gewinnung von kristallinem Morphin aus Mohnkapseln (Methode C)

300 g betragende Portionen der gemahlten, lufttrockenen Mohnkapseln wurden für präparative Zwecke mit 80%igem Äthanol extrahiert. Das Extraktionsverfahren und die Aufarbeitungsmethode des Extraktes sind in einer früheren Mitteilung [4] bereits beschrieben worden.

⁂

Wir möchten an dieser Stelle Herrn Prof. A. GERECS für die Unterstützung der Arbeit, L. DÉCSEI für seine Mitwirkung in der präparativen Arbeit und Frau M. INDRIKOVITS für ihre Beteiligung an der technischen Arbeit unseren Dank aussprechen.

ZUSAMMENFASSUNG

Es wurde festgestellt, daß die polarographische Stufenhöhe des Morphins nach kinetisch erster Ordnung abnimmt, wenn die Nitrosierung bei konstanter Temperatur länger als 5 Minuten vorgenommen wird. Die Abnahme der Stufenhöhe ist auch von der Nitrosierungstemperatur abhängig. Bei diesen Messungen wurde die Nitrosierungsdauer zwischen 5 und 50 Minuten, die Temperatur zwischen 20 und 30 °C geändert.

Diese Untersuchungen wurden auch mit salzsauren Mohnkapseln-Extrakten durchgeführt, wobei festgestellt werden konnte, daß die relative Abnahme der Stufenhöhe in diesem Falle geringer ist, als bei reinem Morphin unter identischen Bedingungen. Dies kann darauf zurückgeführt werden, daß die das Morphin begleitenden Extraktstoffe für einen gegebenen Extrakt, die Stufenhöhe des Morphins unabhängig von der Nitrosierungsdauer um den gleichen Wert erhöhen, während die dem echten Morphingehalt entsprechende Stufenhöhe mit steigender Nitrosierungszeit der Stufenhöhe des reinen Morphins proportional abnimmt.

Es wurde eine Berechnungsmethode angegeben, die es gestattete, den echten Morphingehalt der untersuchten Mohnkapsel-Extrakte, in Kenntnis von zwei zu verschiedenen Nitrosierungszeiten gehörigen Stufenhöhen ohne Trennung der störenden Begleitsstoffe zu berechnen.

LITERATUR

1. BAGGESGAARD-RASMUSSEN, H., HAHN, C. und ILVER, K.: Dansk. Tidskr. Farm **19,** 41 (1945); s. HEYROVSKY, J. und ZUMAN, P.: Bevezetés a gyakorlati polarográfiába (Einführung in die praktische Polarographie; ungarisch). Akadémiai Kiadó, 1955. S. 141.
2. ZSADON, B.: Magy. Kém. Folyóirat **66,** 347 (1960)
3. ZSADON, B. und GERECS, Á.: Magy. Kém. Folyóirat **70,** 49 (1964)
4. GERECS, Á. und ZSADON, B.: Magy. Kém. Folyóirat **71,** 424 (1965)
5. BAGGESGAARD-RASMUSSEN, H.: Bull. Fed. Int. Pharm. **21,** 233 (1947)
6. PFEIFER, S. und KELLER, W.: Pharm. Zentralhalle **95,** 189 (1956)
7. HORÁK, P., HOLUBEK, J., BUMBA, V. und ČEKAN, Z.: Collection Czechoslov. Chem. Commun. **27,** 1037 (1962)
8. EIJO OCHIAI und TOSIHARU NAKAMURA: Berichte **72,** 684 (1939)
9. BAGGESGAARD-RASMUSSEN, H. und BOLL, P.: Acta Chim. Scand. **12,** 885 (1958)
10. LUND, H.: Acta Chim. Scand. **12,** 1444 (1958)
11. GAÁL, GY.: Dissertation 1965; BOGNÁR, R. und GAÁL GY.: Magy. Kém. Folyóirat **69,** 17 (1963)
12. HOLUBEK, J.: Pharm. Zentralhalle **94,** 347 (1955)

Béla ZSADON
Tamás PAÁL
} Budapest, VIII. Múzeum krt 6—8

Acta Chimica Academiae Scientiarum Hungaricae Tomus 57 (3), pp. 335—343 (1968)

CHEMISTRY OF HETEROCYCLIC PSEUDOBASIC AMINOCARBINOLS, XXXIV*

NOTES ON THE SYNTHESIS OF "QUANTRIL" AND ON THE TAUTOMERISM OF β-OXO-CARBOXAMIDES

Cs. SZÁNTAY, L. NOVÁK** and P. SOHÁR***

(Institute of Organic Chemistry. Technical University, Budapest)

Received September 10, 1967

The compound of structure I, known as "Quantril" or "Benzquinamide" is a tranquilizer and a medicine for decreasing blood pressure [1]. It is prepared by the reduction of the oxo-compound of structure **IIa** and acetylation of the resulting alcohol **III**.

Reduction of IIa

Hydrogenation of **IIa** in methanol in the presence of a catalyst (PtO_2) results in an epimeric mixture containing 90% of the alcohol **III**, with the hydroxyl group in axial position, and some of the epimer **IV** [2].

This fact seemed surprising, as in the case of 2-oxo-quinolizidine of similar structure, reductions in basic medium in the presence of PtO_2 always resulted in the thermodynamically more stable derivatives of structure **IV**, with the hydroxyl group in equatorial position [3, 4].

When reducing the ketone **IIa** with sodium borohydride, the ratio of the epimers changed and mainly **IV** was produced. The occurrence of such a difference between these two reduction methods is also inconsistent with previous observations in these series [3, 4].

To investigate this unusual case, **IIa** was spectroscopically studied. The infrared spectrum of its hydrochloride clearly shows the characteristic stretching vibrations of the carbonyl group (1740 cm^{-1}) and the amide group (1650 cm^{-1}) (Fig. 3). On the other hand, both bands practically disappear in the spectrum of the base, and only one single intense band can be seen at 1623 cm^{-1}, as a result of the overlapping bands of the C = C bond and the amide-carbonyl group. The same effect was observed in a chloroform or carbon

* Part XXXIII: L. TŐKE, GY. KALAUS and CS. SZÁNTAY: Acta Chim. Acad. Sci. Hung. **55**, 237 (1968).

** This paper is a part of the dissertation for candidature of L. NOVÁK

*** Pharmaceutical Research Institute, Budapest

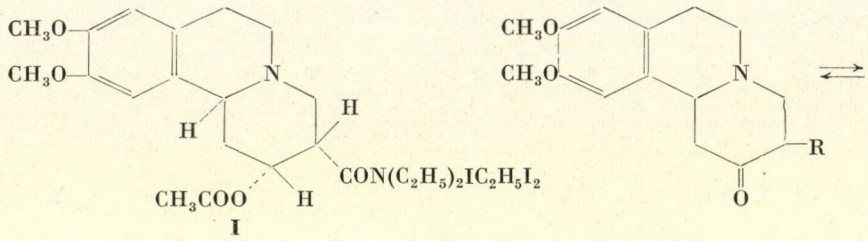

I

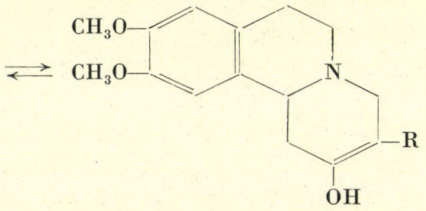

II a, R = $CON(C_2H_5)_2IC_2H_5I_2$
b, R = $COOC_2H_5$
c, R = CN

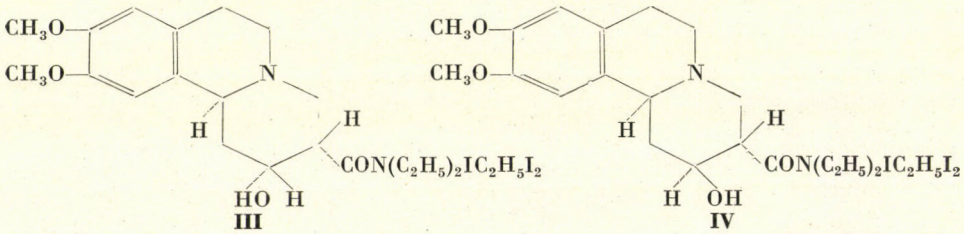

III **IV**

tetrachloride solution of **IIa**. Since, in general, the equilibrium positions of keto-enol tautomers are near in chloroform and methanol solutions [5], it is reasonable to suppose the enol form of **IIa** to predominate in methanol solution, too. Thus, in the catalytic reduction of **IIa** the alcohol is formed by saturating the double bond in the enol form.

The chemisorption on the catalyst of the enol form of **IIa** occurs with higher probability from the sterically less hindered side [4]. If the more stable B/C *trans* ring juncture and the half-chair form of rings B and C are supposed, the molecule is anchored to the catalyst on the side of the lone electron pair of the nitrogen atom (Fig. 1), so this is the probable direction of the hydrogen transfer. Thus the process gives rise to a product of structure **III**, containing the hydroxyl group in axial position.

On the other hand, the reduction with sodium borohydride — corresponding to the character of the reagent — takes place mainly through the keto form. The resulting group, wich contains oxygen-boron bond, owing to its greater space requirement, attempts to assume equatorial position thus facilitating thermodynamical control and the formation of **IV**.

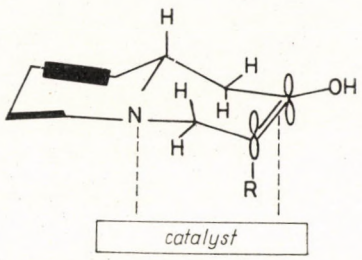

Fig. 1. Chemisorption of IIa on the catalyst

Tautomerism of β-oxo-carboxamides

The phenomenon discussed above directed our attention to the keto-enol tautomerism of β-oxo-carboxamides. Strangely, the literature dealing with this problem is extraordinarily small. Only one amide — acetoacetanilide — was studied in MEYER's [6] classical investigations on the tautomerism of acetoacetic acid derivatives. He found the anilide to be in the pure keto form in the solid state, while in ethanolic solution the equilibrium mixture contains 18% of the enol form. Recently DUDEK and VOLPP [7] have shown, with the help of nuclear megnetic resonance spectroscopy, that even traces of the enol form are absent in N-benzylacetoacetamide.

So literature data seem to contradict our own observations. Thus, to complete our infrared spectroscopic studies, the NMR spectrum of **IIa** was also investigated. The two methyl groups of the ethyl substituents of the amide nitrogen give two separate triplets partly overlapping and resulting in a pseudo-quartet at δ 1.15. The two methyl groups are not equivalent; this may be due to the hindrance of rotation caused by a hydrogen bridge between the hydroxyl group of the enol form and the amide group; or it may be due to the low rotation around the bond between the carbonyl group and the nitrogen atom, which often occurs in amides. The singlet appearing at δ 3.20, which can be integrated as two hydrogens, is characteristic of a CH_2 group present between a nitrogen atom and a -CH = CH-group (*cf.* [8]), but this structure may appear only in the enol form.

In order to find out how general this effect may be acetoacetic diethylamide, (**V**) one of the most simple β-keto amides, was investigated. In the infrared spectrum of this compound an intense C = C stretching band at 1600 cm^{-1} can be seen; the overlapping Amide I bands of the two tautomers appear at 1650 cm^{-1}, at 1730 cm^{-1} the carbonyl band of the ketone is found. The intensities of the bands of the double and the carbonyl group show an approximately equivalent ratio of the two tautomers in compound **V**, in the liquid state as well as in carbon tetrachloride solution.

V

These conclusions are confirmed by the nuclear magnetic resonance spectrum of V (Fig. 2).

In the spectrum obtained in carbon tetrachloride solution, the methyl group of the keto form appears at δ 2.1, and the methyl group of the enol form at δ 1.8. After integration, their ratio shows the presence of about 52% of the

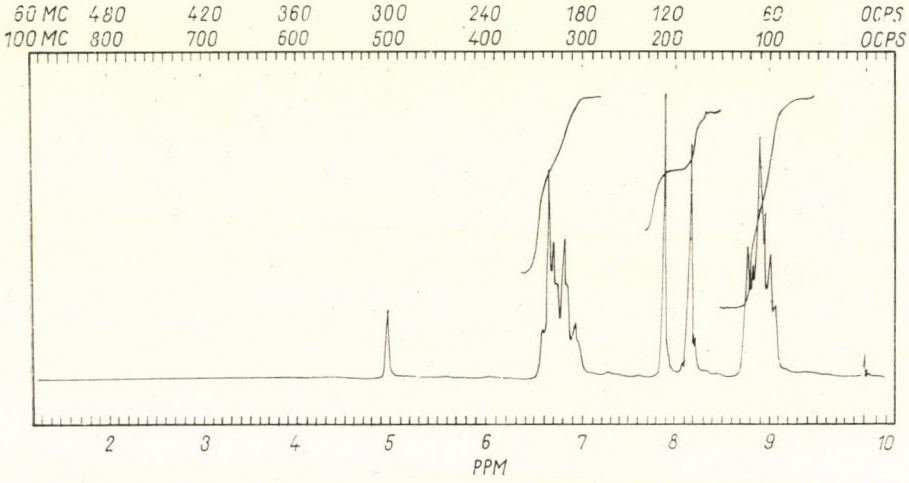

Fig. 2. Nuclear magnetic resonance spectrum of V in CCl_4 solution

keto and 48% of the enol form. The = CH proton of the enol form is clearly seen at δ 5.05.

The NMR spectrum of V in the solid state shows only a slightly different ratio (63 : 37) of the keto and enol forms.

The contradiction between the literature data and our observations is only apparent. In the two papers mentioned [6, 7] N-monosubstituted derivatives were investigated. Stabilization of the keto form is possible in such compounds owing to the effect of a NH . . . O = C-hydrogen bridge. In the case of N-disubstituted amides this effect cannot occur, so the enol form is probably stabilized by the OH . . . $CONR_2$ bridge.

These investigations result in the following conclusion: *Among β-keto acid derivatives, the N-disubstituted amides posses the greatest inclination to enolize.*

Enolization of IIb and IIc

The observations described above prompted us to prepare and investigate other β-keto acid derivatives similar to **II.**

The characteristic infrared bands of compounds **IIa, b, c** are shown in Fig. 3.

In Table I, based on the spectra, the predominant tautomers in the base and salt forms of the different derivatives of **II** are given.

Table I

Predominant (80%) tautomeric forms of **IIa—c**

	IIa	IIb	IIc
Base	enol	enol	keto
Salt	keto	enol	enol

The stretching bands of the conjugated ester carbonyl and the C=C bond of **IIb** are clearly shown in both the base and the salt form (Fig. 3).

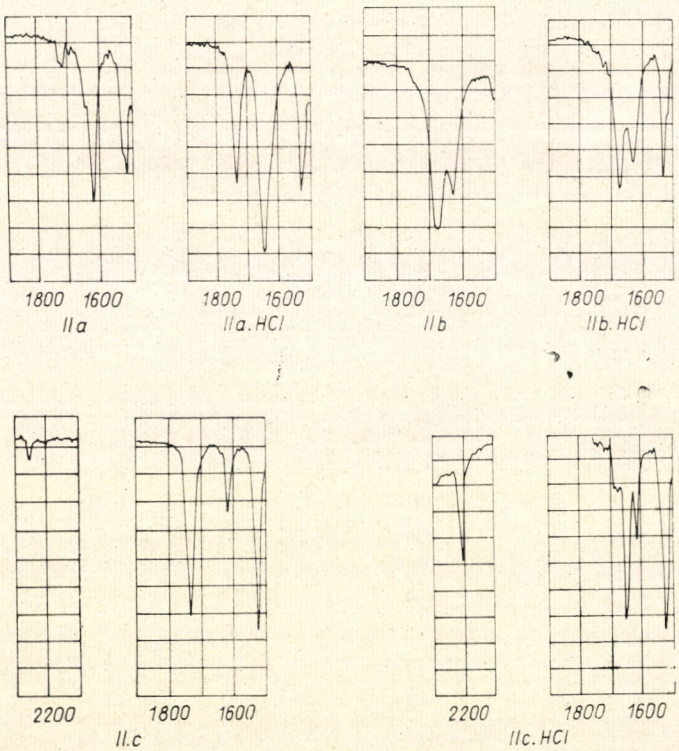

Fig. 3. Characteristic infrared bands of the compounds **IIa—c** and their salts

The cyano band found at 2250 cm^{-1} in the base **IIc** decreases to 2210 cm^{-1} in the salt; the carbonyl band at 1720 cm^{-1} is absent in the salt and instead of it a C=C stretching band appears at 1650 cm^{-1}. It is remarkable that in the spectrum of the salt a very band is seen at 1130 cm^{-1}, which is missing in the spectrum of the base. The intensity of this band decreases in the deuterated salt, and a new band appears at 1110 cm^{-1}; this is probably the C = C —OH(D) band of the enol tautomer. The enolic hydroxyl becomes significantly deuterated, naturally together with the quantitative deuteration of the NH^+ group.

The bases **IIa-c** showed the same behaviour in chloroform or methylene chloride solutions, as given in Table I and so did the salts in methyl cyanide.

The stability of the enol form of bases **IIa-b** is readily explained by the ability to form a hydrogen bridge.

In the case of compound **IIc** there is no way to develop such a hydrogen bond, because of the linearity of the cyano group. So the enolization of β-keto nitriles is generally less. Thus, *e. g.*, the equilibrium mixture of ethyl 2-oxocyclohexanecarboxylate contains 76% [9] of the enol form, and the corresponding nitrile only 10% [10].

In the case of the salts, the stability of the enol form of the keto nitrile **IIc** can again easily be explained. It is known that, in contrast with β-diketo compounds, the enol content of a compound of this type increases with the polarity of the solvent [11]. The high polarity increase due to the salt structure (*cf.* [12]) also considerably increases the mobility of the proton on C-3, and thus the possibility of the development of the enol form. The high enol content of the **IIb** salt can be similarly interpreted.

The stability of the keto form of the salt of **IIa** cannot be explained with certainty. One of the possible explanations may be that the amide group is a suitable electron source to compensate for the electron withdrawing effect of the charged nitrogen atom on the C-3 hydrogen atom, so hinders splitting of the latter as a proton; *i. e.* enolization is prevented.

Preparation of the substances

IIa was prepared by a procedure previously applied by the authors [13], using the reaction of the isoquinoline derivative **VI** and α-methyleneacetoacetic diethylamide (**VII**). Compound **VII**, unknown so far, was obtained from acetoacetic diethylamide and formaldehyde.

IIb was prepared by a procedure given in the literature [14].

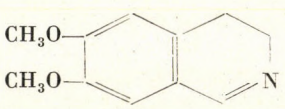

VI

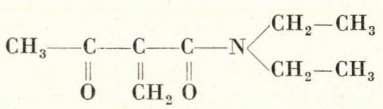

VII

The preparation of the **IIc** nitrile presented a problem. The ring closure by Dieckmann condensation of **IX**, prepared from the ester **VIII** and acrylonitrile, can be carried out in only poor yields using sodium ethoxide.

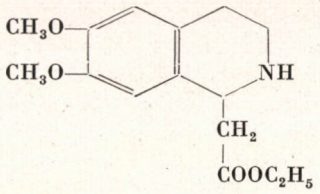

VIII

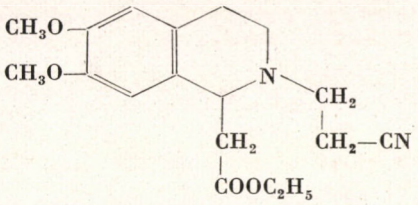

IX

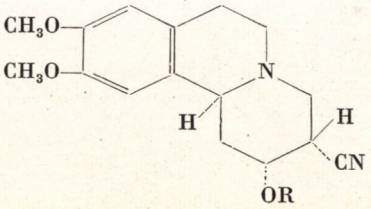

X R=H
XI R=OCCH$_3$

However, the cyclization could be accomplished with sodium dissolved in dimethyl sulphoxide; the condensation of mixed type resulted in about 80% of **IIc**

For the purpose of a pharmacological investigation **XI** was prepared by the reduction of **IIc** (to **X**), and subsequent acetylation.

The pharmacological results. (J. KNOLL, Pharmacological Institute of Medical University, Budapest) showed that the effects of the "Quantril" epimers obtained from **III** and **IV** by acetylation were nearly identical. Compound **X** had no significant effect.

Experimental

The infrared, ultraviolet and NMR spectra were recorded with a Perkin-Elmer 2216, a Unicam SP 600, and an I.N.M.–C.60 instrument, respectively.

α-Methyleneacetoacetic diethylamide (VII)

Acetoacetic diethylamide [15] (100 g) was added dropwise, with continuous stirring, into a solution of sodium acetate (20 g) in 100 ml of 40% formaldehyde. To increase solubility, 10 ml of ethanol was added to the mixture, and it was allowed to stand for 2 hrs at room temperature. The reaction mixture was then poured on water (400 ml), extracted with ether (800 ml) in three portions, and the ether extract dried over magnesium sulphate. After removing the solvent, the remaining substances were fractionated in vacuum, and the fraction boiling at 126—130° 5 torr was collected (21.80 g 20.2%). The product was a colorless liquid with a bad smell, $n_D^{22} = 1.4723$. $C_9H_{15}O_2N$ (169.22). Calcd. C 63.87; H 8.93. Found C 63.59; H 9.04%.

9,10-Dimethoxy-3-(diethylcarbamoyl)-2-oxo-1,2,3,4,6,7-hexahydro-11bH-benzo(a)quinolizine

6,7-dimethoxy-3,4-dihydroisoquinoline (**VI**; 2.00 g: 10 mmole) and α-methyleneacetoacetic diethylamide (**VIII'** 2.3 g; 13 mmole) were allowed to stand for 4 days in a 1 : 1 mixture of ethanol and water (10 ml) at room temperature. The separated crystals were recrystallized from methanol to yield 1.70 g (47.3%), m.p. 150—152° C (lit. [2] m.p.: 150—152° C).

9,10-Dimethoxy-3-(diethylcarbamoyl)-2-acetoxy-1,2,3,4,6,7-hexahydro-11bH-benzo(a)-quinolizine

IIa (12.0 g; 33 mmole) was dissolved in 150 ml of methanol. Sodium borohydride (5.0 g; 132 mmole) was added to the solution during an hour, with vigorous stirring and cooling Stirring was continued for 7 hrs at room temperature. Most of the methanol was evaporated in vacuum, and water and HCl (80 ml each) were added to the residue. The solution was then made alkaline (pH 8—8.5) with 1 *N* sodium hydroxide solution and extracted with 500 ml of benzene. After drying the benzene solution and evaporating the solvent, the residue (11.3 g; 94.5%) was treated with a 1 : 1 mixture of ether and petroleum ether. The resulting mixture of the epimeric alcohols (**III** and **IV**) melted at 125—126° C. This product was allowed to stand for 16 hrs in a mixture of (80 ml) pyridine and acetic anhydride (80 ml) at room temperature.

The oily residue, left after evaporating the solution, was dissolved in 50 ml of water, made alkaline with ammonia, and extracted with 200 ml of benzene. The benzene solution was washed with water, dried, and evaporated in vacuum; the residue was recrystallized from 25 ml of ether. The crystals were washed with ether (10 ml) to obtain 6.75 g (55.6%) of the 2-acetyl derivative of **IV**, m.p. 149—151° C (lit. [2] m.p. 150—151° C).
M.p. of the hydrochloride: 250—251° C.

Evaporation of the ethereal mother liquor of recrystallization gave 0.95 g (7.1%) of **I** ("Quantril"), m.p. 128—131° C (lit. [2] m.p. 130—131.5° C). M.p. of the hydrochloride: 229—231° C.

1-(Ethoxycarbonylmethyl)-2-(β-cyanoethyl)-6,7-dimethoxy-1,2,3,4-tetrahydroisoquinoline (IX)

1-(Ethoxycarbonylmethyl)-6,7-dimethoxy-1,2,3,4-tetrahydroisoquinoline [16] (60.0 g; 215 mmole) was refluxed with freshly distilled acrylonitrile (110 ml) for 16 hrs. After cooling, 100 ml of absolute ether was added, and the solution was extracted with 120 ml of 3 *N* HCl. The acidic extract was made alkaline with conc. ammonia solution and the solidifying product was filtered off (69.5 g; 97.3%). The m.p. of the crude product was 83—84° C; after recrystallization from ether m.p. 86° C was obtained.
$C_{18}H_{24}N_2O_4$ (332.39). Calcd. C 65.04; H 7.28; N 8.43. Found C 64.89; H 7.36; N 8.29%.
Infrared spectrum (KBr): ν_{max} 1725 cm^{-1} (CO); 2250 cm^{-1} (CN).

9,10-Dimethoxy-2-oxo-3-cyano-1,2,3,4,6,7-hexahydro-11bH-benzo(a)quinolizine (IIc)

In a flask equipped with a stirrer and condenser, metallic sodium (1.4 g) was dissolved. with stirring, in absolute dimethyl sulphoxide (30 ml) in dry nitrogen atmosphere. The precipitate (sodium hydroxide) was removed by filtration in nitrogen atmosphere, and an aliquot part of the solution was titrated with 0.1 *N* HCl. The sodium content generally varied between 0.03 and 0.045 g/ml.

The nitrilester **IX** (1.00 g; 3 mmole) was allowed to stand with the above solution of sodium in dimethyl sulphoxide (3 ml; 4 mmole) at 100° C for 3 hrs, in nitrogen atmosphere. After cooling, the mixture was poured on to 10 ml of water, and the solution was neutralized with 5% acetic acid solution. The precipitate was filtered off, washed with water and dried to obtain 0.69 g (80.3%) of **IIc**, m.p. 156—157° C.
$C_{16}H_{18}N_2O_3$ (286.32). Calcd. C 67.11; H 6.34; N 9.78. Found C 66.94; H 6.30; N 9.66%.
Ultraviolet spectrum: λ_{max}^{EtOH} 226 nm (log ε 4.01); 271 nm (log ε 3.81).
M.p. of the hydrochloride: 209—210° C.
$C_{16}H_{19}N_2O_3Cl$ (322.79). Calcd. C 59.53; H 5.93; N 8.68; Cl 10.98. Found C 59.48; H 5.86; N 8.73; Cl 11.21%.
Ultraviolet spectrum: $\lambda_{max}^{H_2O}$ 229 nm (log ε 3.94); 266 nm (log ε 3.81).

9,10-Dimethoxy-2-hydroxy-3-cyano-1,2,3,4,6,7-hexahydro-11bH-benzo(a)quinolizine (X)

IIc (1.00 g; 3.5 mmole) and sodium borohydride (0.25 g; 6.6 mmole) were stirred in ethanol (30 ml) for 6 hrs at room temperature, and 3 *N* HCl (2.5 ml) was then added. After standing for 20 minutes, the solvent was evaporated in vacuum. The residue was dissolved in 10 ml of water, made alkaline with 1 *N* sodium hydroxide solution and shaken with two 15-ml portions of benzene. After drying, the benzene solution was evaporated and the residue recrystallized from 4 ml of ethanol to obtain 0.66 g (65.6%) of a white crystalline substance, m.p. 176—178° C.
$C_{16}H_{20}N_2O_3$ (288.34). Calcd. C 66.64; H 6.99; N 9.72. Found C 66.38; H 7.24; N 9.97%.
M.P. of the hydrochloride: 185—186° C.
$C_{16}H_{21}N_2O_3Cl$ (324.81). Calcd. C 59.16; H 6.51; Cl 10.91. Found C. 58.89; H 6.79; Cl 10.94%.

9,10-Dimethoxy-2-acetoxy-3-cyano-1,2,3,4,6,7-hexahydro-11bH-benzo(a)quinolizine (XI)

The base X (0.90 g; 3.1 mmole) was dissolved in a mixture of 8 ml of acetic anhydride and 8 ml of pyridine. After standing for a day, the mixture was evaporated to dryness. The residue was rubbed with 15 ml of absolute ether, filtered off, and recrystallized from ethanol (8 ml) to give the acetate of XI (0.78 g; 64.4%), m.p. 178—179° C.
$C_{20}H_{26}N_2O_6$ (390.42). Calcd. C 61.52; H 6.71; N 7.18. Found C. 61.53; H 6.67; N 7.42%.
M.p. of the hydrochloride: 253° C.
$C_{13}H_{23}N_2O_4Cl$ (366.84) Calcd. C 58.90; H 7.63; Cl 9.66. Found C 59.14; H 6.31; N 7.54; Cl 9.75%.

The authors' thanks are due to the microanalytical team of the Institute, led by Mrs. L. BALOGH, for the analyses; to Dr. G. DUDEK (Harvard University, Cambridge USA) for valuable discussions; and to the Hungarian Academy of Sciences for sponsoring this work.

SUMMARY

The keto-enol tautomerism of different 2-oxobenzo(a)quinolizidine derivatives carrying an amide, ester or cyano group in position 3 was investigated. The enol content of acetoacetic N-diethylamide, used as a model compound, was determined by means of infrared and nuclear magnetic resonance spectroscopy. This derivative, bearing two substituents on the nitrogen atom, was found to enolize to the highest degree among the β-keto acid derivatives.

REFERENCES

1. SCRIABINE, A., FINGER, K. F., DELAHUNT, C. S., CONSTANTINE, J. W., SCHNEIDER, J. A.: J. Am. Med. Assoc. **184,** 276 (1963); C. A. **59,** 8024 (1963)
2. LOMBARDINO, I. G., MCLAMORE, W. M.: U.S. Pat. 3,055,894; C. A. **58,** 3404 (1963) TRETTER, I. R.: U. S. Pat. 3,053,845; C. A. **58,** 3404 (1963) Belg. Pat. 618,741. Belg. Pat. 621,895
3. BROSSI, A., CHOPARD-DIT-JEAN, L. H., SCHNIDER, O.: Helv. Chim. Acta **41,** 1793 (1958)
4. RADER, Ch. P., WICKS G. E., jr., YOUNG R. L., jr., AARON, H. S.: J. Org. Chem. **29,** 2252 (1964)
5. KABACHNIK, M. I., JOFFE, S. T., VATSURO, K. V.: Tetr. **1,** 317 (1957)
6. MEYER, K. H.: Ber. **45,** 2843 (1912)
7. DUDEK, G. O., VOLPP, B. P.: J. Org. Chem. **30,** 50 (1965)
8. Varian, NMR Spectra Catalog, No. 115, Varian Associates, Palo Alto, California, 1962.
9. DICKMANN, W.: Ber. **55,** 2484 (1912)
10. AUWERS, K., BAHR, Th., FRESE, E.: Ann. **441,** 69, 81 (1925)
11. RUSSEL, P. B., MENTHA, J.: J. Am. Chem. Soc. **77,** 4245 (1955)
12. NOVÁK, L., SOHÁR, P., SZÁNTAY, Cs.: Acta Chim. Acad. Sci. Hung. **54,** 161 (1967)
13. BEKE, D., SZÁNTAY, Cs.: Ber. **95,** 2132 (1962)
14. BROSSI, A., LINDLAR, H., WALTER, M., SCHNIDER, O.: Helv. Chim. Acta **41,** 119 (1958)
15. TRETTER, J. R.: U.S. Pat. 3,105,079; C.A. **60,** 2913 (1964)
16. BATTERSBY, A. R., OPENSHAW, H. T., WOOD, H. C. S.: J. Chem. Soc. **1953,** 2463

Csaba SZÁNTAY
Lajos NOVÁK
Pál SOHÁR
Budapest, XI. Gellért tér 4.

Acta Chimica Academiae Scientiarum Hungaricae Tomus 57 (3), pp. 345—352 (1968)

SYNTHETISCHE LINEARE POLYMERE, XXVIII*

ZUSAMMENHANG ZWISCHEN EINZELNEN SPEZIFISCHEN EIGENSCHAFTEN DER IN DER KETTENMITTE HETEROATOME ODER -ATOMGRUPPEN ENTHALTENDEN OLIGOMEREN POLYMERHOMOLOGEN VERBINDUNGEN UND IHRER MOLEKÜLGRÖSSE**

I. GÉCZY

(Forschungsinstitut für die Textilindustrie, Budapest)

Eingegangen am 23. September 1967

Einleitung

In meinen früheren Mitteilungen [1—10] wurde gezeigt, daß zwischen dem Molekulargewicht linearer polymerhomologer oligomerer Verbindungen und solchen spezifischen Eigenschaften, die von additiven Größen abgeleitet werden können, ganz allgemein der folgende, auch mathematisch beweisbare Zusammenhang besteht:

$$\varphi_{sp} = \frac{a}{M} + b \,, \tag{1}$$

wobei φ_{sp} irgendeine spezifische Eigenschaft (spezifische Refraktion [1], Brechungsindex [2, 3], spezifische Schallgeschwindigkeit [4], spezifisches Parachor [5], spezifisches Refrachor [5], spezifische magnetische Susceptibilität [5], spezifische Viskositätszahl [5], spezifisches Volumen [6], Reziprokschmelzpunkt [7], spezifisches mittleres Dipolmomentquadrat [8], spezifische Polarization [8], spezifische Verbrennungswärme [9], spezifisches Drehungsvermögen [10] usw.) ist. M ist das Molekulargewicht während a und b Konstanten sind, von denen die erste implicit die Kettenendglieder, die letztere explicit die Kettenmittelglieder charakterisieren, und zwar:

$$b = \varphi_k = \frac{\Phi_k}{M_k} \tag{2}$$

$$a = 2M_v(\varphi_v - \varphi_k) = 2(\Phi_v - M_v b) \,, \tag{3}$$

wobei φ dem Zahlenwert der entsprechenden spezifischen, Φ hingegen dem Zahlenwert der entsprechenden molaren Eigenschaften entspricht, während der Index k sich auf die Kettenmittelglieder, der Index v auf die Kettenendglieder bezieht.

* Synthetische lineare Polymere, XXVII: Kolorisztikai Ért. **8**, 221 (1966).

** Vorgetragen an der Konferenz des Vereins Ungarischer Chemiker, Pécs, 26. August 1967.

Es wurde gezeigt, daß Gl. (1) auch auf cyclische polymerhomologe oligomere Verbindungen ausgedehnt werden kann [11]. Die Konstante b kennzeichnet auch in diesem Fall die Kettenmittelglieder und ihr Wert ist mit dem Wert jener Konstante b identisch, die sich auf die lineare Reihe einer ähnlichen Struktur bezieht.

Bei genügend großem Molekulargewicht ($M \to \infty$) kann das Glied a/M auf der rechten Seite der Gl. (1) gegenüber b vernachläßigt werden. In diesem Fall wird die spezifische Eigenschaft allein durch den Zahlenwert der Konstante b bestimmt.

Experimenteller Teil

Gemeinsam bei den bisherigen Untersuchungen war, daß sie sich durchwegs mit linearen bzw. cyclischen oligomeren polymerhomologen Verbindungen solcher Struktur befaßten, deren Zusammensetzung mit der folgenden allgemeinen Formel angegeben werden kann:

$$Y-(M)_n-X \quad \text{bzw.} \quad \underline{(M)_n}\,, \tag{4}$$

wobei M das Kettenglied, n den Polymerisationsgrad und Y und X solche Endgruppen bedeuten, die gleich oder verschieden sein können. Die bisherigen Untersuchungen erstreckten sich aber nicht auf solche polymerhomologe oligomere Verbindungen, deren Zusammensetzung mit der folgenden allgemeinen Formel zu beschrieben ist:

$$Y-(M_n)-R-(M)_n-X, \tag{5}$$

wobei R irgendwelches von den Kettengliedern verschiedene Atom oder Atomgruppe bezeichnet, während die übrigen Zeichen den schon im Text vorgekommenen entsprechen. Für Verbindungen dieser Art war selbst das nicht klar, ob Gl. (1) gültig ist, bzw. inwiefern sie bei polymerhomologen Verbindungen solcher Zusammensetzung verwendbar ist. In der vorliegenden Arbeit wurde daher vor allem auf Grund der Arbeit sowjetischer Forschern eine diesbezügliche Untersuchung einiger in der Literatur neuerdings auffindbaren — mit der Formel (5) zu beschreibenden polymerhomologen oligomeren Verbindungen fortgeführt, näher die Untersuchung der Änderung des Brechnungsindexes, des spezifischen Volumens und der aus diesen beiden berechenbaren spezifischen Refraktion dieser Verbindungen als Funktion der Molekülgröße. Die untersuchten Reihen, nebst Angabe der Quellen der zugehörigen Daten sind in Tabelle I zusammengestellt.

Unter den untersuchten polymerhomologen oligomeren Verbindungen befinden sich sowohl solche mit linearen, als auch solche mit verzweigten Ketten. Die spezifische Refraktion, das Brechungsvermögen und das spezifische Volumen dieser Verbindungen als Funktion des Reziprokwertes der Molekular-

Tabelle I

Die untersuchten, in der Kettenmitte eine Heteroatomgruppe enthaltenden polymerhomologen Reihen und Quelle der Daten über ihren Brechnungsindex und ihr spezifisches Volumen

I.

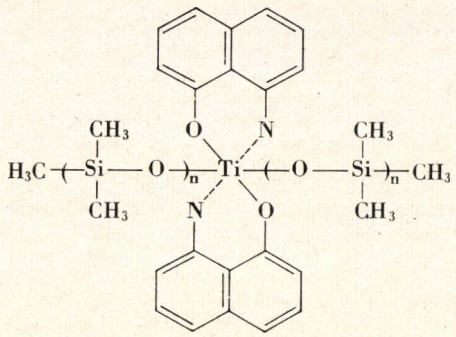

[12] $n = 15, 60, 98, 170, 350$

II.

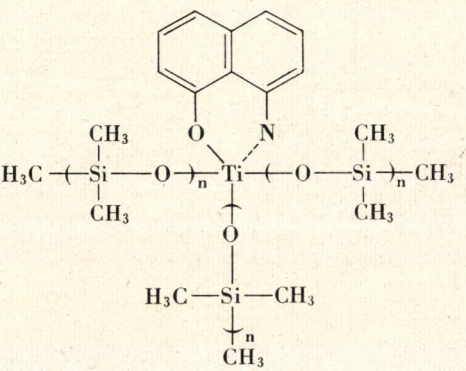

[12] $n = 10, 15, 98, 136, 170$

III.

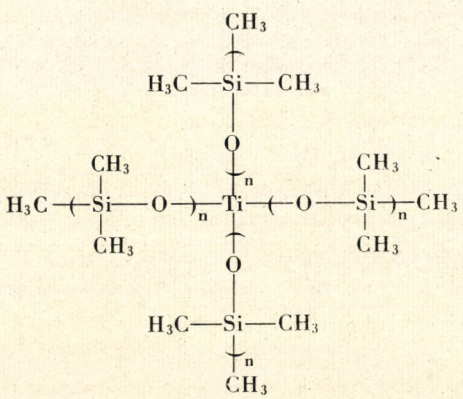

[13] $n = 23, 66, 72$

Fortsetzung der Tabelle I

IV.

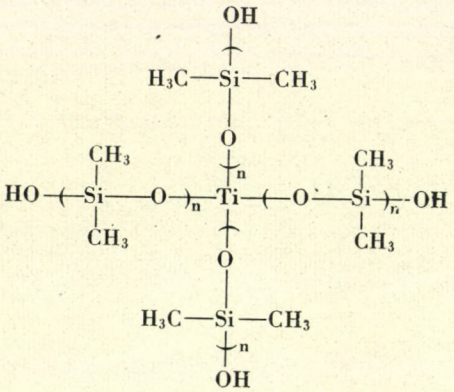

[13] n = 9, 18, 25, 34, 42, 52, 80, 104

IV.a

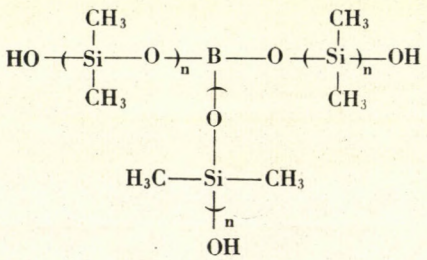

[14*] n = 9, 13, 25, 46, 135, 220

V. $CH_3-(CH_2-)_n-SiH_2-(CH_2)_n-CH_3$

[15] n = 1, 2, 3

VI. $HO-(CH_2)_n-OOC-(CH_2)_4-COOO-(CH_2)_n-OH$

[16] n = 4, 5, 6

VII. $CH_3-(CH_2)_n-OOC-C_6H_4-COO-(CH_2)_n-CH_3$

[17] n = 0, 3, 5, 7, 8, 9

VIII. $CH_3-(CH_2)_n-OOC-C_6H_4-(CH_2)_2-COO-(CH_2)_n-CH_3$

[17] n = 1, 3, 5, 6, 7

* Es sind lediglich Daten über den Brechungsindex bekannt.

größe dargestellt liegen die erhaltenen Punkte mit guter Annäherung auf einer Geraden, wie dies auch aus Abb. 1—3 ersichtlich ist. Ein ähnlicher Zusammenhang ergibt sich auch für die übrigen untersuchten, jedoch wegen Platzmangel nicht dargestellten Fälle (zahlenmäßig 22). Die Werte für die

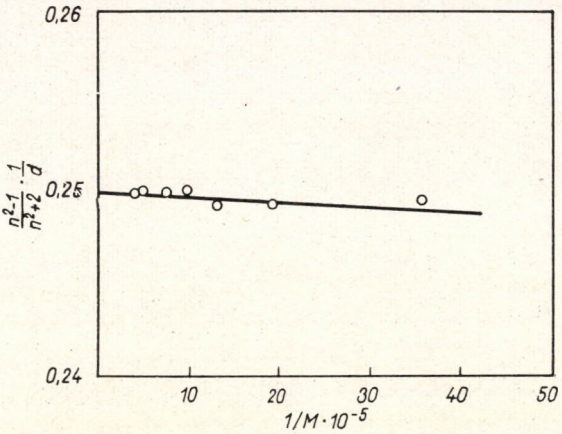

Abb. 1. Spezifische Refraktion von Ti-Dimethylsiloxanen mit OH-Endgruppen, als Funktion des Reziprokwertes des Molekulargewichtes

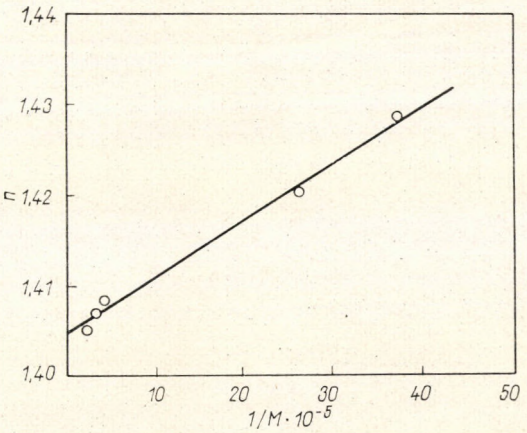

Abb. 2. Änderung des Brechungsindexes von Poly(8-oxy-chinolin-Ti-Dimethylsiloxanen) mit verzweigter Kette als Funktion des Reziprokwertes des Molekulargewichtes

Richtungstangenten und die Achsenabschnitte der für die einzelnen untersuchten spezifischen Eigenschaften erhaltenen Geraden wurden für Polymere verschiedener Struktur nach der Methode der kleinsten Quadrate (*der sog. Durchschnittswerte) berechnet, und in Tabelle II zusammengefaßt. Um Vergleiche zu erleichten, sind auch die in den früheren Arbeiten für die Dimethylsiloxan- und Methylen-Kettenglieder (Gruppen) erhaltenen spezifischen Grenzwerte (der Wert der Konstante *b* in Gl. (1)) angegeben.

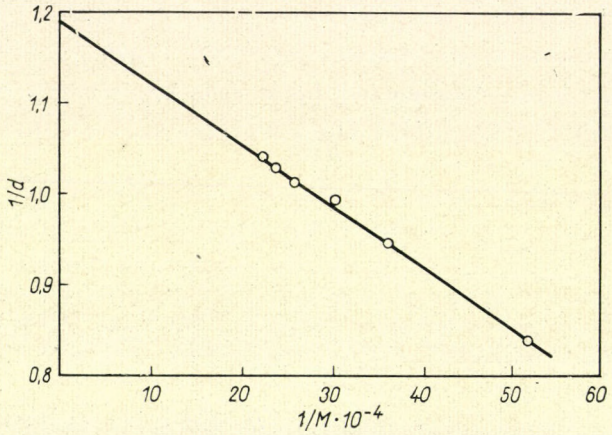

Abb. 3. Änderung des spezifischen Volumens der *o*-Phtalsäureester mit *n*-Alkoholen, als Funktion des Reziprokwertes des Molekulargewichtes

Diskussion der erhaltenen Ergebnisse

Aus Abb. 1—3 sowie aus den untersuchten Fällen kann festgestellt werden, daß sich die Gl. (1) auch zur Beschreibung der von additiven Größen ableitbaren spezifischen Eigenschaften solcher Verbindungen als Funktion der Molekülgröße eignet, die mit der allgemeinen Formel (5) charakterisiert werden können, gleichgültig davon, ob es sich um lineare Moleküle oder solche mit verzweigten Ketten handelt.

Eine nähere Untersuchung der Daten in Tabelle II zeigt, daß die spezifischen Grenzwerte (Konstante *b* in Gl. (1)) der polymerhomologen Reihen **I, II, III, IV** und **IV/a**, sowie der Homologreihen **V, VI, VII** und **VIII,** und die entsprechenden Grenzwerte der Polydimethylsiloxane bzw. der Paraffin-Kohlenwasserstoffe nahezu identisch sind, obwohl im Falle der letzteren die zum Brechungsindex und zum spezifischen Volumen gehörigen *b*-Werte etwas stärker abweichen, was darauf hinweist, daß bei diesen Verbindungen das in die Kette eingebaute Heteroatom oder — atomgruppe auf die Gestaltung der endgültigen Größe dieser Grenzwerte einen gewissen, wenn auch nicht allzu starken Einfluß ausübt.

Wenn nun die mit der bereits früher beschriebenen Methode [18] auf Grund der Gl. (3) berechneten Werte der Konstanten *a* stichprobenartig mit den in Tabelle II enthaltenen Werten verglichen werden, so ergibt sicht bei Verwendung der Gl. (1) auf die spezifische Refraktion (da die zur Berechnung benötigten Inkremente für diesen Fall am ehesten zugänglich sind) für den Wert *a* der polymerhomologen Reihe **I,** mit CH_3- als Endgruppe, 5,08 anstatt 21,58, und für den Wert *a* der Homologreihe **VI,** unter der Annahme, daß beide Endgruppen OH-Gruppen sind, —6,53 gegenüber dem gefundenen Wert von —23,4. Im letzteren Fall ergibt sich auf Grund der Gl. (3) berechnet

Tabelle II

Werte der Konstanten a und b der Gleichung (1) auf Grund der einzelnen untersuchten spezifischen Eigenschaften für Polymere verschiedener Struktur nach der Methode der kleinsten Quadrate (Durchschnittswerte) bestimmt*

	a			*b*		
	n	$1/d$	r_{sp}	n	$1/d$	r_{sp}
I.	99,06*	—105,46*	21,58*	1,403*	1,024*	0,250*
II.	66,93	—82,50	3,01	1,403	1,025	0,250
III.	—13,28	10,92	9,34	1,405	1,027	0,251
IV.	23,92	—67,80	—4,09	1,405	1,023	0,251
IV/a.	13,76	—	—	1,404	—	—
CH_3 | $(Si-O-)_n$ | CH_3	—	—	—	1,403 (2)	1,03 (6)	0,251 (1)
V.	—9,16	32,85	1,39	1,494	1,093	0,332
VI.	—11,55**	—102,97**	—23,40	1,506**	1,260**	0,322
VII.	10,33**	—66,70*	—14,58*	1,463*	1,190*	0,331*
VIII.	10,70	—85,14	—18,81	1,451	1,235	0,336
$-(CH)_2-_n$	—	—	—	1,470 (2)	1,18 (6)	0,331 (1)

** Aus zwei Daten bestimmt

für die Konstante *a* ein Wert von —24,63 ($a = 2/17{,}243 - 89 \times 0{,}332/ = = -24{,}63$), falls man als Endgruppen die Atomgruppen $-(CH_2)_2COO-$ und —OH betrachtet. Dieser direkte Vergleich ist zur Zeit im Falle titanhaltiger Verbindungstypen (**I, II, III, IV**) nicht möglich, da das Inkrement für die Bindung Ti—O nicht zur Verfügung steht.

Die Identität der entsprechenden *b*-Werte sowie der zahlenmäßige Wert der Konstanten *a* können nur dann aufgrund der bisher diskutierten Ergebnisse gedeutet werden, wenn man annimmt, daß sich die Konstanten der Gleichung (1) nicht auf das ganze Molekül der mit der allgemeinen Formel (5) beschriebenen Reihen beziehen, sondern nur auf ein zwischen dem Heteroatom oder -atomgruppe und einer der Endgruppen liegendes Segment des Moleküls. So z. B. im Falle von **III** auf das durch die Formel

$$Ti/_4(-O-\underset{\displaystyle CH_3}{\overset{\displaystyle |}{Si}}-O)_n-\underset{\displaystyle CH_3}{\overset{\displaystyle |}{Si}}-CH_3$$

dargestellte Segment, wo die Atomgruppe $\begin{matrix} CH_3 \\ | \\ (O-Si) \\ | \\ CH_3 \end{matrix}$ als Kettenglied, und $Ti/_4$- bzw. CH_3- als Endgruppen zu betrachten sind oder im Falle von V, auf das Segment $H-Si/2-(CH_2)_n-CH_3$, wo (CH_2) die Kettenmitglieder und $H-Si/_2$- sowie $-CH_3$ die Endgruppen bilden usw. Diese Feststellung gilt natürlich sowohl für Moleküle mit linearen als auch für solche mit verzweigten Ketten.

ZUSAMMENFASSUNG

Ausgehend von Literaturdaten, zeigte der Verfasser, daß die Gl. $\varphi_{sp} = \frac{a}{M} + b$, wobei φ_{sp} irgendeine spezifische Eigenschaft, M das Molekulargewicht, a und b Konstanten bedeuten, auch bei solchen polymerhomologen oligomeren Verbindungen mit linearen oder verzweigten Ketten angewandt werden kann, die mit der folgenden allgemeinen Formel beschrieben werden können:

$$Y-(M)_n-R-(M)_n-X,$$

wobei R irgendwelches zwei- oder mehrwertige Atom oder Atomgruppe ist. Die Konstanten der Gleichung kennzeichnen in diesem Fall das Segment zwischen dem Heteroatom und einer Endgruppe bzw. können sie aus diesen Strukturmerkmalen berechnet werden.

LITERATUR

1. GÉCZY, I.: Acta Chim. Acad.Sci.Hung. **34,** 323 (1962); Magyar Kém. Folyóirat **69,** 312 (1963)
2. GÉCZY, I.: Acta Chim.Acad.Sci.Hung. **37,** 435 (1963); Magy.Kém.Folyóirat **69,** 333 (1963).
3. GÉCZY, I.: Magy. Kém. Folyóirat **70,** 91 (1964); Visokomolekul.Soed. **7,** 642 (1965).
4. GÉCZY, I.: Magy. Kém. Folyóirat **70,** 99 (1964); Chemische Gesellschaft **11,** 86 (1964); Koll. Z., Z. Polymere **201,** 99 (1965).
5. GÉCZY, I.: Magy. Kém. Folyóirat **70,** 156 (1964); Makromol. Chem. **90,** 161 (1966).
6. GÉCZY, I.: Magy. Kém. Folyóirat **70,** 242 (1964); Plaste u. Kautschuk **13,** 11 (1966).
7. GÉCZY, I.: Magy. Kém. Folyóirat **70,** 244 (1964); Zh. Priklad. Khim. **40,** 348 (1967).
8. GÉCZY, I.: Magy. Kém. Folyóirat **71,** 216 (1965); Acta Chim.Acad. Sci.Hung. **45,** 131 (1965).
9. GÉCZY, I.: Kolorisztikai Ért. **8,** 14 (1966); Faserforsch. u. Textiltechn. **17,** 470 (966).
10. GÉCZY, I.: Kolorisztikai Ért. **8,** 221 (1966).
11. GÉCZY, I.: Magy. Kém. Folyóirat **71,** 551 (1965); Polymer Previews **2,** 556 (1966); J. Polym. Sci. (C) **16,** 2991 (1967).
12. ANDRIANOW, K. A., LAWIGIN, I. A.: Visokomolek. Soed. **7,** 1585 (1965).
13. ANDRIANOW, K. A., GOLUBKOW, G. E., JELINEK, W. I., KURASCHEWA, N. A., MANUTSCHAROWA, I. F., LITWINOWA, L. F., ARTEM'EW, B. K.: Visokomol. Soed. **7,** 682 (1965).
14. ANDRIANOW, K. A., JERMAKOWA, M. N.: Izw. Akad. Nauk S.S.S.R. (Khim.) **1966,** 680.
15. Issledowanija w oblasti kremnijorganitscheskich soed. Sb. Statei, Izd. Akad. Nauk S.S.S.R. Moskwa. 1963. S. 231.
16. ZIL'BERMAN, E. N., KULIKOWA, A. E., TEPLJAKOW, N. M.: J.Polym. Sci. **56,** 417 (1962).
17. SUWOROWA, A. I., TAGER, A. A., NOWIKOW, N. I., GOLDIREW, L. N. ESAFOW, W. I., KONOWALOWA, S. G.: Visokomol. Soed. **8,** 1692 (1966).
18. GÉCZY, I.: Magy. Kém. Folyóirat **70,** 249 (1964); Visokomol. Soed. **9,** (B) 81 (1967).

István GÉCZY; Budapest, 62 pf. 182.

INDEX

INORGANIC AND ANALYTICAL CHEMISTRY — ANORGANISCHE UND ANALITISCHE CHEMIE — НЕОРГАНИЧЕСКАЯ И АНАЛИТИЧЕСКАЯ ХИМИЯ

LÉGRÁDI, L.: Mechanism of Adsorption Indication, III. 4-(4'-Nitrophenylazo)-1- naphthol, a New Adsorption Indicator 241

LÉGRÁDI, L.: Mechanism of Adsorption Indication, IV. Combination of the Fajans Indication with the Acid–Base Principle 247

BURGER, K., VÉRTES, A. and PAPP-MOLNÁR, E.: The Nephelauxetic Series and the Order of the Mössbauer Parameters of Iron Complexes 257

TÖLGYESSY, J., BRAUN, T. and VARGA, S.: Some Problems concerning the theory of the Application of Radioactive Kryptonates as Complexometric Indicators 265

PHYSICAL CHEMISTRY — PHYSIKALISCHE CHEMIE — ФИЗИЧЕСКАЯ ХИМИЯ

POKÓ, Z., FODOR, M. and SZABÓ, E.: Formation, Thermal Decomposition and Structure of the System UO_3—H_2O, III. Thermal Decomposition of β-$UO_3 \cdot 2H_2O$ Produced from γ-UO_3 275

LENGYEL, T.: Investigations on Ion Exchange Equilibria with Radioactive Tracer Method, XII. Determination of the Successive Formation Constants of α-Hydroxyisobutyrate Complexes of Europium 291

ERDEY-GRUZ, T. und KUGLER, E.: Über den Wanderungsmechanismus von Wasserstoff- und Hydroxylionen, VIII. Einfluß der Zusammensetzung von Glycerin-Wasser-Gemischen auf die elektrische Leitfähigkeit und Viskosität von gelöstem HCl, KOH, KF und KCl bei 5 und 25 °C 301

KALLÓ, D.: Die katalytisch kinetische Deutung der scheinbar reversiblen Dreieckreaktion erster Ordnung der *n*-Butenisomerisierung 313

ORGANIC CHEMISTRY — ORGANISCHE CHEMIE — ОРГАНИЧЕСКАЯ ХИМИЯ

ZSADON, B. und PAÁL, T.: Über die quantitative polarographische Bestimmung des Morphingehalts von Mohnkapseln 323

SZÁNTAY, Cs., NOVÁK, L. and SOHÁR, P.: Chemistry of Heterocyclic Pseudobasic Aminocarbinols, XXXIV. Notes of the Synthesis of "Quantril" and on the Tautomerism of β-Oxo-Carboxamides 335

GÉCZY, I.: Synthetische lineare Polymere, XXVIII. Zusammenhang zwischen einzelnen spezifischen Eigenschaften der in der Kettenmitte Heteroatome oder -Atomgruppen enthaltenden oligomeren polymerhomologen Verbindungen und ihrer Molekülgröße 345

Printed in Hungary

A kiadásért felel az Akadémiai Kiadó igazgatója — Műszaki szerkesztő: Farkas Sándor

A kézirat nyomdába érkezett: 1968. V. 30. — Terjedelem: 10 (A/5) ív, 61 ábra

68.65738 Akadémiai Nyomda, Budapest — Felelős vezető: Bernát György

ACTA CHIMICA

ТОМ LVII — ВЫП. 3

РЕЗЮМЕ

Механизм адсорбционной индикации, III. Новый адсорбционный индикатор — 4-(4'-нитро-фенил-азо)-I-нафтол

Л. ЛЕГРАДИ

Описывается универсальный аргентометрический индикатор — 4-(4'-нитро-фенил-азо-)-I-нафтол, который может быть использован при титровании ионов хлорида, бромида, иодида, тиоцианида и цианида. Титрование выполняется при pH = 9—10. Индикатор работает на кислотно-основном принципе. Это можно доказать путем установления изменения константы диссоциации адсорбата-красителя при избытке собственных ионов. Подробно обсуждается механизм индикаторного действия.

Механизм адсорбционной индикации, IV. Комбинирование принципа индикации Фаянса с кислотно-основным принципом

Л. ЛЕГРАДИ

Автором описывается новый адсорбционный индикатор — 2-(4'-нитро-фенилазо)-I-нафтол-4-сульфокислота, применяемый при аргентометрическом определении ионов хлорида, бромида, иодида, тиоцианида и цианида. Механизм индикаторного действия является сочетанием адсорбционно-десорбционного процесса с кислотно-основным принципом. Изменение окраски происходит вследствие образования структуры нитроновой кислоты под действием иона серебра или щелочи. Наличие этого типа индикаторного действия можно доказать: а) определением изменения pH при титровании, б) демонстрацией практического постоянства константы диссоциации адсорбата-красителя в избытке анионов и в) адсорбционными измерениями.

Нефелауксетический ряд и ряд параметров Мёссбауэра для комплексов железа

К. БУРГЕР, А. ВЕРТЕШ и Э. ПАП-МОЛНАР

Приводится зависимость между нефелауксетическим влиянием лигандов и параметрами Мёссбауэра для их комплексов железа. На основе приводимых собственных и литературных данных можно наблюдать, что параметры Мёссбауэра для безводных галогенидов, антранилата, гипофосфита, сульфида и диэтил-дитиокарбамата железа(II) соответствуют нефелауксетическому ряду.

Некоторые теоретические проблемы применения радиоактивных вкраплений криптона в качестве индикатора при комплексометрическом титровании

Й. ТЁЛЬДЕШИ, Т. БРАУН и Ш. ВАРГА

Настоящая работа занимается возможностью применения радиоактивных вкраплений криптона в качестве комплексометрических индикаторов. Авторы изучали условия, влияние на выбор радиоактивного вкрапления криптона в качестве индикатора. При выборе индикатора необходимо учитывать все равновесия, как в точке эквивалентности, так и после нее, которые характеризуются кажущимися константами стабильности и произведениями растворимости всех присутствующих в системе комплексов и осадков. Применение выведенных теоретических зависимостей иллюстрируется на конкретном примере выбора и изучения действия радиоактивного вкрапления криптона $Ag10_3$ [^{85}Kr] в качестве индикатора. Индикатор $Ag10_3$ [^{85}Kr] применялся при определении Ca^{2+} путем титрования раствором ЭДТК.

Исследование образования, термического разложения и структуры системы UO_3—H_2O, III. Термическое разложение β-$UO_3 \cdot 2H_2O$, полученного из γ-UO_3:

З. ПОКО, М. ФОДОР и Э. САБО

При определении свойств системы UO_3—H_2O предварительно было исследовано подробно термическое разложение модификаций трёхокисей урана, полученных разными методами. В настоящей работе обсуждаются свойства системы γ-UO_3—H_2O и термическое разложение модификации β-$UO_3 \cdot 2H_2O$, полученного из γ-UO_3. По данным дериватографических исследований было установлено, что продукты гидратации γ-UO_3 отличаются от до сих пор исследованных продуктов гидратации трёхокисей урана. При сопоставлении конечных продуктов гидролиза, проведенного при комнатной температуре, свойства модификаций α-и β-дигидратов наглядно отличаются.

Изучение ионообменных равновесий с помощью радиоактивной индикации, XII. Определение последовательных констант стабильности комплексов европия с α-гидрокси-изомасляной кислотой

Т. ЛЕНДЬЕЛ

Были определены последовательные константы стабильности комплексов европия с α-гидрокси-изомасляной кислотой с помощью жидкого ионообменника — ди-2-этилгексил-фосфорной кислоты. На основе расчетов, проведенных методом Фронеуса и одним из новых методов, были получены следующие значения $\log K_1 = 2{,}70$, $\log K_2 = 2{,}27$ и $\log K_3 = 1{,}55$, находящиеся в хорошем согласии с литературными данными.

О механизме миграции водородного и гидроксидного ионов, VIII. Влияние состава глицерино водных смесей и температуры на электропроводность растворов HCl, KOH, KF и KCl и на их вязкость при температурах 5 и 25°C

Т. ЭРДЕИ-ГРУЗ и Э. КУГЛЕР

Эквивалентная электропроводность раствора HCl в глицерине уменьшается под влиянием небольшого количества воды, при содержании воды 8 мол.% проходит через минимум, а затем увеличивается. Электропроводность растворов KOH, KCl и KF с увеличением содержания воды изменяется в небольшой степени до значений содержания воды, равных 40 мол.% в случае KOH и 60 мол.% в случае KCl и KF, а затем быстро возрастает вплоть до значения, соответствующего водному раствору.

Произведение эквивалентной электропроводности и вязкости в случае глицеринового раствора HCl намного больше, чем в случае водного раствора и сначала резко падает с увеличением содержания воды, между 15—50 мол.% воды почти не изменяется, а затем почти линейно падает. Величина произведения $\Lambda\eta$ достигает минимума при 95 мол.% воды.

Энергия активации электропроводности HCl имеет максимум при 4 мол.% воды, затем уменьшается от 13,8 ккал/моль почти линейно до величины, соответствующей водному раствору. Энергия активации электропроводности растворов KOH, KCl и KF монотонно уменьшается с ростом содержания воды.

На основе экспериментальных результатов можно установить, что в растворах с высоким содержанием глицерина, ионы глицерин-оксония, наряду с гидродинамической миграцией, проводят электрический ток и путем передачи протонов.

Кажется вероятным, что подобно ионам гидроксила в водных растворах, ионы глицерата в глицерине также способны к обмену протонов. В относительно высокой подвижности ионов гидроксила играет роль то, что вследствие несферической симметрии силового поля, они сильнее разрыхляют структуру, чем ионы F^- и Cl^-, которые имеют сферическую симметрию.

Кинетик-каталитическое значение видимо обратимой трехугольной реакции первого порядка изомеризации n-бутенов

Д. КАЛЛО

Кинетика изомеризации *n*-бутенов на твердых кислых катализаторах формально может быть описана схемой обратимой трехугольной реакции; все ступени являются реакциями первого порядка. При интерпретации кинетики каталитического процесса предполагалось образование карбониевого иона и-бутила как общего промежуточного продукта. Согласно этому, реакция на поверхности происходит по следующей схеме:

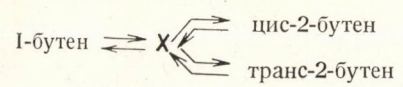

Уравнения для селективности, выведенные на основе этой схемы, формально идентичны феноменологически найденными. Были рассчитаны относительные скорости адсорбции, а также вероятности десорбции отдельных изомеров.

О количественном определении содержания морфина в маковке полярографическим методом

Б. ЖАДОН и Т. ПААЛ

Было установлено, что высота полярогчафической волны морфина уменьшается по кинетическому уравнению первого порядка в том случае, если нитрозирование проводится при постоянной температуре и продолжительность реакции превышает 5 минут. Уменьшение высоты волны также зависит от температуры нитрозирования. При измерениях длительность нитрозирования изменялось в интервале 5—50 мин., а температура между 20 и 30 °C.

Такие же измерения проводились с солянокислыми экстрактами маковки. Было установлено, что относительное уменьшение высоты волны в этом случае меньше, чем для чистого морфина при прочих равных условиях. Это объясняется тем, что примеси, сопровождающие морфин в данном экстракте, увеличивают высоту волны в одинаковой степени, независимо от времени нитрозирования, а высота волны, соответствующая дествительному количеству морфина уменьшается при увеличении времени нитрозирования в той же мере, как и в случае чистого морфина.

Дается метод расчета, с помощью которого можно определить истинное содержание морфина в экстрактах маковки без отделения мешающих веществ, если известны высоты волны при двух различных временах нитрозирования.

Некоторые данные к химии гетероциклических, псевдоосновных аминокарбинолов, XXXIV. Замечания к синтезу «Анантрила» и таутомерии аминов β-оксокарбоновых кислот

Ч. САНТАИ, Л. НОВАК и П. ШОХАР

Изучались условия кето-энольной таутомерии производных 2-оксо-бензо(а)-хинолизидинов, содержащих амидокислотную, эфирную или нитриловую группу в положени 3. С помощью ик- и ЯМР-спектроскопии определялось содержание энольной формы амида N-диэтил-ацетоуксусной кислоты в качестве модельного соединения, и было установлено, что среди производных β-оксокарбоновых кислот в наибольшей степени энолизируется это производное с двумя заместителями на азоте.

Синтетические линейные полимеры, XXVIII. Зависимость между некоторыми удельными свойствами полимерных гомологов — олигомеров, содержащих различные атомы или атомные группы в середине цепи, и размерами молекул

И. ГЕЦИ

На основании литературных данных, автором было показано, что уравнение (I) может быть использовано и для таких олигомерных соединений, являющихся полимерными гомологами с линейной или разветвленной цепочкой, которые можно представить в виде следующей общей формулы:

$$Y-(M)_n-R-(M)_n-X\,,$$

где R — двух- или многовалентный атом или атомная группа. Постоянные в уравнении в этом случае характерны для сегмента, находящегося между атомом или атомной группой, отличающимися от повторяющихся звеньев молекулы, и какой-либо концевой группой; они могут быть определены путем расчета из этих структурных характеристиков.

The Acta Chimica publish papers on chemistry in English, German, French and Russian.

The Acta Chimica appear in volumes consisting of four parts of varying size, 4 volumes being published a year.

Manuscripts should be addressed to

Acta Chimica
Budapest 112/91 Műegyetem

Correspondence with the editors should be sent to the same address.

The rate of subscription is 165 forints a volume. Orders may be placed with "*Kultúra*" Foreign Trade Company for Books and Newspapers (Budapest I., Fő utca 32. Account No. 43-790-057-181) or with representatives abroad.

Les Acta Chimica paraissent en français, allemand, anglais et russe et publient des mémoires du domaine des sciences chimiques.

Les Acta Chimica sont publiés sous forme de fascicules. Quatre fascicules seront réunis en un volume (4 volumes par an).

On est prié d'envoyer les manuscrits destinés à la rédaction à l'adresse suivante:

Acta Chimica
Budapest 112/91 Műegyetem

Toute correspondance doit être envoyée à cette même adresse.

Le prix de l'abonnement est de 165 forints par volume.

On peut s'abonner à l'Entreprise pour le Commerce Extérieur de Livres et Journaux «*Kultúra*» (Budapest I., Fő utca 32. Compte-courant No. 43-790-057-181) ou à l'étranger chez tous les représentants ou dépositaires.

«*Acta Chimica*» издают трактаты из области химической науки на русском, французском, английском и немецком языках.

«*Acta Chimica*» выходят отдельными выпусками разногообъема. 4 выпуска составляют один том. 4 тома публикуются в год.

Предназначенные для публикации рукописи следует направлять по адресу:

Acta Chimica
Budapest 112/91 Műegyetem

По этому же адресу направлять всякую корреспонденцию для редакции.

Подписная цена «*Acta Chimica*» — 165 форинтов за том. Заказы принимает предприятие по внешней торговле книг и газет «*Kultúra*» (Budapest I., Fő utca 32. Текущий счет № 43-790-057-181) или его заграничные представительства и уполномоченные.

44,— Ft

Reviews of the Hungarian Academy of Sciences are obtainable at the following addresses:

ALBANIA
Ndermarja Shtetnore e Botimeve
Tirana

AUSTRALIA
A. Keessing
Box 4886, GPO
Sydney

AUSTRIA
Globus Buchvertrieb
Salzgries 16
Wien I

BELGIUM
Office International de Librairie
30, Avenue Marnix
Bruxelles 5
Du Monde Entier
5, Place St. Jean
Bruxelles

BULGARIA
Raznoiznos
1, Tzar Assen
Sofia

CANADA
Pannonia Books
2. Spadina Road
Toronto 4, Ont.

CHINA
Waiwen Shudian
Peking
P. O. B. 88

CZECHOSLOVAKIA
Artia
Ve Smečkách 30
Praha 2
Poštovná Novinová Služba
Dovoz tisku
Vinohradská 46
Praha 2
Mad'arská Kultura
Václavské nám. 2
Praha I
Poštová Novinová Služba
Dovoz tlače
Leningradská 14
Bratislava

DENMARK
Ejnar Munksgaard
Nörregade 6
Copenhagen

FINLAND
Akateeminen Kirjakauppa
Keskuskatu 2
Helsinki

FRANCE
Office International de Documentation et Librairie
48, rue Gay Lussac
Paris 5

GERMAN DEMOCRATIC REPUBLIC
Deutscher Buch-Export und Import
Leninstraße 16
Leipzig 701
Zeitungsvertriebsamt
Clara Zetkin Straße 62
Berlin N. W.

GERMAN FEDERAL REPUBLIC
Kunst und Wissen
Erich Bieber
Postfach 46
7 Stuttgart S.

GREAT BRITAIN
Collet's Holdings Ltd.
Dennington Estate
London Rd.
Wellingborough, Northants.
Robert Maxwell and Co. Ltd.
Waynflete Bldg. The Plain
Oxford

HOLLAND
Swetz and Zeitlinger
Keizersgracht 471—487
Amsterdam C
Martinus Nijhof
Lange Voorhout 9
The Hague

INDIA
Current Technical Literature
Co. Private Ltd.
India House OPP
GPO Post Box 1374
Bombay I

ITALY
Santo Vanasia
Via M. Macchi 71
Milano
Libreria Commissionaria Sansoni
Via La Marmora 45
Firenze

JAPAN
Nauka Ltd.
92, Ikebukur O-Higashi 1-chome
Toshima-ku
Tokyo
Maruzen and Co. Ltd.
P. O. Box 605
Tokyo-Central
Far Eastern Booksellers
Kanda P. O. Box 72
Tokyo

KOREA
Chulpanmul
Phenjan

NORWAY
Johan Grundt Tanum
Karl Johansgatan 43
Oslo

POLAND
Ruch
ul. Wronia 23
Warszawa

ROUMANIA
Cartimex
Str. Aristide Briand 14—18
Bucureşti

SOVIET UNION
Mezhdunarodnaya Kniga
Moscow G—200

SWEDEN
Almquist and Wiksell
Gamla Brogatan 26
Stockholm

USA
Stechert Hafner Inc.
31, East 10th Street
New York, N. Y. 10003
Walter J. Johnson
111, Fifth Avenue
New York, N. Y. 10003

VIETNAM
Xunhasaba
19, Tran Quoc Toan
Hanoi

YUGOSLAVIA
Forum
Vojvode Mišića broj 1
Novi Sad
Jugoslovenska Knjiga
Terazije 27
Beograd

24. IX. 1968.

Index: 26.007

ACTA CHIMICA

ACADEMIAE SCIENTIARUM HUNGARICAE

ADIUVANTIBUS

L. ERDEY, K. POLINSZKY, G. SCHAY

AC

R. BOGNÁR, GY. BRUCKNER, Z. CSŰRÖS, T. ERDEY-GRÚZ, Z. FÖLDI, M. FREUND, Á. GERECS, GY. HARDY, J. HOLLÓ, Á. KISS, M. KORACH, F. MÁRTA, F. NAGY, E. PUNGOR, Z. SZABÓ, P. TÉTÉNYI, L. VARGHA, K. VAS

REDIGIT

B. LENGYEL

TOMUS 57 FASCICULUS 4

AKADÉMIAI KIADÓ, BUDAPEST

1968

ACTA CHIM. ACAD. SCI. HUNG.

ACTA CHIMICA

A MAGYAR TUDOMÁNYOS AKADÉMIA KÉMIAI TUDOMÁNYOK OSZTÁLYÁNAK IDEGEN NYELVŰ KÖZLEMÉNYEI

SZERKESZTI

LENGYEL BÉLA

TECHNIKAI SZERKESZTŐK

DEÁK GYULA és HARASZTHY-PAPP MELINDA

Az Acta Chimica német, angol, francia és orosz nyelven közöl értekezéseket a kémiai tudományok köréből.

Az Acta Chimica változó terjedelmű füzetekben jelenik meg, egy-egy kötet négy füzetből áll. Évente átlag négy kötet jelenik meg.

A közlésre szánt kéziratok a szerkesztőség címére (Budapest 112/91 Műegyetem) küldendők.

Ugyanerre a címre küldendő minden szerkesztőségi levelezés. A szerkesztőség kéziratokat nem ad vissza.

Az Acta Chimica előfizetési ára kötetenként belföldre 120 Ft, külföldre 165 Ft. Megrendelhető a belföld számára az „Akadémiai Kiadó"-nál (Budapest V., Alkotmány utca 21. Bankszámla 05-915-111-46), a külföld számára pedig a „Kultúra" Könyv- és Hírlap Külkereskedelmi Vállalatnál (Budapest I., Fő utca 32. Bankszámla: 43-790-057-181) vagy annak külföldi képviseleteinél és bizományosainál.

Die Acta Chimica veröffentlichen Abhandlungen aus dem Bereiche der chemischen Wissenschaften in deutscher, englischer, französischer und russischer Sprache.

Die Acta Chimica erscheinen in Heften wechselnden Umfanges. Vier Hefte bilden einen Band. Jährlich erscheinen 4 Bände.

Die zur Veröffentlichung bestimmten Manuskripte sind an folgende Adresse zu senden:

Acta Chimica
Budapest 112/91 Műegyetem

An die gleiche Anschrift ist auch jede für die Redaktion bestimmte Korrespondenz zu richten.

Abonnementspreis pro Band: 165 Forint. Bestellbar bei dem Buch- und Zeitungs-Außenhandels-Unternehmen »*Kultúra*« (Budapest I., Fő utca 32. Bankkonto No. 43-790-057-181) oder bei seinen Auslandsvertretungen und Kommissionären.

Acta Chimica Academiae Scientiarum Hungaricae Tomus 57 (4), pp. 353—362 (1968)

ИЗУЧЕНИЕ РАСПРЕДЕЛЕНИЯ РЕДКИХ ЭЛЕМЕНТОВ МЕЖДУ РАЗЛИЧНЫМИ ФАЗАМИ КАМЕННЫХ МЕТЕОРИТОВ МЕТОДОМ НЕЙТРОНО-АКТИВАЦИОННОГО АНАЛИЗА*

А. К. Лаврухина, Л. Л. Кашкаров, Г. М. Колесов и Л. И. Генаева

(Институт геохимии и аналитической химии им. В. И. Вернадского АН СССР, Москва)

Поступило 2-го августа 1967 г.

В последние годы получили большое развитие работы по изучению химического состава метеоритного вещества. Метеориты, самые малые космические тела Солнечной системы, непрерывно выпадают на поверхность Земли и являются единственными космическими объектами, доступными детальному исследованию в лабораториях.

Метеориты значительно отличаются от земных пород по структуре, а также химическому и фазовому составам. Основными фазами являются силикатная и металлическая; последняя представляет собой железо-никелистые твердые растворы с переменным содержанием никеля (от 3 до 70%). Соотношение фаз в метеоритах различных классов непрерывно изменяется. Железные метеориты состоят преимущественно из никелистого железа, а некоторые типы каменных метеоритов (углистые хондриты, ряд ахондритов) — из силикатного расплава. Своеобразие метеоритного вещества заключается также в наличии у наиболее часто встречающихся типов метеоритов, хондритов хондр — застывших стеклообразных капелек силикатного и железо-никелистого расплавов различных размеров (от нескольких долей миллиметра до нескольких миллиметров).

Для познания процессов, приведших к описанным особенностям метеоритного вещества, необходимы детальные исследования закономерностей распределения элементов между отдельными фазами, металлической и силикатной, между хондрами и межхондровым веществом, между отдельными минералами и т. д.

Решение этой задачи требует применения прежде всего высокочувствительных методов анализа, позволяющих определять малые количества элементов в небольшом количестве пробы. Из всех современных методов анализа для такой цели пригодны только два метода: рентгеноспектральный микроанализ и метод нейтронной активации. С использованием последнего метода в настоящее время появляется все больше данных о среднем содержании редких элементов в метеоритах различных типов. (См., например,

* Доклад на II Международной конференции по физико-химическим методам аналитической химии, 20—23 апреля 1966 г. (г. Будапешт).

сводки [1—3]). Данных о содержании элементов в отдельных фазах метеоритного вещества ничтожно мало. В основном определялось содержание макрокомпонентов — Fe, Co, Mn, Cr, Cu, Mg, Ca, K и Na в отдельных хондрах весом от 0,1 до 71 мг [4—6]. Для редких элементов получены лишь данные о содержании Sc [5], Rb и Sr [6], причем для последних двух элементов брались хондры весом 0,1—0,75 г; определено также содержание Ce, Eu, Sc, Ba, U и P в отдельных обогащенных фракциях темных и светлых разновидностей хондритов Кунашак и Первомайский поселок [7], Ba и U [8], а также Bi, I [9] и F [10] в веществе разновидностей хондритов Pantar и Ensisheim.

В связи и большими трудностями отбора чистых монофазовых и мономинеральных фракций встает вопрос об определении минимального количества пробы, достаточной для точного определения содержания отдельных редких элементов. В настоящей работе рассматривается вопрос о чувствительности определения Sc, Ba, U, Ce и Eu различными вариантами метода нейтронной активации с точностью $\pm 10\%$.

Известно, что величина чувствительности (m) может быть определена по формуле:

$$m = \frac{A_i \cdot N_\tau}{\sigma_{A_i} \cdot a \cdot b \cdot K \cdot J \cdot W \cdot (1 - e^{-\lambda t}) \cdot e^{-\lambda \tau}}, \qquad (1)$$

где A_i — атомный вес, N_τ — минимальная величина измеренной активности ($N_\tau \geqslant 2\Delta$, где Δ — статистическая ошибка определения фона счетчиков), σ_{A_i} — сечение (n, γ)-реакции для i-изотопа, J — поток нейтронов, W — число Авогадро, λ — константа распада, t — время облучения, τ — время, прошедшее от конца облучения до начала счёта активности, a — доля изотопа в естественной смеси, b — поправка на химический выход, K — коэффициент счёта, равный

$$K = \omega \cdot \delta \cdot \left(\sum_{i=1}^{i=n} K_i \cdot g_i \cdot S_i \cdot P_i \cdot l_i\right), \qquad (2)$$

где ω — поправка на телесный угол, δ — поправка на конечные размеры измеряемого образца, K_i — поправка на поглощение излучения в слое покрытия образца, воздухе и веществе окошка счётчика, g_i — поправка на обратное рассеяние от материала подложки, S_i — поправка на поглощение излучения в веществе образца, P_i — доля i-излучения на 1 распад, l_i — разрешающая способность счётчика для i-излучения. Величины определялись экспериментально для всех исследованных изотопов при различной геометрии счёта и с учётом схем распада.

Расчёт проводился для трех вариантов активационного метода при $J = 1{,}10^{13}$ нейтронов/см^2·сек, $b = 1{,}0$ и заданной активности.

I вариант — измерение активности на низкофоновом 4π-счётчике с проточным газом; фон $4 \pm 0{,}5$ имп/мин, $\omega = 0{,}8$; $N_\tau = 1$ имп/мин.

II вариант — измерение на стандартном торцовом счётчике типа МСТ—17 с диаметром окошка 20 мм и фоном 16±2 имп/мин, $\omega = 0{,}05$, $N_\tau = 5$ имп/мин.

III вариант — измерение на сцинтилляционном γ-спектрометре с кристаллом NaJ (Tl) размером 40×40 мм и 100-канальным анализатором импульсов; $\omega = 0{,}4$; $N_\tau =$ в интервале от 10 до 100 имп/мин для γ-линий с различной энергией.

В табл. I в качестве примера приведены величины чувствительности при различном времени облучения для $\tau = 10$ час. Из рассмотрения этих данных следует, что наиболее оптимальным временем облучения является 7 дней (за исключением Eu и Ce при опрепределении по Eu^{152m} и Ce^{143}, соответственно). Наиболее высокая чувствительность достигается при измерениях на низкофоновом 4π-счётчике; особенно она высока для Sc ($\sim 10^{-11}$ г) и Eu ($\sim 10^{-13}$ г). Чувствительность уменьшается примерно на два порядка при измерениях на торцовом счётчике и на γ-спектрометре. Только при определения Ba (по Ba^{131}, распадающемуся путем захвата орбитальных электронов) чувствительность по γ-спектрометрическому варианту достаточно близка к чувствительности 4π-счётчика. Следует также отметить, что γ-спектрометрический вариант менее трудоемок и не требует высокой степени очистки выделенных образцов.

В табл. II приведены данные о минимальных навесках метеоритов, необходимых для определения содержания Sc, Ba, U, Ce и Eu. Они получены при $b = 0{,}5$, $\tau = 10$ час и среднем содержании указанных элементов в каменных и железных метеоритах [1, 2, 3]. Видно, что из проб каменных метеоритов весом 10^{-5}—10^{-3} г могут быть определены Sc, Ce и Eu с точностью ±10% при измерении активности на низкофоновом 4π-счётчике, а Eu (по Eu^{152n}) и на γ-спектрометре. При определении бария минимальная навеска пробы должна составлять около 100 мг для I варианта и ~ 1 г для III варианта. Очень большие навески требуются при определении урана в железных метеоритах (10 г и более), что исключает применение активационного метода для определения содержания этого элемента в отдельных хондрах (вес которых редко превышает 100 мг) и мономинеральных фракциях.

В качестве примера в табл. III приведены наши данные по определению содержания Ce, Eu, Sc, Ba и U в 200 мг пробы светлых и темных разновидностей гиперстеновых хондритов Кунашак и Первомайский поселок. После химического выделения по схеме рис. 1 активность Ce и Sc измерялась на γ-спектрометре соответственно по фотопикам с E = 290 Кэв и E = 880 Кэв (см. рис. 2), Eu — на торцовом счётчике; активность Ba и La^{140} была низкой и могла быть измерена только на 4π-счётчике.

Следует особенно отметить возможность определения очень малых количеств урана и исследование его распределения в различных фазах каменных метеоритов и в железных метеоритах методом регистрации треков

Acta Chim. Acad. Sci. Hung. 57, 1968

Таблица I

Чувствительность определения Sc, Ba, U, Ce *и* Eu *при различном времени облучения*

Элемент	Радиоизотоп	$T_{1/2}$	Сечение активации, барны	Тип распада	$E\beta$ Мэв	$E\gamma$ Кэв	Время облучения	Чувствительность, г		
								I вариант	II вариант	III вариант
Sc	Sc^{46}	85 дней	22±2	β	0,36	880	20 час	$7{,}0 \cdot 10^{-11}$	$5{,}6 \cdot 10^{-9}$	$4{,}2 \cdot 10^{-9}$
						1120;	7 дней	$8{,}8 \cdot 10^{-12}$	$7{,}3 \cdot 10^{-10}$	$5{,}3 \cdot 10^{-10}$
							14 дней	$4{,}5 \cdot 10^{-12}$	$4{,}0 \cdot 10^{-10}$	$2{,}7 \cdot 10^{-10}$
							21 день	$3{,}1 \cdot 10^{-12}$	$2{,}5 \cdot 10^{-10}$	$1{,}8 \cdot 10^{-10}$
							30 дней	$2{,}2 \cdot 10^{-12}$	$1{,}8 \cdot 10^{-10}$	$1{,}4 \cdot 10^{-10}$
Ba	Ba^{11}	11,5 дней	10±1	З. Э	—	122,	20 час	$1{,}5 \cdot 10^{-6}$	$1{,}2 \cdot 10^{-4}$	$1{,}4 \cdot 10^{-5}$
						214,	7 дней	$2{,}1 \cdot 10^{-7}$	$1{,}7 \cdot 10^{-5}$	$1{,}9 \cdot 10^{-6}$
						372,	14 дней	$1{,}3 \cdot 10^{-7}$	$1{,}1 \cdot 10^{-5}$	$1{,}2 \cdot 10^{-6}$
						491,	21 день	$1{,}0 \cdot 10^{-7}$	$8{,}0 \cdot 10^{-6}$	$9{,}0 \cdot 10^{-7}$
							30 дней	$8{,}6 \cdot 10^{-8}$	$6{,}9 \cdot 10^{-6}$	$7{,}8 \cdot 10^{-7}$
U	Ba^{140} ⇄ La^{140}	12,8 дней	107	β^-	0,5; 1,0; 1,8; 1,6	440,	20 час	$1{,}2 \cdot 10^{-8}$	$9{,}6 \cdot 10^{-5}$	$1{,}5 \cdot 10^{-6}$
						820,	7 дней	$1{,}7 \cdot 10^{-9}$	$1{,}4 \cdot 10^{-7}$	$2{,}2 \cdot 10^{-7}$
						1600;	14 дней	$1{,}0 \cdot 10^{-9}$	$8{,}0 \cdot 10^{-8}$	$1{,}3 \cdot 10^{-7}$
						537	21 день	$8{,}0 \cdot 10^{-10}$	$6{,}4 \cdot 10^{-8}$	$1{,}0 \cdot 10^{-7}$
							30 дней	$6{,}8 \cdot 10^{-10}$	$5{,}4 \cdot 10^{-8}$	$8{,}6 \cdot 10^{-8}$
Ce	Ce^{141}	32,5 дней	0,31	β^-	0,44; 0,58	143	20 час	$6{,}4 \cdot 10^{-9}$	$5{,}1 \cdot 10^{-7}$	$4{,}2 \cdot 10^{-6}$
							7 дней	$7{,}9 \cdot 10^{-10}$	$6{,}3 \cdot 10^{-8}$	$5{,}2 \cdot 10^{-7}$
							14 дней	$4{,}2 \cdot 10^{-10}$	$3{,}3 \cdot 10^{-8}$	$2{,}8 \cdot 10^{-7}$
							21 день	$3{,}0 \cdot 10^{-10}$	$2{,}4 \cdot 10^{-8}$	$2{,}0 \cdot 10^{-7}$
							30 дней	$2{,}3 \cdot 10^{-10}$	$1{,}9 \cdot 10^{-8}$	$1{,}5 \cdot 10^{-7}$
	Ce^{143}	33,4 час	0,95		0,71; 1,39	*290*	20 час	$6{,}7 \cdot 10^{-10}$	$5{,}4 \cdot 10^{-8}$	$1{,}0 \cdot 10^{-7}$
Eu	Eu^{152}	9,2 час	1400	ЭЭ; β^-	1,39	*122* 960;	20 час	$7{,}6 \cdot 10^{-14}$	$6{,}1 \cdot 10^{-12}$	$1{,}8 \cdot 10^{-11}$
	Eu^{152}	12,2 года	5500	ЭЭ; β^-	1; 1,5	120, 240	20 час	$2{,}7 \cdot 10^{-9}$	$2{,}2 \cdot 10^{-7}$	$1{,}9 \cdot 10^{-7}$
						340;	7 дней	$3{,}3 \cdot 10^{-10}$	$2{,}6 \cdot 10^{-8}$	$2{,}2 \cdot 10^{-8}$
						1100;	14 дней	$1{,}6 \cdot 10^{-10}$	$1{,}3 \cdot 10^{-8}$	$1{,}1 \cdot 10^{-8}$
						1400;	21 день	$1{,}1 \cdot 10^{-10}$	$8{,}8 \cdot 10^{-9}$	$7{,}3 \cdot 10^{-9}$
							30 дней	$7{,}6 \cdot 10^{-11}$	$6{,}1 \cdot 10^{-9}$	$5{,}0 \cdot 10^{-9}$

Таблица II

Величены минимальных навесок метеоритов, необходимых для определения Sc, Ba, U, Ce *и* Eu

(химический выход — 50%, время охлаждения — 10 час)

Элемент	Время облучения	Минимальный вес пробы, г					
		Каменные метеориты			Железные метеориты		
		I вариант	II вариант	III вариант	I вариант	II вариант	III вариант
Sc	20 час	$1{,}6 \cdot 10^{-5}$	$1{,}3 \cdot 10^{-3}$	$9{,}6 \cdot 10^{-4}$	$7 \cdot 10^{-2}$	5,6	4,2
	7 дней	$2{,}0 \cdot 10^{-6}$	$1{,}6 \cdot 10^{-4}$	$1{,}2 \cdot 10^{-4}$	$8{,}8 \cdot 10^{-3}$	$7{,}1 \cdot 10^{-1}$	$5{,}3 \cdot 10^{-1}$
Ba	20 час	$6{,}6 \cdot 10^{-1}$	$5{,}3 \cdot 10^{1}$	6,2	$1 \cdot 10^{3}$	$8{,}0 \cdot 10^{4}$	$9{,}3 \cdot 10^{3}$
	7 дней	$9{,}3 \cdot 10^{-2}$	7,4	$8{,}3 \cdot 10^{-1}$	$1{,}4 \cdot 10^{2}$	$1{,}1 \cdot 10^{4}$	$1{,}3 \cdot 10^{3}$
U	20 час	1,7	$1{,}4 \cdot 10^{2}$	$2{,}1 \cdot 10^{2}$	$4{,}8 \cdot 10^{1}$	$3{,}8 \cdot 10^{3}$	$6 \cdot 10^{3}$
	7 дней	$2{,}4 \cdot 10^{-1}$	$1{,}9 \cdot 10^{1}$	$3{,}1 \cdot 10^{1}$	6,8	$5{,}4 \cdot 10^{2}$	$8{,}8 \cdot 10^{2}$
Ce (по Ce^{141})	20 час	$1{,}4 \cdot 10^{-2}$	1,2	9,3	6,4	$5{,}1 \cdot 10^{2}$	$4{,}2 \cdot 10^{3}$
	7 дней	$1{,}7 \cdot 10^{-3}$	$1{,}4 \cdot 10^{-1}$	1,2	$7{,}9 \cdot 10^{-1}$	$6{,}3 \cdot 10^{1}$	$5{,}2 \cdot 10^{2}$
Ce (по Ce^{143})	20 час	$1{,}8 \cdot 10^{-3}$	$1{,}4 \cdot 10^{-1}$	$2{,}9 \cdot 10^{-1}$	$8{,}3 \cdot 10^{-1}$	$6{,}6 \cdot 10^{1}$	$1{,}3 \cdot 10^{2}$
Eu (по Eu^{152m})	20 час	$4{,}3 \cdot 10^{-6}$	$3{,}4 \cdot 10^{-4}$	$1{,}0 \cdot 10^{-3}$	$1{,}7 \cdot 10^{-2}$	1,4	4
Eu (по Eu^{152})	20 час	$7{,}3 \cdot 10^{-2}$	5,8	5,1	$2{,}8 \cdot 10^{2}$	$2{,}2 \cdot 10^{4}$	$2 \cdot 10^{4}$
	7 дней	$8{,}9 \cdot 10^{-3}$	$7{,}1 \cdot 10^{-1}$	$5{,}9 \cdot 10^{-1}$	$3{,}5 \cdot 10^{1}$	$2{,}8 \cdot 10^{3}$	$2{,}3 \cdot 10^{3}$

Таблица III

Содержание Ce, Eu, Sc, Ba *и* U *в темных и светлых разновидностях Кунашак и Первомайский поселок*

Метеорит	Распространенность 10^{-6} г/г				
	Ce	Eu	Sc	Ba	U
Кунашак, темная разновидность	1,1±0,3	—	7,4±0,8	5,2±1,5	0,0011±0,004,
светлая разновидность	2,0±0,6	0,089±0,01	8,4±0,6	—	—
Первомайский поселок, темная разновидность	0,7±0,2	0,065±0,01	8,9±0,7	—	—
светлая разновидность	1,3±0,3	0,072±0,01	9,2±0,8	—	—

тяжелых заряженных частиц [11], основанным на визуальном просмотре и подсчёте треков на полированной протравленной поверхности минералов. Например для измерения содержания урана в метеорите Vaca Muerta [12] служили треки осколков деления U^{235}, индуцируемые при захвате тепловых нейтронов. Концентрация урана определялась по формуле

$$C_u \simeq \varrho_i (F \cdot N_v \cdot R \ldots \qquad (3)$$

где ϱ_i—плотность индуцированных треков, F—доля делящихся атомов урана, N_v—атомная плотность минерала и R—средняя толщина слоя образца, на

Облучение образца

Сплавление с Na_2O_2, выщелачивание (H_2O + HCl)

↓ H_2SO_4

$Ba(Sr, Ca)SO_4$	Sc, Р.З.Э., Fe, P		
↓ Na_2CO_3	↓ NH_4OH (избыток)		
$Ba(Sr, Ca)CO_3$	гидроокиси Sc, Р. З. Э., Fe	$[Ni(NH_3)_6]^{2+}$	
HNO_3, дым. HNO_3	8н HCl, D-1×8		
Ca^{2+}, Sr^{2+}, $Ba(NO_3)_2$	Sc, Р. З. Э., P	Fe^{3+}, Co^{2+}	
H_2O, $K_2Cr_2O_7$ CH_3COONa	0,3-0,5н HCl, H_2S (Cu)		
Ca^{2+}, Sr^{2+}, $BaCrO_4$	Sc, Р. З. Э., P	CuS	
Выделение La^{140} из Ba^{140} через 7 дней (U)	10% HNO_3, $(NH_4)_2MoO_4$		
	Sc, Р. З. Э., P	$(NH_4)_3H_4[P(Mo_2O_7)_6]$	
	NH_4OH	10% NH_4OH	
	Гидроокиси Sc, Р. З. Э.	PO_4^{3-} Mo	
	↓ HCl	$MgCl_2$, NH_4Cl NH_4OH	
	0,5н HCl, NH_4CNS Экстракция эфиром	$MgNH_4PO_4$	
	Sc	Р. З. Э.	0,3н. HNO_3, КУ-2
	аммоний тартрат	↓ HF	PO_4^{3-} Mo
	Sc-аммоний тартрат	фториды Р. З. Э.	$MgCl_2$, NH_4Cl NH_4OH
	Sc_2O_3	H_3BO_3 HNO_3	$MgNH_4PO_4$
		↓ NH_4OH, гидроокиси Р. З. Э.	$Mg_2P_2O_7$
		9н HNO_3, $NaBiO_3$ экстракция эфиром	
		Ce^{4+}	0,5н HNO_3 + H_2S
		$H_2C_2O_4$	Р. З. Э. Bi_2S_3
		$Ce_2(C_2O_4)_3$	HF, фториды Р. З. Э.
		CeO_2	H_3BO_3 + HNO_3
			$H_2C_2O_4$, оксалаты Р. З. Э.
			Me_2O_3

Рис. 1. Схема химического анализа каменных метеоритов при определении в них содержания Ba, U, Sc, Р. З. Э.

которой при травлении трек становится видимым. Найдено, [12], что концентрация урана уменьшается в последовательности циркон А < циркон В < витлокит < тридимит < гиперстен < анортит и составляет, например, для последнего [3—9] 10^{-10}г/г.

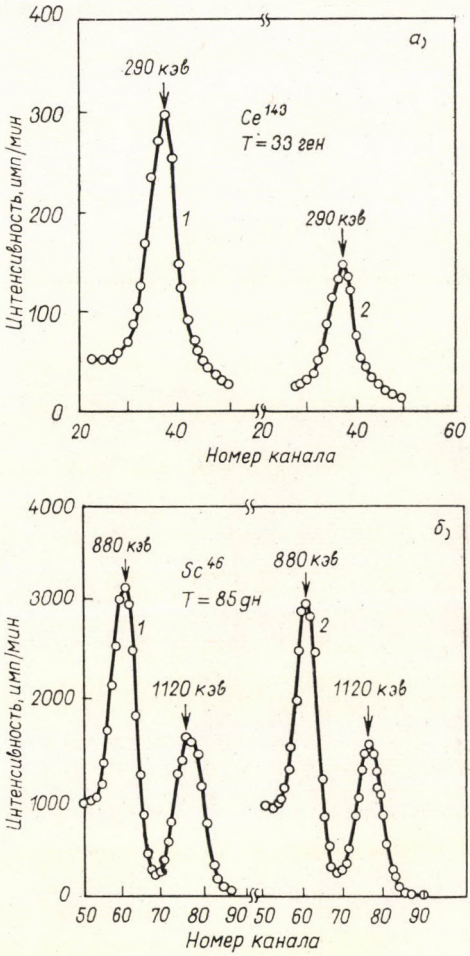

Рис. 2. γ-спектры Ce^{143} (*а*) и Sc^{46} (*б*):
1 — стандарт, 2 — образец

Нами начаты исследования содержания урана и тория в слюдах, тектитах и железных метеоритах. Образцы слюды и тектитов легко обрабатываются и после травления просматриваются в оптический микроскоп в проходящем свете. У слюды используется свежая поверхность после расщепления, а у тектитов — подходящий для просмотра скол или полированная поверхность. На рис. 3 приведены фотографии треков осколков спонтанного деления урана в биотите и тектите (молдавит) с плотностью $\varrho = 1{,}1 \cdot 10^3$ и

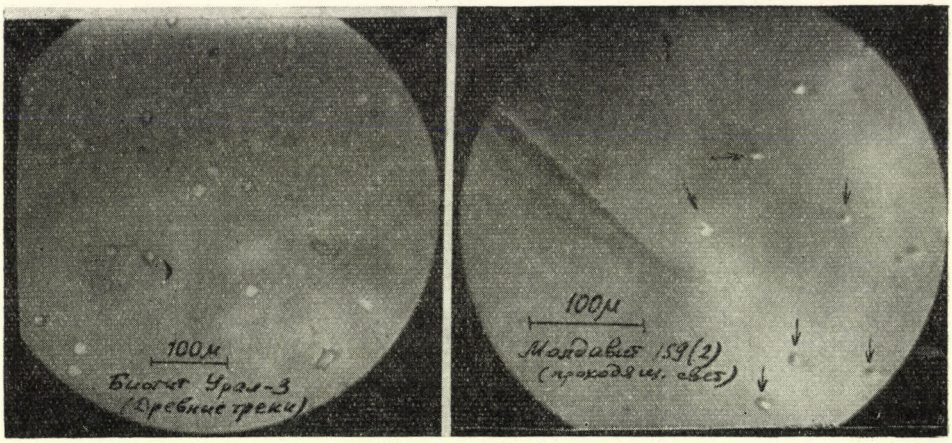

Рис. 3. Треки осколков спонтанного деления в биотите и тектите (молдавит)

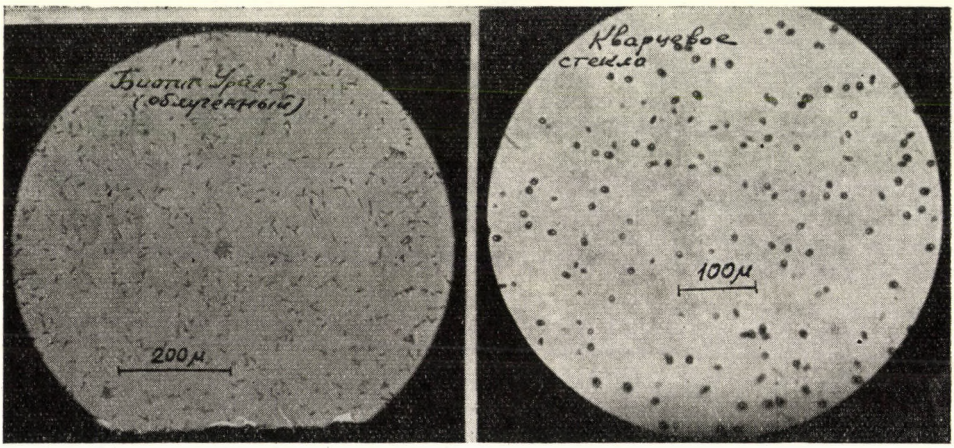

Рис. 4. Индуцированная плотность треков в биотите и в кварцевом стекле (в контакте с поверхностью тектита) равная $1{,}4 \cdot 10^5$ и $7{,}2 \cdot 10^7$ на 1 см² соответственно при интегральном потоке нейтронов 10^{18} нейтрон/см²

15.10^3 треков на 1 см² соответственно. Для определения коцентраций урана и тория образцы последовательно облучаются в потоках нейтронов реактора с различным отношением медленных ($n_м$) и быстрых ($n_б$) нейтронов, определение которых одновременно проводится с помощью эталонных мишеней с электролитически нанесенными слоями U^{235} и Th. Индуцируемые под действием нейтронов треки (см. рис. 4) регистрируются или пленками лавсана (пластиками стекла, кварца), помещенными непосредственно к исследуемой поверхности, или в самом образце. В последнем случае учитывается плотность треков, запасенная в образце в течение геологического времени его существования.

Плотность треков, индуцируемых в потоке нейтронов с отношением $n_м/n_б = K$, записывается как

$$\varrho_i + n_м \cdot W \cdot R \cdot d \cdot \left[\sigma_U^{235} \cdot a \cdot \frac{C_U}{A_U} + \frac{1}{K}\left(\sigma_U^{238} \cdot \frac{C_U}{A_U} + \sigma_{Th} \cdot \frac{C_{Th}}{A_{Th}}\right)\right], \qquad (4)$$

где W — число Авогадро, A_i — атомный вес, R — толщина слоя, равная, для тектитов $1{,}2.10^{-3}$ см [13], d — плотность вещества образца, σ^{235} — эффектив-

Таблица IV

Плотность индуцированных треков в образцах с определенной концентрацией урана (C_U) и тория (C_{Th})

Концентрация урана и тория г/г*	$n_м = n_\sigma$ $2 \cdot 10^{18}$ нейтронов/см²					$n_м = 3{,}5 \cdot 10^{17}$; $n_б = 3{,}9 \cdot 10^{15}$ нейтронов/см				
	ϱ общ. см$^{-2}$	ϱ быст. см$^{-2}$	S см²	ΔC,%*** U	ΔC,%*** Th	ϱ общ. см$^{-2}$	ϱ быст. см$^{-2}$	S см²	ΔC,%** U	ΔC,%** Th
10^{-6}	$8{,}1 \cdot 10^7$	$1{,}24 \cdot 10^7$	0,01	0,1	0,3	$1{,}25 \cdot 10^7$	$2{,}5 \cdot 10^4$	0,01	0,3	0,6
10^{-8}	$8{,}1 \cdot 10^5$	$1{,}24 \cdot 10^5$	*0,01*	*1,1*	*2,8*	$1{,}25 \cdot 10^5$	$2{,}5 \cdot 10^5$	*0,01*	*2,8*	*6,3*
			0,05	0,5	1,3			0,05	1,3	2,8
10^{-10}	$8{,}1 \cdot 10^3$	$1{,}24 \cdot 10^2$	0,1	3,5	9	$1{,}25 \cdot 10^3$	2,5	0,1	9	—
10^{-12}**	405	62	1	5	13	62	0,1	1	13	—

*) При оценке предполагалось $C_U \cong C_{Th}$
**) Интегральный поток нейтронов $n_M = n_б = 10^{19}$ нейтронов/см²
***) Ошибка обусловлена статистической погрешностью определения плотности индуцированных треков

ное сечение деления U^{235} медленными нейтронами, σ^{238} и σ_{Th}-сечения деления U^{238} и Th быстрыми нейтронами, а — доля U^{235} в естественной смеси изотопов урана ($7{,}26 \cdot 10^{-3}$ г/г), C_U и C_{Th} — концентрация урана и тория в образце (в весовых единицах).

Оценка величин C_U и C_{Th}, которые могут быть определены этим методом, приведена в табл. 4. Видно, что концентрация C_U и $C_{Th} \gtrsim 10^{-8}$ г/г может быть определена с точностью до 1% при подсчёте индуцируемых треков на поверхности образца S до 5 мм², если $n_м \cong n_б \cong 2.10^{18}$ нейтрон/см². При этом для исследуемой пластинки толщиной около 0,5 мм вес образца составляет несколько миллиграмм. Концентрация $C_{Th} \lesssim 10^{-8}$ г/г может быть определена только при достаточно больших интегральных потоках быстрых нейтронов ($\sim 10^{19}$ нейтрон/см²) и при просмотре площадей до 1 см².

РЕЗЮМЕ

Расчитана чувствительность нейтронно-активационного определения Sc, Ba, Ce и Eu в образцах каменных и железных метеоритов по активности соответствующих изотопов Sc^{46}, Ba^{131}, Ce^{141} и Ce^{143}, Eu^{152m} и Eu^{152} и Ba^{140}, измеряемой на низкофоновом 4 π-счётчике с проточным газом, на торцовом счётчике типа Гейгера—Мюллера и на сцинтилляционном

γ-спектрометре со 100 канальным анализатором импульсов при различном времени облучения. Определены минимальные навески метеоритного вещества при соответствующем содержании этих элементов в метеоритах, приведены примеры определения Sc, Ba, Ce, Eu и U в темных и светлых разновидностях гиперстеновых хондритов Кунашак и Первомайский поселок.

Обсуждена возможность определения U и Th в слюдах, тектитах и железных метеоритах по трекам осколков деления, индуцируемым реакторными нейтронами.

SUMMARY

The sensitivity of neutron activation analysis for the determination of Sc, Ba, Ce and Eu in stone meteorites and iron meteorites has been calculated. The analysis is based on the measurement of the activity of the isotopes Sc^{46}, Ba^{131}, Ce^{141}, Ce^{143}, Eu^{152m}, Eu^{152} and Ba^{140}. Activities for various times of irradiation were measured with a low-background 4π-counter using carrier gas, with an end-window Geiger—Müller counter, and with a γ-spectrometer equipped with a 100-channel pulse analyzer. The minimum quantity of the meteorite sample to be weighed in at given quantities of the said elements was determined. By way of example, Sc, Ba, Ce, Eu and U analysis results obtained on dark and light variants of hypersten chondrites, found in the vicinity of the places "Kunasak" and "Pervomaiskiĭ Posyolok" are presented. The possibilities of the determination of U and Th in mica, tektites and iron meteorites on the basis of the path of products of nuclear fission, induced by reactor neutrons, is discussed.

ЛИТЕРАТУРА

1. Явнель, А. А.: О распространенности элементов в металлической фазе железных метеоритов и в хондритах. Метеоритика, вып. XXV, изд.-во «Наука», М. 1964, стр. 75.
2. Urey, H. C.: A review of atomic abundances in chondrites and the origin of meteorites. Rev. of Geophysics, **2,** N I, I (1964).
3. Лаврухина, А. К.: Эффекты ядерных реакций, вызванных быстрыми протонами в метеоритах. В сб. Ядерная химия, изд-во «Наука», М., 1965, стр. 7.
4. Keil, K., Fredriksson, K.: The iron, magnesium and calcium distribution in coexisting olivines and rhombic pyroxenes of chondrites. J. Geophys. Res. **69,** N 16, 3487 (1964).
5. Schmitt, R. A., Smith, R. H., Goles, G. G.: Abundances of Na, Se, Cr, Mn, Te, Co and Cu in 218 individual meteoritic chondrules via activation analysis. J. Geophys. Res., **70,** N 10, 1511 (1965).
6. Murthy Rama, V., Compston, W.: Rb—Sr ages of chondrules and ca bonaceous chondrites. J. Geophys. Res., **70,** N 12, 3115 (1965).
7. Лаврухина, А. К., Колесов, Г. М., Каличева, И. С., Акользина, Л. Д.: Активационное определение Ce, Eu, Sc, Ba, U, и P в темных и светлых равновидностях хондритов Кунашак и Первомайский поселок. Геохимия, № 3, 281 (1966 г).
8. Lovering, I. F., Morgan, I. W.: Uranium and thorium abundances in stony meteorites. J. Geophys. Res., **69,** N 10, 1979 (1964).
9. Reed, G. W.: Heavy elements in the Pantar meteorites. J. Geophys. Tes., **68,** N 11, 3351 (1964).
10. Schima Makoto: Fluorine content in meteorites. Scient. Papers Inst. Phys. and Chem. Res., **57,** N 3, 150 (1963).
11. Price, P. B., Walker, R. M.: Observation or fossil particle tracks in natural micas. Nature, **196,** N 4856, 732 (1962).
12. Fleischer, R. L., Naeser, C. W., Price, P. B., Walker, R. M., Marvin, U. B.: Fossile particle tracks and uranium distributions in minerals of Vaca Muerta meteorite. Science, **148,** 629 (1965).
13. Fleischer, R. L., Price, P. B.: Glass dating by fusion fragment tracks. J. Geophys. Res., **69,** N 2, 331 (1964).

A. K. Lavrukhina
L. L. Kaskarov
G. M. Kolesov
L. I. Genaeva

Institut Geokhimii i Analiticheskoi Khimii im. V. I. Vernadskovo AN SSSR, Moskva

Acta Chimica Academiae Scientiarum Hungaricae Tomus 57 (4), pp. 363—371 (1968)

THE CHEMISTRY OF MIXED LIGAND COMPLEXES, III

THE EFFECT OF WATER ACTIVITY ON THE STABILITY OF THE BIS-DIMETHYLGLYOXIMATO-DIIODO-COBALTATE(II) MIXED COMPLEX

K. BURGER, B. PINTÉR, E. PAPP-MOLNÁR and S. NEMES-KÓSA

(Department of Inorganic and Analytical Chemistry, L. Eötvös University, Budapest)

Received September 12, 1967

Studies of complex equilibria in solutions have shown that the values of the equilibrium constants are greatly affected by the composition of the solution; namely, by the solvent, by the concentration and nature of the electrolyte, and by the presence of other complex-forming ligands in the solution, etc. [1].

Some investigations point to the fact that in aqueous solutions a change in water activity alters the values of the equilibrium constants, since metal ions in aqueous solution are normally present in the form of their aquo complexes. If some complex forming ligand is introduced into the solution, it will partly or fully replace the water molecules in the aquo complex, producing mixed or regular complexes [2]. When solid complexes are dissolved in water, a coordination of the water molecules on any unoccupied coordination sites of the metal may also occur.

The significant solubility of the cobalt(II)-dimethylglyoxime complex in water is also based on the formation of a mixed aquo complex. The parent complex, which in the solid state has square planar symmetry, in aqueous solutions binds two water molecules in the direction of the z axis. In an alkaline solution a hydroxo mixed complex of the composition $Me(dmg)_2(OH)_2^{2-}$ and of distorted octahedral symmetry is formed from the aquo complex, after the dissociation of two protons [3]. In our earlier communication we reported on the preparation of mixed complexes, whose composition is analogous to that of the hydroxo and aquo mixed dimethylglyoxime complexes, and which bind halide and pseudohalide ions in the direction of the z axis [4].

An investigation of the mixed complex of cobalt(II)-dimethylglyoxime formed with chloride and bromide has shown [5] that the stability of the mixed complex is influenced not only by the nature of the halide ion, but also by the nature of the alkali cation introduced into the solution together with the halide anion. The stability constants, determined in the presence of various alkali ions, show a decreasing tendency in the direction $Li^+ \rightarrow$ $\rightarrow Rb^+$. According to our calculations the water activity in concentrated salt solutions increases in the same direction, since due to the differ-

ence in the hydration of the various alkali cations, their salts will reduce the water activity of the solution to different degrees. Calculation of the water activity by the ROBINSON—STOKES formula [9] indicates the highest water activity-reducing effect of the lithium ion, and the lowest such effect of rubidium. Because of the low stability of the chloride and bromide mixed complexes, these investigations had to be carried out in 3—6 *M* alkali salt solutions. The formation of the corresponding iodide mixed complexes proceeds in 0.5 *M* solutions. In the latter case no cation dependence of the stability constants was found. We interpret this fact by assuming that in the experiments with concentrated salt solutions, changes in the stability of the complexes might be due to the different degree to which the various alkali ions (with different hydration) affect water activity. In the case of iodide complexes this effect is lacking because of the low concentrations of the solutions.

An unequivocal interpretation of the phenomenon is difficult, since owing to the low stability of the chloride and bromide mixed complexes they will be quantitatively formed only at very high halide ion concentrations (in concentrated salt solution). Thus ions not participating directly in the equilibrium reaction cannot be used for the adjustment of the water activity. Changes in the halide concentration during equilibrium measurement are therefore accompanied by a slight change in water activity. To eliminate this possible source of error, the complex with the composition $Co(dmg)_2HI_2^-$, which is considerably more stable than the chloride and bromide mixed ligand complexes, was chosen as a model of the present experiments. This complex is quantitatively formed in 0.5 *M* iodide solution; thus the water activity can be kept constant within one series of measurements by means of a concentrated solution of salts whose ions do not participate in the equilibrium reaction. In different series of measurements, the water activity of the solution can be altered by altering the concentration of this salt. In this way it can be determined whether the cation effect is primarily due to changed water activity, or electrostatic forces or some other effects also play an important role in it. Owing to the higher stability of this complex, the equilibrium constants can also be determined with a higher accuracy.

Experimental

The equilibrium constants of the equilibria leading to the formation of the mixed complexes

$$Co(dmg)_2H^+ + I^- \rightleftharpoons Co(dmg)_2HI$$

$$Co(dmg)_2HI + I^- \rightleftharpoons Co\,(dmg)_2HI_2^-$$

were determined spectrophotometrically in the presence of

$$1-6\ M\ LiNO_3$$

$$1-5\ M\ NaNO_3$$

$$1-6\ M\ NaClO_4$$

The iodide ion activity in the concentrated salt solutions was calculated from the known iodide ion concentration, with the help of the average activity coefficients of ROBINSON and STOKES [9]. The Co^{2+} concentration was $10^{-4} - 5 \cdot 10^{-5}\ M$, the dimethylglyoxime concentration $5 \cdot 10^{-4}\ M$ (which at the pH value of 6.5 of the experiments ensured the quantitative formation of the complex). The iodide ion concentration was varied between 10^{-4} and $7 \cdot 10^{-1}\ M$. The light absorption of the solutions was measured at 28,200 cm^{-1}, the wave length characteristic of the mixed ligand complex. The concentration of the latter in the solution was calculated from the experimentally determined extinction values. The Bjerrum formation curves [6], $\alpha - \lg [I^-]$, plotted from the experimental data were evaluated by the graphic (curve fitting) method of DYRSSEN and SILLÉN [7, 8] (Figs 1—3). The measured points were fitted to the normalized set of curves,

$$Y = \frac{v^2}{1 + pv + v^2}$$

where $v = K_1 K_2 [I^-]$ and $p = \frac{K_1}{K_2}$ and the stability constants were calculated from the data of the best fitting curve. The values of the stability constants are summed up in Tables I—IV.

For the spectrophotometric measurements a UNICAM SP 700 recording spectrophotometer was used. The pH was adjusted with the help of a Radiometer PHM 4 pH-meter. All reagents used were of analytical grade.

Parallel to the investigation of dimethylglyoxime, the analogous 1,2-cyclohexanedionedioxime (Nioxime) complex was also studied. The parent complex of cobalt(II)-nioxime is similar in structure and properties to that of dimethylglyoxime, it seemed therefore obvious that the first would also form a stable mixed complex with the iodide ion. Preliminary experiments proved fully that with respect to composition and structure the nioxime complex was the perfect analogue of the dimethylglyoxime mixed complex. In these experiments the concentration of Co^{2+} was $10^{-4}\ M$ and that of nioxime $4 \cdot 10^{-4}\ M$. The pH of the solution was adjusted to 6.5. The investigations of this complex were carried out in $1-6\ M\ NaClO_4$ solutions.

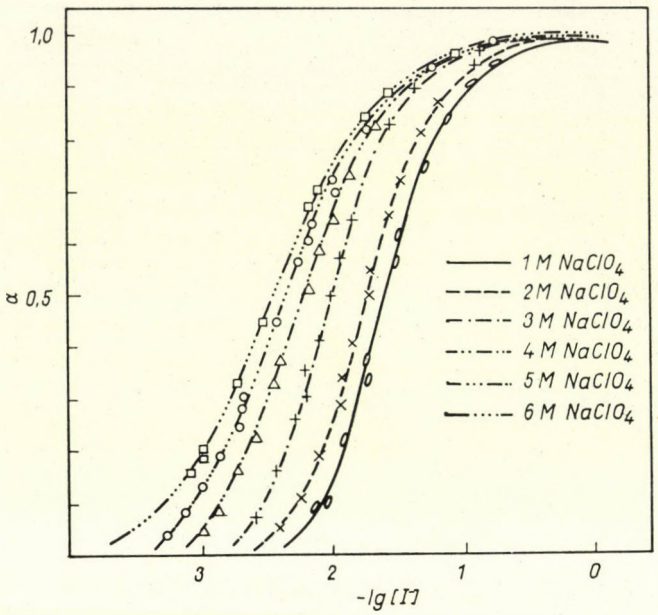

Fig. 1. The Bjerrum formation curves of the bis-dimethylglyoximato-diiodo-cobaltate(II) mixed complex in 1 to 6 *M* sodium perchlorate solutions. (The lines are the normalized curves which best fit the experimental points)

Table I

Stability constants of the bis-dimethylglyoximato-diiodo-cobaltate(II) mixed complex in sodium perchlorate solutions and the water activities of the solutions

$NaClO_4$ concentration *M*,	lg K_1	lg K_2	lg β_2	—lg *a*
1	1.38	1.98	3.36 ± 0.1	0.0148
2	1.54	2.14	3.68 ± 0.1	0.0317
3	1.80	2.40	4.20 ± 0.1	0.0484
4	2.40	2.40	4.80 ± 0.1	0.071
5	3.04	2.44	5.48 ± 0.1	0.095
6	3.86	2.46	6.32 ± 0.1	0.117

The logarithms of the stability constants were plotted against the logarithm of water activity for both complexes (Figs 4—5). The water activity (*a*) was calculated according to ROBINSON and STOKES [9]:

$$\ln a = \frac{\nu \, m w \, \Phi}{1000} \qquad \lg a = \frac{2 \, m \, \Phi}{128}$$

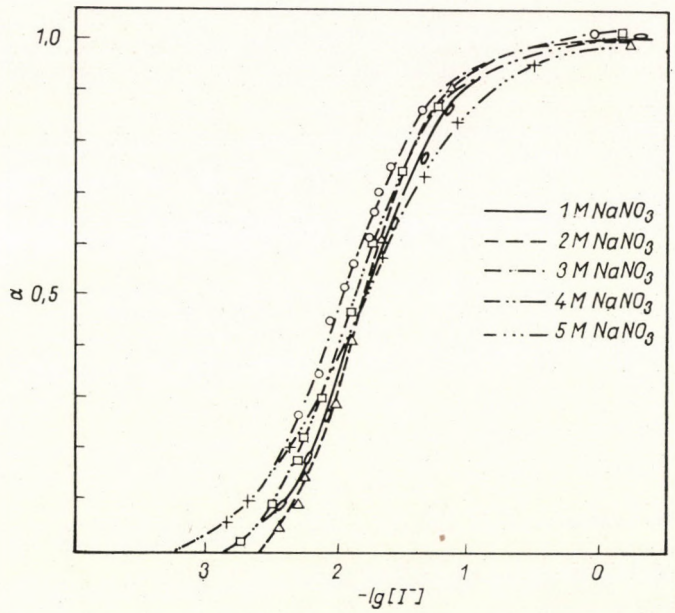

Fig. 2. The Bjerrum formation curves of bis-dimethylglyoximato-diiodo-cobaltate(II) mixed complex in 1 to 5 *M* sodium nitrate solutions. (The lines are the normalized curves which best fit the experimental points)

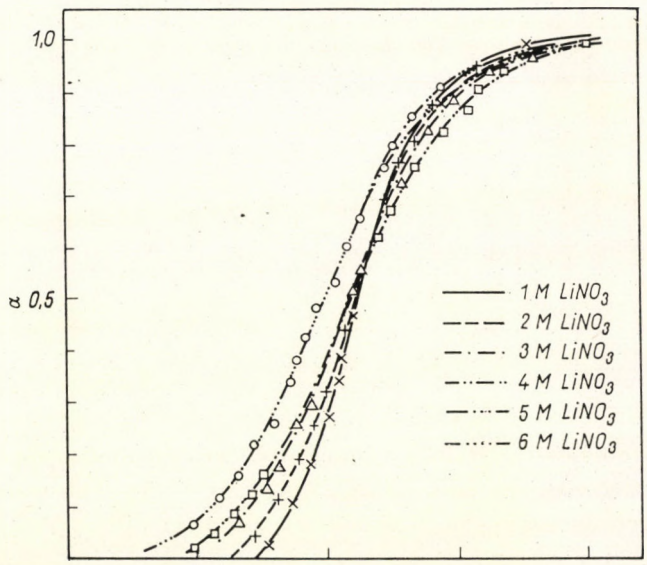

Fig. 3. The Bjerrum formation curves of the bis-dimethylglyoximat o-diiodo-cobaltate(II mixed complex in 1 to 6 *M* lithium nitrate solutions. (The lines are the normalized curves which best fit the experimental points)

Table II

Stability constants of the bis-dimethylglyoximato-diido-cobaltate(II) mixed complex in sodium nitrate solutions and the water activities of the solutions

$NaNO_3$ concentration, M,	lg K_1	lg K_2	lg β_2	—lg a
1	1.56	2.16	3.72 ± 0.1	0.0197
2	1.62	2.22	3.84 ± 0.1	0.027
3	2.20	2.20	4.40 ± 0.1	0.0406
4	2.60	2.00	4.60 ± 0.1	0.0540
5	3.20	1.80	5.00 ± 0.1	0.0665

Table III

Stability constants of the bis-dimethylglyoximato-diiodo-cobaltate(II) mixed complex in lithium nitrate solutions and the water activities of the solutions

$LiNO_3$ concentration M,	lg K_1	lg K_2	lg β_2	—lg a
1	1.58	2.18	3.76 ± 0.1	0.0159
2	2.04	2.04	4.08 ± 0.1	0.0347
3	2.50	1.90	4.40 ± 0.05	0.0561
4	3.24	1.84	5.08 ± 0.04	0.0815
5	3.46	2.06	5.52 ± 0.05	0.106
6	4.04	2.04	6.08 ± 0.05	0.140

Table IV

Stability constants of the bis-nioxime-diiodo-cobaltate(II) mixed complex in sodium perchlorate solutions and the water activities of the solutions

$NaClO_4$ concentration M,	lg K_1	lg K_2	lg β_2	—lg a
1	2.66	2.06	4.72 ± 0.1	0.0148
2	2.80	2.20	5.00 ± 0.05	0.0317
3	2.92	2.32	5.24 ± 0.05	0.0484
4	3.07	2.47	5.54 ± 0.1	0.071
5	3.52	2.12	5.64 ± 0.1	0.095
6	4.00	2.00	6.00 ± 0.05	0.117

where

w = molecular weight of water
v = charge number
m = Raoult concentration
Φ = osmotic coefficient.

Results and discussion

Fig. 4 shows quite clearly that the stability of the mixed ligand complex is proportional to the water activity, independently of the salt used for the adjustment of water activity.

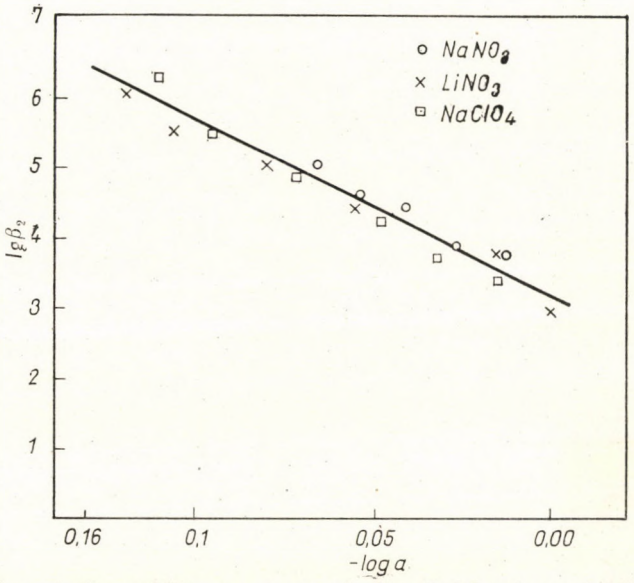

Fig. 4. Logarithm of the stability constants of dimethylglyoxime mixed complex plotted *vs.* the logarithm of the water activities of solutions

Changes in water activity may affect the stabilities of mixed ligand complexes in different ways. In the mixed complex the iodide ions are coordinated in the direction of the z axis, thus substituting water molecules of the aquo mixed complexes; consequently, the stability of the iodide mixed ligand complex depends on the stability of the aquo mixed complex. At low water activities the coordinated water molecules are more readily exchanged by iodide; this is the primary cause of the higher stability of the iodide mixed complex. At the same time, decreased water activity involves the decrease of the hydration of the iodide ion, which facilitates the coordination of the iodide, raising the stability of the mixed complex. Finally a difference between the hydration of the mixed

complex and that of the parent complex might also be assumed. The considerable slope of the curve reflects the manifold effects of the changes in water activity.

Comparison of the successive stability constants determined in solutions of different salt concentrations indicates an increase in the $K_1 : K_2$ ratio with increasing salt concentration. This effect might be explained by a hindering

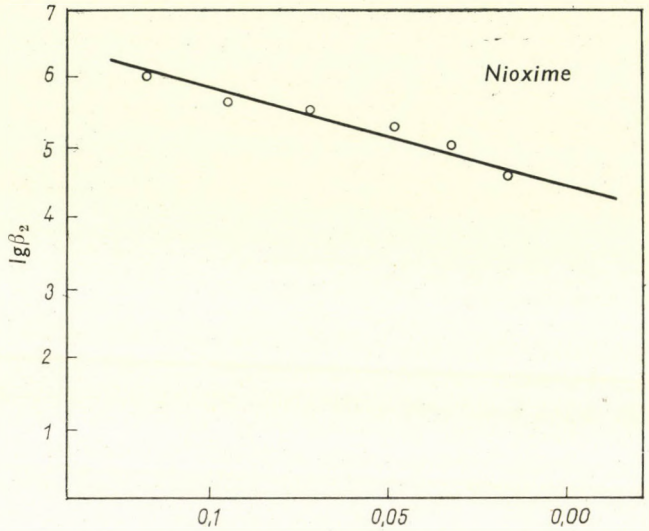

Fig. 5. Logarithm of the stability constants of nioxime mixed complex plotted *vs.* the logarithm of the water activities of solutions

of the second iodide ion to enter the complex as the anion concentration is increased.

Investigation of the nioxime mixed ligand complex led to analogous conclusions, though the straight line in Fig. 5 has a smaller slope. Consequently, changes in water activity have less effect on the stability of this than on the corresponding dimethylglyoxime complex. Apparently, the two six-membered rings of nioxime permit only a lower hydration degree of the complex.

From this, but mainly from the fact that plotting the stability constants in various salt solutions against the water activities of the solutions results in practically a single straight line, we have drawn the conclusion that the "salt effect" (called "cation effect" in our previous paper) has its origin primarily in the change in water activity, and the electrostatic effect of the ions and other factors are only of secondary importance.

SUMMARY

The stability constants of the bis-dimethylglyoximato-diiodo-cobaltate(II) complex were determined in sodium perchlorate, sodium nitrate and lithium nitrate solutions of various concentrations and the water activities of these solutions were calculated. The results indicate an increased stability of the mixed complex with decreasing water activity. The nature of the salt used for the adjustment of a given water activity has no influence on the results.

REFERENCES

1. Beck, M.: The chemistry of complex equilibria (in Hungarian). Akadémiai Kiadó, Budapest, 1965.
2. Beck, M.: Kémiai Közlemények **26,** 353 (1966).
3. Burger, K., Ruff, I.: Talanta **10,** 329 (1963).
4. Burger, K., Ruff, I., Ruff, F.: Proc. Symp. Coord. Chem. Tihany 1964, Akadémiai Kiadó, Budapest, 1965, p. 205.
5. Burger, K., Pintér, B.: J. Inorg. Nucl. Chem. **29,** 1717 (1967).
6. Bjerrum, J.: Metal amine formation in aqueous solution. Copenhagen, 1941.
7. Dyrssen, D., Sillén, L. G.: Acta Chem. Scand. **7,** 663 (1953).
8. Sillén, L. G.: Acta Chem. Scand. **10,** 186 (1956).
9. Robinson, R. A., Stokes, R. H.: Electrolyte Solutions. Butterworths, London, 1959.

Kálmán Burger
Boglárka Pintér
Etelka Papp-Molnár
Sarolta Nemes-Kósa

Budapest, VIII. Múzeum krt. 4/b

Acta Chimica Academiae Scientiarum Hungaricae Tomus 57 (4), pp. 373—376 (1968)

ON THE PARAMETER FORM OF FORCE CONSTANT MATRIX, VII*

THE CLOSEST ASSIGNMENT FORCE CONSTANT MATRIX

P. PULAY

(Department of General and Inorganic Chemistry, L. Eötvös University, Budapest, and Research Group for Inorganic Chemistry of the Hungarian Academy of Sciences, Budapest)

Received November 2, 1967

In the second part of this series [1] the matrix

$$F_0 = G^{-1/2} \Lambda G^{-1/2} \tag{1}$$

was defined as a force constant matrix which reproduces the normal frequencies ν_i and gives the closest assignment between the internal coordinates and the normal coordinates. In Eq. (1) G is the well-known vibrational kinetic energy matrix in momentum representation [2], and Λ is a diagonal matrix with elements $\lambda_i = 4\,\pi^2\,\nu_i^2$. The assignment between internal and normal coordinates is defined by the order of internal coordinates in G and by the order of the diagonal elements in Λ. Independently, the same matrix was proposed by HERRANZ [3, 4].

Neither in our work nor in that of HERRANZ was given, however, a satisfactory proof of the fact that Eq. (1) really gives the closest correspondence between the internal coordinates and the normal ones, assigned to them, because no measure of the closeness of assignment was defined. Our treatment remained heuristic. HERRANZ proved that the L_0 matrix (*i.e.* the transformation matrix from normal coordinates to internal ones), obtained with the force constant matrix (1) has the maximum trace, and that the sum of the squared elements of L is an invariant quantity for any F. From these he concluded that L_0 is the most diagonal of all L matrices, and therefore F_0 gives the closest assignment. This proof is, however, unsatisfactory from two points of view: $tr(L)$ is the sum of the diagonal elements, while the invariant quantity is the sum of the squared elements; the choice of L as the measure of assignment is arbitrary, L^{-1} should have equal rights, as it was discussed in [1].

In the following a reasonable measure of the closeness of assignment will be defined and it will be shown rigorously that in this sense F_0 gives the closest assignment. First define a metric in the linear space of generalized

* Part VI: Acta Chim. Acad. Sci. Hung. **57**, 141 (1968)

coordinates, describing the configuration of the molecule. Let the scalar product of two coordinates q_i and q_j be

$$(q_i, q_j) = G_{ij},$$

i.e. the corresponding G matrix element. This metric satisfies all the requirements of the scalar product in a real Euclidean space: it is symmetric, linear and positive definite.

In normal coordinates, Q_i, the kinetic energy matrix G is the unit matrix, *i.e.* the normal coordinates form an orthonormal set in the sense of the metric defined above.

Our problem is now to orthonormalize the set of internal coordinates $q = (q_1, q_2, \ldots q_n)$, by means of a linear transformation L^{-1} to give the normal coordinates $Q = (Q_1, Q_2, \ldots Q_n)'$, $Q = L^{-1}q$, in such a manner that the differences between q_i und Q_i $(i = 1, 2, \ldots n)$ should be minimal.

These requirements can be formulated as $(Q_i, Q_j = \delta_{ij})$ (orthonormality) and $\sum_i |Q_i - q_i| = \text{minimum}$ (assignment).

This is the problem of symmetric orthogonalization, which was solved by CARLSON and KELLER [5], and LÖWDIN [6]. They have shown that the transformation matrix L^{-1} is the $-1/2$th power of GRAM's matrix of the elements q_i, which is in our case the G matrix:

$$Q = G^{-1/2} q$$

$$L = G^{1/2}.$$

Using the identity

$$F = L^{-1} A L^{-1},$$

we obtain

$$F_0 = G^{-1/2} A G^{-1/2}.$$

So it is proved that F_0 gives the closest assignment between internal and normal coordinates.

We discussed [1] the dependence of F_0 upon scale factors by which the internal coordinates are multiplied. This dependence can be easily understood from Fig. 1, where the two-dimensional case is shown graphically. Here the coordinates are represented by vectors of a plane. Because of the homomorphism of all two-dimensional Euclidean spaces, this figure is an exact representation of the 2 by 2 vibrational problem. In Fig. 1 three different normalizations have been chosen:

a) $|q_1| = 1, \qquad |q_2| = 1,$

b) $|q_1| \gg 1, \qquad |q_2| = 1,$

c) $|q_1| = 1, \qquad |q_2| \gg 1.$

It can be seen that the orthonormalized vectors, corresponding to the normal coordinates Q_1 and Q_2 show a little dependence upon the norms of the internal coordinates q_1 and q_2, and so we must select one of them. We suggest that the "best assignment" should correspond to the case where all the vectors which are to be orthonormalized are normalized to unity prior to orthonormalization. This is the case of Fig. 1a.

In the vibrational problem this corresponds to scaling all the internal coordinates so that $G_{ii} = 1$, computing F_0 and then transforming back to

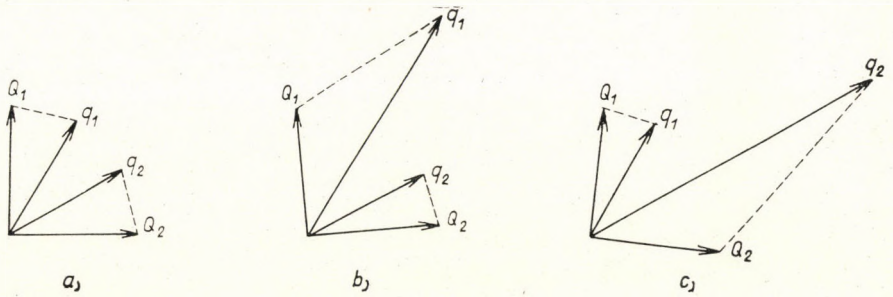

Fig. 1. Scaling effect upon the symmetric orthogonalization of vectors

the original coordinates. This scaling was suggested in [1], again on the basis of a heuristic treatment.

It is hoped that the position of an actual F matrix in the parameter space (see [7]), relative to the "best assignment" defined in this paper and in [1], will be the best measure of the assignment, better than the L matrix or the potential energy distribution. Both of these latter criteria are somewhat arbitrary. Methods for the determination of the position of a given force constant matrix in the parameter space and a thorough discussion of the distribution of the various assignments were given in [8].

When computing general valence force fields from additional data, difficulties often arise from convergence to an incorrect assignment [9]. With the parameter representation method such calculations can be carried out without the danger of getting in the pithole of a wrong assignment, since the assignment can always be easily determined and controlled.

SUMMARY

A reasonable measure of the closeness of the assignation between the internal and normal coordinates of a vibrating molecule has been defined. It has been shown that the force constant matrix $F_0 = G^{-1/2} A G^{1/2}$ corresponds to the closest assignment. The effect of scaling the internal coordinates by numerical factors is discussed and a unique normalization is suggested, where the diagonal elements of the G kinetic energy matrix are equal to 1. The place of an actual force constant matrix in the parameter space is suggested as a rigorous measure of the assignation.

REFERENCES

1. PULAY, P., TÖRÖK, F.: Acta Chim. Acad. Sci. Hung. **47,** 273 (1966).
2. WILSON, E. B., DECIUS, J. C., CROSS, P. C.: Molecular Vibrations. McGraw-Hill, New York, 1955.
3. HERRANZ, J., CASTAÑO, F.: Spectrochim. Acta **22,** 1965 (1966).
4. HERRANZ, J., CASTANO, F.: A. Real. Soc. Espan. Fis. Quim. **A 62,** 199 (1966).
5. CARLSON, B. C., KELLER, J. M.: Phys. Rev. **105,** 102 (1957).
6. LÖWDIN, P.-O.: Advances in Phys. **5,** 1 (1956).
7. PULAY, P., TÖRÖK, F.: Acta Chim. Acad. Sci, Hung. **44,** 287 (1965).
8. TÖRÖK, F.: Acta Chim. Acad. Sci. Hung. **52,** 205 (1967); Acta Chim. Acad. Sci. Hung. To be published.
9. NEEDHAM, D. C., OVEREND, J.: Spectrochim. Acta **22,** 1383 (1966).

Péter PULAY; Budapest, VIII. Múzeum krt. 6—8

Acta Chimica Academiae Scientiarum Hungaricae Tomus 57 (4), pp. 377—383 (1968)

UNTERSUCHUNG DER CHEMISCHEN VORGÄNGE BEI DER KALKBEHANDLUNG DES ROTSCHLAMMES

I. NÁRAY-SZABÓ, I. MAGYAROSY, T. KOTSIS und I. FEHÉR

(Zentralforschungsinstitut für Chemie der Ung. Akademie der Wissenschaften, Budapest und Forschungsinstitut für NE-Metalle Budapest)

Eingegangen am 15. Januar 1968

In Ungarn fallen jährlich etwa 600 000 t Rotschlamm beim Bauxitaufschluß nach BAYER als Nebenprodukt an. Dieses Abfallprodukt hat sich seit Jahrzehnten auf Halden zu vielen Millionen Tonnen vermehrt und seine stetig wachsende Menge ist schon wegen des Platzanspruchs sehr unangenehm. Es enthält aber wertvolle Bestandteile, daher wurden viele Versuche zu seiner Verwertung unternommen.

Der Rotschlamm besteht hauptsächlich aus Fe_2O_3, Al_2O_3, SiO_2 und TiO_2, weiterhin aus chemisch gebundenem und freiem Wasser. Seine mineralische Zusammensetzung ist nur annähernd bekannt; man findet darin in erster Linie Hämatit, ferner verschiedene Natriumaluminiumsilikate, unaufgeschlossene Aluminiumhydroxide bzw. Oxid-Hydroxide und viel amorphen Stoff. Hämatit ist schon im Bauxit vorhanden und beim Aufschluß bleibt er unverändert zurück, ebenso der etwa vorhandene Goethit, FeOOH und der Lepidokrokit derselben Zusammensetzung. Der im Bauxit oft vorkommende Kaolinit liefert beim alkalischen Aufschluß Natriumaluminiumsilikate, wodurch Natronlauge und Tonerde gleichzeitig verloren gehen.

MAGYAROSY und SKUTECZKY [1] vermengen zur Nutzbarmachung des Rotschlammes denselben mit Kalkmilch und Eisenerzpulver und pressen daraus dann bei gewöhnlicher Temperatur Pellets. Die erhaltenen Pellets mit etwa 55% Fe_2O_3 haben eine auffallend große Druckfestigkeit, die 200 $kp.cm^{-2}$ erreichen kann, und vom Gesichtspunkte der Verhüttung äußerst günstig ist. Ihre Herstellungskosten sind gering, im Hochofen können sie mit vollständiger Ausnützung des Eisengehaltes vorteilhaft verhüttet werden und sie erleichtern die Verwendung des in großen Mengen zur Verfügung stehenden staubförmigen Eisenerzes.

Das Ziel unserer Untersuchungen war die Klärung der beim obigen Verfahren zustandekommenden großen Festigkeit.

Desilikation beim Bayer-Verfahren

Da Bauxit immer mehr oder weniger Siliciumdioxid enthält, die Tonerde dagegen möglichst siliciumfrei sein muß, kann nur ein solches Verfahren großtechnisch verwirklicht werden, bei dem das im Bauxit vorhandene SiO_2 nicht in die Tonerde gelangt. Beim pyrogenen Verfahren ist das nicht gesichert, daher wird heute nahezu ausschließlich das BAYERsche Verfahren angewandt. Bei diesem gehen bei der Behandlung mit konzentrierter Natronlauge $Al(OH)_3$ bzw. AlOOH (Böhmit) als Natriumaluminat in Lösung. Es wird auch Siliciumdioxid gelöst, doch werden die ursprünglich entstehenden Natriumsilikate durch die Natriumaluminatlösung als verschiedene feste Natriumaluminiumsilikate ausgefällt und gelangen in den unlöslichen Schlamm. Dieser Vorgang sichert den praktisch genügend niedrigen SiO_2-Gehalt des aus der BAYER-Lauge ausgerührten Aluminiumhydroxids, doch mit einem Verlust von Natronlauge und Tonerde, die in den Rotschlamm gelangen.

Natürlich ist die Industrie bestrebt, diesen Verlust zu verringern; der Bauxit mit niedrigem SiO_2-Gehalt ist daher viel wertvoller. Da aber ein Verlust wegen dem SiO_2-Gehalt keineswegs vermeidbar ist, wäre ein Verfahren, das durch Nutzbarmachung des Rotschlammes einen zusätzlichen Gewinn erzielt, sehr erwünscht.

Früher hat man im Rotschlamm verschiedene Natriumaluminiumsilikat-Phasen angenommen, so z. B. Natrolit usw., aber schon 1946 haben FLINT u. Mitarbeiter [2] gezeigt, daß man es hier mit Verbindungen der Sodalit-Familie zu tun hat. Die Vorgänge des Bauxitaufschlusses haben zahlreiche Forscher untersucht, so GINSBERG u. WEFERS [3], SEIMIYA [4], BREUER, BARSOTTI u. KELLY [5], die ungarischen Autoren LÁNYI [6], MÁTYÁSI u. ORBÁN [7], DUNAY [8, 9], PAPP, MAGYAROSY u. HÉJJA [10], ÜVEGES [11], NEMECZ, SOLYMÁR u. ELEK [12]. Ohne die Ergebnisse dieser Autoren eingehend zu diskutieren, stellen wir zusammenfassend nur soviel fest, daß bei niedrigerer Temperatur, d. h. unter 100 °C sog. LINDEscher Zeolit und BARRERsche Zeolite A und X entstehen; letztere sind aber nicht stabil und wandeln sich zu Hydroxysodalith um. Außerdem erscheint auch der carbonathaltige Cancrinit, wenn Carbonationen zugegen sind. In Anwesenheit anderer Anionen entsteht Nosean (SO_4-haltig) usw. Das haben auch SEIMIYA, weiterhin BREUER und seine Mitarbeiter festgestellt.

Mit unseren eigenen Versuchen wollten wir klären, wie die im Rotschlamm vorhandenen Natriumaluminiumsilikate eine mechanisch feste Bindung bei der Reaktion mit Kalkmilch hervorbringen. Zu diesem Zweck haben wir aus Zettlitzer und Szegilonger (Ungarn) Kaolin durch Behandlung mit Natriumaluminatlauge Na-Al-Silikate hergestellt und dieselben chemisch analysiert. Wir haben diese Produkte mit dem Diffraktometer auf ihre Phasen

untersucht; nachher wurden sie mit Calciumhydroxid behandelt und erneut diffraktometrisch analysiert.

Die Kaoline wurden mit der beim BAYER-Verfahren benützten Natriumaluminatlauge bei 250 °C eine Stunde lang im geschlossenen Autoklaven behandelt, das erhaltene Material dreimal gründlich ausgewaschen und von der schwer filtrierbaren Flüssigkeit durch Zentrifugieren getrennt. Es war schon hier zu sehen, daß ein Teil des Produktes kolloidal ist. Die Analysen der ursprünglichen Kaoline und der bei verschiedenen Lauge : Kaolin-Verhältnissen erhaltenen festen Produkte sind in Tab. I zusammengefaßt. Daraus ersieht man, daß die Zusemmensetzung der durch Behandlung des Kaolinits mit BAYERscher Aluminatlauge erhaltenen Produkte auffallend gleichmäßig ist. Die Daten der Tabelle entsprechen mit geringen Abweichungen der chemischen Formel $Na_4[Al_3Si_3O_{12}OH] \cdot 2H_2O$; das ist Hydroxysodalith mit zwei Molekülen Wasser. Außerdem kann man in den meisten Präparaten eine hexagonale Phase nachweisen, die mit Cancrinit identisch ist, d. h. sie enthält statt Hydroxid CO_3^{2-}- oder HCO_3^--Ionen. Ein in Tab. I unter M 3/3 angeführtes, aus Szegilonger Kaolin hergestelltes Präparat enthielt 3,1% CO_2.

Tabelle I

Zusammensetzung von Kaolinen und der aus ihnen durch Behandlung mit Bayer-Aluminatlauge entstandenen Produkte in %

	Kaoline		Produkte*					
	Zettlitz	Szegilong	M 1/2	M 1/3	M 2/2	M 2/3	M 3/2	M 3/3
H_2O	0,4	0,3	1,4	1,6	0,6	1,0	1,5	1,3
Glühverlust	13,1	11,0	8,8	8,9	9,4	8,8	9,1	8,6
SiO_2	45,9	53,1	33,5	33,2	31,3	33,7	33,1	33,9
Al_2O_3	38,7	33,6	31,3	31,6	31,2	31,2	31,3	31,5
$Fe_2O_3 + TiO_2$	n. b.	n. b.	1,5	1,2	1,2	1,0	1,0	1,1
CaO	n. b.	n. b.	0,4	0,4	0,3	0,4	0,4	0,4
Na_2O	n. b.	n. b.	23,7	24,0	23,9	23,9	23,7	23,2

Zusammensetzung der Aluminatlauge: Na_2O 192,9 g/Liter

Al_2O_3 177,3 g/Liter

* Die Produkte M 3/2 und M 3/3 enthalten auch 3,1% CO_2. Die Präparate M 1/2 u. M 1/3 wurden aus Zettlitzer Kaolin mit dem Molverhältnis $Na_2O : Al_2O_3 = 3{,}72$ dargestellt; M 2/2 u. M 2/3 mit dem Molverhältnis 2,00 u. die Präparate M 3/2 u. M 3/3 aus Szegilonger Kaolin mit dem Molverhältnis 1,65.

Beim Vergleich des Hydroxysodaliths obiger Zusammensetzung mit der Cancrinitphase sieht man, daß die Analysen nur geringe Abweichung zeigen; somit ist die Zusammensetzung von Mischungen solcher Phasen auch nur wenig verschieden:

Hydroxysodalith		Cancrinit
$Na_4[Al_3Si_3O_{12}OH] \cdot 2H_2O$		$Na_4[Al_3Si_3O_{12}HCO_3]$
Na_2O	24,72%	25,45%
Al_2O_3	30,50	31,40
SiO_2	35,87	36,93
H_2O	8,82	1,75
CO_2	—	4,51

Die Zusammensetzungen beider Phasen weichen also nur bezüglich des H_2O- bzw. CO_2-Gehaltes bedeutend voneinander ab und stehen in gutem Einklang mit den Daten der Tabelle I.

Zur Untersuchung der in den Rohstoffen und in den Produkten vorkommenden Phasen haben wir Diffraktogramme von den ursprünglichen Kaolinen und von den durch Aluminatlaugenbehandlung erhaltenen Präparaten verfertigt. Auf diesen kommen starke Linien des Hydroxysodaliths vor; die aus den Reflexionen berechnete Kante der kubischen Elementarzelle beträgt $a = 8{,}993$ Å, die Raumgruppe ist $P\bar{4}3n$, also die gleiche wie beim Sodalith mit $a = 8{,}87$ Å. Letztere Phase enthält Cl^- an Stelle von OH^- unserer Verbindung, aber keine Wassermoleküle. Außer den Linien des Hydroxysodaliths kann man bei allen Präparaten auch diejenigen des Cancrinits ($a = 12{,}60$ Å, $c = 5{,}18$ Å, Raumgruppe $C6_3$) finden. Die relativen Intensitäten sind etwas verschieden, d. h. die Anteile des Hydroxysodaliths und Cancrinits sind wechselnd. Drei oder vier ganz schwache Linien konnten nicht identifiziert werden, diese können aber nur irgendeinen in geringer Menge anwesenden Fremdstoff anzeigen.

Wir können also feststellen, daß in unseren Versuchen aus zwei Kaolinen verschiedener Herkunft und Reinheit durch Behandlung mit BAYER-Lauge ein Gemisch von Hydroxysodalith-Dihydrat und Cancrinit entstanden ist. Man muß noch bemerken, daß in einigen Präparaten schwache Illit-Linien erschienen sind. Illit war in den ursprünglichen Kaolinen in geringer Menge vorhanden und ist bei der obigen Behandlung unverändert geblieben. Linien von Quarz erscheinen in den Diffraktogrammen nicht, der Quarz ist bei der Behandlung also verschwunden (er wurde entweder zu den obigen Phasen umgewandelt oder zu Natriumsilikat aufgelöst).

Durch Vermischen des nach obigem Verfahren erhaltenen Hydroxysodalith-Cancrinit-Pulvers mit verschiedenen Mengen von Calciumhydroxid und Wasser erhielten wir aus dem ursprünglich graubraunen Präparat ein bläulichgraues, pulveriges Produkt. Nach der intensiven Vermischung mit Kalk verfestigte sich das ursprüngliche Material überhaupt nicht, es blieb leicht zerdrückbar. Die Ursache der Abbindung kann also nicht die Reaktion des Hydroxysodaliths oder des Cancrinits mit Kalk sein. Das wird

auch durch die diffraktometrische Untersuchung des Kalk-Hydroxysodalith-Cancrinit-Gemisches bestätigt, da an seinen Diffraktogrammen außer den charakteristischen Linien des Calciumhydroxids und des Calcits, $CaCO_3$, keine neuen Linien auftraten. Es ist möglich, fast sogar sicher, daß die Reaktion mit Kalk im Präparat einen Ionenaustausch verursacht, das führt aber nicht zu einer Abbindung.

Beim Aufschluß nach BAYER entstehen Natriumsilikate (wie auch bei der Herstellung von Wasserglas), weiterhin Aluminiumhydroxid-Gel u. zw. in ziemlich großer Menge. Zur Bestätigung wurde der flüssige Teil des beim Aufschluß erhaltenen, noch nicht gewaschenen Produktes durch Zentrifugieren vom festen Anteil getrennt. Die so erhaltene kolloidale Lösung wurde eingedickt und mit Kalkhydrat vermischt. Wir erhielten eine sich schnell verfestigende kolloidale Masse, deren diffraktometrische Untersuchung nur verschwommene, sehr breite Reflexionen (»Ringe«) ergab, was auf amorphes bzw. äußerst feinkörniges Material hinweist.

Bei der Reaktion des Rotschlammes mit Kalkmilch spielen sich also ähnliche Vorgänge ab wie bei der Abbindung und Verfestigung des Portlandzements. Nach der Vermischung des Rotschlammes mit Kalk stellt sich die Verfestigung schnell, d. h. etwa in einer Viertelstunde ein. Die Abbindung des Portlandzements ist langsamer, das wird aber durch die verlangsamende Wirkung des mit dem Klinker zusammen vermahlenen Gipszusatzes verursacht. Das ist aus technischen Gründen nötig, eine allzu schnelle Abbindung würde nämlich das Einarbeiten des Betons in die Formen unmöglich machen. Die mit Wärmeentwicklung sich abspielende Verfestigung wird durch die Bildung und den Wasserverlust des Tobermorit-Gels hervorgerufen, welche durch die Aufeinanderwirkung des aus dem Zementbrei mit Wasser entstandenen Kieselsäure-Aluminiumhydroxidgels mit Calciumhydroxid zu erklären ist. Eine ähnliche Reaktion spielt sich offenbar auch bei der Wechselwirkung zwischen im Rotschlamm vorliegendem Aluminiumhydroxid und der kolloidalen Kieselsäure mit Kalkmilch ab, was die so entstehende, sehr beträchtliche Festigkeit erklärt.

Der Austausch des im Gitter der kristallinen Silikate vorhandenen Natriums durch Calcium geht zwar auch vor sich, das verursacht aber kleinerlei Abbindung, wie dies auch unsere Erfahrung zeigt.

ZUSAMMENFASSUNG

Der beim Bauxitaufschluß nach BAYER entstehende Rotschlamm bindet nach Vermischung mit Kalkmilch schnell ab und erreicht sehr beträchtliche Festigkeiten. Durch chemische und diffraktrometrische Untersuchung der aus Kaolin mit BAYER-Lauge bei 250 °C entstehenden Produkte und der Reaktion derselben mit Kalkmilch wird gezeigt, daß dadurch keine Festigkeit hervorgebracht wird. Vielmehr bilden sich aus der beim Aufschluß ebenfalls entstehenden kolloiden Kieselsäure und dem Aluminiumhydroxid mit $Ca(OH)_2$ tobermoritähnliche Produkte, die durch Wasserverlust ebenso wie Zementbrei verfestigt werden.

Tabelle II

Diffraktogramme der Aufschlußprodukte von

Zettlitz M 1/2			Zettlitz M 1/3			M 2/2		
2θ	dÅ	I_m	2θ	dÅ	I_m	2θ	dÅ	I_m
8,82	10,017	13	8,87	9,961	11	8,84	9,994	8
13,92	6,356	41	13,91	6,360	31	13,91	6,360	34
19,00	4,667	10	18,98	4,672	9	18,92	4,686	21
19,79	4,482	3				20,30	4,371	2
21.46	4.137	4	21,51	4,127	4	21,37	4.154	5
22,08	4,022	4				22,21	3,999	2
24,30	3,660	40	24,22	3,672	31	24,16	3,680	32
26,81	3,322	6	26,81	3.322	4	26,01	3,422	3
27,55	3,235	15	27,55	3,235	12	27,54	3,236	24
31,48	2,839	3	31,72	2,818	2	31,74	2,817	1
32,64	2,741	10	32,64	2,741	8	32,61	2,743	13
						34,14	2,624	4
34,55	2,594	15	34,68	2,584	10	34,66	2,586	12
						35,74	2,510	4
37,10	2,421	6	37,10	2,421	4	37,06	2,424	8
37,42	2,401	5	37,44	2,400	3	39,73	2,267	3
			41,48	2,175	2	41,48	2,175	2
42,72	2,115	15	42,66	2,117	12	42,74	2,114	13
			45,48	1,993	2	48,31	1,882	2
						50,57	1,803	2
			51,91	1,760	5	51,93	1,759	6
			58,10	1,586	4	58,10	1,586	6
			61,92	1,497	3	61,83	1,499	5
			63,90	1,455	3	63,92	1,455	5

Abkürzungen: Ill = Illit

LITERATUR

1. MAGYAROSY, I., SKUTECZKY, E.: Fémipari Kutató Int. Közl. **6,** 91 (1962).
2. FLINT, E. P. et al.: J. Research Natl. Bur. Standards **36,** 63 (1946).
3. GINSBERG, H., WEFERS, K.: Ang. Chem. **69,** 712 (1957).
4. SEIMIYA, S.: Some properties of red mud. Extractive Metallurgy of Aluminium, Vol. 1. New York—London—Sidney 1963, p. 115.
5. BREUER, R. G., BARSOTTI, L. R., KELLY, A. C.: Extractive Metallurgy of Aluminium, Vol. 1. p. 133.
6. LÁNYI, B.: Kohászati Lapok **87,** 162 (1954).
7. MÁTYÁSI, J., ORBÁN, F.: Almásfüzitői Timföldgyár Kutató Laboratóriumának jelentése (Bericht des Forschungslaboratoriums der Tonerdefabrik in Almásfüzitő [Ung.]). (1962).
8. DUNAY, S.: Timföldgyári hulladékok feldolgozása (Verarbeitung von Abfallprodukten der Tonerdeindustrie [Ung.]. Ausgabe Nr. 2764 des Instituts für Ingenieurfortbildung, Budapest).

Kaolinen mit Bayerscher Aluminatlauge

M 2/3			M 3/2 Sz			M 3/3 Sz			Phase	
2θ	dÅ	I_m	2θ	dÅ	I_m	2θ	dÅ	I_m		hkl
8,84	9,994	8	8,91	9,916	6	8,87	9,961	9	Ill	
13,94	6,360	32	13,91	6,360	30	13,93	6,351	31	H	110
18,96	4,676	20	18,94	4,681	6	19,01	4,664	6	C	101
						19,79	4,482		Ill, H	200
21,42	4,145	5				21,43	4,143	3	C	210
22,10	4,018	2				22,00	4,037	3	H	210
24,26	3,666	34	24,22	3,672	31	24,27	3,664	31	H	211
26,86	3,316	3				26,89	3,312	4	Ill	
27,54	3,236	25	27,62	3,227	6	27,57	3,232	5	C	211
									H	310
32,60	2,744	13	32,59	2,745	7	32,70	2,736	7	C	301
34,19	2,620	4								
34,71	2,582	13	34,66	2,586	12	34,61	2,589	12	H	222
35,65	2,516	4	35,56	2,522	3					
37,10	2,421	9	37,04	2,425	2	37,10	2,421	3	C	401
39,77	2,265	4	37,44	2,400	3	37,52	2,395	4	H	
41,46	2,176	3								
42,74	2,114	12	42,66	2,117	10	42,72	2,115	11	H	411, 330
48,34	1,881	2								
50,50	1,806	3							H	422
51,96	1,758	6	51,86	1,761	5	51,90	1,760	5	H	510
58,10	1,586	6	58,04	1,588	4	58,10	1,586	4	H	440
61,86	1,498	3	61,94	1,497	2	61,90	1,498	2	H	600, 442
63,86	1,456	4	63,84	1,457	3	63,90	1,455	3	H	611, 532
			69,32	1,354	3					

H = Hydroxysodalith, C = Cancrinit

9. DUNAY, S.: Timföldgyári vanádiumiszapok feldolgozása (Verarbeitung von Vanadiumschlämmen der Tonerdeindustrie [Ung.]. Ausgabe Nr. 10 des Instituts für Ingenieurfortbildung, Budapest, 1952).
10. PAPP, E., MAGYAROSY, I., HÉJJA, A.: Acta Techn. Hung. **13**, 33 (1955).
11. ÜVEGES, J.: Fémipari Kutató Int. Közl. **2**, 13 (1958).
12. NEMECZ, E., SOLYMÁR, K., ELEK, S.: Kohászati Lapok, im Druck.
13. BORCHERT, W., KEIDEL, J.: Heidelberg. Beitr. Miner. Petr. **1**, 17 (1947).

István NÁRAY-SZABÓ; Budapest, II. Pusztaszeri út 57/69
István MAGYAROSY, Tivadar KOTSIS, Iván FEHÉR; Budapest, XI. Fehérvári út 144

Acta Chimica Academiae Scientiarum Hungaricae Tomus 57 (4), pp. 385—389 (1968)

АНАЛИЗ ВОЛЬФРАМА МЕТОДОМ НЕЙТРОННОЙ АКТИВАЦИИ, II

ОПРЕДЕЛЕНИЕ СОДЕРЖАНИЯ НАТРИЯ И КАЛИЯ

А. Элек и Э. Сабо

Центральный Институт Физических Исследований Венгерской Академии Наук

Поступило 23-го сентября 1967 г.

С точки зрения активационного анализа вольфрам является неблагоприятной матрицей из-за его хорошей активируемости. В таблице I приведены данные ядерных свойств радиоактивных изотопов вольфрама и определяемых элементов, образующихся в результате (n, γ) реакций. Определением щелочных элементов в вольфраме методом активационного анализа до сих пор занимались немногие. Применяя химическое разрушение матрицы, Косгров и Моррисон разработали метод для отделения вольфрама от нескольких элементов, в том числе от натрия и калия, с применением α-бензоиноксима [1]. Из-за высокой активности самой матрицы (^{187}W), без радиохимических разделений можно определять с достаточной чувствительностью только те элементы, которые обладают, по крайней мере, такой же активируемостью, как сам вольфрам, и которые испускают γ-лучи с энергией больше 1 Мэв. Наряду с радиохимическим отделением натрия, без разрушения образца был определен 1% натрия в натриево-вольфрамовой бронзе Райландом и Фойтом [2]. Также без разрушения образца было определено около 10^{-3}% натрия в металлическом вольфраме Спицыным и сотрудниками [3], и от 10^{-4} до 10^{-3}% натрия, алюминия и кремния Квиттнером и сотрудниками [4, 5]. В образцах, исследованных нами, содержание натрия было $(2 \div 17) \cdot 10^{-4}$%, а калия $(4{,}5 \div 7{,}0) \cdot 10^{-3}$%.

Экспериментальная часть

Установки для облучения и измерения:

Облучение проводилось в реакторе типа ВВР—С Центрального Института Физических Исследований при помощи пневмопочты [6], при потоке нейтронов, равном $5 \cdot 10^{12}$ н/см^2/сек. Снятие сцинтилляционных γ-спектров осуществлялось с помощью γ-спектрометра, состоящего из кристалла **NaJ(Tl)** размером 75 × 75 мм (**Nucl. Ent. IA-4/12 Integral Assembly**) и из многоканального анализатора типа **NTA—256** отечественного производства.

Вольфрамовые спирали и проволочки весом 30 ÷ 100 мг перед облучением обрабатывались 2 н. раствором HNO_3 с целью удаления поверхност-

ных загрязнений. Очищенные образцы и стандарты помещались в разные капсулы из полиамида и облучались в одном общем контейнере в течение 400 сек. В качестве стандартов использовалось 50 мкг натрия в виде сульфата и 500 мкг калия в виде нитрата.

После облучения образцы помещались в платиновую чашку и растворялись в присутствии носителей натрия и калия по 5 мг в 1 мл конц. раствора HF с добавлением нескольких капель конц. раствора HNO_3. Содержание чашки упаривалось досуха на водяной бане, затем остаток растворялся в

Таблица I

Данные ядерных свойств изотопов определяемых элементов и вольфрама [8]

Элемент	Радиоактивный изотоп, образующийся в результате (n, γ) реакции			
	Массовое число	$T_{1/2}$	активность насыщения, расп./сек.г элемента*	тип излучения и энергия γ-квантов, Мэв
Na	24	15,06 ч	$1{,}39 \cdot 10^{10}$	β^-, γ—1,38; 2,76.
K	40	$1{,}29 \cdot 10^9$ л	$4{,}31 \cdot 10^{10}$	β^-, ЭЗ, γ—1,46.
	42	12,44 ч	$1{,}02 \cdot 10^9$	β^-, γ—1,52.
W	181	$1{,}4 \cdot 10^2$ дн	$4{,}52 \cdot 10^7$	ЭЗ
	185	73,2 дн	$2{,}00 \cdot 10^9$	β^-, γ—0,125; . . .
	187	24,1 ч	$3{,}7 \cdot 10^{10}$	β^-, γ—0,134; 0,480; 0,686.

* приведенные значения относятся к потоку медленных нейтронов, равному 10^{12}н/см². сек.

10 мл 1 н. по HF и HNO_3 раствора и пропускался для селективного ионообменного поглощения вольфрама через ионообменную колонку, наполненную анионитом Дауэкс —1×8 в NO_3-форме [7] (высота 12 см, диаметр 0,6 см, скорость протекания 5 мл/см²·мин). После этого колонка промывалась 20 мл дистиллированной воды и собранный в стакан раствор (30 мл), содержащий натрий и калий, помещался на поверхность детектора для снятия γ-спектра.

В предварительных опытах указанное отделение проводилось в присутствии такого же количества неактивного вольфрама и меченных щелочных элементов, и сопоставлением введенной и найденной активностей устанавливалось, что химический выход по калию и натрию является практически 100%-ным. В дальнейшем считали, что нет необходимости применять иные методы для определения химических выходов при анализе отдельных образцов.

Стандарты, облученные вместе с образцами удалялись из капсул вымыванием 0,1 н. раствором HNO_3 и их определенная доля разбавлялась дистиллированной водой до 30 мл, после чего измерялся γ-спектр.

Время измерения γ-спектров состовляло 400 сек. Идентификация изотопов ^{24}Na и ^{42}K проводилась по энергии и по периоду полураспада. Имея

γ-спектры стандартов, определение содержания искомых элементов в образцах вольфрама проводилось декомпонировкой γ-спектров растворов, полученных после отделения матрицы. Спектры декомпонировались в интервале 1,45 ÷ 2,90 Мэв по методу взвешанных наименьших квадратов. На рис. 1 приведены γ-спектры растворов, полученных из двух образцов после селективного поглощения вольфрама, а на рис. 2 приведены γ-спектры стандартов.

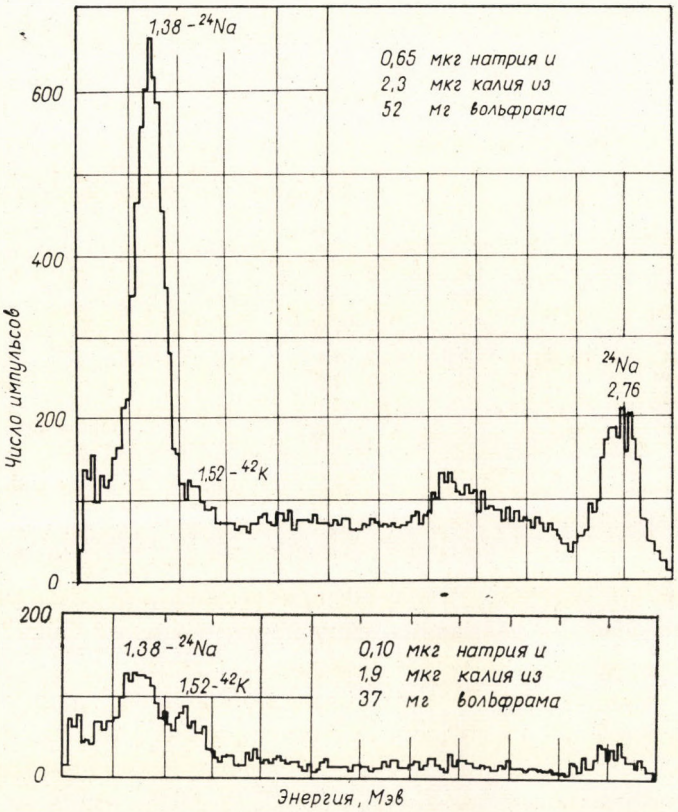

Рис. 1. γ-спектры растворов, полученных после селективного поглощения вольфрама

При данных условиях анализа число импульсов фона при энергии 2,76 Мэв соответствовало числу импульсов, вызванных 0,015 мкг натрия. Выбирая критерием чувствительности анализа то, что число импульсов измеряемой активности должно превышать ошибку фона (в данном случае трехкратную статистическую ошибку), можно сказать, что этим методом 0,005 мкг натрия является определимым ещё с большой надежностью [9].

Чувствительность анализа по калию хуже, чем по натрию, не только из-за худшей активируемости первого, а из-за более интенсивного фона детектора

(^{40}К) и из-за близости фотопика ^{24}Na (1,38 Мэв) к фотопику ^{42}К (1,52 Мэв). Так, $1+5\cdot m_{Na}$ мкг калия давало одинаковое число импульсов по сравнению

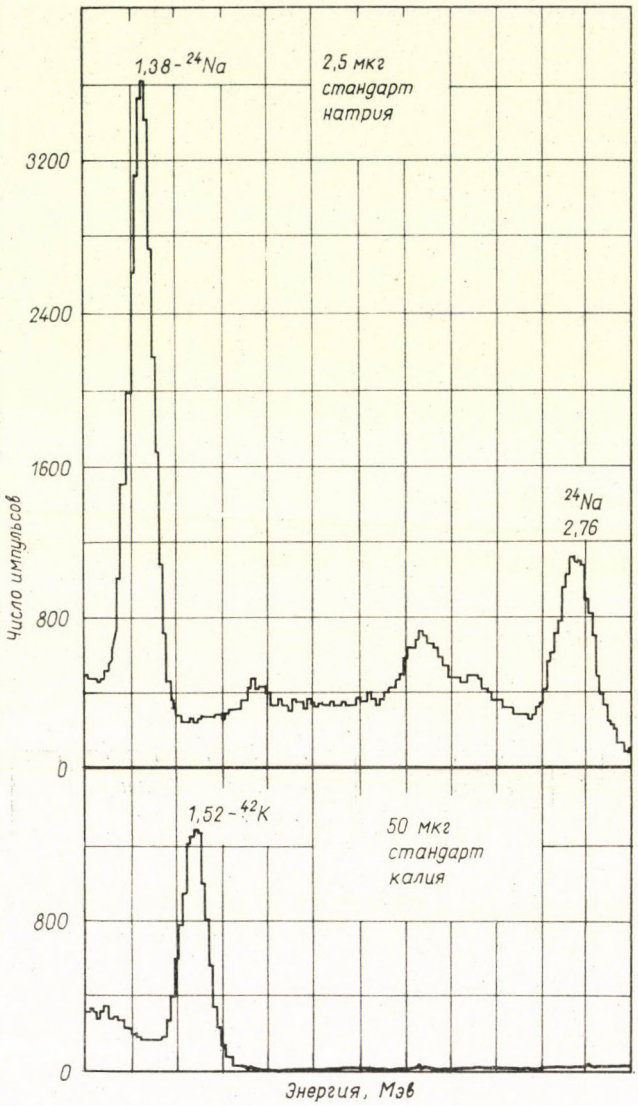

Рис. 2. γ-спектры стандартов натрия и калия

с этими двумя мешающими излучениями. Первый член связан с фоном, а второй с мешающим действием натрия, где m_{Na} обозначает содержание натрия в образце в мкг. По упомянутому критерию чувствительность по калию равняется $0{,}2+0{,}5\cdot m_{Na}$ мкг.

РЕЗЮМЕ

Разработана методика определения содержания натрия и калия в металлическом вольфраме по изотопам ^{24}Na и ^{42}K, применяя химическое разрушение образца и селективное поглощение матрицы путем ионного обмена. Облучение образцов проводилось в реакторе типа ВВР—С при помощи пневмопочты, а снятие γ-спектров осуществлялось с помощью γ-спектрометра, состоящего из кристалла NaJ(Tl) размером 75×75 мм и многоканального анализатора. Чувствительность метода составляет 0,005 мкг натрия и $0{,}2 + 0{,}5 \cdot m_{Na}$ мкг калия, где m_{Na} обозначает количество натрия в образце в мкг.

SUMMARY

A method has been developed for the determination of the sodium and potassium content of tungsten filaments. The samples were irradiated in a WWR-Sz type reactor by means of the pneumatic tube system. After irradiation, a selective separation by ion-exchange of the tungsten was effected. A 3×3 in. NaI(Tl) crystal and a multichannel analyzer were used for the activity measurements of the ^{24}Na and ^{42}K isotopes. Under the given experimental conditions, the sensitivity of the method was 0.005 μg Na and $0.2 + 0.5 \cdot m_{Na}$ — μg K, where m_{Na} denotes the amount of Na in the samples, in μg.

LITERATURE

1. Cosgrove, J. F., Morrison G. H.: Anal. Chem. **29,** 1017 (1957).
2. Reuland, R. J., Voigt, A. F.: Anal. Chem. **35,** 1263 (1963).
3. Спицын, В. И., Глазунов, М. П., Кодочигов, П. Н., Ионов, А. П.: ЖАХ, **18,** 1272 (1963).
4. Quittner, P., Simonits, A., Elek, A.: Talanta, **14,** 417 (1967).
5. Quittner, P.: Acta Chim. Hung., в печати.
6. Csőke, A.: KFKI Közlemények, **13,** 343 (1965).
7. Huff, E. A.: Anal. Chem. **36,** 1921 (1964).
8. Sentfle, F. B., Champion, W. R.: Nuovo Cimento, **3,** (1954).
9. Гунне, Х. Э. Пелекис, Л. Л. в сб.: Нейтронно-активационный анализ. Изд-во Зинатне, Рига 1966.

Antal Elek
Elek Szabó } Budapest, XII. Konkoly Thege út

Acta Chimica Academiae Scientiarum Hungaricae Tomus 57 (4), pp. 391—401 (1968)

DETERMINATION OF REACTION ORDER AND RATE CONSTANTS ON THE BASIS OF THE PARAMETER ESTIMATION OF DIFFERENTIAL EQUATIONS

L. FÁY and A. BALOGH

(University of Chemical Industry, Veszprém, and Hungarian Oil and Gas Research Institute, Veszprém)

Received October 6, 1967

Introduction

The basic task of sciences is to set up hypotheses for explaining observed natural phenomena and to examine whether, by the hypothesis given, the natural phenomenon in question can be described. If so, the hypothesis becomes a natural law until a new phenomenon is found contradicting this hypothesis. Then the establishment of a new hypothesis will be necessary, which can explain both the old phenomenon and the new one.

The recent development of sciences and mathematics has resulted in the presentation of hypotheses and natural laws, usually in a mathematical form. Thus one expects natural laws to describe natural phenomena in a way which is correct not only qualitatively but also quantitatively. Without this requirement the development of science and technology could not have taken place.

In physical chemistry most of the natural phenomena can be written in the form of differential equations. Therefore, checking some hypothesis is usually equivalent to examining whether the solution of the differential equation given is identical with a curve obtained through measurements, or not. If so, it may be said that the natural phenomenon is described by the differential equation set up on the basis of theoretical considerations. The examination of a hypothesis consists, therefore, of the following steps [6]:

1. carrying outi measurements and plotting the experimental results,
2. setting up dfferential equations,
3. solving the differential equations, and
4. comparing the solution with the experimental results.

On performing the first two steps, no difficulty of mathematical nature usually arises, in contradistinction to the steps 3 and 4. In the relatively rare cases when the solution of the differential equations can be written in an analytical form, the difficulty we encounter is the following. One has to choose which one of the solutions obtained is identical with the curve determined experimentally, taking into consideration the errors of measurement. If a

system of linear equations is available, the problem can be solved without any further difficulties. Should the system of equations turn out to be non-linear, the problem may be solved by means of computers, without theoretical difficulties. But if the solution cannot be presented in an analytical form, some method of approximation, particularly that of RUNGE—KUTTA, must be applied. However, using the RUNGE—KUTTA procedure as well as other numerical methods, one has to know the values of all the constants of the differential equations, as otherwise the computation cannot be carried out. These values, however, ought to be determined, after having obtained the solution, from the curve of measurement, possibly taking into consideration the experimental errors. How can this be done? The answer to this question is the subject of the present paper.

1. Exposition of the method

1.1 Ordinary differential equations of the first order

Let us consider a differential equation of the first order, and let us suppose that for the variables x and y experimental data are given. On plotting these data in a system of coordinates, the derivative to each measuring (experimental) point can easily be determined. Thus a system of values of independent and dependent variables as well as of derivatives is obtained

$$x_i, y_i, y'_i \qquad (i = 1, 2, \ldots n) \tag{1}$$

n being the number of the experimental points. Should the differential equation

$$f(x, y, y', c_1, c_2, \ldots c_k) = 0 \tag{2}$$

be fulfilled without errors at the experimental points inserting the value of system (1) into Eq. (2), there would exist n equations for determining the parameters $c_1, c_2, \ldots c_k$. If the function and derivative values at the experimental points are subject to errors, such a system of equations cannot be set up. Let dy_i denote the error of the function values and dy'_i that of the derivatives, then designating the experimental function values by η_i and the respective derivatives by η'_i we have:

$$\begin{aligned} \eta_i &= y_i + dy_i \\ \eta'_i &= y'_i + dy'_i \end{aligned} \qquad (i = 1, 2, \ldots n) \tag{3}$$

by substituting these into Eq. (2) we get

$$\begin{aligned} &f(x_1, \eta_1, \eta'_1, c_1, c_2, \ldots c_k) = \varepsilon_1 \\ &f(x_2, \eta_2, \eta'_2, c_1, c_2, \ldots c_k) = \varepsilon_2 \\ &\vdots \\ &f(x_n, \eta_n, \eta'_n, c_1, c_2, \ldots c_k) = \varepsilon_n \end{aligned} \tag{4}$$

where $\varepsilon_1, \varepsilon_2, \ldots, \varepsilon_n$ denote the errors made by substituting the experimental function and derivative values into the differential equation. According to the principle of least squares, however, the parameters $c_1, c_2, \ldots, c_k$ are chosen to minimize the expression

$$\sum_{i=1}^{n} \varepsilon_i^2 \tag{5}$$

Substituting Eqs (4) into Eq. (5), the parameters can be determined from

$$\Phi(c_1, c_2, \ldots c_k) = \sum_{i=1}^{n} f^2(x_i, \eta_i, \eta_i', c_1, c_2, \ldots c_k) = \min. \tag{6}$$

In case the system of equations

$$\frac{\partial \Phi}{\partial c_i} = 0 \qquad (i = 1, 2, \ldots k) \tag{7}$$

is linear, the parameters may readily be obtained. It is to be noted that this case often occurs if the differential equation cannot be solved by quadrature. *E.g.*, let us consider the differential equation

$$y' = c_1 x^{\alpha} + c_2 y^{\beta} \tag{8}$$

where c_1 and c_2 are parameters to be chosen, α and β being known.

If the system of equations (7) is non-linear, one can proceed in two ways. The first method consists in determining the minimum of the function $\varphi(c_1, c_2, \ldots c_k)$ by means of some procedure for obtaining the extreme values of functions of many variables. (Method of steepest descents: COURANT [7], CURRY [8], HOUSEHOLDER [9], LEVENBERG [10], BOOTH [11]; conjugate gradient method: HESTENS and STIEFEL [12], MARTIN and TEE [13]; "Partan" method: SHAH, BUEHLER, and KEMPTHORNE [14]. Further methods: POWELL [15], DAVIDON [16], FLETCHER and POWELL [1].) The second method consists in solving the system of non-linear equations by means of some method of approximation (*e.g.*, the Newton—Raphson method). In the two latter cases, however, computers must be used. This is the case, for example, when the exponents α and β in Eq. (8) are unknown, and are also to be determined from measurements.

1.2 System of ordinary differential equations

The methods mentioned in the former section can be applied to systems of ordinary differential equations. Let us consider the following system of differential equations:

$$\begin{aligned} f_1(x, y_1, y_2, \ldots y_m, y_1', y_2', \ldots y_m', c_1, c_2, \ldots c_k) &= 0 \\ f_2(x, y_1, y_2, \ldots y_m, y_1', y_2', \ldots y_m', c_1, c_2, \ldots c_k) &= 0 \\ f_m(x, y_1, y_2, \ldots y_m, y_1', y_2', \ldots y_m', c_1, c_2, \ldots c_k) &= 0 \end{aligned} \tag{9}$$

and let the experimental data

$$x_i, \eta_{1i}, \eta_{2i}, \ldots \eta_{mi}, \eta'_{1i}, \eta'_{2i}, \ldots \eta'_{mi} \quad (i = 1, 2, \ldots n) \tag{10}$$

be available. Substituting these into Eq. (9), it is satisfied only if the data (10) are not subject to errors, and the functions y_i $(i = 1, 2 \ldots n)$ are solutions of Eq. (9). Should the function and derivative values satisfying Eq. (9) be subject to errors of measurement, a minimum condition similar to the foregoing section will be set up according to the method of least squares. This minimum condition reads as follows:

$$\Phi(c_1, c_2, \ldots c_k) = \sum_{j=1}^{m} \sum_{i=1}^{n} f_j^2(x_i, \eta_{1i}, \eta_{2i}, \ldots \eta_{mi}, \eta'_{1i}, \eta'_{2i}, \ldots \eta'_{mi}, c_1, c_2, \ldots c_k) = \text{min!}$$

Like in the former section, the parameters $c_1, c_2, \ldots c_n$ can be obtained either by solving the system of equations

$$\frac{\partial \Phi}{\partial c_i} = 0 \qquad (i = 1, 2, \ldots k) \tag{11}$$

or, if these equations are not linear, by an appropriate method mentioned above [1], [7], [8—16]. In the latter case a computer is needed.

1.3 Differential equations of higher order

As known, differential equations of higher order can always be reduced to a system of differential equations of the first order, so that the estimation of the parameters of differential equations of higher order may be performed on the basis of experimental data. In many cases, however, it is not expedient to reduce the equation to a system of equations, all the more because the numerical values of the higher derivatives are needed in any case. They can be determined similarly to the derivatives of the first order. However, when determining higher derivatives by some numerical or graphical method, the fact must be considered that the higher the derivative, the greater the error made. The estimation of parameters can be performed as in the case of differential equations of the first order. If the experimental set of function and derivative values

$$x_i, \eta_i, \eta'_i, \eta''_i, \ldots \eta_i^{(p)} \qquad (i = 1, 2, \ldots k) \tag{12}$$

is available, the parameters $c_1, c_2, \ldots c_n$ of the differential equation

$$f(x, y, y', y'', \ldots y^{(p)}, c_1 c_2, \ldots c_k) = 0 \tag{13}$$

may be computed, as described above, from the minimum condition

$$\Phi(c_1, c_2, \ldots c_n) = \sum_{i=1}^{k} f^2(x_i, \eta_i \eta_i', \eta_i'', \ldots \eta_i^{(p)}, c_1, c_2, \ldots c_k) = \min! \qquad (14)$$

The extreme values are determined as stated above.

2. Application of the method to the determination of reaction order and rate constants

The mathematical procedure introduced above can be applied to determining reaction order and kinetic constants, these quantities being the parameters of the kinetic differential equation. Plotting the concentration as the function of time and determining the slopes belonging to the experimental points graphically, one gets the set of

$$x_i, y_i, y_i', \quad (i = 1, 2, \ldots n)$$

(n being the number of measurements). Hereby on the basis of the rate equations, the estimation of the parameters, *i.e.* the determination of the reaction order and kinetic constants, can be achieved. The application of this method is shown by determining the rate constants and reaction order of the catalytic oxidation of ethylene.

2.1 Determination of reaction order and rate constants in the case of the catalytic oxidation of ethylene

It was pointed out by LEHNER [2] in 1931 that the product of the partial oxidation of ethylene is ethylene oxide. In the same year, LEFORT [3] obtained a patent for the oxidation reaction accomplished in the presence of silver catalyst.

In oxidizing ethylene in the presence of a silver catalyst, ethylene oxide is formed as the main product:

$$C_2H_4 + 1/2\, O_2 \rightarrow C_2H_4O + 29.2\ \text{kcal}\ (280^\circ\ C), \qquad (15)$$

whereas in the complete oxidation of ethylene carbon dioxide is obtained:

$$C_2H_4 + 3\, O_2 \rightarrow 2\, CO_2 + 2\, H_2O + 317\ \text{kcal}\ (280^\circ\ C) \qquad (16)$$

In the presence of a silver catalyst, the ethylene oxide formed in Reaction (15) can be further oxidized:

$$C_2H_4O + 2.5\, O_2 \rightarrow 2\, CO_2 + 2\, H_2O \qquad (17)$$

As to the rate of the formation of ethylene oxide, considering its partial oxidation [4], we have:

$$r_1 = \frac{d[C_2H_4O]}{dt} = k_1 [C_2H_4]^{n_1} - k_2 [C_2H_4O]^{n_2} \tag{18}$$

The rate equation of the formation of carbon dioxide is:

$$r_2 = \frac{d[CO_2]}{dt} = k_3 [C_2H_4]^{n_3} + k_2 [C_2H_4O]^{n_2} \tag{19}$$

where

r_1 = rate of the formation of ethylene oxide (concentration/time),
r_2 = rate of the formation of carbon dioxide (concentration/time),
[] = concentrations of the components formed and taking part in the reaction,
k_1 = rate constant of the formation of ethylene oxide (time^{-1}),
k_2 = rate constant of the oxidation of ethylene oxide (time^{-1}),
k_3 = rate constant of the formation of carbon dioxide (time^{-1}),
n_1, n_2, n_3: constants.
Let be
z_0 = initial concentration of ethylene,
z: = concentration of the unchanged ethylene,
x: = momentary concentration of ethylene oxide,
y: = momentary concentration of carbon dioxide.

Accordingly, the rate equations are:

$$r_1 = \frac{d[x]}{dt} = k_3 [z_0 - z]^{n_1} - k_2 [x]^{n_2} \tag{20}$$

$$r_2 = \frac{1}{2}\frac{d[y]}{dt} = k_3 [z_0 - z]^{n_3} + k_2 [x]^{n_2} \tag{21}$$

By adding the two equations, the rate equation of the reaction of ethylene is obtained:

$$\frac{d[x]}{dt} + \frac{1}{2}\frac{d[y]}{dt} = k_1 [z_0 - z]^{n_1} + k_3 [z_0 - z]^{n_2} \tag{22}$$

Since

$$\frac{d[x]}{dt} + \frac{1}{2}\frac{d[y]}{dt} = \frac{d[z]}{dt} \tag{23}$$

we have

$$\frac{d[z]}{dt} = k_1 [z_0 - z]^{n_1} + k_3 [z_0 - z]^{n_3} \tag{24}$$

Instead of $[z_0 - z]$ we shall use z_t concentration of the ethylene converted further on.

Estimating the parameters k_1, k_3, n_1 and n_3 according to the foregoing, we get

$$\sum_{i=1}^{n} \left[\frac{dz}{dt} - k_1 z_{ti}^{n_1} - k_3 z_{ti}^{n_3} \right]^2 = \min! \tag{25}$$

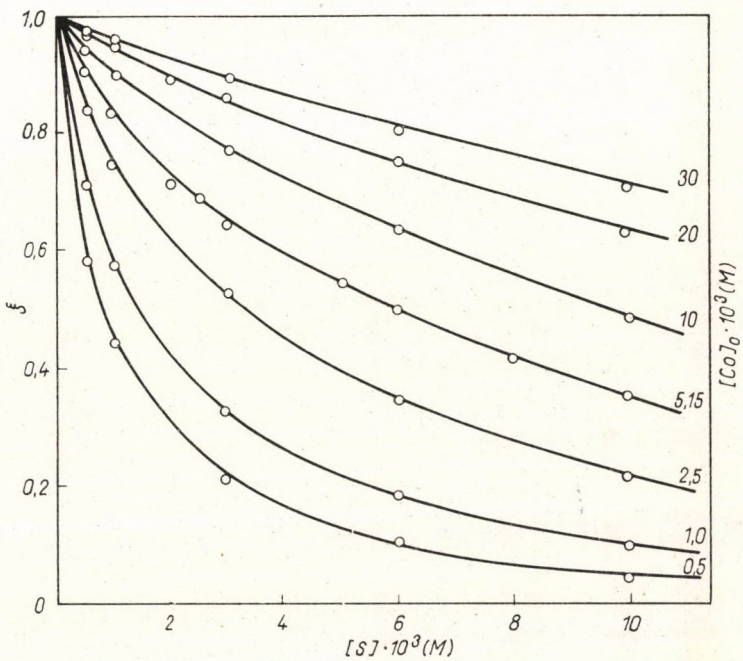

Fig. 1. Ethylene content of the product gas of oxidation at different temperatures as a function of the contact time. Concentration of ethylene in the product gas (mole). Contact time (*s*)

Differentiating the equations according to k_1, k_3, n_1, and n_3, we have:

$$\frac{\partial M}{\partial k_1} = \sum_{i=1}^{n} (z' - k_1 z_{ti}^{n_1} - k_3 z_{ti}^{n_3})\, z_{ti}^{n_1} \tag{26}$$

$$\frac{\partial M}{\partial k_3} = \sum_{i=1}^{n} (z' - k_1 z_{ti}^{n_1} - k_3 z_{ti}^{n_3})\, z_{ti}^{n_3} \tag{27}$$

$$\frac{\partial M}{\partial n_1} = \sum_{i=1}^{n} (z' - k_1 z_{ti}^{n_{i1}} - k_3 z_{ti}^{n_3})\, k_1 z_{ti}^{n_1} \ln z_{ti} \tag{28}$$

$$\frac{\partial M}{\partial n_3} = \sum_{i=1}^{n} (z' - k_1 z_{ti}^{n_1} - k_3 z_{ti}^{n_3})\, k_3 z_{ti}^{n_3} \ln z_{ti} \tag{29}$$

The experimental data needed for the solution of the equations (*i.e.* the graph

of z versus t) are contained in Fig. 1. The ethylene content of the initial gas was $35 \cdot 10^{-3}$ mole, *i.e.*

$$z_0 = 35 \cdot 10^{-3}$$

The computations were carried out from 180° C to 250° C in increments of 10° C, on the basis of the experimental data given. The derivative values were obtained by means of graphical differentiation. Putting the terms (26), (27),

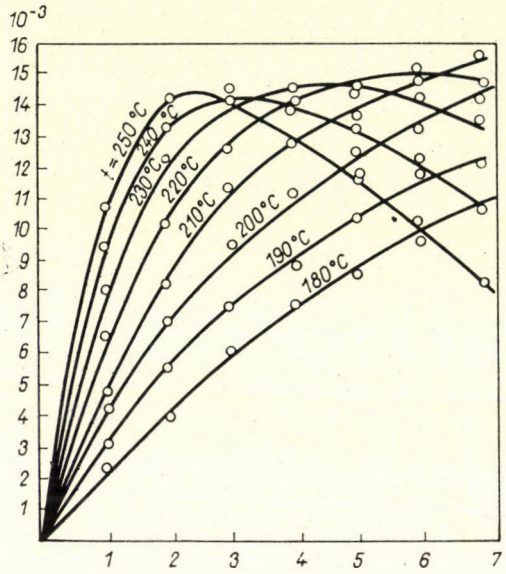

Fig. 2. Computed and measured concentrations of ethylene belonging to different contact times and reaction temperatures. Ethylene oxide formed (mole). Contact time (*s*)

(28), and (29) equal to zero and inserting the values of z_i and z_{t_i}, one gets a system of non-linear equations with four unknowns. This system of equations was solved by a GIER computer with a NOLEQ-3 program given by KJAER [5]. As a result of the computation, the unity (=1) was obtained for the values of both n_1 and n_3, which means that the reactions in the regions investigated must be of the first order. The values of the rate constants k_1 and k_3 are given in Table I.

2.2 Comparison of the values computed with the experimental data

This can easily be done, since in the differential equation (24) to be solved the exponents, both n_1 and n_3, equal the unity (=1). Integrating the equation with the initial conditions

$$z(0) = z_0$$
$$x(0) = 0$$
$$y(0) = 0$$

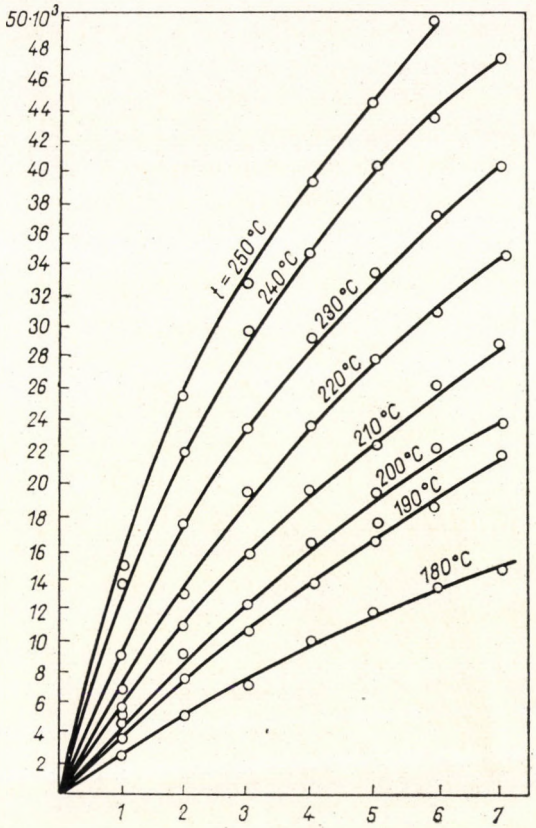

Fig. 3. Computed and measured concentrations of carbon dioxide belonging to different contact times and reaction temperatures. Carbon dioxide formed (mole). Contact time (*s*)

Table I

Temperature °C	Obtained by the method of least squares	
	$k_1[s^{-1}]$	$k_3[s^{-1}]$
180	0.0700	0.0300
190	0.1000	0.0500
200	0.1089	0.1000
210	0.1600	0.1000
220	0.2260	0.1300
230	0.3000	0.1600
240	0.3800	0.2300
250	0.5000	0.2600

we get

$$z = z_0 (1 - e^{-(k_1+k_3)t}) \tag{30}$$

$$x = \frac{k_1 z_0}{k_1 - k_2 + k_3} (e^{-k_2 t} - e^{-(k_1+k_3)t}) \tag{31}$$

$$y = \frac{2z_0}{k_1 + k_3} \left(k_3 - \frac{k_1 k_3}{k_1 - k_2 + k_3} \right) (1 - e^{-(k_1+k_3)t}) - \frac{2z_0 k_1}{k_1 - k_1 + k_3} (e^{-k_2 t} - 1) \tag{32}$$

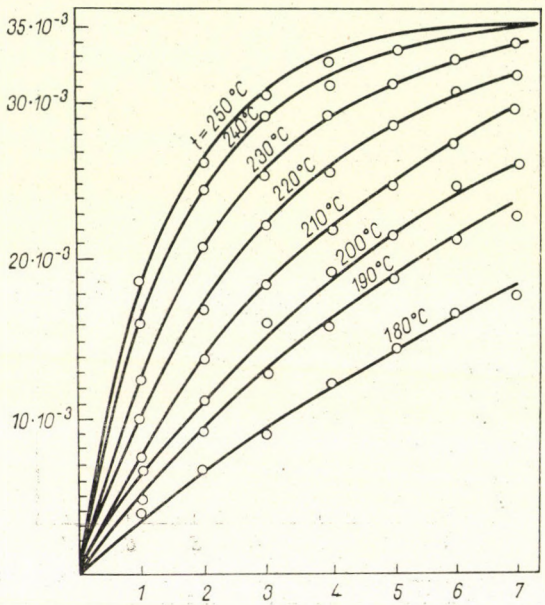

Fig. 4. Computed and measured quantities of ethylene converted, belonging to different contact times and reaction temperatures. Ethylene converted (mole). Contact time (*s*)

The computed and measured values, respectively, are given in Figs 2, 3 and 4. By these the accuracy of the method outlined has been proved, the deviation of the computed and measured values being within the error band.

*

The authors take pleasure in thanking Academician M. FREUND, director of the Hungarian Oil and Gas Research Institute, and Professor A. LÁSZLÓ, head of the Chemical Engineering Department of the University of Chemical Industry, Veszprém, for their valuable help in this work.

SUMMARY

In physical chemistry the problem of checking the correctness of a differential equation by means of experimental data, and of estimating its parameters, often arises. If the differential equation cannot be solved analytically, the solution of the above problem encounters difficulties.

In the present paper a procedure based on the method of least squares is outlined to solve this problem. Minimizing the difference of the computed and measured values, the parameters can be determined either by solving the system of equations obtained by differentiating according to the single variables, or by determining the extreme value directly.

The solution of the above system of equations was achieved in this work by means of a computer. The application of the method is shown in the case of a problem of reaction kinetics. The rate constant and reaction order of the catalytic oxidation of ethylene were determined on the basis of experimental data by means of the method outlined. The rate equation is given as a differential equation that cannot be solved analytically if the reaction order is also unknown. With this method the reaction order and rate constants were determined on the basis of the curve of the ethylene concentration versus time. The differential equation was solved with these computed data and the solution obtained was compared with the experimental results.

REFERENCES

1. Fletcher, R., Powell, M. J. D.: The Computer Journal **6,** 163 (1963).
2. Lehner, S.: J. Am. Chem. Soc. **53,** 3737 (1931).
3. Lefort, F.: Fr. p. 41255, 41810 (1931).
4. Balogh, A.: Dissertation, 1966.
5. Kjaer, J.: Programming of Chemical Calculation, Vol. 2. Numerical Methods for Equations, Polynomials, and Optimization. Haldor Topsoe, Vedbaek, Denmark, 1965, p. 122.
6. Box, G. E. P.: Bull. Inst. International Statistique **36,** (1957).
7. Courant, R.: Bull. Amer. Math. Soc. **49,** 1 (1943).
8. Curry, H. D.: Qu. App. Maths. **2,** 258 (1944).
9. Householder, A. S.: Principles of Numerical Analysis, McGraw-Hill, New York, 1953.
10. Levenberg, K.: Qu. App. Maths. **2,** 164 (1944).
11. Booth, A. D.: Numerical Methods, Butterworths, London, 1957.
12. Hestenes, M. R., Stiefel, E.: J. Res. N. B. S. **49,** 409 (1952).
13. Martin, D. W., Tee, G. J.: The Computer Journal **4,** 242 (1961)
14. Shah, B. V., Buehler, R. J., Kempthorne, O.: Office of Naval Research Report, Nr. 042-207 (No. 2), (1961).
15. Powell, M. J. D.: The Computer Journal **5,** 147 (1962).
16. Davidon, W. C.: A. E. C. Research and Development Report, ANL-5990 (Rev.), (1959).

László Fáy; Veszprém, Csermák Antal utca 7
András Balogh; Veszprém, Schönherz Zoltán út 14

Acta Chimica Academiae Scientiarum Hungaricae Tomus 57 (4), pp. 403—41 0 (1968)

INVESTIGATION OF THE MOLECULAR STRUCTURE OF SULPHURYL CHLORIDE BY SECTOR MICROPHOTOMETER ELECTRON DIFFRACTION

I. HARGITTAI

(Research Laboratory for Chemical Structures of the Hungarian Academy of Sciences, Budapest)

Received November 2, 1967

Introduction

In the present paper the results of a study on the molecular structure of SO_2Cl_2 by the sector microphotometer electron diffraction method are reported.

Recently the molecular structure of $SO_2ClN(CH_3)_2$ was investigated using the electron diffraction sector microphotometer method, with the aim to study the geometric configuration of the trivalent nitrogen atom and that of the hexavalent sulphur atom [1]. Among others, the value of the internuclear distance r(S—Cl) $2.09_4 \pm 0.01$ Å was obtained. Unfortunately, no satisfactory comparison could be made between the determined value and the data published in the literature, partly as there are few such data, and partly because of the contradictions between the available values. As examples, Table I shows some results obtained by PALMER in an important work carried

Table I

r(S—Cl) bond length data

Compound	r(S—Cl), Å	Method*	Ref.
S_2Cl_2	1.99 ± 0.03	VED	[2]
	2.07 ± 0.01	SMED	[3]
SCl_2	1.99 ± 0.03	VED	[2]
	2.006 ± 0.004	SMED	[4]
$SOCl_2$	2.07 ± 0.03	VED	[2]
SO_2Cl_2	1.99 ± 0.02	VED	[2]

* VED: Visual method of electron diffraction
SMED: Sector microphotometer method of electron diffraction

out 30 years ago using the visual method of electron diffraction, and two other data obtained later by sector microphotometer electron diffraction.

As the S—Cl bond length was found to be much longer in the case of $SO_2ClN(CH_3)_2$ than in sulphuryl chloride, it seemed desirable to repeat the electron diffraction molecular structure determination of the latter compound using the sector microphotometer technique and least squares refinement of the parameters.

Method

The sulphuryl chloride used was an "Austranal" product of Loba-Chemie, Austria.

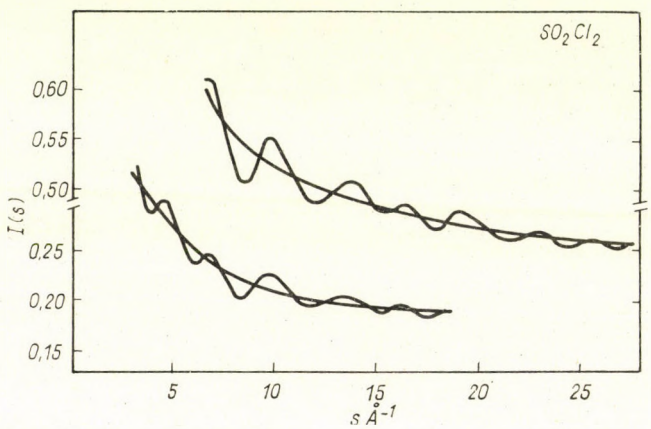

Fig. 1. Total intensity curves obtained by two values of nozzle—plate distance. The background line is shown

The electron diffraction pattern of SO_2Cl_2 vapour was recorded with an apparatus developed from a Zeiss EF4 electron-optical unit in this Laboratory. The nozzle system, cooled trap and photographic camera with rotating sector were described in detail elsewhere [5]. An r^3 sector with a maximum radius of 55 mm, and two gas-nozzle to photographic plate distances of about 285 mm, and 230 mm, respectively, were used. The wave length of the electron beam was about 0.053 Å. A total of 14 electronograms were recorded, and twice three plates, according to two camera distances, were chosen for further evaluation. Traces of the optical density of the diffraction pattern were obtained using a Zeiss GIII fast-photometer, for which a simple device had been constructed that oscillated the plates, as it was described elsewhere [6].

The total intensities obtained at two values of the nozzle – plate distance are shown in Fig. 1. The background line was drawn arbitrarily, trying to follow the trend of the oscillating curve and to get a possibly "smooth" line.

Variations in the background line did not lead to any considerable decrease of the error wave at the beginning of the radial distribution curve (*cf.* F1 in Fig. 3).

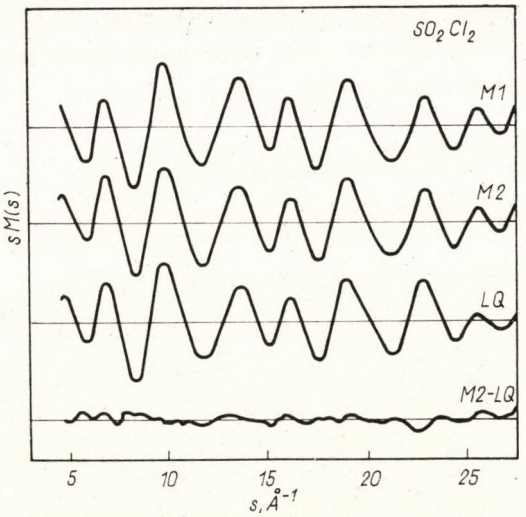

Fig. 2. $sM(s)$ molecular intensity curves. M1 — experimental; M2 — corrected experimental; LQ — as obtained from least squares refinement; M2—LQ — difference curve

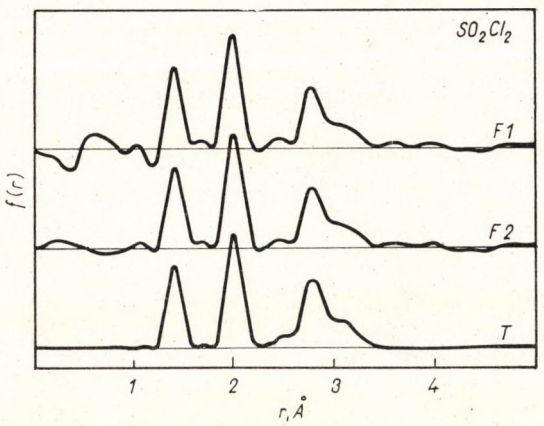

Fig. 3. $f(r)$ radial distribution curves. F1 — calculated from M1; F2 — calculated from M2; T — calculated from the final results

The $sM(s)$ molecular intensity curve M1 in Fig. 2 was obtained in the usual way. Its Fourier-transform, the F1 $f(r)$ radial distribution curve is shown in Fig. 3. In the Fourier transformation the inner part of a theoretical $sM(s)$ curve was used for the range $s = 0.0$ to 4.4 Å^{-1}. It was checked that the choice of the molecular model for which the theoretical curve had been calculated and then used in the extrapolation, did not affect the position of the maxima on the $f(r)$ curve.

There is a significant error wave in the non-structural range 0.0 to 1.20 Å of F1 radial distribution (Fig. 3). Curve M2 of Fig. 2 was obtained by subtracting the inverse Fourier-transform of this error wave from M1. Curve M2 again was subjected to Fourier-transformation and this led to F2 of Fig. 3. This procedure reduced the error wave, but did not affect considerably the structural part of the radial distribution.

Structural analysis

The corrected experimental $f(r)$ curve (F2, Fig. 3) had maxima at $r = 1.41$ Å and 2.01 Å corresponding to the internuclear distances $r(S-O)$ and $r(S-Cl)$, respectively. The compound maximum in the range of 2.25 to 3.40 Å corresponds to the internuclear distances $r(O \ldots O)$, $r(Cl \ldots O)$ and $r(Cl \ldots Cl)$. The small peak at about 2.47 Å corresponds to the first of them, and the second, which has the greatest weight, corresponds to $r(Cl \ldots O)$ and its probable peak is at 2.78 Å.

The least squares refinement of the internuclear distances and mean amplitudes of vibration was carried out on the basis of the corrected experimental $sM(s)$ values (see M2, Fig. 2 and Table II). The corresponding Ural 2 programmes were written [7] based on the literature [8—10].

It should be mentioned that non-nuclear scattering was not taken into account.

The trial structure (Table III), *i.e.* the input parameters in the least squares refinement, was drawn from the experimental radial distribution curve (F2, Fig. 3). Assuming C_{2v} symmetry for the SO_2Cl_2 molecule, four internuclear distances were regarded as independent (r) and the fifth as dependent (d). All five mean amplitudes of vibration (l) were considered independent. In the course of the refinement, the value of $l(O \ldots O)$ appeared to be irrationally small, so it was fixed (0.07 Å) and no longer varied. There was a $b = 0.0024$ value in the weight matrix used in this refinement.

Results and their uncertainties

The results of the least squares refinement are shown in Table III.

The standard deviation of the least squares refinement is also presented here.

When calculating the final uncertainties of the parameters, the possible errors of the theoretical approximation used were not taken into account. (From this point of view the most significant error could arise from the fact that non-nuclear scattering was left out of consideration. It is interesting that repeating the least squares refinement of cyclopropane [10] using the

Table II

sM(s) values of the curve M2 (Fig. 2)

s, Å^{-1}	$sM(s)$	s, Å^{-1}	$sM(s)$	s, Å^{-1}	$sM(s)$
4.6	0.256	12.4	−0.273	20.2	−0.054
4.8	0.282	12.6	−0.171	20.4	−0.130
5.0	0.190	12.8	−0.039	20.6	−0.219
5.2	0.110	13.0	0.073	20.8	−0.301
5.4	0.027	13.2	0.196	21.0	−0.344
5.6	−0.057	13.4	0.296	21.2	−0.352
5.8	−0.154	13.6	0.355	21.4	−0.341
6.0	−0.182	13.8	0.375	21.6	−0.311
6.2	−0.071	14.0	0.334	21.8	−0.273
6.4	0.116	14.2	0.254	22.0	−0.182
6.6	0.310	14.4	0.107	22.2	−0.065
6.8	0.440	14.6	−0.014	22.4	0.027
7.0	0.448	14.8	−0.142	22.6	0.160
7.2	0.364	15.0	−0.240	22.8	0.272
7.4	0.123	15.2	−0.316	23.0	0.337
7.6	−0.007	15.4	−0.243	23.2	0.330
7.8	−0.134	15.6	−0.106	23.4	0.274
8.0	−0.374	15.8	0.035	23.6	0.163
8.2	−0.527	16.0	0.197	23.8	0.036
8.4	−0.554	16.2	0.261	24.0	−0.112
8.6	−0.488	16.4	0.247	24.2	−0.199
8.8	−0.353	16.6	0.177	24.4	−0.255
9.0	−0.174	16.8	−0.006	24.6	−0.250
9.2	0.060	17.0	−0.171	24.8	−0.194
9.4	0.275	17.2	−0.306	25.0	−0.106
9.6	0.474	17.4	−0.392	25.2	−0.009
9.8	0.549	17.6	−0.412	25.4	0.055
10.0	0.578	17.8	−0.348	25.6	0.121
10.2	0.505	18.0	−0.249	25.8	0.135
10.4	0.429	18.2	−0.059	26.0	0.072
10.6	0.275	18.4	0.060	26.2	0.023
10.8	0.038	18.6	0.233	26.4	−0.036
11.0	−0.083	18.8	0.352	26.6	−0.097
11.2	−0.229	19.0	0.415	26.8	−0.105
11.4	−0.343	19.2	0.448	27.0	−0.067
11.6	−0.412	19.4	0.400	27.2	−0.019
11.8	−0.456	19.6	0.256	27.4	0.076
12.0	−0.425	19.8	0.161	27.6	0.184
12.2	−0.364	20.0	0.037		

same set of intensity values and trial structure as in [10], the internuclear distances obtained in this procedure differed from those of [10] very little, namely below 0.001 Å in different directions, but in the case of the mean amplitudes of vibration the difference was 0.01 Å in the order of magnitude, and application of the worse theoretical approximation decreased the mean amplitude values.)

Table III

Results of the least squares refinement

	Trial structure	Results
r(S—O)	1.414	1.4090 ± 0.0018
r(S—Cl)	2.010	2.0108 ± 0.0015
r(O...O)	2.470	2.4853 ± 0.0113
r(Cl...O)	2.784	2.7831 ± 0.0031
d(Cl...Cl)	3.122	3.0810
l(S—O)	0.036	0.0327 ± 0.0038
l(S—Cl)	0.048	0.0449 ± 0.0025
l(O...O)	0.070	0.07 (assumed)
l(Cl...O)	0.066	0.0696 ± 0.0033
l(Cl...Cl)	0.100	0.1090 ± 0.0097

In addition to the standard deviation of the least squares refinement, the scale error was taken into account. The important feature of these relative errors, *i.e.* their approaching equality

$$\sigma(s) \approx \sigma_s(r_{ij}) \approx \sigma_s(l_{ij})$$

was utilized [11], where $s = \frac{4\pi}{\lambda} \sin \frac{\vartheta}{2}$, λ = the wave length, and ϑ = the scattering angle. $\sigma(s)$ was calculated according to the expression

$$\sigma(s) = [\sigma^2(\lambda) + \sigma^2(L) + \sigma^2(m)]^{1/2}$$

where L = the nozzle – plate distance, and m = the magnifying factor of the microphotometer. (TlCl served as a crystal standard, and a Zeiss Abbe comparator and a KM-6 cathetometer were used for the measurements of TlCl diffraction rings and nozzle – plate distances, respectively.) A value of $\sigma(s) \approx 0.2$ was determined, so $\sigma_s(r_{ij}) \approx \sigma_s(l_{ij}) \approx 0.02\%$.

In the case of internuclear distances, this scale error is commensurable with the standard deviation of the least squares refinement and it was added

to it. On the other hand, the scale error, being much less than the standard deviation in the case of the mean amplitudes of vibration, was neglected in the case of the amplitudes.

The final results are shown in Table IV.

Table IV

Final results

	r, Å	l, Å	angles
S—O	1.409 ± 0.005	0.033 ± 0.004	
S—Cl	2.011 ± 0.006	0.045 ± 0.003	
O...O	2.485 ± 0.016	0.07 (assumed)	
Cl...O	2.783 ± 0.009	0.070 ± 0.003	
Cl...Cl	3.08 ± 0.04		
OSO			123 ± 2°
OSCl			107.6 ± 0.6°
ClSCl			100 ± 2°

Comparison of the results with other data

Our results obtained by the sector microphotometer method using least squares refinement are in agreement with PALMER's data [2], if we consider the great uncertainty of the visual method.

The r(S—O) internuclear distance in SO_2Cl_2 is almost equal to that in SO_2F_2, where r(S—O) 1.405 ± 0.003 Å obtained by microwave spectroscopy [12], and less than that in $SO_2ClN(CH_3)_2$ (1.44 ± 0.01 Å) [1] and in $SO_2(N(CH_3)_2)_2$ crystal (1.449 and 1.441 ± 0.005 Å) [13]. The bond angle value OSO 123 ± 2° in SO_2Cl_2 corresponds to that in SO_2F_2 (123°58′ ± 12′) [12].

The lengthening of the r(S—O) internuclear distance observed in $SO_2ClN(CH_3)_2$ may be partly due to the effect of the substitution of a chlorine atom in SO_2Cl_2 by a $N(CH_3)_2$ group, but the problem requires further studies.

*

The author thanks Prof. S. LENGYEL and Dr. L. V. VILKOV for their interest and encouragement. His thanks are also due to mathematicians Mr. J. GERGELY and G. KOSZÓ, workshop foreman Mr. J. HERNÁDI, mechanician Mr. L. HAKLIK and Laboratory assistant Mrs. J. SZILÁGYI for their valuable contribution throughout the course of this work.

SUMMARY

The molecular structure of SO_2Cl_2 was studied by the sector microphotometer electron diffraction method. Using least squares refinement, the following bond lengths and angles were determined: r(S—O) 1.409 $\pm$ 0.005 Å; r(S—Cl) 2.011 $\pm$ 0.006 Å; $\sphericalangle$OSO 123 $\pm$ 2° and $\sphericalangle$OSCl 107.6 $\pm$ 0.6°.

REFERENCES

1. VILKOV, L. V., HARGITTAI, I.: Acta Chim. Acad. Sci. Hung. **52,** 423 (1967).
2. PALMER, K. J.: J. Am. Chem. Soc. **60,** 2360 (138).
3. HIROTA, E.: Bull. Chem. Soc. Japan, **31,** 130 (1958).
4. MORINO, Y., MURATA, Y., ITO, T., NAKAMURA, J.: J. Phys. Soc. Japan **17,** Suppl. B-II, 37 (1962).
5. HARGITTAI, I., HERNÁDI, J., TREMMEL, J.: Jenaer Rundschau **13,** 3 (1968).
6. HARGITTAI, I., HERNÁDI, J.: Jenaer Rundschau, in the press.
7. GERGELY, J.: To be published.
8. HEDBERG, K., IWASAKI, M.: Acta Cryst. **17,** 529 (1964).
9. IWASAKI, M., FRITSCH, F. N., HEDBERG, K.: Acta Cryst. **17,** 533 (1964).
10. BASTIANSEN, O., FRITSCH, F. N., HEDBERG, K.: Acta Cryst. **17,** 538 (1964).
11. VILKOV, L. V.: Zhurnal strukturnoi khimii, **5,** 809 (1964).
12. LIDE, D. R., MANN, D. E., FRISTROM, R. M.: J. Chem. Phys. **26,** 734 (1957).
13. JORDAN, T., SMITH, H. W., LOHR, L. L., Jr., LIPSCOMB, W. N.: J. Am. Chem. Soc. **85,** 846 (1963).

István HARGITTAI; Budapest, VIII. Puskin utca 11—13

Acta Chimica Academiae Scientiarum Hungaricae Tomus 57 (4), pp. 411—423 (1968)

NH STRETCHING VIBRATION BANDS AT WAVE NUMBERS LOWER THAN 3000 cm^{-1}, V*

CYCLIC DIMERIC STRUCTURES, V. QUINAZOLONE DERIVATIVES

P. SOHÁR and I. KÓSA

(Research Institute for Pharmaceutical Chemistry, and Chinoin Pharmaceutical and Chemical Co., Budapest)

Received November 21, 1967

Introduction

In the course of former studies [1] it was found that phthalylhydrazide (**Ic** ⇌ **IIa** ⇌ **IIIa**) and its mono-acylates (**IIb** ⇌ **IIIb**), further dihydrophthal-

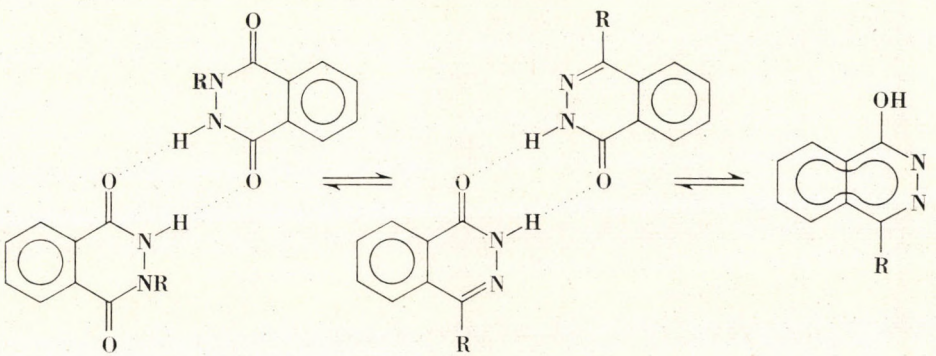

I **II** **III**

a: R = OH
b: R = OAc
c: R = H

azone (**IIc** ⇌ **IIIc**), quinazolinedione (**IVa**) as well as its 3-N-substituted derivatives (**IVb**) associate to form cyclic dimeric structures in the solid phase. In evidence of this, the diffuse NH stretching vibration band with submaxima appears at very low wave numbers, between 3300 and 2400 cm^{-1} [2—4]. In the spectra of these compounds mentioned above, the amide-I band in coalescence with the C=N stretching vibration band is found at about 1670 cm^{-1}, and it is very intensive and broad.

It seemed interesting to examine whether 4(3H)-quinazolinone and its derivatives [5] are also capable to form associated cyclic structures.

* Part IV: SOHÁR, P., NEMES, A.: Acta Chim. Acad. Sci. Hung. **56,** 25 (1968)

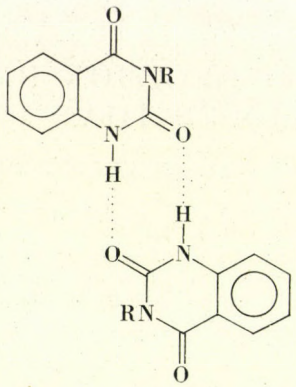

a: R=H
b: R={alkyl / aryl} group

IV

4(3H)-Quinazolinone derivatives

In Spectrum 1, that of 4(3H)-quinazolinone (**V**), the NH stretching vibration (νNH) band is very diffuse, split by sub-maxima, and absorption extends from 3300 to 2300 cm^{-1}. Thus, cyclic dimeric association is present in this case,

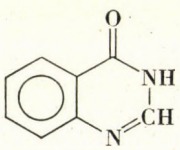

V

too, though not exclusively. The part of the νNH band in the region 3300—3000 cm^{-1} is certainly indicative of molecules that form simple intermolecular hydrogen bonds; as compared to dihydrophthalazone, the ratio of these two kinds of association is shifted towards the latter type. Still more distinct is this shift in the case of the 7-nitro, or 6,8-dichloro analogues (*cf.* Spectra 2 and 3).

Earlier, we have listed the prerequisites of the formation of cyclic dimeric associations [3, 4], of which, for lactams, first place has been given to the chemical character of the amide group and its consequent tendency to form hydrogen bonds. Obviously, owing to the shift towards limiting structure **VI** of the **VI** ↔ **VII** mesomeric system, this tendency is smaller in the 4(3H)-quinazo-

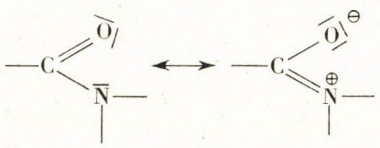

VI **VII**

linone derivatives. The circumstance that the limiting structure **VI** has a greater role in 4(3H)-quinazolinone than in dihydrophthalazone is due to the fact that only the $-I$ effect of the C=N bond affects the amide group in the former while the $+T$ effect of the nitrogen atom adjacent to the amide group largely compensates the $-I$ effect of the C=N bond in the latter [5].

This is very clearly shown by the frequency increase of the amide-I band which, separated from the C=N stretching vibration (νC=N) band that appears invariably at 1670 cm^{-1}, is found here at 1710 cm^{-1}. Since this wave number has to be considered high even for a conjugated ketone, it may be stated that in the instance of 4(3H)-quinazolinone, the mesomeric limiting structure **VI** predominates, and is consequently a true representation of the electron distribution in the molecule.

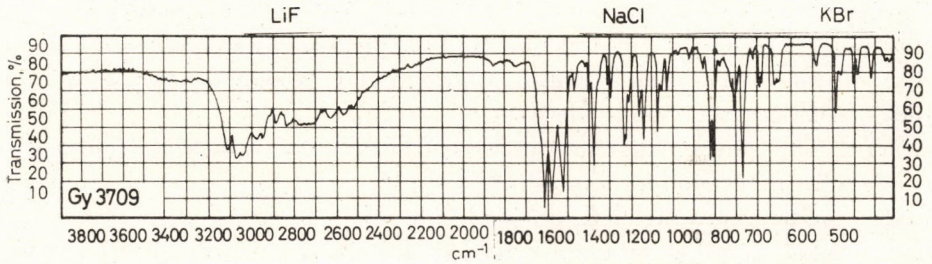

Spectrum 1. 4(3H)-Quinazolinone, in KBr

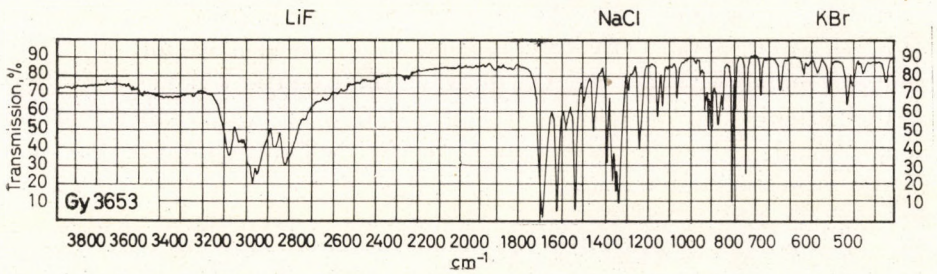

Spectrum 2. 7-Nitro-4(3H)-quinazolinone, in KBr

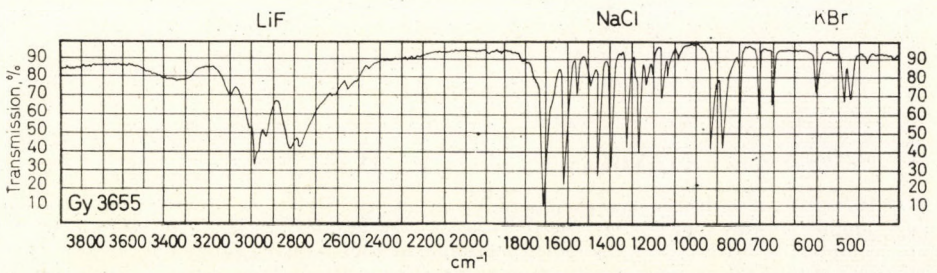

Spectrum 3. 6,8-Dichloro-4(3H)-quinazolinone, in KBr

Clearly, the electrophilic substituents of the condensed aromatic ring exert an effect in this same direction, however, since mesomerism is practically impossible even in the parent compound, the frequency of the amide carbonyl band will not increase any further in the spectra of these derivatives, and a shift in the same direction of the νC=N band will occur (the CN bond order will be increased). Accordingly, the νC=O and νC=N bands of the 7-nitro derivative will overlap and their common maximum will be found at 1695 cm^{-1}. The common maximum of the coalescent band in the case of the 6,8-dichloro compound appears at 1710 cm^{-1}. At the same time, the ratio of the molecules present in simple intermolecular association is increased at the expense of the molecules involved in cyclic dimeric structures.

Thus, in the case of the 4(3H)-quinazolinone molecule the C—N and N—H bonds participate with an amplitude much smaller than the usual in the group vibration extending over the C=O, C—N and N—H bonds (resulting in the appearance of the amide-I band in the sprectra of amides), and therefore the absorption at 1710 cm^{-1} can be approximately assigned to the individual vibration of the C=O bond: this vibration regains its specific bond-frequency character. This phenomenon is similar to the frequency increase found with secondary* amides (imides); in which, however, the two carbonyl vibrations are also coupled, so that instead of individual νC=O vibrations a symmetric-antisymmetric (ν_sC=O and ν_{as}C=O) pair of vibrations will absorb, shifted by an equal degree from the original νC=O frequency value towards higher and lower wave numbers.

4(3H)-Quinazolinone may be regarded as a "secondary" amide where one oxygen atom in the CONCO group has been replaced by nitrogen. This precludes coupling with the νC=O vibration (the frequency values are different); furthermore, the increase of the νC=O frequency is smaller than for secondary amides, since the $-I$ effect of the C=N bond is smaller than that of the C=O group.

4(3H)-Quinazolinone acylates

In order to obtain further evidence, the spectra of 4(3H)-quinazolinone acylates have also been studied.

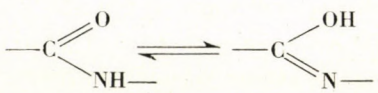

VIII IX

* In contrast with the accepted and incorrect use which designates N-substituted primary amides of the type —CO—NHR as secondary amides, we use the latter term to denote compounds with —CO—N—CO— group. In this sense compounds of the type $R_1CON(COR_2)COR_3$ are tertiary amides, and those of type $RCONR_1R_2$ are N,N-disubstituted primary amides.

Acetylation, and benzoylation gave the N-acyl derivatives of dihydrophthalazone [1, 6]. Greater probability of the mesomeric limiting structure **VII** favours formation of O-acyl derivatives, because this brings about a shift towards the iminohydrin form **IX** of the **VIII** ⇌ **IX** tautomeric equilibrium which, in the case of amides, is generally completely shifted towards structure **VIII**. Thus if our assumption about the relatively low contribution of structure **IX** in 4(3H)-quinazolinone is correct, the exclusive formation of N-acyl compounds is to be expected, and cleavage of the acyl group should be a readily occurring reaction.

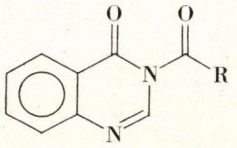

a: R = Me
b: R = Ph

X

This is indeed the fact. Both the acylate (**Xa**) and benzoate (**Xb**) of 4(3H)-quinazolinone are unstable N-acyl compounds which can be used as acylating agents in preparative chemistry [5]. The fact that N-acyl compounds are formed, is supported by the presence of the two carbonyl bands in the spectra. In the case of O-acyl compounds (**XI**), only the carbonyl band of the iminohydrin ester group would appear. The νC=N vibrations would absorb together with the aromatic ring vibrations at about 1600 and 1500 cm^{-1}, thus the νC=N vibration, consequently the νC=N band, could not be discerned separately.

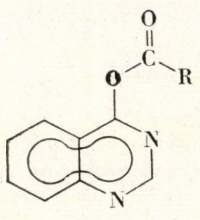

XI

Whether ester bands appear or not, cannot be decided in this case, since the ν_{as}C=O band corresponding to structure **X** and the νC=O band of the iminohydrin ester group of structure **XI** are expected to appear in about the same range of wave numbers; between 1300 and 1200 cm^{-1}, where the absorption of one of the intensive νC—O coupled vibrations of esters is found, strong absorption may be expected also by structure **X**, corresponding to the νC_{Ar}—C(=O) vibration. However, since the band of the two coupled carbonyl vibrations appears both in Spectra 4 and 5 (at 1750 and 1705 cm^{-1} for acetates,

and at 1725 and 1700 cm^{-1} for benzoates), the pertinence of structure **X** can hardly be doubted. The mean values of the $\nu_{as}C{=}O$ and $\nu_{s}C{=}O$ frequencies are 1727.5 and 1712.5 cm^{-1}, respectively. (These would be, approximately, the figures for the individual and nearly identical two $\nu C{=}O$ frequencies without coupling. They are not exactly the same, because the two carbonyls are not equivalent owing to the different structures of the α-substituents,

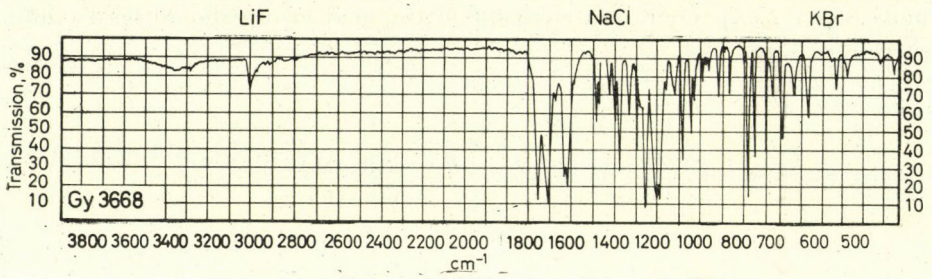

Spectrum 4. N-Acetyl-4(3H)-quinazolinone, in KBr

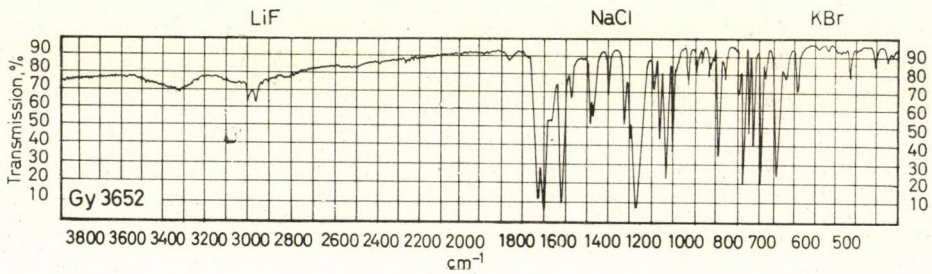

Spectrum 5. N-Benzoyl-4(3H)-quinazolinone, in KBr

especially in the case of N-acetyl-4(3H)-quinazolinone.) The frequency increase due to the $-I$ effect of the substituents is especially clearly discernible if these mean values are compared with those found for the 7-nitro-, and 6,8-dichloro-N-acetyl-4(3H)-quinazolinone derivatives giving 1730, and 1732.5 cm^{-1}, respectively (the frequency of the vibration-pair $\nu_{as}C{=}O - \nu_{s}C{=}O$ is 1760—1700, and 1750—1715 cm^{-1}, respectively; *cf.* Spectra 6, and 7).

It may be noted that the $-I$ effect of the $-C{=}N$ bond is also partly responsible for the relatively high carbonyl frequencies; in view of this, structure **X** could be considered as a "tertiary amide" wherein the oxygen atom of one of the carbonyl groups has been replaced by nitrogen. In systems where three carbonyl groups are linked to the same nitrogen atom and none is conjugated (tertiary amides without a double bond at α-position), especially in cyclic structures where ring strain also increases the frequencies, the coupled carbonyl band of highest frequency appears at very high wave numbers (between 1850 and 1780 cm^{-1} [6, 7]).

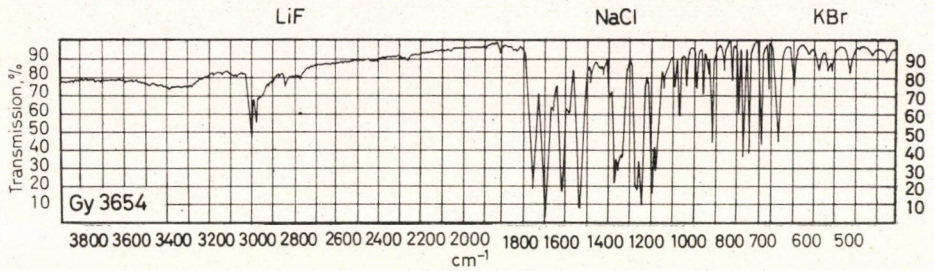

Spectrum 6. N-Acetyl-7-nitro-4(3H)-quinazolinone, in KBr

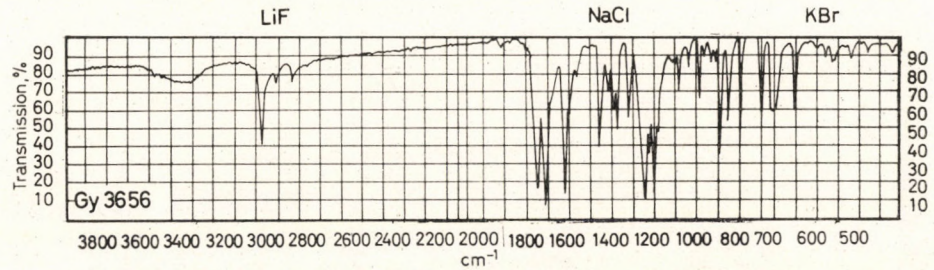

Spectrum 7. N-Acetyl-6,8-dichloro-4(3H)-quinazolinone, in KBr

3-Hydroxy- and 3-acyloxy-4(3H)-quinazolinone derivatives

Great interest is attached to a study of the 3-hydroxy (**XIIa**) and 3-acyloxy (**XIIb**) derivatives of 4(3H)-quinazolinone. In Spectrum 8, that of 3-hydroxy-4(3H)-quinazolinone, the comparatively low wave number of the carbo-

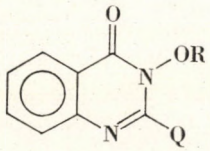

XII

a: R = H Q = H
b: R = Ac Q = H
c: R = H Q = Me
d: R = H Q = Ph

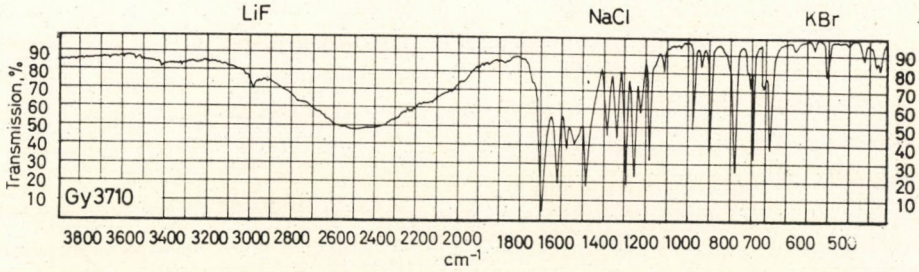

Spectrum 8. 3-Hydroxy-4(3H)-quinazolinone, in KBr

nyl frequency and the relatively high wave number of the $\nu C{=}N$ band (the two coalescent absorptions emerge with a maximum at 1690 cm^{-1}) speaks for the internal ionic structure **XIII**, together with the absorption extending between

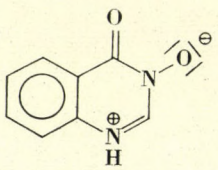

XIII

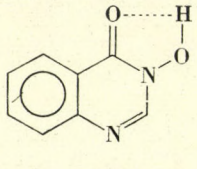

XIV

3000 and 1800 cm^{-1} which is a too low wave number for a νOH band but is very similar to a band characterizing the $\nu(=N^{+}H)$ vibration. A νOH band with this structure can be expected only in the spectra of chelates, or in the formation of an oxonium ion. However, the hydrogen bond of structure **XIV** does not give rise to a chelate band, as evidenced, *e.g.*, by the spectra of hydroxyflavanone derivatives [8]. In the spectrum of 5-hydroxy derivatives of structure **XV** a diffuse νOH absorption at low wave numbers (called thus a "chelate band") is found, while in the spectra of 3-hydroxy compounds of structure **XVI** the νOH band at about 3300 cm^{-1} has relatively well defined contours, thus the presence of a "chelate band" is completely excluded.

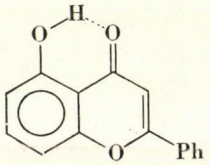

XV

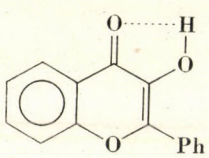

XVI

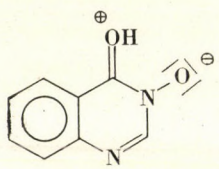

XVII

On the other hand, if structure **XVII** were present, the frequency of the carbonyl band would be lowered, thus also this possibility may confidently be rejected.

Structure **XIII** is supported by the fact that in Spectrum 9, that of the 2-methyl analogue (**XIIc**), the frequencies and shapes of the νOH and the coalesced $\nu C{=}O$ and $\nu C{=}N$ bands are unchanged, while in the case of the 2-phenyl derivative (**XIId**) (Spectrum 10) significant deviations are found. This latter effect is connected with the conjugation of the $N^{+}H{=}C$ bond. If the hydroxyl group were attached to the nitrogen at position 3 (**XIIa**), substitution on the C-2 atom would not perceptibly affect the structure of the νOH band.

The changes in the spectrum of the hydrochloride can also be adduced in evidence for structure **XIII**. In the spectra of the hydrochlorides prepared from the three hydroxy-4(3H)-quinazolinone compounds (Spectra 11, 12 and

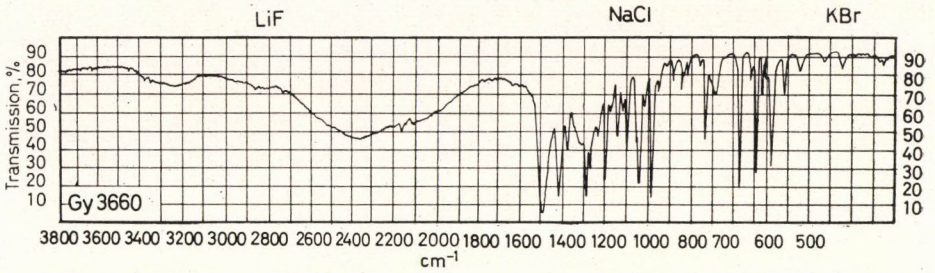

Spectrum 9. 2-Methyl-3-hydroxy-4(3H)-quinazolinone, in KBr

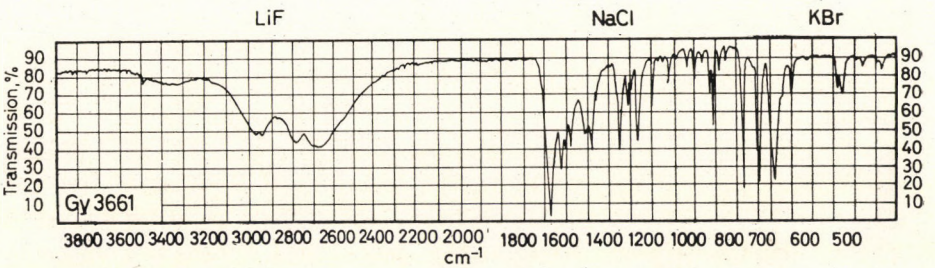

Spectrum 10. 2-Phenyl-3-hydroxy-4(3H)-quinazolinone, in KBr

13) the carbonyl band is shifted in both cases towards the higher, and the νC=N band towards the lower wave numbers, to a considerable degree (the common maxima of the two bands of the bases are found at 1695, 1690, and 1670 cm^{-1}, respectively; for the salts the maxima, shifted in the opposite direction and therefore separated, are to be seen at 1735 and 1655, 1750 and 1650, 1745 and 1640 cm^{-1}, respectively).

If structure **XII** formed in the case of the bases, shifts in the same direction (towards higher wave numbers) of the νC=O and νC=N bands would occur, and the magnitude of the shift should be greater in the case of the νC=N band. For, when a C=N bond is protonated, its order is increased; this, in general, gives rise to an increase by 20 to 60 cm^{-1} in the frequency of the νC=N band [9], obviously in consequence of the shift towards **XVIII** in the mesomeric system **XVIII** ↔ **XIX**. (In the base, the limiting structure **XIX** predominates because of the $+T$ effect of the nitrogen atom, while after

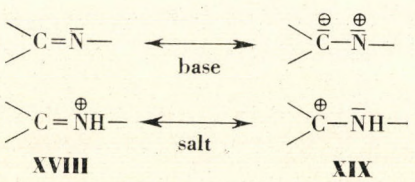

XVIII **XIX**

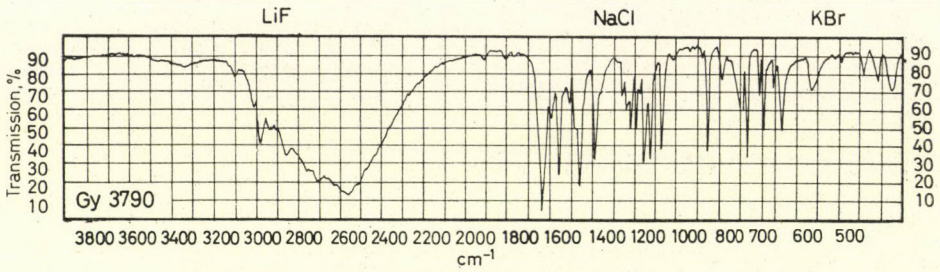

Spectrum 11. 3-Hydroxy-4(3H)-quinazolinone hydrochloride in KBr

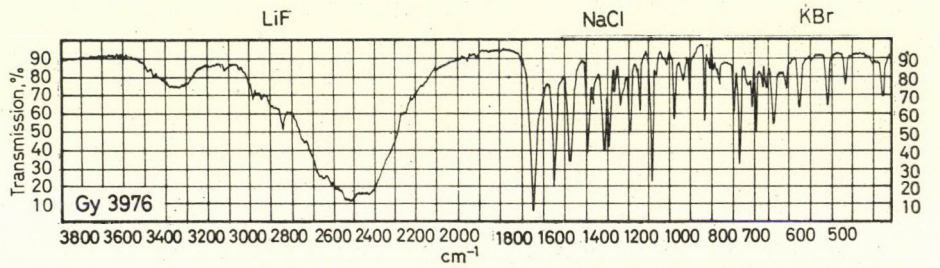

Spectrum 12. 2-Methyl-3-hydroxy-4(3H)-quinazolinone hydrochloride, in KBr

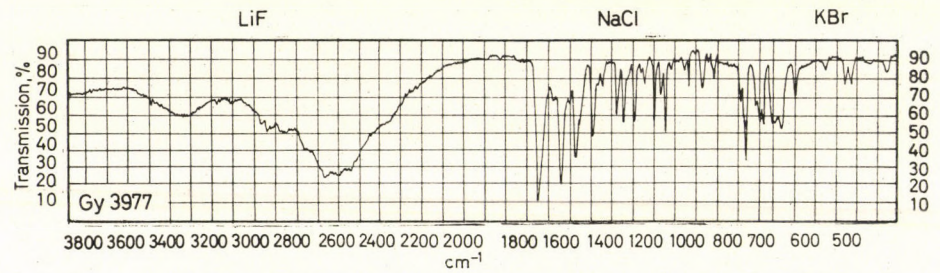

Spectrum 13. 2-Phenyl-3-hydroxy-4(3H)-quinazolinone hydrochloride, in KBr

salt formation the $+T$ effect ceases to operate in consequence of the utilization of the lone electron pair of the nitrogen atom; thus limiting structure **XVIII** becomes preponderant.)

As mentioned above, the $\nu C{=}N$ bands are shifted towards lower wave numbers in the spectra of the salts. Starting with structure **XIII** of the bases, this can be satisfactorily explained. Owing to the inner ionic structure, the increase of the CN bond order and the consequent increase of the $\nu C{=}N$ frequency occurs already in the bases, and this is enhanced by the electron repulsion of the $N{-}O^-$ ion group at position 3. In the course of salt formation, when the base had structure **XII**, the proton will be captured by the oxygen at position 3 and structure **XX** will be formed. The electron affinity of the hydroxyl group at position 3 affects the carbonyl group causing an increase

in the CO bond order and simultaneously in the $\nu C{=}O$ frequency; on the other hand, it renders limiting structure **XIX** more probable thereby lowering the CN bond order and thus the wave number of the $\nu C{=}N$ band.

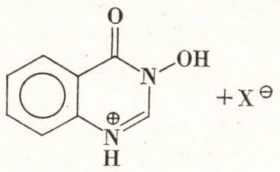

XX

The coalesced νOH and νNH^+ bands emerge between 3200 and 2200 cm^{-1}. The influence produced by the changes in conjugation, due to the presence of the phenyl group at position 2, is well discernible here, too, at least by the different shape of the band (the tendency of the νOH and νNH^+ bands to separate, prevails).

It is interesting to note the extraordinary high ester carbonyl frequency of the 3-acyloxy derivatives (**XIIb**), the like of which has not yet been found in the case of esters. At 1820 cm^{-1} in Spectrum 14, that of the N-acetyl derivative, and at 1790 cm^{-1} in Spectrum 15, that of the N-benzoyl derivative, the bands of cyclic acid anhydrides, acid peroxides, and non-conjugated acid halides, further the carbonyl bands of cyclic tertiary amides emerge [7—11]; However, according to the literature [6, 8—11], in the case of ester carbonyl

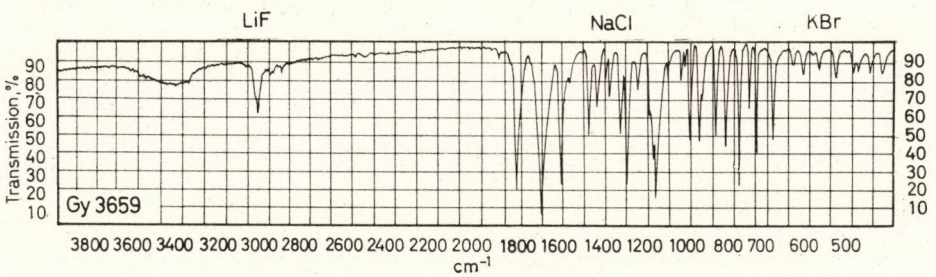

Spectrum 14. 3-Acetoxy-4(3H)-quinazolinone, in KBr

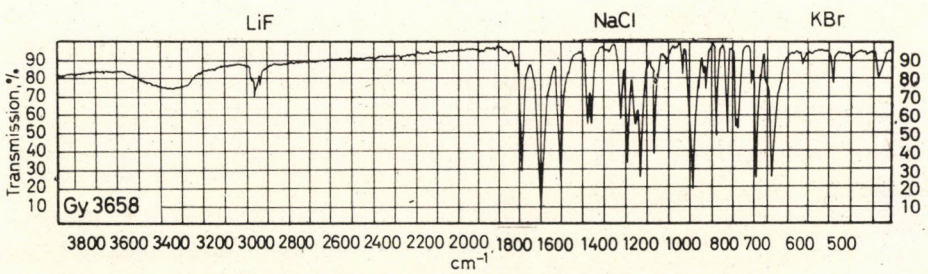

Spectrum 15. 3-Benzoyloxy-4(3H)-quinazolinone, in KBr

1770 cm^{-1} is the upper limit (enol-, phenol-, vinyl-, etc. esters $=C-O-CO-R$) of type. Considering that the $CO-N-O-CO$ group might be regarded as the analogue of an acid peroxide where one of the oxygens has been replaced by anitrogen atom, and since the lesser electron affinity of the nitrogen atom, as compared with that of the oxygen atom, is compensated by the $-I$ effect of the $-C=N$ bond linked to it, and further since the ring structure also increases frequencies, the high frequency of the carbonyl band is quite understandable; of course, the bands of the coupled ester vibrations of the $\nu C-O$ and $\nu C-C$ type [12] do not appear. These bands are replaced by a very intensive band at 1165 cm^{-1} in the acetate, and by very intensive doublet at 990—1000 cm^{-1} in the case of the benzoate, which are due to the various stretching vibrations of the $N-O-C(=O)-C(H_3)$ and $N-O-C(=O)-C_{Ar}$ groups, respectively. The $\nu C=O$ band of the C-4 carbonyl appears at 1700 cm^{-1} ni both spectra, with high intensity. The weak band of $\nu C=N$ at 1670 cm^{-1} si coalesced with the former.

Experimental

The spectra were taken on KBr pellets, with a double-beam UR-10 Zeiss (Jena) infrared spectrometer.

Our thanks are due to Mrs. A. PAP for technical assistance.

SUMMARY

4(3H)-Quinazolinone and its derivatives form cyclic dimeric association structures Conjugation, and with it mesomerism within the amide group are modified as compared to dihydrophthalazone, which is an isomer of 4-quinazolone. The electron displacement, which is general in amides and is directed from the nitrogen towards the oxygen, is repressed in 4(3H)-quinazolinone in consequence of the $-I$ effect of the $-C=N$ bond at position 2. In the case of dihydrophthalazone, the $-I$ effect is compensated by the $+T$ effect of the nitrogen atom of the $-N=C$ group, therefore the mesomerism of the amide group is unperturbed.

The chemical properties of the acyl derivatives are in agreement with the supposed changes in conjugation: the N-acylates of dihydrophthalazone, and 4(3H)-quinazolinone are both obtainable, but the latter are extremely unstable. 3-Hydroxy-4(3H)-quinazolinones have probably an inner salt structure, as it is also shown by the spectra of their hydrochlorides. The extremely high ester carbonyl frequencies (1820, and 1790 cm^{-1}) in the O-acyl derivatives are noteworthy.

REFERENCES

1. SOHÁR, P.: Acta Chim. Acad. Sci. Hung. **40**, 317 (1964).
2. SOHÁR, P.: Magyar Kém. Foly. **71**, 415 (1965). (In Hungarian)
3. SOHÁR, P.: Acta Chim. Acad. Sci. Hung. **54**, 91 (1967).
4. SOHÁR, P.: Infrared Spectroscopic Study of Associations. Post-doctoral Thesis, Budapest, 1964. (In Hungarian)
5. KÓSA, I.: A Study of Quinazolinones. Dr. Techn. Thesis, Budapest, 1968. (In Hungarian)
6. HOLLY, S., SOHÁR, P.: Infrared Spectroscopy. Műszaki Könyvkiadó, Budapest, 1968. (In Hungarian)
7. SOHÁR, P.: Magyar Kém. Foly. **74**, 298 (1968).

8. HOLLY, S., SOHÁR, P.: Practical Infrared Spectroscopy (Láng, L.: Infrared Spectrum Atlas I.) Akadémiai Kiadó (In press).
9. NAKANISHI, K.: Infrared absorption spectroscopy, practical. Holden-Day, San Francisco, 1962.
10. CROSS, A. D.: Introduction to practical infrared spectroscopy. Butterworths, London, 1960.
11. JONES, R. N., SÁNDORFY: C., Infrared and Raman Spectrometry to the Elucidation of Molecular Structure. (Weissberger, A.: Chemical Application of Spectroscopy.) Interscience, New York, 1956.
12. SOHÁR, P., VARSÁNYI, GY.: J. Molecular Structures **1**, 437 (1968).

Pál SOHÁR; Budapest, IV. Szabadságharcosok útja 47/49
Ildikó KÓSA; Budapest, IV. Tó u. 1/5

Acta Chimica Academiae Scientiarum Hungaricae Tomus 57 (4), pp. 425—444 (1968)

NH STRETCHING VIBRATION BANDS AT WAVE NUMBERS LOWER THAN 3000 cm^{-1}, VI*

CYCLIC DIMERIC STRUCTURES, VI. HYDANTOIN DERIVATIVES

P. SOHÁR

(Research Institute for Pharmaceutical Chemistry, Budapest)

Received November 21, 1967

Introduction

The infrared spectra of 5,5-diphenylhydantoin and of its 2- and 4-monothio, and 2,4-dithio derivatives, as well as the spectra of the 1- and 3-monomethyl and 1,3-dimethyl derivatives of the previous compounds have been studied. The possible variants, 16 compounds altogether, were all available. Derivatives that contain methylmercapto groups will be described in another paper [1].

I	a	b	c	d	e	f	g	h	i	j	k	l	m	n	o	p
X	O	O	O	O	S	S	S	S	O	O	O	O	S	S	S	S
Y	O	O	O	O	O	O	O	O	S	S	S	S	S	S	S	S
R_1	H	H	Me	Me	H	H	Me	Me	H	H	Me	Me	H	H	Me	Me
R_2	H	Me	H	Me	H	Me	H	Me	H	Me	H	Me	H	Me	H	Me

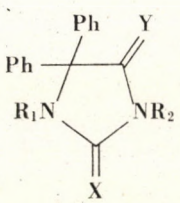

I

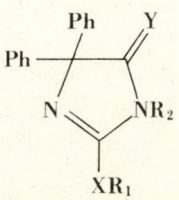

II

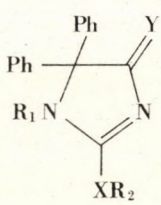

III

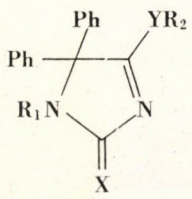

IV

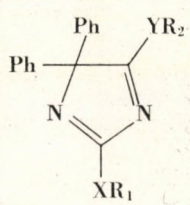

V

* Part V.: Sohár, P., Kósa, I.: Acta Chim. Acad. Sci. Hung. **57**, 411 (1968).

Five tautomers (**I**—**V**) for each of the non-methylated parent compounds **Ia**, **Ie**, **Ii**, and **Im** are possible; of course, the introduction of methyl groups reduces the number of possible tautomers, and the dimethyl derivatives (**Id**, **Ih**, **Il** and **Ip**) allow but the single structure **I**. In compounds where tautomerism is theoretically possible, spectra may furnish the basis for deciding in which tautomeric form or forms a compound is actually present. The problem of tautomerism can be studied on the basis of the amide carbonyl and NH stretching vibration bands.

Spectra of the di-carbonyl compounds

It has been found that, at least under the conditions of obtaining the spectra (in KBr pellets), the amide $\rightleftharpoons$ iminohydrine tautomeric equilibrium is always completely shifted towards the amide form. Therefore, each of the four compounds **Ia**, **Ib**, **Ic**, and **Id** have spectra (Nos 1, 2, 3 and 4, respectively) where a doublet carbonyl stretching vibration (νC=O) band appears in the range between 1800 and 1700 cm^{-1}. Of course, the two maxima cannot be assigned to either of the carbonyl groups at positions 2 or 4, but to the in-phase and out-of-phase (symmetric and antisymmetric) coupled stretching vibrations of the C=O double bond (**VI**, **VII**) [2, 3]. This is suggested by the high frequency value for the maximum that appears at higher wave numbers; and unequivocal evidence for this is furnished by the carbonyl frequency of the mono-thio compounds (see later on). Coupling always occurs [4] when two identical bonds are near enough to each other in a molecule, and the angle made by them is other than 90°. As it is general in the case of cyclic dicarbonyl

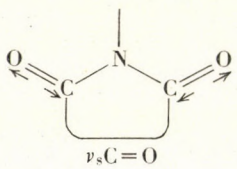

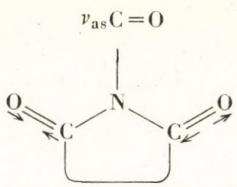

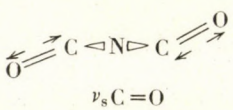

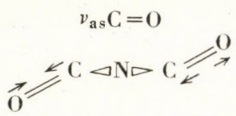

VI **VII** **VIII** **IX**

compounds which do not contain too many members in their ring [5], the band of the coupled symmetric vibration at the lower wave numbers is the more intensive one. This may be explained by the fact that a symmetrical mode of vibration involves a greater change in the dipole moment than its antisymmetric counterpart [2] does. In the case of non-cyclic dicarbonyl

compounds, such as diacylamines, where the carbonyl stretching vibrations are coupled, the change of dipole moment is greater in the more stable *trans* form if the mode of vibration is symmetric (**IX**) than when it is antisymmetric (**VIII**); the situation is, therefore, the opposite, *i.e.* the band appearing at

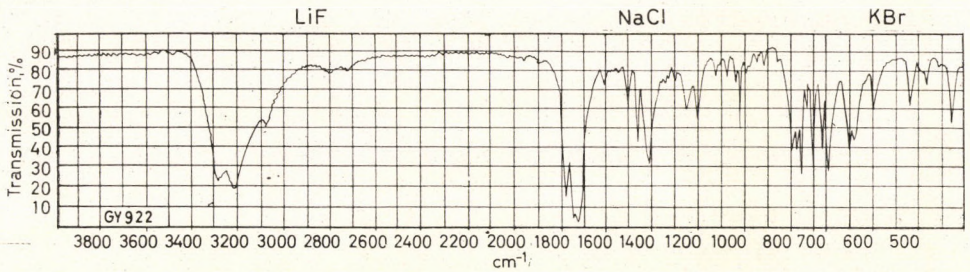

Spectrum 1. 5,5-Diphenylhydantoin, in KBr pellet

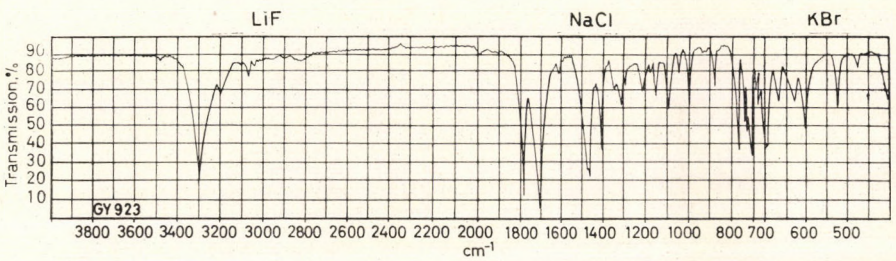

Spectrum 2. 3-Methyl-5,5-diphenylhydantoin, in KBr pellet

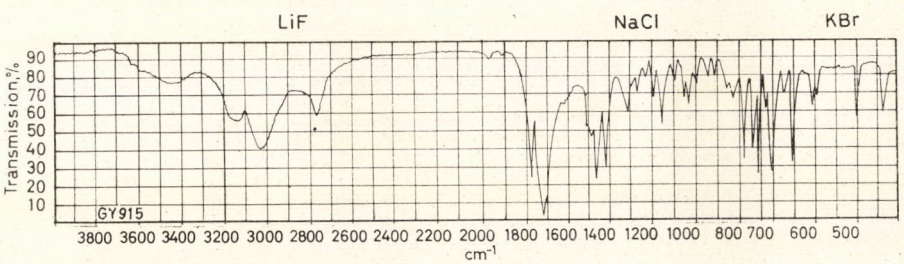

Spectrum 3. 1-Methyl-5,5-diphenylhydantoin, in KBr pellet

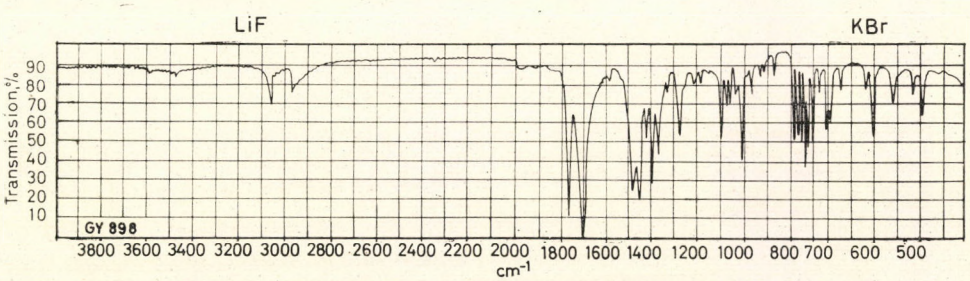

Spectrum 4. 1,3-Dimethyl-5,5-diphenylhydantoin, in KBr pellet

higher wave numbers has greater intensity. In cyclic compounds of not too numerous members in the ring, *trans* arrangement is impossible because of the cyclic structure.

The absolute intensity of the carbonyl bands is further enhanced by the association that makes the C=O double bonds more polar [6] and increases the intensity difference between the two maxima. Both effects are proportional to the strength of the hydrogen bonds [2].

The formation of strong hydrogen bonds can be expected, in the first place, with the more negative carbonyl at position 2 between the two NH groups, and with the more acidic NH group at position 3 between the two carbonyl groups. Thus, much stronger hydrogen bonds can be expected in compounds **Ia** and **Ic** than in **Ib**.

The spectra support these considerations in every respect. The absolute intensity of the carbonyl bands and the relative intensity difference of the two maxima is the smallest in **Id** (Spectrum 4) where no NH group being present, no association occurs. The increase of the intensity and intensity difference observable with compound **Ib** (Spectrum 2) as compared to **Id**, becomes greater in compounds **Ia** and **Ic** (Spectra 1 and 3, respectively; *cf.* also Table I).

The properties of the NH stretching vibration (νNH) bands also support what has been said about the strength of the hydrogen bond. The νNH band, at 3290 cm^{-1} of **Ib** is moderately broad, whereas there is a broad absorption, split in two maxima, in the ranges between 3400 and 3000 cm^{-1}, and 3300 to 2700 cm^{-1}, respectively, in the spectra of **Ia** and **Ic**. In **Ia**, the two bands can be assigned to the two NH groups, the maximum at 3280 cm^{-1} to the more basic one at position 1, and the maximum at 3215 cm^{-1} to that at position 3. In accordance with the presence of two kinds of hydrogen bonds formed with the two NH groups, also the band of the coupled symmetric carbonyl vibration will split in two, and the corresponding maxima are at 1745, and 1725 cm^{-1}, respectively.* Possibly also the splitting of the νNH band in

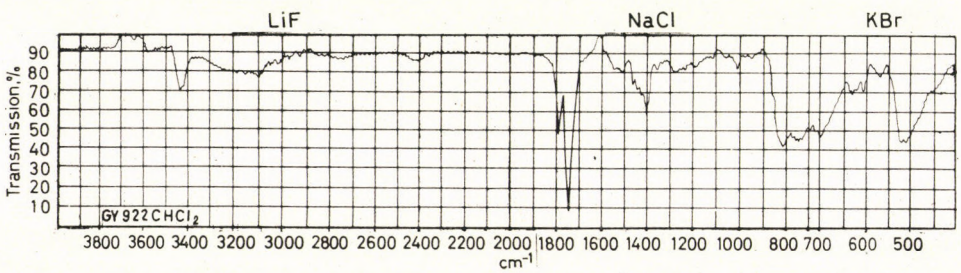

Spectrum 1a. 5,5-Diphenylhydantoin, dissolved in $CHCl_3$

* In the spectra obtained with samples in dilute chloroform solution (Spectrum 1a) no splitting is observed. The band pair of the coupled carbonyl vibrations appear with maxima at 1790 and 1750 cm^{-1}, respectively. The νNH band, equally corresponding to monomeric groups, appears at 3440 cm^{-1}.

Spectrum 3 of **Ic** is in connexion with the formation of the two kinds of hydrogen bonds.

Earlier studies [2, 7—11] have shown that cyclic N-monosubstituted amides (N-unsubstituted lactams) and other similar compounds readily give cyclic dimeric associations. The typical hydrogen bonds of these compounds are characterized by the presence of a specific νNH band in the spectra. The νNH band of the cyclic dimers is rather diffuse, occasionally split into submaxima, and emerges at unusually low wave numbers, generally in the 3200 to 2700 cm^{-1} range.

With unsubstituted hydantoin (and also with the thio derivatives, see later on) such cycles may be formed in three ways (**X**—**XII**), however, structure **XI** is the most probable one.

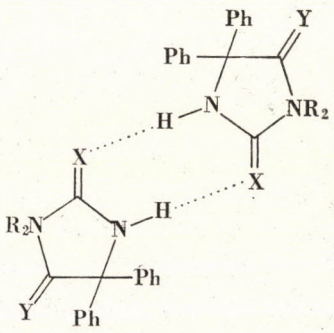

X

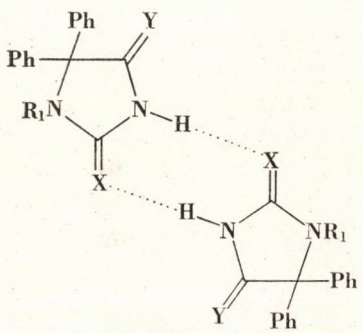

XI

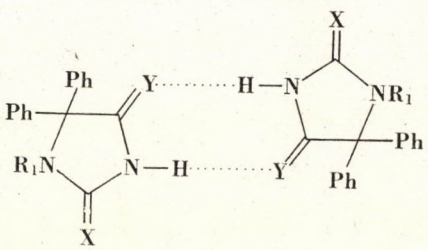

XII

This is so, because, as already mentioned, of the NH groups those at position 3, and of the carbonyls those at position 2, are more susceptible to association on chemical grounds; furthermore, owing to the presence of the bulky 5,5-diphenyl group, the NH groups at position 1 and the carbonyl group at position 4 are under less favourable steric conditions to form hydrogen bonds than are the groups at positions 2 and 3.

Table I

Principal bands in the spectra of 5,5-diphenylhydantoins-thiohydantoins, and their N-methyl derivatives, cm^{-1}

	νNH band		νC=O band		Thioamide bands				
	position 1	position 3	position 2	position 4					
Ia	3820* vs br	3215* vs br	1780* s sh	—	1745 vs br 1725+* vs br	—	—	—	—	—
Ib	3290* vs sh	—	1780+* s sh	—	1710+* vs br	—	—	—	—	—
Ic	—	3140* s br 3030° s br	1775+*° m sh	—	1710+*° vs br	—	—	—	—	—
Id	—	—	1770+□ vs sh	—	1715·□ vs sh	—	—	—	—	—
Ie	3270* s br	3170* s br 3200—2700° w d	—		1755* vs s 1735* vs br	1540 vs br	1270—1230 w br	1170, 1160 vs sh	—	—
If	3270* s br	—	—		1730* vs sh	1520—1495 s br	1290 s sh	1150 s sh	—	—
Ig	—	3300—2900* m br 3100—2700° w d	—		1760□ w sh 1740* vs br	1510—1490 vs br	1300—1280 s br	1145 s sh	—	—
Ih	—	—	—		1740□ vs sh	1405 vs br	1330 vs br	1140 m sh	—	—
Ii	3270* m br	3200—2600° s d	1730° vs br		—	1450 m sh	1260 vs br	—	—	—

Ij	3300*□ m br	—	1765□ vs sh 1740* w sh	—	1450 m sh	1335—1305 vs br	—	—	—
Ik	--	3300—2500° s d	1735° vs br	—	1450 vs br	1300 m sh	—	—	—
Il	—	—	1755□ vs sh	—	1380 s br	1300 m sh	—	—	—
Im	3400 — 2500*° s d		—	—	1550 vs br	1450 — 1435 s br w br coalescence		1230 m br	1150 vs br
In	3300—3100* m br	—	—	—	1525 vs sh	—	—	1325, 1295 vs br	1100, 1090 vs sh
Io	—	3300—2700°* m d	—	—	1520 vs br	1455, 1435 vs br	1400 vs sh	1270 vs sh	1165 vs sh
Ip	—	—	—	—	1510 m br	—	—	1295 vs sh	1110 m sh

vs = very strong; sh = sharp; * = simple intermolecular association;
s = strong; br = broad; ° = cyclic dimeric association;
m = medium; d = diffuse; □ = monomeric (non-associated) group;
w = weak; + = coupled pair of vibrations.

Accordingly, the maximum at about 3150 cm^{-1} in Spectrum 3 is to be assigned to molecules in simple intermolecular association, and that at about 3030 cm^{-1} to molecules in cyclic dimeric association of type **XI**. Most probably, the less intensive band at 2760 cm^{-1} is due to the first overtone of the βNH band at 1450 cm^{-1} in a Fermi resonance with the νNH band, therefore the overtone band is shifted towards lower wave numbers and gains in intensity.

Cyclic dimeric association in compound **Ic** is in connexion with the electron donor effect of the methyl substituent at position 1, which enhances the negative polarization (its tendency to form a hydrogen bond) of the carbonyl at position 2. This is the cause why part of the molecules is in cyclic dimeric association in **Ic**, while in the case of compound **Ia** only simple intermolecular hydrogen bonds are formed.

Spectra of the 2-thio compounds

In the spectra of thioamides, similarly to simple amides, bands of group vibrations appear [10, 12—17]. However, since in a thioamide group, besides the nitrogen atom available for conjugation, a sulphur atom with a free pair of electrons, thus with a similar tendency, is also present, the character of the group vibrations widely differs from molecule to molecule; the smallest change in the structure significantly affects the properties of the spectrum bands [10]. In the case of thiohydantoins the situation is even more complicated, because two nitrogen atoms are linked to the C=S group, not to mention the C=O or C=S substituents at position 4; these latter also participate through their π-electrons in the delocalized electron system which thus involves the entire NC(S)NC(O) or NC(S)NC(S) group. Therefore, no relationship can be expected between the group-vibrations of thiohydantoins and other thioamide or thiourea derivatives, or, in fact, within the group of thiohydantoin derivatives.

In the spectra (Nos 5, 6, 7 and 8) of the 2-thio derivatives there are three bands originating from the group vibration of the NC(S)N moiety. The most intensive band is that in the 1550—1480 cm^{-1} range. There is a band of rather variable intensity between 1350 and 1250 cm^{-1}, and one sharp band of medium intensity in the 1200 to 1100 cm^{-1} range. On the basis of the frequencies and the shifts in various derivatives, these three bands may be assigned to group vibrations whose character is determined mainly by νC=N, νC=S, or νC—N vibrations. It should be added that in the case of thioamides — like in amides — the order of CN bonding will be higher owing to mesomerism (**XIII**↔**XIV**).

However, the limiting structure **XIV** is much more probable here than the analogous structure of simple amides. Therefore, the increase in the CN bond order, and, consequently, the frequency of the stretching vibration of this

bond are significantly higher. (The group vibration band of a similar character in amides, the amide III band, appears at about 1400 cm^{-1}.)

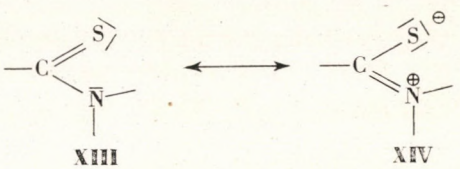

XIII XIV

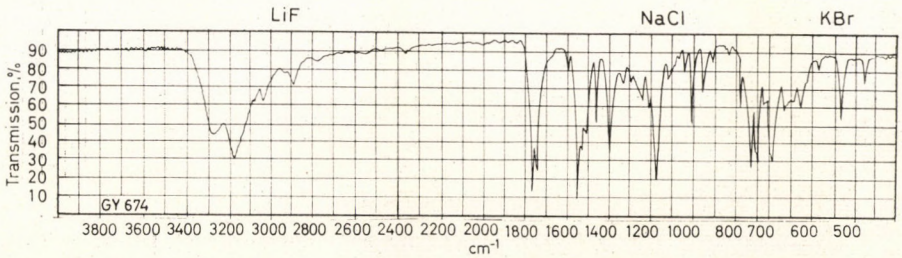

Spectrum 5. 5,5-Diphenyl-2-thiohydantoin, in KBr pellet

In Spectrum 5, that of 5,5-diphenyl-2-thiohydantoin (**Ie**), these three bands emerge at 1540 cm^{-1} (very intensive), between 1270 and 1230 cm^{-1} (weak, diffuse), and with maxima at 1170 and 1160 cm^{-1} (very intensive, sharp doublet). Also the carbonyl band is split (maxima occur at 1755 and 1735 cm^{-1}), and so is the νNH band (diffuse absorption in the 3400 to 2700 cm^{-1} range, with submaxima at 3270, 3170, 3025, 2885 and 2775 cm^{-1}).

All this seems to indicate that two kinds of association structures are present. Tautomerism is out of question, because the high intensity of the νNH band is evidence for the presence of two such groups, further no νSH band is found in the 2600 to 2550 cm^{-1} range [2, 3, 5, 18]. The occurrence of a diffuse νNH band extended towards low wave numbers suggests that a restricted number of the molecules is in cyclic dimeric association and the ring comprises the thiocarbonyl group at position 2, and the NH group at position 3 (type **XI**); at the same time the carbonyl at position 4 is in intermolecular association with the NH group at position 1 (νC=O band at 1775 cm^{-1}, and νNH band at 3270 cm^{-1}). The other, much higher number of molecules form hydrogen bonds of which the participating atoms are the same as before, but instead of ring **XI**, there are only simple intermolecular linkages also between the groups C=S at position 2 and NH at position 3. The corresponding νNH band of the groups at position 3 is shown by a maximum at about 3170 cm^{-1}. Finally, the third part of the molecules (somewhat less than half of the total number) form hydrogen bonds in which the C=O group at 4 and the NH at 3, and the C=S group at 2 and the NH at 1, respectively, take part in establishing the associations. The wave numbers of the NH bands

are roughly the same (more exactly, they coalesce with the bands that correspond to the types of associations mentioned earlier), but the νC=O, and the thioamide bands at about 1260 cm^{-1} are split up (if a strong hydrogen bond is present, the carbonyl frequency is reduced to 1735 cm^{-1}).

These considerations are supported by the spectra (6, 7 and 8) of the N-methyl derivatives. In Spectrum 6, that of the 3-methyl compounds (**If**), the carbonyl frequency at 1730 cm^{-1} and the broad νNH band at 3270 cm^{-1}

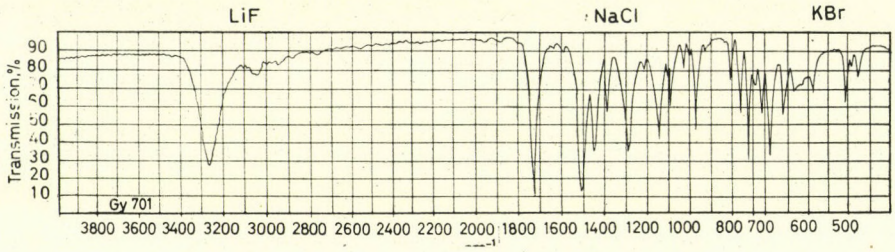

Spectrum 6. 3-Methyl-5,5-diphenyl-2-thiohydantoin in KBr pellet

are evidence for intermolecular association between the C=O group at position 4 and the NH group at position 1.

Two kinds of hydrogen bonds are present in the 1-methyl derivative **Ig**, *viz.* connexions forming cyclic dimers of type **XI**, and bonds between the nitrogen of the NH group at position 3 and the oxygen of the carbonyl group at position 4. The part between 3100 and 2700 cm^{-1} of the diffuse νNH band, and the shoulder at about 1760 cm^{-1} (monomeric groups) of the carbonyl band, respectively, are assigned to the cyclic dimeric association; the part of the higher wave number section (3400 to 2900 cm^{-1}) of the νNH band, and the carbonyl maximum at 1740 cm^{-1} are assigned to the intermolecular hydrogen bond between the groups at positions 3 and 4, in Spectrum 7. The shape of the carbonyl band suggests that hydrogen bonding of the latter type is predominating in the majority of the molecules. These conclusions are supported by the fact that when the substance is recrystallized from some other solvent, say from methanol instead of ethanol and hydrochloric acid, the ratio of the two kinds of associations becomes reversed, and cyclic dimeric associations will preponderate. Accordingly, also the intensity ratio of the two maxima of the νNH and νC=O bands will be inverted (*cf.* Spectrum 7a). Also such samples could be prepared (again through some change in the conditions of crystallization, *viz.* from aqueous hydrochloric acid, followed by very thorough drying), where cyclic dimeric association does not occur at all, and every molecule is equally linked by the NH group at position 3 and the carbonyl at position 4. Of course, in the corresponding spectrum 7b, the band assignable to monomeric carbonyl groups, and the part at wave numbers lower than 2900 cm^{-1} of the νNH band, are absent.

In Spectrum 8 of the 1,3-dimethyl derivative, the carbonyl band is found at 1740 cm^{-1}. The frequency is somewhat lower than in **Ie**, owing to the co-vibrating mass of the methyl substituent at position 3. The same effect can be observed with compound **If**. The thioamide bands appear with all the

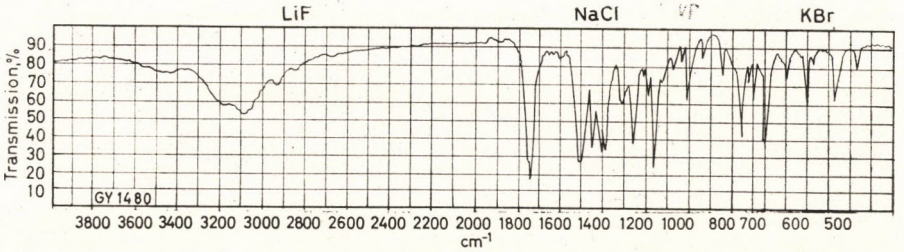

Spectrum 7. 1-Methyl-5,5-diphenyl-2-thiohydantoin, recrystallized from C_2H_5OH + HCl + + H_2O, in KBr pellet

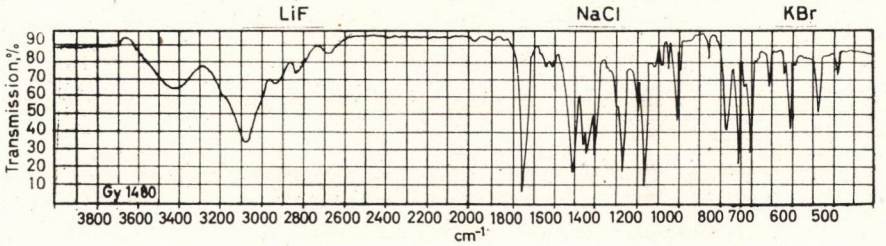

Spectrum 7a. 1-Methyl-5,5-diphenyl-2-thiohydantoin recrystallized from CH_3OH, in KBr pellet

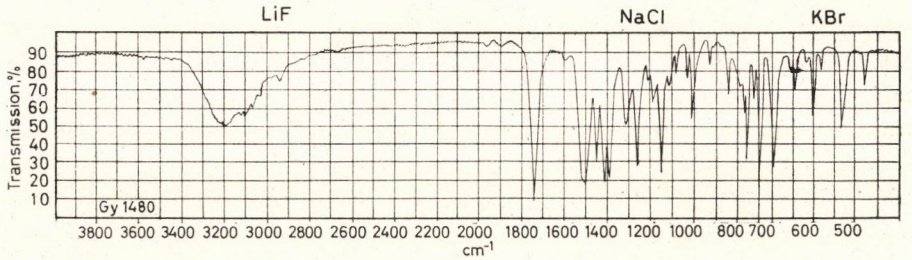

Spectrum 7b. 1-Methyl-5,5-diphenyl-2-thiohydantoin recrystallized from HCl + H_2O and dried for 24 days in vacuum over P_2O_5, in KBr pellet

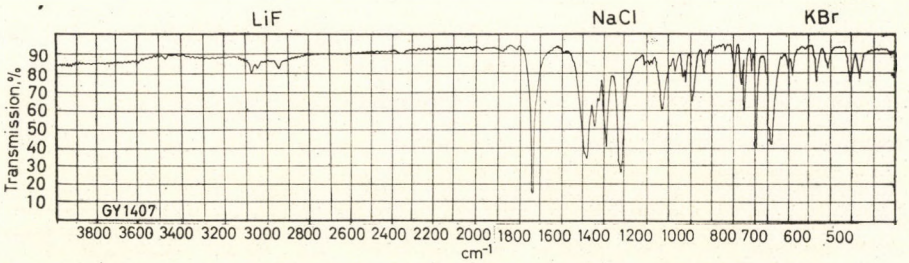

Spectrum 8. 1,3-Dimethyl-5,5-diphenyl-2-thiohydantoin, in KBr pellet

four compounds, and the νC=S band in the middle is intensive and relatively distinct when the group at position 2 is in the monomeric state (compounds **If** and **Ih**). The frequency of the group-vibration of νC—N character is primarily affected by the substitution at position 3, in accordance with the facts that the mesomeric effects which determine the properties of group vibrations play a decisive role primarily within the thioamide group formed by the C=S group at position 2 and the NH group at position 3, and that the NH at position 1 and the carbonyl at position 4 are linked "more loosely" to this system.

The frequency of the νC=O band, that is found between the maxima of the doublet appearing in the spectra of dicarbonyl compounds, shows that the carbonyl vibrations are in fact coupled in the latter compounds [2, 3].

Spectra of the 4-thio compounds

The spectra (Nos 9, 10, 11 and 12) and the association structures of the 4-thio derivatives should show significant deviations from those of 2-thiohydantoins.

This is expected partly because no thiourea group is present in the 4-thio derivatives, therefore, the character of group vibrations will obviously be radically different; further, there is a C=O double bond instead of the thiocarbonyl group at position 2, and this circumstance is favourable for the formation of particularly strong hydrogen bonds. For chemical reasons, as it has been mentioned, the tendency to associate is greater with groups at position 2 than with groups at position 4, and the same may be said about the C=O group when compared to C=S. Thus, in 2-thio compounds, the difference between the carbonyl and thiocarbonyl groups in their tendency to associate is partly equalized owing to their positions, whereas in 4-thio compounds this difference will become greater. Therefore, it can be expected that if the cyclic dimeric association **XI** is indeed a more stable structure than the types **X** and **XII**, this kind of association will be predominant in 4-thio compounds, in contrast with 2-thio compounds where, according to Spectra 5 and 7 of the non-substituted compounds **Ie** and **Ig**, only a small number of molecules will form such hydrogen bonds.

The above considerations are fully supported by the spectra. The three "thioamide bands" characteristic of 2-thio compounds are missing, and other bands appear instead; notably two maxima occur, one between 1450 and 1350, the other between 1350 and 1250 cm^{-1}. In Spectra 9 and 11 of compounds **Ii** and **Ik**, the band of higher wave numbers is of medium intensity and sharpness, the other is very intensive and broad. In the case of compounds **Ij** and **Il** the conditions are reversed: in Spectra 10 and 12, very intensive bands are found between 1450 and 1380 cm^{-1}, and there is a less, but still quite intensive

and sharp maximum at 1300 cm^{-1} in both spectra. These features of the bands — indicating also the character of the vibrations — can be attributed to associations.

The structures of the hydrogen bonds are deducible from the character of the $\nu C{=}O$ and νNH bands. In 1,3-disubstituted compounds (II) no asso-

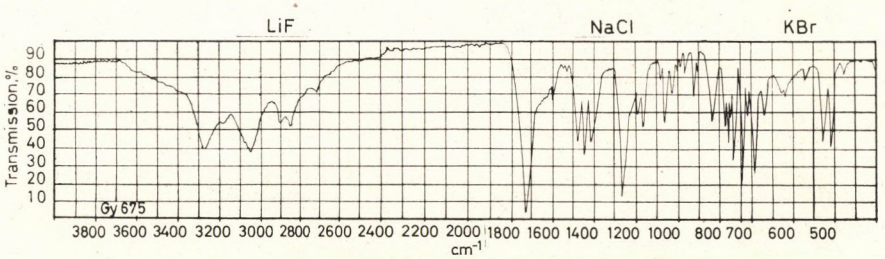

Spectrum 9. 5,5-Diphenyl-4-thiohydantoin, in KBr pellet

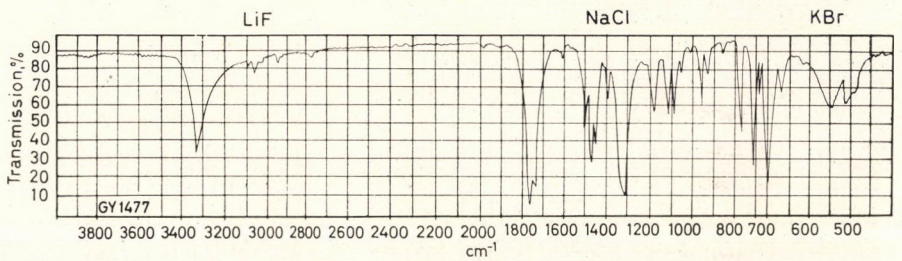

Spectrum 10. 3-Methyl-5,5-diphenyl-4-thiohydantoin, in KBr pellet

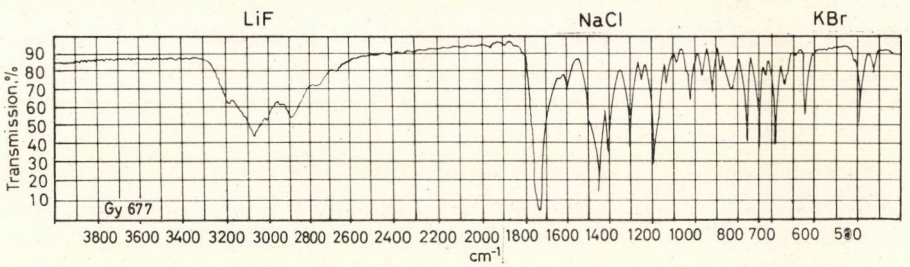

Spectrum 11. 1-Methyl-5,5-diphenyl-4-thiohydantoin, in KBr pellet

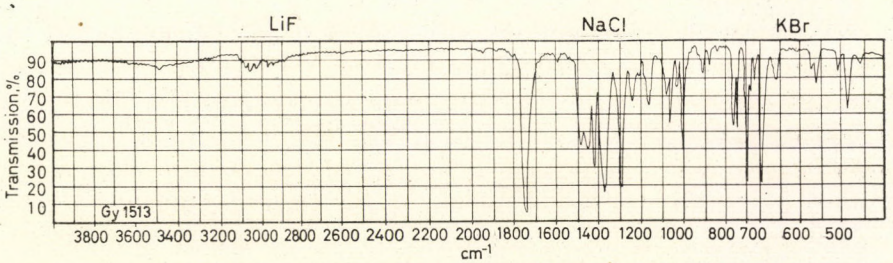

Spectrum 12. 1,3-Dimethyl-5,5-diphenyl-4-thiohydantoin in KBr pellet

ciation is possible, thus the νC=O band is sharp and appears at 1755 cm^{-1} (Spectrum 12). In Spectrum 10 of compound **Ij**, a broad but not diffuse νNH band appears with a maximum at about 3330 cm^{-1}, and its section towards the lower wave numbers is asymmetrically extended. The carbonyl band has a doublet structure: superimposed on the absorption maximum at 1765 cm^{-1} there is a less intensive band at 1730 cm^{-1} (which disappears in spectra recorded on samples dissolved in chloroform; at the same time the νNH band is shifted towards the higher wave number region up to 3450 cm^{-1}, and it becomes sharper; *cf.* Spectrum 10a). All this indicates that the carbonyl group is in

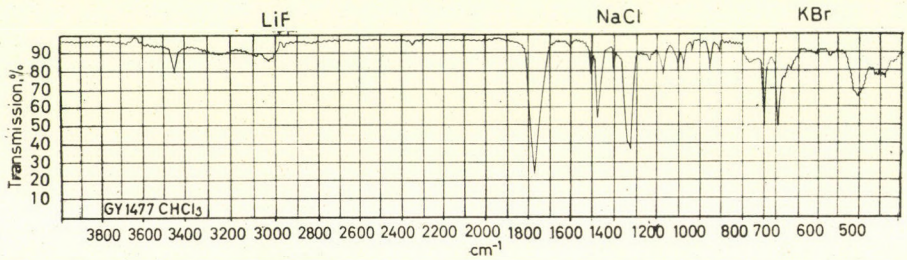

Spectrum 10a. 3-Methyl-5,5-diphenyl-4-thiohydantoin, dissolved in $CHCl_3$

the monomeric state in the great majority of the molecules, and that the NH group at position 1 is associated with the C=S double bond. In some molecules, on the other hand, bonds of the type NH...O=C are formed, and this causes the broadening of the νNH band and the splitting of the νC=O band.

Under the influence of the hydrogen bonds, the **XIII** ↔ **XIV** mesomeric system of thioamides will be altered, and limiting structure **XIV** will become manifest. This gives rise to an increase in the polarity of the bonds. Therefore, if in the spectra of 4-thio compounds such group vibrations absorb whose character is near to the individual bond frequencies, *e.g.*, if a group vibration is present whose properties differ but slightly from the νC=S or νC—N vibrations, it is reasonable to expect that association will increase the intensity of all the bands assignable to thioamide groups. Therefore the frequency of the νC—N type group vibrations will be higher, and the frequencies of vibrations similar to that of νC=S will decrease, owing to the higher probability of structure **XIV**. When Spectra 12 and 10 of compounds **II** and **Ij** are now compared in this respect (no association of any kind is possible in **Ij**), we find some unexpected differences between them. The thioamide band of higher frequency is found at lower wave numbers in Spectrum 10 of compound **Ij** but it is much more intensive, whereas the band of lower wave numbers, though it is more intensive in Spectrum 12 of compound **II**, is not shifted towards lower wave numbers; its frequency even increases a little under the influence of association.

These experimental facts may be interpreted as follows. The two thioamide bands correspond to the asymmetric and symmetric stretching vibrations of the N—C=S group. The ν_{as}N—C=S band is the more intensive when the molecules are in monomeric state; since in the case of a non-polar (symmetric) electron distribution the asymmetric vibration involves greater fluctuations of charge, *i.e.* a greater change of the dipole moment. In associated molecules, where the bond system has become more polar, it is the band of the symmetric vibration that is more intensive. As it is known, the band intensity increases with the second power of the change in dipole moment [6].

Concerning the properties of the thioamide bands, similarity exists between **Ik** and **Il**, and between **Ii** and **Ij**, respectively; thus it is clear that the thioamide group is associated in the case of **Ii**, whereas it is in the monomeric state in **Ik**.

In Spectrum 11 of compound **Ik**, the diffuse band split by sub-maxima, and the one in the 3300—2500 cm^{-1} region (low wave number νNH band), further the relatively low-frequency, very intensive and broad carbonyl band at 1735 cm^{-1}, indicate the formation of dimeric association rings with the participation of the C=O groups at position 2 and that of the NH groups at position 3 (association ring of type **XI**). The uniform association structure is in accord with our earlier statement, deduced from characteristics of the thioamide bands, which said that the thioamide group is in the monomeric state. On the other hand, the cyclic dimeric association of type **XI** that evolves uniformly and according to expectation, is evidence in support of our former assumption concerning the relative stabilities of structures **X**, **XI** and **XII**.

The presence of the low wave number section of the νNH band, and the considerable intensity, low frequency, and broadening of the νC=O band in Spectrum 9 of compound **Ii**, are unequivocal indications of the presence of **XI** type dimers in all the molecules also of this compound. The characteristics of the thioamide bands, together with the broad νNH band (assignable to the NH group at position 1) which has a maximum at 3270 cm^{-1} pointing again to association, indicate that at the same time intermolecular hydrogen bonds are also formed by the NH groups at position 1 and the C=S groups at position 4.

Spectra of the 2,4-dithio compounds

When spectra 13, 14, 15 and 16 of the dithio compounds are compared with the spectra either of 2-thio derivatives or of 4-thio derivatives, a radically different structure of the thioamide band system is again observed. The stretching vibrations of the C=S double bonds at positions 2 or 4 can become coupled (similarly to the carbonyl vibrations in hydrations), but also independently of this and owing to the more pronounced tendency of sulphur atoms

for tautomerism, it is probable that group vibrations extend over the entire N(H)C(S)N(H)C(S) bond system. This is the reason why these spectra have bands other than those of mono-thiohydantoins. Obviously, association will again significantly affect the character of the bands (frequencies, intensities, width, etc.). The probability of the formation of cyclic dimers of type **XI** will be less than in the case of 4-thiohydantoins, since the C=S group is less prone to form hydrogen bonds than carbonyl (the 2-substituent carbonyl that participates in the **XI**-type ring in 4-thiohydantoins). On the other hand, compared to 2-thio compounds this probability is higher, since at position 4 the compara-

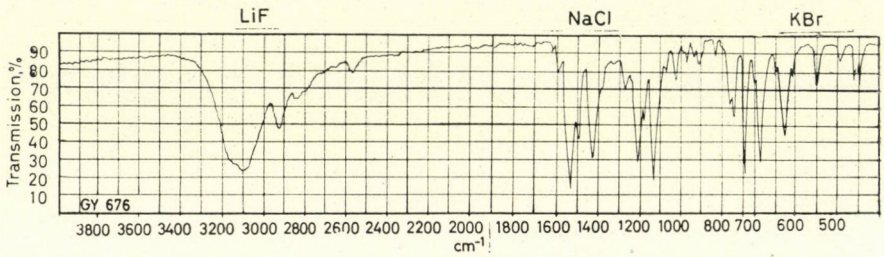

Spectrum 13. 5,5-Diphenyl-2,4-dithiohydantoin, in KBr pellet

tively less electronegative C=S double bond has taken the place of the carbonyl group, and this allows the formation of stronger hydrogen bonds.

In accordance with the foregoing, as an indication of at least partial cyclic dimeric associations, the νNH band is diffuse and extended towards the lower wave numbers down to 2600 cm^{-1} in Spectra 13 and 15 of compounds **Im** and **Io**, respectively. In the case of **Im**, the band of the NH group at position 1 does not become separate, but the intensity is much higher than in Spectrum 15 of compound **Io**, and the maximum is at 3160 cm^{-1} instead of 3080 cm^{-1}, showing that the νNH band of the more basic group at position 1 emerges at higher wave numbers.

Also in the case of the 3-methyl derivative (**In**), the band (Spectrum 14) of the NH group at position 1 is broader in the dithiohydantoin series, in accordance with the formation of stronger hydrogen bonds. This is the consequence of the weaker electronegativity of the thiocarbonyl group.

A combined, or an overtone, band appears in coalescence with the νNH absorptions in the spectra of compounds **Im**, **Io** and **In**, at 2930, 2885 and 3000 cm^{-1}, respectively. Probably these are combinations of vibrations of the frequencies 1530 and 1440 cm^{-1}, or of 1520 and 1400 cm^{-1}, or it corresponds to the overtone of the 1520 cm^{-1} band.

There appears an intensive band at 1550—1500 cm^{-1} in the spectra of all the four dithiohydantoin compounds, which originates from the thioamide group. The weak stretching vibration band at 1500 cm^{-1} of the aromatic

rings is also coalesced in the maximum. The character of the vibration is revealed by the changes of relative intensities in the four spectra. The band is the strongest in Spectrum 13 of compound **Im**, that contains two NH groups; it is the weakest in Spectrum 16 of compound **Ip**, that contains no NH group. Further, it is more intensive in the case of compound **Io** (NH at position 3) than in **In** (where the less polar NH group at position 1 is present which can give rise to relatively weak bands only). All this unequivocally suggests that in-plane deformation (βNH) vibrations of the NH groups are one of the main contributors to the appropriate group vibration. The fact that the band is

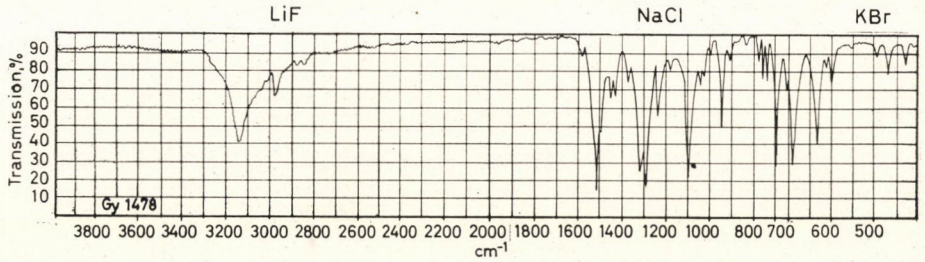

Spectrum 14. 3-Methyl-5,5-diphenyl-2,4-dithiohydantoin, in KBr pellet

comparatively intensive and shifted only slightly (by 20 to 40 cm^{-1}) towards lower wave numbers in the spectrum of **Ip**, containing no NH groups, shows that besides the βNH vibrations, the stretching vibration of the C—N bond (whose order is increased according to the **XIII**—**XIV** mesomerism), or one of the stretching vibrations of the C—N=S group, is also a main component of the group vibration assignable to this band. In spectra of compounds **Im** and **Io**, a rather intensive, broad, and with the latter, a doublet type absorption is found at 1450 cm^{-1}. This band is absent in the spectra of **In** and **Ip**. Thus the band is assignable to the NH group at position 3, and it is due to an individual bond frequency (βNH).

In Spectrum 15 of compound **Io**, further three intensive, sharp bands appear with maxima at 1400, 1270 and 1165 cm^{-1}. These bands are present also in Spectrum 13 of compound **Im**, the first in coalescence with the band at about 1450 cm^{-1}, and the other two at about 1230 and 1150 cm^{-1}, *i.e.* at lower wave numbers than in **Io**. All the three bands are broader than in Spectrum 15 of compound **Io**.

This allows the conclusion that these bands are attributable to the complex vibrations of the NCS group containing the carbon and nitrogen atoms at positions 4 and 3, respectively. In the case of **Im**, the maxima are widened owing to the association established by the participation of the thiocarbonyl group at position 4. In compound **Io**, hydrogen bonds are formed unequivocally

between groups NH at position 3 and C=S at position 2, therefore, the thiocarbonyl group at position 4 is in the monomeric state. The frequency drop in the two lower wave number bands brought about by association, indicates a vibration mode that is near to that of the νC=S bond frequency. With respect to the corresponding group vibration, the increased frequency of the band of the highest wave number is evidence for a νC—N vibration mode (the prevalence of limiting structure **XIV**, which is more probable because of association, involves an increase in the CN bond order).

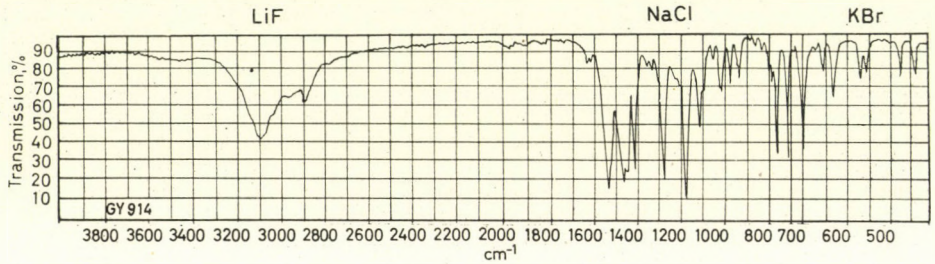

Spectrum 15. 1-Methyl-5,5-diphenyl-2,4-dithiohydantoin, in KBr pellet

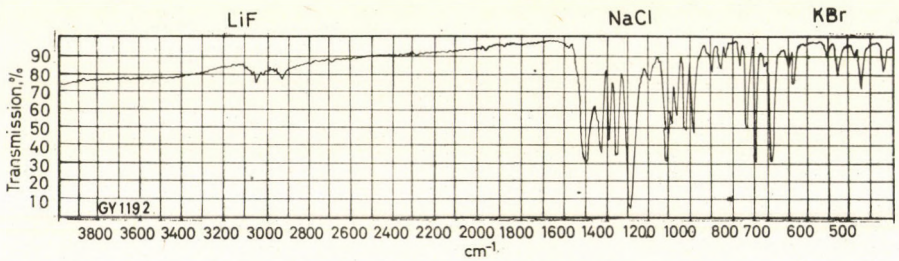

Spectrum 16. 1,3-Dimethyl-5,5-diphenyl-2,4-dithiohydantoin, in KBr pellet

In addition to the band, already discussed, at 1520 cm^{-1} in Spectrum 14 of compound **In**, an intensive doublet with maxima at 1325 and 1295 cm^{-1} is found together with an intensive band at 1100 cm^{-1}, which has a well discernible shoulder at about 1090 cm^{-1}. The presence of these two bands may probably be ascribed to the coupling of the vibrations of the two NCS groups; the four maxima might belong to the in-phase and out-of-phase ν_{as}NCS and ν_{s}NCS vibrations. The frequency value corresponds to a νC=S vibration with a bond order decreased in consequence of mesomerism. However, it is also possible that splitting and the shoulder are due to the simultaneous presence both of associated and monomeric groups. Since only one NH group is present, only one of the two C=S bonds — obviously that at position 2 — can participate in an association.

Spectrum 16 of compound **Ip** has only two maxima of somewhat lower intensity and at a smaller distance apart, at 1295 and at 1100 cm^{-1}. This decreased intensity is especially conspicuous in the band assigned to the symmetric mode of vibration. This fact supports the latter possibility. (Earlier we have pointed out that association in an asymmetric—symmetric vibration pair increases the band intensity mainly of the latter by making the bond system more polar.)

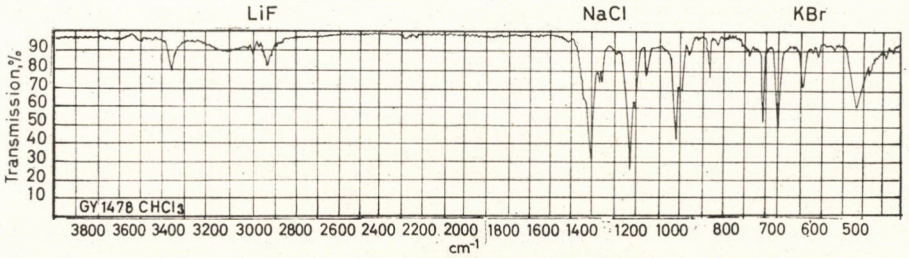

Spectrum 14a. 3-Methyl-5,5-diphenyl-2,4-dithiohydantoin, dissolved in $CHCl_3$

Definitive evidence is furnished by Spectrum 14a of compound **In** dissolved in chloroform. Here only two bands with maxima at 1230 and 1105 cm^{-1} are found: the νNH band appears with a wave number higher by 300 cm^{-1}, at 3440 cm^{-1}.

*

Besides the above-discussed bands of the C=O, C=S, and NH groups, or of greater units composed of these, the bands of the aromatic rings and those of the methyl groups can also be identified in the spectra of hydantoins and thiohydantoins. These are generally weak with the exception of the out-of-plane deformation vibration bands of the aromatic CH bonds and of the aromatic rings at about 750 and 700 cm^{-1}; they appear in the ranges expected. Some further weak bands, due to heterocycles and aromatic rings, or to the deformation vibrations of the groups mentioned, are present but cannot be unequivocally assigned.

Experimental

The spectra (of samples in KBr pellets, or when dissolved to about 0.1 mole per litre, in 0.1 mm NaCl cuvettes) were recorded with a Zeiss UR-10 (Jena) double-beam infrared spectrometer.

The compounds mentioned had been synthesized, according to methods described [19—23],* by Dr. J. NYITRAI and Dr. K. ZAUER, of the Organic Chemistry Department, Technical University, Budapest, under the direction of Professor K. LEMPERT, to all of whom my thanks are due for having made these substances available for study. For technical assistance I thank my collaborators, Mrs. A. PAP, Miss E. HORVÁTH and Miss K. KURUNCZI.

* K. LEMPERT, and K. ZAUER are the first to have synthesized compound **Ik** [24].

SUMMARY

The infrared spectra of 5,5-diphenylhydantoin, and its thio- and N-methyl derivatives have been studied. It has been found that all these compounds are in the di-carbonyl (carbonyl-thio-carbonyl, or dithio-carbonyl) forms; tautomers containing iminohydrin or thio-imino-hydrin groups are not formed. The carbonyl vibrations in the di-carbonyl compounds are coupled, and their characteristics are affected by associations. In the thio derivatives, the thioamide, thiourea, and thioimide groups show specific group-vibration bands with widely varied structures. In the spectrum of the 2-thio compounds three bands, characteristic of the group N(H)C(S)N(H), appear in the 1550—1480, 1350—1250 and 1200—1100 cm^{-1} ranges. In the spectrum of the 4-thio compounds two thioamide bands appear in the 1450—1350 and 1350—1250 cm^{-1} ranges. In the spectrum of 2,4-dithiohydantoins there is one intensive band between 1550 and 1500 cm^{-1}. In the spectra of the two compounds containing the NH group at position 3, there appears an intensive maximum also at about 1450 cm^{-1}. These two compounds give rise to three further bands assignable to the thioamide group, between 1435 and 1400, 1270 and 1230, and 1165 and 1150 cm^{-1}, respectively. In the spectra of the two derivatives containing 3-methyl groups, two bands appear at about 1300 and 1100 cm^{-1}, respectively.

The association pattern is rather variable. In the first place, the carbonyls at position 2 and the NH at position 3 are those which form strong hydrogen bonds. Some of the compounds can form cyclic dimeric association.

This is the exclusive form of association in the two 4-thio-3-non-substituted compounds, whereas only a part of the molecules of the corresponding 2-thio derivatives becomes united by this form of association. A variety of simple intermolecular associations is possible between the other molecules and between the groups at positions 1 and 4.

REFERENCES

1. SOHÁR, P., NYITRAI, J., ZAUER, K., LEMPERT, K.: Acta Chim. Acad. Sci. Hung. (In press)
2. SOHÁR, P.: Infrared Spectroscopic Study of Association Structures. (Post-doctoral Thesis) Budapest, 1964 (in Hungarian).
3. SOHÁR, O., NYITRAI, J., ZAUER, K.: Association and tautomerism in some derivatives of hydantoin. Paper presented at the Conference of the Hungarian Chemical Society, Sopron, 1965 (In Hungarian).
4. VARSÁNYI, GY.: Organic Chemical Spectroscopy. Felsőoktatási Jegyzetellátó, Budapest, 1958 (In Hungarian).
5. NAKANISHI, K.: Infrared absorption spectroscopy, practical. Holden-Day, San Francisco, 1962.
6. HERZBERG, G.: Molecular spectra and molecular structure. Akadémiai Kiadó, Budapest, 1959 (In Hungarian).
7. SOHÁR, P.: Acta Chim. Acad. Sci. Hung. **40,** 317 (1964).
8. SOHÁR, P., FARKAS, L.: Acta Chim. Acad. Sci. Hung. **54,** 79 (1967).
9. SOHÁR, P.: Acta Chim. Acad. Sci. Hung. **54,** 91 (1967).
10. SOHÁR, P., NEMES, A.: Acta Chim. Acad. Sci. Hung. **56,** 25 (1968).
11. SOHÁR, P., KÓSA, I.: Acta Chim. Sci. Acad. Hung. **57,** 411 (1968).
12. JENSEN, K. A., NIELSEN, P. H.: Acta Chem. Scand. **20,** 597 (1966).
13. RAO, C. N. R., VENKATARAGHAVAN, R.: Spectrochim. Acta **18,** 541 (1962).
14. RAO, C. N. R., VENKATARAGHAVAN, R., KASTURI, T. R.: Can. J. Chem. **42,** 36 (1964).
15. SUZUKI, I.: Bull. Chem. Soc. Japan **35,** 1286, 1449 (1962).
16. KAKIMOTO, S., SEYDEL, J., WEPE, E.: Tuberk. Forsch. Borstel, Jahresber. **5,** 233 (1961).
17. YAMAGOUCHI, A., PENLAND, R. B., MIZUSHIMA, S., LANE, T. J., CURRON, C., QVAGLIANO, J. V.: J. Am. Chem. Soc. **80,** 527 (1958).
18. CROSS, A. D.: Introduction to practical infrared spectroscopy. Butterworths, London, 1960.
19. CARRINGTON, H. C., WARING, W. S.: J. Chem. Soc. **1950,** 354.
20. BILTZ, H.: Chem. Ber. **41,** 1379 (1908).
21. LONG, L. M., MILLER, C. A., TRAUTMANN, H. D.: J. Am. Chem. Soc. **70,** 902 (1948).
22. BILTZ, H.: Chem. Ber. **42,** 1792 (1909).
23. HENZE, H. R., SMITH, P. E.: J. Am. Chem. Soc. **65,** 1090 (1943).
24. LEMPERT, K., ZAUER, K.: Acta Chim. Acad. Sci. Hung. **47,** 391 (1966).

Pál SOHÁR; Budapest, IV. Szabadságharcosok útja 47/49

Acta Chimica Academiae Scientiarum Hungaricae Tomus 57 (4), pp. 445—451 (1968)

L'UTILISATION DES OLÉFINES PLUS ÉLEVÉES DE CRAQUAGE DANS L'OXO-SYNTHÈSE*

L. MARKÓ et M. FREUND

(Institut Hongrois du Pétrole et du Gaz Naturel, Budapest et Veszprém)

Reçu le 8 Mars 1968

Du point de vue des matières premières de la pétrochimie nous n'avons attribué jusqu'à présent que peu d'attention aux oléfines d'un poids moléculaire plus élevé, résultant des procédés thermiques de craquage, et ceci pour deux raisons:

1. — Les produits contenant des oléfines obtenus par le craquage thermique sont d'une composition très compliquée et en plus, relativement à la structure de ces oléfines très peu de données ont été publiées jusqu'ici.

2. — Les oléfines de craquage contiennent toujours des composés de soufre qui en maints cas font échec aux procédés catalytiques modernes.

Au cours de travaux exécutés à l'Institut Hongrois du Pétrole et du Gaz Naturel nous avons élaboré une technique modifiée de l'oxo-synthèse qui n'est pas susceptible au contenu de soufre des oléfines employées comme matière première et qui, en plus, offre la possibilité de produire directement des alcools primaires en traitant des oléfines, de l'oxyde de carbone et de l'hydrogène [1, 2]. En premier lieu notre technologie se prête au traitement des oléfines obtenues par le craquage du pétrole, mais peut aussi utiliser d'autres oléfines comme matières premières [3]. Jusqu'à présent nous avons le plus d'expériences avec les oléfines C_7 et les alcools octyliques préparés à partir de ces dernières; c'est pourquoi, dans ce qui suit nous n'allons traiter que des résultats y relatifs.

Poursuivant nos recherches, nous nous sommes occupés en détail de la structure des oléfines des produits de craquage pouvant être prises en considération comme matière première et de celles des alcools primaires préparés a partir de ces dernières. Sur le Tableau N° 1, nous avons présenté la composition d'oléfines C_6 et C_7 de fractions bouillant de 70 à 110 °C, des essences produites par le craquage sélectif thermique de trois différents pétroles bruts. Les différents types d'oléfines ont été déterminés par la spectroscopie infrarouge [4]; les hydrocarbures des oléfines individuelles par la chromatographie combinée à gaz et à liquide.

* Présenté par M. FREUND au 7e Congrès Mondial du Pétrole à Mexico le 5 Avril 1967.

Les données se rapportant aux types d'oléfines et à la composition individuelle des hydrocarbures oléfiniques ne fournissent d'informations que relativement à 40—80 % du contenu d'oléfines de l'essence de craquage. Par conséquent, vu les difficultés analytiques, ces données ne peuvent être considérées comme complètes. Cependant même ainsi elles sont suffisantes pour déterminer que les oléfines — quoique représentant des composés bien compliqués — consistent en premier lieu en oléfines α, et à l'intérieur de celles-ci les oléfines individuelles qui peuvent être démontrées sont surtout le *n*-hexène-1 et le *n*-heptène-1. Mettant en parallèle ce fait avec les données de la littérature [5] se rapportant aux propylènes dimères ou aux propylènes-butilènes oligomères d'un poids moléculaire similaire, il est évident que les oléfines de craquage C_6—C_7 sont généralement d'une chaîne bien moins ramifiée.

D'ailleurs cette différence se manifeste aussi dans la structure des oxo-alcools préparés à partir de ces oléfines. Le Tableau N° 2 contient la proportion de groupe CH_3/CH_2 de quelques oxo-alcools C_8 de notre production et d'un produit mis en circulation par une maison étrangère; elles ont été déterminées à l'aide de la spectroscopie infra-rouge [6]. La proportion CH_3/CH_2 est qualitativement caractéristique de la ramification moyenne du mélange isomérique de l'alcool octylique parce que plus un octanol contient des chaînes latérales,

Tableau I

Composition des oléfines C_6 et C_7 d'une fraction d'essence de craquage

Origine du pétrole brut craqué		Hongrie		Roumanie		Union Soviétique	
Fraction d'essence	Contenu en oléfines %	37		42		37	
	Contenu en soufre %	0,67		0,02		0,18	
Distribution des oléfines selon les types	Doubles liaisons à l'extrémité de la chaîne, % relatif	52		39		36	
	en partie vynile ,,		48		35		31
	en partie vynilidène ,,		4		4		5
	Doubles liaisons intérieures ,,	12		—		19	
	en partie cis ,,		4		—		4
	en partie trans ,,		8		—		15
	Dérivés d'éthylène trisubstitués ,,	16		—		15	
Composition individuelle des oléfines	Oléfines *n*-C_6 et *n*-C_7 ,,	27,8		44,5		19,8	
	en partie oléfines α ,,		26,2		27,7		13,6
	en partie oléfines intér. ,,		1,6		16,8		6,2
	Oléfines *iso*-C_6 et *iso*-C_7 ,,	19,2		20,3		18,5	
	Oléfines C_6 et C_7 à noyaux ,,	2,9		7,4		2,7	

plus cette proportion sera grande. Naturellement cette détermination est aussi valable pour les chaînes d'hydrocarbure en général.

On peut voir que, comparés aux produits préparés à partir d'oléfines oligomères, les oxo-alcools obtenus à partir des oléfines de craquage thermique ont le plus souvent des chaînes moins ramifiées. Par conséquent leur qualité atteint tout au moins celle de ces dernières. Selon nos expériences les alcools C_8 provenant des oléfines de craquage se prêtent aussi bien à la préparation des plastifiants de PVC du type dioctylphtalate que les autres alcools octyliques de type différent ayant été mis en circulation dans ce but. La résistance thermique, la flexibilité, la résistance à la rupture et la résistance électrique des PVC plastifiés par des dioctylphtalates produits à partir de nos alcools atteignent et même en quelque cas surpassent celle des échantillons plastifiés par des dioctylphtalates d'une autre origine. L'utilisation des oléfines de craquage thermique comme matière première de l'oxo-synthèse n'était pas possible par les technologies connues jusqu'ici, étant donné que le soufre contenu dans la matière première entrave l'hydrogénation contact-catalytique des aldéhydes, produits par l'hydroformylation des oléfines [7]. Donc, concernant cette matière première, il s'imposait d'élaborer une technique différente de celle employée jusqu'à présent.

Nous avons déjà plusieurs fois donné un compte rendu du fait que, par la modification des circonstances de réaction de l'hydroformylation de l'oléfine (par l'augmentation de la pression partielle de l'oxyde de carbone et de la température), on peut hydrogéner en alcools les aldéhydes ainsi formés [1, 8, 9]. Ce procédé dénommé par nous «synthèse directe de l'alcool» peut donc réaliser en une seule opération les deux réactions suivantes:

$$R-CH=CH_2 + CO + H_2 \rightarrow R-CH_2-CH_2-CHO$$

$$R-CH_2=CH_2 - CHO + H_2 \rightarrow R-CH_2-CH_2-CH_2OH$$

Tableau 2

Ramification de chaîne des molécules de quelques oxo-alcools

Origine de l'oxo-alcool	Matière première oléfinique	Origine de la matière première	La proportion de groupe CH_3/CH_2 de l'oxo-alcool
Préparé sur base de nos expériences	Fractions d'essence de craquage thermique	Hongrie	0,23
		Roumanie	0,20
	Essence Fischer—Tropsch, *n*-α-oléfines	Allemagne Dém.	0,11
«Alcool isooctylique» de production étrangère	$C_3 + C_4$ oligomères	—	0,41

Ces deux réactions sont catalysées par des carbonyles de cobalt, lesquels exercent leur action sous forme de catalyseurs homogènes dissous dans le mélange de réaction. L'hydrogénation d'aldéhydes selon la deuxième équation de réaction diffère donc fondamentalement et théoriquement des hydrogénations d'aldéhydes usitées jusqu'à présent, par le fait même qu'elle constitue un procédé catalytique homogène et non hétérogène.

On sait que les catalyseurs de l'hydrogénation hétérogène perdent leur activité en présence de différentes contaminations, notamment des inhibiteurs de catalyse. Parmi les inhibiteurs de catalyseurs les composés du soufre sont un des groupes les plus connus, en présence desquels l'hydrogénation en alcool des aldéhydes n'était jusqu'à présent pas possible [7] par un procédé applicable aussi dans la pratique. La littérature contenait des données contradictoires relativement à la façon dont les composés de soufre influencent l'hydrogénation homogène catalytique d'aldéhyde et en même temps l'hydroformylation [9]. Étant donné, cependant, qu'il s'agit ici d'une hydrogénation catalytique fondamentalement différente, il semble donc justifié d'examiner cette question à fond.

Nous avons démontré qu'en fonction de leur structure les composés organiques soufrés empêchent l'hydrogénation catalytique homogène des aldéhydes en présence des catalyseurs de cobalt-carbonyle [11]. L'action inhibitrice de composés soufrés examinés par nous s'accroît selon l'ordre suivant: thioéthers saturés, thiophène $<$ tétrahydrothiophène $<$ allylthioéthers $<$ mercaptans, disulfures, thiophénol $<$ sulfure de carbone.

Les deux premiers membres de la série, donc les thioéthers saturés et le thiophène, sont en pratique sans effet.

L'effet inhibiteur de catalyse des composés organiques soufrés augmente dans un ordre similaire, lors de l'hydroformylation des oléfines [5]. Cela indique que l'action inhibitrice peut être expliquée par les réactions entre les composés soufrés et les carbonyles de cobalt catalysant les deux réactions. Selon nos expériences les composés nocifs de soufre réduisent considérablement la concentration des carbonyles de cobalt dissous dans le mélange de réaction de la synthèse, et indispensables du point de vue de la catalyse. Ils conduisent en même temps vers la formation de résidus solides contenant du soufre et du cobalt. De ce fait nous pouvons conclure, et d'ailleurs cela a été déjà prouvé, que sous les circonstances de réaction de la synthèse les composés nocifs de soufre catalytiquement inactif transforment essentiellement les carbonyles de cobalt en sulfure de cobalt.

Selon nos mesurages 50—90 % des composés soufrés se trouvant dans les oléfines de craquage thermique sont des composés du type thioéther et thiophène, c'est-à-dire que du point de vue de l'hydroformylation de l'oléfine et de l'hydrogénation de l'aldéhyde, ils peuvent être considérés comme étant inertes. Les 10 % à 50 % subsistant sont présents sous forme de merceptans

et de disulfures, l'élimination desquels — particulièrement celle des disulfures — est impossible de résoudre simplement. Afin d'élaborer une technologie appropriée au traitement des oléfines de craquage soufrées, il s'imposait que nous nous occupions en détail des réactions des mercaptans et disulfures avec les carbonyles de cobalt. Afin d'obtenir un meilleur aspect des différentes circonstances, nous avons naturellement étendu nos expériences à d'autres composés de soufre, mais nous ne désirions pas maintenant nous occuper en détail des résultats obtenus.

Nous avons démontré que les dicobalt-octacarbonyles et les mercaptans ou bien les disulfures réagissent déjà à une température ambiante, ce qui cause la formation de différents dérivés de carbonyles de cobalt contenant du soufre [12]. Parmi ces complexes ceux ayant une composition de $Co_3(CO)_9S$ et $Co_3(CO)_6(S)(SR)$ se sont avérés les plus importants, parce qu'on a prouvé que les mercaptans et les disulfures, dans les conditions de l'hydroformylation et de l'hydrogénation des aldéhydes, transforment les carbonyles de cobalt catalytiquement actifs en ces complexes [2]. Ces dérivés du carbonyle de cobalt sulfurés sont d'une part catalytiquement inactifs, ils peuvent donc être considérés comme des catalyseurs inhibés, d'autre part, pendant la formation du sulfure de cobalt, ils se décomposent graduellement, ce qui aboutit à la séparation et à la désactivation finale du cobalt.

En dehors des complexes mentionnés nous sommes à même de produire et d'identifier de nombreux autres dérivés soufrés de carbonyles de cobalt, maix ceux-ci ne sont intéressants que du point de vue de la chimie des complexes [13].

Comme il apparaît de la formule le $Co_3(CO)_9S$ et le $Co_3(CO)_6(S)(SR)$ contiennent un atome de soufre solitaire. Ce qui indique que les carbonyles de cobalt peuvent extraire du soufre des mercaptans et des disulfures. On a pu prouver qu'au cours de ce procédé, le groupe d'alkyls des mercaptans et des disulfures se transforme en premier lieu en hydrocarbures saturés selon la formule de réactions schématique suivante [12]:

$$RSH(RSSR) \xrightarrow{Co_2(CO)_8} RH,\ R-R$$

Sur base de nos connaissances, cette désulfuration se manifeste sous les conditions les plus modérées, en relation avec les méthodes connues jusqu'à présent, c'est-à-dire que les réactions susmentionnées se produisent à une température ambiante, comme nous l'avons d'ailleurs déjà mentionné.

L'effet inhibiteur qui s'exerce donc sur l'hydroformylation des mercaptans et des disulfures et sur l'hydrogénation homogène catalytique des aldéhydes s'explique finalement par le fait que, par les complexes de carbonyles de cobalt soufrés, il transforme les carbonyles de cobalt catalytiquement actifs en sulfide de cobalt. En face de cet état de choses, la question est de savoir pour quelle raison il ne se forme pas de nouveau du $Co_2(CO)_8$ catalytiquement

actif à partir du sulfure de cobalt sous les conditions de la synthèse, similairement que à partir de plusieurs autres composés de cobalt.

Cette question peut être tranchée par de simples calculs thermodynamiques. Il est possible de calculer que la variation de l'enthalpie libre des réactions entre les sulfures de cobalt et les oxydes de carbone est tellement désavantageuse que la concentration nécessaire du carbonyle de cobalt ne peut être garantie qu'à des pressions extrêmement élevées [2]. La formation du sulfure de cobalt doit donc être considérée comme une réaction irréversible dans les circonstances de réaction de l'hydroformylation ou bien de la synthèse directe de l'alcool.

Il s'ensuit que selon nos connaissances présentes la formation du sulfure de cobalt ne peut point être évitée au cours de la transformation des oléfines de craquage contenant des mercaptans et des disulfures. Donc en traitant de pareilles matières premières, il faut toujours compter avec la désactivation partielle du catalyseur. Cependant, nous sommes arrivés à résoudre ce problème du point de vue pratique et technologique, indépendamment de ce fait. La circonstance que l'inhibition des catalyseurs de carbonyle de cobalt n'est au juste qu'une réaction stœchiométrique, nous est venue en aide ici au cours de ce procédé: les mercaptans et les disulfures de cobalt, proportionnellement à leur quantité, se transforment eux-mêmes en hydrocarbures saturés et inertes. Donc les carbonyles de cobalt qui subsistent peuvent ensuite exercer leur action catalytique sans difficulté. Ceci est essentiellement différent des procédés catalytiques hétérogènes, ou déjà la moindre quantité d'inhibiteur peut causer la désactivation complète du lit de catalyseur.

Cette différence virtuelle offre une possibilité pour la solution pratique. En effet si on emploie un catalyseur de cobalt d'une quantité suffisamment grande, on peut traiter des matières premières d'un pourcentage de soufre variable. Une partie du cobalt désulfurise partiellement la matière première, c'est-à-dire que simultanément avec la formation du sulfure de cobalt, il élimine les mercaptans et les disulfures nocifs, tandis que l'autre partie, sous forme de catalyseur, assure l'hydroformylation et la réduction de l'aldéhyde.

Nous avons réussi à réaliser ce principe sous forme d'un procédé continu. La recirculation économique du cobalt est essentielle, étant donné qu'il faut régénérer le sulfure de cobalt ainsi formé. Notre procédé a été réalisé dans une usine pilote d'une capacité annuelle de quelques centaines de tonnes.

RÉSUMÉ

Jusqu'à présent on n'a attribué que peu d'attention aux oléfines plus élevées obtenues par le procédé de craquage thermique comme matière première pour l'oxosynthèse.

Basé sur l'hydrogénation catalytique homogène des aldéhydes, on a réussi à développer un procédé continu pour l'oxo-synthèse directe des alcools. Ce procédé n'est pas susceptible à l'empoisonnement catalytique par des composés sulfuriques, représentant par ce fait un trait caractéristique très important du point de vue de l'utilisation industrielle des oléfines de craquage qu'on peut facilement obtenir à partir du pétrole.

RÉFÉRENCES

1. BERTY, J., OLTAY, E., MARKÓ, L.: Chem. Techn. (Berlin) **9**, 283 (1957).
2. FREUND, M., MARKÓ, L.: Brennst. Chemie **46**, 100 (1965).
3. FREUND, M., MARKÓ, L., LAKY, J.: Acta Chim. Acad. Sci. Hung. **31**, 77 (1962). Riv. Combustibili **16**, 334 (1962); Revue de Chimie **7**, 863 (1962).
4. BÉLAFI, L., BOR, G.: Magyar Ásványolaj és Földgáz Kísérleti Intézet Közleményei **8**, 9 (1967).
5. KARLINSZKY, L., ZÖLLNER, GY., MATOLCSY, G.: Acta Chim. Acad. Sci. Hung. **40**, 445 (1964).
6. BÉLAFI, L., BOR, G.: Magyar Ásványolaj és Földgáz Kísérleti Intézet Közleményei **6**, 27 (1965).
7. WEISSER, O., LANDA, S., PECKA, K.: Chem. Techn. (Berlin) **16**, 463 (1964).
8. BERTY, J., MARKÓ, L.: Acta Chim. Acad. Sci. Hung. **3**, 177 (1953).
9. MARKÓ, L.: Magyar Ásványolaj és Földgáz Kísérleti Intézet Közleményei **2**, 228 (1961).
10. GEMESSMER, A.: D. B. Pat. 881 645 (Chem. Verwertungsgesellschaft Oberhausen (1941); WENDER, I., LEVIN, R., ORCHIN, M.: J. Am. Chem. Soc. **72**, 4375 (1950); WENDER, I., ORCHIN, M.: J. Am. Chem. Soc. **72**, 4842 (1950); MACHE, V.: Chem. Zvesti **15**, 181 (1961); ALDRIDGE, C. L., JONASSEN, N. B.: J. Am. Chem. Soc. **85**, 886 (1963).
11. LAKY, J., SZABÓ, P., MARKÓ, L.: Acta Chim. Acad. Sci. Hung. **46**, 247 (1963).
12. KLUMPP, E., MARKÓ, L., BOR, G.: Chem. Ber. **97**, 926 (1964).
13. MARKÓ, L., BOR, G., KLUMPP, E., MARKÓ, B., ALMÁSY, G.: Chem. Ber. **96**, 955 (1963); MARKÓ, L., BOR, G., KLUMPP, E.: Angew. Chem. **75**, 248 (1963); KHATTAB, S. A., MARKÓ, L., BOR, G., MARKÓ, B.: J. Organometal. Chem. **1**, 373 (1964); KLUMPP, E., BOR, G., MARKÓ, L.: Chem. Ber. **100**, 1451 (1967).

László MARKÓ
Mihály FREUND
Veszprém, Wartha V. u. 4—6.

Acta Chimica Academiae Scientiarum Hungaricae Tomus 57 (4), pp. 453—459 (1968)

BOOK REVIEWS — BUCHBESPRECHUNGEN — РЕЦЕНЗИИ КНИГ

Optical Rotatory Dispersion and Circular Dichroism in Organic Chemistry. Including Applications from Inorganic Chemistry and Biochemistry. (Editor: G. SNATZKE). Proceedings of NATO Summer School held at Bonn, 24 September—1 October 1965. Heydn and Son Ltd. London, 1967, pp. 416.

Physical methods of measurements, developing at a rapid pace, play a role of steadily increasing importance in the solution of structural and stereochemical problems in organic chemistry. In the last decade the methods of optical rotatory dispersion (ORD) and circular dichroism (CD) have found wide-spread application in the research of optically active compounds. Though both phenomena have been known since the years of the last century, they were not put to general use, owing to the lack of adequate instruments. The last decade witnessed essential changes in this field. Several convenient instruments (spectropolarimeter, dichrograph) became commercially available, and, as a consequence of this fact, the number of publications dealing with the investigation and possible applications of optical rotatory dispersion and circular dichroism suddenly increased.

In view of the great interest of organic chemists in the possibilities offered by these methods, a Summer School was organized at Bonn by Prof. G. SNATZKE in the autumn of 1965. The lectures delivered at this School have now been published in book form, as requested by the participants of the School.

Consequently, the present work is not a monograph, but the printed collection of a series of lectures; however, it combines the advantages offered by both types of presentation in a successful way. On the one hand, it was possible to gather at this School the most prominent research workers of the two methods from all over the world. Thus, the reader is acquainted with these methods not through the meditation of only one, however brilliant, researcher but by comparing the opinions of a number of different authors, he may form a relatively objective picture of the field. On the other hand, the structure of the book resembles that of a monograph, as the successive chapters (lectures) are linked to each other to give a didactically homogeneous train of ideas.

The first quarter of the book, which contains altogether 23 chapters (lectures), comprises a general introduction by P. CRABBÉ and C. D. DJERASSI and the lectures of A. MOSCOWITZ and S. F. MASON dealing with the theory of the Cotton effect. These are followed by a critical survey, by F. WOLDBYE, of the types of instruments available for the time being, and of the principles of their operation. This chapter is of particular practical value for research workers.

In the other parts of the work, the scope of the application of optical rotatory dispersion and circular dichroism are presented. This part is classified according to the most important chromophore functional groups, starting with the carbonyl compounds, which have been investigated most thoroughly (W. KLYNE), through conjugated systems (K. MISLOW), to a discussion of the chromophore derivatives of "transparent" compounds (B. SJÖBERG). Several chapters are devoted to the effects which can be attained in optical rotatory dispersion and in circular dichroism by variations of the medium (A. RASSAT, A. MOSCOWITZ) and the temperature (G. SNATZKE), and possibilities of utilizing these effects are pointed out. The general discussions are complemented by chapters summarizing experiences obtained in the determination of the steric structures (secondary structure) of particular groups of compounds, such as inorganic complexes (F. WOLDBYE, S. F. MASON), polypeptides and proteins (E. R. BLOUT), and high polymers (P. PINO).

The organic chemist who is getting acquainted with this field finds useful help in some lectures which compare the scope of applications of ORD and CD with each other, and with other, better known, physical methods (NMR).

The examples discussed in the lectures, corresponding to the fields which have been most thoroughly investigated so far, relate mainly to steroids and terpenes. This, however, does not prevent generalization of the regularities, or their applicability to other groups of compounds.

Though some of the material contained in the book has been available in other monographs, the present collection offers the marked advantage that it contains more than final and finished research results and finally established opinions. The lectures truly reflect the current problems of methods which have passed the initial stage and are in the process of dynamic development. In addition to examples illustrating routine use, a number of other fields of possible applications are also discussed, where only the first steps have been made so far; attention is called to some challenging problems awaiting solution, such as those in the field of the magnetic measurement of optical activity (MORD and MCD).

Consequently, this interesting series of lectures presents useful information on a high level to all readers interested in broadening the scope of application of the two methods, and to those who desire to learn and use methods of optical rotatory dispersion and circular dichroism as routine procedures in the elucidation of the fine structure of optically active organic molecules.

I. PINTÉR

G. H. NANCOLLAS: Interaction in Electrolytic Solutions. Elsevier, Amsterdam, 1966, X + pp. 214

The title of this interesting book is a bit misleading because from among the vast number of different types of interactions in electrolytic solutions only the problems of ion-pair formation are treated thoroughly, and some important types of complexes are not mentioned at all.

The book consists of six Chapters and an Appendix containing seven Tables. The Introduction clearly summarizes the basic information on the structure of water and on the ionic theories. The following two Chapters deal with the experimental methods and calculation procedures for the determination of equilibrium constants. Although the treatment is very lucid it is unlikely that a novice will be able to make use of the methods without consulting other books or the original research papers.

The most valuable parts of the book are Chapters 4 and 5 in which the relationships involving the equilibrium constants and the thermodynamic properties of complexes are clearly traeted. In the recent developments in these fields the author himself played a prominent role.

The concluding Chapter treats some mechanistic aspects of complex formation; however this part is too short to give an adequate account on this extremely important area.

Each Chapter is followed by a well chosen list of important references. In the Appendix reliable thermodynamic functions for a number of complex systems are tabulated.

The typography of this readable book is excellent. The book is a valuable contribution to the literature of solution chemistry and particularly recommended to advanced students interested in this field.

M. T. BECK

Elementbildung und Korrosion, Band 19. Verlag Chemie, GMBH, Weinheim/Bergstr. 1967. 171 S., 216 Abb. und 30 Tab.

Die 19. Korrosions-Veröffentlichung des Verlags Chemie, mit den einzelnen Vorlesungen der in Frankfurt am Main am 28. und 29. Oktober 1965 gehaltenen Vortragsserie, ist erschienen. Die Vortragsserie behandelt die Entstehungsmöglichkeiten der Korrosionselemente. Im ersten Artikel gibt H. KAESCHE einen Überblick über die Rolle der Korrosionselemente in den elektrochemischen Korrosionsvorgängen. Zwei Vorlesungen befassen sich mit der Rolle der Grundmetalle und ihrer Metallüberzüge. E. RAUB zeigt, wie die in diesen Fällen auftretende Korrosion durch den Sauerstoffgehalt des Elektrolyts beeinflußt bzw. wie über den Sauerstoffgehalt des Elektrolyts der Verlauf der Korrosion kontrolliert werden kann. E. EBERIUS studierte das System Fe(Zn)Minium in Abhängigkeit vom pH-Wert, unter Berücksichtigung des aus dem Minimum gebildeten Bleis. Er weist darauf hin, daß im Falle von Zinküberzügen kein Minium verwendet werden darf.

Strukturelle Heterogenitäten spielen bei der Entstehung von Korrosionselementen eine wichtige Rolle. So konnten z. B. HOFMANN und Mitarbeiter feststellen, daß die Korrosionsbeständigkeit in Schwefelsäure durch den Kupfergehalt von Blei gesteigert wird, während

Nickel auf die interkristalline Korrosion entschieden fördernd wirkt. Hartblei hat vorteilhafte Eigenschaften, reines Blei weniger. Interessant ist die Feststellung, daß die in Schwefelsäure ausgebildete Schutzschicht des Bleis in Ermüdungsversuchen allmählich zugrunde ging. H. E. BÜHLER untersuchte die Cr-Ni-Stähle vom Gesichtspunkt der Stofftextur-Heterogenität, während A. BÄUMEL die beim Schweißen von Stahl auftretenden selektiven Korrosionsvorgänge studierte. Er fand, daß an unlegiertem Stahl zwischen der nicht vollständig entzunderten Platte und der Schweißfläche ein Korrosionselement gebildet wird. Die Schweißnaht korrodierte. Eine Korrosion konnte jedoch auch zwischen entzunderter Platte und Schweißstelle beobachtet werden. Bei Mn-Cr-Stählen scheidet sich in einer bestimmten Entfernung von der Naht Chromcarbid aus, bzw. in Meerwasser tritt eine interkristalline Korrosion auf. Interkristalline Korrosion kann auch an den Schweißstellen des mit Al gemilderten Stahls beobachtet werden. Er befaßt sich auch mit der Frage, wie die Ausscheidung von Chromcarbid vermieden werden kann, und welchen Einfluß das Delta-Ferrit auf das Korrosionsverhalten von austenitischen geschweißten Werkstücken ausübt.

E. FOT studierte die Graphitisation von Gußeisen im Falle von verschiedenen Gußeisensorten und verschiedenen Angriffsmedien. H. LÜDIGER zeigt die Rolle der verschiedenen Strukturbildner und der Mischkristalle beim elektrochemischen Ätzen.

Die Arbeit von W. R. FISCHER befaßt sich mit dem Schutz mittels Lokalkathoden. Wenn Metalle, die passiviert werden können, mit Lokalkathoden in Berührung kommen, erhalten sie einen anodischen Schutz, falls die kritische passivierende Stromdichte durch den Kathodenvorgang erzeugt wird. Platinmetalle sind besonders gute Lokalkathoden sowie auch Kohle und Halbleiter-Oxyde. Von diesen genügt bereits eine geringe Menge. Die kathodisch wirkenden Komponenten können in das Metall legiert oder auch mit diesem von außen her in Berührung gebracht werden.

Die durch das Metall und die darauf befindliche Schutzschicht gebildeten Korrosionselemente werden im Rahmen einer separaten Gruppe behandelt.

G. HERBSLEB studierte beim Eisen und bei den Cr-Ni-Stählen die Möglichkeiten der an mit einer Passivischicht überzogenen Metallen auftretenden Lochkorrosion. L. GRAF beobachtete bei homogenen Mischkristallen eine Elementbildung. Er stellte fest, daß ein Element gebildet werden kann, wenn das Legierungsmetall edler als das Grundmetall ist und nicht gelöst oder in gewissen Fällen auf die Mischkristalle wieder ausgeschieden wird. Ferner können Korrosionselemente entstehen, wenn die gebildeten Korrosionsprodukte edler sind als das Mischkristall. Die mit Korrosionsprodukten bedeckten Oberflächen sind kathodisch und können auch zu Spannungskorrosion führen.

H. GRAFEN untersuchte den Einfluß der Deckschicht auf die durch Spannungskorrosion entstandenen Risse und stellte fest, daß solche Risse vor allem dort auftreten, wo die Deckschicht fehlerhaft ist.

Zwei Artikel beschäftigen sich mit den Konzentrationselementen. H. RICKERT studierte mit galvanostatischer Methode Blei- bzw. Zinkelektroden in Chromat- und Phosphatlösungen. Er fand aktive und passive Zonen und beobachtete bei den aktiven Zonen eine Auflösung des Metalls (es trat Lochkorrosion auf). Die praktischen Erfahrungen über das gleichzeitige Auftreten von aktiven und passiven Zonen stehen mit der Theorie in Einklang. Bei der Lösung ist die Stromdichte an den aktiven Stellen der Konzentration der die Deckschicht bildenden Amine in der Lösung proportional und der Dicke der Nernstschen Diffusionsschicht umgekehrt proportional. Bei ständiger Berührung ist die Oberfläche der aktiven Zone dem angelegten Anodenstrom proportional, wobei das Elektrodenpotential einen von der Stromstärke unabhängigen Wert besitzt.

Interessant sind die Versuche von G. HEIM. Dieser Autor arbeitete zur Untersuchung der im Boden sich bildenden Makroelemente eine Laboratoriumsmethode aus. Die in der Schlacke/Sand Grenzfläche der experimentellen Rohrleitung gemessenen Stromstärken waren in der Größenordnung von 500 μA. Außer den elektrochemischen Gesetzmäßigkeiten müssen dabei auch die geometrischen Bedingungen beachtet werden.

Schließlich befassen sich einige Arbeiten mit der Bildung von Konzentrationselementen in der Praxis.

W. G. VON BAECKMANN untersuchte die entlang der Rohrleitungen sich bildenden Makro-Korrosionselemente und beschrieb zahlreiche praktische Fälle.

O. VON FRANQUÉ beobachtete die Möglichkeit einer Lochkorrosion von Kupfer im Trinkwasser. Er studierte die Wirkung der durch verschiedene Oberflächenbehandlungen des Kupfers entstehenden Schutzschichten auf die Potentiale. C. DROTSCHMANN stellte fest, daß die in NH_4Cl auftretende Korrosion des Zinks bei Leclanché-Elementen ein sehr wichtiger Vorgang ist, wobei man eine gewisse Inhibitorwirkung beobachten kann. In $MgCl_2$-Lösungen können Deckschichten ausgebildet werden, die eine Schutzwirkung besitzen. Die Korrosion wird auch durch Proteine inhibitiert. Ferner muß auch die Reinheit des Zinks beachtet werden. H. DETER-

MAN untersuchte den Einfluß von großen Belüftungszellen bei Schiffen in Meerwasser, und verglich diese Korrosion mit der korrosionverursachenden Wirkung des auf der Stahloberfläche zurückgebliebenen Zunders.

Die Zusammenstellung liefert für Fachleute, die sich mit theoretischen oder praktischen Korrosionsproblemen beschäftigen, sehr nützliche Daten.

GY. BÁCSKAI

G. TÖLG: *Chemische Elementaranalyse mit kleinsten Proben.* Verlag Chemie GMBH. Weinheim/Bergstr., 1968. 227 S., 66 Abb. und 5 Tab.

Der Ausdruck »mit kleinsten Proben« im Titel des Buches von G. TÖLG bedeutet Stoffmengen von weniger als 100 Mikrogramm (10^{-4} g), wie sie in der sog. Ultramikroanalyse zu quantitativen Bestimmungen verwendet werden.

Nachdem F. PREGL und seine Schüler in den ersten dreißig Jahren des Jahrhunderts die Mikromethoden der Elementaranalyse und der Bestimmung von funktionellen Gruppen unter Verwendung von Stoffmengen von 1—10 mg ausgearbeitet hatten, mußten diese Verfahren schon bald verfeinert werden, und zwar nicht nur in bezug auf Genauigkeit, sondern auch hinsichtlich ihrer Empfindlichkeit, da in der Forschung organischer Naturstoffe und wegen der rapiden Entwicklung der molekularen Biologie dies zu einer dringenden Forderung wurde. Zur Lösung einiger Aufgaben im Ultramikro-Maßstab (so z. B. zur Bestimmung des Stickstoffgehaltes organischer Verbindungen) waren auch früher schon geeignete Methoden bekannt, die den Anforderungen der Ultramikroanalyse Rechnung tragende systematische Revision der Verfahren der Elementaranalyse wurde jedoch erst vor etwa 10 Jahren von R. BELCHER und seinen Mitarbeitern begonnen. Auch G. TÖLG beruft sich im Vorwort seines Buches auf diesen Autor. TÖLG schreibt, daß R. BELCHER seine eigenen Methoden in seinem 1966 erschienenen Buch zwar bereits beschrieben hat, trotzdem hielt er es für notwendig, diese besonderen Methoden, ergänzt mit seinen eigenen, in Form einer Monographie zusammenzufassen.

Das Vorwort des Buches beschreibt die an diese Spezialverfahren gestellten Anforderungen und die Leistungsfähigkeit der bisher ausgearbeiteten Methoden. Tabellen geben an, welche Stoffmengen zur Bestimmung der einzelnen Elementarbestandteile organischer Verbindungen notwendig sind, nach welchem Prinzip gearbeitet wird, und wie groß der Fehler der einzelnen Methoden ist. Die Tabellen enthalten ferner die Literaturquellen, wo die Methoden beschrieben sind.

Der Erste Abschnitt des Buches behandelt die Fragen der Einwaage und der Behandlung der Stoffe. Die analytischen Ultramikro-Waagen ermöglichen zwar die Wägung mit einer absoluten Genauigkeit von weniger als 10 Nanogramm (10^{-8} g), doch ist die Belastbarkeit dieser Waagen sehr klein (nur etwa 1 mg), und sie sind auf äußere Einwirkungen (Erschütterungen, Staub, Temperaturschwankungen) sehr empfindlich. Für die Praxis werden jedoch auch solche Ultramikro-Waagen gebaut, mit denen 200—400 mg der Substanz bei einer absoluten Genauigkeit von 10—50 Nanogramm gewogen werden können. Dieser Abschnitt ist auch vom Gesichtspunkt der Praxis von Bedeutung, da die Leser mit der Aufstellung und Behandlung der Ultramikro-Waagen vertraut gemacht werden, und jene speziellen und sinnreichen Methoden kennenlernen, mit welchen bei der Ultramikroanalyse die Stoffe gelöst, die Flüssigkeiten gemessen, verdünnt und titriert oder verdünnte Lösungen konzentriert werden. Die Methoden der Verbrennung von organischen Substanzen ist in der Ultramikroanalyse von besonderer Bedeutung. Die gute Zusammenstellung dieses Abschnitteiles zeugt von der genauen Kenntnis der Literatur und von den praktischen Erfahrungen des Verfassers.

Etwa 4/5 des Umfanges des Buches stellt der ausführliche Methodische Teil dar, in dem die zur quantitativen Bestimmung der in den organischen Verbindungen vorliegenden Elementarbestandteile geeigneten Methoden der Reihe nach so eingehend beschrieben werden, daß die Bestimmungen auf Grund dieser Beschreibungen vorgenommen werden können.

Das Buch ist nicht nur für jene eine nützliche Lektüre, die daraus die Ultramikroanalyse kennenlernen wollen, sondern auch für die, die sich auf diesem Spezialgebiet der organisch-chemischen Analyse betätigen; erfahrene Analytiker werden daraus viel wertvolles Wissensmaterial schöpfen können.

L. MÁZOR

I. GYARMATI: *Non-equilibrium thermodynamics* (in Hungarian). Műszaki Kiadó, Budapest, 1967. pp. 160.

The book deals with the fundamental principles and basic equations of non-equilibrium (irreversible) thermodynamics on the basis of the general theory of classical continua.

Since this task now belongs to the actual and unsolved problems of physics, in GYARMATI's book a contribution is given to the treatment of certain fundamental problems, in addition to a summary of known results. This, however, can only be done if the field-theoretical basis of thermodynamics is developed keeping in mind the requirements of classical field theory. Therefore, in Chapter I the fundamentals of classical field theory are outlined.

Chapter II deals with the total system of balance equations of the classical field theory, paying particular attention to the derivation of balance equations of multicomponent superposed media.

Chapter III treats the general development of ONSAGER's non-equilibrium thermodynamics. After the local formulation of the first and second laws, the entropy balance equations are determined. These are followed by the total development and analysis of the system of ONSAGER's linear laws and reciprocal relations.

In Chapter IV the properties of non-equilibrium potential functions (dissipation functions) are discussed, and the variational principle equivalent to the ONSAGER theory (the principle of the least dissipation of energy) is formulated for continua in a general form. The alternative forms of the variational principle recognized recently by the author are given, which proved to be very productive from both the theoretical and practical points of view.

In Chapter V the principle of minimum entropy production is treated and the relation of this principle to ONSAGER's principle is clarified. It is shown that the principle of minimum entropy production is only an alternative formulation of ONSAGER's principle valid for stationary states. With the aid of the variational principle valid for stationary cases, the general theory of stationary states is discussed, and the classification of stationary systems is given. The general conditions of stationarity for the case of heat conduction, multicomponent diffusion, chemical reactions, etc., are determined, and the stability of such cases is examined.

In Chapter VI the FOURIER equation of heat conduction, the total set of equations of multicomponent isothermal diffusion, and the NAVIER—STOKES equation of viscous flow are derived from the new representation of the principle of least dissipation of energy recognized by the author. It is proved by this derivation of the specified equations that the new representation is more productive than ONSAGER's original one, furthermore, it makes possible the formulation of the new integral principle of thermodynamics. After the general formulation of the new integral principle of thermodynamics, it is shown that the EULER—LAGRANGE equations are equivalent to the total system of the transport equations. As the direct application of the integral principle transport equations describing different non-isotherm and cross effects are also dealt with. Finally, the relations between the thermodynamical integral principle and the field-theoretical representant of the HAMILTON principle are given, and attention is called to several similarities and essential differences. It is proved by the derivation of the practically important transport equations that the true variational principle of thermodynamics is represented by the new integral principle.

In the Appendix a brief summary of the used mathematical apparatus is to be found.

E. BERECZ

Neuere Methoden der präparativen organischen Chemie, Band V. Herausgegeben von Wilhelm FOERST) Verlag Chemie, Weinheim/Bergstrasse, 1967. 280 S.

Der stürmischen Entwicklung der präparativen organischen Chemie, dem immer wieder und in raschem Nacheinander erfolgenden Auffinden und Ausbau neuerer Synthesemöglichkeiten und der Erforschung neuer Reaktionsweisen entsprechend folgen die einzelnen Beiträge der Reihe der »Neueren Methoden« in der »Angewandten Chemie« einander in immer kürzeren Zeitabständen. So kommt es, daß auch der fünfte Sammelband dieser Reihe nicht lange auf sich warten ließ und knapp ein halbes Jahr nach dem Erscheinen des vierten Bandes* nunmehr ebenfalls vorliegt.

* s. Acta Chim. Acad. Sci. Hung. **53,** 422 (1967).

Vier — oder, wenn man die des Schwefels auch zu dieser Verbindungsklasse rechnet, fünf — der sieben, in dem fünften Bande enthaltenen und seit ihrem ursprünglichen Erscheinen in der »Angewandten Chemie« wieder auf den neuesten Stand gebrachten Beiträge befassen sich mit der Verwendung bzw. Synthese elementorganischer Verbindungen. Dies entspricht völlig der immer bedeutenderen Rolle, die diese Verbindungsklasse in der organisch-chemischen Forschung und Produktion neuerdings spielt.

Es handelt sich um die folgenden Beiträge: »Neue Reaktionen von Phosphinalkylenen und ihre präparativen Möglichkeiten« von H. J. BESTMANN (52 Seiten) und daran in vielen Punkten anknüpfend die »Synthese natürlich vorkommender Fettsäuren durch sterisch kontrollierte Carbonyl-Olefinierung« von L. D. BERGELSON und M. M. SCHEMJAKIN (der erste sowjetische Beitrag zu dieser Reihe! — 21 Seiten); »Die Silylierung als Hilfsmittel in der organischen Synthese« von L. BIRKOFER und A. RITTER (25 Seiten); Natrium- und Kaliumorganische Verbindungen« von M. SCHLOSSER (64 Seiten) und schließlich »Organische Synthesen mit Imiden des Schwefeldioxyds« von G. KRESZE und W. WUCHERPFENNIG (41 Seiten).

Die Namen der Autoren — alle bekannte Forscher oder sogar Pioniere auf dem von ihnen zusammengefaßten Gebiete — bürgen für das Niveau der Beiträge.

Auch die beiden restlichen Beiträge, die sich nicht mit elementorganischen, sondern mit »gewöhnlichen« organischen Verbindungsklassen beschäftigen, nämlich die »Synthesen mit heterocyclischen Amiden (Azoliden)« von H. A. STAAB und W. ROHR (41 Seiten) und »Synthesen mit s-Triazin« von Ch. GRUNDMANN, dem Vertreter der USA im vorliegenden Bande (29 Seiten), sind von Experten verfaßt, deren Namen sich eines nicht minderen Wohlklanges erfreuen.

Die Bedeutung der behandelten Synthesemethoden, Reaktionen und Verbindungsklassen ist wohlbekannt, so daß sich eine diesbezügliche Würdigung erübrigt. Der Überblick über die Fülle der Anwendungsmöglichkeiten und neueren Entwicklungsrichtungen der behandelten Methoden und Verbindungen, die dem Leser der einzelnen Beiträge gewährt wird, versetzt ihn jedoch immer wieder ins Staunen, auch wenn er einen großen Teil der Originalarbeiten und eventuell auch frühere Zusammenfassungen über die einzelnen behandelten Gebiete kennt.

Der Band wird sich — der Rezensent ist davon überzeugt — nicht nur in den Bibliotheken von Lehr-, Forschungsinstituten und chemischen Werken, sondern auch in den Privatbibliotheken der Organiker einen festen und wichtigen Platz sichern.

K. LEMPERT

Team of authors of the Working Committee for Catalysis of the Hungarian Academy of Sciences: *Contact Catalysis* (in Hungarian). Akadémiai Kiadó, Budapest, 1966.

In the rapid development of the chemical industry of today, a prominent role has been played by the results attained in kinetic studies on catalytic processes, including contact catalysis. The importance of kinetic investigations has been emphasized even more so by the necessity of meeting the requirements in the automation of industrial processes and in increasing their efficiency.

In the field of contact catalysis, despite the results of intense research work carried out in recent years, there are still a number of kinetic problems to be solved, mainly concerning the mechanism of elementary processes taking place on catalyst surfaces and the properties of catalysts. There are a great number of monographs in world literature that survey the results and problems related to one or more details of this field. However, none of them published up to now can be regarded as a comprehensive work of the theoretical fundamentals, giving useful advice as regards practical applications.

The present work differs in this sense from all the monographs published so far, and it is therefore of a pioneer character not only in Hungarian, but also in world literature, in that it discusses the important basic problems of the entire field of contact catalysis and outlines the possibilities of its utilization in practice, and thus offers a comprehensive survey for experts who are active in this field. The authors of the work, by all means, deserve credit for this fact alone. Moreover, if one considers the fact that this book — by starting with fundamental knowledge and guiding the reader up to large-scale industrial applications — serves as useful reference, first and foremost, for those who are only beginning to get acquainted with this field of research, but also for experts actively engaged in industry, can one really appreciate the significance and practical value of it.

The structure of the book, consisting of seven chapters, well fits the aims set by the authors. Since the catalysts used in this field of catalysis are of solid substances, therefore the primary requirement is to know the structure and properties of such solids in order to elucidate and interpret the mechanism of the processes taking place on the catalysts. Accordingly, in Chapter I, the electron structure of metals and semiconductors is discussed, and the ways of interpretation of the electric, magnetic and surface properties of catalysts on the basis of their electron structures are presented.

Chapter II is entirely devoted to one important elementary process of contact catalysis, namely to adsorption. The most essential fundamental concepts are given along with examples selected from the field of physical adsorption. Their presentation in this manner greatly facilitates the understanding of the techniques used in catalytic investigations based on the principles of adsorption, and lastly, but not least, gives a summary of their applicability. The discussion of the mechanism of chemisorption on the basis of modern electron theory furnishes valuable information for a deeper understanding of the causes that result in various processes taking place in the presence of catalysts.

Chapter III is concerned with the ways in which chemical conversions occur, with the parameters determining them, and with the relation existing between the changes occurring in the properties of the catalyst during use and the catalytic process.

Chapter IV starts with the basic concepts concerning the rates of chemical reactions. This is followed by a discussion of the regularities of the course of catalytic reactions as compared with heterogeneous reactions. Subsequently, the methods applied for the experimental determination of reaction rates, and the ways of experimental checking of theoretically derived rate equations are presented through some well-selected examples.

Chapters V, VI and VII contain material perhaps most readily and directly utilizable by experts working in industrial plants. Chapter V deals with the changes occurring in the properties of the catalysts, with the parameters influencing the various effects exerted by the catalysts, and also with the description of the types of catalysts. Chapter VI discusses, in detail, the aspects of the selection of suitable catalysts, the various possible ways of preparing them experimentally, and the methods of investigation suitable for studying their various properties. In the last chapter, Chapter VII, the modes of the practical application of contact catalytic processes are presented. Accordingly, this chapter contains useful information regarding the methods for the experimental determination of the parameters of processes taking place in contact catalytic reactors, as well as some aspects concerning the planning and optimization of such reactors.

On the basis of the language and style, both being good and consistent, it would be hard to tell that the book was compiled from works written by various authors. This is mainly to the credit of the reviewer and to that of the editors. There are, however, some repetitions to be found in various parts of the book, though, as such, are not necessarily disadvantageous, nevertheless, they could have been avoided by more careful editing. Moreover, certain parts of Chapter I do not appear to be quite in accord — not as much as regards their content, but rather in their way of wording — with the primary aim set, and successfully attained in other chapters, namely, "to facilitate the work of experts in practice and that of research workers".

Detailed references to literature given at the end of each chapter give valuable aid to readers who desire more detailed information concerning some of the more particular problems. There are excellently compiled author and subject indexes. The publishers are to be congratulated for the attractive appearance of the book.

F. MÁRTA

INDEX

INORGANIC AND ANALYTICAL CHEMISTRY — ANORGANISCHE UND ANALYTISCHE CHEMIE — НЕОРГАНИЧЕСКАЯ И АНАЛИТИЧЕСКАЯ ХИМИЯ

Лаврухина, А. К., Кашкаров, Л. Л., Колесов, Г. М, Генаева, Л. И.: Изучение распределения редких элементов между различными фазами каменных метеоритов методом нейтроно-активационного анализа. LAVRUKHINA, A. K., KASKAROV, L. L., KOLESOV, G. M. and GENAJEVA, L. I.: Investigation of the Distribution of Rare Elements between the Various Phases of Stone Meteorites by Neutron Activation Analysis) 353

BURGER, K., PINTÉR, B., PAPP-MOLNÁR, E. and NEMES-KÓSA, S.: The Chemistry of Mixed Ligand Complexes, III. The Effect of Water Activity on the Stability of the Bis-Dimethylglyoximato-Diiodo-Cobaltate(II) Mixed Complex 363

PULAY, P.: On the Parameter Form of Force Constant Matrix, VII. The Closest Assignment Force Constant Matrix 373

NÁRAY-SZABÓ, I., MAGYAROSY, I., KOTSIS, T. und FEHÉR, I.: Untersuchung der chemischen Vorgänge bei der Kalkbehandlung des Rotschlammes 377

PHYSICAL CHEMISTRY — PHYSIKALISCHE CHEMIE — ФИЗИЧЕСКАЯ ХИМИЯ

Элек, А. и *Сабо, З.:* Анализ вольфрама методом нейтронной активации II. Определение содержания натрия и калия. ELEK, A. and SZABÓ, E.: Investigation of Tungsten by Neutron Activation Analysis, II 385

FÁY, L. and BALOGH, A.: Determination of Reaction Order and Rate Constants on the Basis of the Parameter Estimation of Differential Equations 391

HARGITTAI, I.: Investigation of the Molecular Structure of Sulphuryl Chloride by Sector Microphotometer Electron Diffraction 403

SOHÁR, P. and KÓSA, I.: NH Stretching Vibration Bands at Wave Numbers Lower than 3000 cm^{-1}, V. Cyclic Dimeric Structures, V. Quinazolone Derivatives 411

SOHÁR, P.: NH Stretching Vibration Bands at Wave Numbers Lower than 3000 cm^{-1}, VI. Cyclic Dimeric Structures, VI. Hydantoin Derivatives 425

ORGANIC CHEMISTRY — ORGANISCHE CHEMIE — ОРГАНИЧЕСКАЯ ХИМИЯ

MARKÓ, L. et FREUND, M.: L'utilisation des oléfines plus élevées de craquage d ans l'oxosynthèse 445

Book Reviews — Buchbesprechungen — Рецензии книг 453

Printed in Hungary

A kiadásért felel az Akadémiai Kiadó igazgatója — Műszaki szerkesztő: Farkas Sándor

A kézirat nyomdába érkezett: 1968. VI. 21. — Terjedelem: 9,75 (A/5) ív, 74 ábra

68.65842 Akadémiai Nyomda, Budapest — Felelős vezető: Bernát György

ACTA CHIMICA

ТОМ. LVII — ВЫП. 4

РЕЗЮМЕ

Химия смешанных комплексов, III. Влияние активности воды на стабильность смешанных бис-диметил-глиоксимато-дииодных комплексов кобальта II

К. БУРГЕР, Б. ПИНТЕР, Э. ПАПП-МОЛНАР и Ш. НЕМЕШ-КОША

Определялась стабильность бис-диметил-глиоксимато-дииодного комплекса кобальта(II) в растворах с различными концентрациями перхлората натрия, нитрата натрия, и нитрата лития. Были рассчитаны активности воды в различных растворах. Было установлено, что стабильность смешанных комплексов возрастает с уменьшением активности воды растворов. Использование различных солей для получения заданной активности воды не сказывается на результатах.

О параметрической форме матрицы силовых постоянных, VII. Наиболее близкая ассигнация матрицы силовых постоянных

П. ПУЛАИ

Определялось разумное измерение близости ассигнаций между внутренними и нормальными координатами колеблющихся молекул. Было показано, что матрица силовых постоянных $F_0 = G^{-1/2} \Lambda G^{-1/2}$ соответствует наиболее близкой ассигнации. Рассматривалось влияние обмера нормальных координат с помощью численных факторов, и предлагалась единая нормализация для случаев, когда диагональные элементы матрицы кинетической энергии G равны 1. Полагалось, что место матрицы действительных силовых постоянных в параметровом пространстве является точной мерой ассигнаций.

Изучение процессов, протекающих при известковой обработке красного шлама

И. НАРАИ-САБО, И. МАДЬАРОШИ, Т. КОЧИШ и И. ФЕХЕР

Красный шлам, образующийся при разработке бокситов по Байеру, при смешивании с известковым молоком затвердевает и достигает значительной твердости. На основе химических и дифрактометрических исследований было установлено, что реакция продуктов, образующихся при обработке каолина щелочью Байера при температуре 250 °C, с известковым молоком не приводит к затвердеванию. Однако, при разработке каолин, находящийся в бокситах, образуется и коллоидная кремневая кислота и гидрокись алюминия, которые, реагируя с $Ca(OH)_2$, дают продукты подобные тоберториту и, теряя воду, затвердевают так же как, и цементовое тесто.

Определение порядка реакции и констант скоростей на основе приблизительной оценки параметров дифференциальных уравнений

Л. ФАЙ и А. БАЛОГ

В области физической химии часто возникает проблема доказательства правильности составленного дифференциального уравнения на основе результатов измерений, а также оценки параметров этого дифференциального уравнения. Если аналитическое решение дифференциального уравнения не известно, то резрешение этой проблемы сталкивается с трудностями.

В настоящей работе представляется прием, основанный на методе наименьших квадратов и позволяющий разрешить вышеупомянутую проблему. Из условия наименьшего расхождения расчетных и измеренных величин, параметры могут быть определены как с помощью решения системы уравнений, полученной дифференцированием в частных производных по переменным, так и с помощью непосредственного определения граничных значений функции.

В настоящей работе решение системы уравнений проводилось с помощью счетной машины. Использование метода иллюстрировано на примере расчета по реакционной кинетики. Определение константы скорости в уравнении скорости для каталитического окисления этилена и порядка реакции на основе данных измерений производилось с помощью описанного метода. Если полагать, что порядок реакции не известен, то уравнение скорости представляет собой дифференциальное уравнение, не имеющее аналитического решения. С помощью нашего метода из хода кривых изменения концентрации этилена во времени определялись порядок реакции и константы скорости. На основе рассчитанных данных решалось дифференциальное уравнение, и решение сравнивалось с результатами измерений.

Электронографическое секторно-микрофотометрическое исследование строения молекулы SO_2Cl_2

И. ХАРГИТТАИ

Было исследовано строение молекулы SO_2Cl_2 электронографическим секторно-микрофотометрическим методом. Следующие длины связи и валентные углы были определены с помощью метода наименьших квадратов: I(S—O) 1,409 $\pm$ 0,005 Å, I(S—Cl) 2,011 $\pm$ 0,006 Å $\sphericalangle$ OSO 123 $\pm$ 2° и $\sphericalangle$ OSCl 107,6 $\pm$ 0,6°.

Полоса валентных колебаний NH в области волновых чисел, меньших 3000 $см^{-1}$, V. Циклические димеры, V. Производные хиназолона

П. ШОХАР и И. КОША

4(3H)-хиназолинон и его производные ассоциируются в форме циклического димера. Условия сопряжения, и вместе с этим и мезомерия внутри амидной группы изменяются интересно по сравнению с дигидрофталазоном, являющимся структуральным изомером 4-хиназолона. Было установлено, что общее для амидов смещение электрона от атома азота в направлении атома кислорода, вследствие эффекта-I связи —C = N в положении 2, затрудняется в 4(3H)-хиназолиноне, в то время как в дигидрофталазоне эффект + *T* атома азота группы —N=C компенсирует эффект-I, и в результате мезомерия амидной группы осуществляется свободно.

Структура ацильных производных и их химические свойства находятся в согласии с заключениями, сделанными на основе изменений в условиях сопряжения, поскольку в случае дигидрофталазона могут быть получены как O- так и N-ацилаты, в то время как из 4(3H)-хиназолинона получаются лишь очень неустойчивые N-ацилпроизводные. 3-

гидрокси-4(3H)-хиназолиноны, вероятно, обладают структурой внутренней соли, что подтверждается и спектрами их солянокислых солей. Следует отметить исключительно высокую эфирнокарбонильную частоту (около 1820 и 1790 $см^{-1}$) их O-ацильных производных.

Полоса валентных колебаний группы NH в области волновых чисел, меньших 3000 $см^{-1}$, VI. Циклические димеры, VI. Производные хидантоина

П. ШОХАР

Исследовались ик-спектры 5,5-идфенил-хидантоина, а также его тио- и N-метил-производных. Было установлено, что все соединения находятся в диоксо- (или оксотиоксо- и дитиоксо-)форме; таутомеры, содержащие иминогидринные (тиоиминогидринные) группы, не образуются. В случае диоксосоединений колебания карбонильной группы накладываются друг к другу. Условия ассоциации влияют на свойства полос наложенных колебаний. В случае тиопроизводных тиоамидные, тиокарбамидные и тиоимидные группы обладают характерными полосами колебаний, структура которых весьма разнообразна. В спектре 2-тио-соединения наблюдаются три полосы, характерные для группы N(H)C(S)N(H), и находящиеся в интервалах 1550—1480, 1350—1250 и 1200—1100 $см^{-1}$. Для 4-тиосоединений наблюдаются две тиоамидные полосы в интервалах 1450—1350 и 1350—1250 $см^{-1}$. В спектре 2,4-дитио-хидантоина в интервале 1550—1500 $см^{-1}$ имеется интенсивная полоса. В случае тех двух соединений, которые обладают группой NH в 3-ем положении также появляется интенсивный максимум и в области около 1450 $см^{-1}$. Для этих двух соединений были обнаружены также и три дополнительные полосы в интервалах 1435—1400, 1270—1230 и 1165—1150 $см^{-1}$ за счет тиоамидной группы. В спектрах двух 3-метил-производных обнаружены две полосы в области около 1300—1100 $см^{-1}$.

Условия ассоциации многообразны. В первую очередь, образуют карбонильная группа в положении 2 и NH-группа в положении 3 сильные водородные связи. В случае некоторых соединений возможна также ассоциация циклических димеров. Поэтому, если для двух соединений 4-тио-3-незамещенных производных, это единственная форма ассоциации, то у соответствующих 2-тио-производных она существует лишь для некоторой доли молекул, а для остальной доли молекул возможные различны простые интермолекулярные ассоциации между группами в положениях 1 и 4.

Использование высокомолекулярных олефинов бензина крекинга в качестве исходного вещества для оксо-синтеза

Л. МАРКО и М. ФРАЙНД

Среди исходных веществ для оксо-синтеза мало изучались до сих пор олефины с более высокими молекулярными весами, являющиеся продуктами термического крекинга.

Исходя из этих олефинов, с помощью гомогенного каталитического гидрирования образующихся олефинов удалось разработать непрерывный одноступенчатый промышленный процесс оксо-синтеза, приводящий непосредственно к образованию спирта. Яды катализаторов, как, например, серные соединениия, не оказывают влияния на процесс, что является очень важным с точки зрения возможности использования олефинов, легко получаемых при крекинге нефти для целей оксо-синтеза.

The Acta Chimica publish papers on chemistry in English, German, French and Russian.

The Acta Chimica appear in volumes consisting of four parts of varying size, 4 volumes being published a year.

Manuscripts should be addressed to

Acta Chimica
Budapest 112/91 Műegyetem

Correspondence with the editors should be sent to the same address.

The rate of subscription is 165 forints a volume. Orders may be placed with "*Kultúra*" Foreign Trade Company for Books and Newspapers (Budapest I., Fő utca 32. Account No. 43-790-057-181) or with representatives abroad.

Les Acta Chimica paraissent en français, allemand, anglais et russe et publient des mémoires du domaine des sciences chimiques.

Les Acta Chimica sont publiés sous forme de fascicules. Quatre fascicules seront réunis en un volume (4 volumes par an).

On est prié d'envoyer les manuscrits destinés à la rédaction à l'adresse suivante:

Acta Chimica
Budapest 112/91 Műegyetem

Toute correspondance doit être envoyée à cette même adresse.

Le prix de l'abonnement est de 165 forints par volume.

On peut s'abonner à l'Entreprise pour le Commerce Extérieur de Livres et Journaux «*Kultúra*» (Budapest I., Fő utca 32. Compte-courant No. 43-790-057-181) ou à l'étranger chez tous les représentants ou dépositaires.

«*Acta Chimica*» издают трактаты из области химической науки на русском, французском, английском и немецком языках.

«*Acta Chimica*» выходят отдельными выпусками разного объема. 4 выпуска составляют один том. 4 тома публикуются в год.

Предназначенные для публикации рукописи следует направлять по адресу:

Acta Chimica
Budapest 112/91 Műegyetem

По этому же адресу направлять всякую корреспонденцию для редакции.

Подписная цена «*Acta Chimica*» — 165 форинтов за том. Заказы принимает предприятие по внешней торговле книг и газет «*Kultúra*» (Budapest I., Fő utca 32. Текущий счет № 43-790-057-181) или его заграничные представительства и уполномоченные.

Reviews of the Hungarian Academy of Sciences are obtainable at the following addresses:

ALBANIA

Ndermarja Shtetnore e Botimeve
Tirana

AUSTRALIA

A. Keesing
Box 4886, GPO
Sydney

AUSTRIA

Globus Buchvertrieb
Salzgries 16
Wien I

BELGIUM

Office International de Librairie
30, Avenue Marnix
Bruxelles 5

Du Monde Entier
5, Place St. Jean
Bruxelles

BULGARIA

Raznoiznos
1, Tzar Assen
Sofia

CANADA

Pannonia Books
2, Spadina Road
Toronto 4, Ont.

CHINA

Waiwen Shudian
Peking
P. O. B. 88

CZECHOSLOVAKIA

Artia
Ve Smečkách 30
Praha 2

Poštovná Novinová Služba
Dovoz tisku
Vinohradská 46
Praha 2

Mad'arská Kultura
Václavské nám. 2
Praha I

Poštová Novinová Služba
Dovoz tlače
Leningradská 14
Bratislava

DENMARK

Ejnar Munksgaard
Nörregade 6
Copenhagen

FINLAND

Akateeminen Kirjakauppa
Keskuskatu 2
Helsinki

FRANCE

Office International de Documentation et Librairie
48, rue Gay Lussac
Paris 5

GERMAN DEMOCRATIC REPUBLIC

Deutscher Buch-Export und Import
Leninstraße 16
Leipzig 701

Zeitungsvertriebsamt
Clara Zetkin Straße 62
Berlin N. W.

GERMAN FEDERAL REPUBLIC

Kunst und Wissen
Erich Bieber
Postfach 46
7 Stuttgart S.

GREAT BRITAIN

Collet's Holdings Ltd.
Dennington Estate
London Rd.
Wellingborough. Northants.

Robert Maxwell and Co. Ltd.
Waynflete Bldg. The Plain
Oxford

HOLLAND

Swetz and Zeitlinger
Keizersgracht 471—487
Amsterdam C

Martinus Nijhof
Lange Voorhout 9
The Hague

INDIA

Current Technical Literature
Co. Private Ltd.
India House OPP
GPO Post Box 1374
Bombay I

ITALY

Santo Vanasia
Via M. Macchi 71
Milano

Libreria Commissionaria Sansoni
Via La Marmora 45
Firenze

JAPAN

Nauka Ltd.
92, Ikebukur O-Higashi 1-chome
Toshima-ku
Tokyo

Maruzen and Co. Ltd.
P. O. Box 605
Tokyo-Central

Far Eastern Booksellers
Kanda P. O. Box 72
Tokyo

KOREA

Chulpanmul
Phenjan

NORWAY

Johan Grundt Tanum
Karl Johansgatan 43
Oslo

POLAND

RUCH
ul. Wronia 23
Warszawa

ROUMANIA

Cartimex
Str. Aristide Briand 14—18.
Bucureşti

SOVIET UNION

Mezhdunarodnaya Kniga
Moscow G—200

SWEDEN

Almquist and Wiksell
Gamla Brogatan 26
Stockholm

USA

Stechert Hafner Inc.
31, East 10th Street
New York, N. Y. 10003

Walter J. Johnson
111, Fifth Avenue
New York, N. Y. 10003

VIETNAM

Xunhasaba
19, Tran Quoc Toan
Hanoi

YUGOSLAVIA

Forum
Vojvode Mišića broj 1
Novi Sad

Jugoslovenska Knjiga
Terazije 27
Beograd